



Universidad de Oviedo
Universidá d'Uviéu
University of Oviedo

Departamento de Química Orgánica e Inorgánica

Programa de Doctorado: Síntesis y Reactividad Química

***Catalytic Coupling Processes of Silylated Unsaturated Systems,
Initiated by Carbophilic Activation***

Sergio Fernández González

Tesis Doctoral

2022



Universidad de Oviedo
Universidá d'Uviéu
University of Oviedo

Departamento de Química Orgánica e Inorgánica

Programa de Doctorado: Síntesis y Reactividad Química

***Catalytic Coupling Processes of Silylated Unsaturated Systems,
Initiated by Carbophilic Activation***

Sergio Fernández González

Memoria presentada para optar al grado de Doctor en Química orgánica con
Mención de Doctor Internacional

Dissertation submitted to apply for the degree of Doctor of Philosophy in
Organic Chemistry with Internacional Doctor Mention



RESUMEN DEL CONTENIDO DE TESIS DOCTORAL

1.- Título de la Tesis	
Español/Otro Idioma: <i>Procesos catalíticos de acoplamiento de sistemas insaturados sililados, iniciados mediante activación carbófila</i>	Inglés: <i>Catalytic Coupling Processes of Silylated Unsaturated Systems, Initiated by Carbophilic Activation</i>
2.- Autor	
Nombre: Sergio Fernández González	DNI/Pasaporte/NIE:
Programa de Doctorado: Síntesis y Reactividad Química	
Órgano responsable: Universidad de Oviedo	

RESUMEN (en español)

La presente memoria se encuentra dentro del campo de la Catálisis Organometálica, y más en concreto en la catálisis homogénea de oro(I). En ella se encuentran recogidos los resultados obtenidos durante el estudio de la reactividad de sistemas sililados insaturados, como los propargilsilanos, en presencia de catalizadores carbófilos. En base al tipo de transformación descrita, este documento se ha dividido en cuatro capítulos bien diferenciados.

El primer capítulo describe los resultados alcanzados en la primera propargilación de derivados carbonílicos, catalizada por complejos de oro(I), a partir de propargilsilanos. El estudio de dicha transformación ha permitido describir una metodología altamente eficiente y en condiciones suaves para la generación de silil éteres homopropargílicos. Su análisis exhaustivo ha permitido además determinar el mecanismo por el cual transcurre, identificando como intermedio clave un complejo organometálico de tipo σ -aleniloro(I). De hecho, la participación de dicha especie pudo ser confirmada empíricamente, representando el primer ejemplo aislado de este tipo de complejos de oro(I) con actividad catalítica.

El segundo capítulo se centra en la descripción de primera reacción catalítica de bispropargilación desoxigenativa, empleando para ello complejos de oro(I) como catalizadores. En él se describe la síntesis diastereoselectiva de derivados de 9,9-bispropargilxantenos a partir de xantonas y propargilsilanos. Asimismo, ha sido posible obtener de forma selectiva productos de monopropargilación, bispropargilación simétrica y bispropargilación no simétrica, a través de la modulación del disolvente de reacción. Este capítulo también ilustra el potencial sintético de los productos obtenidos, representado mediante diversas derivatizaciones de los mismos.

El tercer capítulo recoge los resultados obtenidos en el estudio de una síntesis "one-pot" de 2-silil-4,5-dihidrofuranos, catalizada por complejos de oro(I), a partir de propargilsilanos y carbonilos. Dicha reacción consta de tres etapas consecutivas: propargilación, hidrólisis de un silil éter y cicloisomerización de un intermedio de tipo 1,4-alquínol. Adicionalmente, se ha conseguido llevar a cabo una isomerización cis-trans de los productos obtenidos ajustando las condiciones del proceso, suponiendo ésta la cuarta etapa consecutiva de esta metodología. Por otra parte, la realización varios experimentos de deuteración, así como una gráfica de Hammett, apoyan la propuesta mecanística aquí recogida.

En el cuarto capítulo se describe una síntesis "one-pot" de derivados de benzofulvenos cocatalizada por un complejo de oro(I) y un ácido de Lewis, a partir de propargilsilanos y derivados de benzofenona. Dicha metodología implica tres pasos de reacción consecutivos: propargilación, eliminación e hidroarilación de tipo Nazarov. La influencia del ácido de Lewis ha demostrado ser crucial en dicha transformación, proponiéndose la coordinación del mismo al contraión del complejo de oro(I), aumentando así su electrofilia y potenciando la actividad catalítica del mismo. Estudios mecanísticos detallados, incluyendo experimentos estequiométricos de RMN a baja temperatura, han permitido apoyar por primera vez dicha hipótesis.



RESUMEN (en Inglés)

This Dissertation is included within the area of Organometallic Catalysis, and more specifically using gold(I) homogeneous catalysis. It contains the results obtained during the study of the reactivity of unsaturated silylated systems, such as propargylsilanes, in the presence of carbophilic catalysts. Regarding the type of organosilicon reagent studied and the transformation described, this document has been divided into four well-differentiated chapters.

Chapter I describes the results achieved in the first propargylation of carbonyl derivatives, catalyzed by gold(I) complexes, from propargylsilanes. The study of this transformation allowed to describe a highly efficient methodology under mild conditions for the generation of homopropargylic silyl ethers. The exhaustive analysis of this reaction permitted also to determine in detailed way the mechanism it occurs through, identifying a η^3 -allenylgold(I) complex as the key intermediate. In fact, the participation of this species could be empirically confirmed, representing the first isolated example of this type of gold(I) complexes with catalytic activity.

Chapter II is focused on the first catalytic deoxygenative bispropargylation reaction, using gold(I) complexes as catalysts. This study made possible to describe the diastereoselective synthesis of 9,9-bispropargylxanthene derivatives from xanthenes and propargylsilanes. Moreover, it has been possible to selectively obtain monopropargylation, symmetric bispropargylation and non-symmetric bispropargylation products, by modulating the solvent of the reaction. This chapter also illustrates the synthetic potential of the obtained products, represented by several derivatization reactions.

Chapter III collects the results obtained in the study of a one-pot intermolecular synthesis of 2-silyl-4,5-dihydrofurans, by means of gold(I) catalysis, from propargylsilanes and carbonyl compounds. This reaction consists of three consecutive stages: propargylation, hydrolysis of a silyl ether and cycloisomerization of a 1,4-alquinol intermediate. Additionally, it has been possible to carry out a cis-to-trans isomerization of the obtained products by adjusting the process conditions, adding the fourth consecutive gold(I)-catalyzed stage to this methodology. Moreover, several deuteration experiments, as well as a Hammett plot, support the mechanistic proposal herein collected.

Chapter IV summarizes a one-pot gold(I)-Lewis-acid cocatalyzed synthesis of benzofulvene scaffolds, starting from propargylsilanes and different benzophenones derivatives. The described methodology involves three consecutive reaction steps: propargylation, elimination and Nazarov-type hydroarylation. The influence of the Lewis acid has proven to be crucial in this transformation, proposing its coordination to the counterion of the gold(I), increasing therefore its electrophilicity and enhancing its catalytic activity. More detailed mechanistic studies, including several low temperature NMR stoichiometric experiments, have supported this hypothesis for the first time.

**SR. PRESIDENTE DE LA COMISIÓN ACADÉMICA DEL PROGRAMA DE DOCTORADO
EN SÍNTESIS Y REACTIVIDAD QUÍMICA**

Agradecimientos

Antes de empezar a escribir esta memoria, me dije a mí mismo que no iba a escribir este apartado. Y aquí estoy, reescribiendo mis palabras una y otra vez. El motivo para ambas cosas no es la falta de personas a las que estar agradecido después de cinco años, sino la imposibilidad de expresar a todas y cada una de ellas mi gratitud sin dejarme a nadie en el tintero. Al empezar esta etapa, un gran maestro me dijo que “la tesis es un trabajo duro que se asemeja a recorrer un largo y complicado camino lleno de baches y bifurcaciones, cada día hay que recorrer un poco del camino con trabajo duro y constante”. Doy fe de ello, y espero haber sabido estar a la altura de sus enseñanzas. También remarcó varias veces que dicho camino no se recorre solo, siempre están tus directores, compañeros, familia y amigos, a veces aguantando tus problemas sin entenderlos.

Una vez dicho esto, me gustaría empezar por agradecer a mis directores, Alfredo y Javier (Santa), la forma en que han sabido guiarme en esta etapa tan importante, siendo “jefes” cercanos, con paciencia, comprensión, ganas de enseñar y sentido del humor (esto último que no falte). Gracias por todo, he aprendido muchísimo y he disfrutado todo el proceso.

En cuanto al grupo de compañeros, amigos y familiares que me han acompañado, podría casi escribir otra tesis si os mencionase individualmente. Siento meteros en el mismo saco, pero creo que es lo más práctico. Gracias a todos por estar a mi lado en los buenos y en los malos momentos, incluso para tomar un vermú o una cerveza si la ocasión lo requería (que generalmente así era); por aconsejarme y apoyarme en momento difíciles; por las buenas críticas, que me han ayudado a crecer profesional y personalmente; por sacarme una carcajada en medio de un duro trabajo; y por haber podido conocer las personas tan maravillosas que hay en este mundillo de la Química.

Acknowledgements

Before I started writing this Dissertation, I told myself not to write this section. And here I am, rewriting my words over and over again. The reason for both is not the lack of people to be grateful to after five years, but the impossibility of expressing my gratitude to each one of them without forgetting anyone in that process. At the beginning of this stage, a great teacher told me that "the thesis implies hard work, like traveling a long and complicated road full of potholes and crossroads, every day you have to travel a little bit of the road with hard and constant work". I can testify it, and I hope I have lived up to his teachings. He also stressed several times that you don't travel this path on your own, your directors, colleagues, family and friends are always there, sometimes listening to your problems without understanding them.

Once I said this, I would like to start by thanking my directors, Alfredo and Javier (Santa), for the way in which they have been able to guide me in this important stage, being close "bosses", with patience, understanding, desire to teach and sense of humor (this one should never lack). Thank you for everything, I have learned a lot and I have enjoyed the whole process.

Regarding the group of colleagues, friends and relatives who have accompanied me, I could almost write another thesis if I mentioned you individually. I'm sorry to put you in the same bag, but I think it's the most practical thing to do. Thank you all for being by my side during good and bad times, even drinking a vermouth or a beer if the occasion required it (it usually did); for advising and supporting me through difficult times; for the good reviews, which have helped me to grow professionally and personally; for making me laugh in the middle of a hard job; and for having been able to meet the wonderful people within this Chemistry world.

Resumen

La presente memoria se encuentra dentro del campo de la Catálisis Organometálica, y más en concreto en la catálisis homogénea de oro(I). En ella se encuentran recogidos los resultados obtenidos durante el estudio de la reactividad de sistemas sililados insaturados, como los propargilsilanos, en presencia de catalizadores carbofílicos. En base al tipo de transformación descrita, este documento se ha dividido en cuatro capítulos bien diferenciados.

El primer capítulo describe los resultados alcanzados en la primera propargilación de derivados carbonílicos, catalizada por complejos de oro(I), a partir de propargilsilanos. El estudio de dicha transformación ha permitido describir una metodología altamente eficiente y en condiciones suaves para la generación de silil éteres homopropargílicos. Su análisis exhaustivo ha permitido además determinar el mecanismo por el cual transcurre, identificando como intermedio clave un complejo organometálico de tipo σ -alenooro(I). De hecho, la participación de dicha especie pudo ser confirmada empíricamente, representando el primer ejemplo aislado de este tipo de complejos de oro(I) con actividad catalítica.

El segundo capítulo se centra en la descripción de primera reacción catalítica de bispropargilación desoxigenativa, empleando para ello complejos de oro(I) como catalizadores. En él se describe la síntesis diastereoselectiva de derivados de 9,9-bispropargilxantenos a partir de xantonas y propargilsilanos. Asimismo, ha sido posible obtener de forma selectiva productos de monopropargilación, bispropargilación simétrica y bispropargilación no simétrica, a través de la

modulación del disolvente de reacción. Este capítulo también ilustra el potencial sintético de los productos obtenidos, representado mediante diversas derivatizaciones de los mismos.

El tercer capítulo recoge los resultados obtenidos en el estudio de una síntesis “one-pot” de 2-silil-4,5-dihidrofuranos, catalizada por complejos de oro(I), a partir de propargilsilanos y carbonilos. Dicha reacción consta de tres etapas consecutivas: propargilación, hidrólisis de un silil éter y cicloisomerización de un intermedio de tipo 1,4-alquínol. Adicionalmente, se ha conseguido llevar a cabo una isomerización *cis-trans* de los productos obtenidos ajustando las condiciones del proceso, suponiendo ésta la cuarta etapa consecutiva de esta metodología. Por otra parte, la realización varios experimentos de deuteración, así como una gráfica de Hammett, apoyan la propuesta mecanística aquí recogida.

En el cuarto capítulo se describe una síntesis “one-pot” de derivados de benzofulvenos cocatalizada por un complejo de oro(I) y un ácido de Lewis, a partir de propargilsilanos y derivados de benzofenona. Dicha metodología implica tres pasos de reacción consecutivos: propargilación, eliminación e hidroarilación de tipo Nazarov. La influencia del ácido de Lewis ha demostrado ser crucial en dicha transformación, proponiéndose la coordinación del mismo al contraíón del complejo de oro(I), aumentando así su electrofilia y potenciando la actividad catalítica del mismo. Estudios mecanísticos detallados, incluyendo experimentos estequiométricos de RMN a baja temperatura, han permitido apoyar por primera vez dicha hipótesis.

Summary

This Dissertation is included within the area of Organometallic Catalysis, and more specifically using gold(I) homogeneous catalysis. It contains the results obtained during the study of the reactivity of unsaturated silylated systems, such as propargylsilanes, in the presence of carbophilic catalysts. Regarding the type of organosilicon reagent studied and the transformation described, this document has been divided into four well-differentiated chapters.

Chapter I describes the results achieved in the first propargylation of carbonyl derivatives, catalyzed by gold(I) complexes, from propargylsilanes. The study of this transformation allowed to describe a highly efficient methodology under mild conditions for the generation of homopropargylic silyl ethers. The exhaustive analysis of this reaction permitted also to determine in detailed way the mechanism it occurs through, identifying a η^2 -allenylgold(I) complex as the key intermediate. In fact, the participation of this species could be empirically confirmed, representing the first isolated example of this type of gold(I) complexes with catalytic activity.

Chapter II is focused on the first catalytic deoxygenative bispropargylation reaction, using gold(I) complexes as catalysts. This study made possible to describe the diastereoselective synthesis of 9,9-bispropargylxanthene derivatives from xanthenes and propargylsilanes. Moreover, it has been possible to selectively obtain monopropargylation, symmetric bispropargylation and non-symmetric bispropargylation products, by modulating the solvent of the reaction. This chapter

also illustrates the synthetic potential of the obtained products, represented by several derivatization reactions.

Chapter III collects the results obtained in the study of a one-pot intermolecular synthesis of 2-silyl-4,5-dihydrofurans, by means of gold(I) catalysis, from propargylsilanes and carbonyl compounds. This reaction consists of three consecutive stages: propargylation, hydrolysis of a silyl ether and cycloisomerization of a 1,4-alquinol intermediate. Additionally, it has been possible to carry out a *cis-to-trans* isomerization of the obtained products by adjusting the process conditions, adding the fourth consecutive gold(I)-catalyzed stage to this methodology. Moreover, several deuteration experiments, as well as a Hammett plot, support the mechanistic proposal herein collected.

Chapter IV summarizes a one-pot gold(I)-Lewis-acid cocatalyzed synthesis of benzofulvene scaffolds, starting from propargylsilanes and different benzophenones derivatives. The described methodology involves three consecutive reaction steps: propargylation, elimination and Nazarov-type hydroarylation. The influence of the Lewis acid has proven to be crucial in this transformation, proposing its coordination to the counterion of the gold(I), increasing therefore its electrophilicity and enhancing its catalytic activity. More detailed mechanistic studies, including several low temperature NMR stoichiometric experiments, have supported this hypothesis for the first time.

Index

Introduction	1
General background	5
1 Silicon catalysis.....	7
1.1 Properties of silicon. Organosilicon compounds.....	7
1.2 Silicon species as Lewis acids in catalysis	13
1.3 Silylium cations as synergistic promoters	20
2 Gold catalysis.....	23
2.1 Properties of Gold. Relativistic Effects.	23
2.2 Homogenous gold catalysis. Important factors	28
2.3 Gold-catalyzed transformations involving carbon-carbon multiple bonds.....	41
Chapter I: Gold-catalyzed propargylation of carbonyl compounds. Isolation of a σ-allenylgold(I) complex.....	55
1 Introduction	57
2 Bibliographic background.....	59
2.1 General reactivity of propargylsilanes	59
2.2 Coupling reactions between propargylsilanes and carbonyl compounds.....	63
2.3 Propargylation reactions of carbonyl compounds	66
2.4 σ -Allenylgold complexes in homogeneous gold catalysis	69
3 Results and discussion.....	73
4 Conclusions	93
Chapter II: Gold-catalyzed bispropargylation reaction. Synthesis of 9,9-bispropargylxanthene derivatives.....	95
1 Introduction	97
2 Bibliographic background.....	99
2.1 Xanthenes, xanthidrols and xanthenes	99
2.2 Catalytic nucleophilic bis-additions to carbonyl compounds.....	103
3 Results and Discussion	107
4 Conclusions	133

Chapter III: Gold-catalyzed synthesis of 2-silyl-4,5-dihydrofurans	135
1 Introduction	137
2 Bibliographic background	139
2.1 Dihydrofurans in organic synthesis	139
2.2 Gold-catalyzed isomerization of 1,4-alkynols	143
2.3 Gold(I)-catalyzed ring-opening <i>cis-to-trans</i> isomerization processes	146
3 Results and discussion	149
3.1 Synthesis of 2-silyl-4,5-dihydrofurans.....	149
3.2 <i>Cis-to-trans</i> isomerization of 2-silyl-4,5-dihydrofurans	155
4 Conclusions	169
Chapter IV: Lewis acid enhancement of a gold(I) complex activity. One-pot synthesis of benzofulvene derivatives.....	171
1 Introduction.....	173
2 Bibliographic background.....	175
2.1 Additive effects in homogeneous catalysis	175
2.2 Gold-additive-cocatalyzed processes	176
3 Results and discussion.....	187
4 Conclusions.....	209
General conclusions	211
Experimental section.....	215
1 General Aspects	217
1.1 General Considerations	217
1.2 Instrumental Techniques	218
2 Experimental Procedures.....	219
2.1 Synthesis of propargylsilanes	219
2.2 Experimental procedures described in Chapter I	226
2.3 Experimental procedures described in Chapter II	259
2.4 Experimental procedures described in Chapter III	315
2.5 Experimental procedures described in Chapter IV	351

<i>Annex I: Nuclear Magnetic Resonance (NMR) spectra.....</i>	<i>389</i>
1 Chapter I.....	391
2 Chapter II.....	428
3 Chapter III.....	472
4 Chapter IV.....	512
 <i>Annex II: Crystallographic data</i>	 <i>543</i>

Introduction

The following Dissertation lies within the field of Organic Synthesis, particularly in the area of homogenous transition metal catalysis.

Catalysis has become a key tool for chemists to achieve more selective and sustainable methodologies during the last decades. Particularly, noble-metal-based catalysts play a key role in ton-scale industrial processes, due to the plethora of reactions that they can afford.

In this regard, gold catalysis has experienced the called “golden rush” over the last years, and the applications and transformations developed using gold catalysts have grown exponentially. Our research group felt attracted some years ago for this kind of processes, expanding the gathered knowledge with interesting contributions in this area.

The results described along this Dissertation are focused on the carbophilic activation of unsaturated organosilicon compounds, specially propargylsilanes. The activation of these systems by gold species has allowed to obtain, through a synergistic gold-silylium-catalyzed propargylation, different structures bearing the propargyl moiety, and, in several cases, their further transformations in a one-pot manner using the same catalyst. The mechanisms of these transformations have been extensively studied, isolating sometimes interesting intermediates.

This Dissertation has been divided into four Chapters and a General background section.

This General background has been split into two parts: the first one discloses the general aspects of the properties of organosilicon compounds and some examples of silicon catalysis, meanwhile the second one summarized the chemical properties of gold, and representative examples in gold homogenous catalysis.

The obtained results have been gathered as follows:

- Chapter I: Gold-catalyzed propargylation of carbonyl compounds. Isolation of a σ -allenylgold(I) complex.
- Chapter II: Gold-catalyzed bispropargylation reaction. Synthesis of 9,9-bispropargylxanthene derivatives.
- Chapter III: Gold-catalyzed synthesis of 2-silyl-4,5-dihydrofurans.
- Chapter IV: Lewis acid enhancement of a gold(I) complex activity. One-pot synthesis of benzofulvene derivatives.

Finally, an Experimental section describes the synthetic procedures followed during this study and the characterization data of the obtained compounds. In addition, two different Annexes at the end gather the recorded NMR spectra and the X-Ray Diffraction data obtained.

General background

1 Silicon catalysis

1.1 Properties of silicon. Organosilicon compounds

Silicon was firstly isolated in the XIX century by Berzelius. This element is located on the fourteenth group and the third period of the Periodic Table of the Elements. It possesses an atomic number of $Z = 14$ and its electronic configuration is $[\text{Ne}] 3s^2 3p^2$. It is the eighth most abundant element in the Milky Way and the second one in The Earth's crust.¹

Organosilicon reagents are those organic species that contain at least one silicon atom in their structure. As well as its neighbour carbon, silicon has four valence electrons, being capable of forming four covalent bonds after sp^3 hybridization. However, silicon-based chains are not so favourable as carbonated ones, because of the poor $3p$ orbitals overlap. This is reflected by the high instability of silicon-silicon multiple bonds, although several examples have been described.²

The behaviour of organosilicon derivatives is closely related with the nature of the carbon-silicon bond and it is determined by six important properties of the silicon atom, as follows:

¹ Corey, J. Y. *Organic Silicon Compounds*, **1989**, 2-49.

² For further details in organosilicon species with multiple bonds see: Baceiredo, A.; Kato, T. in *Organosilicon Compound (2017)*. Eds: Lee, V. Y; Elsevier Inc., Amsterdam, **2017**, 533-618.

1. Electronegativity. Silicon is less electronegative than carbon and hydrogen atoms (1.90 in the Pauling scale, compared to 2.55 and 2.20, respectively). Therefore, carbon-silicon bonds are more polarized than carbon-hydrogen ones, turning organosilicon species into electrophiles through the silicon, and nucleophiles through the carbon position.

2. β -Stabilizing effect of carbocations. This feature was the origin of several controversies thirty years ago, but it is commonly accepted nowadays. Many computational and experimental studies have demonstrated that, if the carbon-silicon bond can achieve a *trans* coplanar disposition, a stabilizing interaction between the $\sigma_{\text{C-Si}}$ bonding molecular orbital and the empty p_z orbital of the carbocation takes place. This is the interaction commonly known as hyperconjugation, and it is a consequence of carbon-silicon bond polarization (Figure 1).³

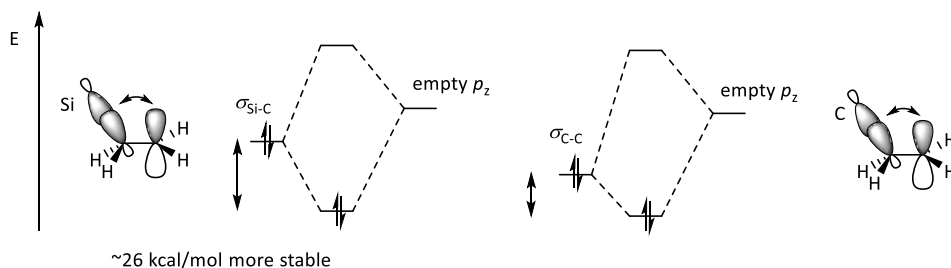


Figure 1: Energy comparison between β -effect and usual hyperconjugation.

As stated before, organosilicon reagents usually behave as ‘masked’ C-nucleophiles, and β -silicon effect is highly determining in the reaction regioselectivity. In Figure 2, usual reactivity for different unsaturated silanes towards electrophiles is shown.⁴

³ a) Wierschke, S. G.; Chandrasekhar, I.; Jorgensen, W. L. *J. Am. Chem. Soc.* **1985**, *107*, 1496-1500; b) Lambert, J. B.; Zhao, Y.; Emblidge, R. W.; Salvador, L. A.; Liu, X.; So, J.; Chelius, E. C. *Acc. Chem. Res.* **1999**, *32*, 183-190.

⁴ Curtis-Long, M. J.; Aye, Y. *Chem. Eur. J.* **2009**, *15*, 5402-5416.

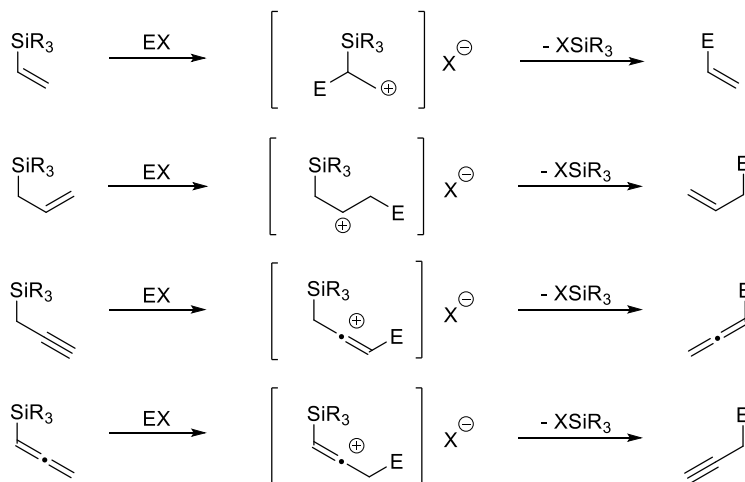
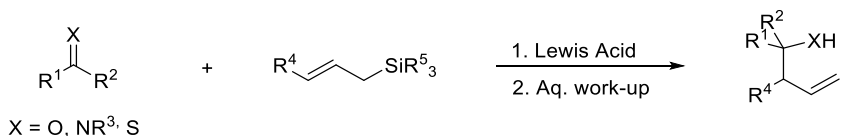


Figure 2: Usual reactivity of unsaturated silanes as nucleophiles.

Taking advantage of these two properties, electronegativity and β -stabilizing effect of carbocations, organosilicon compounds have been widely employed in organic synthesis, since their reactivity is usually more predictable than the observed for common organometallic reagents. One of the first described examples was the allylation of carbonyls employing allylsilanes, known as the Hosomi-Sakurai reaction, whose general behaviour with allylsilanes is represented in Scheme 1.⁵ Thus, the carbonylic compound is activated by its coordination to the Lewis acid catalyst, generating a more electrophilic specie. Then, the allylsilane reacts, as shown before, through nucleophilic attack and protodesilylation to yield the final products.



Scheme 1: General scheme of Hosomi-Sakurai reaction for allylsilanes.

⁵ For selected examples, see: a) Momiyama, N.; Nishimoto, H.; Terada, M. *Org. Lett.* **2011**, 2126-2129; b) Lade, J. J.; Pardeshi, S. D.; Vadagaonkar, K. S.; Murugan, K.; Chaskar, A. C. *RSC Adv.* **2017**, 7, 8011-8033.

3. α -Stabilizing effect of carbanions. This interesting property can be attributed to three main factors (Figure 3). First, an orbitalic interaction between the molecular orbitals σ_{C-M} and σ_{C-Si}^* , which results in a stabilization of the bonding molecular orbital σ_{C-M} . Second, an overlap between the filled sp^3 hybridized atomic orbitals at the carbon atom and the empty $3d$ orbitals of the silicon atom. And finally, the inductive effects generated, since silicon is a larger and more polarizable atom than carbon.⁶

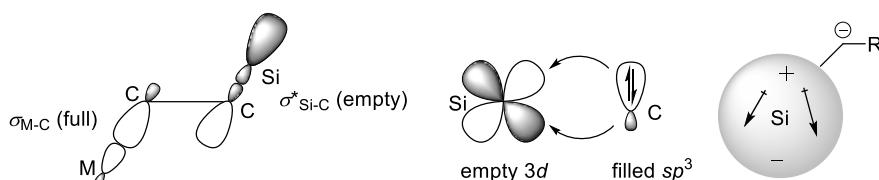
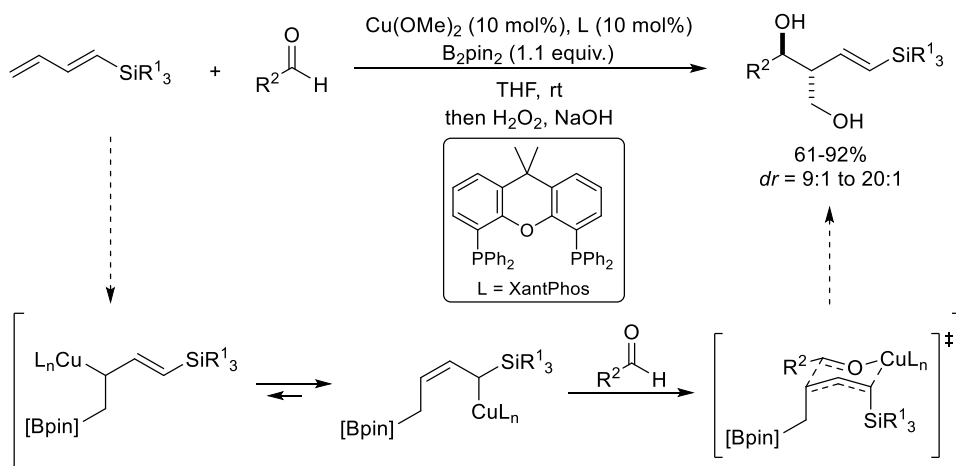


Figure 3: Illustration of the three main factors responsible for the α -silicon effect.

α -Silicon effect has been considered by many authors less relevant compared to the β -effect. However, it is well-known that metalation processes in this position are favoured, and sometimes can even drive the reaction outcome, as it is shown in Scheme 2. For this example of a hydroborylation-allylation process, the α -silicon effect proved to be crucial, by driving the metalation regioselectivity.⁷



Scheme 2: Copper(II)-catalyzed hydroborylation-allylation of aldehydes.

⁶ Brinkman, E. A.; Berger, S.; Brauman, J. I. *J. Am. Chem. Soc.* **1994**, *116*, 8304-8310.

⁷ Gao, S.; Chen, M. *Chem. Sci.* **2019**, *10*, 7554-7560.

4. Bond length. Given that, for the formation of a carbon-silicon bond, silicon uses $3sp^3$ hybrid orbitals and, on the other hand, carbon employs $2sp^3$, the simple carbon-silicon bond average distance is quite longer than C-C bond (1.89 Å vs. 1.54 Å). For this reason, silyl substituents are less sterically demanding than their carbon counterparts.⁸

5. Bond dissociation energy and heteroatom affinity. The average dissociation energy for carbon-silicon single bonds lies around 76 kcal/mol. This value is just 6-7 kcal/mol lower than the average energy for a carbon-carbon single bond, indicating a higher reactivity. Following a logical trend, organosilicon reagents are less reactive than their analogous germanes (57 kcal/mol), stannanes (46 kcal/mol) and plumbanes (31 kcal/mol).⁹

However, some heteroatom-silicon bonds are usually slightly stronger than carbon-silicon or silicon-hydrogen bonds (Table 1), acting in many reactions as the main driving force.⁴ This may be the result of an overlap between the empty $3d$ orbitals of silicon and the $2p$ lone pairs of the respective heteroatoms, giving to that bonds a character of partial double bonds. Additionally, given the electronegativity and size of these elements, it has been also proposed an ionic component for these bonds.¹⁰

Bond	Bond strength (kcal/mol)	Bond length (Å)
Si-H	90 (in Me ₃ Si-H)	1.48
Si-C	65-89 (in Me ₃ Si-CH ₃) ^{8,11}	1.85
Si-O	108 (in Me ₃ Si-OMe)	1.66
Si-F	135 (in Me ₃ Si-F)	1.57

Table 1: Bond dissociation energies and lengths for some Si-X bonds.

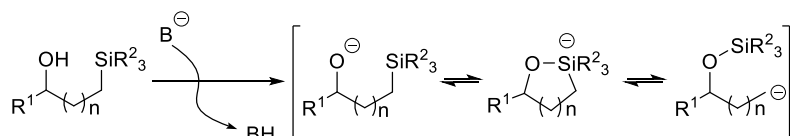
⁸ Pawlenko, S. in *Organosilicon Chemistry* (1986); Eds: Gruyter, Walter. Gruyter & Co.; Berlín, 1986, 1, 7.

⁹ Walsh, R. *Acc. Chem. Res.* **1981**, *14*, 246-252.

¹⁰ Klare, H. F. T.; Oestreich, M. *Dalton Trans.* **2010**, *39*, 9176-9184.

¹¹ There is controversy about these values, due to the different variety of methodologies employed for their measurement.

One example of this behaviour could be the rearrangement described by Brook in 1974,¹² whose general mechanism is depicted in Scheme 3. As it can be seen, when an alkoxide anion is generated in an organosilane, a direct intramolecular attack of the oxygen atom to the silicon centre takes place, generating a cyclic hypervalent silicon (property discussed in the next paragraph), and finally the carbon-silicon bond is dissociated to generate a carbanion. In this behaviour, three intermediates are in equilibrium, so it is also possible to form a C-Si bond breaking a Si-O bond (retro-Brook Rearrangement), depending on the reaction conditions.



Scheme 3: General mechanism for a Brook Rearrangement.

6. Hypervalence ability. The silicon atom possesses 3d empty orbitals relatively lower in energy compared to the carbon atom. This property allows an expansion of its coordination number through a rehybridization to form penta- and hexacoordinated species. This key property can lead to several reactive pathways unreachable for carbon species, since Lewis acidity of the silicon and nucleophilicity of the substituents will dramatically change depending on the number and the nature of the silicon substituents (Figure 4).¹³

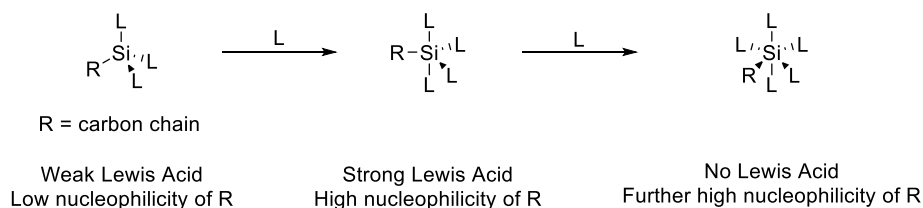


Figure 4: Lewis acidity and nucleophilicity tendency for hypervalent silicon species.

¹² Brook, A. G. *Acc. Chem. Res.* **1974**, *7*, 3, 77-84.

¹³ a) Ramsden, C. A. *Chem. Soc. Rev.* **1994**, *23*, 111-118; b) Rendler, S.; Oestreich, M.; *Synthesis* **2005**, *11*, 1727-1747.

1.2 Silicon species as Lewis acids in catalysis

Silanes were widely studied as protecting groups due to their stability, especially for alcohols, and also as selective nucleophiles, as stated before.⁴ However, their role as Lewis acids was one of the latest studied. The capability of an organosilane compound to behave as Lewis acid is closely related to two out of the six previously mentioned features, as follows: hypervalence ability and electronegativity. In this sense, their coordination to unsaturated systems generates strong electrophiles that can react with smooth nucleophiles. From bibliographic research, it can be observed that only two types of organosilicon reagents have been used as Lewis acid catalysts: highly acidic neutral silanes and silylium species. Several examples of both types of catalysis will be mentioned under these lines.

1.2.1 Neutral silanes as Lewis acid catalysts

Although tetracoordinated silicon species, especially tetraalkylsilanes, are poor electrophiles, their Lewis acidity can be increased by introducing perfluorinated moieties, strained chains, electron-withdrawing groups, heteroatoms, or a combination of them.¹⁴ Some representative neutral silanes of this type with enhanced Lewis acidity are depicted below (Figure 5).

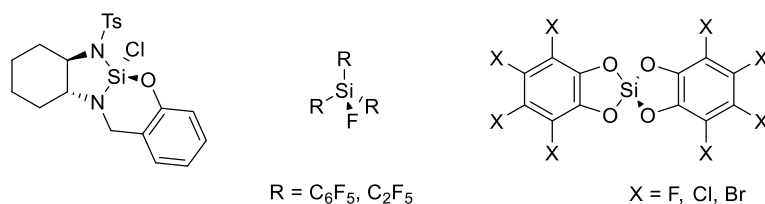


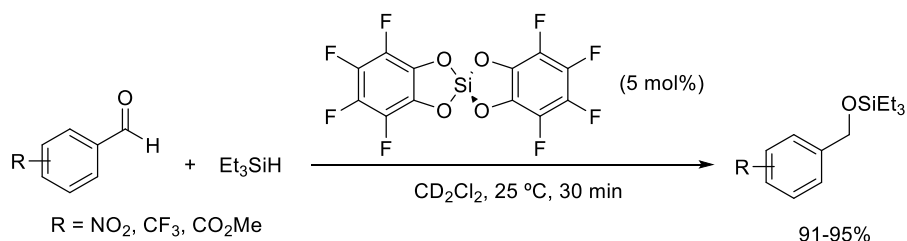
Figure 5: Examples of neutral silicon catalysts with enhanced Lewis acidity.

The catalytic use of these reagents was unexplored¹⁵ until Tilley and co-workers described in 2014 the hydrosilylation reaction of aromatic electron-poor aldehydes,

¹⁴ For further information see: a) Dilman, A. D.; Ioffe, S. L. *Chem. Rev.*, **2003**, *103*, 733-772; b) Hrdina, R.; Opekar, F.; Roithova, J.; Katora, M. *Chem. Commun.* **2009**, *17*, 2314-2316; c) Chalifoux, W. A.; Reznik, S. K.; Leighton, J. L. *Nature*, **2012**, *487*, 86-89.

¹⁵ Hartmann, D.; Schädler, M. *Chem. Sci.* **2019**, *10*, 7379-7388.

catalyzed by a highly acidic biscathecolsilane (Scheme 4).¹⁶ In this transformation, the coordination of the aldehyde to the highly acidic silicon atom generates a super electrophile, easing a transition state where the hydrosilylation step takes place in a concerted manner, without generating silylium species.



Scheme 4: Hydrosilylation reaction catalyzed by a highly acidic neutral silane.

1.2.2 Silylium species as catalysts

Silylium cations are tricoordinated species of tetravalent silicon. To be more precise, they should be called donor-stabilized silylium-like ions, since only three examples of 'naked' silylium ions have been described to date (Figure 6).¹⁷ For all of them, the ²⁹Si-NMR spectra exhibit high unshielded shifts, around 220-230 ppm.

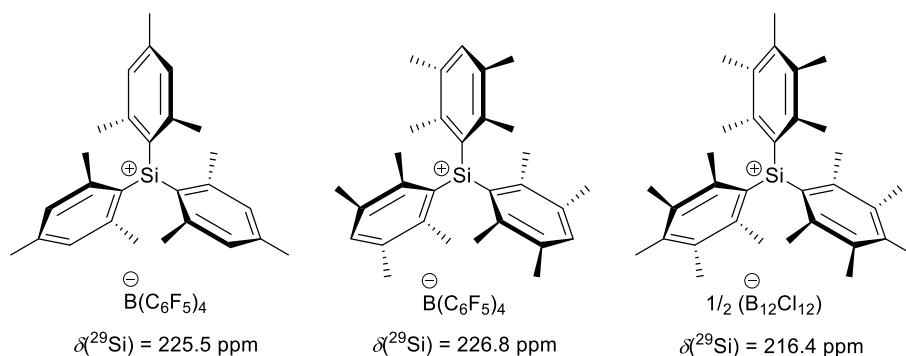


Figure 6: Described 'naked' silylium cations.

¹⁶ Liberman-Martin, A. L.; Bergman, R. G.; Tilley, T. D. *J. Am. Chem. Soc.* **2015**, *137*, 5328-5331.

¹⁷ a) Lambert, J. B.; Zhao, Y. *Angew. Chem. Int. Ed. Engl.* **1997**, *36*, 400-401; b) Lambert, J. B.; Lin, L. *J. Org. Chem.* **2001**, *66*, 8537-8539; c) Schäfer, A.; Reißmann, M.; Jung, S.; Schäfer, A.; Saak, W.; Brendler, E.; Müller, T. *Organometallics* **2013**, *32*, 4713-4722.

This type of compounds behaves very different in solution from their analogue carbocations, being more electrophilic, showing high carbo-, oxo- and fluorophilicity.¹⁸ Thus, their coordination to heteroatoms or C-C multiple bonds generates 'super-electrophiles' that react with smooth nucleophiles. New methods to prepare these reagents have helped this area to emerge, and it stands as a promising alternative for transformations where metal catalysts fail.¹⁹

Silylium Lewis acids have been common reagents, promoters and catalysts during decades, demonstrating great performance in transformations ranging from C-C and C-heteroatom bond-forming reactions, to oxidations and reductions. In the following pages, some examples of this behaviour that evidence the relevance of this type of compounds are described.

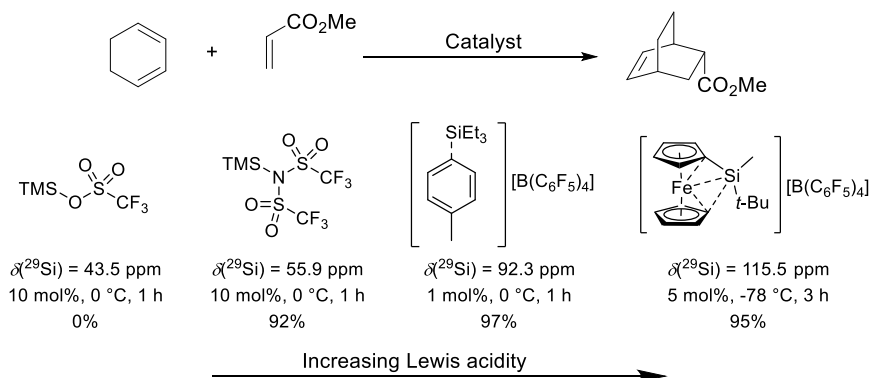
1.2.2.1 C-C and C-heteroatom bond-forming silylium catalysis

Starting the description with C-C bond forming reactions, one of the first reported silylium catalysts for these processes was trimethylsilyl trifluoromethanesulfonate, TMSOTf.²⁰ However, it proved to be non-acidic enough for some reactions. Thus, new generations of catalysts with enhanced reactivity were discovered, and their Lewis acidity can be easily correlated to their ²⁹Si-NMR shifts.¹⁰ In Scheme 5, a comparison between the catalytic activity of some silylium catalysts for the Diels-Alder cycloaddition between methyl acrylate and 1,3-cyclohexadiene is depicted.¹⁹

¹⁸ Walker, J. C. L.; Klare, H. F. T.; Oestreich, M. *Nat. Rev. Chem.* **2020**, *4*, 54-62.

¹⁹ Klare, H. F. T.; Albers, L.; Süsse, L.; Keess, S.; Müller, T.; Oestreich, M. *Chem. Rev.* **2021**, *121*, 5889-5985.

²⁰ a) Dilman, A. D.; Ioffe, S. L. *Chem. Rev.* **2003**, *103*, 733-772; b) Shaykhutdinova, P., Keess, S.; Oestreich, M. *Organosilicon Chemistry: Novel Approaches and Reactions* (eds Hiyama, T. & Oestreich, M.) 131-170. (Wiley- VCH, **2019**).



Scheme 5: Comparison between different silylium catalysts in a Diels-Alder reaction.

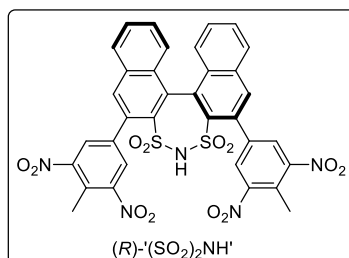
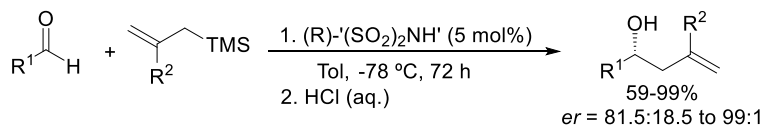
Moreover, advances in this field include the use of chiral silicon centres or chiral counterions to introduce enantioselectivity in this kind of cycloaddition reactions, obtaining promising results.²¹

It is important to mention, that most of the described reactions under the name of silylium catalysis are not strictly so. For the process, to be truly catalytic, silylium catalyst should be regenerated, so isotopic labels would be retained. However, a non-reactive silane is usually generated, and a second source must supply a new silylium specie to reactivate the process. For this reason, silylium catalysts are usually employed along with organosilicon nucleophiles, and must be considered in that cases as facilitators instead of catalysts.

Following this way, isolation of unstable silylium catalysts is not always necessary, as they can be in situ prepared from silyl nucleophiles. A good example of this reactivity is shown in Scheme 6 and describes an enantioselective Hosomi-Sakurai allylation of aldehydes. In this transformation, the catalyst has been generated using a chiral sulfonylimide.²²

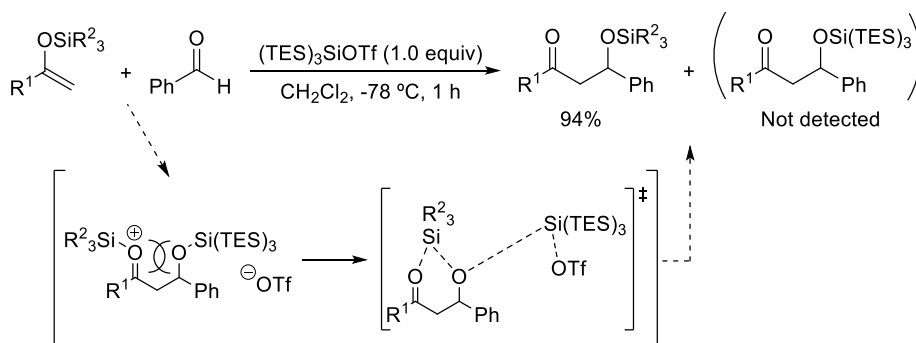
²¹ a) Sakaguchi, Y.; Iwade, Y.; Sekikawa, T.; Minami, T.; Hatanaka, Y. *Chem. Commun.*, **2013**, 49, 11173-11175; b) Gatzemeier, T.; van Gemmeren, M.; Youwei, X.; Höfler, D.; Leutzschand, M.; List, B. *Science* **2016**, 351, 949-952.

²² Mahlau, M.; García-García, P.; List, B. *Chem. Eur. J.* **2012**, 18, 16283-16287.



Scheme 6: Enantioselective silylium-catalyzed Hosomi-Sakurai allylation of aldehydes.

It should be also mentioned, as an early successful result, the silylium-catalyzed aldol reaction described by Noyori and co-workers.²³ For this type of processes, silyl moieties, in both nucleophile and catalyst, must match to avoid the formation of crossed products. However, the use of 'supersilyl' groups can overcome this problem, due to the steric hindrance of these species, promoting chemoselective transfer of less bulky silyl moieties (Scheme 7).²⁴



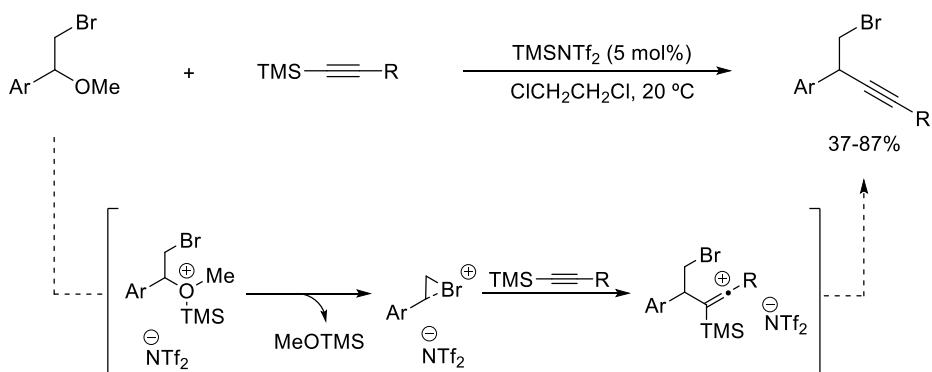
Scheme 7: Promising results obtained with 'supersilyl'-silylium catalysts.

Another example of silylium facilitators in C-C bond formation reactions employing smooth nucleophiles is depicted in Scheme 8. In this case, silylium activation of (2-bromo-1-methoxyethyl)arenes generates an anchimerically

²³ Murata, S.; Suzuki, M.; Noyori, R. *Tetrahedron Lett.* **1980**, *21*, 2527-2528.

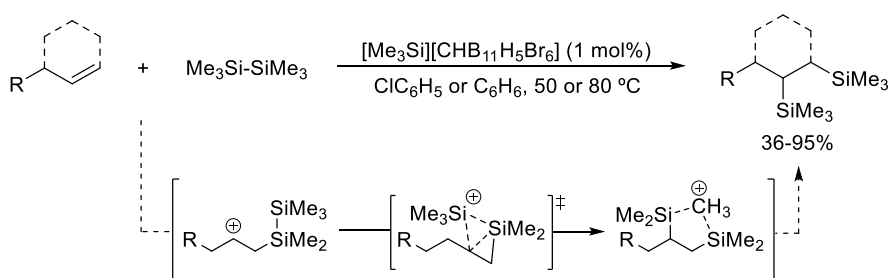
²⁴ Sai, M.; Akakurab, M.; Yamamoto, H. *Chem. Commun.* **2014**, *50*, 15206-15208.

stabilized carbocation, which is then trapped by an alkynylsilane, producing a new silylium facilitator.²⁵



Scheme 8: Silylium-catalyzed alkyynylation of (2-bromo-1-methoxyethyl)arenes.

Finally, as a representative example of carbon-heteroatom bond formation, Scheme 9 summarizes the silylium-catalyzed disilylation of alkenes reported by Oestreich and co-workers.²⁶ As it is described, the reaction begins through the abstraction of a methyl group from the disilane by the superelectrophilic catalyst, generating a silyl-silylium species that is able to activate the olefin. After that, a [1,3]-silyl shift leads to the final products, upon activation of another molecule of disilane through a methyl-bridged transition state. It is worth to remark, that this kind of transition states has not been reported yet with transition-metal species.



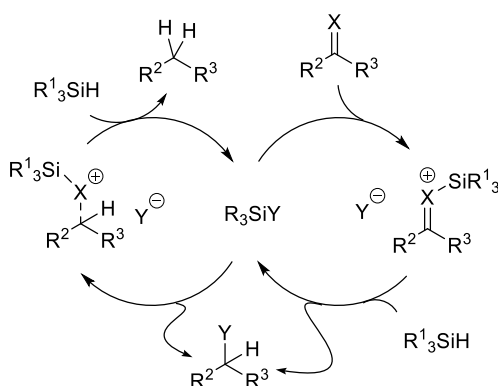
Scheme 9: Olefin disilylation with disilanes through silylium catalysis.

²⁵ Rubial, B.; Ballesteros, A.; González, J. M. *Eur. J. Org. Chem.* **2018**, *45*, 6194-6198.

²⁶ Wu, Q.; Roy, A.; Irran, E.; Qu, Z. -W.; Grimme, S.; Klare, H. F. T.; Oestreich, M. *Angew. Chem. Int. Ed.* **2019**, *58*, 17307-17311.

1.2.2.2 Oxidative and reductive silylium catalysis

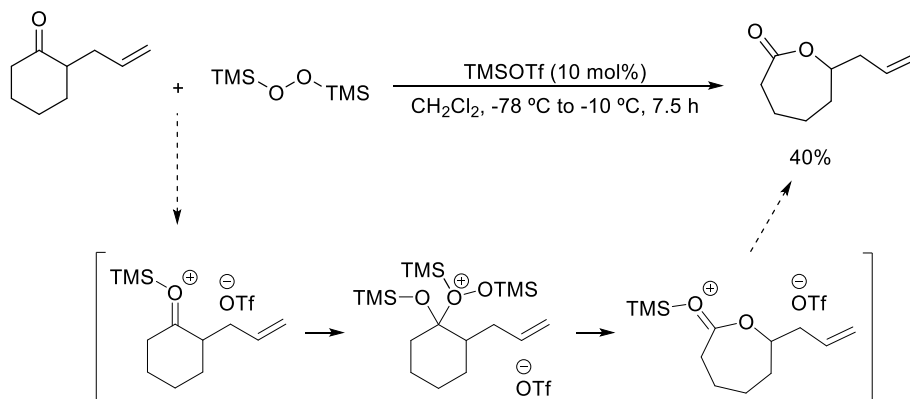
Many reduction reactions, such as C(sp³)-F hydrodefluorination, carbonyl and ether deoxygenation, and C=X (X = O, F) hydrosilylation, have been developed with silylium facilitators.^{20b} Since all of them follow a similar mechanistic pattern, a general catalytic cycle can be postulated, and it is represented in Scheme 10. Thus, activation of the heteroatom by silylium cations ease a hydride transfer from a silane, generating a new silicon-based Lewis Acid. In the second step, the same sequence of activation-hydride-transfer takes place with a second molecule of silane achieving the complete loss of the heteroatom, formally reducing the starting material.



Scheme 10: Catalytic cycle for silylium-catalyzed reduction reactions.

On the contrary, oxidation reactions catalyzed or promoted by silylium species have received less attention than reduction ones. A representative example of this sort of transformations is represented in Scheme 11. Thus, the reaction takes place upon silylium activation of the 2-allylcyclohexanone, followed by nucleophilic attack of the peroxy-siloxane and later rearrangement. The overall process can be considered as a formal Baeyer-Villiger oxidation.²⁷ It is highly remarkable that the olefin remained unaltered under these conditions, in contrast to other common methodologies.

²⁷ Suzuki, M.; Takada, H.; Noyori, R. *J. Org. Chem.* **1982**, *47*, 902-904.



Scheme 11: Example of a silylium-catalyzed selective Baeyer-Villiger type oxidation.

1.3 Silylium cations as synergistic promoters

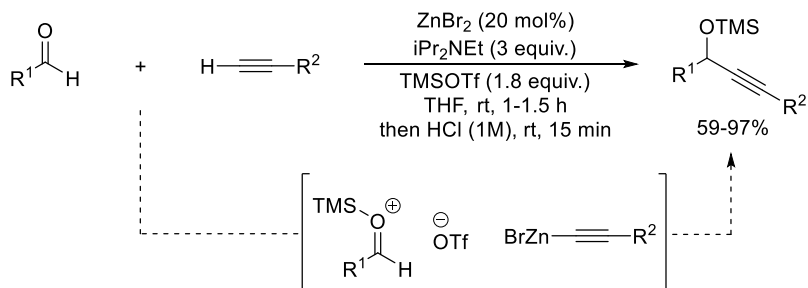
A catalytic process can be considered synergistic when both, nucleophile and electrophile, are activated at the same time by two separated and different catalysts, to afford a single transformation. This procedure can lead to previously inaccessible chemical transformations, improve the efficiency of described reactions, and even achieve or enhance the selectivity.²⁸

Silylium species have been used in synergic processes with organometallic reagents since some years ago. However, these transformations usually required stoichiometrical amounts because they do not use an organosilane as nucleophile, avoiding silylium regeneration.

In the example given below (Scheme 12), an alkynylation process of aldehydes is represented.²⁹ Thus, under basic conditions, a zinc(II) acetylide is generated from a terminal alkyne, and this reagent reacts with the silylium-activated aldehyde to afford the propargyl silyl ether, which is then hydrolyzed under acidic conditions to afford the corresponding propargyl alcohol.

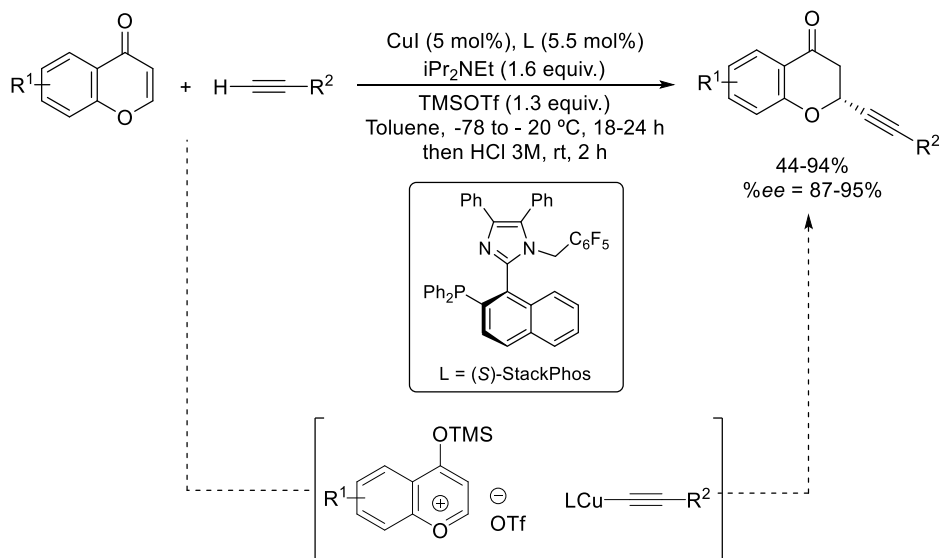
²⁸ Allen A. E.; MacMillan, D. V. C. *Chem. Sci.* **2012**, *3*, 633-658.

²⁹ Downey, C. W.; Mahoney, B. D.; Lipari, V. R. *J. Org. Chem.* **2009**, *74*, 2904-2906.



Scheme 12: Zn(II)-catalyzed alkyne-aldol reaction of silyloxy-activated aldehydes.

This methodology has also been used for the enantioselective alkyne-aldol reaction of chromones (Scheme 13).³⁰ Similarly to the example described before, a copper(I) acetylide is generated from a terminal alkyne in the presence of an organic base, and this reagent reacts with the benzopyrylium intermediate via Michael addition.



Scheme 13: Enantioselective Michael alkyne-aldol reaction via Cu(I)-silylium synergic activation.

³⁰ DeRatt, L. G.; Pappoppula, M.; Aponick, A. *Angew. Chem. Int. Ed.* **2019**, *58*, 8416-8420.

Recent advances in this field involve catalytic in-situ generation of the activating silylium cations using a transition metal catalyst and a silylated compound. Thus, starting from unsaturated organosilane species, the Lewis acid activation of a multiple bond by the metallic complex triggers the formation of the silylium intermediate which, in turn, carries out synergically a second Lewis acid activation. In this sense, gold complexes still play a key role in these transformations thanks to their ability to activate carbon-carbon multiple bonds. For this reason, due to the close relationship with the research developed in the present dissertation, several examples of this behaviour will be disclosed during the next section.

2 Gold catalysis

2.1 Properties of Gold. Relativistic Effects.

Attending to the position occupied by gold in the Periodic Table of the Elements (Group 11, atomic number: $Z = 79$) and its electronic configuration ($[\text{Xe}] 4f^{14} 5d^{10} 6s^1$), it is not simple to fully understand its physical properties. The same problem appears in the study of its chemical behaviour towards C-C multiple bonds, compared to elements in the same Group (Cu and Ag, along with Au, the called *coinage* metals) or nearby (Rh, Pd, Ir and Pt). To explain both, it becomes necessary to introduce the concept known as *relativistic effects*.³¹

Relativistic effects are described as the divergences between calculated values employing models in quantum chemistry considering or not the Theory of Relativity, formulated by Albert Einstein in 1905.³² Paul Dirac, in 1929, was one of the first chemists that employed the term *relativity* referred to electron quantum theory, but also underestimating it in the consideration of atomic and molecular structure against Coulomb forces.³³ Since then, among several contributors to quantum chemistry, only Bertha Swirles (1935)³⁴ described a relativistic model until

³¹ a) Autschbach, J. *J. Chem. Phys.* **2012**, *136*, 150902-150917; b) Pyykkö, P. *Annu. Rev. Phys. Chem.* **2012**, *63*, 45-64.

³² Einstein, A. *Annalen der Physik* **1905**, *17*, 891-921.

³³ Dirac, P. A. M. *Proc. R. Soc. A.* **1929**, *123*, 714-733.

³⁴ Swirles, B. *Proc. R. Soc. A.* **1935**, *152*, 625-649.

more recent works in the 1970s decade, when the relativistic effects were observed in heavy elements.³⁵

For an appropriate treatment, the attention should be turned to one of the most familiar results in this theory and its relationship with relativistic Bohr atomic radius (a_{rel}), both of them outlined in Equation 1.

$$m_{rel} = \frac{m_0}{\sqrt{1-(v_e/c)^2}} \quad a_{rel} = \frac{\hbar}{m_{rel} \cdot c \cdot \alpha}$$

Equation 1: Relativistic mass (m_{res}) and relativistic Bohr radius (a_{rel}) equations.

The first equation relates relativistic mass (m_{rel}) with the uncorrected mass (m_0), taking into account electron speed (v_e). The second one shows the relation between the relativistic Bohr atomic radius (a_{rel}) and the relativistic mass, being c the speed of light constant, \hbar the reduced Planck's constant and α the fine-structure constant.

From a qualitative point of view, nuclei with larger charge -or atomic number- will boost electrons speed, thus increasing relativistic mass and decreasing relativistic Bohr atomic radius. This also means, that electrons in orbitals s and p will be closer to the nucleus, shielding electrons from orbitals d and f . In other words, orbitals s and p get contracted while d and f suffer an expansion.

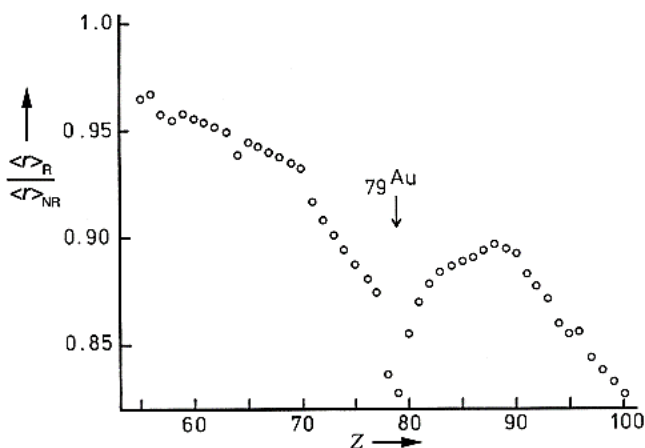


Figure 7: Relativistic and non-relativistic 6s radii ratio vs. atomic number Z.

³⁵ a) Pitzer, K. S. *Acc. Chem. Res.* **1979**, *12*, 271-276; b) Pyykkö, P. *Chem. Rev.* **1988**, *88*, 563-594.

In Figure 7 it is clearly shown that relativistic effects are stronger for heavier elements, in particular for Pt ($Z = 78$) and gold ($Z = 79$).³⁶ With these considerations it is possible now to explain most of the special chemical properties of organoaurated species.

- Contraction of orbital 6s and expansion of 5d result in a strong interaction of gold atom with its ligands, in comparison with the other coinage metals.³⁷ For this reason, gold(I) complexes usually exhibit bicoordinated linear geometry with 14 electrons, while Cu(I) and Ag(I) form tri- or tetraordinated complexes. On the other hand, gold(III) complexes tend to adopt square-planar geometry with 16 electrons.

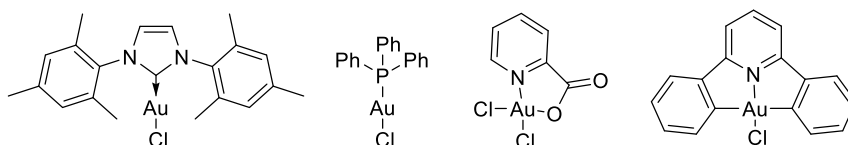


Figure 8: Some examples of common gold(I) and gold(III) complexes.

It is worth to mention that, despite different inorganic and organic gold species have been described with oxidation states ranging from -1 to +6,³⁸ gold chemistry is dominated by gold(I) and gold(III) complexes.

- Another experimental fact derived from this distortion is the called 'aurophilicity', a trend of gold complexes to aggregate forming Au-Au interactions.³⁹ Aurophilic bonds lengths range from 2.50 to 3.50 Å, with a strength of 7-12 kcal/mol, comparable to some hydrogen bonds.

³⁶ Leyva-Pérez, A.; Corma, A. *Angew. Chem. Int. Ed.* **2012**, *51*, 614-635.

³⁷ a) Gorin, D. J.; Toste, F. D. *Nature*, **2007**, *446*, 395-403; b) Autschbach, J.; Sekierski, S.; Seth, M.; Schwerdtfeger, P.; Schwarz, W. H. E. *J. Comput. Chem.* **2002**, *23*, 804-813.

³⁸ Lin, J.; Zhang, S.; Guan, W.; Yang, G.; Ma, Y. *J. Am. Chem. Soc.* **2018**, *140*, 9545-9550.

³⁹ Schmidbaur, H.; Schier, A. *Chem. Soc. Rev.*, **2012**, *41*, 370-412.

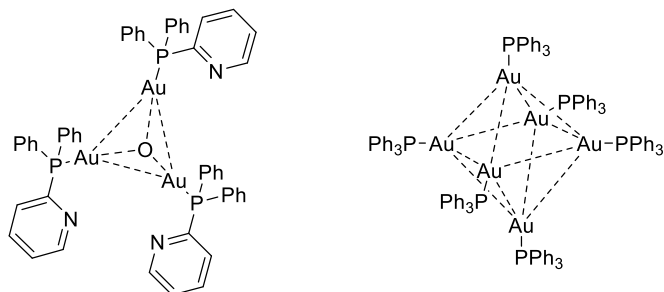
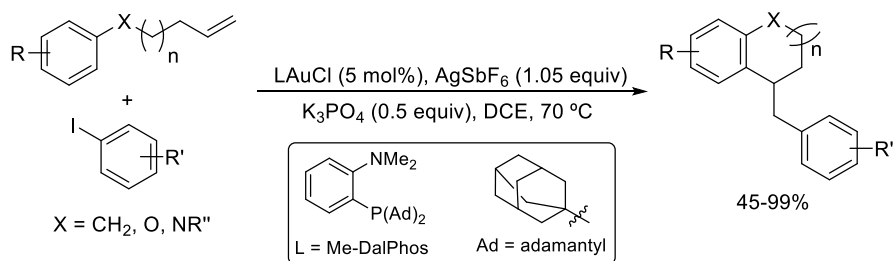


Figure 9: Two examples of described gold(I) clusters stabilized by aurophilic bonds.

- The first ionization potential of gold is larger than expected, 9.22 eV, in comparison with the other elements in the same group (7.72 eV for copper and 7.57 eV for silver).⁴⁰
- Experimental and computational studies show that oxidative addition, for Au(I) complexes, and reductive elimination, in Au(III) species, are highly disfavoured, so redox cycles between them are hard to achieve.⁴¹ However, even though it remains as a challenging area, several examples of this reactivity have been achieved. As a representative example a gold(I)-gold(III) redox catalytic cycle for a consecutive intra- and inter diarylation of alkenes is shown in Scheme 14.⁴²



Scheme 14: Example of a process catalyzed by a gold(I)-gold(III) redox system.

⁴⁰ Cronje, S.; Djordjevic, B.; Schuster, O.; Schmidbaur, H. *Chem. Phys.* **2005**, *311*, 151-161.

⁴¹ Huang, B; Hu, M.; Toste, F. D. *Trends Chem.* **2020**, *2*, 707-720.

⁴² Chintawar, C. C.; Yadav, A. K.; Patil, N. T. *Angew. Chem. Int. Ed.* **2020**, *59*, 11808-11813.

- In addition, as a consequence of the relativistic effects, the 5d orbital expansion causes less electron-electron repulsion, so electrons are more delocalized, making Au(I) species less nucleophilic than their Ag(I) or Cu(I) analogues.
- Taking into account the 6s and 6p orbitals contractions, another important aspect to consider is the lowering of the LUMO. This effect makes gold atom a better Lewis acid than silver or copper. In fact, computational studies⁴³ have demonstrated that orbital 6s of a gold(I) phosphine complex is responsible for the binding of a second ligand. Compared to the same silver(I) or copper(I) complexes, this bicoordinated specie is more stabilized (Table 2). Moreover, gold cation is large, diffuse, and capable of sharing charge with the ligand. Therefore, its interactions should be driven by orbitalic instead of charge control, making gold(I) a soft Lewis acid with preference for π -systems like C-C multiple bonds.

Compound	$r_{(M-P)}$ (Å)	ΔE (kJ/mol)
[Au(PH ₃) ₂] ⁺	2.291	267.4
[Au(PH ₃) ₂] ⁺ <i>Non Relativistic</i>	2.696	120.9
[Ag(PH ₃) ₂] ⁺	2.447	160.4
[Cu(PH ₃) ₂] ⁺	2.224	210.1

Table 2: Optimized bond distances r and Dissociation energies ΔE for the dissociation $[M(PH_3)_2]^+ \rightarrow [M(PH_3)]^+ + PH_3$.

From a catalytic point of view, activation of alkynes with gold complexes is more common than activation of alkenes. Computational studies did not give light to this point, since they predict that [ethene-Au]⁺ complex is approx. 10 kcal/mol more stabilized than the [ethyne-Au]⁺.⁴⁴ For this reason, it can be thought that the discrimination could lie in the nucleophile.

⁴³ Schwerdtfeger, P.; Hermann, H. L.; Schmidbaur, H. *Inorg. Chem.* **2003**, *42*, 1334-1342.

⁴⁴ Nechaev, M. S.; Rayon, V. M.; Frenking, G. *J. Phys. Chem. A.* **2004**, *108*, 3134-3142.

It is known that alkynes have lower HOMOs and LUMOs than their alkenes analogues, being less nucleophilic and more electrophilic.⁴⁵ If this 'rule' works for the corresponding gold complexes, this could be the origin of the called 'alkynophilicity' in gold catalysis.

Although carbophilic Lewis acidity of gold complexes is mainly due to relativistic effects in the metal atom, it is important to clarify that these are not the only variable that should be considered in homogeneous gold catalysis, since the catalysts are usually organometallic cationic complexes instead of single atoms. For this reason, other different factors related with the nature of these species with transcendental influence in gold homogeneous catalysis will be considered in the next section.

2.2 Homogenous gold catalysis. Important factors

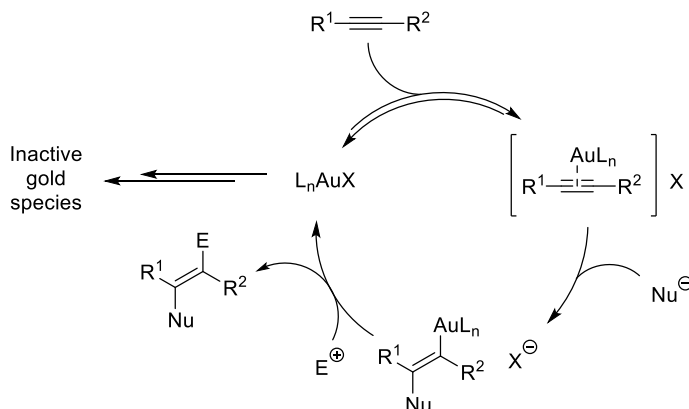
Selective carbophilic activation of unsaturated carbon-carbon bonds has become a powerful synthetic tool for organic chemists during the last decades. Currently, it still stands as a very active research field due to the plethora of transformations accessible following this methodology, allowing to enlarge the molecular complexity in a controlled manner. Among the great variety of carbophilic activators, gold complexes have drawn even higher attention nowadays. Since this dissertation is closely related to this kind of transformations, some general aspects are discussed below.

Gold catalysis field has exponentially grown thanks to the description of novel catalytic transformations, involving non-expected key organoaurated intermediates that have been proposed and sometimes even isolated. However, the issues that lead to those reaction pathways, and affect the efficiency or selectivity of these processes, are not always easy to identify and understand.⁴⁶

⁴⁵ Fleming, I. *Frontier Orbitals and Organic Chemical Reactions*. 1976, 23-32.

⁴⁶ Lu, Z.; Li, T.; Mudshinge, S. R.; Xu, B.; Hammond, G. B. *Chem. Rev.* **2021**, *121*, 8452-8477.

As a rough approximation, it could be proposed that most of the gold-catalyzed transformations, involving carbon-carbon triple bond activation, occur through a few key steps (Scheme 15).



Scheme 15: Mechanism of a model gold-catalyzed reaction initiated by alkyne activation.

First, π -coordination of the catalyst to the C-C multiple bond reduce the electronic density of the π -cloud, changing its nucleophilic character towards an electrophilic one. In a second step, a nucleophile could attack the activated unsaturated system generating a vinyl-gold intermediate (or alkyl for alkenes) following Markovnikov's rule. Finally, the organoaurated specie would react with an electrophile, usually a proton (protodeauration), recovering the catalyst. It is important to mention that, along with the catalytic cycle, gold catalysts can suffer poisoning reactions, leading to non-catalytically active species.

However, even considering this mechanism as general, the choice of the best gold catalyst seems quite random sometimes, since there are no clear rules that foresee its performance for each step. In this sense, and motivated by these facts, several research groups have focused their attention on studying which factors can influence this catalytic cycle and how to design more efficient gold-catalyzed transformations. As the result of these studies, three main factors have emerged as crucial considerations for these transformations, as follows: the properties of the ligand, the nature of the counterion and the presence of an additive.

2.2.1 Ligand-dependent effects

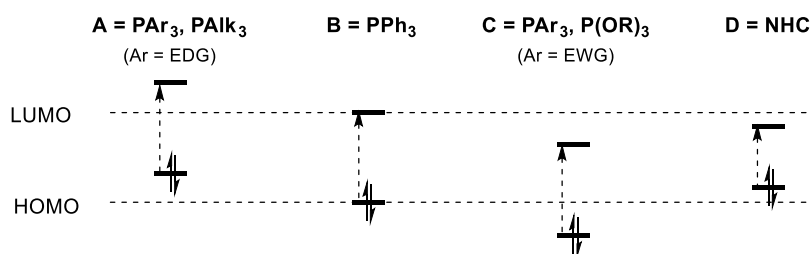
It has been extensively investigated and demonstrated, that the properties and catalytic performance of organometallic complexes can be widely tuned by changing the nature of the ligands attached to the metal. In this regard, the field of gold catalysis represents no exception, being the study of the ligand influence the deepest investigated effect in gold catalysis by far.

Generally speaking, two important features characterize ligands influence: the electronic and the steric parameters. Many times, they are equally important and usually complement each other, but in other occasions one of them prevails. Since phosphorous based and *N*-Heterocyclic Carbenes (NHCs) ligands are currently the most popular ligands employed in homogeneous gold catalysis, a brief comparison between them is given below.

2.2.1.1 Electronic properties

Usually, the major electronic influence of a ligand is related to its σ, π -donation and π -accepting capabilities. These are closely related with their frontier orbitals: a higher energy of the HOMO implies a stronger electron-donating ability, and a stronger the accepting ability is favoured by a lower energy of the LUMO.⁴⁷

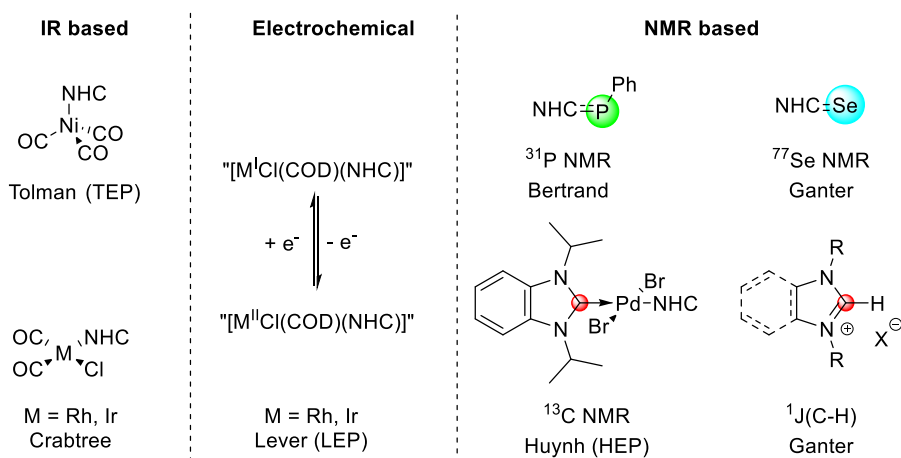
In a schematic representation (Figure 10) and taking triphenylphosphine as a reference (**B**), trialkyl phosphines and triaryl phosphines with electron-donating groups (**A**) and NHCs (**D**) present higher in energy HOMOs. On the other hand, triaryl phosphines with electron-withdrawing groups, phosphites and phosphoramidites have LUMOs of lower energy (**C**). Therefore, from a qualitative point of view, the first ones could be described as 'electron-rich' and the last ones as 'electron-poor' ligands.



⁴⁷ Huynh, H. V. *Chem. Rev.* **2018**, *118*, 9457-9492.

Figure 10: Qualitative representation of the frontier orbitals of four generic ligands.

Over the years, several methodologies have been employed to try to quantify these electronic properties. For this purpose, the Tolman Electronic Parameter (TEP) was early introduced by this author in 1970 to try to analyze the electronic nature of several phosphines,⁴⁸ and it is based on IR spectroscopy. Thus, for a given phosphine ligand (L), it measures the vibration frequency of the carbonyl groups (ν) of nickel complex $L\text{-Ni}(\text{CO})_3$, prepared from the corresponding phosphine and $\text{Ni}(\text{CO})_4$. Although this procedure was later applied to some NHCs, it presented important disadvantages (toxicity of the reagents, instability of some complexes...). These drawbacks were overcome by other methodologies as it is represented in Figure 11.²² This wide range of experimental procedures allowed chemists to create a library of several values and different approaches to compare several ligands depending on the requirements needed regardless their nature.

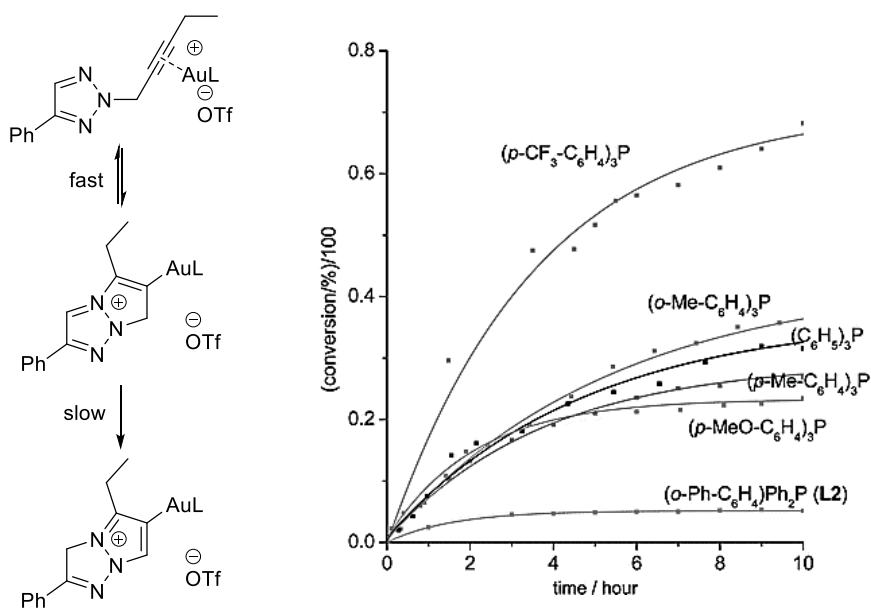
**Figure 11:** Described methods for evaluating electronic properties of NHCs.

With these considerations, in the case of gold catalysis, it has been always commonly accepted that 'electron-rich' ligands should stabilize cationic intermediates and ease the last step (nucleophilic attack to an electrophile). On the contrary, the 'electron-poor' ones should increase Lewis acidity of the complex, thus favouring π -coordination to the C-C multiple bond and the subsequent nucleophilic attack. In this sense, it is worth to mention the research work carried

⁴⁸ Tolman, C. A. *J. Am. Chem. Soc.* **1970**, *92*, 2953-2956.

out by Xu and coworkers,⁴⁹ where the authors studied activation, protodeauration and deactivation steps for model substrates to confirm this hypothesis.

For studying the electrophilic activation of an alkyne, they needed to find a resistant to protodeauration model substrate, to prevent interferences in the outcome. They turned their attention to a *N*2-propargylic triazole capable of forming a gold(I) triazolium salt upon gold(I) activation, for which protodeauration step proved to be slow enough (Scheme 16). Despite the authors assume that many other uncontrollable factors could be operating, they found a good correlation for reaction progression and initial rate, both decreasing along with the increasing electronic density in the ligand, with the only exception of biaryl phosphine ligand (L2), in which steric properties seem to be crucial as well.

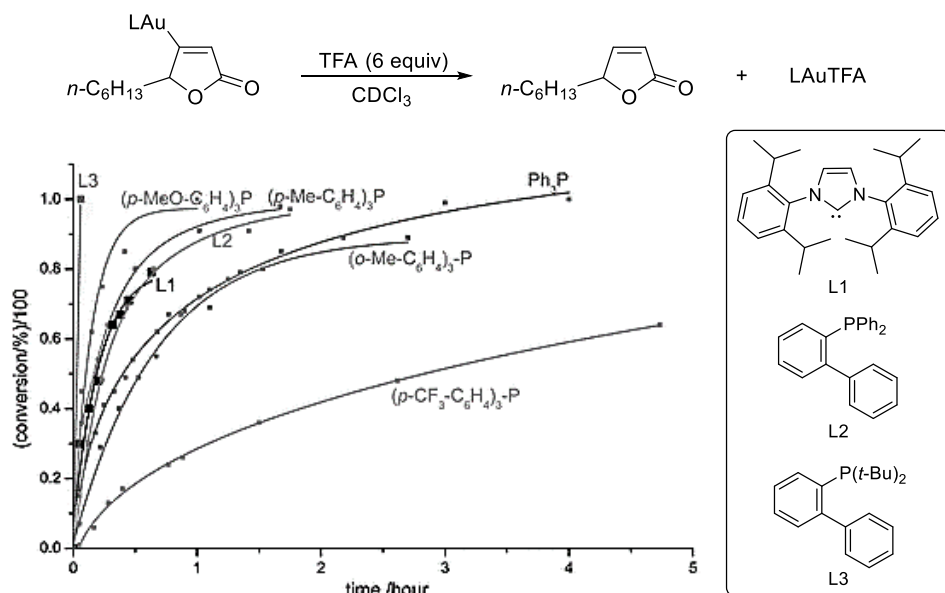


Scheme 16: Model reaction studied for alkyne activation with different ligands.

For the protodeauration study, they chose a cyclic vinylgold(I) complex, as these species are common intermediates in gold catalysis that, in last term, experience protodeauration to furnish the final products. Trifluoroacetic acid was selected as model proton source, since it is acidic enough to protodeaurate the model substrate in an easily measurable lapse of time. As inferred from the results

⁴⁹ Wang, W.; Hammond, G. B.; Xu, B. *J. Am. Chem. Soc.* **2012**, *134*, 5697-5705.

exposed in Scheme 17, similar results to the alkyne activation were obtained for protodeauration step, since they demonstrated that, in fact, ‘electron-rich’ type ligands accelerate the process. However, the steric hindrance seems not be as important as for the activation step, since the biarylphosphine ligand L2 sticks perfectly with the expected trend according to its electronic properties. These experimental results were later supported by computational studies carried out by Belanzoni.⁵⁰



Scheme 17: Model protodeauration reaction studied and obtained results.

Many other works tried to separately investigate electronic ligand effects in gold catalysis, as linear geometry of gold(I) complexes should diminish steric interactions. Most of them failed, because, as proved by the last two exposed results for biaryl phosphines, these effects cannot be easily avoided for bulkier ligands, at least for the so far studied model reactions.⁵¹

⁵⁰ Gaggioli, C. A.; Ciancaleoni, G.; Zuccaccia, D.; Bistoni, G.; Belpassi, L.; Tarantelli, F.; Belanzoni, P. *Organometallics* **2016**, *35*, 2275-2285.

⁵¹ Christian, A. H.; Niemeyer, Z. L.; Sigman, M. S.; Toste, F. D. *ACS Catal.* **2017**, *7*, 3973-3978.

2.2.1.2 Steric influence

The ligand volume can also exert an important influence in gold catalysis through the non-bonding interactions between different parts of the reactant and the catalyst. Sometimes this effect can drastically determine the conformation and reactivity, affecting the outcome of the process.

Again, Tolman was the first author that proposed, in 1977, an experimental parameter to quantify the volume of a ligand and try to estimate its steric influence with the so-called Tolman Cone Angle (ϕ).⁵² However, this parameter can only be undoubtedly measured for symmetrical phosphines, so its use is limited (Figure 12).

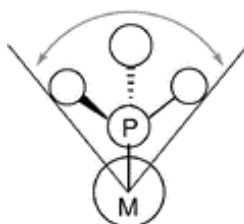


Figure 12: Graphic definition of the Tolman Cone Angle.

More recently, Cavallo and Nolan described a new parameter that could be used for both phosphorous-based and NHCs ligands bonded to a metallic centre. They defined the Percent Buried Volumen ($\%V_{bur}$) as the percentage of the total volume of a sphere occupied by the ligand bonded to the metal, at an average distance (usually 2.00 Å).⁵³ In Figure 13 are described the values of this parameter for four common gold(I) chloride complexes, employed in this dissertation.

⁵² Tolman, C. A. *Chem. Rev.* **1977**, *77*, 313-348.

⁵³ a) Hillier, A. C.; Sommer, W. J.; Yong, B. S.; Petersen, J. L.; Cavallo, L.; Nolan, S. P. *Organometallics* **2003**, *22*, 4322-4326; b) Clavier, H.; Nolan, S. P. *Chem. Commun.* **2010**, *46*, 841-861.

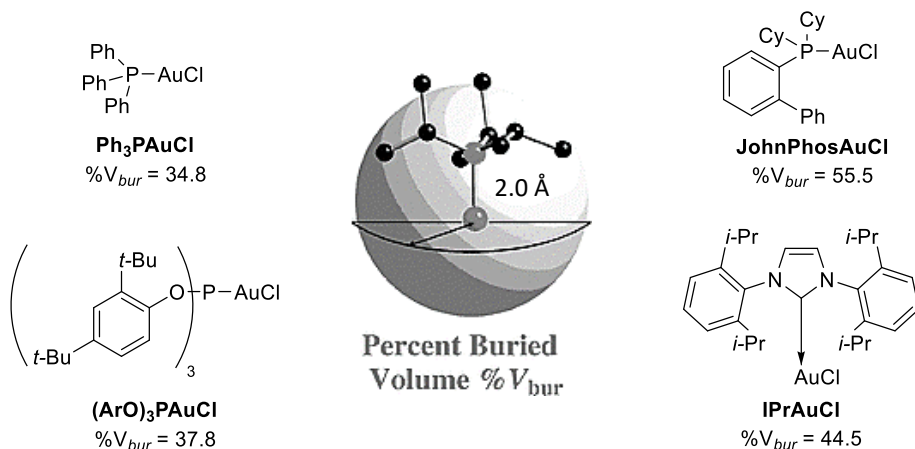


Figure 13: Percent Buried Volume values of four common gold(I) chloride complexes.

The results obtained for this parameter were so promising that in 2009 the free web application SambVca was developed by Cavallo and co-workers.⁵⁴ This computational tool calculates the Percent Buried Volume of a ligand in a defined complex, using the experimentally obtained data from an X-Ray Diffraction analysis.

2.2.2 Counterion-depending effects

In contrast to ligand-depending effects, counterions roles in gold catalysis have been less investigated and sometimes remained not very clear and surrounded by ambiguity. Given that they can seriously affect reactivity, chemo- and regioselectivity, it became clear the need for a deeper understanding. However, only few years ago, systematic studies of counterions started to be carried out. In this context, contributions by Bandini, Hashmi and Hammond are highly remarkable.^{46,55}

⁵⁴ Poater, A.; Cosenza, B.; Correa, A.; Giudice, S.; Ragone, F.; Vittorio Scarano, V.; Cavallo, L. *Eur. J. Inorg. Chem.* **2009**, *13*, 1759-1766.

⁵⁵ a) Jia, M.; Bandini, M. *ACS Catal.* **2015**, *5*, 1638-1652; b) Schiefl, J.; Schulmeister, J.; Doppiu, A.; Wörner, E.; Rudolph, M.; Karch, R.; Hashmi, A. S. K. *Adv. Synth. Catal.* **2018**, *360*, 3949-3959.

At the beginning of the study of gold catalysis, halides raised as the most common counterions, since they form strong bonds with gold generating stable complexes. However, this stability is translated to a high energetic barrier to be overcome in catalysis, as linear gold(I) complexes need a free coordination site to activate unsaturated systems. Thus, new generations of less-coordinating counterions came on stage (Table 3), being Tf_2N^- , TfO^- , SbF_6^- and BAr^{F_4-} the most widely employed.

Halides	O-based	N-based	B-/Al-based	C-based	Others
Cl^-	TsO^-	$(\text{PhSO}_2)_2\text{N}^-$	BAr^{F_4-}	CN^-	SbF_6^-
Br^-	MsO^-	Tf_2N^-	BF_4^-	HCTf_2^-	PF_6^-
I^-	TFA^-		$\text{B}(\text{C}_6\text{F}_5)^-$	Tf_3C^-	
	TfO^-		$[\text{Me}_3\text{NB}_{12}\text{Cl}_{11}]^-$	$\text{TsC}(\text{CN})_2^-$	
	ClO_4^-		$\text{Al}[\text{OC}(\text{CF}_3)_3]_4^-$		
	Phosphates				

Table 3: Common counterions in homogenous gold catalysis.

Although it may appear intuitive at first sight for some cases, classifying these counterions in order to rationalize their behaviour is a very complex task. In the next paragraphs several factors attributable to counterions will be described, being all of them relevant for each gold-catalyzed reaction, as follows: gold- and proton-affinity of the counterion, stability of the complex, and space distribution of the ionic pair.

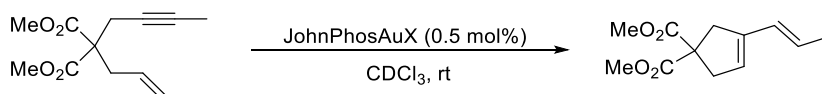
2.2.3 Gold- and proton-affinity of counterions

As mentioned before, the counterion gold-affinity can be a critical barrier to activate alkenes and alkynes. To date, three pioneering works tried to measure this influence through computational and NMR studies.⁵⁶ In a more recent work, Hammond and co-workers defined a new parameter, the Gold Afinittity Index (GAI),

⁵⁶ a) Kovács, G.; Ujaque, G.; Lledós, A. *J. Am. Chem. Soc.* **2008**, *130*, 853-864; b) Zhdanko, A.; Maier, M. E. *ACS Catal.* **2014**, *4*, 2770-2775.

using calculated dissociation energy for some of the most common counterions in gold catalysis.⁵⁷

With this index in hand, counterion effect for an example of gold(I)-catalyzed 1,6-enyne cycloisomerization was rationalized with good matching between the theoretical predictions and the experimental observations (Table 4).



X	Gold Affinity Index (GAI)	Relative initial rate
AcO ⁻	6.1	0.0
TsO ⁻	2.4	1.0
BF ₄ ⁻	0.5	7.1
SbF ₆ ⁻	0	21
Tf ₃ C ⁻	0.2	32
Al[OC(CF ₃) ₃] ₄ ⁻	≈0	42

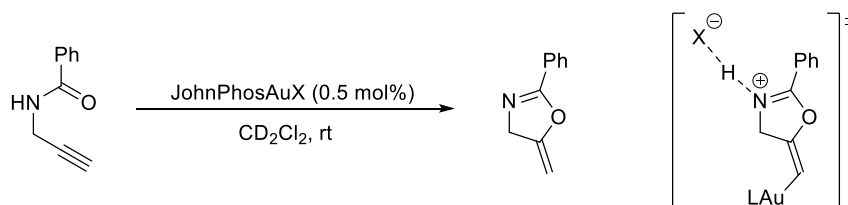
Table 4: GAI applied to a 1,6-enyne gold(I)-catalyzed cycloisomerization.

On the other hand, when an active proton is involved in the mechanism, the ability of the counterion to carry this proton can be also decisive. Thus, Laurence and co-workers studied this capability introducing the Hydrogen Bond Basicity Index (HBI) for some counterions, based on calculated hydrogen bonding energies. This parameter was later extended by Hammond,⁴⁶ finding that this indicator is usually more accurate than pK_a, although it has no good correlation with GAI.

As an example, HBI was also used for rationalizing counterion effect in a gold(I)-catalyzed cyclization of a propargyl amide, where proton-transfer is a key step, and the results are summarized in Table 5. Although the experimentally observed initial ratios for the gold SbF₆⁻ and Tf₃C⁻ complexes catalyzed reactions do not match with the expected ones probably due to other factors, the values found for AcO⁻, TfO⁻ and NTf₂⁻ complexes can be easily rationalized. In the case of the AcO⁻ anion, the HBI is extremely high, meaning that the proton is strongly bonded, in agreement with pK_a of the acetic acid in comparison with the other superacids of the table, preventing the protodeauration step. In the case of triflate and triflimide, it would

⁵⁷ Lu, Z.; Han, J.; Okoromoba, O. E.; Shimizu, N.; Amii, H.; Tormena, C. F.; Hammond, G. B.; Xu, B. *Org. Lett.* **2017**, *19*, 5848-5851.

be not easy to predict the effect attending only to their close pK_a values (-11.4 for TfOH and -11.9 for HNTf₂). However, the higher HBI of the triflate anion suggests that it can abstract the proton from the nitrogen atom in the transition state better than the triflimidate one. Thus, the combination of its higher HBI along with its acidity makes this anion a better 'proton carrier' than the other ones shown.



X	pK_a (in 1,2-DCE)	Hydrogen Bonding Basicity Index (HBI)	Relative initial rate
AcO ⁻	15.5	10	0.0
TfO ⁻	-11.4	3.4	5.1
Tf ₂ N ⁻	-11.9	1.0	0.9
SbF ₆ ⁻	-	2.8	1.0
Tf ₃ C ⁻	-16.4	0	1.0

Table 5: HBI applied to a propargylamide gold(I)-catalyzed isomerization.

2.2.4 Stability of the gold complex

It is well-known that, for different gold complexes with the same ligand, counterions can play crucial roles in their decay process, and in last term in the reaction outcome. This effect was studied by Hammond and co-workers in the decay process of cationic gold complexes with different counterions in the presence of cyclohexene (Figure 14).⁴⁶ However, they could not undoubtedly assess the role of the anion, being not well-established yet.⁵⁸

⁵⁸ a) Laurence, C.; Brameld, K. A.; Graton, J. r. m.; Le Questel, J.-Y.; Renault, E. *J. Med. Chem.* **2009**, *52*, 4073-4086; b) Kumar, M.; Jasinski, J.; Hammond, G. B.; Xu, B. *Chem. Eur. J.* **2014**, *20*, 3113-3119.

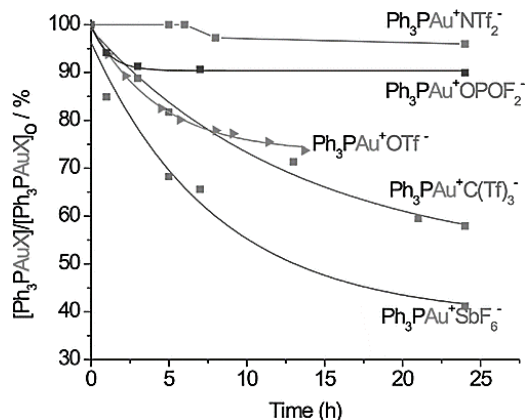


Figure 14: Comparison between different gold complexes in a decay process.

In general, experimental observations suggest that cationic gold complexes bearing less coordinating counterions are usually very unstable⁵⁹ and some of them impossible to isolate without a stabilizing molecule, usually a nitrile.

2.2.5 Ion pairing in gold catalysis

Another factor that can deeply impact in the reaction outcome is ion pairing, since gold-catalyzed processes involve several coordination-decoordination steps around the gold atom, the ligand, the counterion and the unsaturated system. However, this effect has been scarcely investigated because it is not always easy to understand and predict.

In an interesting work, Macchioni and Zuccaccia⁶⁰ demonstrated by DFT and NMR experiments that there are three possible cation/anion orientations once the unsaturated system is coordinated. If the anion remains close to the alkene/alkyne (Figure 15, *right*), the reaction takes place; on the contrary, when it stays near to

⁵⁹ a) Raabe, I.; Krossing, I. *Angew. Chem. Int. Ed.* **2004**, *43*, 2066-2090; b) Mézailles, N.; Ricard, L.; Gagosz, F. *Org. Lett.* **2005**, *7*, 4133-4136.

⁶⁰ a) Zuccaccia, D.; Belpassi, L.; Tarantelli, F.; Macchioni, A. *J. Am. Chem. Soc.* **2009**, *131*, 3170-3171; b) Ciancaleoni, G.; Belpassi, L.; Tarantelli, F.; Zuccaccia, D.; Macchioni, A. *Dalton Trans.* **2013**, *42*, 4122-4131.

the ligand (Figure 15, *left*) the reaction slows or is even shut down,⁶¹ although the authors do not extensively rationalized this observation.

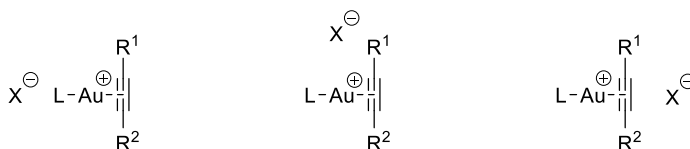


Figure 15: Possible orientations in gold(I)-alkyne π -complexes in solution.

Of course, electronic and steric properties of the ligand, solvent's polarity and temperature also determine these space dispositions, so many authors state that it is necessary to find the perfect match for all of them to improve the catalytic cycle.⁶²

2.2.6 Additive-depending effects

Additives have been widely employed in transition metal catalysis to improve both: yield and selectivity; and sometimes even generate a dramatical change in the second one.⁶³ During the last years, gold catalysis has not fallen behind in this field, but there was a lack of gathering data until very recently.⁴⁶ As these effects are closely related with the study carried out in *Chapter IV*, they will be further discussed in the corresponding section of this memory.

⁶¹ Biasiolo, L.; Ciancaleoni, G.; Belpassi, L.; Bistoni, G.; Macchioni, A.; Tarantelli, F.; Zuccaccia, D. *Catal. Sci. Technol.* **2015**, *5*, 1558-1567.

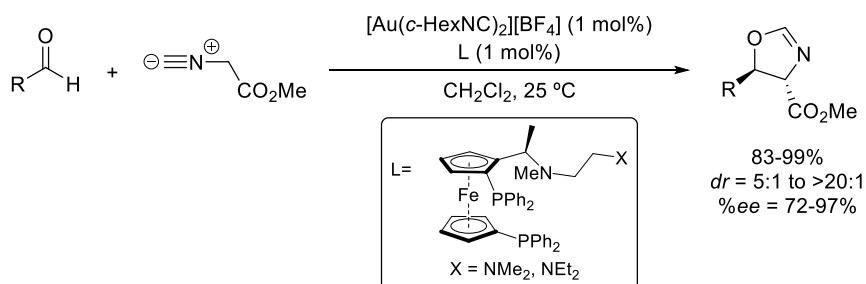
⁶² a) Biasiolo, L.; Del Zotto, A.; Zuccaccia, D. *Organometallics* **2015**, *34*, 1759-1765; b) Schießl, J.; Schulmeister, J.; Doppiu, A.; Wörner, E.; Rudolph, M.; Karch, R.; Hashmi, A. S. K. *Adv. Synth. Catal.* **2018**, *360*, 2493-2502.

⁶³ Becica, J.; Döbereiner, G. E. *Org. Biomol. Chem.* **2019**, *17*, 2055-2069.

2.3 Gold-catalyzed transformations involving carbon-carbon multiple bonds

Few metals have been so attractive as gold in the human history. It has been largely employed in jewellery and decorative items, given its characteristic glow and yellow colour, and its resistance to tarnishing and corrosion.

However, in the field of catalysis, gold was considered as a 'dead' metal for decades, until the first example of homogenous gold catalysis was described by Ito and Hayashi in 1986, an enantioselective synthesis of dihydrooxazoles (Scheme 18).⁶⁴ Since then, gold catalysis has evolved until stating nowadays as a key tool for the activation of organic species, growing exponentially with increasing complexity and selectivity.



Scheme 18: First example of homogeneous gold(I) catalysis, by Ito and Hayashi.

The wide range of reported gold-catalyzed transformations makes them hard to compile and classify. For this reason, due to its relationship with the thematic of this memory I decided to focus only on transformations involving C-C multiple bonds activation followed by nucleophilic attack and/or rearrangements. Other interesting transformations such as gold redox catalysis,⁴¹ activation of diazo compounds,⁶⁵ cycloheptatrienes⁶⁶ or cyclopropenes,⁶⁷ or gold catalysis as oxophilic Lewis acid will not be discussed.

⁶⁴ Ito, Y.; Sawamura, M.; Hayashi, T. *J. Am. Chem. Soc.* **1986**, *108*, 6405-6406.

⁶⁵ For recent reviews see: a) Wei, F. et al. *Sci. Bull.* **2015**, *60*, 1479-1492; b) Ma, B.; Liu, L.; Zhang, J. *Asian J. Org. Chem.* **2018**, *7*, 2015-2025.

⁶⁶ For further information see: Mato, M.; García-Morales, C.; Echavarren, A. M. *ChemCatChem* **2019**, *11*, 53-72.

The reactions described here have been divided into two groups depending on the coordination mode of the gold catalysts to the active site: π -activation or σ -activation of alkynes.

2.3.1 π -Activation of alkynes

As explained in the previous section, π -complexation of alkynes by gold complexes leads to electrophilic systems that undergo nucleophilic additions following Markovnikov regioselectivity rules.

Given the different nature of nucleophiles involved in gold catalysis, I decided to address the description of representative examples of these transformations, starting from alkynes, splitting them into four groups: addition of heteronucleophiles; addition of carbonucleophiles and 1,n-enyne cycloisomerization; migration of propargylic carboxylates; and formation of α -oxo and α -imino-carbenes.

2.3.1.1 Addition of heteronucleophiles

The seminal examples of this carbophilic activation were described by Teles and Tanaka using gold(I) complexes,⁶⁸ and Utimoto through gold(III) species,⁶⁹ proving their efficiency as catalysts for the hydration of alkynes through addition of *O*-nucleophiles. Since then, even more robust hydration processes have been described.⁷⁰ In this sense, a comparison in terms of efficiency between different gold-catalyzed methodologies has been performed by Zuccaccia and co-workers, who recently described a highly efficient solvent- and silver-free gold(I)-catalyzed hydration of alkynes.⁷⁰

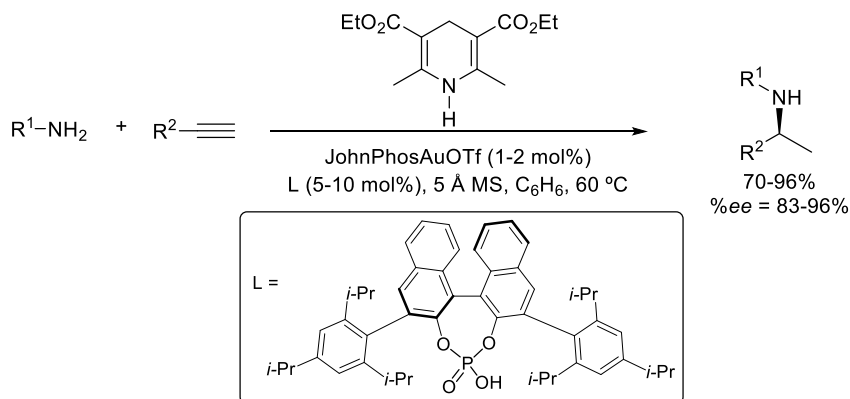
⁶⁷ For recent reviews see: a) Miege, F.; Meyer, C.; Cossy, J. *Beilstein J. Org. Chem.* **2011**, *7*, 717-734; b) Vicente, R. *Chem. Rev.* **2021**, *121*, 1, 162-226.

⁶⁸ a) Teles, J. H.; Brode, S.; Chabanas, M. *Angew. Chem. Int. Ed.* **1998**, *37*, 1415-1418; b) Mizushima, E.; Sato, K.; Hayashi, T.; Tanaka, M. *Angew. Chem. Int. Ed.* **2002**, *41*, 4563-4565.

⁶⁹ Fukuda, Y.; Utimoto, K. *J. Org. Chem.* **1991**, *56*, 3729-3731.

⁷⁰ a) Marion, N.; Ramón, R. S.; Nolan, S. P. *J. Am. Chem. Soc.* **2009**, *131*, 448-449; b) Brill, M.; Naha, F.; Gómez-Herrera, A.; Zinser, C.; Cordes, D. B.; Slawin, A. M. Z.; Nolan, S. P. *ChemCatChem* **2017**, *9*, 117-120; c) Gatto, M.; Belanzoni, P.; Belpassi, L.; Del Zotto, A.; Tarantelli, F.; Zuccaccia, D. *Green Chem.* **2018**, *20*, 2125-2134; d) Gatto, M.; Del Zotto, A. Segato, J.; Zuccaccia, D. *Organometallics* **2018**, *37*, 4685-4691.

A similar development can be observed for gold-catalyzed hydroamination processes. This type of reactions was earlier described by Utimoto.⁷¹ As a proof of these reactions' efficiency, an example involving sequential hydroamination and enantioselective transfer hydrogenation is described in Scheme 19.⁷²



Scheme 19: Gold(I)-catalyzed hydroamination and transfer hydrogenation of alkynes.

Following this trend, one of the most studied gold-catalyzed processes have been intramolecular addition of heteronucleophiles to C-C multiple bonds, mainly for the formation of *O*- and *N*-heterocyclic compounds. Homopropargyl alcohols and amines have been widely used for this purpose, but, as these reactions are closely related with the present dissertation, some examples will be further disclosed in *Chapter III*.

On the other hand, carbonyl compounds and their *N*-derivatives (imines, oximes, hydrazones...) can also act as suitable nucleophiles for heterocycles synthesis under gold catalysis.⁷³

⁷¹ a) Fukuda, Y.; Utimoto, K.; Nozaki, H. *Heterocycles* **1987**, *25*, 297-300; b) Y. Fukuda, Y.; Utimoto, K. *Synthesis* **1991**, *11*, 975-978.

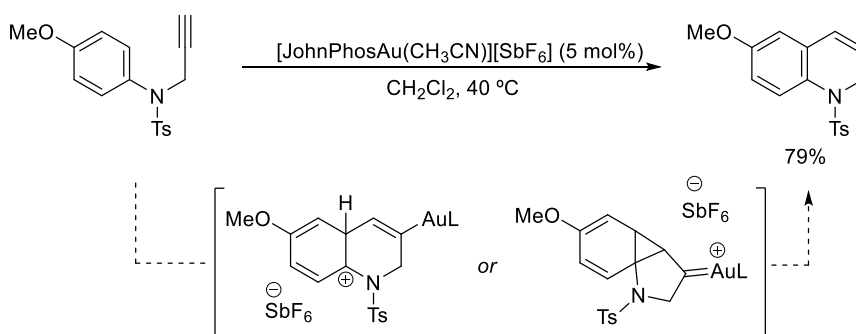
⁷² Liu, X.-Y.; Che, C.-M. *Org. Lett.* **2009**, *11*, 4204-4207.

⁷³ For selected examples, see: a) Belting, V.; Krause, N. *Org. Biomol. Chem.* **2009**, *7*, 1221-1225; b) Teng, T.-M.; Das, A.; Huple, D.B.; Liu, R.-S. *J. Am. Chem. Soc.* **2010**, *132*, 12565-12567; c) Leyva-Pérez, A.; Cabrero-Antonino, J. R.; Cantín, A.; Corma, A. *J. Org. Chem.* **2010**, *75*, 7769-7780; d) Guven, S.; Ozer, M. S.; Kaya, S.; Menges, N.; Balci, M. *Org. Lett.* **2015**, *17*, 2660-2663; e) Zimin, D. P.; Dar'in, D. V.; Rassadin, V. A.; Kukushkin, V. Y. *Org. Lett.* **2018**, *20*, 4880-4884.

2.3.1.2 Addition of carbonucleophiles. 1,*n*-Enynes cycloisomerization.

Carbon-carbon bond-forming reactions through addition of C-nucleophiles to alkynes have also been studied in gold catalysis, being hydro(hetero)arylation and alkene-alkyne cycloaddition the most common transformations.⁷⁴

Hydroarylation reactions can operate following two different mechanisms although with similar energetic barriers. The reaction could occur via direct Friedel-Crafts alkenylation or, in an alternative pathway, via formation of a cyclopropyl gold carbene intermediate. In Scheme 20, an intramolecular hydroarylation of an *N*-aryltosylpropargylamide takes place to furnish a 1,2-hydroquinoline derivative.⁷⁵



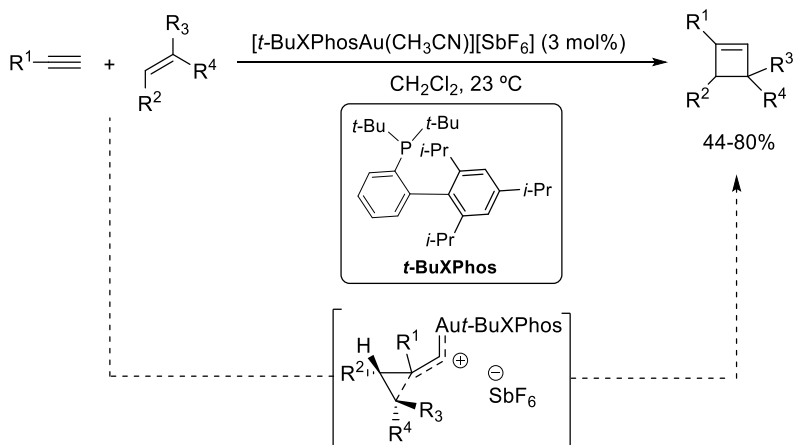
Scheme 20: Intramolecular hydroarylation of an *N*-aryl-tosyl-propargylamide.

As an example of alkene-alkyne cycloaddition, in Scheme 21 is outlined a gold-catalyzed cyclobutene formation through a formal [2+2] cycloaddition.⁷⁶ For these reactions, regiochemical outcomes agree with the formation of distorted cyclopropyl intermediates, which evolve through ring expansion.

⁷⁴ a) Muratore, M. E.; Homs, A.; Obradors, C.; Echavarren, A. M. *Chem. Asian J.* **2014**, 9,306-3082; b) Muratore, M. E.; Echavarren, A. M. *PATAI's Chemistry of Functional Groups*, **2014**.

⁷⁵ Martín-Matute, B.; Nevado, C.; Cárdenas, D. J.; Echavarren, A. M. *J. Am. Chem. Soc.* **2003**, 125, 5757-5766.

⁷⁶ López-Carrillo, V.; Echavarren, A. M. *J. Am. Chem. Soc.* **2010**, 132, 9292-9294.



Scheme 21: Gold(I)-catalyzed [2+2] cycloaddition of alkynes and alkenes.

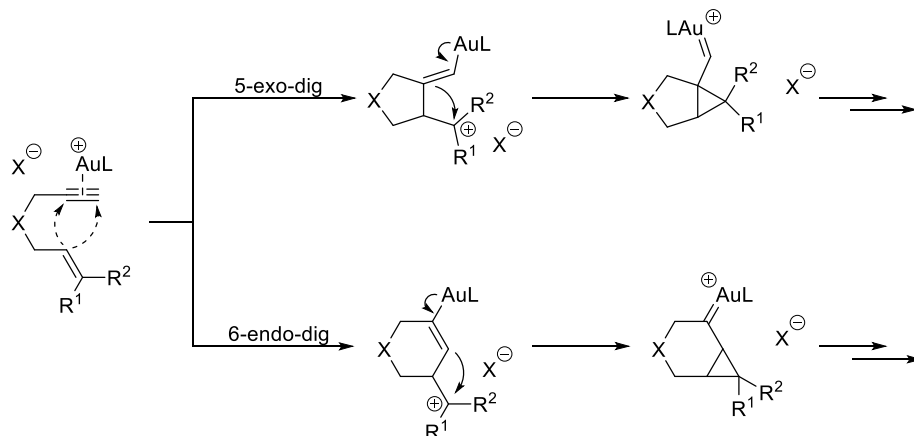
However, the most representative and deeply studied gold(I)-catalyzed C-C bond-forming reactions are 1,*n*-enyne,⁷⁷ allenyne and allenene cycloisomerizations,⁷⁸ being the first substrates the most studied ones. First, it should be mentioned that, for other transition metals, these transformations proceed *via* simultaneous coordination of the alkene and the alkyne, usually followed by migratory insertion or metallacycle formation.⁷⁹ As gold(I) complexes structures are linearly bicoordinated, this activation is prevented, so they go through different mechanistic pathways, usually involving carbene intermediates and skeletal rearrangements.

Among them, 1,6-enynes have been the most studied reagents in terms of mechanism, and, in the absence of nucleophiles or other 'directing' groups, they proceed through 5-*exo*-dig or 6-*endo*-dig cyclization (Scheme 22).

⁷⁷ For selected reviews of 1,*n*-enyne cycloisomerization see: a) Obradors, C.; Echavarren, A. M. *Acc. Chem. Res.* **2014**, *47*, 902-912; b) Dorel, R.; Echavarren, A. M. *Chem. Rev.* **2015**, *115*, 9028-9072; c) Marín-Luna, M.; Nieto, O.; Silva, C. *Front. Chem.* **2019**, *7*, 1-22.

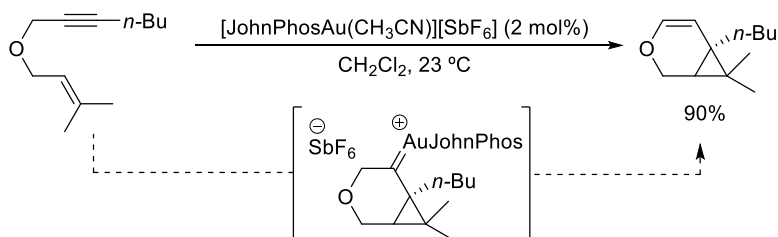
⁷⁸ For some examples of 1,*n*-allenene and allenene cycloisomerizations see: a) Aubert, C.; Fensterbank, L.; García, P.; Malacria, M.; Simmoneau, A. *Chem. Rev.* **2011**, *111*, 1954-1993; b) Cañeque, T.; Truscott, F. M.; Rodríguez, R.; Maestri, G.; Malacria, M. *Chem. Soc. Rev.* **2014**, *43*, 2916-2926.

⁷⁹ For selected examples of 1,*n*-enyne cycloisomerization catalyzed by other transition metals, see: a) Aubert, C.; Buisine, O.; Malacria, M. *Chem. Rev.* **2002**, *102*, 813-834; b) Marinetti, A.; Jullien, H.; Voituriez, A. *Chem. Soc. Rev.* **2012**, *41*, 4884-4908; c) Muratore, M. E.; Homs, A.; Obradors, C.; Echavarren, A. M. *Chem. Asian. J.* **2014**, *9*, 3066-3082; d) Stathakis, C. I.; Gkizis, P. L.; Zografos, A. L. *Nat. Prod. Rep.* **2016**, *33*, 1093-1117.



Scheme 22: Mechanistic proposals for gold(I)-catalyzed cycloisomerization of 1,6-enynes.

Professor Echavarren's has been one of the groups with higher contributions to develop these transformations, carrying out systematically bibliographic, experimental and computational studies, and catalyst design to improve reaction selectivity.⁸⁰ A simple example of this type of rearrangements is depicted in Scheme 23. Thus, starting from simple accessible allyl propargyl ether, an oxabicyclic compound is obtained in the presence of a gold(I) catalyst.⁸¹ A 6-*endo*-dig cyclization, carbene formation and C-H insertion would explain the reaction outcome.

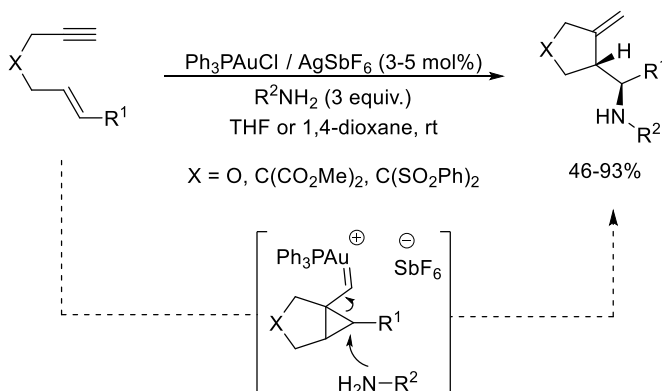


Scheme 23: Gold(I)-catalyzed cycloisomerization of a 1,6-enyne.

⁸⁰ For selected examples see: a) Jiménez-Núñez, E.; Echavarren, A. M. *Chem. Rev.* **2008**, *108*, 3326-3350; b) Pérez-Galán, P.; López-Carrillo, V.; Echavarren, A. M. *Contrib. Sci.* **2010**, *6*, 143-153; c) Zuccarello, G. et al. *J. Am. Chem. Soc.* **2019**, *141*, 11858-11863; d) Zuccarello, G.; Zanini, M.; Echavarren, A. M. *Isr. J. Chem.* **2020**, *60*, 360-372.

⁸¹ Harrak, Y.; Simonneau, A.; Malacria, M.; Gandon, V.; Fensterbank, L. *Chem. Commun.* **2010**, *46*, 865-867.

Along with skeleton rearrangements, common reactivity of 1,*n*-enynes involves intra- or intermolecular trapping of the cyclopropyl gold carbenes *via* cyclopropanation, C-H insertion or nucleophilic addition. As an illustrative example of these transformations, an aminocyclization of 1,6-enynes is described in Scheme 24. After formation of the cyclopropyl gold carbene intermediate, conjugated addition of the amine furnish the final product.⁸²



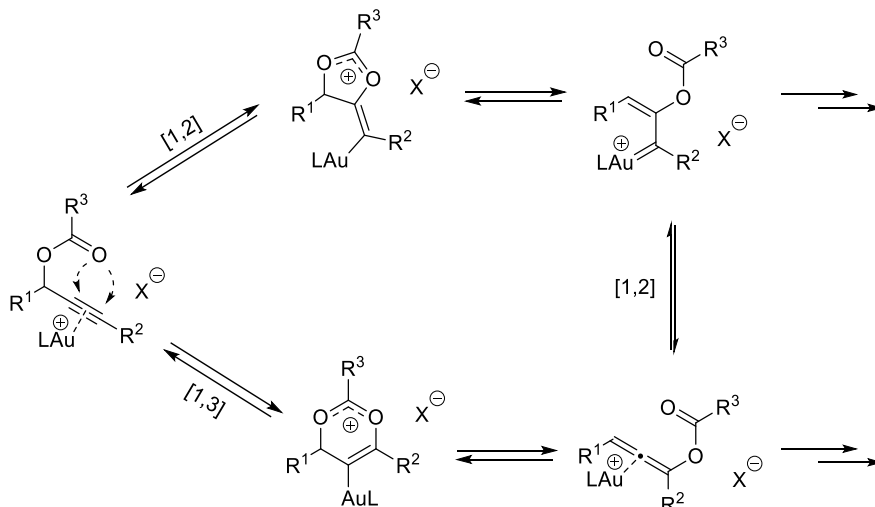
Scheme 24: Cycloisomerization of a 1,6-enyne followed by intermolecular trapping.

2.3.1.3 Propargyl carboxylate migrations

Carboxylates derived from propargylic alcohols or propargylamines have been considered privileged structures, given they are easily accessible and present a high synthetic potential.⁸³ These substrates can undergo two different pathways upon gold carbophilic activation: [1,2] or [1,3]-carboxy migration. In Scheme 25 this divergent evolution has been outlined. Thus, the first one evolves through 5-*exo*-dig and generates a gold carbene intermediate, while the second one, through 6-*endo*-dig cyclization, furnishes a carboxyallene π -complex, able to rearrange through a new [1,2] migration to the previously mentioned carbene intermediate.

⁸² Leseurre, L.; Toullec, P. Y.; Genêt, J.-P.; Michelet, V. *Org. Lett.* **2007**, *9*, 4049-4052.

⁸³ For selected examples see: a) Marion, N.; Nolan, S. P. *Ang. Chem. Int. Ed.* **2007**, *46*, 2750-2752; b) Shu, X. -Z.; Shu, D.; Schienebeck, C. M.; Tang, W. *Chem. Soc. Rev.* **2012**, *41*, 7698-7711; c) Tejedor, D.; Mendez-Abt, G.; Cotos, L.; Garcia-Tellado, F. *Chem. Soc. Rev.* **2013**, *42*, 458-471; d) Kumar, R. K.; Bi, X. *Chem. Comm.* **2016**, *52*, 853-868.



Scheme 25: General gold(I) activation of propargylic carboxylates.

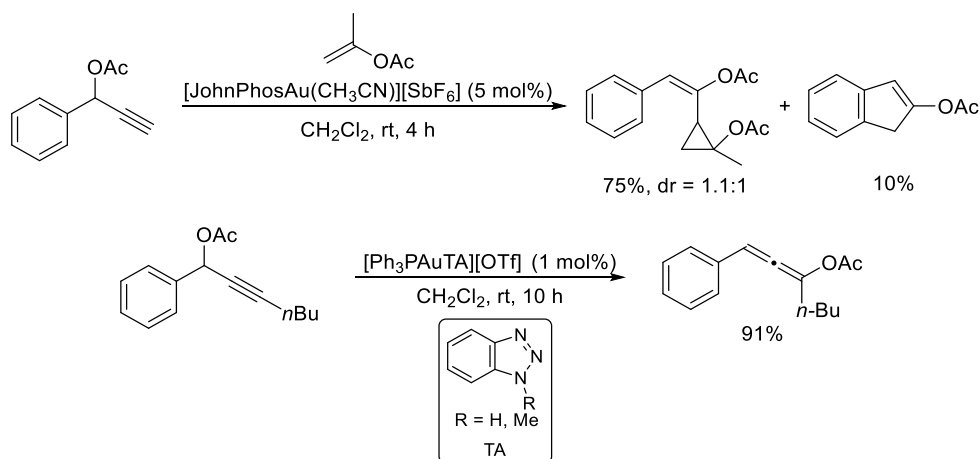
Computational studies performed on this type of reactions⁸⁴ have proven that two factors determine which vinylgold intermediate is more favourable, as follows: electronic and steric factors at the C_β of the alkyne. Thus, electron-rich aryl rings and bulky alkyl substituents should favour [1,3]-migration since they stabilize positive charge in C_β. On the other hand, hydrogen or electron-withdrawing groups should favour [1,2]-migration.

However, further experimental and computational results have demonstrated that both mechanisms can operate simultaneously until an equilibrium between both vinylgold intermediates is reached.⁸⁵ Many times, the reaction outcome strongly depends on the further reactivity of both intermediates, so it can be driven carefully choosing coupling partners, catalyst and conditions. This way, in Scheme 26 two gold(I)-catalyzed transformations of similar propargylacetates are represented. For the first one, the presence of a terminal alkyne favours a [1,2]-

⁸⁴ Soriano, E.; Marco-Contelles, J. *Chem. Eur. J.* **2008**, *14*, 6771-6779.

⁸⁵ For experimental evidence see: a) Sherr, B. D.; Toste, F. D. *J. Am. Chem. Soc.* **2004**, *126*, 15978-15979; b) Gandon, V.; Lemièrre, G.; Hours, A.; Fensterbank, L.; Malacria, M. *Angew. Chem. Int. Ed.* **2008**, *47*, 7534-7538; c) Mauleón, P.; Krinsky, J. L.; Toste, F. D. *J. Am. Chem. Soc.* **2009**, *131*, 4513-4520; b) Marion, N.; Lemièrre, G.; Correa, A.; Costabile, C.; Ramón, R. S.; Moreau, X.; de Frémont, P.; Dahmane, R.; Hours, A.; Lesage, D.; Tabet, J. -C.; Goddard, J. -P.; Gandon, V.; Cavallo, L.; Fensterbank, L.; Malacria, M.; Nolan, S. P. *Chem. Eur. J.* **2009**, *15*, 3243-3260. For computational studies see: Correa, A.; Marion, N.; Fensterbank, L.; Malacria, M.; Nolan, S. P.; Cavallo, L. *Angew. Chem. Int. Ed.* **2008**, *47*, 718-721.

migration followed by the cyclopropanation of an olefin (only 10% of intramolecular C-H insertion was observed).⁸⁶ However, with a butyl group on the acetylenic carbon a [1,3]-migration is favoured, yielding an acetoxyallene efficiently.⁸⁷



Scheme 26: Examples of [1,2]- and [1,3]-acetoxy migration for propargylacetates.

It is worth to mention that similar results have been described with multiple propargyl derivatives such as (thio)acetals, amides, sulfonamides... Also, a wide range of functional groups in the propargylic and acetylenic positions are tolerated, and they can be easily combined with external nucleophiles. Therefore, very different skeletons can be achieved under gold catalysis starting from these simple reagents, standing as promising substrates in total synthesis.⁸⁸

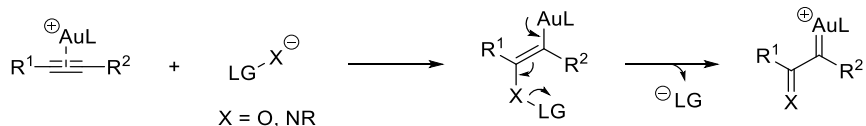
2.3.1.4 Formation of α -oxo and α -imino gold carbene complexes

When the heteronucleophile possess a leaving group attached to the heteroatom, nucleophilic attack to an alkyne followed by retrodonation (*push-pull*) leads to gold carbenes with a double C-heteroatom bond at *alpha* position (Scheme 27). Thus, *O*-nucleophiles generate α -oxo carbenes and *N*-nucleophiles α -imino-carbenes, being the first ones more studied in the bibliography.

⁸⁶ Sperger, C. A.; Tungen, J. E.; Fiksdahl, A. *Eur. J. Org. Chem.* **2011**, 20, 3719-3722.

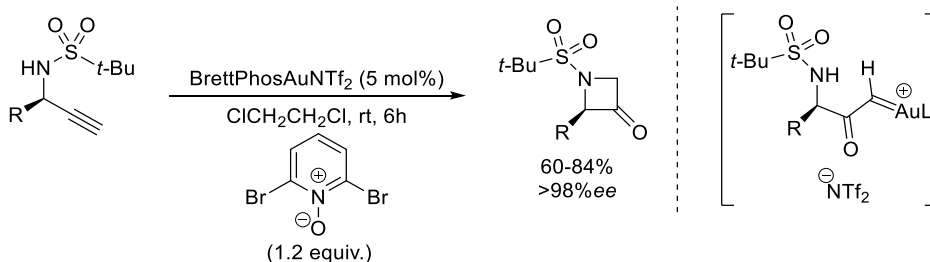
⁸⁷ Wand, D. *Org. Lett.* **2011**, 13, 2618-2621.

⁸⁸ Mouriès-Mansuy, V.; Fensterbank, L. *Isr. J. Chem.* **2018**, 58, 586-595.



Scheme 27: Generation of α -oxo and α -imino gold(I) carbenes.

Two simple examples of these transformations are depicted below. In Scheme 28, a highly efficient synthesis of azetidin-3-ones is described.⁸⁹ Intermolecular oxidation of the alkyne with a pyridine *N*-oxide derivative produces an α -oxo carbene intermediate that can be trapped by the sulfonamide group, yielding the final products. Chirality, which can be easily introduced at the substrates, is retained, stating this transformation as an excellent route to access these structures within few steps.

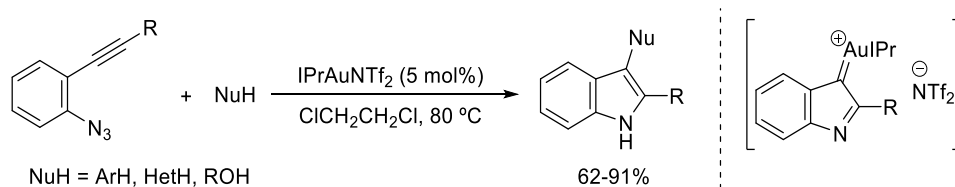


Scheme 28: Synthesis of azetidin-3-ones *via* α -oxo gold(I) carbene complexes.

As an example of heterocycle formation through the participation of an α -imino carbene complex, a synthesis of 3-substituted indoles from *o*-alkynylphenyl azides is represented in Scheme 29. Intramolecular generation of the α -imino carbene by addition of the azide and nitrogen extrusion is followed by intermolecular nucleophilic trapping, furnishing the final products.⁹⁰

⁸⁹ Ye, L.; He, W.; Zhang, L. *Angew. Chem. Int. Ed.* **2011**, *50*, 3236-3239.

⁹⁰ Lu, B.; Luo, Y.; Liu, L.; Ye, L.; Wang, Y.; Zhang, L. *Angew. Chem. Int. Ed.* **2011**, *50*, 8358-8362.

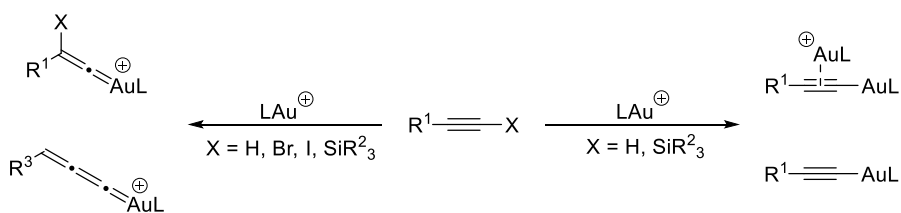


Scheme 29: Synthesis of indoles through α -imino gold(I) carbene complexes.

As shown, this strategy allows accessing these valuable intermediates from simple unsaturated systems and suitable substrates. Many evolution pathways of the carbene intermediates have been described; and several α -oxo and α -imino carbene precursors have been reported, with leaving groups ranging from simple nitrogen to more complex organic chains. Therefore, they are highly desirable alternatives to potentially explosive diazo compounds and valuable tools for the synthesis of heterocycles.⁹¹

2.3.2 σ -Activation of alkynes. Gold acetylides

Along with the previously described π -activation, terminal alkynes, alkynylsilanes and 1-haloalkynes can experiment σ -activation in the presence of a gold catalyst. In this sense, different key intermediates have been formulated, as follows: monometallic acetylides and σ,π -bimetallic complexes, vinylidenes and higher order cumulenes (Scheme 30).



Scheme 30: σ - and σ,π -activations of alkynes by gold(I) complexes.

⁹¹ For selected reviews of α -oxo carbenes, see: a) Zhang, L. *Acc. Chem. Res.* **2014**, *47*, 877-888; b) Bhunia, S.; Ghosh, P.; Patra, S. R. *Adv. Synth. Catal.* **2020**, *362*, 3664-3708. For selected review of α -imino carbenes, see: c) Aguilar, E.; Santamaría, J. *Org. Chem. Front.* **2019**, *6*, 1513-1540; d) Zhao, X.; Rudolph, M.; Asiri, A. M.; Hashmi, A. S. K. *Front. Chem. Sci. Eng.* **2020**, *14*, 317-349.

Although all these species have attracted attention during the last years because of their interesting reactivity,⁹² only the role in catalysis of gold acetylides generated from alkynylsilanes will be discussed, since it is closely related with the present dissertation.

The first gold(I) π -complexes of alkynylsilanes were isolated by Toste and Russell.⁹³ Employing an alkynylsilane-tethered phosphine, Toste obtained a dimeric complex (Figure 16, *left*), whose X-ray structure showed that gold atoms are unsymmetrically coordinated, closer to the C_{β} with the silyl moiety in both alkynes while.

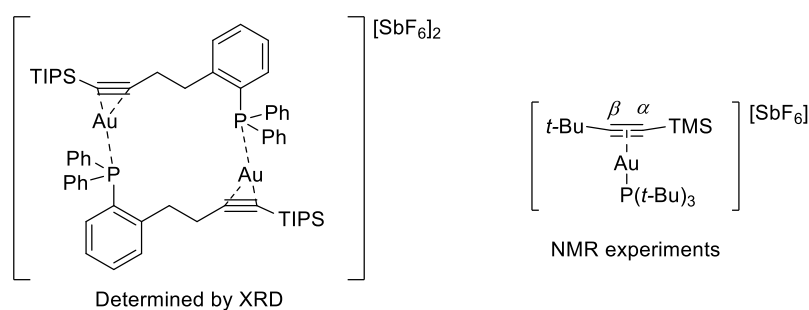


Figure 16: π -Gold(I) complexes of alkynylsilanes.

On the other hand, Russell and co-workers isolated a monomeric gold complex using a smaller silylacetylene (Figure 16, *right*). Despite its geometry could not be accurately determined, ^{29}Si -NMR and ^{13}C -NMR studies of this complex proved a deshielding of the silicon signal, in comparison with the non-coordinated alkynylsilane (-5.2 ppm respect to -18.8 ppm), and for the C_{β} (from 116.5 to 132.8 ppm), suggesting the same result observed by Toste. Russell and co-workers also isolated and characterized different gold(I) acetylides, starting from the same precursors. After silyl group removal with fluoride sources, and depending on the stoichiometry, they found mono-, bi-, tri- and tetra-aurated intermediates.^{93b} Considering these results, they formulated a mechanism for the *slippage* of the silyl moiety to form a gold acetylide complex, as follows (Scheme 31).

⁹² For selected reviews see: a) Gimeno, A. et al. *Chem. Eur. J.* **2014**, *20*, 683-688; b) Halliday, C. J. V.; Lynam, J. M. *Dalton Trans.* **2016**, *45*, 12611-12626; c) Gagosz, F. *Synthesis* **2019**, *51*, 1087-1099.

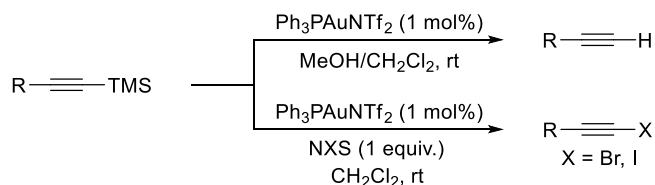
⁹³ a) Shapiro, N.; Toste, F. D. *PNAS* **2008**, *105*, 2779-2782; b) Hooper, T. N.; Green, M.; Russell, C. A. *Chem. Commun.* **2010**, *46*, 2313-2315.



Scheme 31: Slippage in the gold(I) acetylide formation from alkynylsilanes.

Thus, after π -coordination of the gold complex to the alkyne, the β -silicon effect (see *Properties of silicon. Organosilicon compounds*) favours incipient positive charge formation on the C_β . This feature results in a transference of positive charge from gold atom to the silicon one, making it more electrophile. Thus, abstraction of the silyl group, cleaving C-Si bond, generates the corresponding gold(I) acetylide.

However, when a weakly coordinating anion assists the C-Si bond cleavage, a reactive silylium source is *in situ* generated, allowing further reactivity. The first example of this approach, reported by Sheppard, only permitted simple protonation and halogenation of the gold(I) acetylide, employing methanol or *N*-halosuccinimide (NXS) as electrophiles sources (Scheme 32).⁹⁴

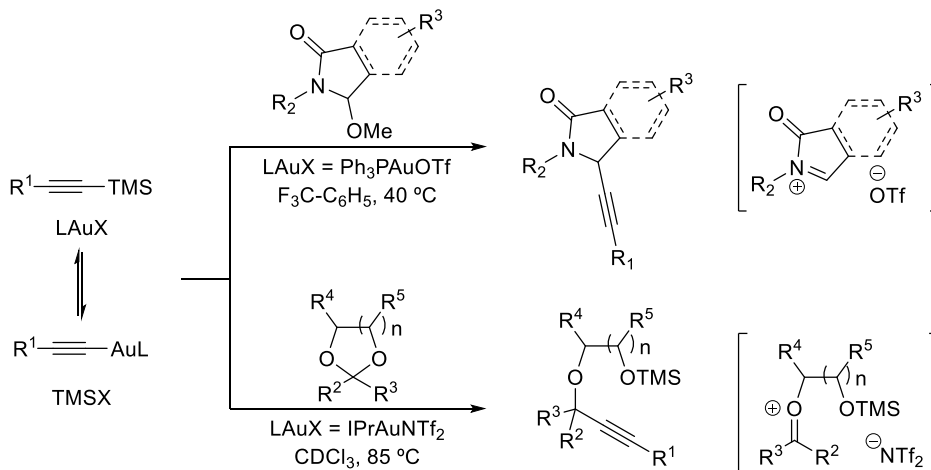


Scheme 32: Gold(I)-catalyzed proto- and halodesilylation of trimethylsilylalkynes.

More interestingly, some advances have been developed in this area during the last decade with the discovery of catalytic synergistic processes with C-C bond formation, involving silylium species acting as *in situ* generated facilitators. In this sense, Dalla and co-workers described the catalytic alkynylation of cyclic *N,O*- and *O,O*-acetals with alkynylsilanes (Scheme 33).⁹⁵ These transformations proceeds via gold(I) acetylide, after slippage of the silyl group, forming a silylium specie that can active the corresponding ketal.

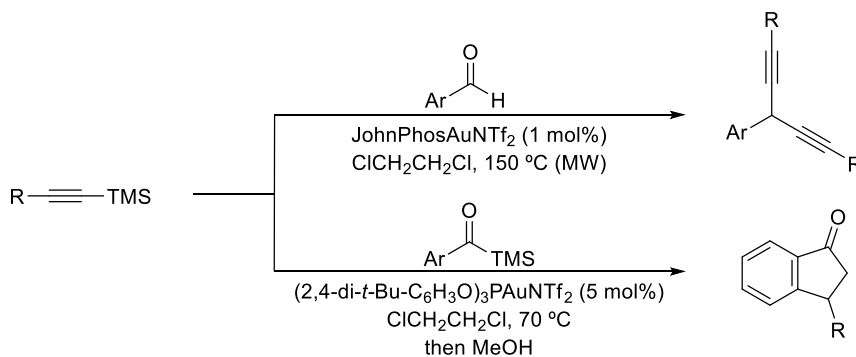
⁹⁴ Starkov, P.; Rota, F.; D'Oyley, J. M.; Sheppard, T. D. *Adv. Synth. Catal.* **2012**, *354*, 3217-3224.

⁹⁵ a) Michalska, M.; Songis, O.; Taillier, C.; Bew, S. P.; Dalla, V. *Adv. Synth. Catal.* **2014**, *356*, 2040-2050; b) Berthet, M.; Songis, O.; Taillier, C.; Dalla, V. *J. Org. Chem.* **2017**, *82*, 9916-9922.



Scheme 33: Gold(I)-catalyzed alkynylation of acetals with alkynyltrimethylsilanes.

Our research group also reported several examples of this type of reactivity, consisting in the addition of trimethylsilylalkynes to aromatic aldehydes or acylsilanes, yielding respectively bis(alkynyl)arylmethanes or indanones.⁹⁶ General reaction conditions are shown in Scheme 34, but, considering that these transformations are closely related with the present dissertation, mechanistic issues will be further discussed in *Chapter I* and *Chapter II*.



Scheme 34: Gold(I)-catalyzed addition of alkynyltrimethylsilanes to aromatic aldehydes (bisalkynylation) and acylsilanes (indanone synthesis).

⁹⁶ a) Rubial, B.; Ballesteros, A.; González, J. M. *Adv. Synth. Catal.* **2013**, *355*, 3337-3343; b) González, J.; Santamaría, J.; Ballesteros, A. *Angew. Chem. Int. Ed.* **2015**, *54*, 13678-13681; c) Rubial, B.; Ballesteros, A.; González, J. M. *Eur. J. Org. Chem.* **2018**, *45*, 6194-6198.

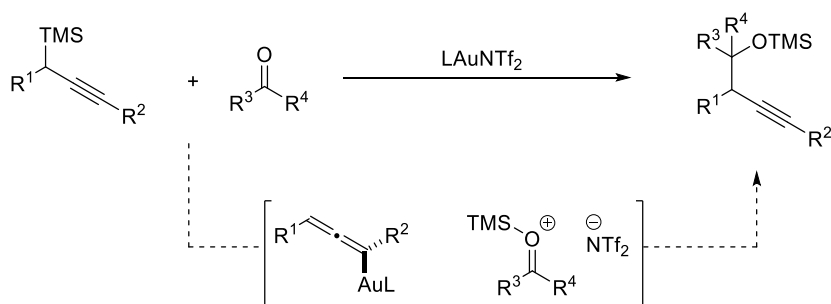
Chapter I:

Gold-catalyzed propargylation of carbonyl compounds.

Isolation of a σ -allenylgold(I) complex.

1 Introduction

This chapter summarizes the results obtained in the first gold(I)-catalyzed propargylation of carbonyl compounds starting from propargylsilanes. The mentioned transformation allows propargylation of the carbonyl group under mild conditions and with excellent yields. The reaction mechanism was studied and involves the formation of a σ -allenylgold(I) intermediate and the synergistic activation of the carbonyl group by trimethylsilylbistriflimide, the Lewis acid generated during the process (Scheme 1.1).



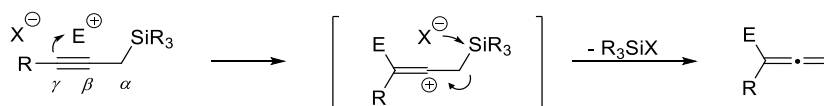
Scheme 1.1: Propargylation of carbonyl compounds *via* gold(I) catalysis.

It is worth to mention that the σ -allenylgold intermediate was isolated and fully characterized by NMR techniques. In addition, its mechanistical role was also proved, becoming the first catalytically relevant σ -allenylgold(I) complex confirmed in the literature.

2 Bibliographic background

2.1 General reactivity of propargylsilanes

As stated in the General background, silicon atom and C-Si bond properties make organosilicon reagents more predictable in terms of regioselectivity than other organometallic analogues. In this vein, the nucleophilic character of propargylsilanes.¹ As illustrated in Scheme 1.2, propargylsilanes usually react as nucleophiles through the C γ , regioselectively incorporating an allenyl moiety to the electrophile. This reaction proceeds through a carbocationic intermediate, and the later evolution of this species depends on the properties of the silyl moiety.



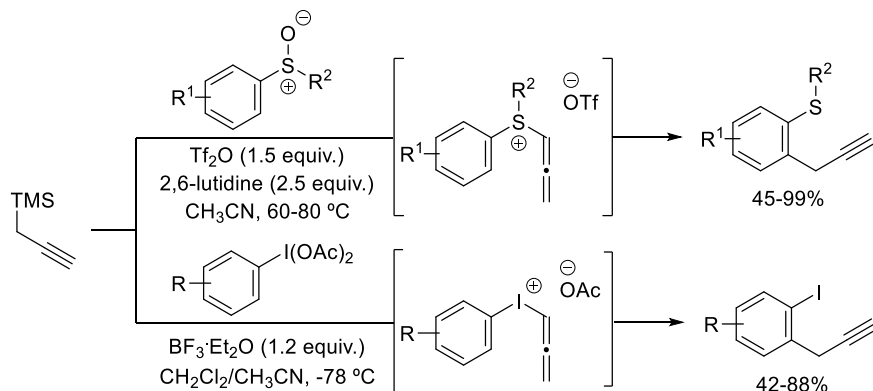
Scheme 1.2: Common mechanism for a propargylsilane nucleophilic attack.

As representative examples of this type of reactivity, in Scheme 1.3 two transformations described by Procter and Shafir are represented.² Both processes consist in directed *ortho*-propargylation of arylsulfoxides and aryliodanes, respectively. Activation of the sulfoxide or iodane leads to very electrophilic S(IV)

¹ Curtis-Long, M.; Aye, Y. *Chem. Eur. J.* **2009**, *15*, 5402-5416.

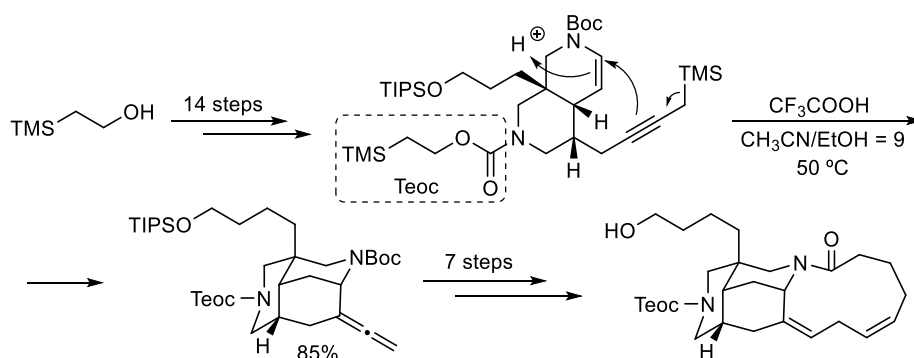
² a) Eberhart, A. J.; Shrivs, H. J.; Álvarez, E.; Carrèr, A.; Zhang, Y.; Procter, D. J. *Chem. Eur. J.* **2015**, *21*, 7428-7434; b) Izquierdo, S.; Bouvet, S.; Wu, Y.; Molina, S.; Shafir, A. *Chem. Eur. J.* **2018**, *24*, 15517-15521.

and I(III) species, furnishing allenyl intermediates upon propargylsilane nucleophilic attack. Further evolution through an electrocyclic rearrangement, similar to a classical Claisen one, generates the final products.



Scheme 1.3: *Ortho*-propargylation of arylsulfoxides and iodanes with propargylsilanes.

In addition, the high stability of propargylsilane, has made them useful in total synthesis.³ Scheme 1.4 shows their participation in the total synthesis of Madangamine derivatives, an interesting family of pentacyclic alkaloids with cytotoxicity against some human cancer cell lines.⁴ An acid-promoted cyclization of a propargylsilane emerged as one of the key steps for this methodology.



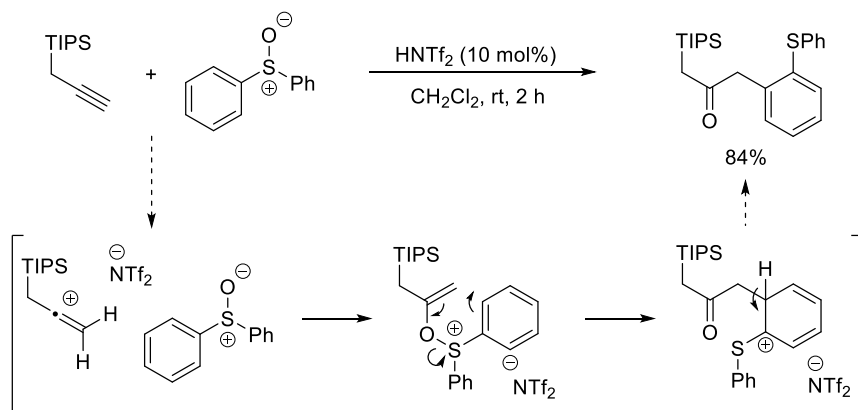
Scheme 1.4: Synthesis of a precursor in the total synthesis of Madangamines.

³ a) Langkopf, E.; Schinzer, D. *Chem. Rev.* **1995**, *95*, 1375-1408; b) Schinzer, D.; Ringe, K.; Jones, P. G.; Döring, D. *Tetrahedron Lett.* **1995**, *36*, 4051-4054.

⁴ Takahiro, S.; Yanagita, Y.; Nagashima, Y.; Takikawa, S.; Kurosu, Y.; Matsuo, N.; Miura, K.; Simizu, S.; Sato, T.; Chida, N. *Bull. Chem. Soc. Jpn.* **2019**, *92*, 545-571.

However, further studies in the chemistry of propargylsilanes show two different possible evolutions that do not imply the loss of the silyl moiety: an intra- or intermolecular trapping by a nucleophile of the carbocation intermediate, or a [1,2]-silyl migration.

A very recent example of a transformation involving an intermolecular trapping of the β -silylvinyl cation is the triflimide-catalyzed synthesis of α -silyl ketones starting from propargylsilanes and sulfoxides developed by Maulide.⁵ For this reaction, the acid catalyst activate the propargylsilane instead of the sulfoxide, in an opposite way to the previously mentioned example (Scheme 1.3).^{2a} Thus, the oxygen atom of the sulfoxide reacts with the β -silyl-stabilized carbocation, generating a highly reactive intermediate that undergoes a rearrangement to give the final ketone (Scheme 1.5).



Scheme 1.5: Synthesis of α -silyl- α -arylketones from propargylsilanes and sulfoxides.

As mentioned above, a different type of evolution of the cationic intermediate involves a non-vertical stabilization of the vinyl carbocation through [1,2]-silyl migration. Miginiac *et al.*⁶ described this process early in the 1980s, and other representative examples were recently developed by Turks.⁷ Interestingly, Ferreira

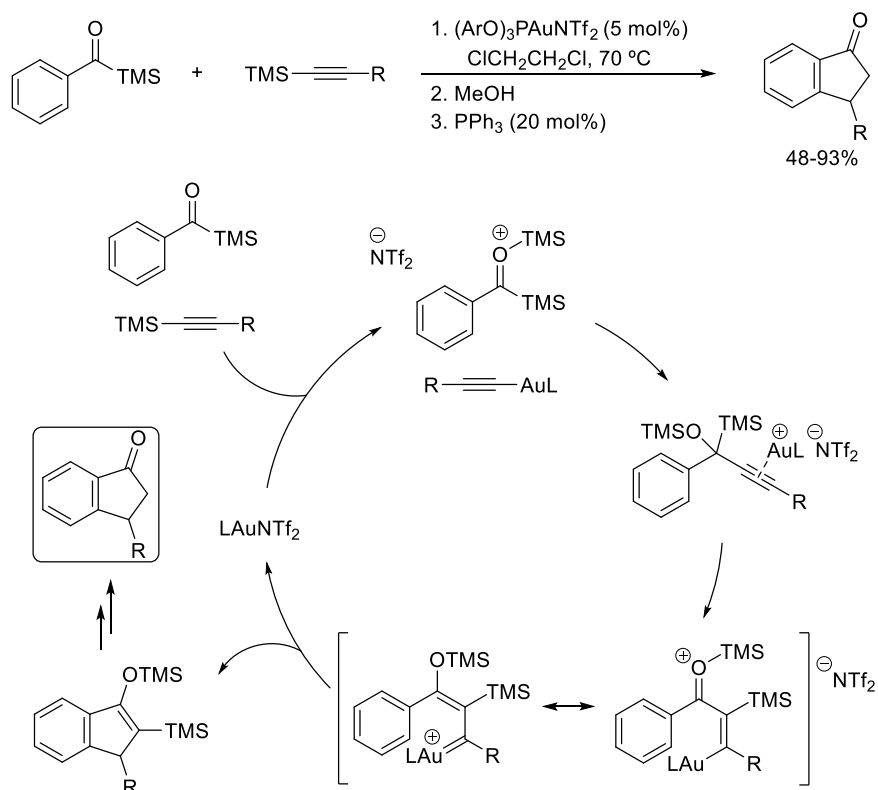
⁵ Pons, A.; Michalland, J.; Zawodny, W.; Chen, Y.; Tona, V.; Maulide, N. *Angew. Chem. Int. Ed.* **2019**, *58*, 17303-17306.

⁶ Pernet, J.; Mesnard, D.; Miginiac, L. *Tetrahedron Lett.* **1982**, *23*, 4083-4086.

⁷ a) Puriņš, M.; Mishnev, A.; Turks, M. *J. Org. Chem.* **2019**, *84*, 3595-3611; b) Beļunieks, R.; Puriņš, M.; Kumpiņš, V.; Turks, M. *Chemistry of Heterocyclic Compounds* **2021**, *57*, 20-25.

and co-workers reported that this [1,2]-silyl migration can be also assisted by a vicinal heteroatom.⁸

In this sense, our research group also contributed to enrich this kind of transformations by describing a gold(I)-catalyzed synthesis of indanones through the reaction of alkynyl- and acylsilanes (Scheme 1.6).⁹ In this case, σ -activation of the trimethylsilylalkyne generates a gold(I) acetylide (see *General background*) while synergically activating the acylsilane. Upon addition of the acetylide, a propargylsilane intermediate is formed. Subsequently, π -activation of the C-C triple bond promotes a [1,2]-silyl migration assisted by the trimethylsilyloxy group. This process gives rise to a γ -alkoxy and β -silyl stabilized gold(I) vinylcarbene, which evolves by C-H activation of the arene ring to yield an indene derivative.

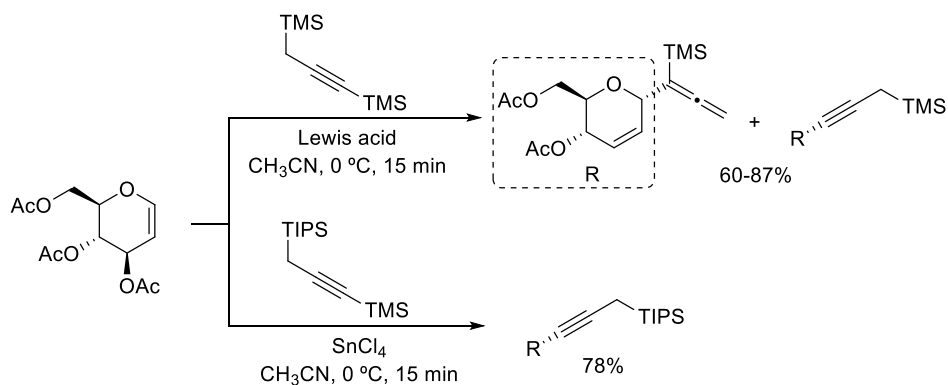


Scheme 1.6: Gold(I)-catalyzed coupling of alkynyl- and acylsilanes.

⁸ Rooke, D. A.; Ferreira, E. M. *J. Am. Chem. Soc.* **2010**, *132*, 11926-11928.

⁹ González, J.; Santamaría, J.; Ballesteros, A. *Angew. Chem. Int. Ed.* **2015**, *54*, 13678-13681.

A special family of propargylsilanes, the 1,3-bisilylated propyne derivatives, have also attracted attention during the past decades. Due to the combined properties of alkynyl- and propargylsilanes, they are even more nucleophilic, but the reactivity depends on the nature of both silyl moieties. As a representative example of this behaviour, Isobe and co-workers described the Lewis acid catalyzed reaction between these nucleophiles and glucals to obtain mixtures of allenic and acetylenic products (Scheme 1.7).¹⁰ As shown, with similar silyl groups, the reactivity depends on the Lewis acid employed. However, if the propargylsilane moiety is bulkier and more stable than the other one, alkynylsilane prevails as the main reactive group leading to alkynylated products regioselectively. A similar behaviour has been later described by the same group.¹¹



Scheme 1.7: Allenylation/alkynylation of glucals employing 1,3-bisilylated propynes.

2.2 Coupling reactions between propargylsilanes and carbonyl compounds

The most exploited and historically developed reaction of propargylsilanes has been their coupling with carbonylic compounds to yield allenic alcohols.¹² As it was explained before, these transformations occur regioselectively through the γ -

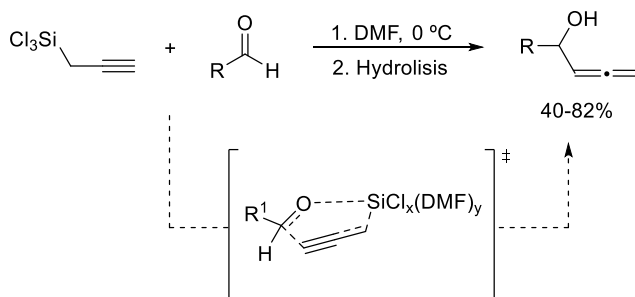
¹⁰ a) Isobe, M.; Phoosaha, W.; Saeeng, R.; Kira, K.; Yenjai, C. *Org. Lett.* **2003**, *25*, 4883-4885;
b) Huang, G.; Isobe, M. *Tetrahedron*, **2001**, *57*, 10241-10246.

¹¹ Saeeng, R.; Sirion, U.; Sahakitpichan, P.; Isobe, M. *Tetrahedron Lett.* **2003**, *44*, 6211-6215.

¹² Hashmi, A. S. K. *Modern Allene Chemistry*, **2004**, *1*, 2-3.

carbon of the C-C triple bond respect to the silicon atom. Due to the commonly low reactivity of this moiety, these reactions usually require activation of the propargylsilane by a Lewis base or activation of the carbonyl compound by a Lewis acid. A wide range of examples have been reported including the participation of transition metal complexes among the last ones.

Starting with base-promoted allenylations, they usually occur through formation of an hypervalent silicon intermediate. As explained in the *General background*, the higher the coordination number of the silicon centre, the higher the nucleophilicity of the carbonated chain. In this regard, DMF-promoted coupling between aldehydes and propargyl(trichloro)silanes, to generate allenylalcohols, is an interesting example of this type of processes (Scheme 1.8).¹³ Mechanistically, the formation of silicon hypervalent species is proposed after DMF coordination to the propargylsilane. This highly reactive intermediate could interact with the aldehyde through a six-centered transition state to generate the corresponding product. The asymmetric version of this transformation has been also carried out, either starting from enantiopure propargyl(trichloro)silanes¹⁴ or using optically active Lewis bases.¹⁵



Scheme 1.8: Propargylsilane-aldehyde coupling, promoted by DMF.

On the other hand, Lewis acid catalyzed reactions of propargylsilanes with carbonyls and their derivatives came out to the bibliography during the 1980s,

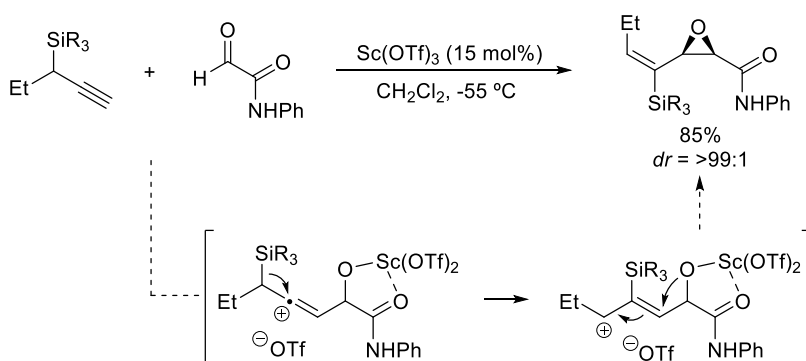
¹³ Schneider, U.; Sugiura, M; Kobayashi, S. *Tetrahedron*, **2006**, 62, 496-502.

¹⁴ Marshall, J. A.; Adams, N. D. *J. Org. Chem.* **1997**, 62, 8976-8977.

¹⁵ Nakajima, M.; Saito, M; Hashimoto, S. *Tetrahedron Asymmetry* **2002**, 13, 2449-2452.

closely related to the Hosomi-Sakurai work on allyl- and allenylsilanes.¹⁶ Most of these transformations proceed through a similar mechanism as the previously described furnishing allenylalcohols, but the carbonyl group is the activated counterpart to increase its electrophilicity. In addition to some non-metallic Lewis acid catalyzed processes,¹⁷ a lot of other examples with representative metals, such as Al(III)¹⁸ or Sn(IV),¹⁹ and mainly transition metals have been described. Although TiCl₄ has been the most employed one,²⁰ some works using Sc(III)²¹ and Zn(II)^{17a} can be found in the literature, usually in stoichiometric amounts.

As shown in the previous section, propargylsilanes can also evolve without releasing the silyl moiety, by trapping the carbocationic intermediate or through [1,2]-silyl migration processes. Regarding the second possibility, a work that deserves to be highlighted was carried out by Evans (Scheme 1.9).²² Thus, using scandium(III) triflate as catalyst, addition of propargylsilane is followed by a [1,2]-silyl migration and, in contrast to the previous example, the resulting carbocation is trapped furnishing highly functionalized epoxides.



Scheme 1.9: Synthesis of epoxides catalyzed by Sc(OTf)₃.

¹⁶ Hosomi, A.; Sakurai, H. *Tetrahedron Lett.* **1976**, *17*, 1295-1298.

¹⁷ a) Schmitt, A.; Reissig, H. *Eur. J. Org. Chem.* **2000**, *23*, 3893-3901; b) Schinzer, D.; Kabbara, J.; Ringe, K. *Tetrahedron Lett.* **1992**, *33*, 8017-8018.

¹⁸ Schinzer, D.; Sttfein, J.; Solyom, S. *J. Chem. Soc., Chem. Commun.* **1986**, *154*, 829-830.

¹⁹ Thebtaranonth, C.; Thebtaranonth, Y. *Tetrahedron* **1990**, *46*, 1385-1489.

²⁰ Schinzer, D.; Dettmer, G.; Ruppelt, M.; Solyom, S.; Steffen, J. *J. Org. Chem.* **1988**, *53*, 3823-3828.

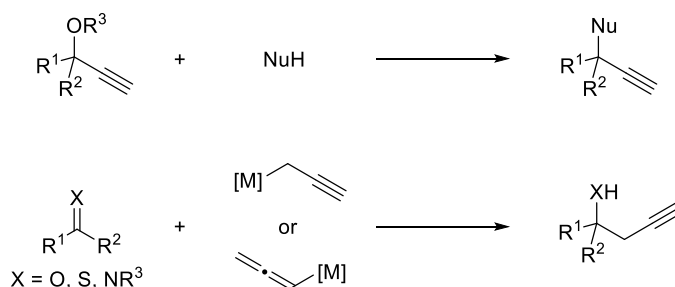
²¹ Clive, D. L. J.; He, X.; Postema, M. H. D.; Mashimbye, M. J. *J. Org. Chem.* **1999**, *64*, 4397-4410.

²² Evans, D. A.; Aye, Y. *J. Am. Chem. Soc.* **2007**, *129*, 9606-9607.

2.3 Propargylation reactions of carbonyl compounds

Transformations that introduce a propargyl group in a molecule are considered as very valuable tools in organic synthesis. Among them, propargylation reactions forming carbon-carbon single bonds have been studied since decades ago due to their usually mild conditions, functional group tolerance and high synthetic potential of the products they afford.²³

It is well established a rough classification depending on the electrophilic or nucleophilic character of the propargyl synthon. The first ones usually employ direct nucleophilic substitution of propargyl alcohols or their derivatives (Scheme 1.10, *top*), while the second consist in the addition of σ -allenyl or σ -propargyl metal complexes to carbonyl compounds (Scheme 1.10, *bottom*).



Scheme 1.10: Types of C-C bond-forming propargylations.

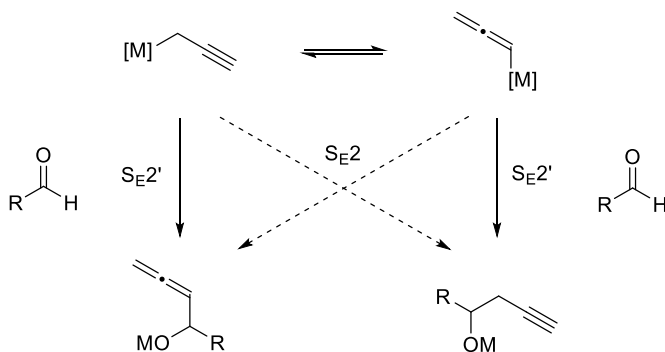
The reaction of σ -allenyl or σ -propargyl metal complexes with carbonyl derivatives or nitro-olefins yields homopropargylic alcohols, amines, amides, sulfides or nitro compounds. Due to the topic of this dissertation, some examples of this type of reactivity will be discussed.

Probably the first described example of this type of transformations was the employment of allenyl Grignard reagents in 1950 by Prévost *et al.*,²⁴ although this powerful tool still attracts nowadays attention in organic synthesis. Regioselectivity in these transformations is usually a common problem, due to the in-situ isomerization between allenic and propargylic organometallic reagents. Some other factors, such as the nature of the metallic centre, the steric hindrance and

²³ Chang-Hua, D.; Xue-Long, H. *Chem. Rev.* **2011**, *111*, 1914-1937.

²⁴ Prévost, C.; Gaudemar, M.; Honigberg, J. C. R. *Hebd. Seances Acad. Sci.* **1950**, *230*, 1186-1188.

the electrophile nature have proved to be also important for the process. For carbonyl derivatives, many experimental and computational studies prove that these intermediates react through S_E2' pathways giving mixtures of alcohols,²⁵ although a S_E2 is proposed for other transformations (Scheme 1.11).²⁶



Scheme 1.11: Different addition mechanisms for allenyl/propargylmetals.

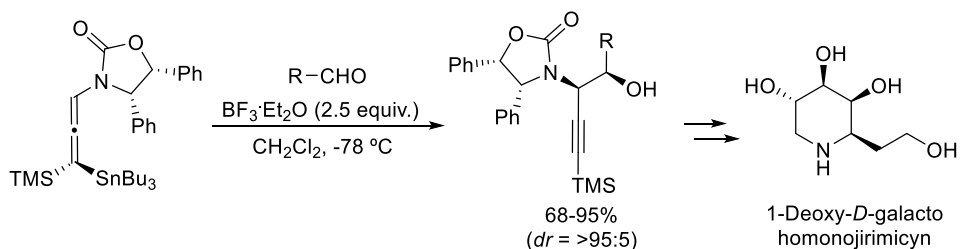
A very common way to overcome this problem consists in the use of preformed σ -allenylmetal reagents that do not isomerize or, as an alternative, selectively in situ generate them from an adequate propargyl moiety, tuning the electronic properties of the precursor and the metal.

Several examples have been reported employing stable allenylstannanes, boranes or silanes in combination with stoichiometric or catalytic amounts of Lewis acids.²³ As an example of this, Scheme 1.12 shows a key step in the synthesis of an azasugar.²⁷ The enantiomerically pure starting material contains allenamide, allenylstannane and allenylsilane moieties. Although allenamide should attack through the central carbon of the allene, β -silicon effect and carbon-tin bond dissociation are able to drive the reaction outcome. Thus, after activation of the aldehyde, a nucleophilic attack of the allene occurs from the α position of the amide, which allows further *syn/anti* selectivity in the transition state.

²⁵ For further information, see: Marshall, J., Gung, B. and Grachan, M. *Synthesis and Reactions of Allenylmetal Compounds*. **2021**.

²⁶ Yanagisawa, A.; Suzuki, T.; Koide, T.; Okitsu, S.; Arai, T. *Chem. Asian J.* **2008**, *3*, 1793-1800.

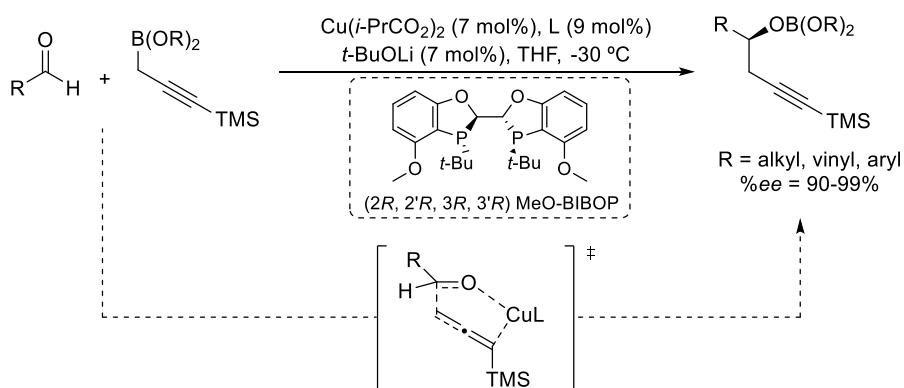
²⁷ Achmatowicz, M.; S. Hegedus, L. S. *J. Org. Chem.* **2004**, *69*, 2229-2234.



Scheme 1.12: Selective synthesis of azasugars employing allenyltin propargylation.

Propargyl halides and propargylboranes are usually starting materials for these processes, and their activation through oxidative addition, in the case of halides, or base-assisted carbophilic activation, in the case of boranes, leads to *in situ* formation of organometallic allenyl complexes. As this second type of activation is closely related with the results described in the present *Chapter 1*, an example is given below.

In Scheme 1.13 a propargylation process of carbonyls with propargylboronic esters is represented.²⁸ First, activation of the boronic esters in the presence of copper alkoxide takes place, generating an allenylcopper(I) complex. The α -silicon effect stabilizes the intermediate with the carbon-copper bond in that position, preventing allenyl-propargyl isomerization. Then, the addition of the organocopper intermediate to the aldehyde gives rise to the final product.



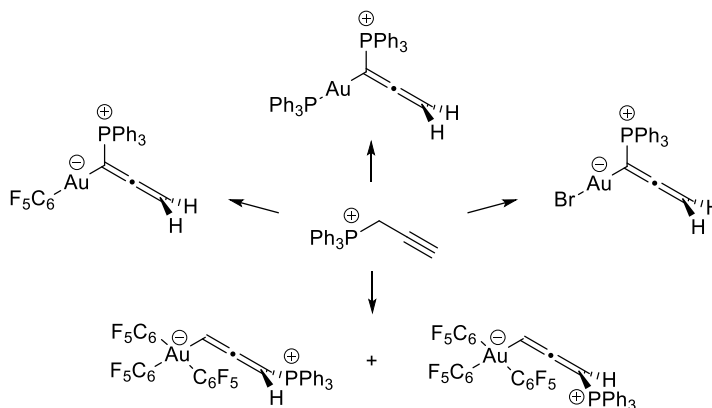
Scheme 1.13: Copper(I)-catalyzed propargylation of carbonyls with propargylboronates.

²⁸ Fandrick, D. R.; Fandrick, K. R.; T. Reeves, J. T.; Tan, Z.; Tang, W.; Capacci, A. G.; Rodríguez, S.; Song, J. J.; Lee, H.; Yee, N. K.; Senanayake, C. H. *J. Am. Chem. Soc.* **2010**, *132*, 7600-7601.

2.4 σ -Allenylgold complexes in homogeneous gold catalysis

As stated in the *General background*, gold(I) and gold(III) complexes have proved to be useful catalysts promoting a wide range of different organic transformations. Regarding to this, a lot of organogold intermediates have been proposed to support mechanisms insights, but their isolation and characterization is still now a challenging topic.

In this sense, although several σ -allenyl-transition-metal complexes have been isolated and studied,²⁹ σ -allenylgold complexes were firstly described only few years ago.³⁰ Starting from propargyltriphenylphosphonium salts, Gimeno and coworkers were able to obtain the allenyl species, by addition of a suitable gold(I) or gold(III) precursor, under basic conditions (Scheme 1.14).

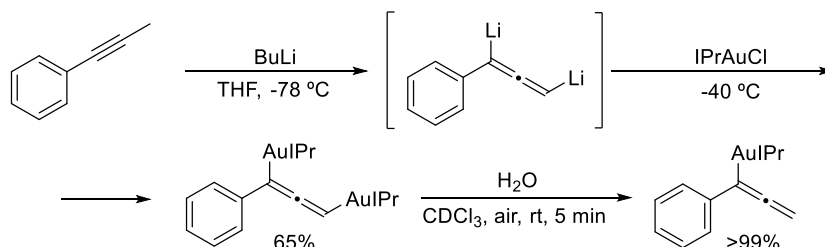


Scheme 1.14: Reported σ -gold(I) and gold(III) allenyl complexes.

²⁹ For selected examples of other isolated σ -allenyl transition metal complexes, see: a) Goodfellow, R. J.; Green, M.; Mayne, N.; Rest, A. J.; Stone, F. G. A. *J. Chem. Soc. A* **1968**, 177-180; b) Johnson, M. D.; Mayle, C. *J. Chem. Soc. D*, **1969**, 192-192; c) Matsuzaka, H.; Koizumi, H.; Takagi, Y.; Nishio, M.; Hidai, M. *J. Am. Chem. Soc.* **1993**, *115*, 10396-10397; d) Wouters, J. M. A.; Klein, R. A.; Elsevier, C. J.; Haming, L.; Stam, C. H. *Organometallics* **1994**, *13*, 4586-4593; e) Werner, H.; Fluegel, R.; Windmueller, B.; Michenfelder, A.; Wolf, J. *Organometallics* **1995**, *14*, 612-618; f) Barluenga, J.; Trabanco, A. A.; Flórez, J.; García-Granda, S.; Llorca, M.-A. *J. Am. Chem. Soc.* **1998**, *120*, 12129-12130; g) Werner, H.; Wiedemann, R.; Laubender, M.; Windmüller, B.; Steinert, P.; Gevert, O.; Wolf, J. *J. Am. Chem. Soc.* **2002**, *124*, 6966-6980; h) Hughes, R. P.; Larichev, R. B.; Zakharov, L. N.; Rheingold, A. L. *Organometallics* **2006**, *25*, 3943-3947; i) Zhang, S.; Zhang, W.-X.; Zhao, J.; Xi, Z. *J. Am. Chem. Soc.* **2010**, *132*, 14042-14045; j) Santiago, A.; Gómez-Gallego, M.; de Arellano, C. R.; Sierra, M. A. *Chem. Commun.* **2013**, *49*, 1112-1114.

³⁰ Johnson, A.; Laguna, A.; Gimeno, M. C. *J. Am. Chem. Soc.* **2014**, *136*, 12812-12815.

A few years later, Hashmi's research group also managed to obtain a dinuclear NHC-gold(I) allenyl complex starting from bis organolithium reagents.³¹ The behaviour of this organometallic species against protonation led to the formation of a mononuclear allenyl derivative, as it can be seen in Scheme 1.15. Both species, mono- and dinuclear, were isolated and fully characterized by NMR techniques, representing the only reported examples after the previously mentioned work. However, in both cases, their reactivity against other electrophiles remained unexplored.



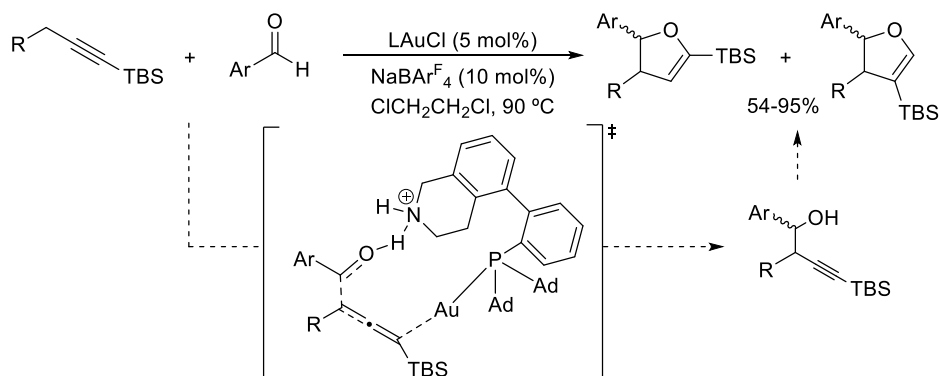
Scheme 1.15: Synthesis and protonation of σ -dinuclear gold(I)-allen-1,3-diyli complex.

In this regard, Professor Zhang's group proposed, for the first time, the participation of a σ -allenylgold(I) complex in the isomerization of terminal alkynes to 1,3-dienes, although intermolecular reactivity for this organogold complex remained locked.³² Nevertheless, working on the ligand design for this process, they were finally able to achieve an intermolecular reaction for the mentioned organogold complex: the first gold(I)-catalyzed propargylation and cycloisomerization of aromatic aldehydes with silyl-protected alkynes, yielding a mixture of 2- and 3-silyl-4,5-dihydrofurans (Scheme 1.16).³³ Although they could not isolate the proposed allenylmetal, several computational studies suggest the participation of this intermediate.

³¹ Zargaran, P.; Mulks, F. F.; Rudolph, M.; Rominger, F.; Hashmi, A. S. K. *Organometallics* **2019**, *38*, 1524-1533.

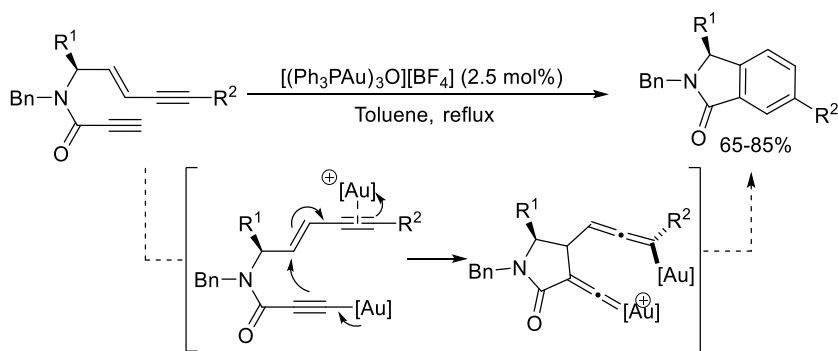
³² Wang, Z.; Wang, Y.; Zhang, L. *J. Am. Chem. Soc.* **2014**, *136*, 8887-8890.

³³ Li, T.; Zhang, L. *J. Am. Chem. Soc.* **2018**, *140*, 17439-17443.



Scheme 1.16: First reported gold(I)-catalyzed propargylation of aromatic aldehydes.

Finally, another interesting example of gold catalysis evoking the participation of a σ -allenylgold(I) intermediate has been reported very recently by Hyland and co-workers.³⁴ In this case, the key intermediate would consist in a dinuclear gold(I) vinylidene and allenyl complex (Scheme 1.17). However, this intermediate would be too reactive to be isolated, experimenting an intramolecular cycloisomerization reaction to furnish the final product.



Scheme 1.17: Dual gold(I)-catalyzed cycloaromatization of non-conjugated *E*-enediynes.

Taking all this into account, it is necessary to remark that σ -allenylgold(I) complexes remain underexplored as key intermediates in gold catalysis, because their catalytical role in different transformations could not be unambiguously proved and the reactivity for the isolated complexes was not studied.

³⁴ Zamani, F.; Babaahmadi, R.; F. Yates, B. F.; G. Gardiner, M. G.; Ariafard, A.; Pyne, S. G.; Hyland, C. J. T. *Angew. Chem. Int. Ed.* **2019**, *58*, 2114-2119.

3 Results and discussion

Regarding the results previously obtained in our research group in gold catalysis with silylalkynes, which involved either σ -activation of an alkynyltrimethylsilane³⁵ or σ and π -activation of an α -trimethylsilyloxy propargylsilane,^{35b} we decided to study the reactivity of bis-silylated systems towards electrophiles under gold catalysis. In that sense, 1,3-bis(trimethylsilyl)-3-phenyl-1-propyne **1.1a** was chosen as model substrate (Figure 1.1).

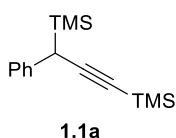
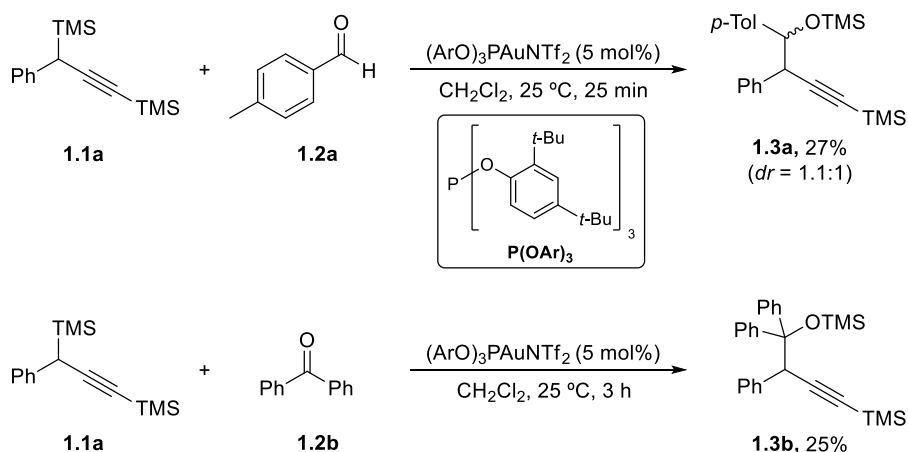


Figure 1.1: Model propargylsilane **1.1a**.

Initially we carried out the reaction of model substrate **1.1a** with *p*-tolualdehyde **1.2a** in the presence of a 5 mol% of a phosphite gold(I) catalyst, (ArO)₃PAuNTf₂, employing dichloromethane as solvent. After 25 min of reaction, at room temperature, homopropargyl silyl ether **1.3a** was isolated in a 27% yield from the reaction mixture and as a 1.1:1 mixture of diastereoisomers (Scheme 1.18, top). Additionally, to find out if ketones were also suitable electrophiles, the reaction

³⁵ a) Rubial, B.; A. Ballesteros, A.; González, J. M. *Adv. Synth. Catal.* **2013**, *355*, 3337-3343; b) González, J.; Santamaría, J.; Ballesteros, A. *Angew. Chem. Int. Ed.* **2015**, *54*, 13678-13681.

was also carried out under similar reaction conditions using benzophenone **1.2b** as electrophile. After 3 hours, compound **1.3b** was isolated in a 25% yield (Scheme 1.18, bottom).



Scheme 1.18: Gold-catalyzed propargylation of *p*-tolualdehyde and benzophenone.

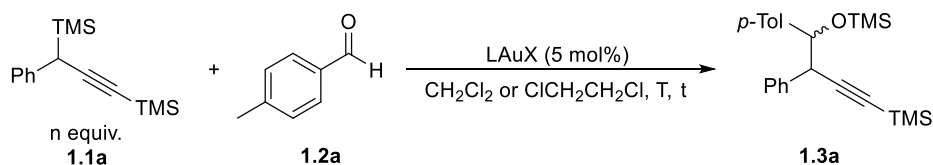
Both compounds were characterized by several NMR techniques and their structure was doubtlessly determined by an X-ray diffraction experiment on a single monocrystal obtained from a dichloromethane:methanol solution of compound **1.3b** (Figure 1.2).



Figure 1.2: Structure of homopropargyl silyl ether **1.3b**

The described results represent an insertion of the carbon-oxygen bond of the carbonyl compound into the carbon-silicon bond of the propargylsilane, through a propargylation process. On the other hand, regarding that gold-catalyzed propargylation was underexplored, since a single example has been described in the literature, we decided to focus our efforts on exploring this reaction.

In order to optimize the yield of the formation of homopropargyl silyl ethers **1.3**, several reaction conditions (temperature, stoichiometry, gold catalyst and reaction time) were analyzed and the results are described in Scheme 1.19.



Entry	LAuX	Equiv.	T	t	%Yield ^[a]	dr
1	(ArO) ₃ PAuNTf ₂	1	25 °C	20 min	27	1.1:1
2	(ArO) ₃ PAuNTf ₂	3	25 °C	20 min	80*	1.1:1
3	IPrAuNTf ₂	3	25 °C	20 min	42	1.1:1
4	JohnPhosAuNTf ₂	3	25 °C	20 min	20	1.1:1
5	PicAuCl ₂	3	25 °C	20 min	NR	-
6	Ph ₃ PAuCl/AgNTf ₂	3	25 °C	20 min	68	1.1:1
7	Ph ₃ PAuNTf ₂	3	25 °C	20 min	64	1.1:1
8	AgNTf ₂	3	25 °C	20 min	NR	-
9	(ArO) ₃ PAuNTf ₂	3	40 °C	20 min	61	1.1:1
10	(ArO) ₃ PAuNTf ₂	3	-40 °C	1 h	77	1.1:1

^[a]Determined by ¹H-NMR using dibromomethane as internal standard. *Isolated yield.

Scheme 1.19: Screening of the reaction conditions.

From the screening reported in Scheme 1.19 it can be inferred that employing equimolecular quantities of both reagents resulted in the formation of only a 25% of the desired product (*Entry 1*) with formation of allenylsilane **1.4**, alkyne **1.5** and alkynylsilane **1.6a** in a roughly 75% yield jointly, probably due to the decomposition of the starting propargylsilane **1.1a** (Figure 1.3). Also, a reaction blank was performed yielding quantitatively both by-products. It was possible to overcome this problem using three equivalents of propargylsilane **1.1a**, coming up to an 80% isolated yield of homopropargyl silyl ether (*Entry 2*).

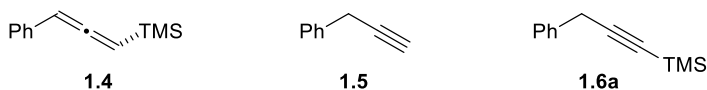
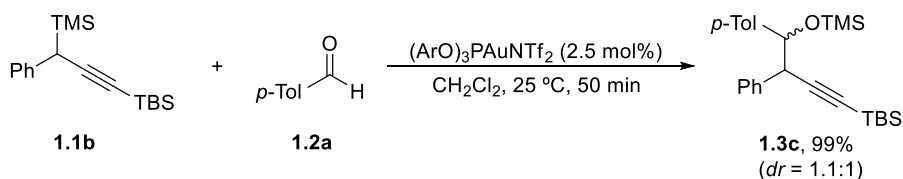


Figure 1.3: By-products identified in the studied reaction.

The effect of the gold catalyst ligands was also studied, using conventional gold(I) and gold(III) complexes which cover, in a representative way, different terms of electronic and steric hindrance properties (*Entries 3-7*). Notably, the diastereoisomeric ratio remained unchanged in all the cases, when the formation of **1.3a** was observed. Therefore, the initially chosen gold(I) phosphite complex proved to give the best result. The use of a silver salt in the absence of a gold complex led to no conversion of the starting materials (*Entry 8*). Finally, it is remarkable that reaction takes place even at $-40\text{ }^{\circ}\text{C}$ in one hour with almost the same performance (*Entry 9*). However, at $40\text{ }^{\circ}\text{C}$ the formation of unidentified by-products diminishes the yield of the desired product (*Entry 10*), so we decided to adopt $25\text{ }^{\circ}\text{C}$ as the optimal temperature for the reaction.

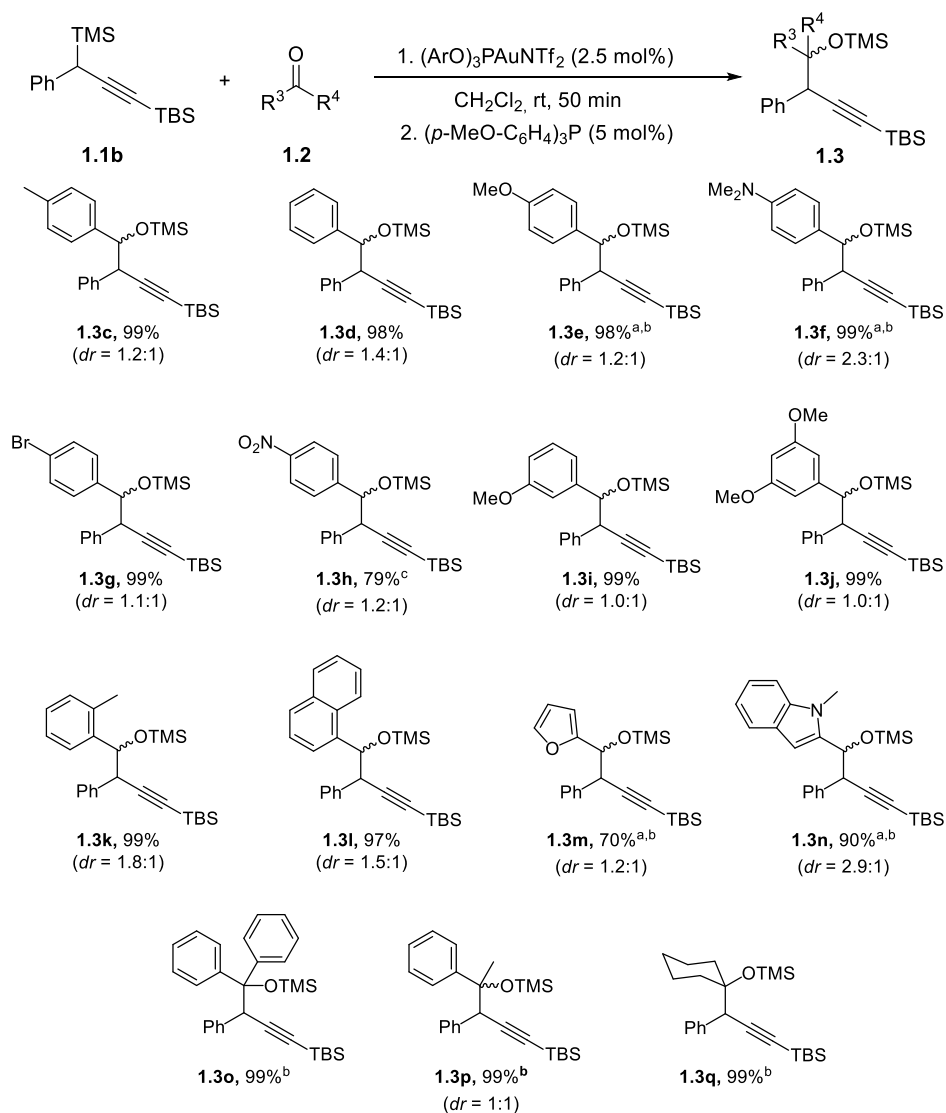
Moreover, the replacement of the trimethylsilyl group of the acetylenic position by a *tert*-butyldimethylsilyl one improves the reaction performance, probably due to the higher stability of the starting material and the final products. In this vein, it was possible to employ an almost equimolecular quantity of **1.1b** (1.2 equivalents), lowering catalyst loading to 2.5 mol% and obtaining the silyloxy compound **1.3c** in quantitative yield, as a 1.1:1 mixture of diastereoisomers (Scheme 1.20). A new ligand screening was also performed under these conditions and, once again, $(\text{ArO})_3\text{PAuNTf}_2$ complex resulted to be the best choice (see *Experimental Section*).



Scheme 1.20: Synthesis of homopropargyl silyl ether **1.3c**.

Once a protocol with the optimal reaction conditions was established, the effects of the substituents in the carbonyl reagent were studied, using **1.1b** as model propargylsilane (Scheme 1.21). In the course of this study, it was also found that the addition of a phosphine at the end of the reaction avoids further undesired

transformations by deactivating the gold catalyst, so we decided to add a 5 mol% of tris-(*p*-methoxyphenyl)phosphine for that purpose.



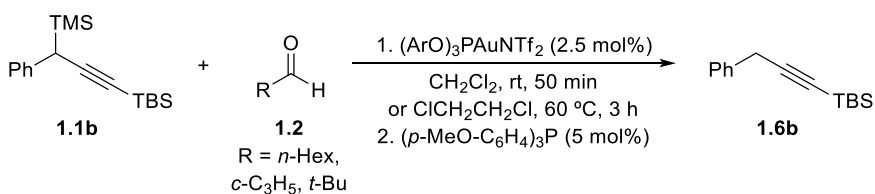
^aReaction performed at -20 °C; ^b3 h of reaction; ^c5 mol% of gold(I) catalyst.

Scheme 1.21: Scope of the reaction in terms of carbonyl compound **1.2**.

As it can be observed, the propargylation reaction takes place satisfactorily for aromatic aldehydes (**1.3c-n**), and both aromatic and aliphatic ketones (**1.3o-q**). The reaction also tolerates a wide range in terms of substitution pattern of the aromatic ring of carbonyl compound **1.2**, ranging from electron-donating (**1.3c,e-f,i-**

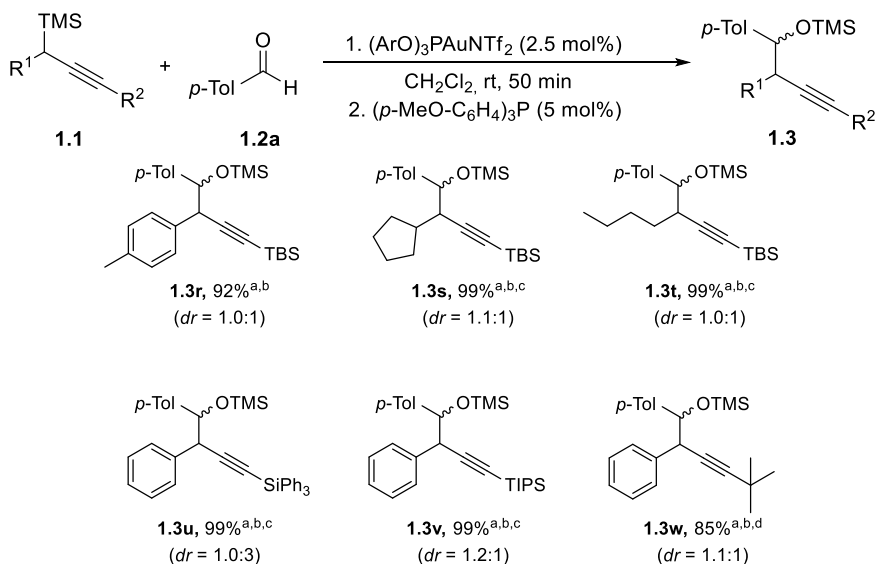
k) and electron-withdrawing groups (**1.3g-h**) to heterocyclic derived aldehydes (**1.3m-n**). Additionally, *ortho*-substituted benzaldehydes performed the reaction perfectly, furnishing homopropargyl silyl ethers **1.3k-l**. Excellent yields were observed in all the cases with no significative dependence on the reaction time among aldehydes and among ketones.

Aliphatic aldehydes like hexanal, cyclopropylcarbaldehyde and pivaldehyde were also tested, but only desilylation of the starting material was observed (Scheme 1.22). In the first two cases, this could happen because of the presence of acidic protons in alpha position to the activated carbonyl group. However, no aldolic condensation products were observed in any case. For pivaldehyde, probably the high steric demand of the *tert*-butyl group prevents the reaction, so the propargylsilane undergoes slowly protodesilylation.



Scheme 1.22: Tested aliphatic aldehydes.

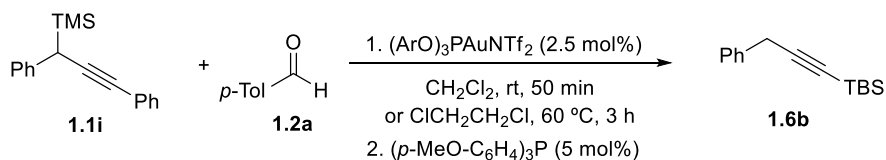
From the point of view of propargylsilanes **1.1**, certain degree of variability could be also employed in their gold-catalyzed propargylation reactions toward *p*-tolualdehyde **1.2a** (Scheme 1.23). In this sense, the *p*-tolyl derivative worked in a similar way to the model substrate (**1.3r**). On the other hand, aliphatic propargylsilanes gave similar results although they required higher catalyst loadings and longer reaction times (**1.3s-t**). Additionally, propargylsilane bearing bulkier silyl groups like triisopropylsilyl (TIPS) or triphenylsilyl worked surprisingly well in the formation of propargylsilyl ethers, as compounds **1.3u** and **1.3v** could be obtained after 16 h of reaction in almost quantitative yield. Finally, in an effort to determine if a silyl moiety in the acetylenic position is required or not, the reaction was performed with a *tert*-butyl derivative yielding propargylation product **1.3w** in high yield.



^a3 equivalents of propargylsilane **1.1**; ^b5 mol% of catalyst; ^c16 h of reaction; ^d3 h of reaction

Scheme 1.23: Scope in terms of the propargylsilane **1.1**.

Along with the *tert*-butyl acetylene derivative, propargylation with a phenyl substituted propargylsilane was examined, but only protodesilylation process was observed, probably due to the high instability of the starting material (Scheme 1.24).

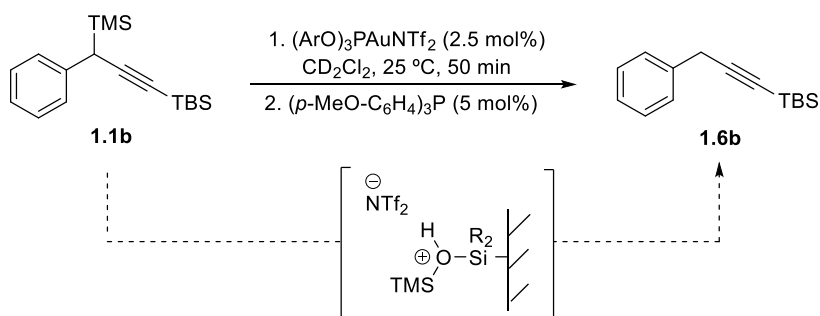


Scheme 1.24: Attempt to use a 1,3-diphenylpropargylsilane for propargylation.

Remarkably, for the last three successful examples, starting from propargylsilanes bearing bulkier silyl groups or with a *tert*-butyl group in the acetylenic position, the reaction must be carried out in a polypropylene tube, placed inside the corresponding Schlenk, to observe the formation of the homopropargyl silyl ethers **1.3u-w**. When the process is set in a simple Schlenk under argon atmosphere, protodesilylation of the starting propargylsilanes **1.1** is observed. Although the mechanistic studies will be further discussed, it is important to explain in advance that this requirement arises from the formation of

a very reactive silylium species, trimethylsilylbistriflimide (TMSNTf₂), during the transformation. Due to the high oxophilicity of these intermediates, the silanol groups of the glassware surface can be activated, releasing triflimide (HNTf₂).³⁶ Apparently, these substrates that present lower reactivity towards propargylation, only suffering protodesilylation reaction.

This hypothesis can be supported by a blank reaction of the model propargylsilane **1.1b** in the presence of the gold(I) phosphite and under the standard reaction conditions using methylene chloride-*d*₂ as solvent (Scheme 1.25). After 50 min of reaction, the alkynylsilane **1.6b** was the only observed product, even though all the reagents were carefully lyophilized and the solvent was freshly distilled under inert atmosphere. Moreover, no deuterium label was observed in the final product, indicating that the solvent is not the proton source in this protodesilylation process.

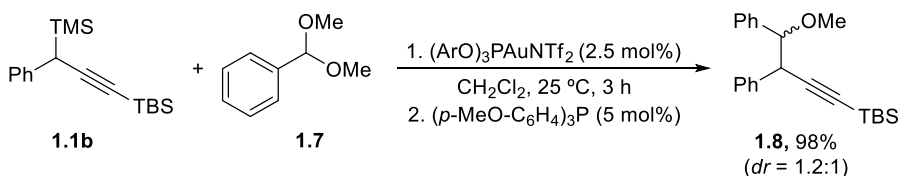


Scheme 1.25: Hypothesis about proton source in the reaction.

Once we found out the importance of avoiding glassware free silanols using a propylene tube, we repeated some of the experiments that previously failed, probably due to the lower reactivity of the starting materials. In this regard, the reactions using aliphatic aldehydes (Scheme 1.22) or a propargylsilane bearing a phenyl group at the acetylenic position (Scheme 1.24) were tested once again. The use of a polypropylene tube did not report positive results for all of them.

³⁶ Wilson, K.; Clark, J. H. *Pure Appl. Chem.* **2000**, 72, 1313–1319.

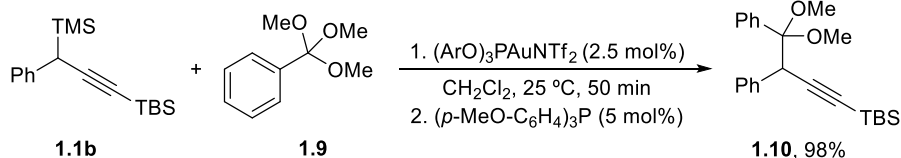
In order to broaden the scope of this transformation, we tested other related carbonyl derivatives, under the standard reaction conditions, using propargylsilane **1.1b**. As shown in Scheme 1.26, dimethylacetal of benzaldehyde **1.7** was also suitable electrophiles, generating homopropargyl methylether **1.8** in excellent yield.



Scheme 1.26: Gold-catalyzed propargylation of a benzaldehyde acetal.

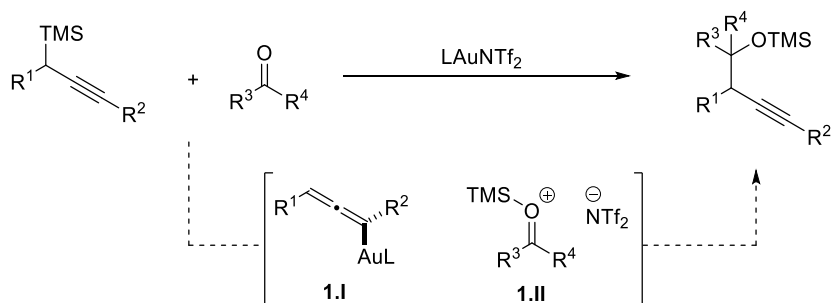
Finally, carboxyl derivatives were also tested, such as benzoyl chloride, methyl benzoate or dimethylbenzamide. Though, all of them remained unreactive even using a propylene tube or heating at 60 °C. This lack of reactivity could be attributed to two features: first, carboxyl carbocations are more stabilized than carbonyl ones; and second, the reactive carbon is more sterically demanding than the carbonylic analogues.

However, trimethyl orthobenzoate **1.9**, an ester acetal, was a suitable electrophile for this transformation (Scheme 1.27). In fact, homopropargyl dimethylacetal **1.10** was obtained in almost quantitative yield under the standard reaction conditions, and it could be isolated and characterized. This result points out that steric hindrance around the reactive carbonylic carbon of the TMSNTf₂-activated carbonyl derivative is probably the main obstacle for esters and amides to undergo propargylation.



Scheme 1.27: Synthesis of homopropargyl acetal **1.10** from an orthobenzoate.

At this point, we focused our efforts on determining the mechanism pathway for this novel transformation. Regarding the previously mentioned Zhang's gold-catalyzed propargylation reaction,³⁷ we envisioned a similar mechanistic pathway, whose key intermediates are outlined in Scheme 1.28.



Scheme 1.28: Key proposed intermediates for the gold-catalyzed propargylation.

In a similar way to Zhang's work, the activation of the propargylsilane **1.1** would generate a σ -allenylgold(I) intermediate **1.I**, although in this case is due to the abstraction of the TMS group, probably by the triflimidate anion. Moreover, the organosilicon species formed could in turn synergistically activate the carbonyl group (intermediate **1.II**), facilitating the consecutive nucleophilic attack. However, considering that very active silylium species with high oxo- and carbophilicity³⁸ are generated during the catalytic process, another possible route could involve the participation of the gold catalyst as a slow silylium generator, being the silylium cation the real promoter for this transformation. This alternative mechanism would imply the formation of allenylsilane **1.III** as intermediate, instead of σ -allenylgold(I) complex **1.I** (Figure 1.4). Then, the oxophilic activation of the carbonyl compound (intermediate **1.II**) would ease the nucleophilic attack of allenylsilane **1.III**.

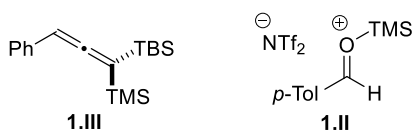


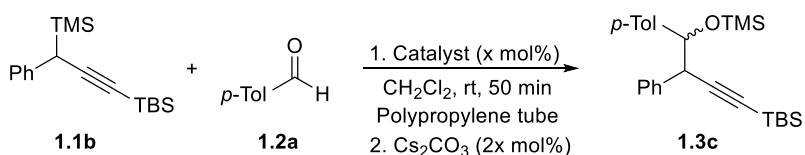
Figure 1.4: Possible key intermediates for the silylium-catalyzed propargylation.

³⁷ Li, T.; Zhang, L. *J. Am. Chem. Soc.* **2018**, *140*, 17439-17443.

³⁸ Walker, J. C. L., Klare, H. F. T.; Oestreich, M. *Nat. Rev. Chem.* **2020**, *4*, 54-62.

Therefore, it became necessary at this point to determine if gold(I)-silylium catalysis was the only operating route; if silylium promotion was the working mechanism while the proposed σ -allenylgold(I) complex **1.III** represented only a resting state; or, as a third alternative, both routes participate at the same time.

With this goal in mind, propargylsilane **1.1b** and *p*-tolualdehyde **1.2a** were chosen once again as model substrates, and different amounts of HNTf₂ and TMSNTf₂ were tested as promoters, using dichloromethane as solvent, at room temperature. The results of this study are summarized in Scheme 1.29. During the study it was observed that the addition of cesium carbonate at the end of the reaction avoids further decomposition, deactivating the silylium catalyst.



Entry	Catalyst	x mol%	%yield of 1.3c ^a
1a	TMSNTf ₂	0.1	<5
1b	HNTf ₂	0.1	0
2a	TMSNTf ₂	0.5	10
2b	HNTf ₂	0.5	0
3a	TMSNTf ₂	1	16
3b	HNTf ₂	1	0
4a	TMSNTf ₂	2.5	20
4b	HNTf ₂	2.5	0
5a	TMSNTf ₂	5	Decomposition
5b	HNTf ₂	5	Decomposition

^aYield determined by ¹H-NMR using dibromomethane as internal standard.

Scheme 1.29: Screening of the conditions for silylium catalysis.

As shown in *Entry 4a*, trimethylsilyl bistriflimide can promote the propargylation reaction, but at a much lower extent than in combination with gold(I) catalysis. However, triflimide itself does not promote it, even considering that substoichiometric amounts of silylium should be generated by protodesilylation of

propargylsilane **1.1b**.³⁹ Moreover, it is important to remark that the propargylation reaction does not take place, using either HNTf₂ or TMSNTf₂ as promoters, if the transformation is carried out in a glass Schlenck instead of a polypropylene tube. In that case, only protodesilylation process of propargylsilane **1.1b** is observed.

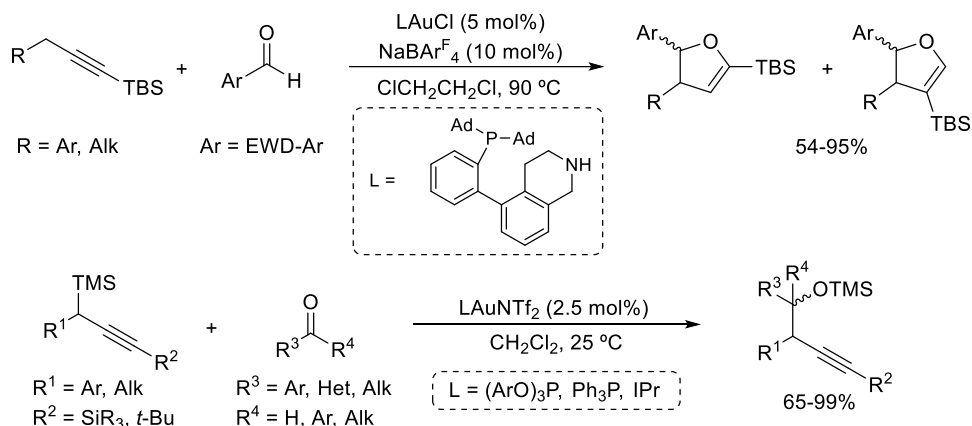
Thus, even though the possibility of both mechanisms operating at the same time cannot be doubtlessly ruled out, synergistic gold(I)-silylium catalysis seems to be the truly mechanism pathway, given the 'special' conditions needed for the highly sensitive silylium catalysis and the lower yield observed in comparison with the employment of the gold(I) phosphite complex.

Considering all the described results, this transformation represented the second example of a gold(I)-catalyzed propargylation reaction, being reported the first one by Professor Zhang and co-workers only four months earlier (Scheme 1.30).³² However, it presented some important differences compared to the results developed by these authors, as follows:

- The introduction of a trimethylsilyl moiety at the propargylic position turned the process more efficient and easier to control, as the intermediate homopropargyl alcohols could be isolated as silyl ethers.
- Moreover, the reaction tolerated a wide range of substituents with different electronic properties at various positions of the starting materials.
- Remarkably, the reaction took place in high yield employing propargylsilanes with bulkier TIPS and triphenylsilyl groups, and also with a *tert*-butyl group in the acetylenic position.
- Our process was more accessible regarding the gold catalysts, given that 'regular' commercially available gold(I) complexes could perform it, such as IPrAuNTf₂, Ph₃PAuNTf₂ or (ArO)₃PAuNTf₂.
- In addition, it also represented the first example of gold(I)-silylium synergistic catalysis employing propargylsilanes, since the previously reported examples of this cooperative catalysis have been only described for alkynylsilanes.^{35,40}

³⁹ Mahlau, M.; García-García, P.; List, B. *Chem. Eur. J.* **2012**, *18*, 16283-16287.

⁴⁰ a) Michalska, M.; Songis, O.; Taillier, C.; Bew, S. P.; Dalla, V. *Adv. Synth. Catal.* **2014**, *356*, 2040-2050; b) Berthet, M.; Songis, O.; Taillier, C.; Dalla, V. *J. Org. Chem.* **2017**, *82*, 9916-9922.



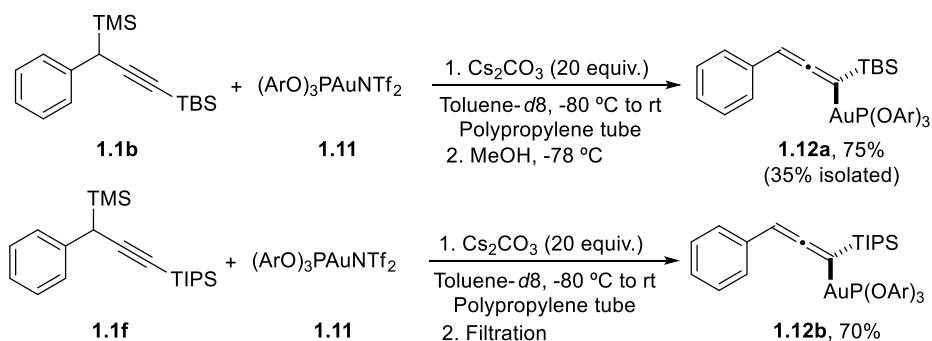
Scheme 1.30: Comparison between Zhang's propargylation and the developed process.

❖ Isolation and characterization of σ -allenylgold(I) complex **1.1**

In an attempt to validate our mechanistic proposal with experimental evidences, several experiments were carried out to isolate σ -allenylgold(I) intermediate **1.III**. For that purpose, we employed stoichiometric amounts of silylated propargylsilane **1.1b** and gold(I) phosphite **1.11**, in freshly dried toluene-*d*₈ as solvent to perform NMR analysis. Considering the potential protodesilylation issue due to the glassware free silanols that we observed during the study of the reaction scope (Scheme 1.25),³⁶ we set all the experiments in a polypropylene tube and at low temperature, to avoid the decomposition of TMSNTf₂. However, the use of glass NMR tubes caused protodesilylation at -78 °C. Given the high rate of that side reaction even at low temperatures, we considered that any attempt to avoid HNTf₂ generation should be performed in the presence of an external base.

Experimentally, the reaction was carried out in dry toluene-*d*₈ at -80 °C, inside a plastic polypropylene tube and in the presence of 20 equivalents of cesium carbonate as base. Formation of σ -allenylgold(I) complex **1.12a** was observed in a 75% yield. After removing the cesium carbonate by filtration, this pure organogold(I) complex was obtained as a white solid by precipitation in dry methanol at -78 °C in a 35% yield (Scheme 1.31, *top*), allowing its full characterization by several mono- and bidimensional NMR techniques. It was also possible to obtain the corresponding σ -allenylgold(I) complex **1.12b** starting for

propargylsilane **1.1f**, under the same conditions, and characterize it after partial purification (Scheme 1.31, *bottom*).



The most representative signal for complex **1.12a** on the $^1\text{H-NMR}$ spectrum is the phosphorus coupled allenic proton, with a chemical shift of 5.43 ppm and a coupling constant of $^5J_{\text{H-P}} = 8.4$ Hz (Figure 1.5). Regarding the aliphatic area of the spectrum, three sets of tert-butyls can be observed at 1.51, 1.21 and 1.09 ppm, corresponding the two first to the phosphite ligand and the third one to the TBS moiety. Finally, the two methyl groups give a single signal at 0.22 ppm.

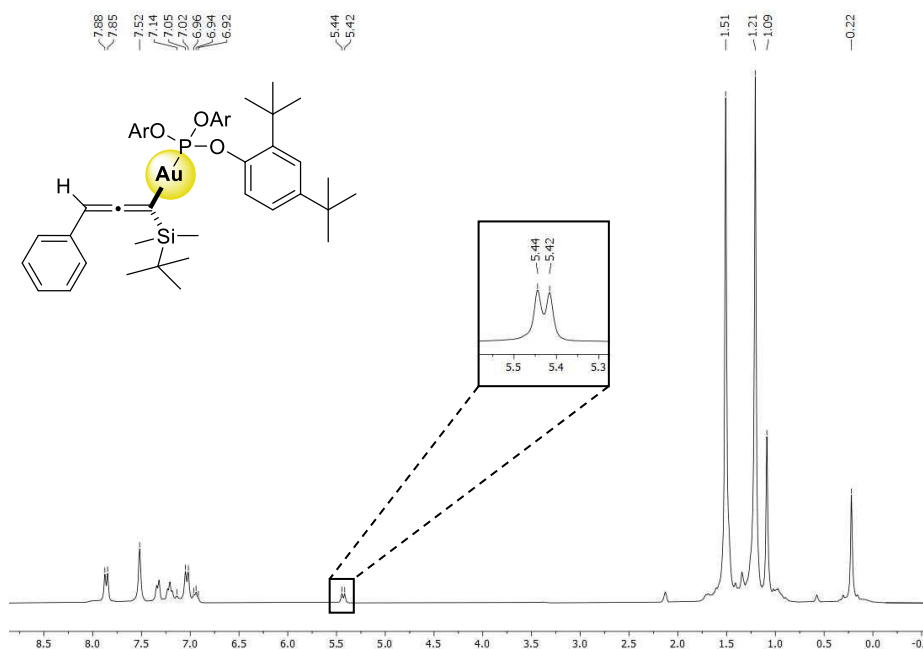


Figure 1.5: $^1\text{H-NMR}$ spectrum of σ -allenylgold(I) complex **1.12a**.

Attending to the ^{13}C -NMR spectrum (Figure 1.6), three representative signals for complex **1.12a** were identified: the phosphorus-coupled central carbon of the allene moiety (C_A , $\delta = 203.9$ ppm, $J_{\text{C-P}} = 10.8$ Hz), the gold-bounded terminal allenic carbon (C_B , $\delta = 108.0$ ppm, $J_{\text{C-P}} = 140.6$ Hz), and the terminal C-H allenic carbon (C_C , $\delta = 75.1$ ppm, $J_{\text{C-P}} = 11.4$ Hz).

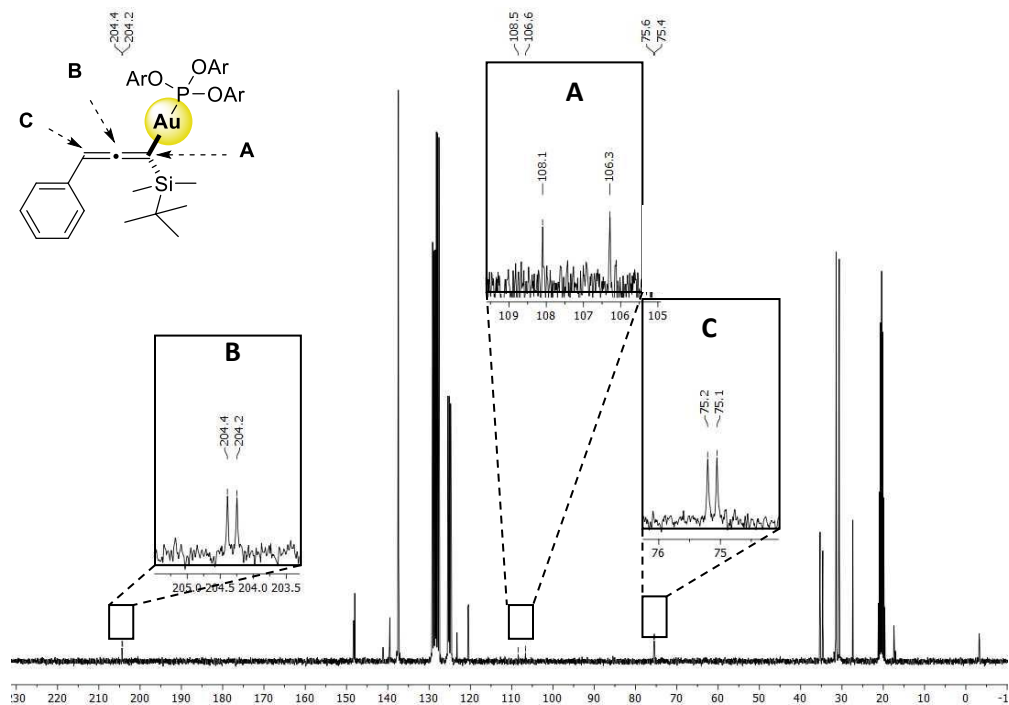


Figure 1.6: ^{13}C -NMR spectrum of σ -allenylgold(I) complex **1.12a**.

The assignment of these carbons could be achieved combining the information obtained by different mono- and bi-dimensional NMR experiments. The DEPT-135 and the Heteronuclear Single Quantum Coherence (HSQC) experiments confirmed that the ^1H signal at 5.43 ppm belong to a CH carbon at 75.1 ppm, lying this shift in the typical area for terminal allenic carbons with an aromatic substituent. Particularly, the Heteronuclear Multiple Bond Correlation (HMBC) experiment was extremely useful, as three key long-distance C-H couplings can be observed (Figure 1.7): between the allenic hydrogen atom at C_C and C_A (2J) and C_B (3J), and also between gold-bounded carbon C_A and TBS-methyl hydrogen atoms (3J).

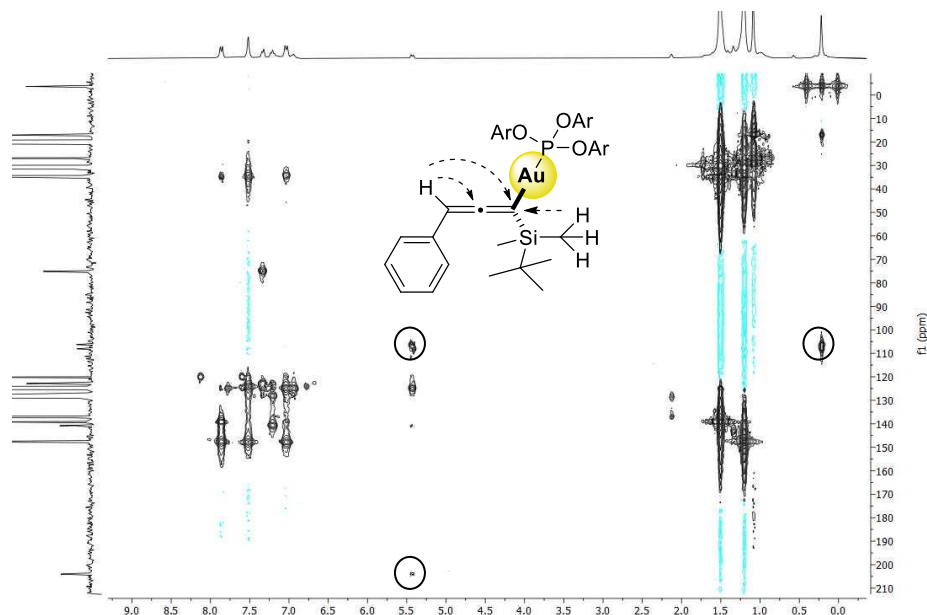


Figure 1.7: HMBC spectrum of σ -allenylgold **1.12a**.

On the other hand, the ^{31}P -NMR spectrum of σ -allenylgold(I) complex **1.12a** exhibits a single signal with a significant downfield shift, from 92.3 ppm for LAuNTf_2 to 137.6 ppm (Figure 1.8). In addition, a proton-coupled ^{31}P experiment was performed, observing a splitting of the signal into a doublet with $J_{\text{P-H}} = 8.4$ Hz, as expected regarding at the previously obtained ^1H spectrum (Figure 1.5).

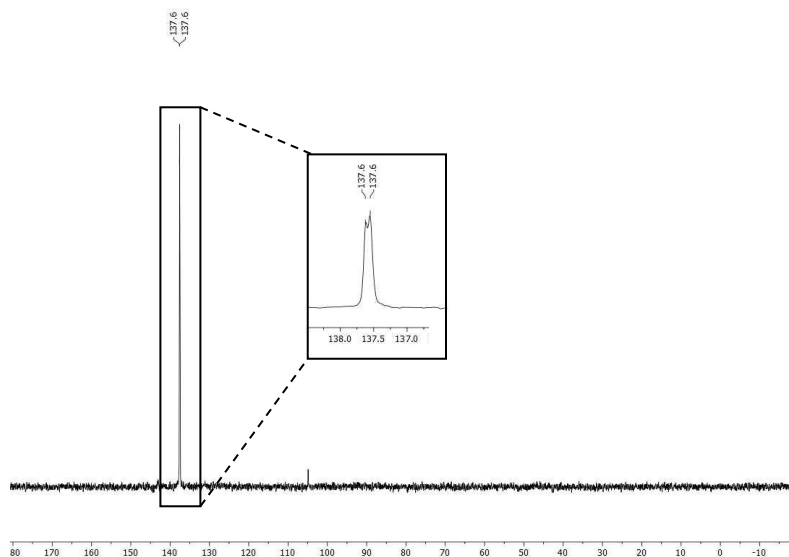
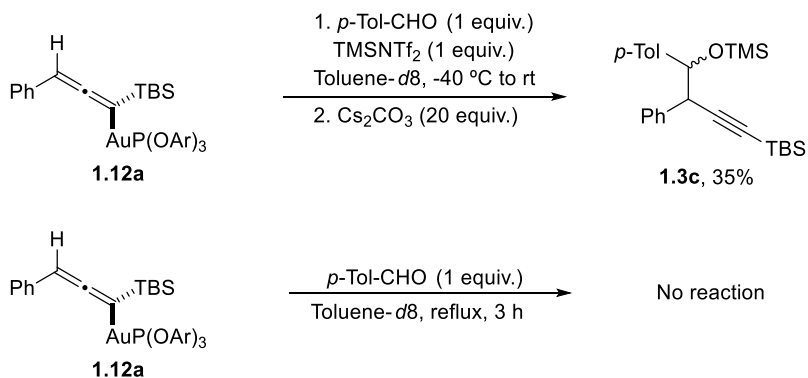


Figure 1.8: ^{31}P -NMR spectrum of σ -allenylgold(I) complex **1.12a**.

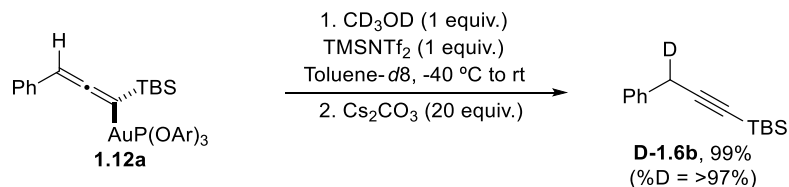
Finally, the organogold complex **1.12a** was analyzed by infrared spectroscopy using an ATR-FTIR apparatus. Among all the characteristic bands, the two most representative would be $\nu = 1884$ and 1863 cm^{-1} , lying within the expected area for the carbon-carbon double bonds of allene derivatives.

As the next step, we decided to evaluate its role in the catalytic cycle of the propargylation reaction. Thus, attending to the mechanistic proposal, we performed a stoichiometric reaction adding intermediate **1.12a** to a preformed solution of TMSNTf₂-activated *p*-tolualdehyde in toluene-*d*8 at -40 °C, resulting in the formation of the expected homopropargyl silyl ethers **1.3c** in moderate yield (Scheme 1.32). However, the absence of TMSNTf₂ did not lead to the formation of the expected product even at high temperature, confirming the need for a synergistic activation to facilitate the nucleophilic attack of σ -allenylgold(I) intermediate **1.12a**.



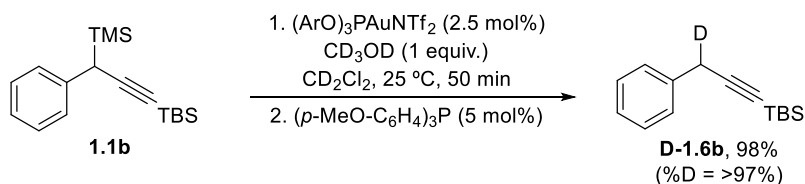
Scheme 1.32: Stoichiometric experiments starting from σ -allenylgold(I) complex **1.12a**.

We also performed a stoichiometric reaction between intermediate **1.12a** and DNTf₂ (generated from TMSNTf₂ and CD₃OD) in toluene-*d*8 at -40 °C (Scheme 1.33). Under these conditions, the corresponding deuterated alkynylsilane **D-1.6b** was obtained in almost quantitative yield, indicating therefore that non-deuterated alkynylsilane **1.6a** is formed as by-product through S_E2' protonation of σ -allenylgold(I) complex **1.12a**.



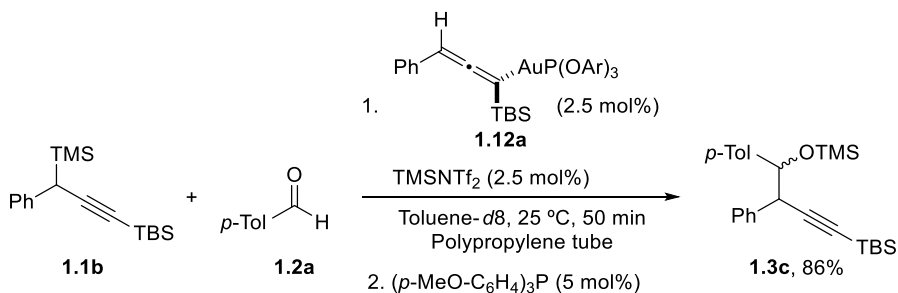
Scheme 1.33: Stoichiometric deuteration reaction of σ -allenyld(I) complex **1.12a**.

Similarly, when fully deuterated methanol- d_4 is used as a controlled proton source, alkynylsilane **D-1.6b** can be isolated in 98% under the standard reaction conditions with a deuteration percentage over 97% (Scheme 1.34). This result also suggests that hydroxyl groups on the glassware surface can be a plausible proton source, although they are less reactive, given the huge ratio between free silanols on the glassware surface and methanol- d_4 .



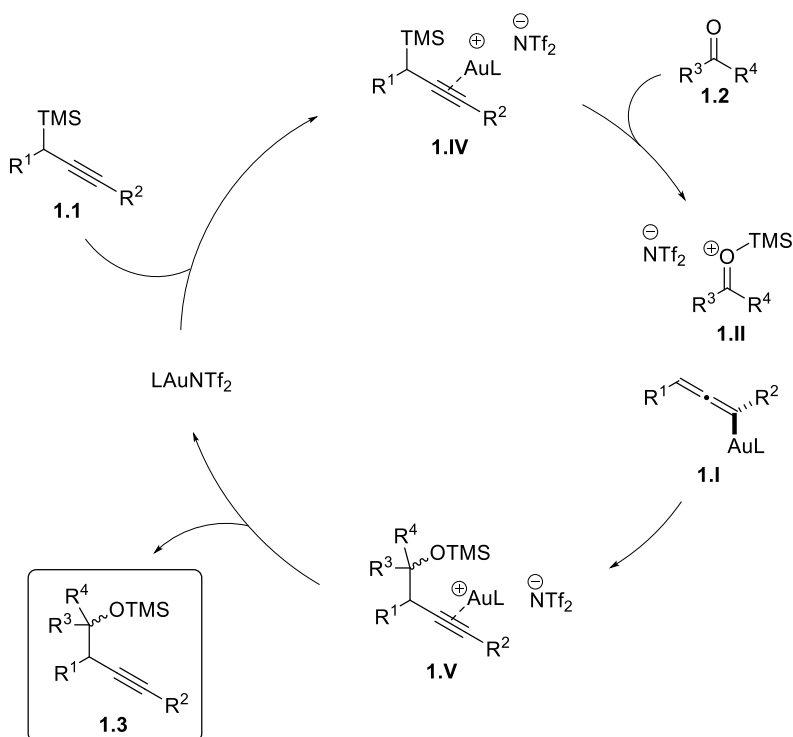
Scheme 1.34: Gold-catalyzed deutero-desilylation reaction of propargylsilane **1.1b**.

Finally, a successful catalytic propargylation could be also carried out starting from model propargylsilane **1.1b** and *p*-tolualdehyde **1.2a** using a 2.5 mol% of a combination of σ -allenyld(I) complex **1.12a** and TMSNTf_2 , as precatalysts. As shown in Scheme 1.35, the expected homopropargyl silyl ethers **1.3c** were obtained in a great 86% yield.



Scheme 1.35: Catalytic propargylation using intermediate **1.12a** and TMSNTf_2 .

Taking into account all the previously described results, our initial hypothesis about the catalytic cycle seemed to be the most plausible. Therefore, we envisioned a catalytic cycle for representing the mechanistic pathway of this transformation, where the key steps would consist in the formation of a σ -allenylgold(I) complex while synergistically activating the carbonyl compound. This mechanistic proposal is outlined in Scheme 1.36.



Scheme 1.36: Mechanistic proposal for the formation of homopropargyl silyl ethers **1.3**.

This transformation could start via coordination of the gold(I) catalyst to the alkyne, forming the π -complex intermediate **1.IV**. This intermediate **1.IV** could then evolve towards the formation of the σ -allenylgold(I) intermediate **1.I**, after carbon-silicon bond cleavage, following the expected regioselectivity for a propargylsilane nucleophilic attack.⁴¹ This behaviour might be enabled by the participation of the triflimidate anion, generating TMSNTf₂. The carbonyl compound could also assist to

⁴¹ Curtis-Long, M.; Aye, Y. *Chem. Eur. J.* **2009**, *15*, 5402-5416.

this C-Si bond breakage, being in turn synergistically activated³⁵ (intermediate **1.II**) and facilitating a nucleophilic attack from intermediate **1.I**, through a S_E2' pattern and generating intermediate **1.V**. Finally, coordination of the gold(I) catalyst to a new molecule of propargylsilane **1.1** would release the observed homopropargyl silyl ethers **1.3** and restart the catalytic cycle.

In summary, it has been described a high-yielding gold(I) catalyzed propargylation reaction, starting from carbonyl compounds and propargylsilanes. This transformation is proposed to occur through formation of a key σ -allenylgold(I) complex. Indeed, this elusive organogold intermediate was isolated and characterized by several NMR techniques, and its role in the catalytic process was empirically proved. Although these organometallic species have been previously reported by Gimeno and Hashmi, and proposed as intermediates in gold catalysis by Zhang and Hyland, this σ -allenylgold(I) complex represented the first example whose participation in a gold(I)-catalyzed transformation was unambiguously demonstrated by isolation and control experiments.

4 Conclusions

It has been described a gold-catalyzed propargylation of carbonyl compounds, using propargylsilanes as nucleophiles. The reaction proceeds under smooth conditions using a phosphitegold(I) triflimidate complex as the catalyst. These results represent the second reported example of gold-catalyzed propargylation and the first one using conventional ligands.

A general methodology for the synthesis of homopropargyl silyl ethers has been accomplished with excellent yields and total atom economy. Moreover, this transformation tolerates a wide range in the substitution pattern of aromatic aldehydes and different aliphatic and aromatic ketones, along with certain variability in the nature of the propargylsilane.

The proposed mechanism for this transformation evokes the formation of a σ -allenylgold intermediate, while generating a highly electrophilic silylium source. This would represent the first example of a synergistic gold(I)-silylium catalysis starting from propargylsilanes.

The elusive σ -allenylgold(I) intermediate could be isolated and characterized by several mono- and bidimensional NMR techniques. Its catalytic role was proved by several stoichiometric experiments, representing the first σ -allenylgold(I) complex to be synthesized and identified as a true reaction intermediate in a catalytic transformation.

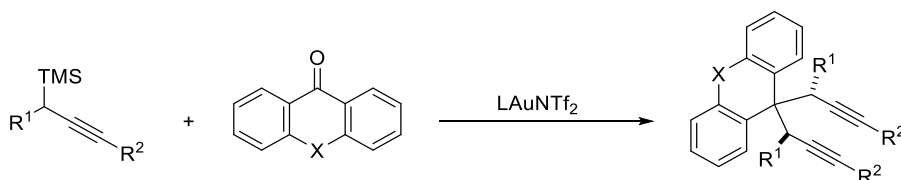
Chapter II:

Gold-catalyzed bispropargylation reaction.

Synthesis of 9,9-bispropargylxanthene derivatives

1 Introduction

This section summarizes the first catalytic deoxygenative bispropargylation process described in the literature. This transformation, catalyzed by gold(I) complexes, diastereoselectively generates 9,9-bispropargylxanthene structures with excellent yields (Scheme 2.1).



Scheme 2.1: Gold-catalyzed diastereoselective bispropargylation of xanthone derivatives.

As an extension of the propargylation reaction described in *Chapter I*, a sequential addition of two equivalents of allenylgold(I) intermediates to synergically activated xanthone explains the reaction outcome. In fact, selective mono- or bispropargylation processes can be easily controlled by solvent tuning, allowing isolation of silyl-protected xanthidols or non-symmetrical xanthenes. Moreover, these 1,6-diynes have been employed as starting materials for further organic transformations.

2 Bibliographic background

2.1 Xanthenes, xanthidols and xanthenes

9*H*-Xanthene-9-ones or xanthenes are natural occurring molecules found as secondary metabolites in some families of plants, fungi and lichens.¹ They possess a tricyclic dibenzo[*b,e*]pyrone core and, depending on the substituents, they can be classified into six different groups: simple, glycosylated, prenylated, lignoids, bisxanthenes and miscellaneous. In Figure 2.1, one example of each of the first four groups of naturally occurring xanthenes are given.

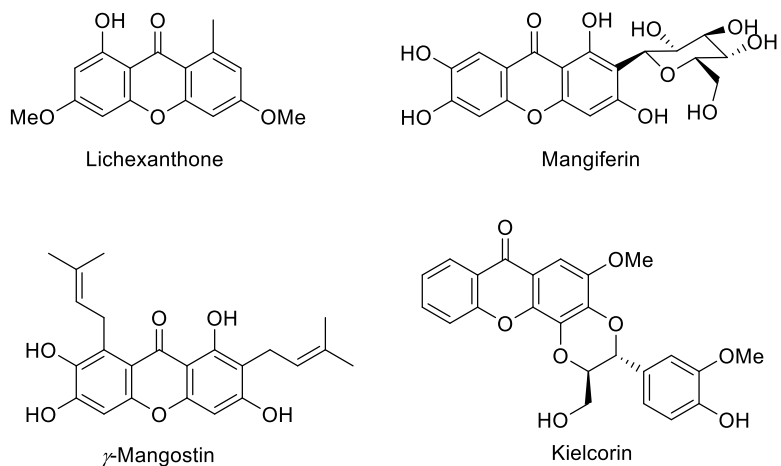


Figure 2.1: Examples of naturally occurring xanthenes.

¹ Vieira, L. M. M.; Kijjoa, A. *Curr. Med. Chem.* **2005**, *12*, 2413-2446.

Their reduced forms, xanthinol and xantheno, do not have the same occurrence, and only few examples have been recently reported,² so most of them are synthetically obtained.

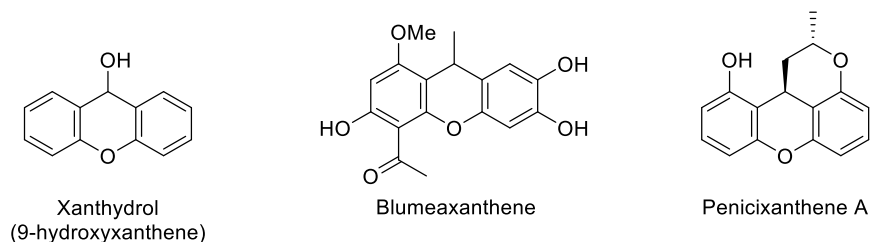


Figure 2.2: Examples of xanthinol and xanthenes found in nature.

Xanthonoids are in general privileged scaffolds, not only because of the great variety of complex structures found in nature, but also because of their interesting properties. Most of them present biological activity as neuroprotectors, antibacterials, antiparasitics or pesticides, and recent studies focused their attention in 9-substituted xanthenes and xanthidols as potent pharmaceuticals.³ Also, they have proved their versatility as chemosensors, molecular switches, organic dyes, building blocks in material science, catalysts, etc.⁴ A well-known example consist in Fluorescein (Figure 2.3), employed as fluorophore in forensics to detect traces of blood stains.⁵

² a) Cao, J. Q.; Yao, Y.; Chen, H.; Qiao, L.; Zhou, Y. Z.; Pei, Y. H. *Chin. Chem. Lett.* **2007**, *18*, 303-305; b) Richardson, S. N.; Nsiama, T. K.; Walker, A. K.; McMullin, D. R.; Miller, J. D. *Phytochemistry* **2015**, *117*, 436-443; c) Bai, M.; Zheng, C.-J.; Nong, X.-H.; Zhou, X.-M.; Luo, Y.-P.; Chen, G.-Y. *Mar. Drugs* **2019**, *17*, 649-657.

³ For a representative review, see: Maia, M.; Resende, D. I. S. P.; Durães, F.; Pinto, M. M. M.; Sousa, E. *Eur. J. Med. Chem.* **2021**, *210*, 113085-113104.

⁴ For selected examples see: a) Umemoto, S.; Im, S.; Zhang, J.; Hagihara, M.; Murata, A.; Harada, Y.; Fukuzumi, T.; Wazaki, T.; Sasaoka, S.; Nakatani, K. *Chem. Eur. J.* **2012**, *18*, 9999-10008; b) Grzelakowska, A.; Kolińska, J.; Zakłós-Szydab, M.; Sokołowska, J. *J. Photochem. Photobiol. A Chem.* **2020**, *387*, 112153-112163; c) Wiel, M. K. J.; Feringa, B. L. *Tetrahedron* **2009**, *65*, 4332-4339; d) Villada, J. D.; D'Vries, R.; Macías, M.; Zuluaga, F.; Chaur, M. N. *New J. Chem.* **2018**, *42*, 18050-18058; e) Kushida, Y.; Nagano, T.; Hanaoka, K. *Analyst* **2015**, *140*, 685-695; f) Shabir, G.; Saeed, A.; Channar, P. A. *Mini-Reviews Org. Chem.* **2018**, *15*, 166-197.

⁵ Budowle, B.; Leggitt, J. L.; Defenbaugh, D. A.; Keys, K. M.; Malkiewicz, S. F. *J. For. Sci.* **2000**, *45*, 1090-1092.

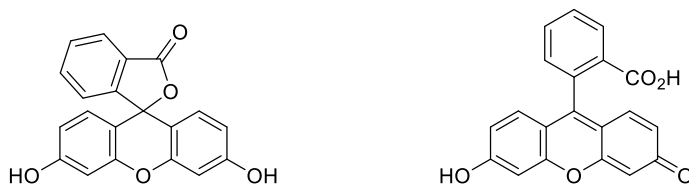
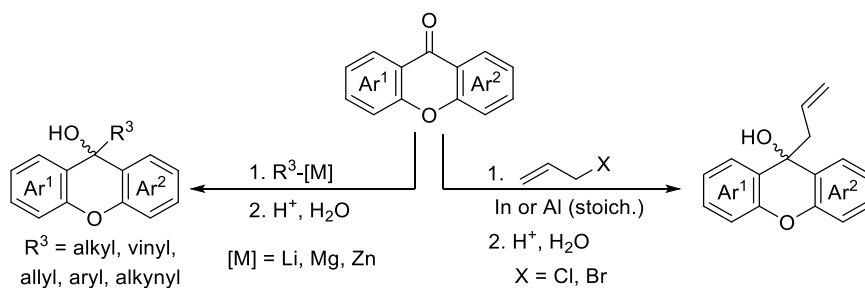


Figure 2.3: Two possible structures of fluorescein.

Several synthetic routes have been described for accessing substituted xanthydrols and xanthenes, including reduction or additions to xanthone precursors. As this section is focused on the synthesis of 9-substituted xanthydrols and 9,9-disubstituted xanthenes *via* nucleophilic addition to xanthenes, a brief discussion related to this topic is given below.

The most common strategy for the synthesis of xanthydrol derivatives starting from xanthenes consists in the addition of organometallic reagents followed by an aqueous work-up (Scheme 2.2, *left*).⁶ Other approaches consist in Barbier-type reactions with allyl halides using metals, such as In or Al, *in situ* generating the nucleophile (Scheme 2.2, *right*).⁷ As major disadvantages, all these methodologies require stoichiometric amounts of organometallic reagents and usually harsh conditions, but, given the wide range of readily accessible nucleophiles, several alkyl-, alkenyl-, allyl-, alkynyl- and arylxanthydrols can be obtained in a simple way.

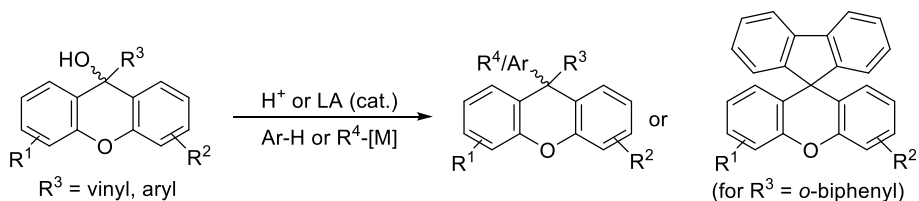


Scheme 2.2: Approaches for the synthesis of xanthydrols from xanthenes.

⁶ For selected examples see: a) Giri, R.; Goodell, J. R.; Xing, C.; Benoit, A.; Kaur, H.; Hiasa, H.; Ferguson, D. M. *Bioorg. Med. Chem.* **2010**, *18*, 1456-1463; b) Hogan, D. T.; Sutherland, T. C. *J. Phys. Chem. Lett.* **2018**, *9*, 2825-2829; c) Hirata, R.; Torii, A.; Kawano, K.; Futaki, S.; Imayoshi, A.; Tsubaki, K. *Tetrahedron* **2018**, *74*, 3608-3615.

⁷ a) Preite, M. D.; Pérez-Carvajal, A. *Synlett* **2006**, *19*, 3337-3339; b) Preite, M. D.; Jorquera-Geroldi, H. A.; Pérez-Carvajal, A. *ARKIVOC* **2011**, *7*, 380-388.

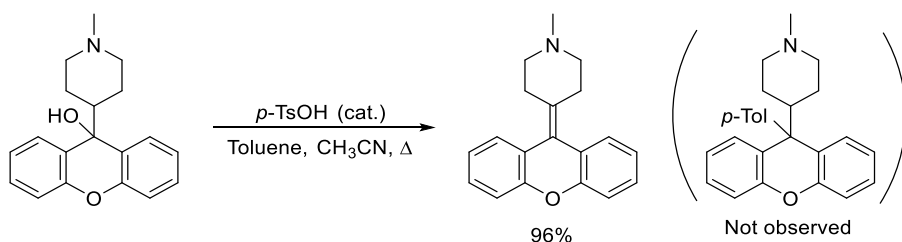
Moreover, xanthydrols can be used for obtaining non-symmetrically disubstituted xanthenes or spirocycles. Generally, treatment of xanthydrols with strong Bronsted or Lewis acids leads to stable xanthylium intermediates, which can be trapped by aryl rings, inter- or intramolecularly (Scheme 2.3). In addition, other organometallic reagents can be also employed, increasing functional group variety.



Scheme 2.3: Synthesis of 9,9-disubstituted xanthenes from xanthydrols.

Other strategies that complement these results are based in transforming hydroxyl into a better leaving group, as acetate or tosylate, to incorporate C-nucleophiles such as aryls or enols from enolizable ketones.⁸

However, only 9-aryl- or 9-vinylxanthydrols are suitable for these procedures, since 9-alkyl substituted ones furnish just elimination products, known as xanthylienes. One example of transformation of xanthydrols into xanthylienes is represented in Scheme 2.4. Although the reaction takes place in a non-polar solvent as toluene, the carbocation undergoes a E1 process faster, rather than the Friedel-Crafts alkylation shown in Scheme 2.3.⁹

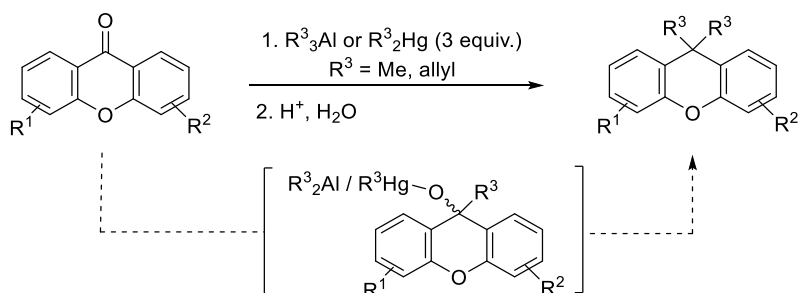


Scheme 2.4: Formation of a xanthyliene derivative under acidic conditions.

⁸ Kavala, V.; Murru, S.; Das, G.; Patel, B. K. *Tetrahedron* **2008**, *64*, 3960-3965.

⁹ Birman, V. B.; Chopra, A.; Ogle, C. A. *Tetrahedron Lett.* **1996**, *37*, 5073-5076.

For achieving 9,9-bisalkylated xanthenes starting from xanthenes, only two examples, both of them employing stoichiometric strategies, have been described. In these cases, highly reactive organoaluminanes¹⁰ or acutely toxic alkylmercury reagents¹¹ act as potent alkylating agents to furnish xanthydrils, and then, as Lewis acids to introduce the second alkyl moiety (Scheme 2.5).



Scheme 2.5: Bisalkylation processes of xanthenes to obtain 9-9-bisalkylxanthenes.

It is worth to mention that no propargylated xanthydrils or xanthenes have been reported to date, despite the great synthetic potential offered by these groups and the possible interesting properties they could bear.

2.2 Catalytic nucleophilic bis-additions to carbonyl compounds

The addition of organometallic reagents to carbonyl compounds has been a powerful and widely used tool in organic synthesis over decades. Classical procedures used to be stoichiometric and not always easy to control, so the development of worthwhile catalytic versions for these transformations became a challenging quest.¹²

Although catalyzed monoaddition reactions are well studied, selective introduction of two equivalents of these nucleophiles in the same carbonylic atom has not always received the same attention. In this sense, only isolated examples of

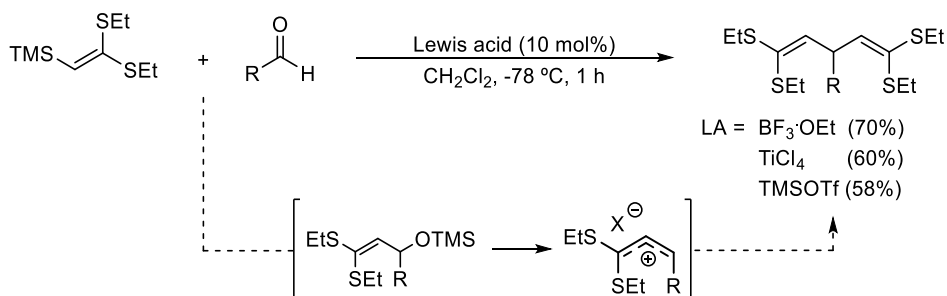
¹⁰ Olech, K.; Gutkowski, R.; Kuznetsov, V.; Roszak, S; Soloduch, J.; Schuhmann, W. *ChemPlusChem* **2015**, 80, 679-687.

¹¹ Oishi, M. In *Science of Synthesis*, **2004**, 7, 261-385.

¹² Nguyen, K. D.; Park, B. Y., Luong, T., Sato, H., Garza, V. J.; Krische, M. J. *Science* **2016**, 354, 300-306.

catalytic bisvinylation, bisallylation and bisalkynylation reactions of carbonyls have been described.

Okauchi and co-workers described the single example reported to date of a deoxygenative bisvinylation reaction of aldehydes, promoted by a Lewis acid catalyst (Scheme 2.6).¹³ The key for this transformation lies in the starting material, a β,β -bis(ethylthio)vinylsilane, in which the thioether moieties increase the nucleophilic character of the usually less reactive vinylsilane. Moreover, these groups can also assist the silyloxy abstraction and stabilize the carbocationic intermediate, easing the second vinylation reaction.



Scheme 2.6: Catalytic bisvinylation of aldehydes.

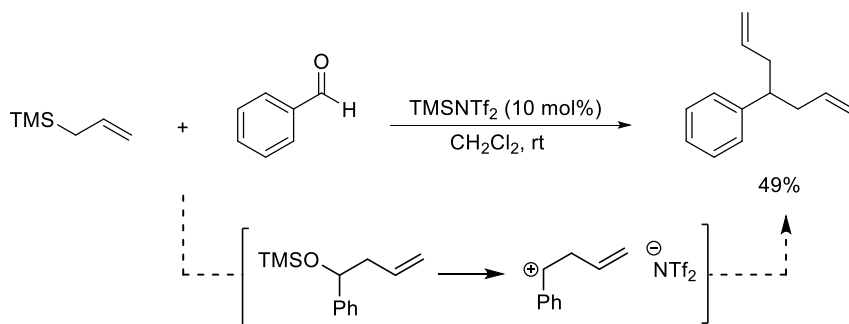
In the field of catalytic bisallylation, three independent deoxygenative examples have been reported in the literature, employing trimethylallylsilane as allylating reagent, and an acid catalyst in all cases (TMSNTf_2 ,¹⁴ YbCl_3 ,¹⁵ or a proton source¹⁶). However, bisallylated compounds were obtained as by-products, or from very specific compounds, since no deeper optimization or scope investigation were carried out. In addition, only non-substituted allyl chain was employed, so no information about selectivity in this process was gathered. In Scheme 2.7, the first reported bisallylation process is depicted.

¹³ Okauchi, T.; Tanaka, T.; Minami, T. *J. Org. Chem.* **2001**, *66*, 3924-3929.

¹⁴ Ishii, A.; Kotera, O.; Saeki, T.; Mikami, K. *Synlett* **1997**, *10*, 1145-1146.

¹⁵ Fang, X.; Watkin, J. G.; Warner, B. P. *Tetrahedron Lett.* **2000**, *41*, 447-449.

¹⁶ Murugan, K.; Chen, C. *Tetrahedron Lett.* **2011**, *52*, 5827-5830.



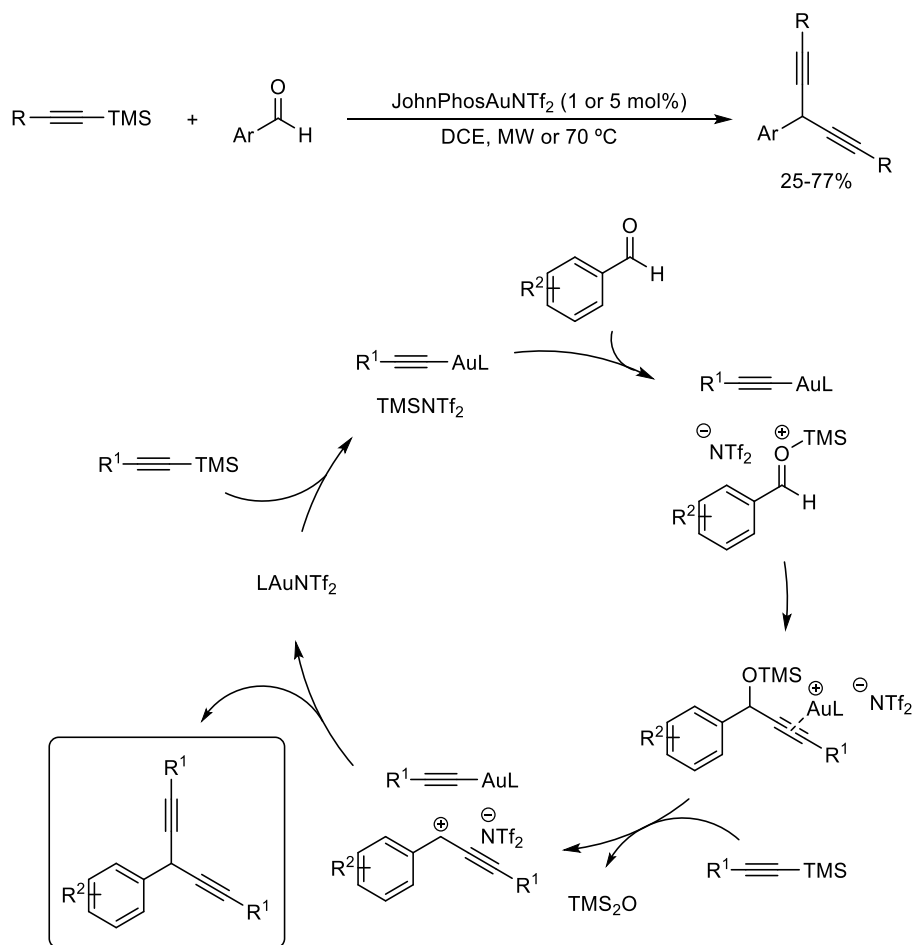
Scheme 2.7: First reported catalytic deoxygenative bisallylation reaction.

Related to catalytic bisalkynylation processes, two examples of this methodology have been reported to date, being the first example by Kuninobu, Takai and Ishii,¹⁷ and yielding 1,4-diyne upon aromatic aldehydes deoxygenation. The authors demonstrated that Au(I) and Re(I) catalysts promote the first alkynylation to the activated aldehyde, but second alkynylation is only due to the rhenium catalyst.

A similar bisalkynylation procedure was later developed by our research group,¹⁸ proving that the synergic gold(I)-silylium catalysis can effectively promote this transformation under proper conditions. In Scheme 2.8 a mechanistic proposal for this reaction is outlined. As stated in previous sections (see *General background*), the σ -activation of the alkynylsilane by the gold(I) catalyst generates a gold(I) acetylide and trimethylsilyltriflimide (TMSNTf₂). This strong silylating agent could activate the benzaldehyde derivative, facilitating the addition of the gold(I) acetylide and generating a propargyl silyl ether as intermediate. Then, the formation of a second gold(I) acetylide would release another molecule of TMSNTf₂, generating a carbocationic intermediate, upon activation of the silyl ether, and promoting the second addition to furnish the final product.

¹⁷ Kuninobu, Y.; Ishii, E.; Takai, K. *Angew. Chem. Int. Ed.* **2007**, *46*, 3296-3299.

¹⁸ Rubial, B.; A. Ballesteros, A.; González, J. M. *Adv. Synth. Catal.* **2013**, *355*, 3337-3343.



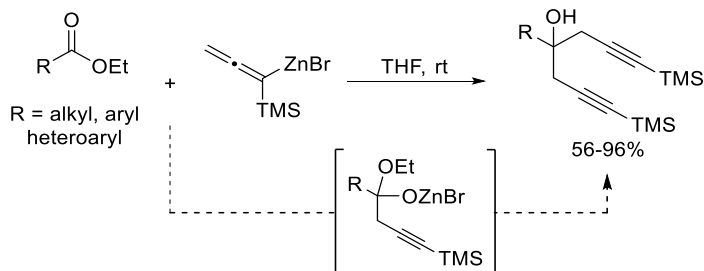
Scheme 2.8: Gold(I)-catalyzed bisalkynylations of aromatic aldehydes.

Regarding to catalytic bispropargylation processes, they remain unexplored, and only a few stoichiometric examples have been reported in the literature. These reactions did not attract much attention since they were developed as an alternative approach to bisallylation reactions, in order to improve their selectivity.

Oestreich and Sempere-Culler reported the first bispropargylation of unactivated esters with organozinc(II) reagents.¹⁹ As shown in Scheme 2.9, an equilibrium between allenyl- and propargylzinc can be proposed, but allenic form predominates due to the α -silicon effect. Therefore, coordination of the metal

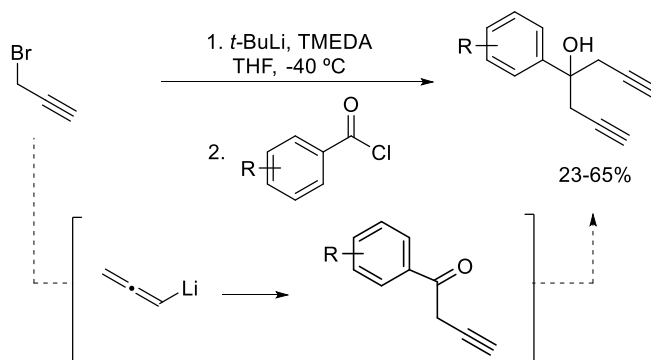
¹⁹ Oestreich, M.; Sempere-Culler, F. *Chem. Commun.* **2004**, 6, 692-693.

center to the carboxy group leads to a six-membered transition state, driving regioselectivity to propargylation. After the first addition, a zinc alkoxide is released, generating an homopropargyl ketone which is further propargylated to a bis-homopropargyl alcohol. The same authors described later a second approach to this family of processes, starting from cyclic acetal derivatives of salicylic acid, and the same organozinc(II) reagents.²⁰



Scheme 2.9: Bispropargylation of unactivated esters with organozinc reagents.

Finally, another synthetic method was described a few years ago, employing propargyl bromide and acyl chlorides (Scheme 2.10).²¹ This procedure consists in two steps initiated by halogen-lithium exchange to generate an allenyllithium reagent. Then, a careful control of the temperature drives the reaction to selective propargylation, instead of allenylation. Two consecutive propargylations furnish the expected bishomopropargyl alcohols with good selectivity.



Scheme 2.10: Bispropargylation of acyl chlorides with allenyllithium.

²⁰ Oestreich, M.; Sempere-Culler, F.; Machotta, A. B. *Angew. Chem. Int. Ed.* **2005**, *44*, 149-152.

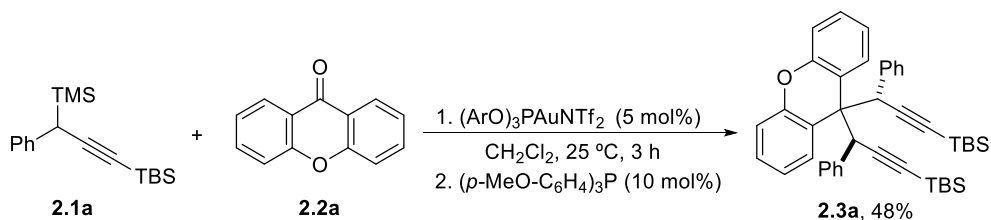
²¹ Vázquez, S.; Cabezas, J. A. *Tetrahedron Lett.* **2014**, *55*, 1894-1897.

As it can be inferred, there is a lack of development in these transformations, since stoichiometrical amounts of highly reactive and moisture-sensitive organometallic reagents are required. Moreover, contrary to the previously described bisvinilation and bisallylation reactions, only carboxy groups have been employed, yielding bishomopropargyl alcohols instead of non-oxygenated 1,6-diynes.

3 Results and Discussion

Regarding the results described in *Chapter I*, for the gold(I)-catalyzed propargylation of carbonyl compounds, we decided to test xanthone **2.2a** as a potentially suitable electrophile. Given that no 9-propargylxanthidrols have been reported to date, we envisioned that this robust protocol could open the door to these unexplored structures.

With this target in mind, we chose propargylsilane **2.1a** and xanthone **2.2a** as model substrates, and started the study using similar conditions to the gold(I)-catalyzed propargylation process described in *Chapter I*. Therefore, to a solution of these substrates **2.1a** and **2.2a** in dichloromethane, a 5 mol% of phosphitegold(I) triflimidate was added at room temperature. After 3 hours of reaction, under these conditions, 9,9-bispropargylxanthene **2.3a** was identified as a single diastereoisomer and isolated in a 48% yield from the crude reaction mixture, instead of the expected 9-propargylxanthidrol silyl ether (Scheme 2.11).



Scheme 2.11: Synthesis of 9,9-bispropargylxanthene **2.3a**.

9,9-Bispropargylated xanthene derivative **2.3a** was fully characterized by several mono- and bidimensional NMR techniques. Its structure was confirmed, and the relative stereochemistry of both stereocentres was assigned without any doubt, through an X-ray diffraction experiment on a single monocrystal, obtained by crystallization from a dichloromethane:methanol solution (Figure 2.4).

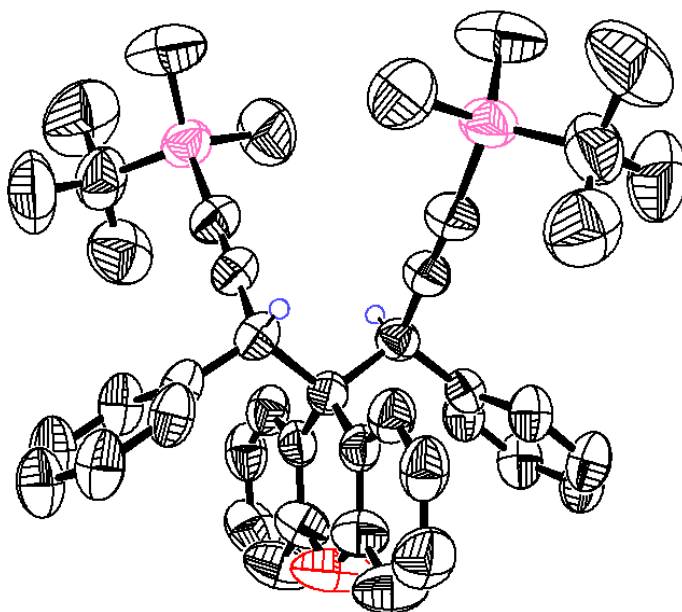
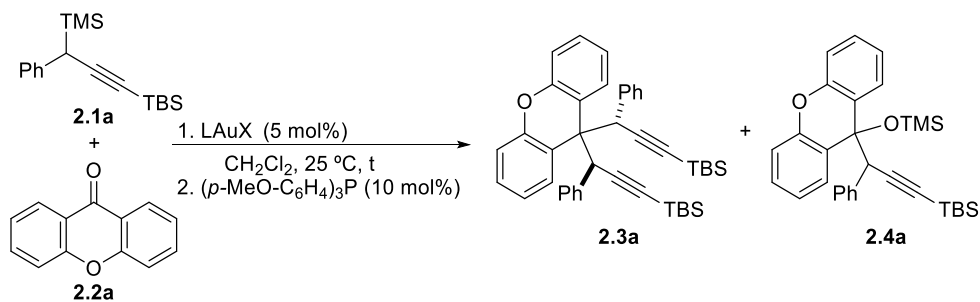


Figure 2.4: Structure of 9,9-bispropargylxanthene **2.3a**.

As far as we can ascertain, this is the first example of a catalytic consecutive nucleophilic deoxygenative bispropargylation process. Moreover, the reaction seemed to be completely diastereoselective. Considering the interest of this transformation, we decided to study it in a more detailed way.

First, in an attempt to optimize the model reaction conditions between propargylsilane **2.1a** and xanthone **2.2a**, different gold(I) catalysts were tested, along with variations in the reaction time and number of equivalents of **2.1a**, as at least two equivalents of propargylsilane **2.1** should be needed. The outcome of this study is summarized in Scheme 2.12.



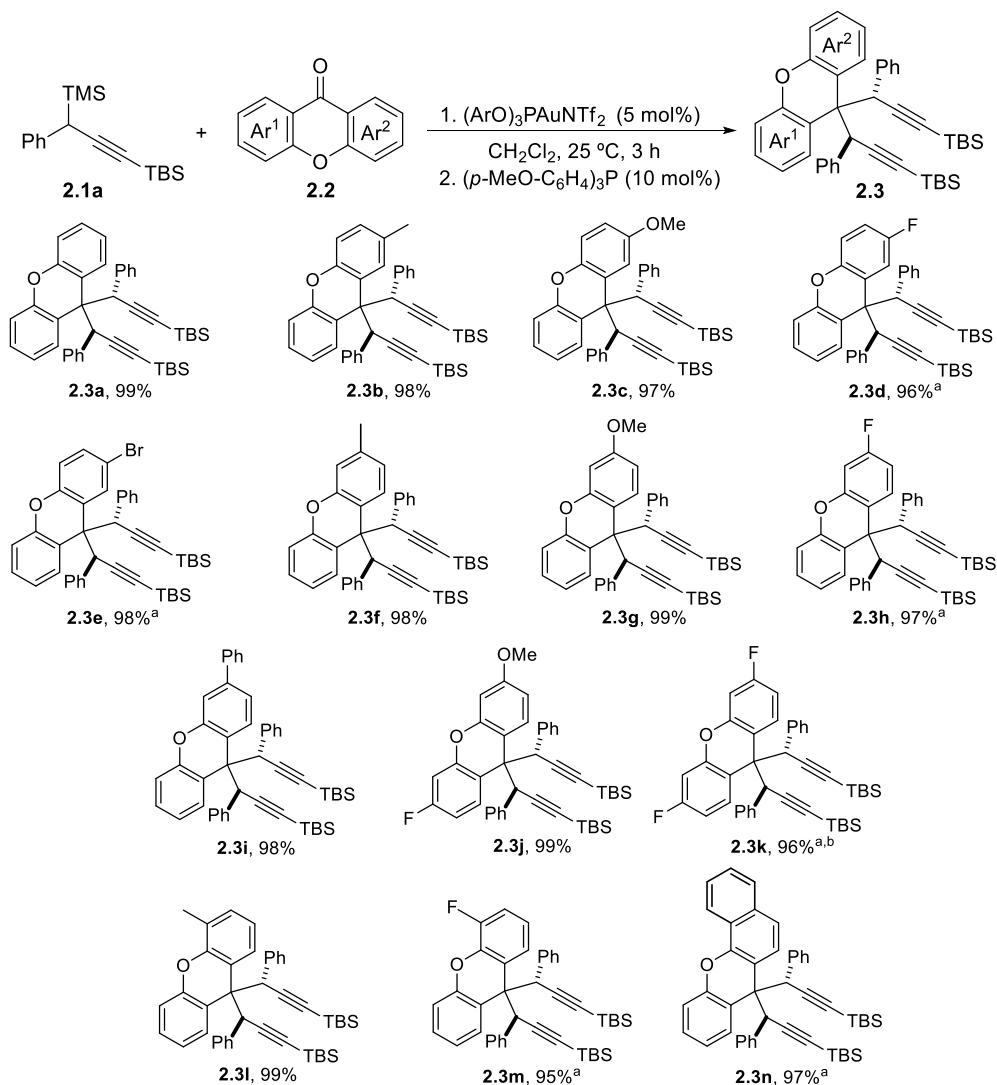
Entry	LAuX	n equiv.	T (°C)	t	% 2.3a ^a	% 2.4a ^a
1	(ArO) ₃ PAuNTf ₂	2.4	25	3 h	89	9
2	(ArO) ₃ PAuNTf ₂	3	25	3 h	99*	-
3	Ph ₃ PAuNTf ₂	3	25	3 h	99	-
4	IPrAuNTf ₂	3	25	3 h	21	75
5	JohnPhosAuNTf ₂	3	25	3 h	NR	NR
6	PicAuCl ₂	3	25	3 h	NR	NR
7	(ArO) ₃ PAuNTf ₂	3	25	1 h	41	59

^aDetermined by ¹H-NMR using dibromomethane as internal standard. *Isolated yield.

Scheme 2.12: Screening of the gold(I)-catalyzed bispropargylation reaction.

As it can be seen in Scheme 2.12, increasing the number of equivalents to 2.4 (*Entry 1*) improved the yield to an excellent 89%, along with another product which was identified as monopropargyl xanthinol silyl ether **2.4a**. Fortunately, quantitative yield was obtained employing three equivalents of propargylsilane **2.1a** (*Entry 2*). A modification in the gold(I) catalyst only decreased the obtained amount of 9,9-bispropargylxanthene **2.3a** in favour of compound **2.4a** (*Entry 4*) or even completely stopped the reaction (*Entries 5-6*). Although triphenylphosphinegold(I) triflimidate also performed the reaction quantitatively (*Entry 3*), phosphitegold(I) triflimidate was chosen as the best catalyst due to its higher stability towards storage. Finally, shorter reaction time only afforded product **2.3a** in a 41% yield, along with xanthinol derivative **2.4a** (*Entry 7*).

Once we established a representative procedure for the bispropargylation of xanthone **2.2a**, we decided to study the behaviour of the reaction in terms of the substitution pattern in the aromatic ring of this family of compounds (Scheme 2.13).



^a6 hours of reaction, ^bReaction performed at 60 °C.

Scheme 2.13: Scope of the bispropargylation reaction in terms of xanthone derivatives **2.2**.

From Scheme 2.13 can be observed that the yields were excellent in all the cases and all the products were obtained as a single diastereoisomer, indicating that the bispropargylation process is totally diastereoselective. The bispropargylation reaction tolerated a wide range of substrates in terms of substitution pattern of the xanthone ring **2.2**, from electron-donating (products **2.3b-c,f-g,i,j,l**) to electron-withdrawing groups (products **2.3d-e,h,k,m**), or a combination of both in different rings (product **2.3j**). Finally, the reaction of an

extended polycyclic xanthone was also successful (product **2.3n**). As outlined in Scheme 2.13, longer reaction times were required for xanthenes bearing electron-withdrawing groups (products **2.3d-e,h,k,m**) to complete the transformation.

As a limitation for this process, it was found that 1,3-dimethylxanthone and 2-nitroxanthone yielded only the corresponding diastereoisomeric mixtures of xanthyrol silyl ethers **2.4o-p** in almost quantitative yield respectively, instead of the expected 9,9-bispropargylxanthenes (Figure 2.5). Therefore, the presence of *ortho* substitution or strong electron-withdrawing groups seemed to be responsible of the inhibition of the second propargylation step.

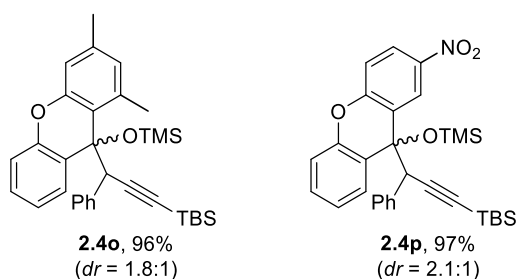
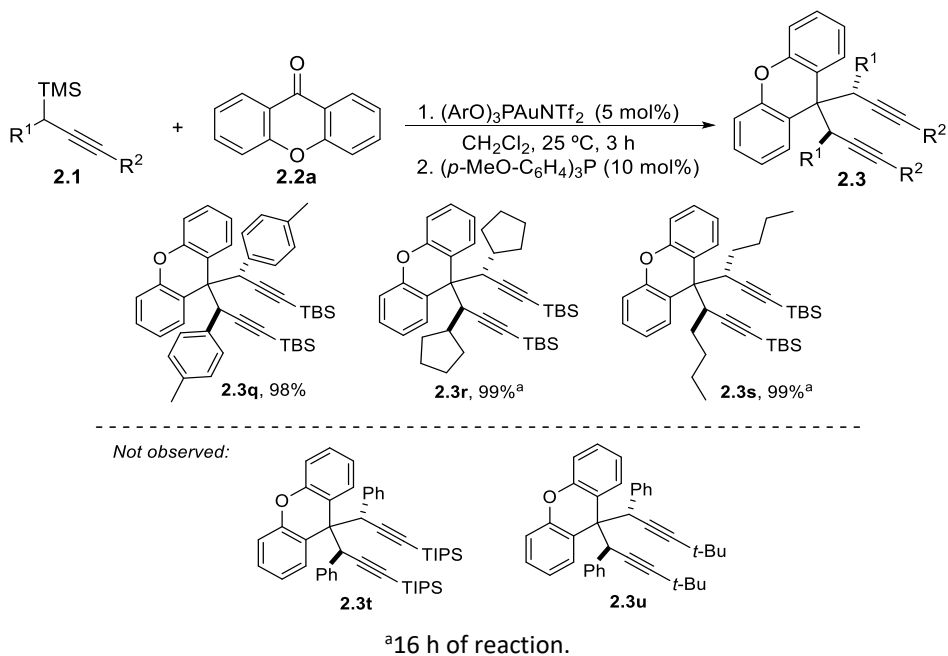


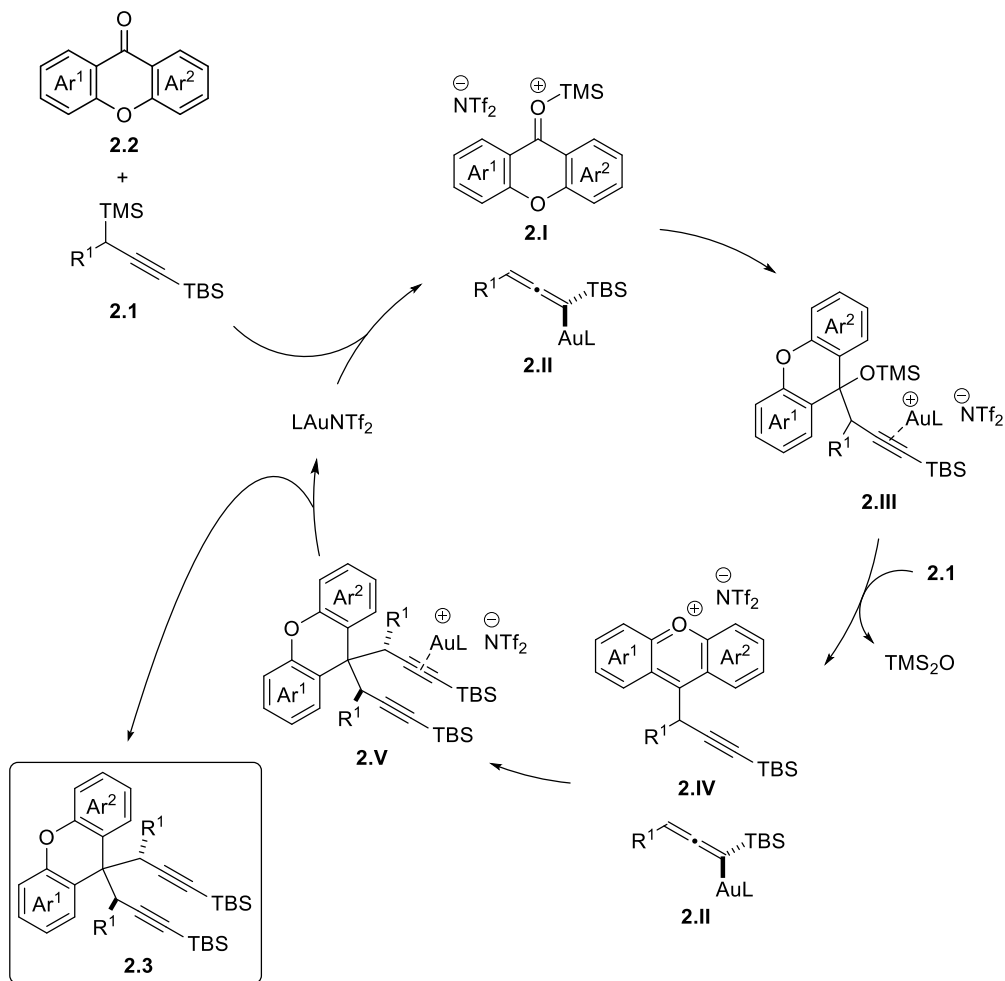
Figure 2.5: Observed xanthyrol silyl ethers **2.4o-p**.

Finally, other propargylsilanes **2.1**, bearing a *p*-tolyl group or an aliphatic chain at the propargylic position, performed the reaction well, as 9,9-bispropargylxanthenes **2.3q-s** were obtained in almost quantitative yields and with total diastereoselectivity (Scheme 2.14). However, the presence of a bulkier alkynylsilyl group like triisopropylsilyl (TIPS) inhibited the reaction even at higher temperature. Finally, a propargylsilane derivative bearing an alkynyl *tert*-butyl group was also tested, but no positive results were observed. This outcome agreed with the lower reactivity described in *Chapter I* for these substrates in their reaction with benzophenones, since they required higher catalyst loadings and/or longer reaction times.



Scheme 2.14: Scope of the bispropargylation process with different propargylsilanes **2.1**.

With these results in hand, and the knowledge gathered from the observations described in *Chapter I*, we envisioned a catalytic cycle for this transformation that is outlined in Scheme 2.15. Thus, the mechanistic proposal for this reaction could be initiated by σ -activation of propargylsilane **2.1** to generate the σ -allenylgold(I) intermediate **2.II**. This interaction would generate TMSNTf_2 , that could in turn synergistically activate xanthone **2.2**. This step would enable the nucleophilic addition of the allenylgold(I) **2.II** to intermediate **2.I**, furnishing a xanthydiol silyl ether **2.III**. Next, the activation of a second molecule of propargylsilane **2.1a** by the gold catalyst could trigger the release of a molecule of hexamethyldisiloxane, affording xanthylium intermediate **2.IV** and a new σ -allenylgold(I) complex **2.II**. Finally, a second propargylation step would yield the 9,9-bispropargylxanthene **2.3**, while restarting the catalytic cycle.



Scheme 2.15: Mechanistic proposal for the formation of 9,9-bispropargylxanthene **2.3**.

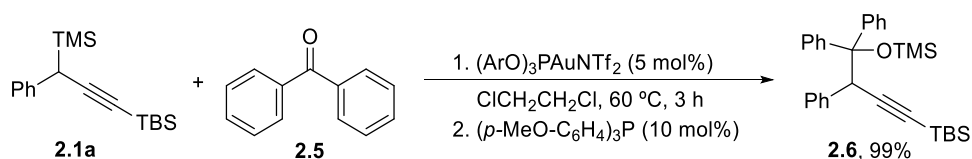
In an effort to rationalize the required structural and electronic properties of the carbonyl compound for this transformation, it was necessary to turn our attention to the role of the xanthone core in the mechanism. Compared to the carbonyl derivatives we tested for the gold-catalyzed propargylation process (see *Chapter I*), xanthone derivatives **2.2** present some important features:

- The three-dimensional structure of these ketones is completely flat due to the bridge between rings, making them less hindered than the non-bridged benzophenone analogues.

- An aromatic dibenzopyrylium (xanthylium) intermediate **2.I** is proposed to be generated upon TMSNTf₂ activation of the carbonyl group. This intermediate could be more stable than the carbocation generated for aromatic aldehydes or ketones. After the first propargylation, another xanthylium intermediate **2.IV** could be generated by consecutive activation, probably enabling the second nucleophilic attack of another σ -allenylgold(I) complex **2.II**.
- The oxygen atom bridging both phenyl rings could assist the release of the hexamethyldisiloxane molecule, through donation of the lone pair of electrons.

Attempting to determine if all these structural and electronical aspects were required for the transformation, a set of experiments was carried out using propargylsilane **2.1a** as model substrate.

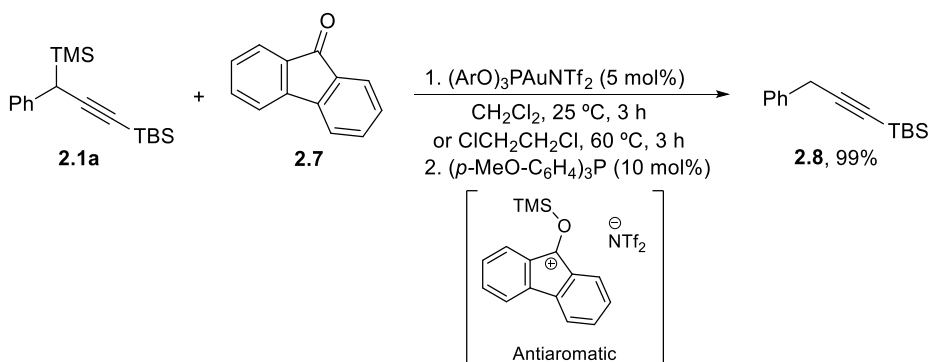
- As reported in *Chapter I*, treating a mixture of benzophenone **2.5** and model propargylsilane **2.1a**, under the same conditions, only yielded the expected homopropargyl silyl ether **2.6**. Even at higher temperature (60 °C), no bispropargylation product was observed (Scheme 2.16). The electron-rich 4,4'-dimethoxybenzophenone was also tested under the same conditions, since both methoxy groups should stabilize the carbocationic intermediate and assist the hexamethyldisiloxane molecule release. However, a different kind of reactivity was observed, leading to a new transformation that will be further discussed in *Chapter IV*, but it was not detected any amount of bispropargylated compound. Considering these results, we deduced that a bridged system could be required.



Scheme 2.16: Attempts of bispropargylating benzophenone **2.5**.

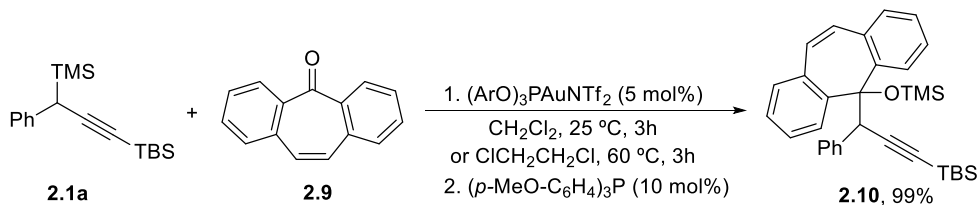
- Next, a solution of 9-fluorenone **2.7** and propargylsilane **2.1a** were treated under the standard conditions, but alkynylsilane **2.8**, coming from protodesilylation of **2.1a**, was the only observed product. Carrying out the reaction at higher temperature did not overcome this issue (Scheme 2.17). This result could arise from the instability of the potential antiaromatic carbocationic intermediate that should be formed upon silylium-activation of fluorenone **2.7**.

Thus, apart from the bridged flat structure, the generation of a stable carbocation seemed to be also needed.



Scheme 2.17: Bispropargylation tests employing 9-fluorenone **2.7**.

- Regarding the previous results, we envisioned that dibenzosuberone could be a suitable ketone for experimenting the bispropargylation process. In this sense, their possibility to form a stable dibenzotropilyum carbocation upon silylium-activation could play a key role. Nevertheless, the gold-catalyzed reaction between propargylsilane **2.1a** and ketone **2.9** only afforded the monopropargylation product **2.10**, either under the standard conditions or increasing the temperature (Scheme 2.18). Presumably, the initial carbonylic carbon is not so accessible in this case for a second nucleophilic attack or TMSNTf_2 activation, due to the larger seven-membered ring structure, and its boat conformation.²²

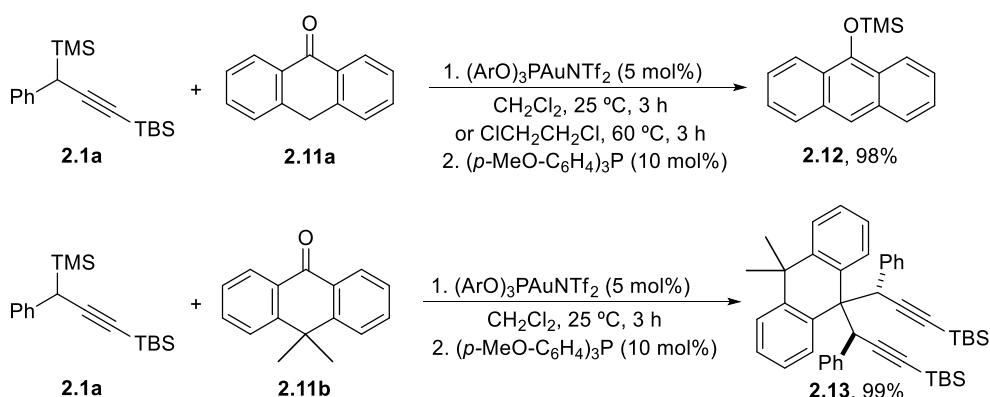


Scheme 2.18: Study of bispropargylation process for a seven-membered ring ketone.

²² Dastan, A.; Kilic, H.; Nurullah Saracoglu, N. *Synthesis* **2018**, 50, 391-439.

Taking into account all these outcomes, it seemed clear that the unique flat-tricyclic structure of xanthone was crucial for the second propargylation step to take place. Finally, it became necessary to determine if the lone pair of electrons, coming from the oxygen atom in xanthone **2.2**, was also essential to promote the reaction. Hence, we tested analogues of xanthone derivatives with two different bridging moieties lacking an available pair of electrons: anthrones (carbon-bridged) and thioxanthone-10,10-dioxide (SO₂-bridged).

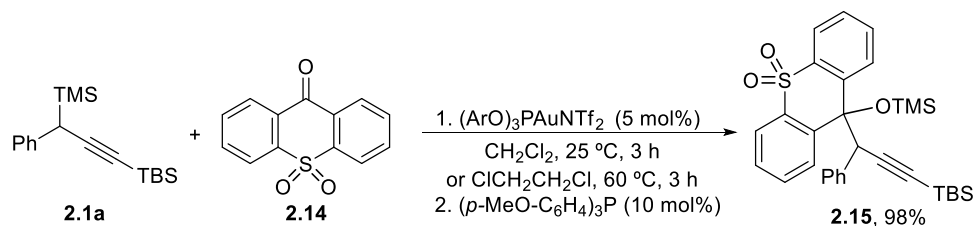
Thus, when anthrone **2.11a** was tested under the standard conditions, complete protodesilylation of propargylsilane **2.1a** was observed, along with the formation of anthracene derivative **2.12**, which was identified in 98% yield from the crude mixture by NMR (Scheme 2.19, *top*). The formation of this product could be explained considering the tautomeric anthracene-9-ol form of **2.11a**.²³ To overcome this issue, we employed 5,5-dimethylanthrone **2.11b** as electrophile, and in this case a successful bispropargylation was achieved, giving rise to bispropargylanthrene **2.13** as a single diastereoisomer (Scheme 2.19, *bottom*).



Scheme 2.19: Performed tests using anthrone derivatives **2.11**.

For thioxanthone-10,10-dioxide **2.14**, the propargylation reaction took place under the standard conditions to generate the corresponding homopropargyl silyl ether **2.15**, which was isolated in 98% yield (Scheme 2.20). However, bispropargylation reaction did not occur, even at higher temperature.

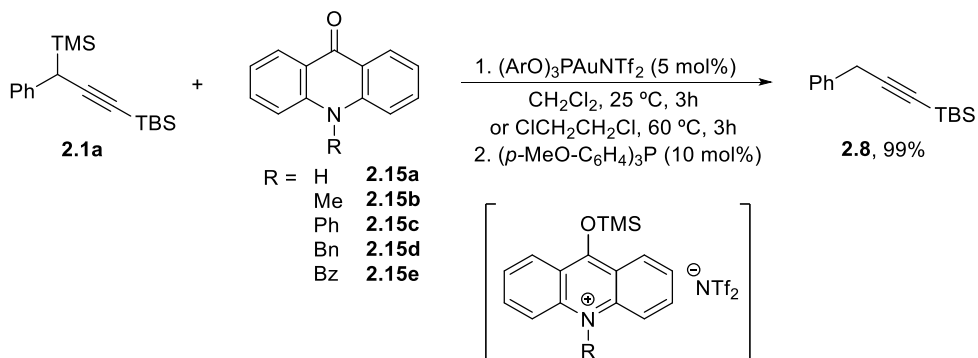
²³ Similar results were observed under homogeneous gold catalysis, starting from alkyne silanes and alcohols. For further information, see: Starkov, P.; Rota, F.; D'Oyley, J. M.; Sheppard, T. D. *Adv. Synth. Catal.* **2012**, *354*, 3217-3224.



Scheme 2.20: Monopropargylation of thioxanthone-10,10-dioxide **2.14**.

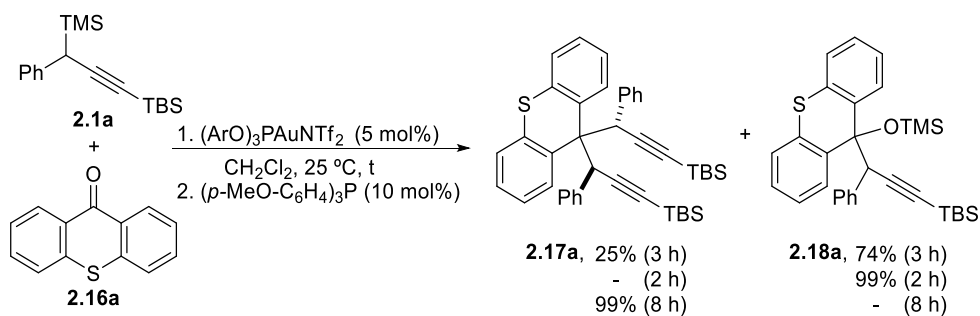
The lack of reactivity for thioxanthone-10,10-dioxide **2.14**, in terms of the formation of the bispropargylated compound, supports a plausible participation of the aromatic xanthylium intermediate **2.V**. In this vein, both bridging moieties ($-\text{SO}_2-$ and $-\text{C}(\text{Me})_2-$) do not possess available lone electron pairs, so the formed carbocationic intermediate would be less stabilized compared to the one obtained for other xanthone derivatives. However, the presence of methyl groups in the anthrone derivative **2.11b** could stabilize the carbocationic intermediate through hyperconjugation, explaining the different reactivity compared to derivative **2.14**. Thus, it seemed that the presence of a lone electron pair from a bridging heteroatom is not required for the bispropargylation reaction. However, the great applicability of xanthonoids in different fields, along with their straightforward synthesis, drove our attention to the use of these carbonyl compounds.

For this reason, two other analogues of xanthenes were tested as electrophiles: acridones (nitrogen-bridged) and thioxanthenes (sulfur-bridged). Thus, when *N*-unprotected acridone **2.15a** was treated under the standard conditions, only protodesilylation of **2.1a** was observed, presumably due to the coordination of TMSNTf_2 to the *N*-H group and releasing of HNTf_2 . However, using several derivatives **2.15b-e** bearing different *N*-protecting groups (methyl, phenyl, benzyl and benzoyl, respectively) did not overcome this issue, since all of them did not react under the standard conditions, or even heating at 60 °C (Scheme 2.21). Probably, the major stability of the presumable acridinium intermediates avoid the first propargylation step due to their lower electrophilicity, provoking the slow protodesilylation of σ -allenylgold(I) intermediate **2.II** by HNTf_2 .



Scheme 2.21: Attempts to use acridones **2.15** for bispropargylation reaction.

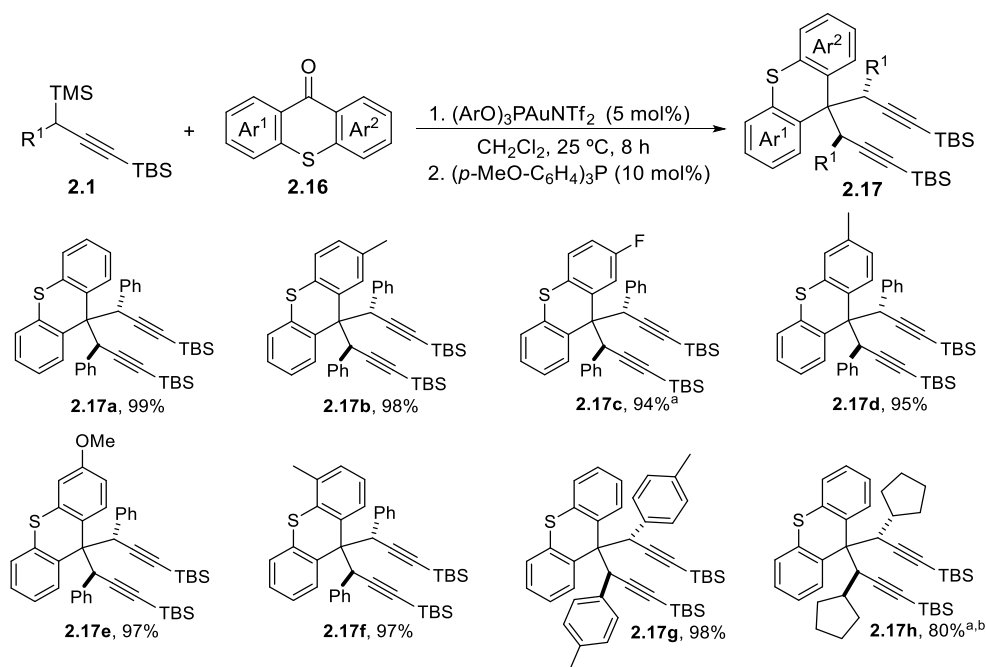
On the other hand, when we tested the reaction employing thioxanthone **2.16a** as carbonyl compound, 9,9-bispropargylated thioxanthene **2.17a** was isolated in 25% yield as a single diastereoisomer, along with a 74% yield of thioxanthodiol silyl ether **2.18a** (Scheme 2.22). The exclusive formation of each compound could be achieved with an exhaustive control of the reaction time. Thus, shorter reaction time gave rise to the exclusive formation of thioxanthodiol silyl ether **2.18a**, while longer reaction time afforded the diastereoisomerically pure 9,9-bispropargylthioxanthene **2.17a** in an almost quantitative yield.



Scheme 2.22: Gold-catalyzed mono- and bispropargylation of thioxanthone **2.16a**.

Regarding this behaviour, we studied the scope of the bispropargylation reaction in terms of the thioxanthone **2.16** and propargylsilane **2.1** structures, considering that this transformation required longer reaction times than for xanthone analogues. From Scheme 2.23 can be observed that, as previously observed for xanthenes **2.3**, the yields were excellent in all the cases, with total diastereoselectivity. The presence of different electron-donating (**2.17b-d,f**) and an electron-withdrawing fluorine group (**2.17e**) worked perfectly in both *meta* and

para position respect to the carbonyl, requiring the fluorinated thioxanthone even longer reaction time to be completed. Additionally, other different substituted aromatic propargylsilanes **2.1b** or aliphatic propargylsilane **2.1d** afforded the corresponding xanthenes **2.17g-h** in very good yields. Once again, the lower reactivity of aliphatic propargylsilanes was demonstrated, as the latest example required 16 h of reaction at 60 °C.



^a16 hours of reaction, ^bReaction performed at 60 °C.

Scheme 2.23: Scope of thioxanthone derivatives **2.14** for bispropargylation reaction.

Similarly to the behaviour of xanthenes **2.2**, it was found that the presence of strong electron-withdrawing groups in *meta* position of thioxanthenes **2.16** completely inhibited the second propargylation step, even at higher temperature, generating thioxanthodiol silyl ether **2.18i-j** in almost quantitative yield (Figure 2.6). These outcomes follow a good trend considering the lower reactivity shown by model thioxanthone **2.16a**.

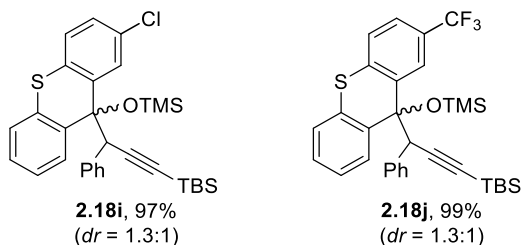


Figure 2.6: Thioxanthanol silyl ethers **2.18** obtained instead of the corresponding thioxanthene derivatives **2.17**.

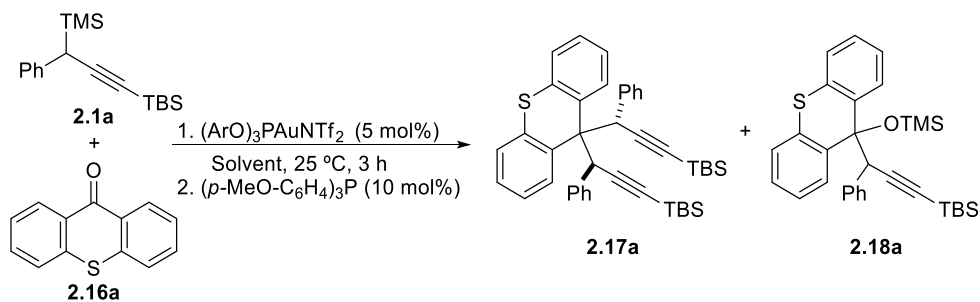
Therefore, the use of xanthenes or thioxanthenes and propargylsilanes, in the presence of a gold complex, allowed us to describe the first catalytic deoxygenative bispropargylation reaction of carbonyl compounds.

This methodology proceeds in a high yielding and totally diastereoselective way, allowing to obtain a wide range of 9,9-bispropargylxanthenes and 9,9-bispropargylthioxanthenes with different substitution pattern and electronic properties.

In addition, it was found that the process does not require the presence of a bridging heteroatom with lone pairs of electrons, also opening the door to the bispropargylation of 9,9-disubstituted anthrone derivatives.

❖ Monopropargylation and non-symmetrical bispropargylation reactions

Coming to this point and considering the behaviour of model thioxanthone **2.14a** towards the propargylation reaction (Scheme 2.22), we envisioned that different reaction conditions could allowed us to selectively obtain monopropargylxanthidrol **2.4** or thioxanthidrol silyl ethers **2.18**, regardless the substitution pattern in the aromatic rings. For this purpose, thioxanthone **2.16a** and propargylsilane **2.1a** (three equivalents) were chosen as model substrates for a new screening with different solvents (Scheme 2.24)



Entry	Solvent	%yield 2.17a ^a	%yield 2.18a ^a
1	CH ₂ Cl ₂	25	74
2	CH ₂ Cl ₂ ^b	-	98*
3	ClCH ₂ CH ₂ Cl	20	78
4	CHCl ₃	<5	95
5	Hexane	-	36
6	Toluene	-	99*
7	CH ₃ CN	-	95
8	1,4-Dioxane	-	98

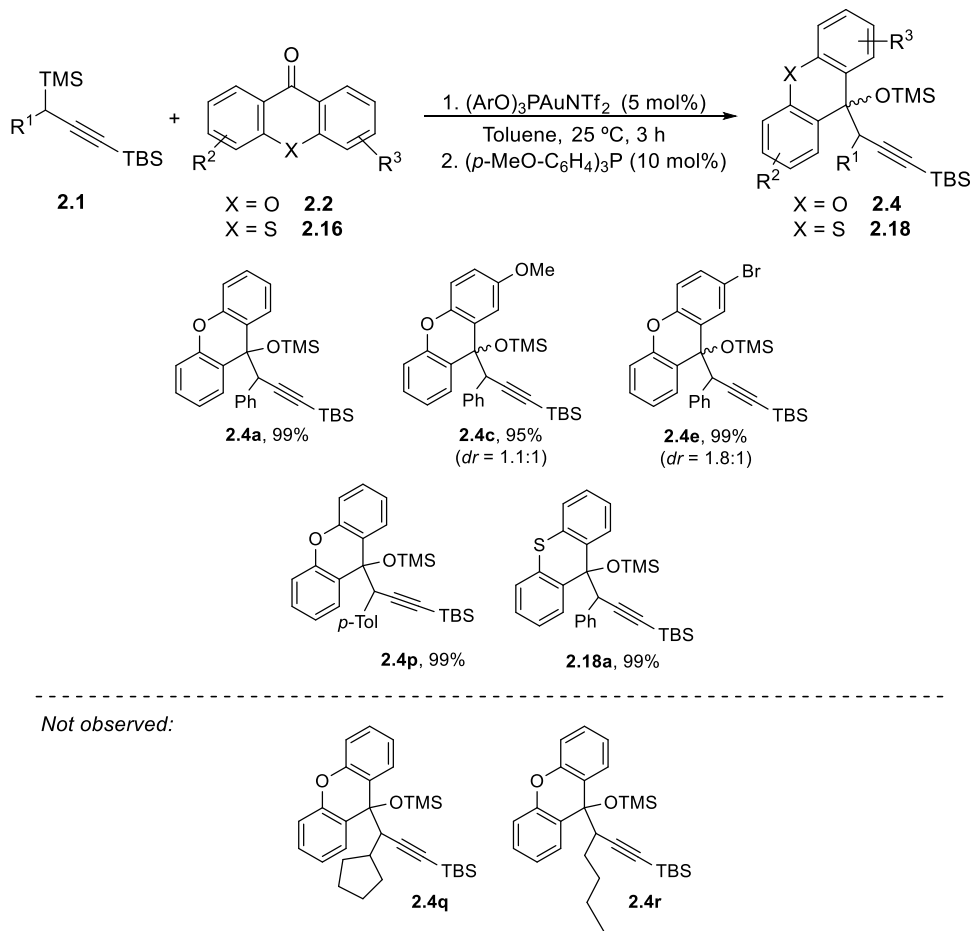
^aYield determined by ¹H-NMR using dibromomethane as internal standard. ^b2 h of reaction.

*Isolated yield.

Scheme 2.24: Solvent screening using thioxanthone **2.14a** as model substrate.

As it can be inferred from Scheme 2.24, non-polar solvents, such as hexane and toluene (*Entries 5-6*), and some coordinating non-chlorinated polar solvents, such as acetonitrile and 1,4-dioxane (*Entries 7-8*), prevent the second propargylation step. Moreover, it was also possible to reduce the amount of propargylsilane **2.1a** to 1.2 equivalents. Considering these results, toluene was chosen as optimum solvent for the selective monopropargylation process.

Once we established this model protocol, we turned our attention to the synthesis of representative examples of xanthrol silyl ethers **2.4** and thioxanthrol silyl ether **2.16a**. Thus, the reaction of different xanthenes **2.2** and thioxanthone **2.16a** with various aromatic and aliphatic propargylsilanes **2.1** was tested, and the results of this study are depicted in Scheme 2.25.

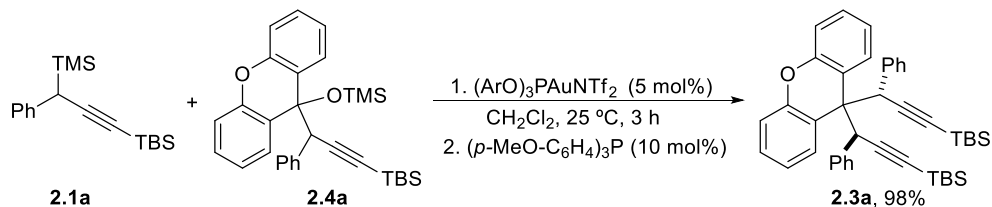


Scheme 2.25: Scope of the monopropargylation process.

In all the cases, the desired xanthydiol silyl ethers **2.4a,c,e,p** and thioxanthydiol silyl ether **2.18a** were obtained in almost quantitative yields, without any erosion of the yield due to bispropargylation reaction, even for xanthone **2.2a**, thioxanthone **2.11** or xanthone derivatives bearing strong electron-donating groups (compound **2.4e**). However, following this methodology it was not possible to obtain the corresponding xanthydiol silyl ethers **2.4q-r**, from aliphatic propargylsilanes.

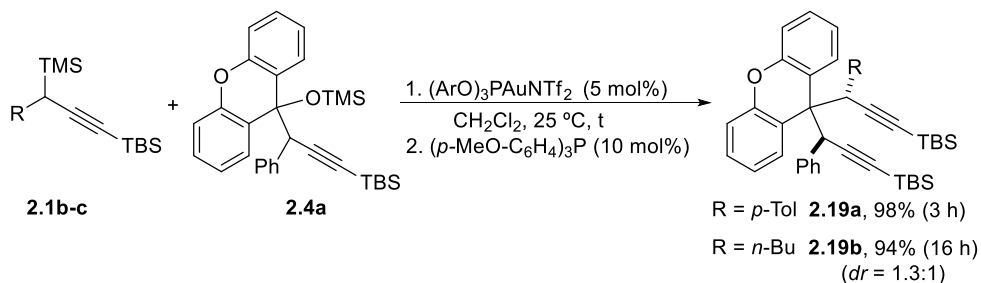
Once we were able to selectively isolate xanthydiol silyl ethers **2.4**, we headed our efforts to support their role as intermediates in the bispropargylation reaction, as outlined in the mechanistic proposal (Scheme 2.15). Therefore, a methylenechloride solution of xanthydiol silyl ether **2.4a** and propargylsilane **2.1a**

was treated under the standard gold-catalyzed bispropargylation conditions, generating 9,9-bispropargylxanthene **2.3a** in 98% yield, with total diastereoselectivity, and supporting our mechanistic proposal (Scheme 2.26).



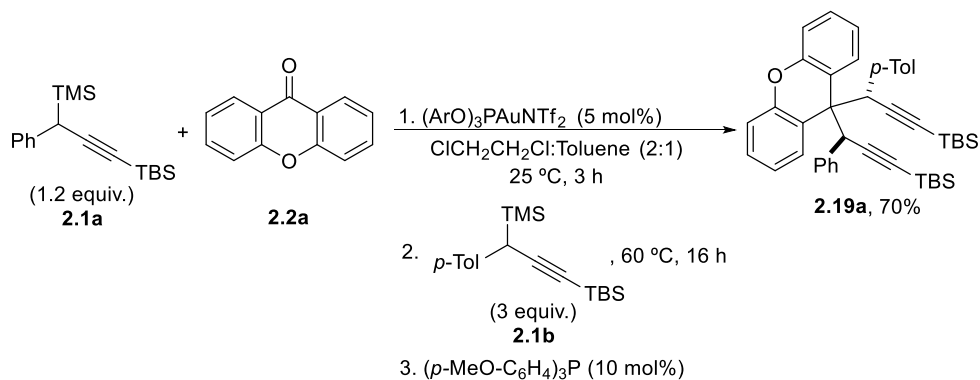
Scheme 2.26: Gold(I)-catalyzed synthesis of xanthene **2.3a** from xanthidrol **2.4a**.

The possibility of obtaining monopropargylated derivatives, through solvent modification, could also open the door to non-symmetrically bispropargylated xanthenes, isolating first the xanthidrol silyl ether **2.4** and introducing in a second step a different propargylsilane **2.1**. With this goal in mind, mixtures of xanthidrol silyl ether **2.4a** and propargylsilanes **2.1b-c** were treated under the standard reaction conditions, obtaining diastereoisomerically pure xanthene **2.19a** after 3 h, and xanthene **2.19b** as a mixture of two diastereoisomers after 16 h, in 98% and 94% yield, respectively (Scheme 2.27).



Scheme 2.27: Gold-catalyzed non-symmetrical propargylation of compound **2.4a**.

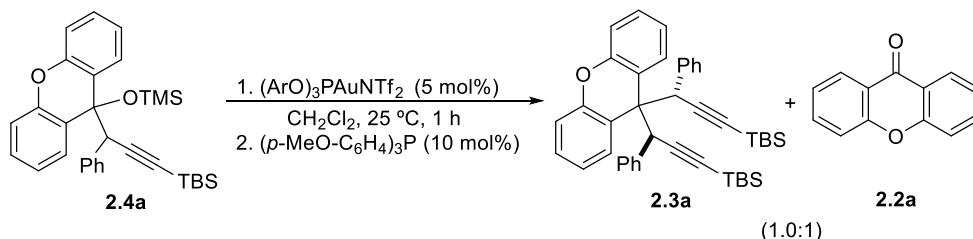
In addition, this procedure could also be optimized to establish a one-pot procedure for the synthesis of compound **2.19a** in a 70% yield, involving a double 'non-symmetrical' propargylation reaction, in an ordered and consecutive way, through the use of a mixture of 1,2-dichloroethane and toluene in a 2:1 ratio (Scheme 2.28).



Scheme 2.28: One-pot non-symmetrical bispropargylation reaction of xanthone **2.2a**.

❖ Disproportionation reaction of xanthidrol silyl ether **2.4a**.

During the optimization process for the one-pot non-symmetrical bispropargylation, it was found that xanthidrol silyl ether **2.4a** reacted, under the standard conditions, in the absence of propargylsilane **2.1a** to generate a mixture of 9,9-bispropargylxanthene **2.3a** and xanthone **2.2a**, in a roughly 1.0:1 ratio (Scheme 2.29). This transformation represents a formal disproportionation of xanthidrol silyl ether **2.4a** to afford the ‘oxidized’ xanthone **2.2a** and the ‘reduced’ xanthene **2.3a**.

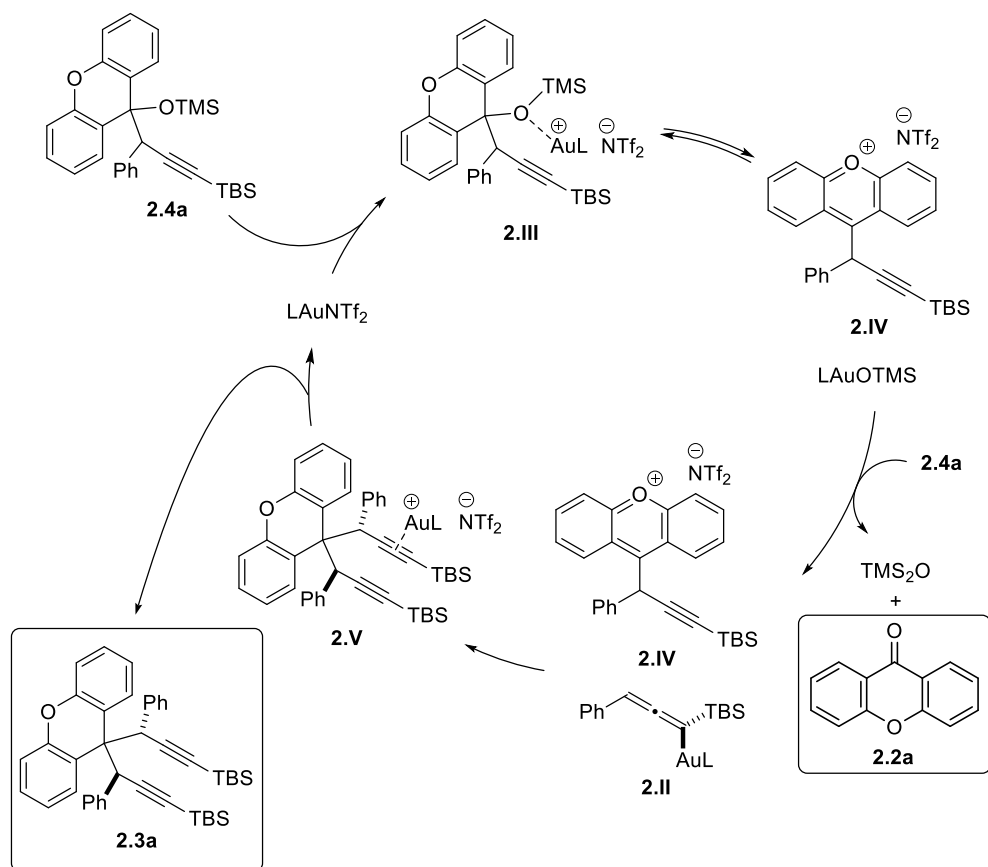


Scheme 2.29: Gold(I)-catalyzed disproportionation reaction of xanthidrol silyl ether **2.4a**.

In this regard, it is also interesting to mention a recently described disproportionation reaction of xanthidrols, without substitution at the carbon C9.²⁴ The authors found out that the treatment of these molecules with titanium

²⁴ Shi, Z.; Chen, S.; Xiao, Q.; Yin, D. *J. Org. Chem.* **2021**, *86*, 3334-3343.

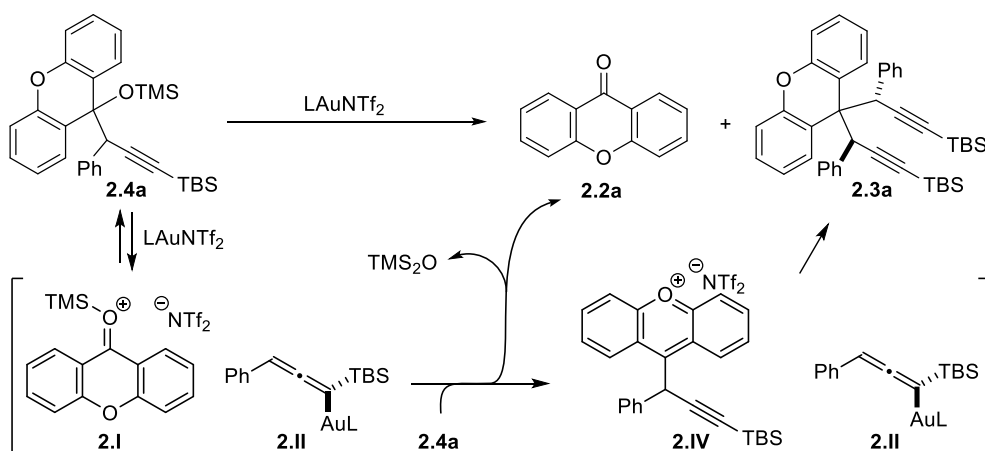
tetrachloride generated xanthenes and xanthenes. Several deuterium-labelled experiments suggested the formation of a xanthenylium carbocation upon acidic activation, followed by hydride transfer from another xanthidrol molecule, as the most probable mechanism. With this information in hand, we envisioned a possible mechanistic route for our observation, as outlined in Scheme 2.30.



Scheme 2.30: Mechanistic proposal for disproportionation reaction.

The process could be initiated by coordination of the gold(I) complex to the silyl ether moiety, acting as an oxophilic Lewis acid, leading to an equilibrium with stable xanthenylium intermediate **2.IV** and gold(I) trimethylsilyloxyate. This gold complex could desilylate a new molecule of xanthidrol silyl ether **2.4a**, which in turn would experiment a retropropargylation reaction to generate σ -allenyngold(I) complex **2.II** and xanthone **2.2a**. Finally, the propargylation process of xanthenylium **2.IV** and gold-decoordination of intermediate **2.V** would furnish the corresponding 9,9-bispropargylxanthene **2.3a**.

However, a different mechanistic pathway, considering a carbophilic activation of xanthrol silyl ether **2.4a**, could also be proposed as briefly described in Scheme 2.31. Thus, π -activation of the alkynylsilane moiety of **2.4a** by the gold(I) complex (intermediate **2.III**), could promote a retropropargylation reaction, generating σ -allenylgold(I) complex **2.II** and xanthylium intermediate **2.I**. Then, through coordination equilibria, another molecule of xanthrol silyl ether **2.4a** would be activated by the TMSNTf_2 , releasing xanthone **2.2a** and hexamethyldisiloxane, leading to xanthylium intermediate **2.IV** and converging with the previously proposed mechanism.

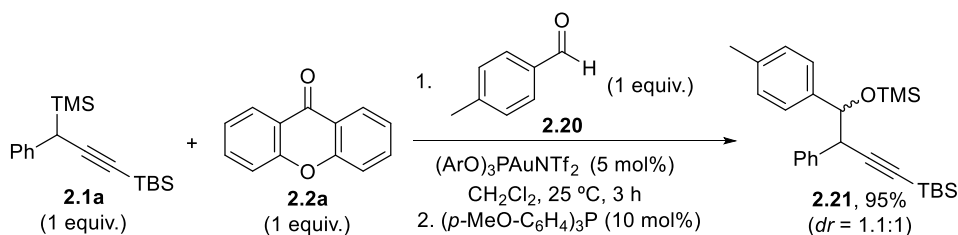


Scheme 2.31: Mechanistic proposal based on carbophilic activation of **2.4a**.

The main difference between both possibilities lies in the formation or not of TMSNTf_2 , a highly reactive silylium species. If TMSNTf_2 is generated, an external and more reactive carbonyl could be activated and propargylated, achieving a formal transpropargylation reaction. However, if silylium is not involved in the reaction mechanism, no transpropargylation product would be observed, as allenylgold(I) intermediates do not react with non-activated carbonyl compounds even in refluxing toluene (see Chapter I). Therefore, we envisioned that carrying out the disproportionation process in the presence of a suitable carbonyl compound could give some light about the mechanism.

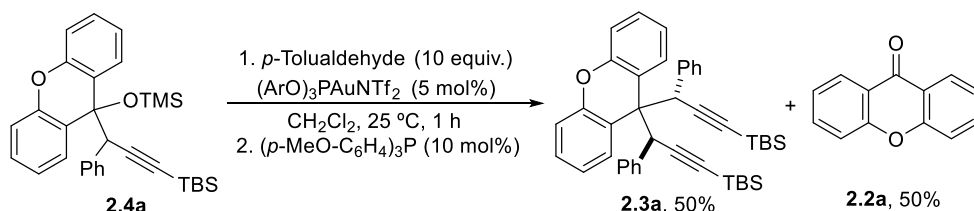
With this target in mind, in order to find an appropriate carbonyl derivative, a competition reaction between *p*-tolualdehyde **2.20** and xanthone **2.2a** was previously carried out under standard propargylation conditions, using model propargylsilane **2.1a** as nucleophile (Scheme 2.32). As result, aldehyde **2.20** was

propargylated in a full extension to give homopropargyl silyl ethers **2.21**, while xanthone **2.2a** did not react at all.



Scheme 2.32: Competition experiment between *p*-tolualdehyde **2.20** and xanthone **2.2a**.

Once we confirmed the faster reaction ratio for *p*-tolualdehyde **2.20** compared to xanthone **2.2a**, a disproportionation reaction of model xanthidrol silyl ether **2.4a** was carried out in the presence of 10 equivalents of *p*-tolualdehyde **2.20** (Scheme 2.33). In this experiment, 9,9-bispropargylxanthene **2.3a** and xanthone **2.2a** were obtained in a 50% yield each. The absence of traces of homopropargyl silyl ether **2.21** presumably supports the no-participation of TMSNTf₂ in this process, and the mechanistic proposal for the disproportionation reaction described in Scheme 2.30 could be operating.



Scheme 2.33: Disproportionation reaction in the presence of *p*-tolualdehyde **2.20**.

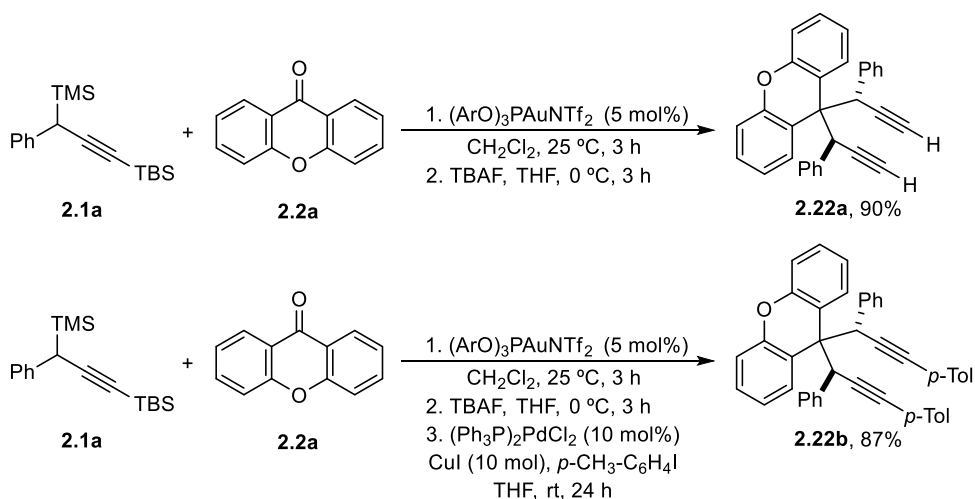
❖ Further synthetic transformations

Given the utility of 1,6-diynes in organic synthesis,²⁵ 9,9-bispropargyl xanthene skeleton could represent an interesting analogue which has not been reported yet.

²⁵ For selected reviews, see: a) Singidi, R. R.; Kutney, A. M.; Gallucci, J. C.; RajanBabu, T. V. *J. Am. Chem. Soc.* **2010**, *132*, 13078-13087; b) Xuan, J.; Studer, A. *Chem. Soc. Rev.* **2017**, *46*, 4329-4346; c) Marín-Luna, M; Nieto-Faza, O.; Silva-López, C. *Front. Chem.* **2019**, *296*, 1-22.

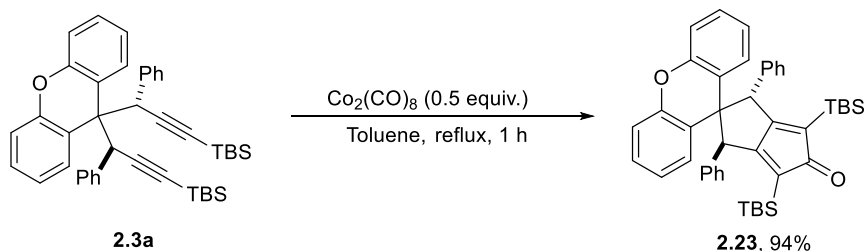
In this regard, derivatizations of 9,9-bispropargylxanthene **2.3a** were carried out to illustrate the synthetic potential of these molecules.

In a first approach, a simple silyl deprotection using tetrabutylammonium fluoride was *in situ* achieved after the gold catalytic cycle, without isolation of the intermediate 9,9-bispropargylxanthene **2.3a**. Following this methodology, xanthene **2.22a** was obtained in 90% yield (Scheme 2.34, *top*). Additionally, *in situ* deprotection followed by a double Sonogashira reaction was also successful, yielding xanthene **2.22b** in a high 87% yield (Scheme 2.34, *bottom*). This procedure could be considered as complementary to the bispropargylation process, since propargylsilanes **2.1** bearing an aryl group at the acetylenic position did not perform the gold-catalyzed propargylation reaction (*see Chapter I*).



Scheme 2.34: One-pot synthesis of 9,9-bispropargylxanthenes **2.22a-b**.

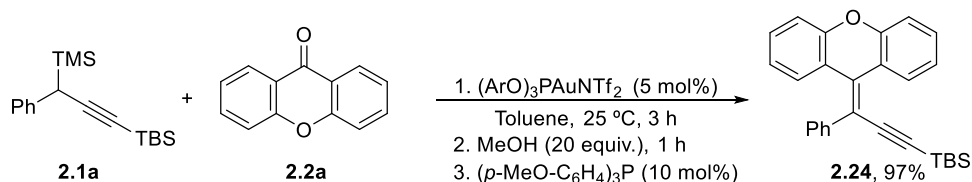
On the other hand, the possibility of accessing to spirocyclic structures through an intramolecular carbonylative [2+2+1] cyclization was also explored. Therefore, treating 9,9-bispropargylxanthene **2.3a** with cobalt octacarbonyl in refluxing toluene yielded compound **2.23** in 94% yield (Scheme 2.35). The structure of the spirocyclic cyclopentadienone **2.23** was confirmed by several NMR experiments.



Scheme 2.35: Intramolecular carbonylative [2+2+1] cyclization of xanthene **2.3a**.

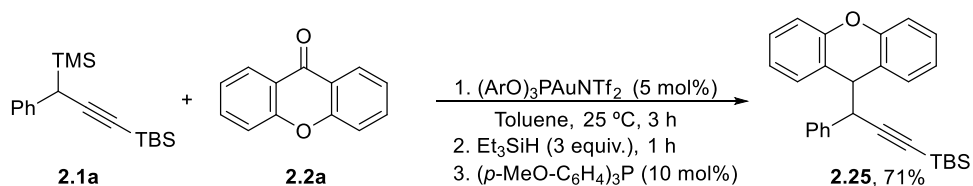
Additionally, considering that as far as we can ascertain no examples of 9-propargylxanthidols have been reported to date, we decided to also study their synthetic applicability.

In a first attempt, we decided to in situ deprotect xanthidol silyl ether **2.4a**, generated by selective gold-catalyzed monopropargylation reaction, adding methanol at the end the reaction. However, the desired xanthidol could not be isolated, as a dehydration reaction took place to generate xanthylidene **2.24** in 97% yield (Scheme 2.36), whose structure was determined by NMR experiments.



Scheme 2.36: One-pot synthesis of xanthylidene **2.24**.

Finally, given that there are no reported examples of 9-propargylxanthenes, we also considered the possibility of carrying out a monopropargylation reaction followed by in situ reduction of the xanthidol silyl ether. For this purpose, we added three equivalents of triethylsilane as reductant after the gold-catalyzed monopropargylation reaction of xanthone **2.2a**. Fortunately, 9-propargylxanthene **2.25** was obtained in a 71% yield (Scheme 2.37).



Scheme 2.37: One-pot synthesis of 9-propargylxanthene **2.25**.

In summary, starting from xanthone derivatives **2.2** or thioxanthone derivatives **2.16** and propargylsilanes **2.1**, it was possible to selectively obtain, under gold(I) catalysis, a collection of different xanthene derivatives with no bibliographic precedents (Figure 2.7). In this regard, 9-propargylxanthidols **2.4**, 9-propargylthioxanthidols **2.18**, xanthylidene **2.24**, 9-propargylxanthene **2.25**, 9,9-bispropargylxanthenes **2.3-2.22** and 9,9-bispropargylthioxanthenes **2.17** were obtained in a one-pot manner.

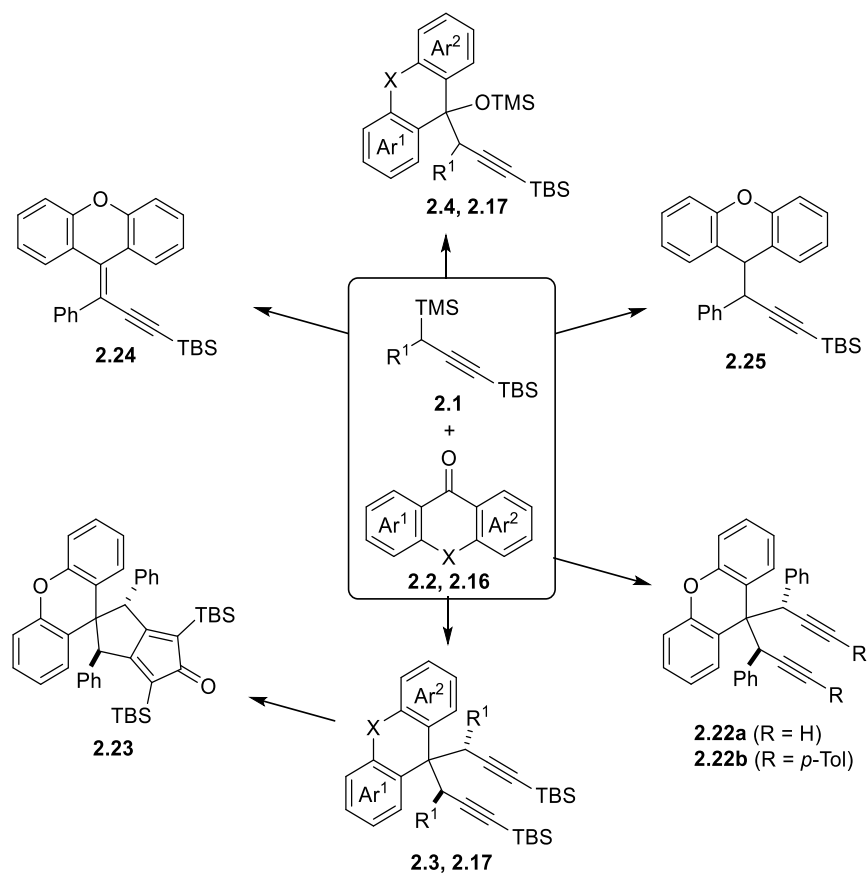


Figure 2.7: Different xanthenoid derivatives obtained from simple xanthone **2.2a**.

4 Conclusions

The first catalytic deoxygenative bispropargylation reaction has been described. The reaction is performed under mild conditions by a phosphitegold(I) triflimidate as catalyst, using xanthone derivatives as electrophiles and propargylsilanes as nucleophiles.

The mechanistic proposal for this transformation involves a synergistic gold(I)-silylium catalysis, involving the participation of two equivalents of a σ -allenylgold(I) and two different xanthenylium carbocations as intermediates. The stability of these intermediates is supposed to favour the second propargylation step, as several control experiments have demonstrated.

It has been developed a simple and totally diastereoselective protocol for the synthesis of 9,9-bispropargylxanthene and thioxanthene derivatives, in excellent yields. The transformation also tolerates a wide range of substitution pattern of xanthenes and thioxanthenes, as well as different aromatic and aliphatic propargylsilanes.

A selective monopropargylation reaction, achieved by solvent tuning, has been described for the synthesis of several propargylxanthanol and thioxanthanol silyl ethers, and the role of these compounds as reaction intermediates has been proved. In addition, this methodology has allowed to obtain some non-symmetrically substituted 9,9-bispropargylxanthenes in a stepwise or one-pot manner.

The gold(I)-catalyzed formal disproportionation reaction of a 9-propargylxanthrol silyl ether has been detailed, obtaining a 9,9-bispropargylxanthene and xanthone under mild conditions. Several control experiments allowed us to determine that this reaction occurs through oxophilic activation of the xanthrol, followed by a transpropargylation reaction.

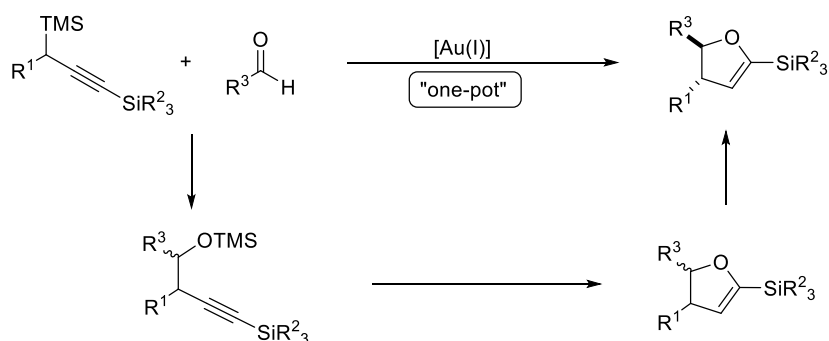
Further functionalization of the obtained 9,9-bispropargylxanthene derivatives have also been carried out to illustrate their synthetic potential, giving rise to a family of xanthenoid derivatives.

Chapter III:

Gold-catalyzed synthesis of 2-silyl-4,5-dihydrofurans

1 Introduction

In this Chapter is described a gold-catalyzed procedure for the synthesis of *trans*-2-silyl-4,5-dihydrofurans starting from propargylsilanes and aromatic aldehydes. It involves four steps: a) propargylation process as described in Chapter I; b) deprotection of a homopropargyl silyl ether; c) cycloisomerization of a 1-alkyn-4-ol and d) *cis-to-trans* isomerization (Scheme 3.1).



Scheme 3.1: Transformation studied in this Chapter.

The reaction can be also carried out in a *one-pot* manner without erosion of the yield. In addition, several isotopically labelled experiments, intramolecular trapping of a proposed intermediate and a Hammett plot, have been performed to experimentally support the mechanistic proposal.

2 Bibliographic background

2.1 Dihydrofurans in organic synthesis

Oxygenated five-membered rings are very important structures in natural occurring products.¹ In this field, dihydrofurans, which can be classified according to the dihydro unit position in the cycle as 2,3- or 2,5-dihydrofurans, frequently appear as a subunit in molecules with biological activity. Apparently, 2,5-dihydrofurans are more common scaffolds in nature than their isomers, and can be found in compounds ranging from simple molecules, as the antibiotic Furanomycin,² to complex structures, such as the cytotoxic agent Eleutherobin (Figure 3.1).³

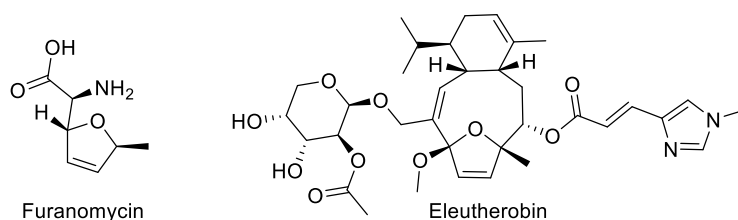


Figure 3.1: Examples of naturally occurring 2,5-dihydrofurans.

¹ a) Majumdar, K. C.; Chattopadhyay, S. K. *Heterocycles in Natural Product Synthesis*; Wiley-VCH: Weinheim, **2011**, 99; b) Jacques, R.; Pal, R.; Parker, N. A.; Sear, C. E.; Smith, P. W.; Ribaucourt, A.; Hodgson, D. M. *Org. Biomol. Chem.* **2016**, *14*, 5875-5893.

² Kang, S. H.; Lee, S. B. *Chem. Commun.* **1998**, 761-762.

³ Lindel, T.; Jensen, P. R.; Fenical, W.; Long, B. H.; Casazza, A. M.; Carboni, J.; Fairchild, C. R. *J. Am. Chem. Soc.* **1997**, *119*, 8744-8745.

On the other hand, 2,3-dihydrofurans are less common in the skeleton of biomolecules, but they also appear with a wide range of complexity and biofunctionality. Two examples of this type of compounds are given in Figure 3.2, such as Azadirachtin, which is used as a potent insecticide;⁴ and Glabramycin C, a strong antibiotic agent against *Streptococcus pneumoniae*.⁵

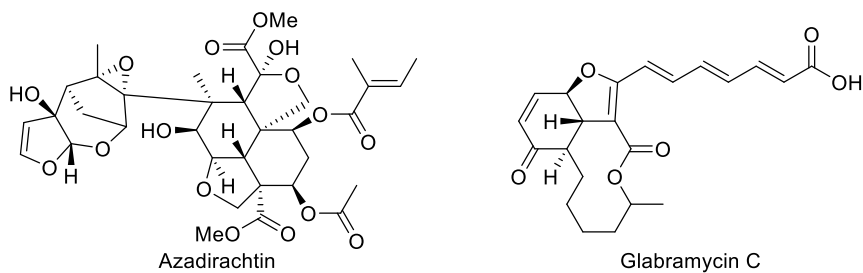
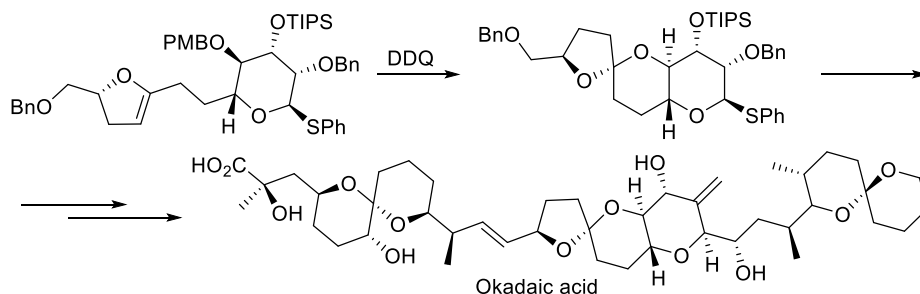


Figure 3.2: Natural products with a 2,3-dihydrofuran subunit.

Both isomers have proved to be interesting synthons in organic synthesis, as they can be easily functionalized, reduced and oxidized. However, 2,3-dihydrofurans own an additional synthetic potential compared to their counterparts, arising from their enol ether character, that allows to access to attractive complex spirocyclic skeletons.⁶ As an illustrative example, in Scheme 3.2 is described this type of behaviour in the synthesis of Okadaic acid.⁷ Thus, after the DDQ-induced PMB deprotection of its precursor, a spontaneous spiroacetalization of the 2,3-dihydrofuran moiety furnishes the key intermediate of this route.



Scheme 3.2: Spiroacetalization of a 2,3-dihydrofuran in the synthesis of Okadaic acid.

⁴ Mordue(Luntz), A. J.; Nisbet, A. J. *An. Soc. Entomol. Brasil* **2000**, *29*, 615-632.

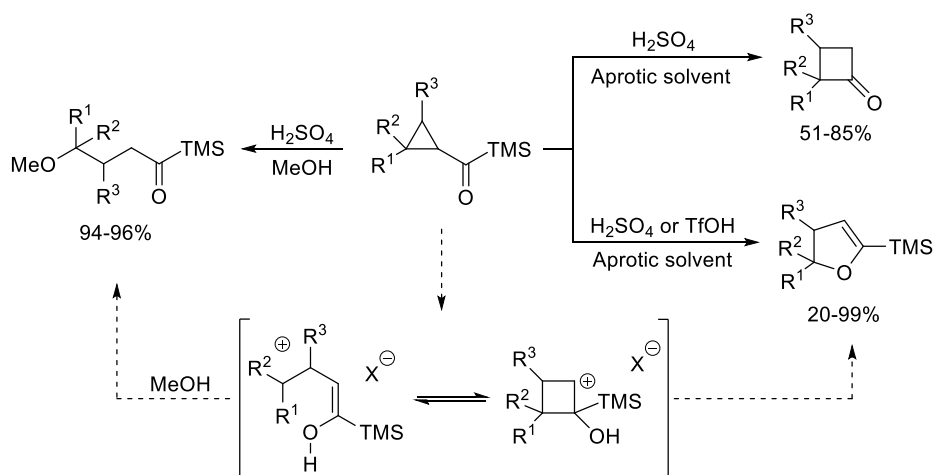
⁵ Jayasuriya, H.; Zink, D.; Basilio, A.; Vicente, F.; Collado, J.; Bills, G.; Goldman, M. L.; Motyl, M.; Huber, J.; Dezeny, G.; Byrne, K.; Singh, S. B. *J. Antibiot.* **2009**, *62*, 265-269.

⁶ Chupakhin, E.; Babich, O.; Prosekov, A.; Asyakina, L.; Krasavin, M. *Molecules* **2019**, *24*, 4165-4201.

⁷ Fuwa, H.; Sakamoto, K.; Muto, T.; Sasaki, M. *Tetrahedron* **2015**, *71*, 6369-6383.

Regarding the experimental conditions for the generation of 2,3-dihydrofurans, since the first direct synthesis was described by Gianturco in 1965,⁸ a wide range of synthetic strategies have been designed for this target. Transition metal catalysts, oxophilic and carbophilic, are key tools in most of these studies, although metal-free procedures have also been described.⁹

A very representative protocol of the metal-free approaches to these compounds, based in a ring-expansion reaction, was described by Nakajima and co-workers.¹⁰ Thus, starting from cyclopropyl acylsilanes, activation by a Brønsted acid catalyst leads to a cyclobutyl carbocation intermediate, with two possible evolution pathways depending on the substituents and the solvent, generating γ -methoxyacylsilanes, cyclobutanones or 2-silyl-4,5-dihydrofurans (Scheme 3.3).



Scheme 3.3: Acid-catalyzed ring-opening of cyclopropyl acylsilanes.

On the other hand, Danheiser¹¹ and Evans¹² illustrated perfectly how to obtain these scaffolds from allenylsilanes and carbonyl compounds in an intermolecular

⁸ Gianturco, M. A.; Friedel, P.; Flanagan, V. *Tetrahedron Lett.* **1965**, *23*, 1847-1852.

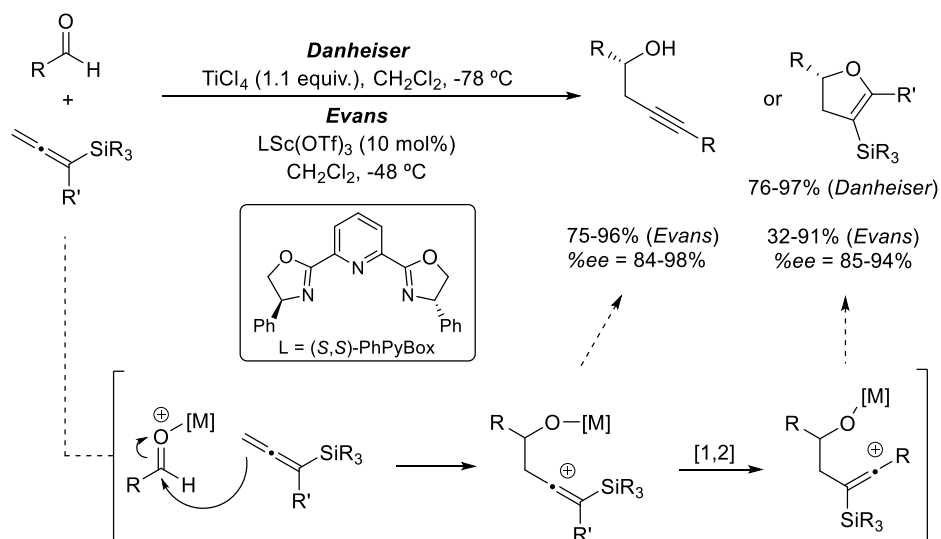
⁹ Kilroy, T. G.; O'Sullivan, T. P.; Guiry, P. J. *Eur. J. Org. Chem.* **2005**, 4929-4949.

¹⁰ a) Nakajima, T.; Segi, M.; Mituoka, T.; Fukute, Y.; Honda, M.; Naitou, K. *Tetrahedron Lett.* **1995**, *36*, 1667-1670; b) Honda, M.; Naitou, T.; Hoshino, H.; Takagi, S.; Segi, M.; Nakajima, T. *Tetrahedron Lett.* **2005**, *46*, 7345-7348.

¹¹ Danheiser, R. L.; Kwasigroch, C. A.; Tasi, Y.-M. *J. Am. Chem. Soc.* **1985**, *107*, 7233-7235.

¹² Evans, D. A.; Sweeney, Z. K.; Rovis, T.; Tedrow, J. S. *J. Am. Chem. Soc.* **2001**, *123*, 12095-12096.

way, employing oxophilic transition metal catalysts (Scheme 3.4). In this regard, the activation of the carbonyl group by coordination of the catalyst allows nucleophilic attack of the allenylsilane. When the silyl substituent is bulky enough, a [1,2]-silyl migration takes place, leading to the final products after ring closing. In the example reported by Evans, the proposed homopropargyl silyl ether could be in situ hydrolyzed, and isolated as the corresponding alcohols, or cycloisomerized to obtain 3-silyl-4,5-dihydrofurans. For both derivatives, high enantiomeric excesses and yield were achieved employing an enantiopure scandium(III) catalyst.

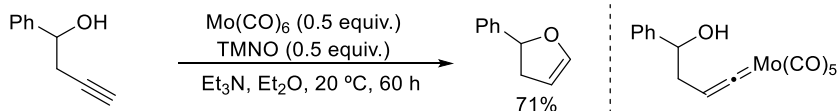


Scheme 3.4: Intermolecular synthesis of 3-silyl-4,5-dihydrofurans.

Finally, carbophilic activation to furnish these compounds is also possible, as reported for the first time by McDonald and co-workers.¹³ In this work, in-situ generated (pentacarbonyl)(trimethylamine)molybdenum(0), from molybdenum(0) hexacarbonyl and trimethylamine *N*-oxide (TMNO), can promote 1-alkyn-4-ols cycloisomerization through formation of a vinylidene intermediate (Scheme 3.5). Similar methodologies invoking these intermediates, upon σ -activation of the alkyne, have been described for different transition metals, such as Rh¹⁴ and Ru.¹⁵

¹³ McDonald, F. E.; Connolly, C. B.; Gleason, M. M.; Towne, T. B.; Treiber, K. D. *J. Org. Chem.* **1993**, *58*, 6952-6953.

¹⁴ Trost, B. M.; Rhee, Y. H. *J. Am. Chem. Soc.* **2003**, *125*, 7482-7483.

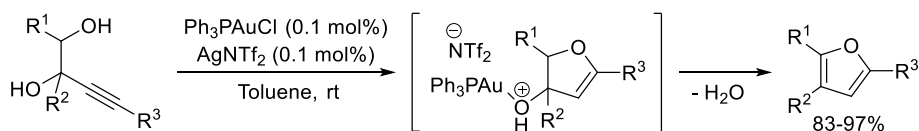


Scheme 3.5: First described carbophilic cycloisomerization of 1,4-alkynols.

Catalytic π -activation of alkynes with carbophilic transition metals, such as gold or platinum, has become a powerful tool for the synthesis of heterocycles. One of the most studied reactions of this family is the intramolecular alkoxylation of alkynes, being the cycloisomerization of 1,*n*-alkynols particularly interesting for obtaining oxygenated heterocycles with different ring sizes. As this *Chapter* is focused on the synthesis of 2,3-dihydrofurans through gold(I)-catalyzed 1,4-alkynol cyclization, some aspects of this reaction are discussed below.

2.2 Gold-catalyzed isomerization of 1,4-alkynols

In comparison to their higher homologues, cycloisomerization of 1,4-alkynols has received less attention from a synthetic point of view, in the field of homogeneous gold catalysis. In contrast, they have been widely employed for further cascade transformations, especially aromatization to furans and acetalization. An example of cyclization-aromatization is given in Scheme 3.6. Thus, after the hydroalkoxylation of the alkyne, the gold(I) catalysts can act as an oxophilic Lewis acid, assisting the dehydration process to obtain the aromatic five-membered ring.¹⁶ This methodology has been also used for synthesizing a thiamine diphosphate (biologically active form of Vitamin B1) analogue.^{16c}

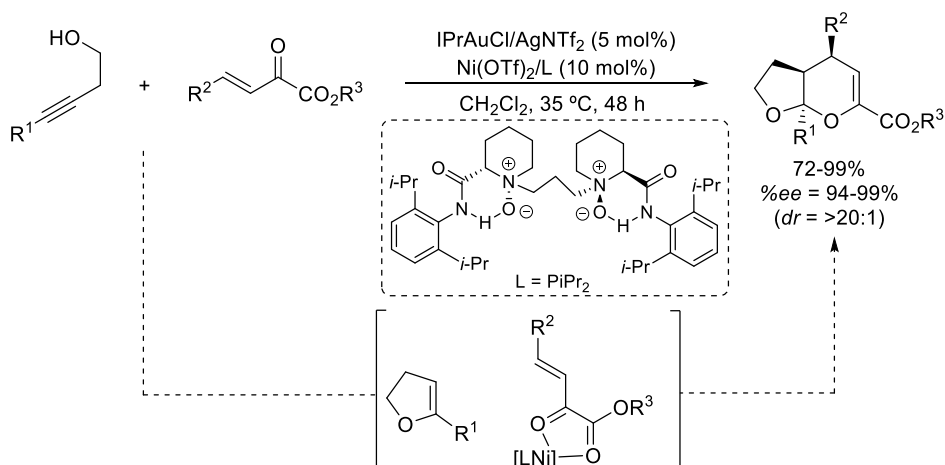


Scheme 3.6: Gold-catalyzed synthesis of furans from alkynyl diols.

¹⁵ a) Liu, P. N.; Su, F. H.; Wen, T. B.; Sung, H. H.-Y.; Williams, I. D.; Jia, G. *Chem. Eur. J.* **2010**, *16*, 7889-7897; b) Cai, T.; Yang, Y.; Li, W. -W.; Qin, W. -B.; Wen, T. B. *Chem. Eur. J.* **2018**, *24*, 1606-1618.

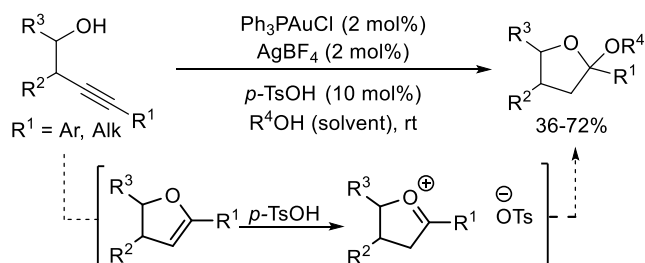
¹⁶ a) Aponick, A.; Li, C.-Y.; Malinge, J.; Marques, E. F. *Org. Lett.* **2009**, *11*, 4624-4627; b) Egi, M.; Azechi, K.; Akai, S. *Org. Lett.* **2009**, *11*, 5002-5005; c) Iqbal, A.; Sahraoui, E. H.; Leeper, F. J. *Beilstein J. Org. Chem.* **2014**, *10*, 2580-2585.

As another interesting example of 2,3-dihydrofurans synthesis followed by further evolution, a recent work for the synthesis of bicyclic *O,O*- and *N,O*-acetals, through gold(I)/nickel(II) bimetallic catalysis, can be mentioned.¹⁷ As it is outlined in Scheme 3.7, starting from a simple 1,4-alkynol, a 2,3-dihydrofuran intermediate is obtained via gold(I) catalysis. Then, after activation of the ester derivative by a nickel catalyst, an inverse electron-demand hetero Diels-Alder reaction occurs.



Scheme 3.7: Gold(I)/Nickel(II) bimetallic catalysis for the synthesis of bicyclic fused acetals.

In a work closely related with the present dissertation, a remarkable transformation for the synthesis of 2-alkoxytetrahydrofurans was described by Belting and Krause.¹⁸ In this case, a Brønsted acid is used for boosting acetal formation in a multicomponent reaction (Scheme 3.8). This transformation proves, that gold(I) activation of the enol ether is also possible, as the final products are obtained even in the absence of the acid, although in longer reaction times.



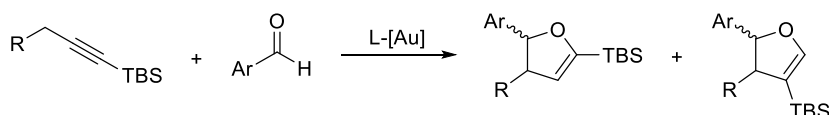
Scheme 3.8: Gold(I)-catalyzed cyclization-acetalization of 1,4-alkynols.

¹⁷ Hu, B.; Li, J.; Cao, W.; Lin, Q.; Yang, J.; Lin, L.; Liu, X.; Feng, X. *Adv. Synth. Catal.* **2018**, *360*, 2831-2835.

¹⁸ Belting, V.; Krause, N. *Org. Lett.* **2006**, *8*, 4489-4492.

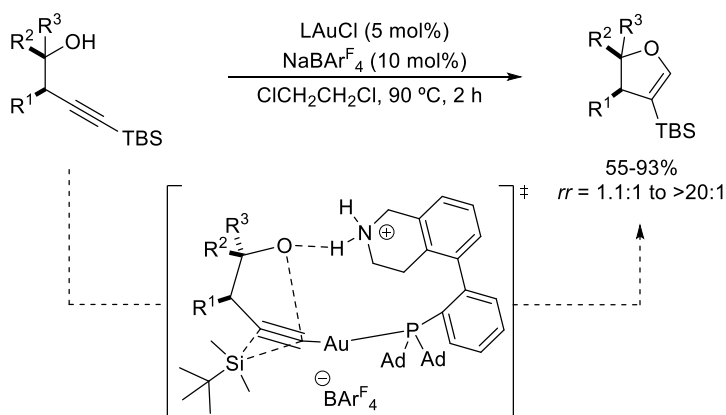
Finally, focusing in the use of alkynylsilanes, scarce examples of gold-catalyzed cyclizations of 1-silyl-1,*n*-alkynols have been reported.¹⁹

In this sense, Zhang's group described a synthesis of 2-silyl- and 3-silyl-substituted 4,5-dihydrofurans, already mentioned in *Chapter I*, which is summarized in Scheme 3.9.²⁰ However, this methodology was not regio- or diastereoselective, since the [1,2]-silyl migration was not under control and the mixture of *cis/trans* diastereoisomers were always obtained.



Scheme 3.9: Gold(I)-catalyzed propargylation-cycloisomerization of aromatic aldehydes.

Further research reported by the same group described a regioselective cycloisomerization of *syn*-1-silyl-1-alkyn-4-ols to *cis*-3-silyl-4,5-dihydrofurans through a controlled [1,2]-silyl migration (Scheme 3.10).²¹ Careful design of the gold catalyst (see transition state; Ad = adamantyl) and the reaction conditions favoured this transformation, although *anti*-alkynols remained unreactive.



Scheme 3.10: Gold(I)-catalyzed intramolecular synthesis of *cis*-3-silyl-4,5-dihydrofurans.

¹⁹ Hashmi, A. S. K.; Schafer, S.; Wolfle, M.; Gil, C. D.; Fischer, P.; Laguna, A.; Blanco, M. C.; Gimeno, M. C. *Angew. Chem. Int. Ed.* **2007**, *46*, 6184-6186.

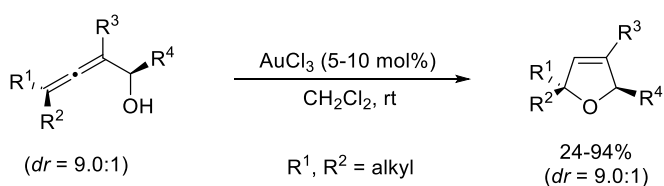
²⁰ Li, T.; Zhang, L. *J. Am. Chem. Soc.* **2018**, *140*, 17439-17443.

²¹ Li, T.; Yang, Y.; Li, B.; Bao, X.; Zhang, L. *Org. Lett.* **2019**, *21*, 7791-7794.

It is worth to mention that these two works contributed to enlarge the number of synthetic approaches to 3-silyl-4,5-dihydrofurans, both inter- and intramolecular, respectively. However, selective intermolecular synthesis of 2-silyl-4,5-dihydrofurans remained unexplored.

2.3 Gold(I)-catalyzed ring-opening *cis-to-trans* isomerization processes

As previously stated, gold-catalyzed cycloisomerization reactions of alkynes or allenes bearing an heteronucleophile are valuable tools for the stereoselective construction of heterocycles. Moreover, these transformations usually proceed with total transfer of the pre-existing stereochemistry (Scheme 3.11).²²



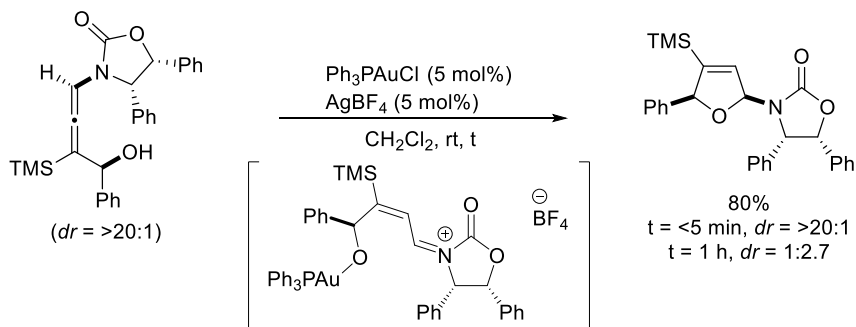
Scheme 3.11: Stereoretentive cyclization of α -allenols.

However, several examples have been reported involving a loss of the chirality transfer, probably due to gold-catalyzed ring opening-closing mechanisms.²³ In this sense, an interesting example of gold-catalyzed cyclization of hydroxy allenamides was reported by Hyland and Hegedus.²⁴ They found out that allenamide reacts in the presence of a gold(I) catalyst to yield *cis*-2,5-dihydrofurans with excellent regioselectivity (Scheme 3.12). However, longer reaction times led to a mixture of *cis-trans* isomers, indicating a ring-opening after coordination of the gold catalyst eased by assistance of the nitrogen atom.

²² Hoffmann-Röder, A.; Krause, N. *Org. Lett.* **2001**, *3*, 2537-2538.

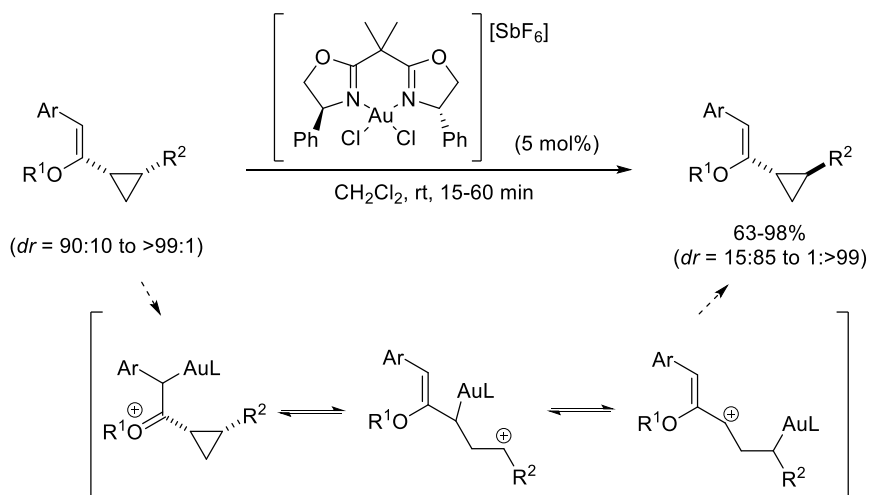
²³ a) Yeager, A. R.; Min, G. K.; Porco, J. A.; Schaus, S. E. *Org. Lett.* **2006**, *8*, 5065-5068; b) Deutsch, C.; Gockel, B.; Hoffmann-Röder, A.; Krause, N. *Synlett* **2007**, *11*, 1790-1794; c) Sawama, Y.; Sawama, Y.; Krause, N. *Org. Lett.* **2009**, *11*, 5034-5037.

²⁴ Hyland, C. J. T.; Hegedus, L. S. *J. Org. Chem.* **2006**, *71*, 8658-8660.



Scheme 3.12: Catalytic cyclization-isomerization of an allenamide-allenol.

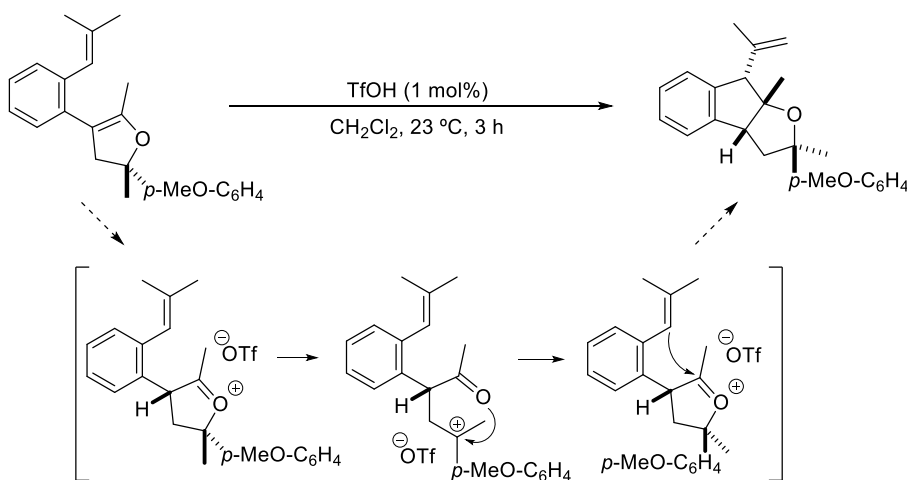
In addition to the mentioned transformations involving an oxophilic activation of the substrates, Fiksdahl and co-workers described a gold-catalyzed *cis-to-trans* isomerization of vinylcyclopropanes, by presumable carbophilic activation (Scheme 3.13).²⁵ The authors proposed that, following usual enol ether reactivity, the first step could imply a nucleophilic attack to the gold complex affording an oxonium intermediate. Then, consecutive metallotropic rearrangements, involving C-C bond dissociation, lead to a carbocationic intermediate, achieving *trans* configuration after ring-closing.



Scheme 3.13: Gold-catalyzed *cis-to-trans* isomerization of vinylcyclopropanes.

²⁵ Reiersølmoen, A. C.; Østrem, E.; Fiksdahl, A. *Eur. J. Org. Chem.* **2018**, 25, 3317-3325.

However, this type of epimerization has never been observed for 2,3-dihydrofurans under gold catalysis, even considering their great applicability for studying the hydroalkoxylation mechanism. To the best of our knowledge, a single example of *cis-to-trans* isomerization reaction, catalyzed by a Brønsted acid, of 2,3-dihydrofurans can be found,²⁶ and it is depicted in Scheme 3.14.



Scheme 3.14: Acid-catalyzed isomerization-alkylation of 2,3-dihydrofurans.

The strongly acidic catalyst generates an oxonium intermediate, following the reactivity pattern of enol ethers. Then, a transitory cleavage of the carbon-oxygen bond takes place, generating a carbocationic intermediate and, after free rotation along the single bond and ring-closure, the epimerized fused tetrahydrofuran is obtained.

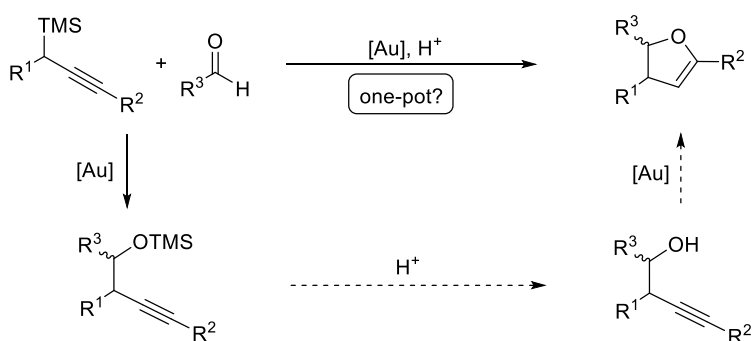
²⁶ Li, C.-W.; Lin, G.-Y.; Liu, R.-S. *Chem. Eur. J.* **2010**, *16*, 5803-5811.

3 Results and discussion

3.1 Synthesis of 2-silyl-4,5-dihydrofurans

Taking into account the results reported in *Chapter I* for the high-yielding gold-catalyzed propargylation of carbonyl compounds, we envisioned the possibility of involving a second catalytic cycle to form 2-silyl-4,5-dihydrofurans, interesting molecules without any selective one-pot synthesis described in the literature.

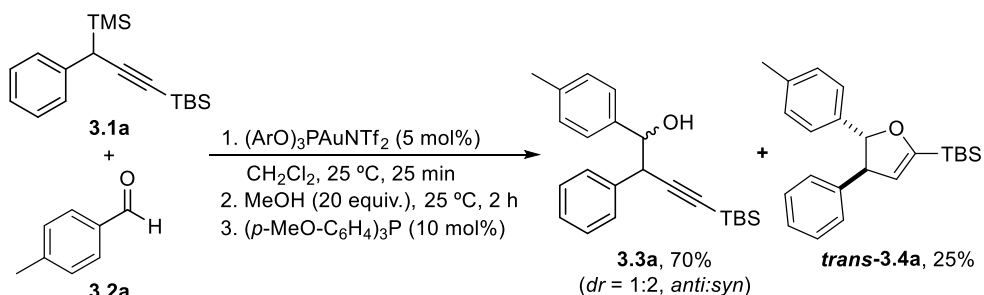
As a working hypothesis for this transformation, the gold(I) complex, after catalyzing the propargylation reaction, could desilylate the homopropargyl silyl ether in the presence of a proton source, and in turn activate the alkynylsilane moiety for the cycloisomerization step (Scheme 3.15).



Scheme 3.15: Working hypothesis for the one-pot synthesis of 2-silyl-4,5-dihydrofurans.

With this target in mind, we decided to start the study employing propargylsilane **3.1a** and *p*-tolualdehyde **3.2a** as model substrates, following the

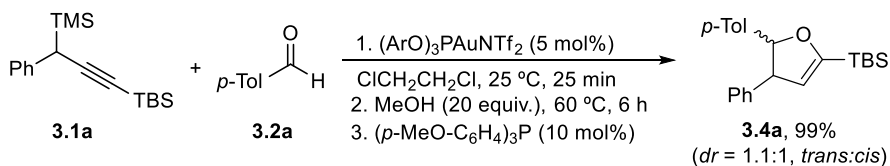
optimized conditions for the propargylation process (see *Chapter I*). In a second step, we tested methanol as proton source for hydroxyl group deprotection (Scheme 3.16). Finally, a 10 mol% of (*p*-MeO-C₆H₄)₃P was added at the end of the reaction to inactivate the catalyst and avoid potential decomposition processes.



Scheme 3.16: Initial results for the studied transformation.

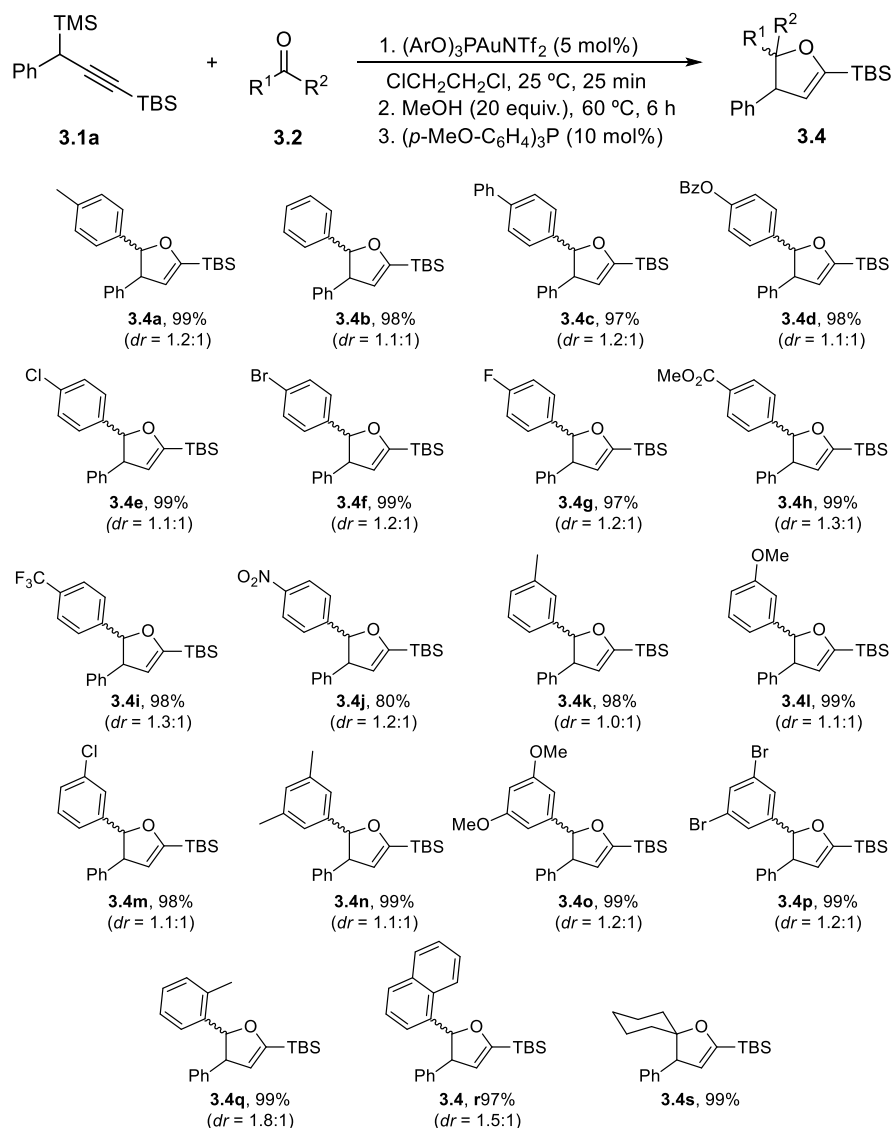
After two hours of reaction with methanol, at room temperature, we observed a complete solvolysis of the silyl ether to generate homopropargyl alcohols **3.3a** and the incipient formation of the target 2-silyl-4,5-dihydrofurans **3.4a**. Relevantly, only the *anti*-isomer seems to cycloisomerize under these conditions to furnish **trans-3.4a**. Longer reaction times (from eight to sixteen hours) at room temperature gave exclusively a mixture of **syn-3.3a** and **trans-3.4a**. The structure and stereochemical assignments were determined by selective NMR techniques, including selective nOe experiments

Next, after optimizing the reaction conditions for improving the cycloisomerization step, we decided to carry out the whole process in 1,2-dichloroethane, with a 5 mol% of the gold(I) catalyst and heating the mixture at 60 °C after methanol addition. Following this procedure, dihydrofurans **3.4a** were obtained after six hours of reaction in quantitative yield and as almost equimolecular amount of both *cis/trans* isomers (Scheme 3.17).



Scheme 3.17: Gold(I)-catalyzed *one-pot* propargylation-deprotection-cyclization.

With these results in hand, we decided to explore the scope of the reaction employing suitable carbonyls **3.2** and different propargylsilanes **3.1**. First, we tested the behaviour of the cyclization for different aromatic aldehydes²⁷ and ketones (Scheme 3.18).

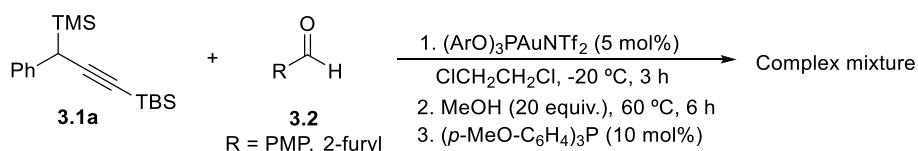


Scheme 3.18: Scope of the reaction in terms of carbonyl compound **3.2**.

²⁷ As mentioned in *Chapter I*, aliphatic aldehydes do not perform propargylation reaction due to the presence of acidic protons in *alpha* to the carbonyl group.

As it can be inferred from Scheme 3.18, the reaction proceeded with excellent yields starting from aromatic aldehydes as benzaldehyde and also with arene rings with a wide range of substitution pattern. In this sense, excellent yields were obtained with benzaldehyde derivatives bearing electron-donating (**3.4a-c,k-l,n-o,q**) to electron-withdrawing (**3.4d-j,m,p**). Similarly, 1-naphthaldehyde was also suitable for dihydrofurans formation (**3.4r**).

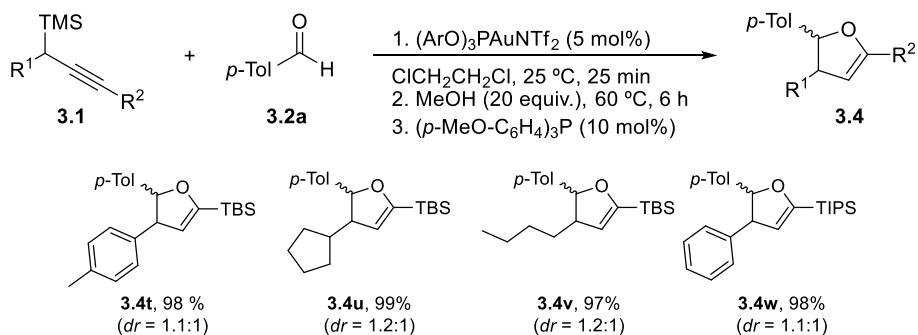
However, aromatic aldehydes bearing strong electron-donating groups in *para* position of the arene ring or heterocyclic aldehydes gave rise to complex mixtures (Scheme 3.19).



Scheme 3.19: Limitations in the carbonyl nature of the studied reaction.

Related to aromatic ketones, such as benzophenone or acetophenone derivatives, they did not cyclize under these conditions but reacted in a different way. This transformation will be further discussed in *Chapter IV*. However, an aliphatic ketone such as cyclohexanone gave rise to the corresponding spirocyclic compound **3.3s** in almost quantitative yield.

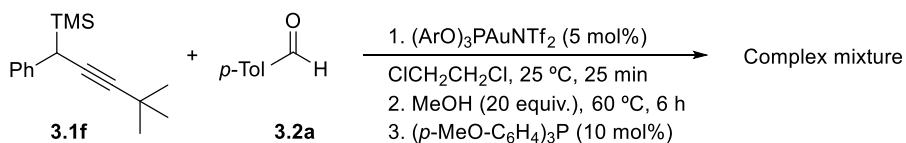
As the next step, we tested the reactivity of different propargylsilanes **3.1b** which proved to be suitable for propargylation step, changing the substituents at the propargylic carbon and also at the acetylenic position (Scheme 3.20).



Scheme 3.20: Scope of the reaction in terms of propargylsilane **3.1** substitution pattern.

As expected, *p*-tolyl substituted propargylsilane furnished product **3.4t** in high yield. Also, different aliphatic propargylsilanes worked well (products **3.4u-v**), and even a bulkier silyl group as TIPS group in the alkyne moiety was tolerated (**3.4w**).

A propargylsilane with a *tert*-butylalkynyl derivative **3.1f** was also tested. However, this system was not suitable for this transformation, leading again to a complex mixture (Scheme 3.21). This outcome is in agreement with previous studies, as 1-*tert*-butyl-1,4-alkynols did not isomerize to the corresponding dihydrofurans under gold catalysis.²⁸

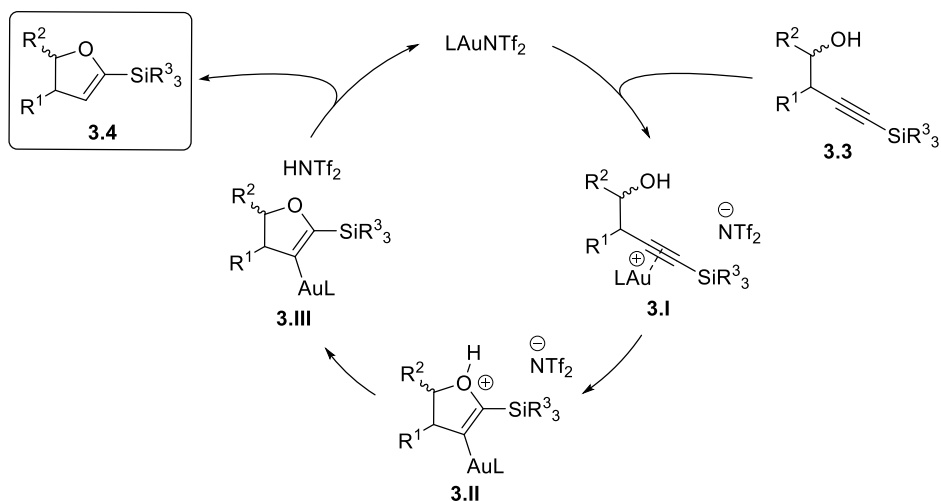


Scheme 3.21: Limitations in the propargylsilane scope of the reaction.

The reported results show the great applicability of this methodology for the synthesis of 2-silyl-4,5-dihydrofurans, in an intermolecular way, starting from a broad variety of aldehydes or aliphatic ketones, and propargylsilanes. As it has been described, the reaction occurs in a one-pot procedure with excellent yields and in a regioselective manner. In contrast to Zhang's group reported gold(I)-catalyzed propargylation,²⁹ only 2-silyl-4,5-dihydrofurans were obtained in all the cases, and no traces of 3-silyl-4,5-dihydrofurans formation were observed. Taking this into account, a mechanism pathway through 5-*endo*-dig cyclization, after deprotection of the homopropargyl silyl ethers, could be formulated, as follows (Scheme 3.22).

²⁸ Belting, V.; Krause, N. *Org. Lett.* **2006**, *8*, 4489-4492.

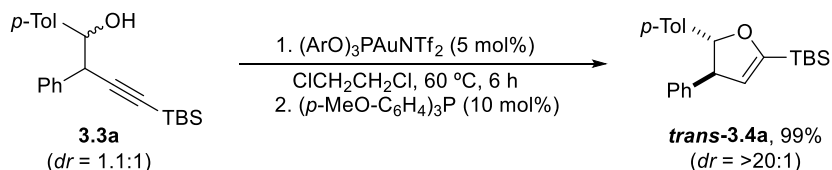
²⁹ Li, T.; Zhang, L. *J. Am. Chem. Soc.* **2018**, *140*, 17439-17443



Scheme 3.22: Proposed mechanism for the cycloisomerization of 1-silyl-1,4-alkynols **3.3**.

After gold(I)-catalyzed propargylation and methanolysis of the trimethylsilyloxy group, the C-C triple bond of homopropargyl alcohols **3.3** could be activated by the same catalyst via π -coordination (intermediate **3.I**). This coordination would facilitate the hydroxyl group nucleophilic attack, generating intermediate **3.II**. Finally, HNTf₂ formation and proto-deauration of vinylgold(I) intermediate **3.III** would furnish 2-silyl-4,5-dihydrofuran skeleton **3.4** in a selective way.

To check our mechanistical hypothesis, homopropargyl alcohols **3.3a** were synthesized, through gold-catalyzed propargylation followed by an acidic hydrolysis, and isolated as a mixture of diastereoisomers in a close to 1:1 ratio. Next, homopropargyl alcohols **3.3a** were tested under the standard reaction conditions, but in the absence of methanol, due to protodesilylation was already performed in a previous step (Scheme 3.23).



Scheme 3.23: Gold-catalyzed cyclization of alkynols **3.3a** in the absence of methanol.

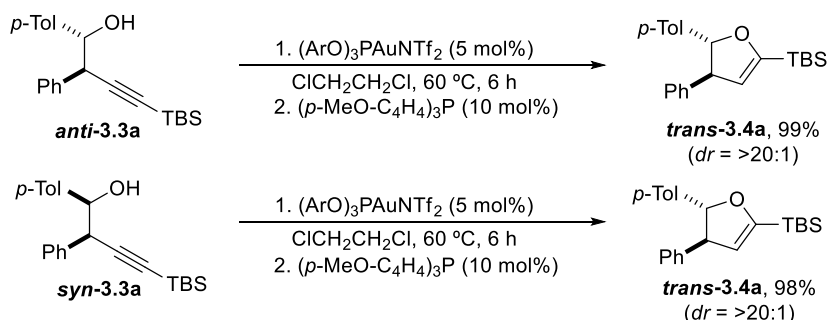
Surprisingly, although gold-catalyzed cycloisomerization of *anti*-**3.3a** should generate *trans*-**3.4a**, and similarly *syn*-**3.3a** should give rise to the corresponding

cis-3.4a, it was observed the formation of **trans-3.4a** as the only diastereoisomer, in a quantitative manner. This result allowed us to establish a hypothetical and unexpected *cis-to-trans* isomerisation of the corresponding 2-silyl-4,5-dihydrofurans **3.4** in the presence of the gold catalyst.

As indicated in the introduction of this chapter, no *cis-to-trans* isomerization reactions of 2,3-dihydrofurans have been reported under homogeneous gold catalysis, so at this point we decided to initiate a deep exploration of this process.

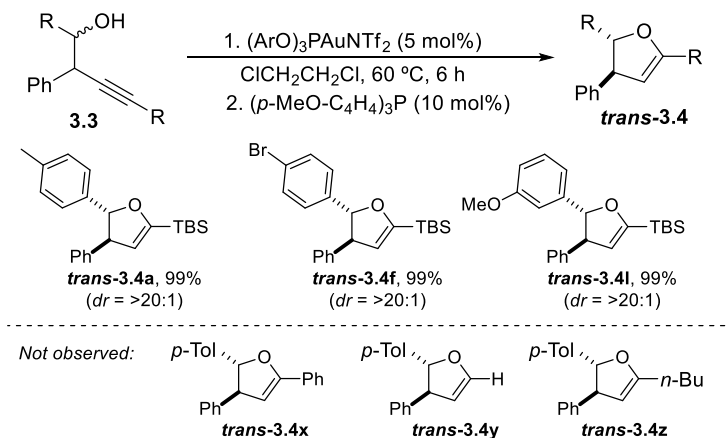
3.2 *Cis-to-trans* isomerization of 2-silyl-4,5-dihydrofurans

As a preliminary study of this transformation, we explored the cyclization of the model homopropargyl alcohols **syn-3.3a** and **anti-3.3a**. These compounds were obtained through the corresponding gold-catalyzed propargylation of *p*-toluolaldehyde, followed by acidic hydrolysis and chromatographic separation. Thus, independent cycloisomerization of each diastereoisomer was carried out discretely, treating a 1,2-dichloroethane solution of them with a 5 mol% of the catalyst at 60 °C, for six hours (Scheme 3.24).



Scheme 3.24: Cyclization of diastereoisomerically pure alkynols in the absence of methanol.

As thought, alkynol **anti-3.3a** afforded **trans-3.4a** quantitatively (Scheme 3.24, top). However, **syn-3.3a** gave rise to the same adduct **trans-3.4a** (Scheme 3.24, bottom). Similar results were obtained employing different mixtures of alkynol precursors **3.3** under the same reaction conditions (Scheme 3.25). Regardless the electronic properties in the aryl group at carbon-C5, *trans*-dihydrofurans **trans-3.4** were obtained within six hours as the only diastereoisomers.

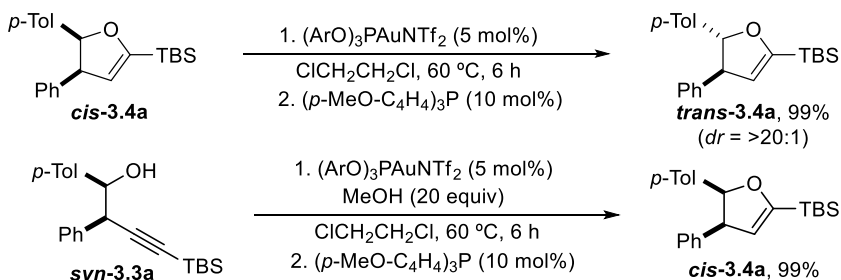


Scheme 3.25: Synthesis of *trans*-dihydrofurans **trans-3.4** starting from alkynols **3.3**.

In addition, to investigate if the silyl moiety is required for this isomerization to occur, three different alkynols **3.3**, not affordable through gold-catalyzed propargylations, were synthesized by other means. However, after gold treatment the reaction only gave rise to complex mixtures under the reaction conditions or even at room temperature, instead of the expected *trans*-dihydrofurans **trans-3.4x-z** (Scheme 3.25, *bottom*). These outcomes indicated that a silyl-protected alkyne seems to be necessary for the process to take place.

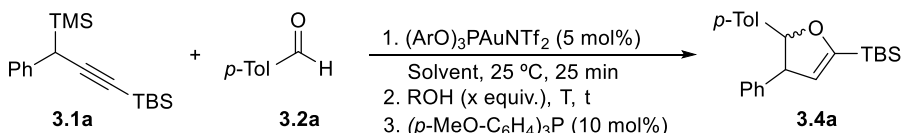
Next, attempting to determine if isomerization reaction happens before or after alkynol cyclization, *cis*-2-silyl-4,5-dihydrofuran **cis-3.4a** was also treated under the standard gold catalytic conditions in the absence of methanol. As shown in Scheme 3.26 (*top*), *trans*-2-silyl-4,5-dihydrofuran **trans-3.4a** was obtained as the only product, indicating that isomerization occurs after dihydrofurans formation. Finally, cycloisomerization of alkynol **syn-3.3a** or treatment of *cis*-dihydrofuran **cis-3.4a** under these conditions, but in the presence of methanol (20 equivalents), resulted in the obtention of the corresponding *cis*-dihydrofuran **cis-3.4a** as the only diastereoisomer (Scheme 3.26, *bottom*). Thus, methanol seems to inhibit *cis-to-trans* isomerization, in agreement with the results obtained by Krause.³⁰

³⁰ Belting, V.; Krause, N. *Org. Lett.* **2006**, *8*, 4489-4492.



Scheme 3.26: *Cis-to-trans* isomerization and isolation of model *cis*-dihydrofuran **cis-3.4a**.

Considering all the variables involved in this transformation, we envisioned that a careful choice of the reaction conditions could allow a *one-pot* gold(I)-catalyzed propargylation, protodesilylation, cyclization and *cis-to-trans* isomerization. Using the best gold catalyst already established for the one-pot synthesis of dihydrofurans previously described, we decided to modify the solvent, the amount of proton source and its nature, the reaction time and even the temperature in a quest for the final target (Table 3.1). Once again, propargylsilane **3.1a** and *p*-tolualdehyde **3.2a** were chosen as model substrates.



Entry	Solvent	ROH	Equiv.	T	t	%Yield ^a	dr (trans:cis)
1	ClCH ₂ CH ₂ Cl	MeOH	20	60	6 h	99	1.1:1
2	ClCH ₂ CH ₂ Cl	MeOH	10	60	6 h	99	1.1:1
3	ClCH ₂ CH ₂ Cl	MeOH	1	60	6 h	99	1.1:1
4	ClCH ₂ CH ₂ Cl	MeOH	1	60	16 h	99	1.1:1
5	ClCH ₂ CH ₂ Cl	MeOH	1	80	6 h	99	1.1:1
6	ClCH ₂ CH ₂ Cl	<i>t</i> -BuOH	1	60	6 h	99*	>20:1
7	ClCH ₂ CH ₂ Cl	<i>t</i> -BuOH	5	60	6 h	98	5:1
8	ClCH ₂ CH ₂ Cl	<i>t</i> -BuOH	5	60	16 h	98	>20:1
9	ClCH ₂ CH ₂ Cl	<i>t</i> -BuOH	1	40	6 h	75	2:1
10	ClCH ₂ CH ₂ Cl	<i>t</i> -BuOH	1	60	3 h	99	>20:1
11	CH ₃ CN	<i>t</i> -BuOH	1	60	6 h	81	1.8:1
12	CHCl ₃	<i>t</i> -BuOH	1	60	6 h	99	1.1:1

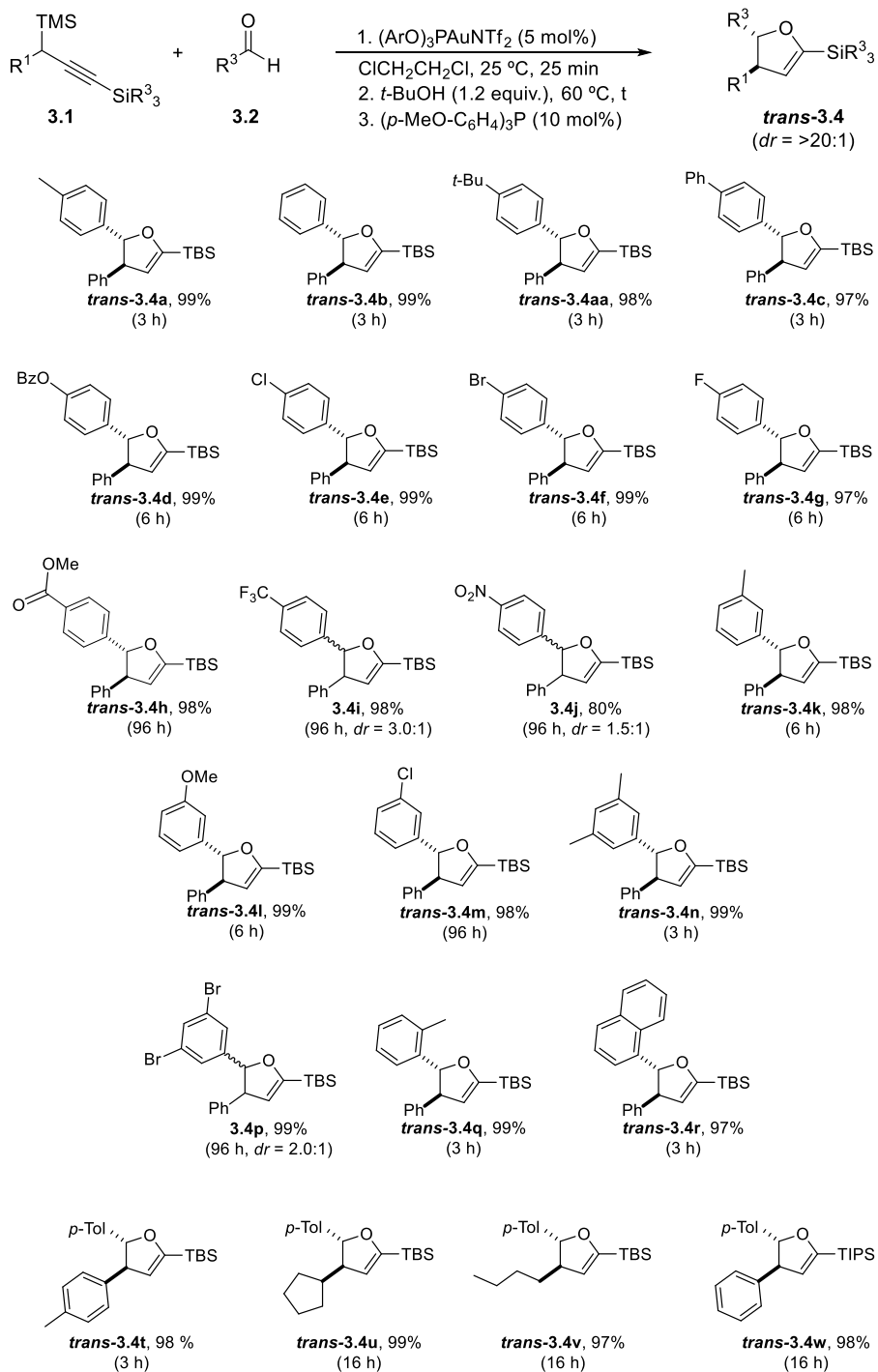
^aDetermined by ¹H-NMR using dibromomethane as internal standard. *Isolated yield.

Table 3.1: Screening of the reaction conditions for the *one-pot* process.

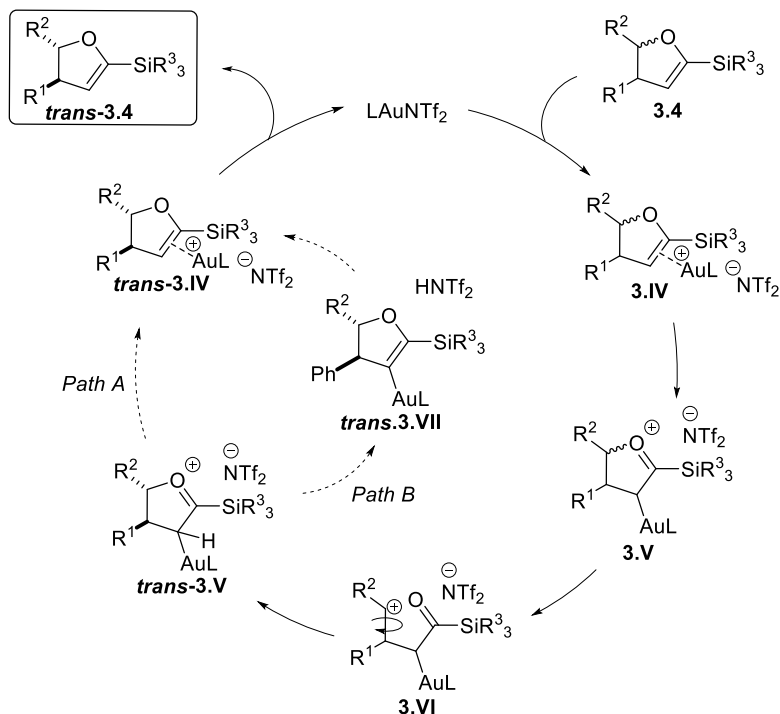
From Table 3.1, it can be inferred that when methanol was used as the proton source, no isomerization was observed even decreasing its amount until only a stoichiometric quantity (*Entries 1-3*). Longer reaction time (*Entry 4*) or higher temperature (*Entry 5*) gave no good results either. Fortunately, the use of a bulkier alcohol, such as *tert*-butanol, led to the desired goal, allowing a complete isomerization using a single equivalent (*Entry 6*). It was also checked that the use of large amounts of this alcohol does not prevent isomerization, although the reaction becomes slower (*Entries 7-8*). At lower temperature, alkynols did not react completely to yield the final dihydrofurans, so the higher dr is due to the different rate between them (*Entry 9*). Moreover, it was possible to reduce the reaction time to only three hours (*Entry 10*). Finally, we tested the influence of other solvents that have been demonstrated suitable for propargylation, such as acetonitrile and chloroform. However, they inhibited *cis-to-trans* isomerization even after six hours of reaction (*Entries 11-12*).

Regarding these outcomes, we tested a similar collection of propargylsilanes **3.1** and aldehydes **3.2** that worked well for the one-pot synthesis of 2-silyl-4,5-dihydrofurans **3.4**. Under the optimized reaction conditions, we found a strong dependence between the reaction rate and the electronic properties of the aromatic aldehydes, so reaction times were optimized for each example (Scheme 3.27).

As it is described in Scheme 3.27, the gold-catalyzed *one-pot* transformation, including propargylation, ether cleavage, cyclization and *cis-to-trans* isomerization worked perfectly in almost all the cases, furnishing *trans*-2-silyl-4,5 dihydrofurans **trans-3.4** with excellent yields. It is worth to mention that, for comparable aromatic aldehydes (**trans-3.4a-h,x**), the presence of electron-donating groups (**trans-3.4a-c,x**) required shorter reaction times than their analogues bearing electron-withdrawing groups (**trans-3.4d-h**). In addition, the use aliphatic propargylsilanes (dihydrofurans **trans-3.4u-v**), or a bulkier triisopropylsilyl group (**trans-3.4w**), required longer reaction times to be completed. Finally, for three specific dihydrofurans (**trans-3.4i,j,p**), all of them with strong electron-withdrawing groups at the arene ring, good diastereoisomeric ratios could not be achieved even after 96 hours of reaction, whereas longer reaction times (7 days) only led to decomposition of the final products.

Scheme 3.27: Scope of the *one-pot* synthesis of *trans*-dihydrofurans **trans-3.4**.

Taking all these results into account, and the work developed by Krause,³⁰ a mechanistic proposal for the gold(I)-catalyzed *cis-to-trans* isomerization step could be formulated, and it is outlined in Scheme 3.28.



Scheme 3.28: Mechanistic proposal for the gold-catalyzed *cis-to-trans* isomerization.

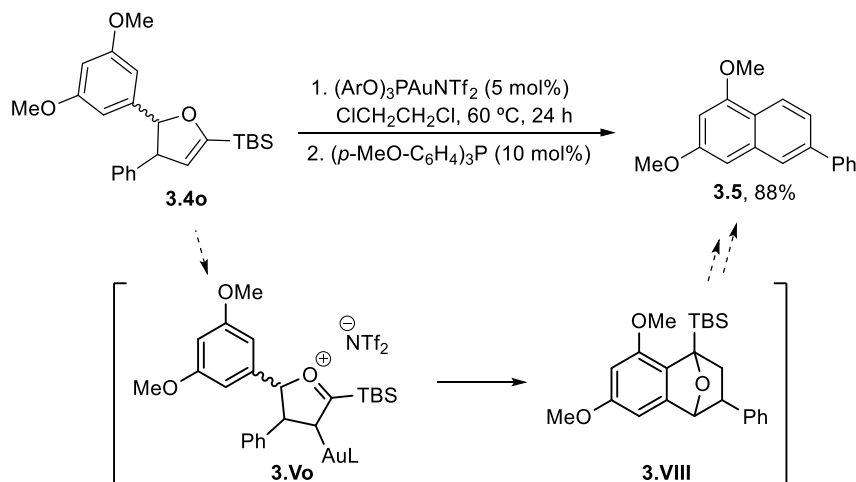
Thus, after one-pot formation of the diastereomeric mixture of dihydrofurans **3.4**, from the corresponding propargylsilanes **3.1** and benzaldehydes **3.2**, the gold catalyst could form a π -complex coordinating the double bond of the dihydrofuran (intermediate **3.IV**), leading to the formation of α -oxonium alkylgold(I) intermediate **3.V**. Then, a transient cleavage of the benzylic carbon-oxygen bond of this intermediate would generate carbocationic intermediate **3.VI**, stabilized by the presence of the aryl ring. The formation of this intermediate **3.VI**, with free rotation along C4-C5 single bond, could be the key step for the isomerization process. Finally, reclosure of the heterocycle through a nucleophilic attack of the oxygen to the carbocation would take place, yielding the more stable *trans*- α -oxonium alkylgold(I) intermediate **trans-3.V**. At this point, two different evolution pathways could be envisioned: a direct gold(I) elimination to generate π -complex intermediate **trans-3.IV** (Path A), releasing afterwards the catalyst and initiating a

new catalytic cycle; or by counterion-assisted deprotonation to form vinylgold(I) intermediate **trans-3.VII** and triflimide (Path B), which would finally suffer protodeauration achieving intermediate **trans-3.IV**.

At this point, multiple control experiments were designed and carried out to confirm our mechanistical hypothesis. The experiments are grouped in different sections, depending on the key steps from Scheme 3.28 we targeted to prove.

• **Oxonium intermediate 3.V. Role of the methanol.**

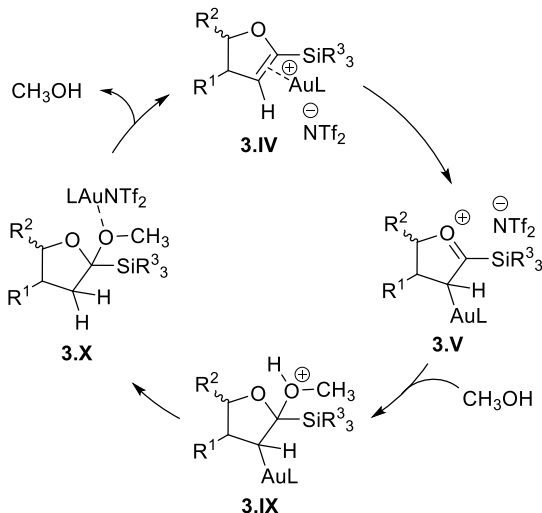
An experimental observation that seemed to agree with the participation of oxonium intermediate **3.V** was the formation of naphthalene derivative **3.5**, starting from a diastereomeric mixture of dihydrofurans **3.4o** synthesized from an electron-rich benzaldehyde, under the standard reaction conditions (Scheme 3.29). In this case, an intramolecular attack of the arene ring to the electrophilic carbon C2 of the oxonium species **3.Vo**, followed by a dehydration-aromatization process of intermediate **3.VIII**, could explain the formation of naphthalene derivative **3.5**.



Scheme 3.29: Formation of naphthalene derivative **3.5** starting from **3.4o**.

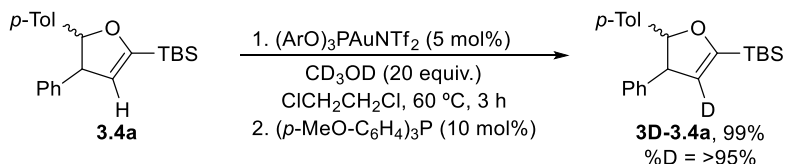
In a similar manner, it can be envisioned that the interaction between intermediate **3.V** and methanol, less bulky and better nucleophile than *tert*-butanol, could interrupt the catalytic cycle for the isomerization (Scheme 3.30). This way, a nucleophilic attack to the electrophilic carbon C2 of the oxonium intermediate **3.V** would generate the silylacetal intermediate **3.X** after

protodeauration of intermediate **3.IX**. This species could be unstable under the reaction conditions, losing methanol, probably by assistance of the gold(I) complex, to regenerate the initial dihydrofuran **3.4** preventing *cis-to-trans* isomerization.



Scheme 3.30: Possible role of methanol in avoiding isomerization process.

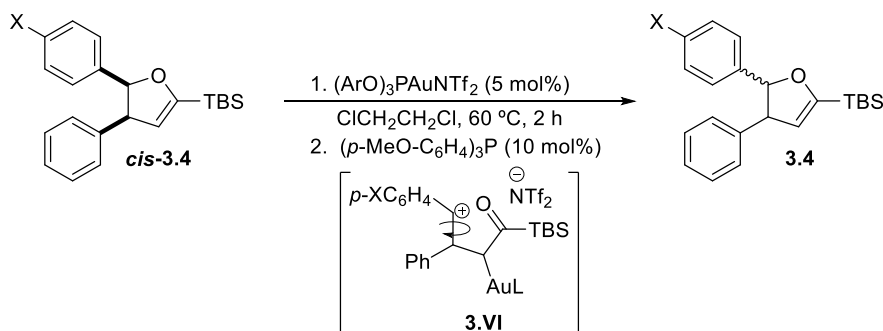
To support this hypothesis, we treated a *cis-trans* mixture of dihydrofurans **3.4a** in the presence of an excess of methanol-*d*₄, to gain some insight of the role of this reagent (Scheme 3.31). After three hours of reaction, a complete proton-deuterium exchange at carbon C3 was observed, with no significative change in the initial diastereoisomeric ratio of the dihydrofurans mixture. This result agrees with our previously explained hypothesis (Scheme 3.30), as the large excess of methanol-*d*₄ would lead to complete deuteration after consecutive addition-dehydration steps.



Scheme 3.31: Deuteration of model dihydrofurans **3.4a** in the presence of CD₃OD.

• **Carbocationic intermediate 3.VI**

Regarding the key step for the isomerization reaction, the hypothesis of a temporary carbon-oxygen bond cleavage with formation of cationic intermediate **3.VI** (Scheme 3.28), could be supported by the different observed ratios in the isomerization process depending on the electron-donating or electron-withdrawing abilities of the arene ring (see Scheme 3.27). In an effort to demonstrate the formation of a positive charge at carbon C5, we decided to run a Hammett-type analysis, starting from a representative collection of *cis*-dihydrofurans **cis-3.4** synthesized by our developed methodology. This way, a set of *cis*-to-*trans* isomerization experiments were carried out under the standard reaction conditions but shorter reaction times (two hours). The crude mixtures were analyzed by ¹H-NMR to determine the isomerization ratio (Table 3.2). Using the diastereoisomeric ratio for **cis-3.4a** (X = H) isomerization as reference, the relative rate constants were obtained with the relative diastereoisomeric ratios, and then plotted the logarithm of these relative rate constants against tabulated σ values,³¹ for each functional group (Figure 3.3).



Compound	X	trans:cis	k/k ₀	log(k/k ₀)	σ
3.4d	Ph	16.7:1	4.065	0,609	- 0.18
3.4b	Me	17.5:1	4.280	0,631	- 0.17
3.4a	H	4.1:1	1.000	0,000	0.00
3.4h	F	1:2.1	0.508	-0,294	0.06
3.4f	Cl	1:3.6	0.068	-1,167	0.23
3.4g	Br	1:3.0	0.081	-1,092	0.23

Table 3.2: Representative examples and obtained values.

³¹ Hansch, C.; Leo, A.; Taft, R. W. *Chem. Rev.* **1991**, *91*, 165-195.

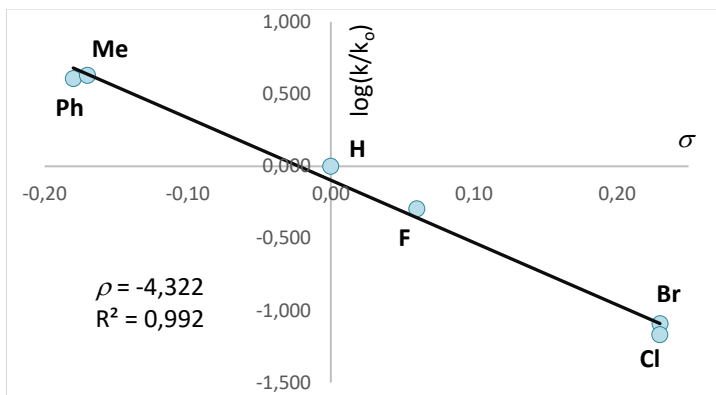
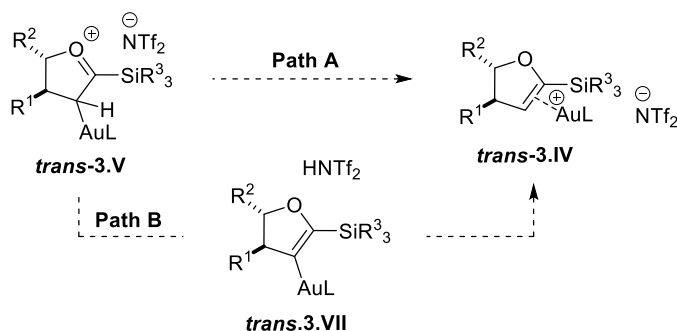


Figure 3.3: Hammett plot for the *cis-to-trans* isomerization reaction.

A good fit ($R^2 = 0.992$) was obtained, in the Hammett plot, for the linear correlation of the experimental values (Figure 3.3). Additionally, the negative slope of the plot (ρ), whose value of -4.453 can be considered of high intensity, is in agreement with the formation of a positive charge in the transition state of the rate determining step. This fact supports the participation of intermediate **3.VI**, as a positive charge is created (Scheme 3.28). Moreover, the transformation stage of intermediate **3.V** into intermediate **3.VI** could be considered the rate limiting step.

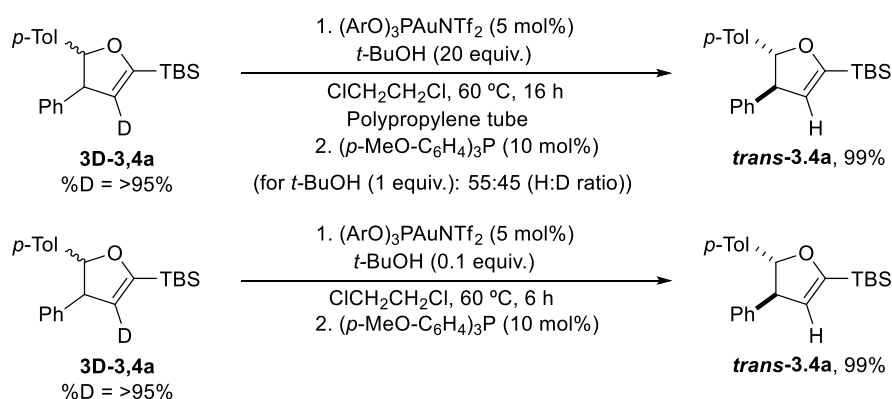
- **Oxonium intermediate *trans*-3.V. Direct deauration vs. protodeauration**

Regarding the final step of the isomerization process, two different mechanistic hypotheses could be proposed starting from oxonium intermediate ***trans*-3.V**, as summarized in Scheme 3.32: direct deauration with formation of π -complex ***trans*-3.IV** (*Path A*), or deprotonation towards vinylgold(I) intermediate ***trans*-3.VII** and triflimide (HNTf₂), followed by protodeauration (*Path B*).



Scheme 3.32: Possible pathways for the formation of intermediate ***trans*-3.IV**.

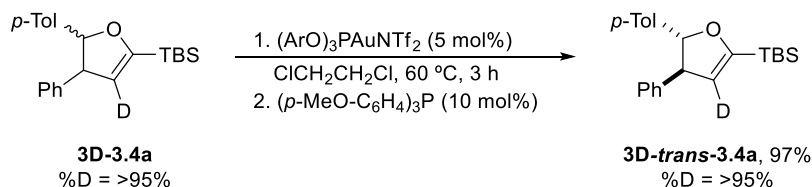
Aiming to distinguish between them, we performed an isomerization reaction inside a propylene tube of a deuterated mixture of 4,5-dihydrofurans **3D-3.4**, synthesized as depicted in Scheme 3.31, in the presence of a large excess of *tert*-butyl alcohol and the gold catalyst (Scheme 3.33, *top*). Under these conditions, a complete disappearance of the deuterium label was observed, but when a single equivalent of *tert*-butyl alcohol was used, 45% of the deuterium-labelled compound was observed, as statistically expected. These outcomes can support the formation of triflimide and vinylgold intermediate **trans-3.VII**, which would explain the proton-deuterium exchange. However, when the same experiment was carried out with only 0.1 equivalents of *tert*-butyl alcohol, but in a regular glassware, a complete *cis-to-trans* isomerization and scrambling of the deuterium label was observed (Scheme 3.33, *bottom*). This result would also agree with the formation of HNTf₂ during the catalytic process, and the proton source could be the free silanols on the glassware walls, as previously described (see *Chapter I*).



Scheme 3.33: Isomerization experiments of C3-deuterated dihydrofurans **3D-3.4a**.

These results opened the door to another mechanistical possibility: formation of vinylgold complex **3.VII** as resting state, while a proton catalyzed *cis-to-trans* isomerization takes place. In fact, the isomerization of a diastereoisomeric mixture of dihydrofurans **3.4a** to **trans-3.4** can be accomplished by a 5 mol% of HNTf₂, at room temperature, in only one hour. Nevertheless, naphthalene derivative **3.5** could not be synthesized using different amounts of triflimide as catalyst, due to decomposition issues of the starting dihydrofurans **3.4o**. This outcome allowed us to discard this catalysis as major contribution to the one-pot process, although it can coexist.

On the other hand, the process can happen with no significant loss of deuterium in the C3 position when the reaction is performed in the absence of *tert*-butyl alcohol (Scheme 3.34, *bottom*). This result also pointed out to the no formation of triflimide in the course of the reaction, arising direct deauration of intermediate **trans-3.V** with formation of π -complex **trans-3.IV** (*Path A*) as the most plausible mechanism.



Scheme 3.34: Isomerization experiments of C3-deuterated dihydrofurans **3D-3.4a**.

- **Other mechanistic possibilities**

However, another plausible mechanism would involve an isomerization of the dihydrofurans carbon-carbon double bond along the ring (Figure 3.4), losing the diastereoisomery first and the generating the most stable isomer, the *trans*-2-silyl-4,5-dihydrofuran in a second stage. To explore this possibility, we synthesized C4 and C5 deuterium labelled dihydrofurans **4D-3.4a** and **5D-3.4b**, using a deuterium labelled propargylsilane and aldehyde respectively, and treated them under the isomerization reaction conditions in the presence of *tert*-butyl alcohol (Scheme 3.35). In both cases, the diastereoisomeric mixture of dihydrofurans gave rise to the corresponding *trans* isomer without deuterium scrambling, implying no proton exchange during the epimerization. These outcomes agreed with our mechanistic proposal and discard a reaction pathway through carbon-carbon double bond isomerization.

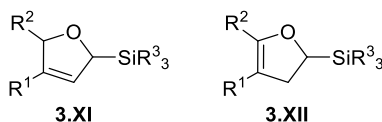
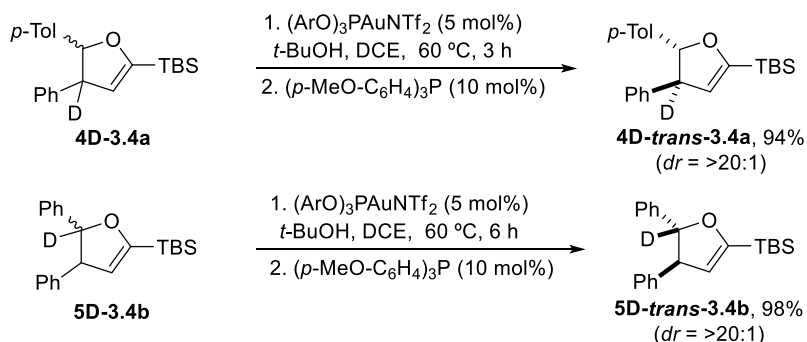


Figure 3.4: Possible intermediate isomeric dihydrofurans by C-C double bond isomerization.



Scheme 3.35: Isomerization reaction of 4- and 5-deuterium labelled dihydrofurans.

Finally, another possibility that could not be ruled out was an isomerization process due to the gold(I)-assisted carbon-oxygen bond cleavage at C5 with formation of a gold(I) enolate intermediate **3.XIII** (Figure 3.5). This type of reaction has been previously reported by Krause for 2,5-dihydrofurans with intermolecular nucleophilic trapping of the carbocationic intermediate.³²

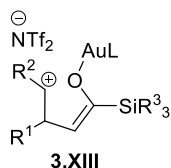


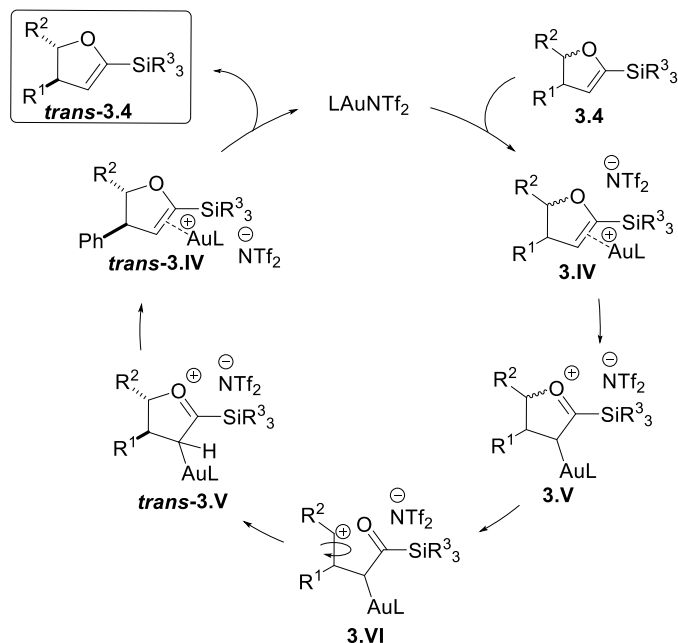
Figure 3.5: Possible gold(I) enolate intermediate **3.XIII**.

However, when we used a more oxophilic gold(III) picolinate complex instead of the gold(I) phosphite under the standard conditions, no isomerization reaction took place at all. This result, although it does not allow to discard a carbon-oxygen bond cleavage through gold-oxygen coordination, does not point at this possibility.

Considering all the obtained results, it can be inferred that the most plausible mechanism corresponds to the one represented in Scheme 3.36. Several results supported the participation of intermediates **3.V**, **3.VI**, and *trans*-**3.V**, allowing to discard other mechanistic pathways involving carbon-carbon double bond

³² Sawama, Y.; Sawama, Y.; Krause, N. *Org. Lett.* **2009**, *11*, 5034–5037.

isomerization or a vinylgold(I) intermediate formation. However, the presence of an oxophilic activation or a proton catalytic cycle cannot be completely discarded, although the outcomes showed them as unlikely possibilities.



Scheme 3.36: Most plausible mechanism for the *cis-to-trans* isomerization.

In summary, the obtained results have demonstrated that a high-yielding intermolecular synthesis of 2-silyl-4,5-dihydrofurans, starting from aldehydes and propargylsilanes, can be accomplished by a gold(I) catalyst in a one-pot manner. The silyl moiety seemed to be crucial for the feasibility of this transformation. Additionally, a control of the reaction condition allows to obtain the pure *trans* isomers through gold-catalyzed *cis-to-trans* isomerization, whose key steps consist in ring-opening, rotation along a single carbon-carbon bond and ring-closing processes.

4 Conclusions

A novel one-pot, selective gold-catalyzed synthesis of 2-silyl-4,5-dihydrofurans from aromatic aldehydes and propargylsilanes has been described, representing the first intermolecular example for accessing these structural motifs. Moreover, pure *trans* isomers can also be obtained in a one-pot manner depending on the reaction conditions.

Differently decorated *trans*-2-silyl-4,5-dihydrofurans have been synthesized using this methodology. The process tolerated a wide range of substituents with different electronic properties, allowing to obtain these compounds in high yields and diastereoisomeric pure.

The reaction involves four consecutive gold(I) catalyzed reactions in a one-pot procedure, as follows: propargylation, silyl ether deprotection, alkynol cycloisomerization and *cis-to-trans* dihydrofuran isomerization.

A deep study of the *cis-to-trans* dihydrofuran isomerization has also been performed. The mechanistic proposal for that process involves the participation of alkylgold(I) oxonium intermediates, and also a carbocationic intermediate through temporal carbon-oxygen bond cleavage. These hypotheses are supported by experimental observations, several deuterium labelled experiments and a Hammett type study. A carbocationic intermediate, which allows free rotation along C4-C5 bond, seems to participate in the rate-determining step.

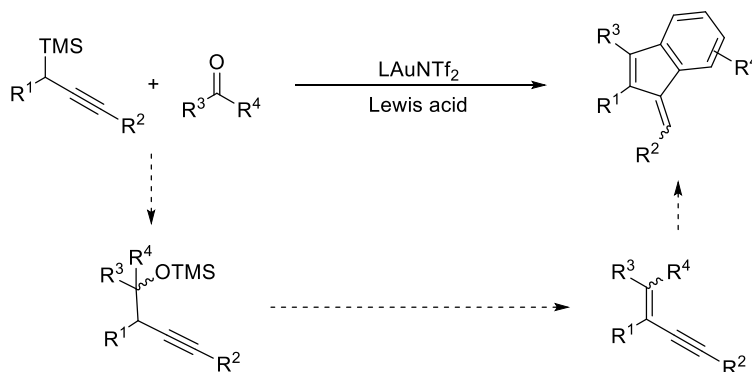
Chapter IV:

Lewis acid enhancement of a gold(I) complex activity.

One-pot synthesis of benzofulvene derivatives

1 Introduction

This Chapter summarizes the results for the synthesis of substituted benzofulvenes using a combination of a gold(I) catalyst and a Lewis acid. The process consists in a one-pot propargylation, elimination, and Nazarov-type cyclization through a carbocationic σ -allenylgold(I) intermediate (Scheme 4.1).



Scheme 4.1: One-pot synthesis of benzofulvenes through gold(I)-Lewis acid catalysis.

Several control experiments allowed us to determine that the Lewis acid catalyst plays an important role in this transformation, as it 'modifies' the counterion nature increasing the activity of the gold complex.

2 Bibliographic background

2.1 Additive effects in homogeneous catalysis

During decades, additives has been employed in homogeneous organometallic catalysis, facilitating new reactivities or improving activity or selectivity of reported transformations.¹ Although their roles cannot always be assessed, two main groups can be identified when combining metallic catalysts and additives: tandem catalysis and cocatalysis.

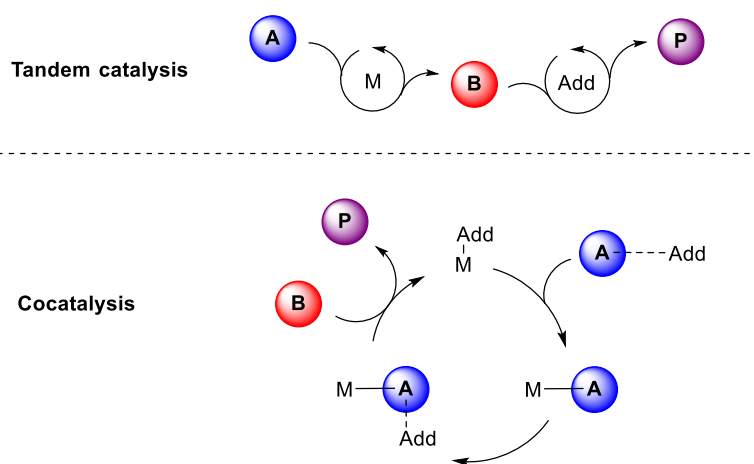


Figure 4.1: Tandem catalysis vs. cocatalysis with additives.

¹ Wang, C.; Xi, Z. *Chem. Soc. Rev.* **2007**, *36*, 1395-1406.

As it is shown in Figure 4.1 (*top*), when the additive is able to perform a separated catalytic cycle without influencing the metal-catalyzed one, it is called tandem catalysis. These processes are usually much easier to rationalize and relate with the nature of the additive. On the contrary, cocatalysis is invoked when both catalysts operate within the same catalytic cycle (Figure 4.1, *bottom*). In this case, role-assessment is not always possible for the additive, as it can participate in several key steps, interacting with substrates and/or metallic catalysts.

As previously explained in *Chapter I*, gold catalysis remains nowadays as a hot area of research, given the great number of transformations reported during the last years. In this sense, mechanistic investigations in gold-catalyzed processes represent a challenging topic, even for well-known transformations, since the catalysis outcome is usually difficult to explain attending to all the variables. In this sense, counterion and additive effects have been less investigated in comparison with the influence caused by ligand-tuning (see *General background*). A systematic study was initiated only few years ago, and it is worth to mention the contributions of Hammond and Xu in collecting and reviewing these results.

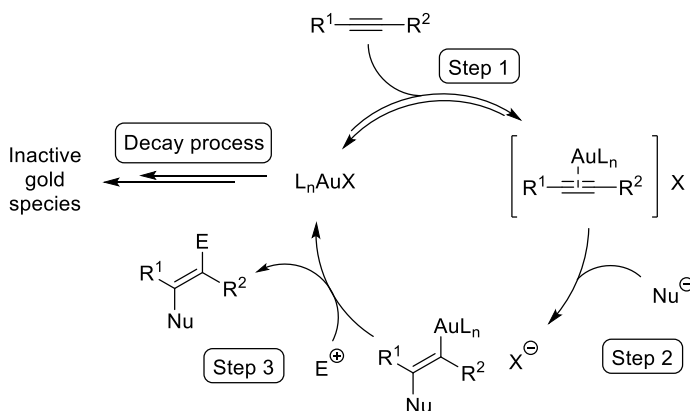
Given that the results reported in the present Chapter are strongly influenced by gold/additive cocatalysis, representative examples, in which the role of the cocatalyst could be determined, will be discussed in the next section.

2.2 Gold-additive-cocatalyzed processes

A wide range of additives has been employed in gold catalysis during last years, including nitrogenated bases, Brønsted and Lewis acids, salts... This way, Hammond and Xu classified them, attending to their role in the catalytic process, into four groups:² hydrogen bonding acceptors, activators/reactivators, acidic cocatalysts and promoters. However, they do not discard that other not-yet-reported roles could exist.

For this dissertation, we decided to follow this classification to mention some representative examples. In order to clarify further explanations, the general and simplest catalytic cycle proposed for gold catalysis involving alkyne activation is once again depicted in Scheme 4.2.

² Lu, Z.; Li, T.; Mudshinge, S. R.; Xu, B.; Hammond, G. B. *Chem. Rev.* **2021**, *121*, 8452-8477.



Scheme 4.2: General mechanism in gold-catalyzed transformations of alkynes.

2.2.1 Hydrogen bonding acceptors

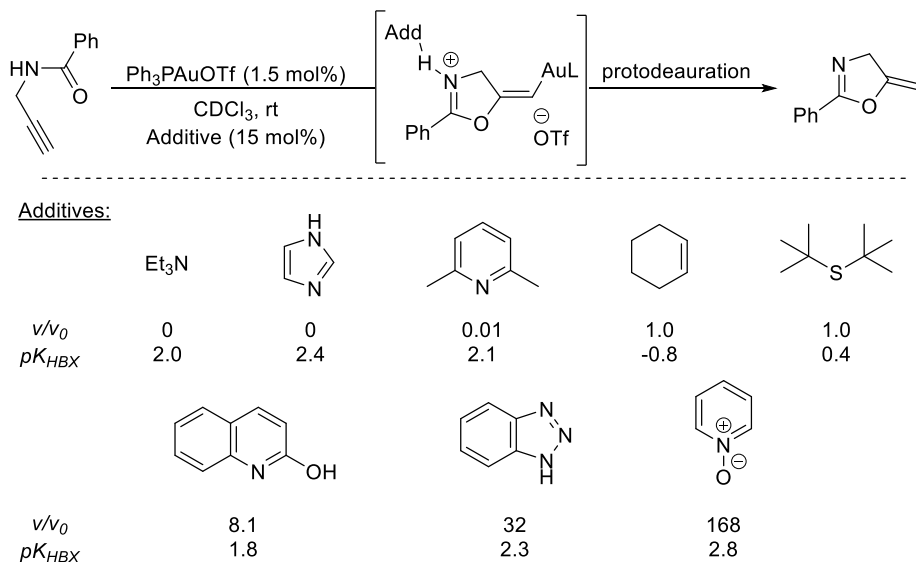
As it was explained for gold counterions (see *General background*), the ability of an additive to transfer an active proton can have a deep impact on the reaction outcome (Scheme 4.2, *Step 3*). However, additives with this ability can also bind the gold complex, competing with the unsaturated system, and stabilize it decreasing its reactivity (Scheme 4.2, *Step 1*). Depending on the balance between both effects, the reaction can be even shutted down.

In this sense, Hammond and co-workers studied a gold(I)-catalyzed cyclization of a propargyl amide taking into account the relative rate in the presence or absence of different additives³ and also the pK_{HBX} (Hydrogen Bonding Index)⁴ for each additive, using *tert*-butylsulfide as reference (Scheme 4.3). Protodeauration, the rate limiting step, should be eased by the addition of additives with high pK_{HBX} , because they can interact with the acidic proton of the proposed intermediate, acting as a carrier. However, some additives with high pK_{HBX} , such as triethylamine, imidazole or 2,6-lutidine, inactivate the reaction, because they also present high aurophilicity. In this regard, benzotriazole and pyridine *N*-oxide significantly accelerate the reaction. This can be due to the existence of a dynamic coordination

³ Wang, W.; Kumar, M.; Hammond, G. B.; Xu, B. *Org. Lett.* **2014**, *16*, 636-639.

⁴ a) Laurence, C.; Brameld, K. A.; Graton, J. R. M.; Le Questel, J.-Y.; Renault, E. *J. Med. Chem.* **2009**, *52*, 4073-4086; b) Okoromoba, O. E.; Han, J.; Hammond, G. B.; Xu, B. *J. Am. Chem. Soc.* **2014**, *136*, 14381-14384; c) Han, J.; Lu, Z.; Flach, A. L.; Paton, R. S.; Hammond, G. B.; Xu, B. *Chem. Eur. J.* **2015**, *21*, 11687-11691.

equilibrium that assist the protodeauration and do not strongly struggle with π -coordination of the alkyne (Scheme 4.2, Step 2). Additionally, benzotriazoles offer two different possibilities that can be very useful in homogenous gold catalysis: stabilizing simple unstable gold complexes and tuning their catalytic activity without changing the ligand properties.⁵



Scheme 4.3: Additive effect in hydrogen-bonding assisted protodeauration.

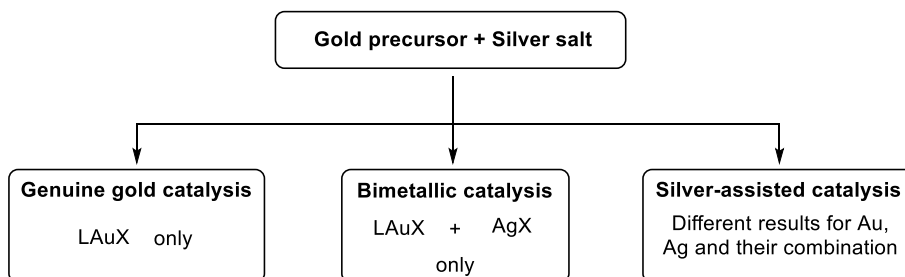
2.2.2 Additives as catalyst generators/regenerators

Gold halides are the most employed precursors of active gold catalysts due to their stability. However, the high affinity of the halide to the gold atom usually prevents its catalytical activity. The most employed additives to overcome this problem are silver salts through a counterion exchange. However, several studies have demonstrated that silver salts are in occasions not so innocent,⁶ as the called

⁵ Wang, D.; Gautam, L. N. S.; Bollinger, C.; Harris, A.; Li, M.; Shi, X. *Org. Lett.* **2011**, *13*, 2618-2621.

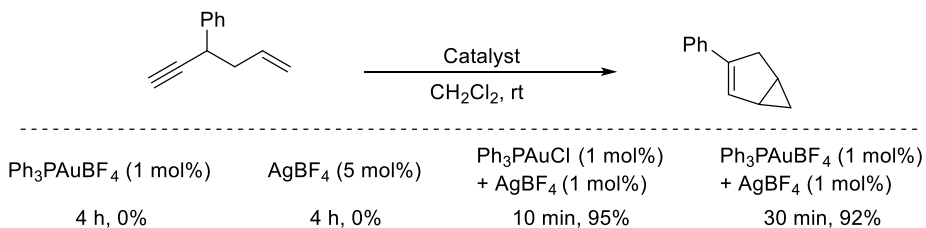
⁶ a) Weber, D.; R. Gagné, M. R. *Org. Lett.* **2009**, *11*, 4962-4965; b) Schmidbaur, H.; Schier, A. *Z. Naturforsch.* **2011**, *66*, 329-350; c) Zhu, Y.; Day, C. S.; Zhang, L.; Hauser, K. J.; Jones, A. C. *Chem. Eur. J.* **2013**, *19*, 12264-12271.

silver-effect is present in many cases.⁷ Different experimental results have demonstrated that some reactions are not efficiently promoted by a gold catalyst generated through the silver method, due to a mixture of both silver and gold species. Shi and co-workers distinguished three possibilities: genuine gold catalysis, bimetallic catalysis and silver-assisted catalysis (Scheme 4.4).^{7a}



Scheme 4.4: Types of gold catalysis in the presence of a silver salt.

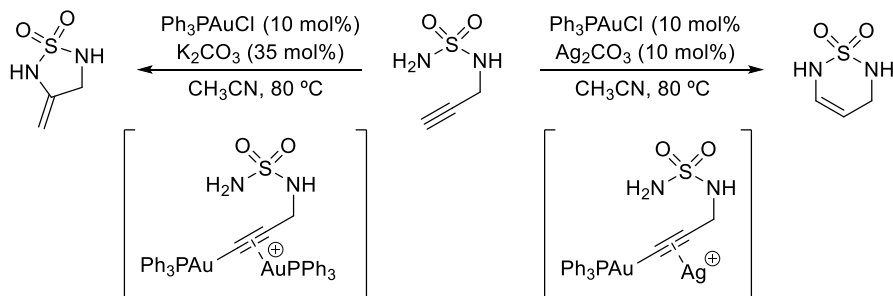
In the case of bimetallic catalysis, these authors demonstrated through ³¹P-NMR that the addition of different amounts of silver salts lead to different complexes. Additionally, removal or not of the precipitated silver chloride, after silver treatment of a gold(I) chloride, leads to a different complex than when it remains in suspension. This observation was tested in several model reactions, such as the isomerization of a 1,5-enyne depicted in Scheme 4.5. As it can be seen, neither gold or silver catalyst promotes the reaction, but the combination of gold(I) chloride or tetrafluoroborate with silver salt, efficiently furnished the formation of the final bicyclic product.



Scheme 4.5: Different outcomes in a bimetallic gold-silver-catalyzed transformation.

⁷ a) Wang, D.; Cai, R.; Sharma, S.; Jirak, J.; Thummanapelli, S. K.; Akhmedov, N. G.; Zhang, H.; Liu, X.; Petersen, J. L.; Shi, X. *J. Am. Chem. Soc.* **2012**, *134*, 9012-9019; b) Homs, A.; Escofet, I.; Echavarren, A. M. *Org. Lett.* **2013**, *15*, 5782-5785; c) Zhdanko, A.; Maier, M. E. *ACS Catal.* **2015**, *5*, 5994-6004.

Interestingly, as a remarkable example of silver-assisted catalysis, a regiodivergent hydroamination of a propargyl sulfuric diamide can be mentioned (Scheme 4.6). Thus, when the reaction is carried out in the absence of silver, a 5-*exo-dig* cyclization takes place via gold σ,π -activation of the alkyne. However, formation of a gold(I) acetylide and π -activation with the silver salt leads to a 6-*endo-dig* cyclization product.⁸



Scheme 4.6: Regiodivergent alkyne hydroamination due to the silver effect.

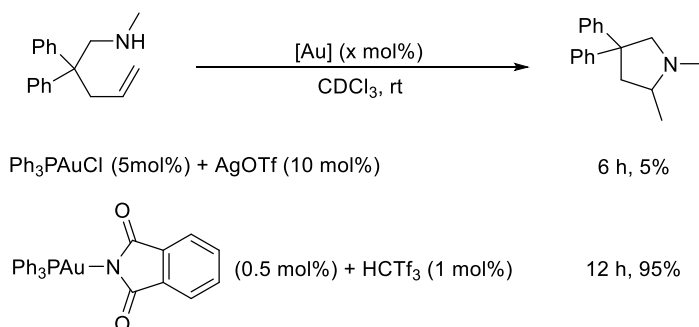
An alternative strategy, regarding the ‘traditional’ halide-scavenge with silver salts, consist in the use of Brønsted or Lewis acids which could act following two distinct trends: as slow and reversible counterion exchangers or coordinating impurities that potentially would poison the gold catalytic cycle.

Treatment of alkyl-, aryl- or hydroxygold complexes with Brønsted acids is a well-known methodology to generate gold complexes with catalytic activity, although they usually require strong acids.⁹ In this sense, Hammond and co-workers designed a methodology involving a combination of a gold(I) phthalimide

⁸ Veguillas, M.; Rosair, G. M.; Bebbington, M. W. P.; Lee, A.-L. *ACS Catal.* **2019**, *9*, 2552-2557.

⁹ a) Teles, J. H.; Brode, S.; Chabanas, M. *Angew. Chem. Int. Ed.* **1998**, *37*, 1415-1418; b) Mizushima, E.; Hayashi, T.; Tanaka, M. *Org. Lett.* **2003**, *5*, 3349-3352; c) Gaillard, S.; Slawin, A. M. Z.; Nolan, S. P. *Chem. Commun.* **2010**, *46*, 2742-2744; d) Gaillard, S.; Bosson, J.; Ramón, R. S.; Nun, P.; Slawin, A. M. Z.; Nolan, S. P. *Chem. Eur. J.* **2010**, *16*, 13729-13740; e) Tzouras, N. V.; Saab, M.; Janssens, W.; Cauwenbergh, T.; Van Hecke, K.; Nahra, F.; Nolan, S. P. *Chem. Eur. J.* **2020**, *26*, 5541-5551; f) Gasperini, D.; Collado, A.; Gómez-Suárez, A.; Cordes, D. B.; Slawin, A. M. Z.; Nolan, S. P. *Chem. Eur. J.* **2015**, *21*, 5403-5412.

with a Brønsted acid (Scheme 4.7).¹⁰ Although the phthalimido gold(I) complex possesses no catalytic activity due to the strong gold-nitrogen bond, the proton affinity of the phthalimide leads to a counterion shuffling equilibrium and generating an active catalyst. In addition, this strategy opens the door to more efficient processes in which reactivity can be easily tuned by changing the nature of the Brønsted acid.



Scheme 4.7: Gold-Brønsted-acid-catalyzed hydroamination of an alkene.

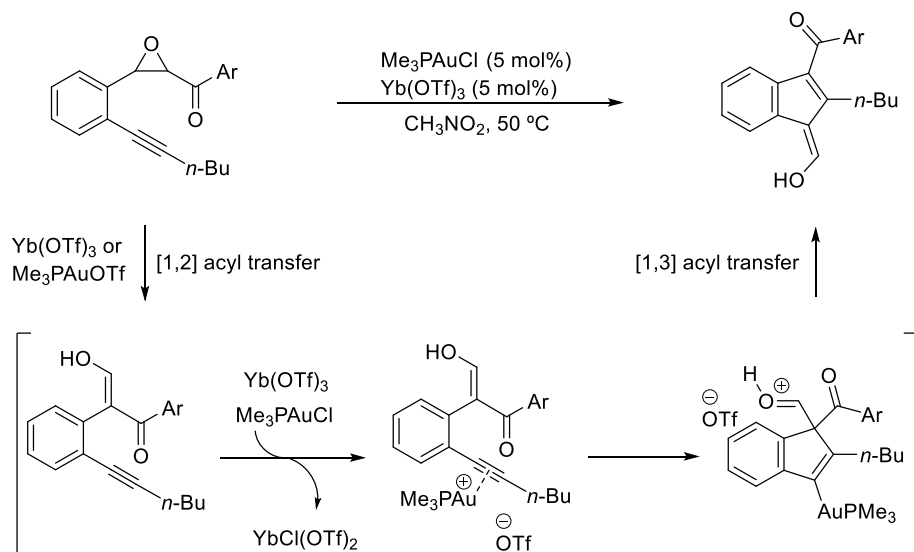
On the other hand, Lewis acids can also act as cocatalysts in gold-catalyzed reactions.¹¹ The synthesis of indene derivatives through gold(I)-Yb(OTf)₃ cocatalyzed rearrangement of *o*-alkynyl styrene epoxides, described by Shi and Die, represent an interesting example of gold halide activation using a metallic Lewis acid (Scheme 4.8).¹² The authors found that either gold or ytterbium catalyst can efficiently promote the initial [1,2]-acyl transfer, but only

¹⁰ Han, J.; Shimizu, N.; Lu, Z.; Amii, H.; Hammond, G. B.; Xu, B. *Org. Lett.* **2014**, *16*, 3500-3503.

¹¹ For selected examples, see: a) Wang, X.; Yao, Z.; Dong, S.; Wei, F.; Wang, H.; Xu, Z. *Org. Lett.* **2013**, *15*, 2234-2237; b) Subba Reddy, B. V.; Rajashekhar Reddy, M.; Yarlagadda, S.; Ravikumar Reddy, C.; Ravi Kumar, G.; Yadav, J. S.; Sridhar, B. *J. Org. Chem.* **2015**, *80*, 8807-8814; c) Wang, B.; Liang, M.; Tang, J.; Deng, Y.; Zhao, J.; Sun, H.; Tung, C.-H.; Jia, J.; Xu, Z. *Org. Lett.* **2016**, *18*, 4614-4617; d) Liang, M.; Zhang, S.; Jia, J.; Tung, C.-H.; Wang, J.; Xu, Z. *Org. Lett.* **2017**, *19*, 2526-2529; e) Gong, J.; Wan, Q.; Kang, Q. *Adv. Synth. Catal.* **2018**, *360*, 4031-4036; f) Fernández, P.; Alonso, P.; Fañanás, F. J.; Rodríguez, F. *Eur. J. Org. Chem.* **2018**, *29*, 3957-3964; g) Purgett, T. J.; Dyer, M. W.; Bickel, B.; McNeely, J.; Porco, J. A. *J. Am. Chem. Soc.* **2019**, *141*, 15135-15144; h) Dhote, P. S.; Ramana, C. V. *Org. Lett.* **2019**, *21*, 6221-6224.

¹² Dai, L.-Z.; Shi, M. *Chem. Eur. J.* **2010**, *16*, 2496-2502.

trimethylphosphinegold(I) triflate promotes the second isomerization step, albeit with poor yields due to its instability. However, the combination of both catalysts boosts the reaction rate, presumably through slow formation of trimethylphosphinegold(I) triflate, avoiding its fast decomposition.

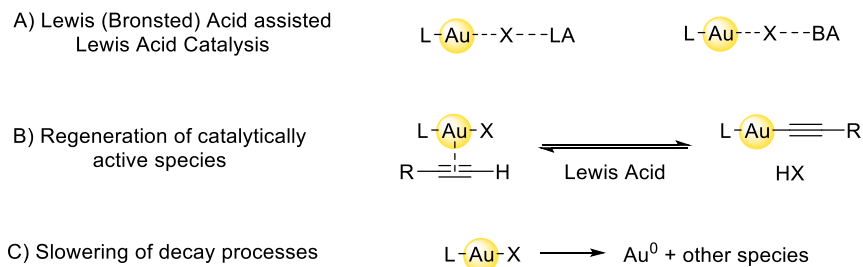


Scheme 4.8: Gold(I)- $\text{Yb}(\text{OTf})_3$ -catalyzed rearrangement of alkynyl epoxides.

2.2.3 Acidic cocatalysts

Different Brønsted and Lewis acids can be used in combination with catalytically active gold complexes to improve their performance. In this sense, Hammond and co-workers carried out different studies with model reactions to gain some light in these transformations.¹³ Although they found no consistent effectiveness and were unable to describe a detailed mechanistic of how these additives work, they propose three different roles for acidic cocatalysts, depicted in Scheme 4.9.

¹³ Barrio, P.; Kumar, M.; Lu, Z.; Han, J.; Xu, B.; Hammond, G. B. *Chem. Eur. J.* **2016**, *22*, 16410-16414.



Scheme 4.9: Proposed roles for acidic cocatalysts in gold catalysis.

Thus, following the concept of Brønsted (and Lewis) acid-assisted Lewis acid catalysis introduced by Yamamoto,¹⁴ the acidic additive could coordinate one of the gold ligands or the counterion, increasing its electrophilicity (Scheme 4.9, *top*). This could speed up the coordination step to the unsaturated system (Scheme 4.2, *Step 1*). A second possibility would be preventing the formation of non-reactive gold acetylides terminal alkynes from terminal alkynes (Scheme 4.9, *medium*). The last role could be related to the influence of the cocatalyst in decomposition processes of the gold catalyst (Scheme 4.9, *bottom*). In this sense, Hammond's group reported that gold(I) complexes experience disproportionation reactions furnishing non-active gold species.¹⁵

Considering the first type of potential influence, no examples have been reported to date involving coordination of the counterion, as far as we can ascertain. It is worth to mention that this behaviour is closely related to the results described in this Chapter.

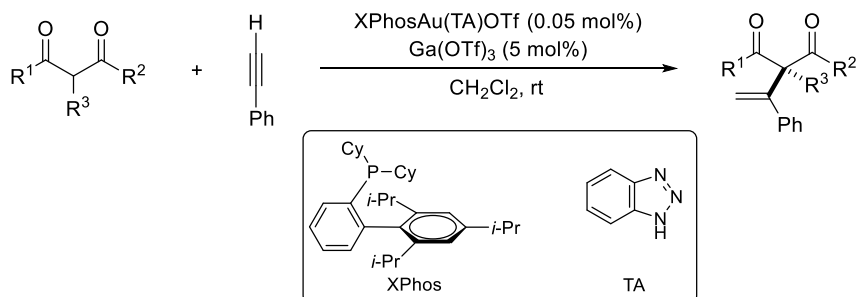
On the contrary, a very representative example of gold catalyst activation through coordination to one of the ligands has been reported by Shi and co-workers.¹⁶ In this work, an intermolecular synergistic gold(I)-Ga(III)-catalyzed Nakamura reaction is described (Scheme 4.10). Several experiments demonstrated that the reaction does not proceed well for the gold-silver combination due to the catalyst instability, and addition of a benzotriazole as additive only slowed the reaction down. However, the use of Ga(OTf)₃ as cocatalyst, along with the

¹⁴ Yamamoto, H.; Futatsugi, K. *Angew. Chem. Int. Ed.* **2005**, *44*, 1924-1942.

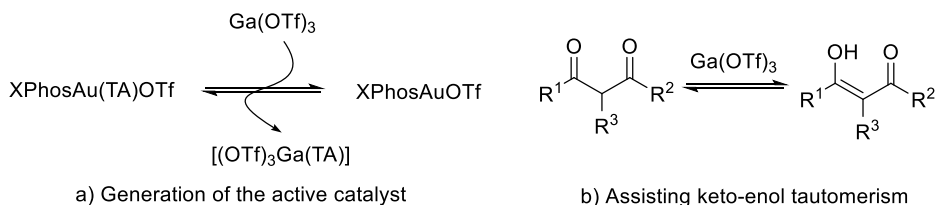
¹⁵ Kumar, M.; Jasinski, J.; Hammond, G. B.; Xu, B. *Chem. Eur. J.* **2014**, *20*, 3113-3119.

¹⁶ Xi, Y.; Wang, D.; Ye, X.; Akhmedov, N. G.; Petersen, J. L.; Shi, X. *Org. Lett.* **2014**, *16*, 306-309.

benzotriazolyl gold(I) complex, dramatically increases the performance. For this transformation, two roles have been set for the Ga(III) catalyst: coordination to the benzotriazole, generating the active catalyst; and coordination to the 1,3-dicarbonyl compound, easing keto-enol tautomerism.



Proposed roles:



Scheme 4.10: Gold(I)-Ga(OTf)₃ catalyzed Nakamura reaction.

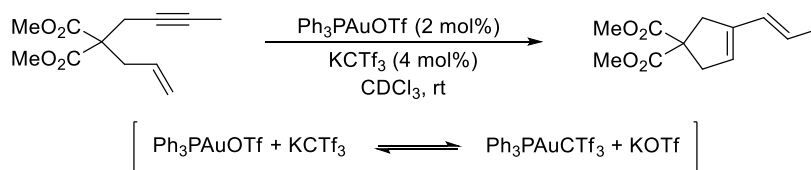
Finally, for the other two mechanistic roles, preventing gold-acetylide formation or decomposition processes, no examples can be undoubtedly assigned yet, since they are not always easy to confirm.

2.2.4 Promoters

Although there are no rules to predict stability of the different complexes, it is well-known that poorly coordinating counterions usually require the use of stabilizing molecules to prevent decomposition processes.⁶ However, these complexes usually exhibit higher reactivity due to its greater electrophilicity.

In this sense, Hammond and co-workers envisioned that the use of (CTf₃) as counterion could increase the efficiency in some gold-catalyzed reaction, due to the low gold-affinity and coordination capability of this anion, although the preparation of such complexes could be challenging. However, they also foresaw

that a counterion shuffling could take place between a stable preformed catalyst and KCTf_3 , due to soft-soft and hard-hard interaction in ion pairing. They called this reagent a 'promoter' since it does not interact with other acidic or basic species in the reaction. They tested their hypothesis in the gold(I)-catalyzed cycloisomerization of a 1,6-enyne (Scheme 4.11).¹⁷ The reaction rate of silver-formed $\text{Ph}_3\text{PAuCTf}_3$ was observed to be only slightly higher than using KCTf_3 as additive, and both of them perform the cycloisomerization several times faster than the original triflate complex.

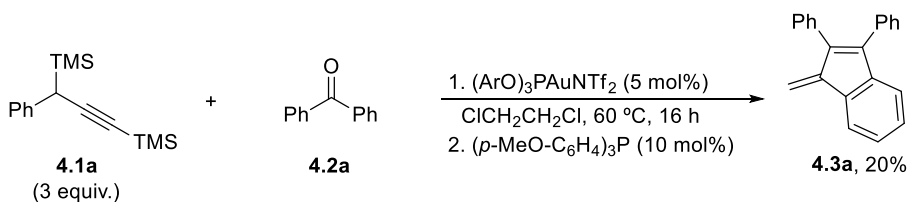


Scheme 4.11: Example of an additive acting as promoter in a gold-catalyzed reaction.

¹⁷ Han, J.; Lu, Z.; Wang, W.; Hammond, G. B.; Xu, B. *Chem. Commun.* **2015**, 51, 13740-13743.

3 Results and discussion

During our studies of the gold(I)-catalyzed propargylation of synergistically activated carbonyl derivatives, we found out, that the reaction of 3 equivalents of propargylsilane **4.1a** with benzophenone, at 60 °C for 24 h, led to a complex mixture of products. From that mixture, benzofulvene derivative **4.3a** was identified and isolated in a 20% yield (Scheme 4.12). To the best of our knowledge, this result would represent the first intermolecular gold-catalyzed synthesis of a benzofulvene derivatives.¹⁸

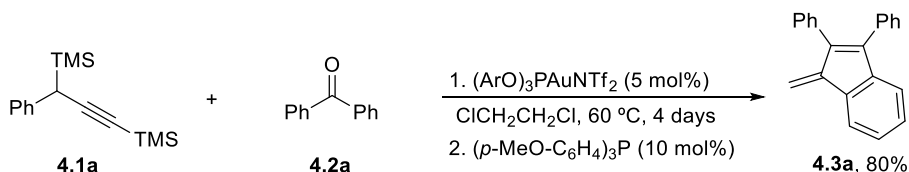


Scheme 4.12: Benzofulvene derivative obtained.

Considering that this product could arise from an intramolecular arylation via 5-*exo-dig* cyclization, we decided to investigate this transformation. For this purpose, propargylsilane **4.1a** and benzophenone **4.2a** were chosen as the model substrates.

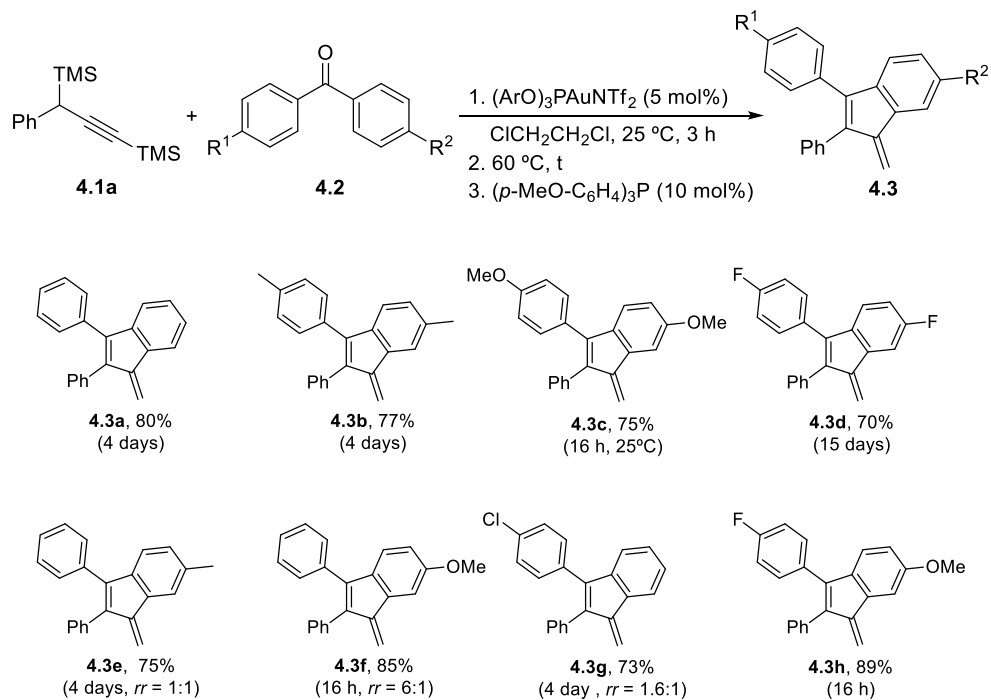
¹⁸ For other gold-catalyzed synthesis of benzofulvenes, see: Hashmi, A. S. K.; Braun, I.; Noesel, P.; Schaedlich, J.; Wietek, M.; Rudolph, M.; Rominger, F. *Angew. Chem. Int. Ed.* **2012**, *51*, 4456-4460; b) Álvarez, E.; Miguel, D.; García-García, P.; Fernández-Rodríguez, M. A.; Rodríguez, F.; Sanz, R. *Synthesis* **2012**, *44*, 1874-1884; c) Plajer, A. J.; Ahrens, L.; Wietek, M.; Lustosa, D. M.; Babaahmadi, R.; Yates, B.; Ariafard, A.; Rudolph, M.; Rominger, F.; Hashmi, A. S. K. *Chem. Eur. J.* **2018**, *24*, 10766-10772.

The reaction was carried out in the presence of a 5 mol% of $(\text{ArO})_3\text{PAuNTf}_2$, which gave the best results for the propargylation process, in 1,2-dichloroethane. After the propargylation step, the reaction mixture was heated at 60 °C for four days, showing full conversion of the starting materials and yielding benzofulvene **4.3a** in a good 80% yield (Scheme 4.13).



Scheme 4.13: Best conditions found for the synthesis of benzofulvene **4.3a**.

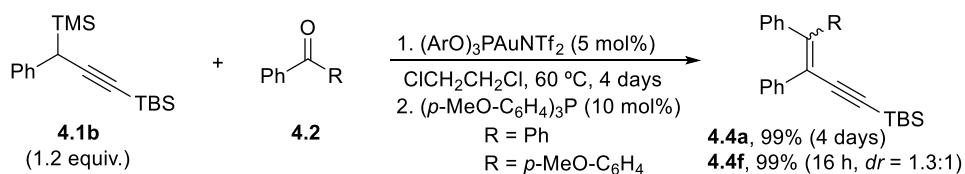
Once it was observed that the intramolecular hydroarylation requires long heating periods, we studied the scope of this reaction in terms of the carbonyl compound, adjusting the reaction time for each example (Scheme 4.14).



Scheme 4.14: Scope of the synthesis of benzofulvenes **4.3**.

As it is shown from symmetrical benzophenones, the reaction is strongly dependent on the electronic properties, ranging the time to achieve full conversion from 16 h (at 25 °C) for 4,4'-dimethoxybenzophenone **4.2c** to 15 days in the case of electron-poor 4,4'-difluorobenzophenone **4.2d**. On the other hand, the behaviour of the reaction towards non-symmetrically substituted benzophenones was also studied. In most of the cases, the products were obtained as a mixture of regioisomers, such as benzofulvenes **4.3e-g**, in good trend with the difference in the electronic properties between both arene rings, and always favouring the hydroarylation from the electron-richer arene ring. In this sense, benzophenone **4.2h**, with an electron-donating and an electron-withdrawing group in different arenes, showed complete regioselectivity in the formation of benzofulvene **4.3h**.

Then, we envisioned the use of a more stable propargylsilane, replacing the acetylenic trimethylsilyl group in **4.1** by a more robust *tert*-butyldimethylsilyl group (propargylsilane **4.1b**), would improve the propargylation step and therefore the overall yield of the reaction, while reducing the number of equivalents (see Chapter I). Initially, benzophenone derivatives **4.2** were tested under the optimized reaction conditions, using 1.2 equivalents of propargylsilane **4.1b** (Scheme 4.15). However, instead of the expected benzofulvenes, 1,3-enynes **4.4a,f** were observed in almost quantitative yield. These products would arise from a dehydration of the initially generated homopropargyl silyl ether, and could be considered as an intermediate in the formation of benzofulvenes **4.3**.

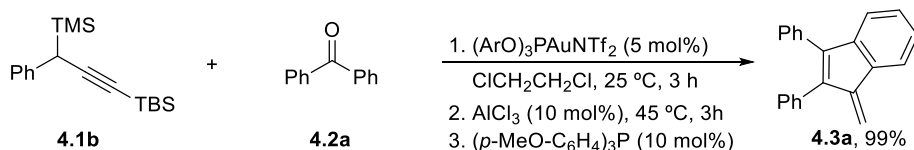


Scheme 4.15: Unexpected formation of 1,3-enynes **4.4a,f**.

After this observation, we considered, among other alternatives, the addition of a Lewis acid catalyst after propargylation step¹⁹ to facilitate the dehydration process and perhaps the subsequent cyclization. In an initial attempt, propargylsilane **4.1a** and benzophenone **4.2a** were dissolved in dry 1,2-dichloroethane and treated with the phosphite-gold(I) triflimide complex at 25 °C. After 3 hours, a 10 mol% of AlCl₃ was added and the reaction was stirred for

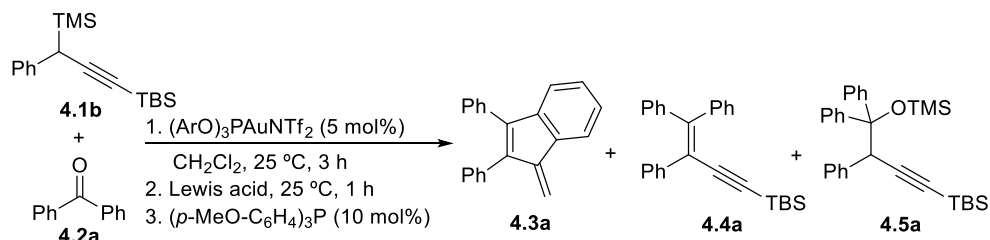
¹⁹ We observed that the presence of AlCl₃ inhibited the propargylation step.

another 3 hours at 45 °C (Scheme 4.16). Following this methodology, benzofulvene **4.3a** was obtained in almost quantitative yield. It is remarkable the influence of the aluminum chloride, as **4.3a** was obtained at 45 °C in only 3 hours, compared to the previously mentioned 4 days required for its synthesis at 60 °C, in absence of AlCl₃.



Scheme 4.16: Model gold(I)/Lewis acid-catalyzed reaction studied.

With this promising result in hand, we explored the use of different Lewis acids under milder conditions to be able to establish a comparison between AlCl₃ and a potentially better catalyst. For this purpose, the model reaction was carried out in dichloromethane and kept at 25 °C for only one hour after the addition of the Lewis acid. The results of this study are summarized in Scheme 4.17.



Entry	Lewis acid	4.5a (%) ^[a]	4.4a (%) ^[a]	4.3a (%) ^[a]
1	None	99	-	-
2	Yb(OTf) ₃	99	-	-
3	Zn(OTf) ₂	52	47	-
4	Sc(OTf) ₃	20	74	<5
5	Ga(OTf) ₃	13	82	<5
6	Cu(OTf) ₂	-	81	14
7	InCl ₃	-	86	11
8	GaCl ₃	-	60	32
9	AlCl ₃	-	50	49
10	AlBr ₃	-	89	10

^[a]Determined by ¹H-NMR using dibromomethane as internal standard.

Scheme 4.17: Screening of different Lewis Acids as cocatalysts.

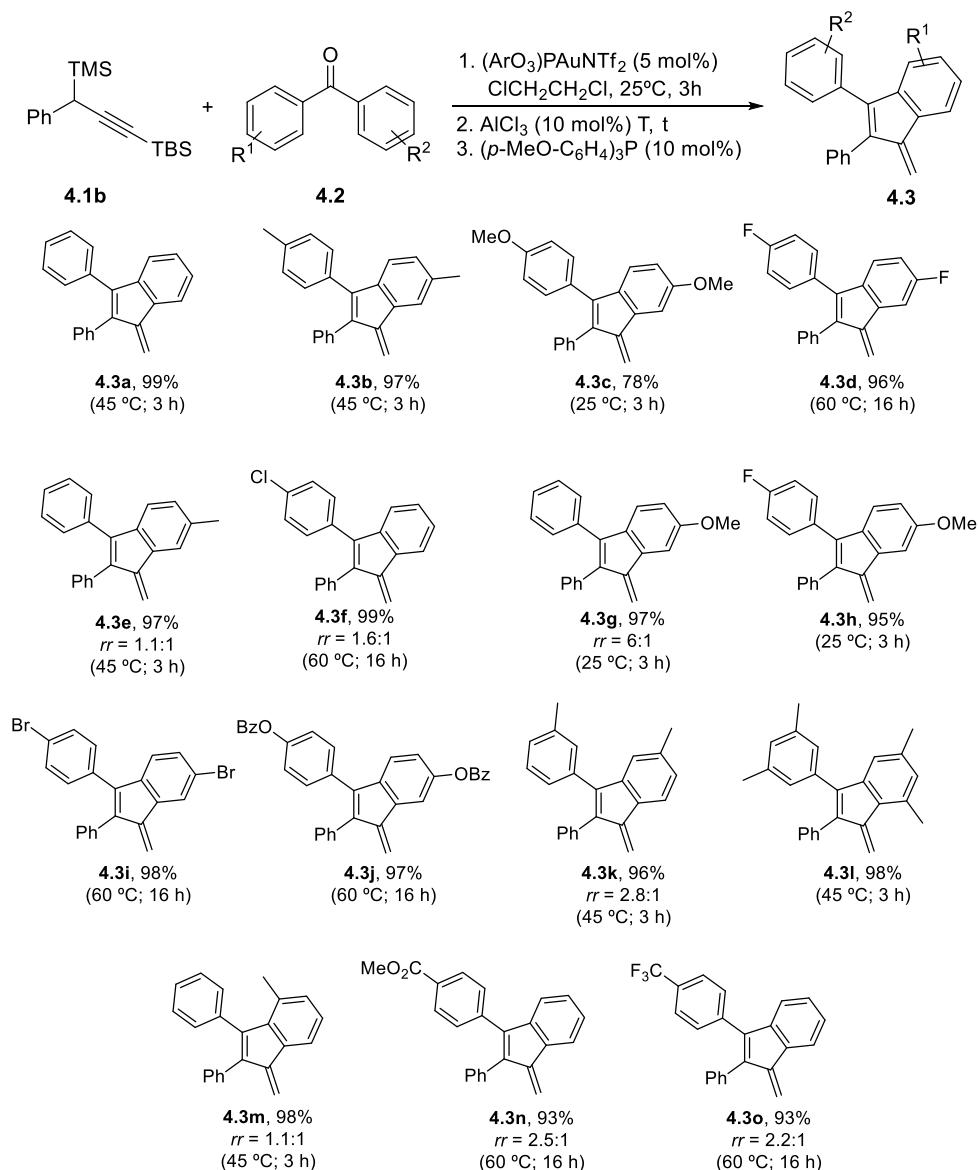
Among all the cocatalysts tested, aluminum trichloride arose as the best option (*Entry 9*), being able to achieve a roughly 50% of benzofulvene **4.3a** and enyne **4.4a**. Other metallic triflates mostly afforded 1,3-enyne **4.4a** (*Entries 3-5*) or even did not promote dehydration step (*Entry 2*). Only copper(II) triflate furnished benzofulvene **4.3a** in a low 14% yield (*Entry 6*). Interestingly, the use of less acidic aluminum bromide yielded the desired product in a much lower yield (*Entry 10*). The same trend was observed for gallium and indium chlorides (*Entries 7-8*), finding that the final yields are in good trend with the decreasing Lewis acidity of these halides in comparison with aluminum trichloride.²⁰ Regarding these results, aluminum trichloride was chosen as the best option for this *one pot* procedure, due to its effectiveness.

Once optimized the reaction conditions, the next stage consisted in the study of the scope of the reaction in terms of structure of the carbonyl compound **4.2** (Scheme 4.18). The reaction performed well for benzophenone derivatives with different substitution patterns, ranging from electron-donating to electron-withdrawing groups, with excellent yields in all the cases. The reaction temperature and time were optimized for each example, and are given below.

It is worth to mention that, for benzophenones bearing electron-withdrawing groups (**4.3d**, **4.3f**, **4.3i-j** and **4.3n-o**) it was necessary to heat at 60 °C for 16 hours to achieve full conversion. In particular, it is highly remarkable that the use of Au(I)-Al(III) combination allowed to obtain benzofulvene **4.3d** in higher yield and under milder conditions (45 °C instead of 60 °C) in 16 h instead of the previously reported 15 days. On the contrary, the reaction for benzophenones with strong electron-donating groups took place even at 25 °C after the addition of the aluminum trichloride (**4.3c**, **4.3g** and **4.3h**).

Additionally, the isomeric ratios observed for benzofulvenes **4.3e**, **4.3g**, **4.3f** and **4.3h** matched perfectly with the previously obtained in the absence of aluminum trichloride (Scheme 4.14), supporting the existence of a similar mechanistic pathway in both cases. For the rest of the examples, the same trend in terms of regioselectivity was observed: the major isomer corresponds to the hydroarylation of the more nucleophilic arene ring, and the isomers ratio depends on the difference of nucleophilicity between both arenes.

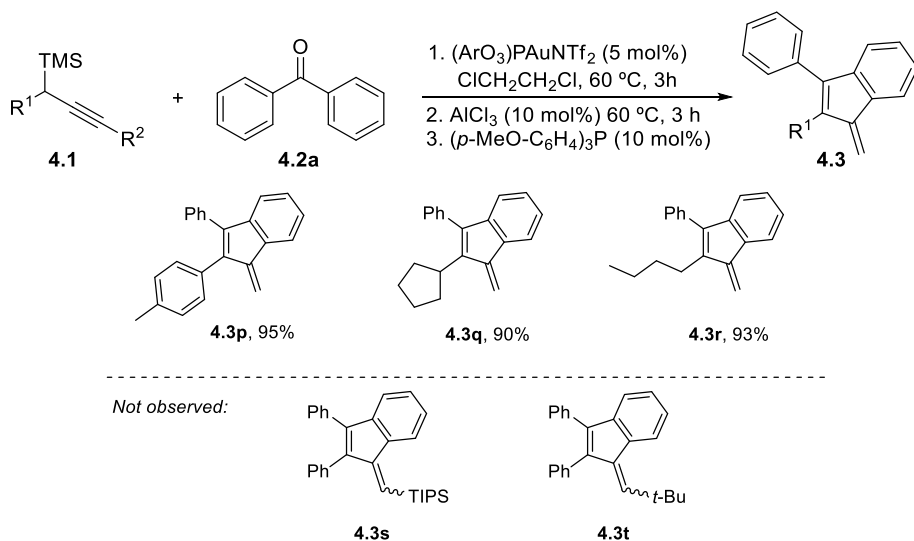
²⁰ Satchell, D. P. N.; Satchell, R. S. *Chem. Rev.* **1969**, *69*, 251-278.



Scheme 4.18: Scope of benzofulvene formation with different carbonyl compounds **4.2**.

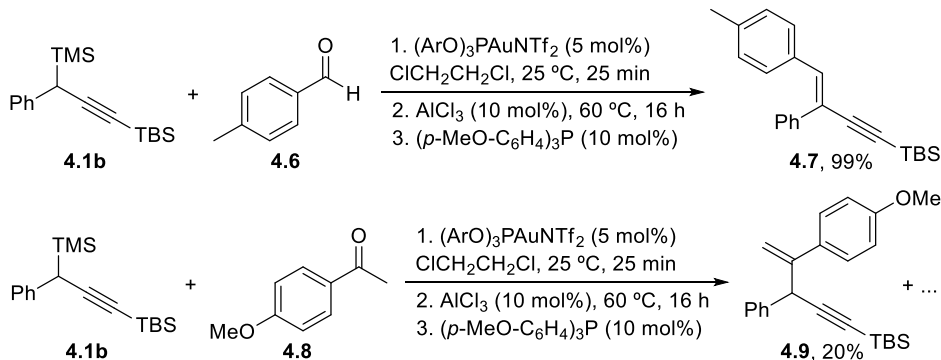
Next, we studied the scope of this transformation employing propargylsilanes **4.1** with different substituents at the propargylic position. It is important to remark that, in all these cases, it was necessary to use three equivalents of propargylsilane **4.1** and heat at 60 °C for the propargylation step, due to the lower reactivity of these derivatives. As depicted in Scheme 4.19, *p*-tolyl, cyclopentyl and butyl groups were also well tolerated, furnishing benzofulvenes **4.3ap-r** in excellent

yields. Nevertheless, propargylsilanes bearing a bulkier triisopropylsilyl group (TIPS) or a *tert*-butyl group in the acetylenic position did not furnish the expected benzofulvenes **4.3s** and **4.3t**. In both cases, only protodesilylation of the starting material took place, demonstrating once again their lower reactivity towards propargylation reaction (see Chapter I).



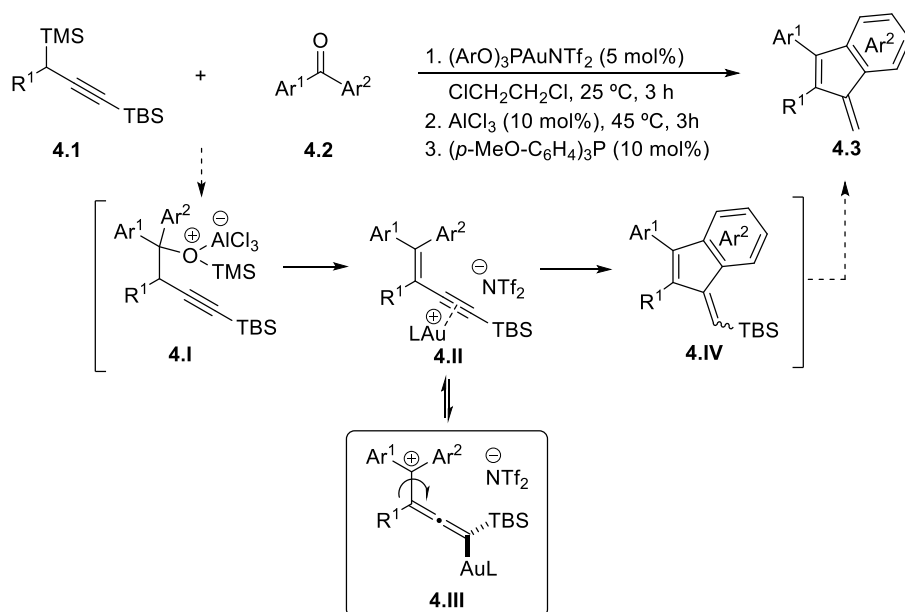
Scheme 4.19: Scope in terms of the propargylsilane **4.1**.

The use of an aromatic aldehyde led to no cyclization product. Thus, for *p*-toluylaldehyde **4.6**, the corresponding 1,3-enyne **4.7** was obtained as the only product even heating at 60 °C for 16 hours (Scheme 4.20). Additionally, the use of 4-methoxyacetophenone **4.8** only afforded the expected benzofulvene in less than a 5% yield. However, a mixture of different products was observed, presumably the *Z:E* isomers of the corresponding 1,3-enyne along with other by-products. As a very relevant compound, among them 1,4-enyne **4.9** was isolated.



Scheme 4.20: Limitation of the reaction for benzaldehydes and acetophenones.

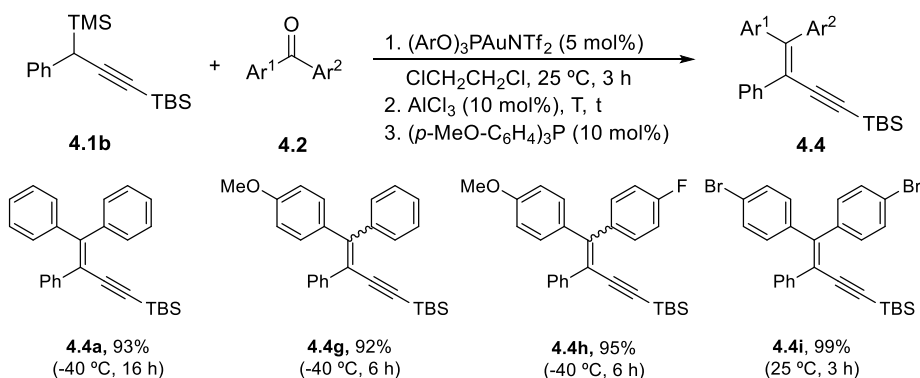
These results gave important hints about the mechanism of this transformation, because the emergence of 1,3-enyne **4.7** and 1,4-enyne **4.9** could support a reaction pathway through the formation of a positive charge at the benzylic position. Moreover, it was proven that two aryl rings are required for this transformation to occur, probably due to the higher stability of the mentioned carbocation. Therefore, we envisioned a mechanistical proposal in which these structures could be considered as intermediates, as it is summarized in Scheme 4.21.



As it is described, the Lewis acid should coordinate the silyl ether (intermediate **4.I**) easing the dehydration step and generating the corresponding 1,3-enynes **4.4** and **4.7**. Dehydration through the terminal methyl group for acetophenone **4.6b** would generate 1,4-enyne **4.8**. Next, only for of benzophenones **4.2**, diaryl substituted intermediate **4.II**, generated by coordination of the gold complex, could be in equilibrium with a carbocationic σ -allenylgold(I) intermediate **4.III**. This key carbocationic σ -allenylgold(I) **4.III** could explain the regioselectivity of the reaction, as it allows free rotation along the C-C single bond, allowing a preferential attack

from the more nucleophilic arene ring. Finally, a Nazarov-type cyclization²¹ would be responsible of silyl-benzofulvene **4.IV** formation, finishing with a protodesilylation step.

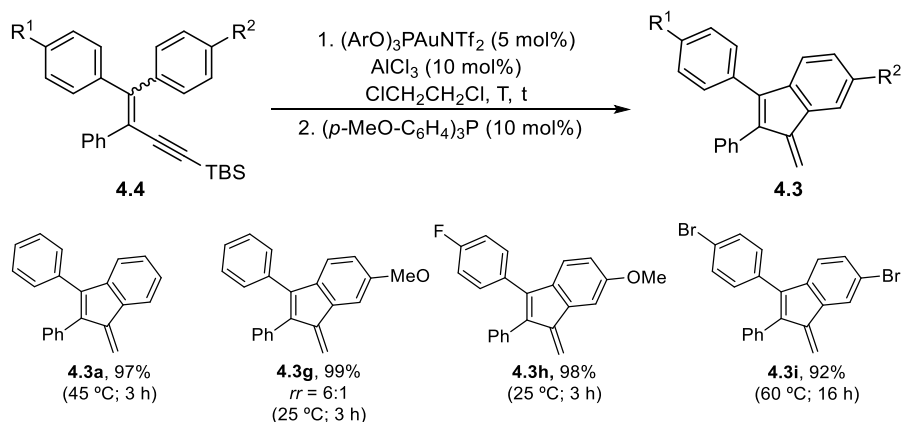
To confirm our hypothesis, we tried to trap different 1,3-enynes **4.4** under gold(I)-AlCl₃ catalysis. Fortunately, under milder reaction conditions, we were able to get a collection of 1,3-enynes **4.4** with different substitution patterns at the aromatic rings (Scheme 4.22). For non-symmetrically substituted enynes **4.4g,h,i**, a mixture of the *Z:E* isomers was observed in all the cases, in a close to 1:1 ratio. We also observed that enynes with electron-donating groups required lower temperatures and shorter reaction times to be formed.



Scheme 4.22: *One pot* gold-catalyzed synthesis of different 1,3-enynes **4.4**.

Next, 1,3-enynes **4.4a,g,h,i** were tested under the optimized reaction conditions for the formation of benzofulvenes **4.3a,g,h,i**, using 10 mol% of AlCl₃, attempting to observe the proposed silyl-benzofulvenes **4.IV**. Nevertheless, benzofulvenes **4.3** instead of **4.IV** were obtained with excellent yields in all the cases (Scheme 4.23). It is worth to mention that regioisomeric ratios in the final products agreed with the *one pot* process and differed from the initial *Z:E* mixture, supporting the participation of the allenic intermediate **4.III**.

²¹ Cordier, P.; Aubert, C.; Malacria, M.; Lacôte, E.; Gandon, V. *Angew. Chem. Int. Ed.* **2009**, *48*, 8757-8760.

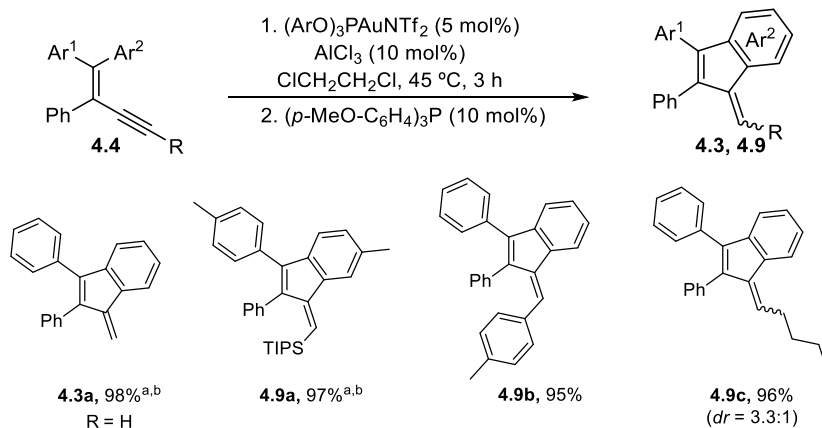


Scheme 4.23: Gold(I)/AlCl₃-catalyzed cyclization of 1,3-enynes **4.4**.

Although 1,3-enynes **4.4** could be confirmed as reaction intermediates for the one-pot synthesis of benzofulvenes, surprisingly no silyl-benzofulvenes **4.IV** were observed, despite there were no proton sources that allow protodesilylation step. Considering the role played by the silanol groups on the glassware surface in undesired protodeauration observed in *Chapter I*, we carried out the reaction in a polypropylene tube, but no silyl-benzofulvenes **4.IV** were observed at all.

Additional experiments to confirm our proposal, while determining if an alkynylsilyl moiety is required for this transformation, consisted in removing the TBS group or replacing it by more robust TIPS group, an arene ring or an alkyl chain. With this idea in mind, 1,3-enynes **4.4u-w**, not accessible through propargylation reaction, were synthesized by other means,²² and tested under the optimized reaction conditions. As shown in Scheme 4.24, other silyl groups, alkyl and aryl substituents, as well as a terminal alkyne, worked perfectly. It should be noted that, for bulkier and more robust TIPS group (**4.4s**), Z-silyl-benzofulvene **4.9a** was obtained in almost quantitative yield with total diastereoselectivity. This result suggests that silyl-benzofulvenes are true reaction intermediates and their instability towards protodesilylation triggers the final step. Moreover, the use of an aryl and alkyl substituent indicates that the presence of a silyl moiety is not a requirement for benzofulvene formation. Stereochemistries of the major isomer of benzofulvenes **4.9a-c** were determined by NMR nOe experiments. Finally, it is also important the result obtained for the terminal alkyne.

²² Miguel-Ávila, J.; María Tomás-Gamasa, M.; Mascareñas, J. L. *Angew. Chem. Int. Ed.* **2020**, *59*, 17628-17633.



^aReaction performed at 25 °C; ^b1 h of reaction.

Scheme 4.24: Cyclization of enynes **4.4f-i** with different alkynyl moieties.

❖ Mechanism determination. Role of the Lewis acid

Once it was confirmed the participation of 1,3-enynes **4.4** and silyl-benzofulvenes **4.9** as intermediates, we focused our efforts in determining the role played by the Lewis acid in the catalytic process. Considering the reported Lewis acid effects in gold catalysis, we envisioned two possibilities for the present transformation: a tandem AlCl_3 -gold(I) catalysis, performing aluminum trichloride the dehydration step and the gold(I) complex the cyclization process, or a cocatalysis through generation of a more active gold catalyst.

Initially, we carried out a set of control experiments with this goal in mind. First of all, we observed that neither gold(I) catalyst nor aluminum trichloride were competent to independently achieve the full catalytic process under the standard reaction conditions, either from homopropargyl silyl ether **4.5a** or 1,3-enyne **4.4a** (Figure 4.2). These results allowed us to discard a hypothetical tandem mechanism.

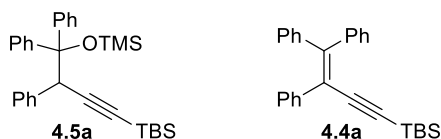
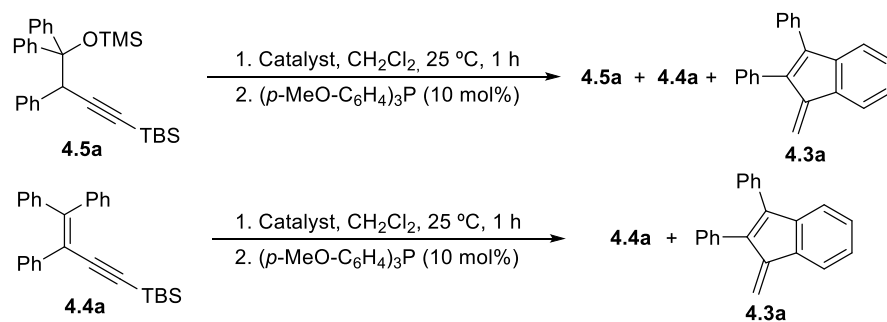


Figure 4.2: Homopropargyl silyl ether **4.5a** and 1,3-enyne **4.4a** for control experiments.

Heading now to investigate a possible interaction between both catalytical species, a 1:1 mixture of AlCl_3 and the gold(I) complex was stirred in dry CD_2Cl_2 , for

Several control experiments were set aiming to identify the true catalytically active species. Considering that the propargylation process only requires the gold(I) catalyst, we studied dehydration and cyclization steps. Thus, homopropargyl silyl ether **4.5a** or 1,3-enyne **4.4a** were dissolved in dry CD_2Cl_2 and treated with the species involved in the equilibrium, and the results are summarized in Table 4.1.



Entry	Catalyst	Alkyne	% 4.5a ^a	% 4.4a ^a	% 4.3a ^a
1	(ArO) ₃ PAuNTf ₂ (5 mol%) + AlCl ₃ (10 mol%)	4.5a	-	-	99
		4.4a	-	-	99
2	(ArO) ₃ PAuNTf ₂ (5 mol%) + AlCl ₃ (5 mol%)	4.5a	65	27	7 ^b
		4.4a	-	37	60
3	(ArO) ₃ PAuNTf ₂ (5 mol%)	4.5a	99	-	-
		4.4a	-	99	-
4	AlCl ₃ (10 mol%)	4.5a	99	-	-
		4.4a	-	99	-
5	(ArO) ₃ PAuCl (5 mol%)	4.5a	99	-	-
		4.4a	-	99	-
6	Cl ₂ AlNTf ₂ (5 mol%) ^c	4.5a	68	28	-
		4.4a	-	90	7
7	HNTf ₂ (2.5 mol%) ^c	4.5a	-	84	15
		4.4a	-	72	27
8	(ArO) ₃ PAuCl (5 mol%) + AlCl ₃ (5 mol%)	4.5a	72	22	<5
		4.4a	-	91	7
9	(ArO) ₃ PAuCl (5 mol%) + Cl ₂ AlNTf ₂ (5 mol%)	4.5a	-	33	65
		4.4a	-	-	99

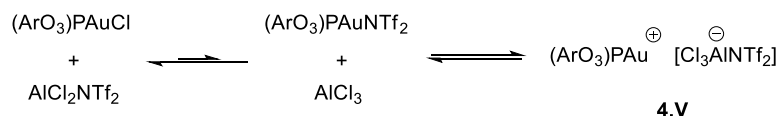
^aYield determined by ¹H-NMR using dibromomethane as internal standard; ^b45% after 3 h at 45 °C; ^cThe use of 5 mol% of HNTf₂ resulted in decomposition products.

Table 4.1: Control experiments starting from silyl ether **4.5a** and enyne **4.4a**.

- First, the reaction was carried out in the presence of both catalysts, using 5 mol% of the gold complex and 10 mol% of AlCl₃, (*Entry 1*), leading to quantitative formation of benzofulvene **4.3a**. The use of a 5 mol% of AlCl₃ moderately diminished the yield (*Entry 2*), presumably indicating a possible equilibrium between the isolated catalysts and the active species.
- Independently using (ArO)₃PAuNTf₂ (*Entry 3*) or AlCl₃ (*Entry 4*) led to no positive result, as previously mentioned. Additionally, phosphite-gold(I) chloride complex (*Entry 5*) also behaved as a catalytically inert complex, just as expected.
- The use of a 5 mol% of freshly prepared Cl₂AlNTf₂ (*Entry 6*) showed low activity, affording benzofulvene **4.3a** in very low yield, and also 1,3-enyne **4.4a** in 28% yield starting from **4.5a**.
- We envisioned that a Brønsted acid catalysis could exist, due to the dehydration process, operating as a background catalysis or even as the true catalytic cycle. Various experiments carried out using triflimide (HNTf₂) seem to support the idea of a minor background catalysis, since benzofulvene **4.3a** was observed in lower yields, compared to the Au(I)-Al(III) combination (*Entry 7*). For this reason, enhanced gold-catalysis seems to be the responsible of this transformation, although a slight background proton catalysis cannot be completely discarded and avoided.
- We also tested a mixture of the phosphite-gold(I) chloride and AlCl₃ as catalyst (*Entry 8*). For this combination, the elimination and cyclization steps take place, albeit with a lower rate. However, this result strongly supports our idea since no other equilibrium but the counterion abstraction could be operating in the catalyst activation, given that counterion shuffling would generate the same gold(I) chloride. Moreover, a similar result has been described in the literature using a phosphine-gold(I) complex and gallium trichloride.²⁵
- Finally, a combination of the phosphite-gold(I) chloride and Cl₂NTf₂ should represent the closest scenario to the catalytic system, and indeed, it worked as expected, generating the final benzofulvene **4.3a** in quantitative yield, starting from 1,3-enyne **4.4a** (*Entry 8*).

²⁵ Joost, M.; Gualco, P.; Coppel, Y.; Miqueu, K.; Kefalidis, C. E.; Maron, L.; Amgoune, A.; Bourissou, D. *Angew. Chem. Int. Ed.* **2014**, *126*, 766-770.

It should be noted that $(\text{ArO})_3\text{PAuNTf}_2$, AlCl_3 , $(\text{ArO})_3\text{PAuCl}$ and $\text{AlCl}_2\text{NTf}_2$ are non-competent catalysts by themselves, leading to lower or no formation of benzofulvene **4.3a**. Thus, we considered the hypothetical existence of a second equilibrium as the proposed, but not doubtlessly observed, by Hammond and co-workers²⁶ involving a counterion abstraction to generate a more electrophilic gold complex **4.V** by decreasing the coordinative ability of the triflimidate anion (Equation 4.2). This species **4.V** would explain the enhancement in the catalytic activity of the gold complex, that follows a good trend with the Lewis acidity for comparable additives. This outcome would be different from the previously reported gold(I) chloride activations by Lewis acid,²⁷ since a simple counterion-exchanged did not allow to explain the experimental results.



Equation 4.2: Proposed equilibrium including more electrophilic species **4.V**.

Coming up to this point, we focussed our efforts in finding direct experimental evidence to support our hypothesis. Considering that the equilibrium was highly displaced at room temperature towards gold(I) chloride and $\text{AlCl}_2\text{NTf}_2$ formation, we envisioned that several low temperature NMR experiments might gave us a chance to directly observe complex **4.V** or its coordination to an intermediate 1,3-enyne **4.4**. 1,3-Enyne **4.4s** was chosen as model substrate, considering the greater robustness of its triisopropylsilyl group, and, after preliminary attempts, $-85\text{ }^\circ\text{C}$ as the optimum temperature for the experiments (Figure 4.4).

²⁶ Lu, Z.; Li, T.; Mudshinge, S. R.; Xu, B.; Hammond, G. B. *Chem. Rev.* **2021**, *121*, 8452-8477.

²⁷ For selected examples, see: a) Dai, L.-Z.; Shi, M. *Chem. Eur. J.* **2010**, *16*, 2496-2502; b) Guerinot, A.; Fang, W.; Sircoglou, M.; Bour, C.; Bezenine-Lafollee, S.; Gandon, V. *Angew. Chem. Int. Ed.* **2013**, *52*, 5848-5852; c) Fang, W.; Presset, M.; Guerinot, A.; Bour, C.; Bezenine-Lafollee, S.; Gandon, V. *Org. Chem. Front.* **2014**, *1*, 608-613; d) Fang, W.; Presset, M.; Guerinot, A.; Bour, C.; Bezenine-Lafollee, S.; Gandon, V. *Chem. Eur. J.* **2014**, *20*, 5439-5446.

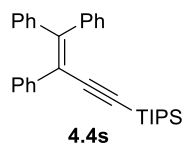


Figure 4.4: 1,3-Enyne **4.4s** employed for low temperature NMR experiments.

First, the species involved in the equilibrium (Equation 4.2) were dissolved in CD_2Cl_2 , and the solutions were discretely analyzed at $-85\text{ }^\circ\text{C}$ by ^1H , ^{31}P - and ^{19}F -NMR. For that purpose, two different mixtures were prepared at room temperature, cooled down and studied: $(\text{ArO})_3\text{PAuNTf}_2 + \text{AlCl}_3$ and $(\text{ArO})_3\text{PAuCl} + \text{AlCl}_2\text{NTf}_2$, corresponding to both sides of the proposed equilibrium. The resulting ^{31}P -NMR spectra are gathered in Figure 4.5.

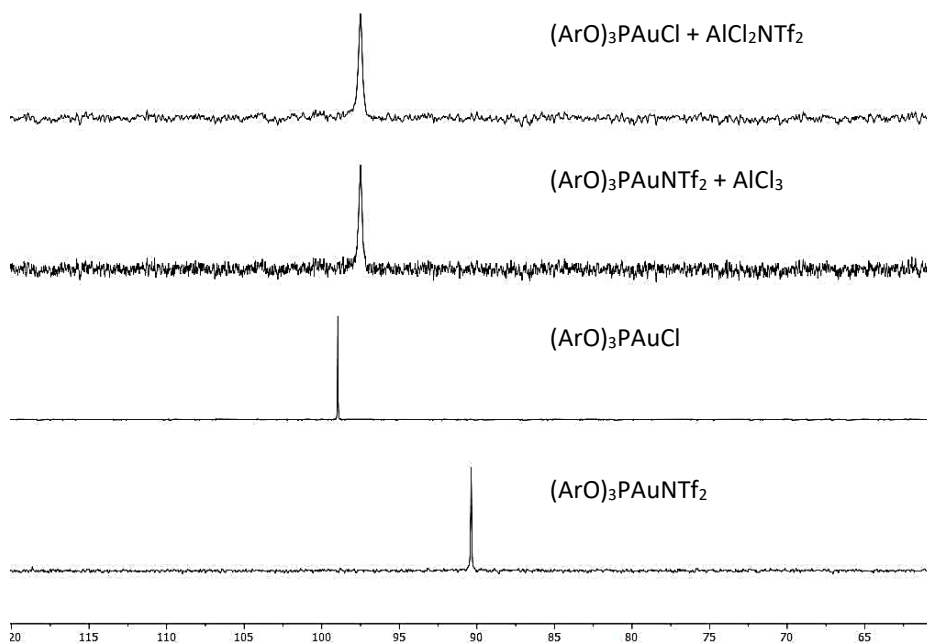


Figure 4.5: Low temperature ^{31}P -NMR spectra.

From these experiments it could be deduced that both mixtures $(\text{ArO})_3\text{PAuNTf}_2 + \text{AlCl}_3$ and $(\text{ArO})_3\text{PAuCl} + \text{AlCl}_2\text{NTf}_2$ led to the same outcome, since they presented identical ^{31}P -NMR signal (97.5 ppm). Indeed, those signals clearly differed from the ones corresponding to each of the free parent species $(\text{ArO})_3\text{PAuCl}$ (99.0 ppm) and $(\text{ArO})_3\text{PAuNTf}_2$ (90.4 ppm). Because of this, we proposed that the new signal at 97.5

ppm could correspond to the catalytically active specie **4.V**, not observed at room temperature (Figure 4.3).

On the other hand, the same coincidence was also observed in the ^{19}F -NMR spectra for both gold-aluminium combinations, appearing a new ^{19}F signal at -76.0 ppm, clearly distinguishable from the parent compounds $(\text{ArO})_3\text{PAuNTf}_2$ and $\text{AlCl}_2\text{NTf}_2$ (Figure 4.6). We could assign this peak to the aluminate anion $[\text{Cl}_3\text{AlNTf}_2]^-$. The presence of other small peaks could correspond to other aluminate anions bearing triflimide subunit with different stoichiometry.²⁸

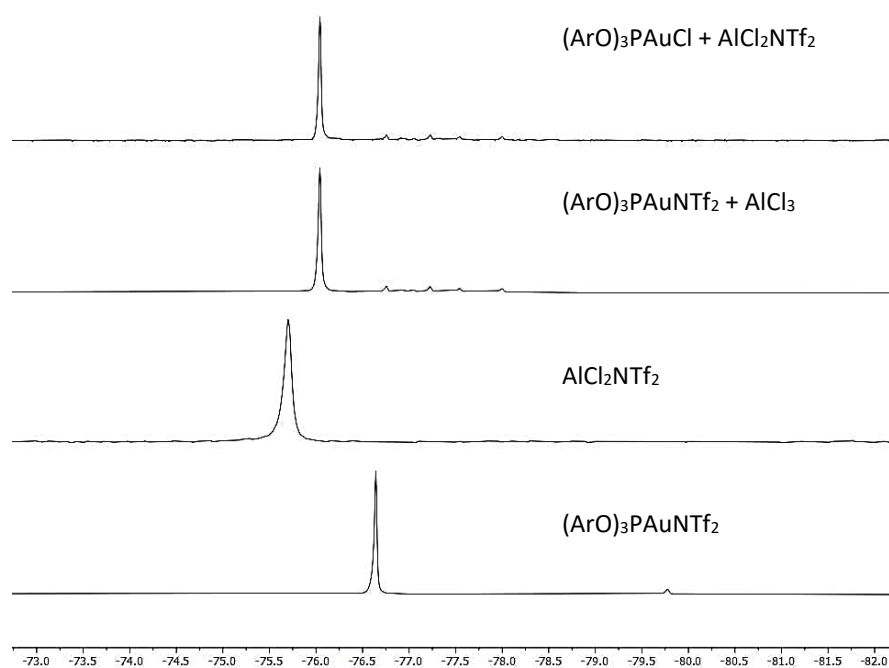


Figure 4.6: Low temperature ^{19}F -NMR spectra.

Afterwards, different mixtures of 1,3-enyne **4.4s** with each of the possible gold(I) catalysts were prepared and analyzed by ^{31}P -, ^{19}F and ^{13}C -NMR at $-85\text{ }^\circ\text{C}$. Attending first to the ^{31}P -NMR spectra, collected in Figure 4.7, it became clear that all the experiments with a coordinative gold(I) complex showed the same peak at 99.5 ppm, which would correspond to the cationic gold-enyne species, differing in

²⁸ Rodopoulos, T.; Smith, L.; Horne, M. D.; R  ther, T. *Chem. Eur. J.* **2010**, *16*, 3815-3826.

each case with $(\text{ArO})_3\text{PAuNTf}_2$ (90.4 ppm), $(\text{ArO})_3\text{PAuCl}$ (99.0 ppm) and potential complex **4.V** (97.5 ppm). Only the mixture of 1,3-enyne **4.4s** and $(\text{ArO})_3\text{PAuCl}$ presented a different behaviour, indicating the obtained value of 98.9 ppm that no coordination to the 1,3-enyne **4.4s** took place.

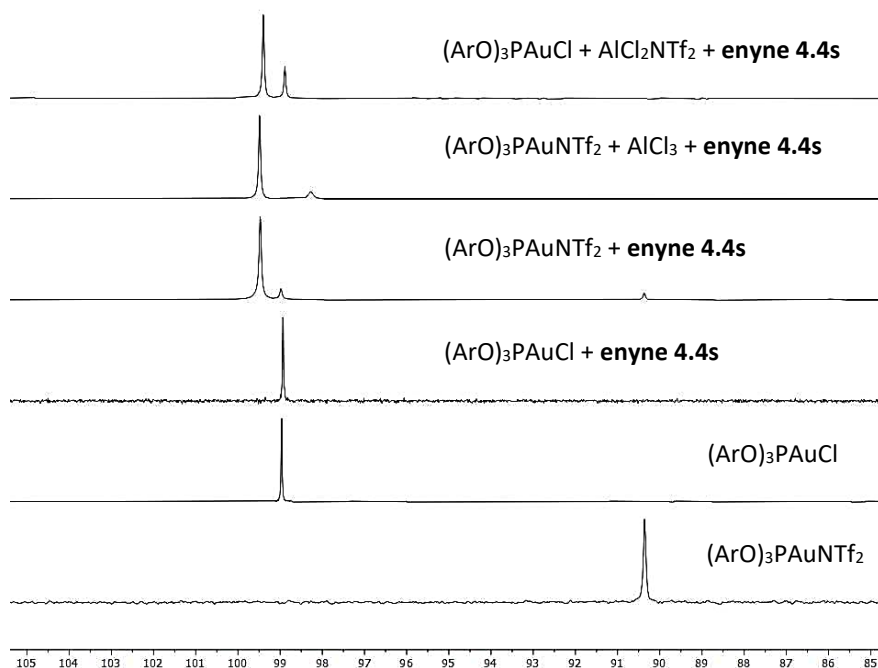


Figure 4.7: Low temperature ^{31}P -NMR spectra of gold-enyne complexes.

Therefore, for the 1,3-enyne **4.4s** coordination of the mixtures $(\text{ArO})_3\text{PAuNTf}_2 + \text{AlCl}_3$ and $(\text{ArO})_3\text{PAuCl} + \text{AlCl}_2\text{NTf}_2$, and also for the coordinated $(\text{ArO})_3\text{PAuNTf}_2$, we considered that the nature of the cationic units is identical. Moreover, this hypothesis could be confirmed by ^{13}C -NMR, as all of them showed the same chemical shifts.

Fortunately, the ^{19}F -NMR experiments of the mixtures were more illustrative, as the observed chemical shifts exhibited significant differences among them, proving the distinct nature of the anionic entity, and the spectra are collected in Figure 4.8.

The most notable observation is the presence of a new signal at -76.3 ppm for both gold-aluminum mixtures, different from the free parent compounds, $(\text{ArO})_3\text{PAuNTf}_2$ (-76.6 ppm) and $\text{AlCl}_2\text{NTf}_2$ (-75.7 ppm), and more remarkable, very different from the mixture $(\text{ArO})_3\text{PAuNTf}_2 + \text{enyne } \mathbf{4.4s}$ (-80.0 ppm). Thus, these

results supported the presence of the same anion for both gold-aluminum mixtures, with a significant downfield difference with the one observed for the complex $(\text{ArO})_3\text{PAuNTf}_2 + \text{enyne } \mathbf{4.4s}$, lacking AlCl_3 . Regarding this, we proposed the coordination of the triflimidate anion by a molecule of AlCl_3 to generate an aluminate counterion. This trend agreed also with the experimental observation described by R ther and co-workers.²⁸

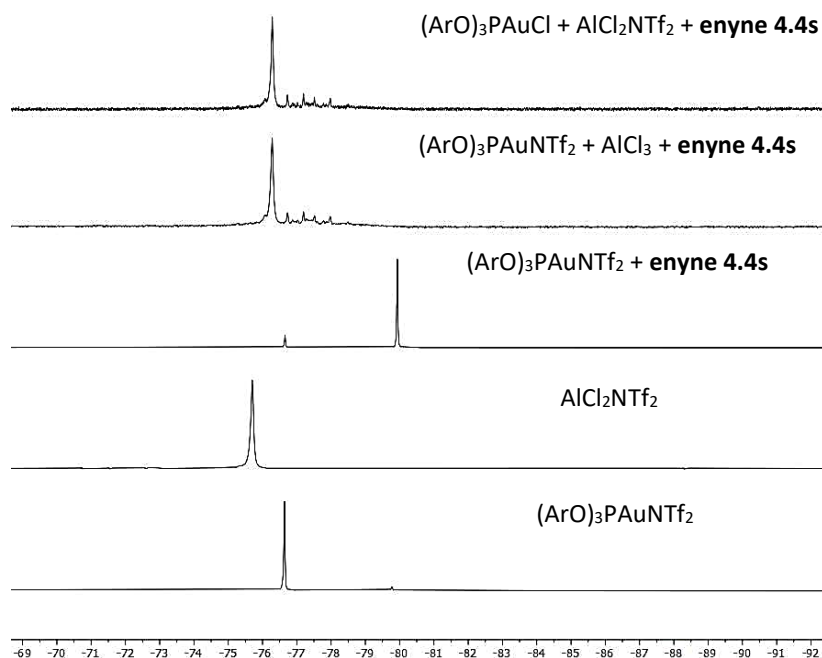
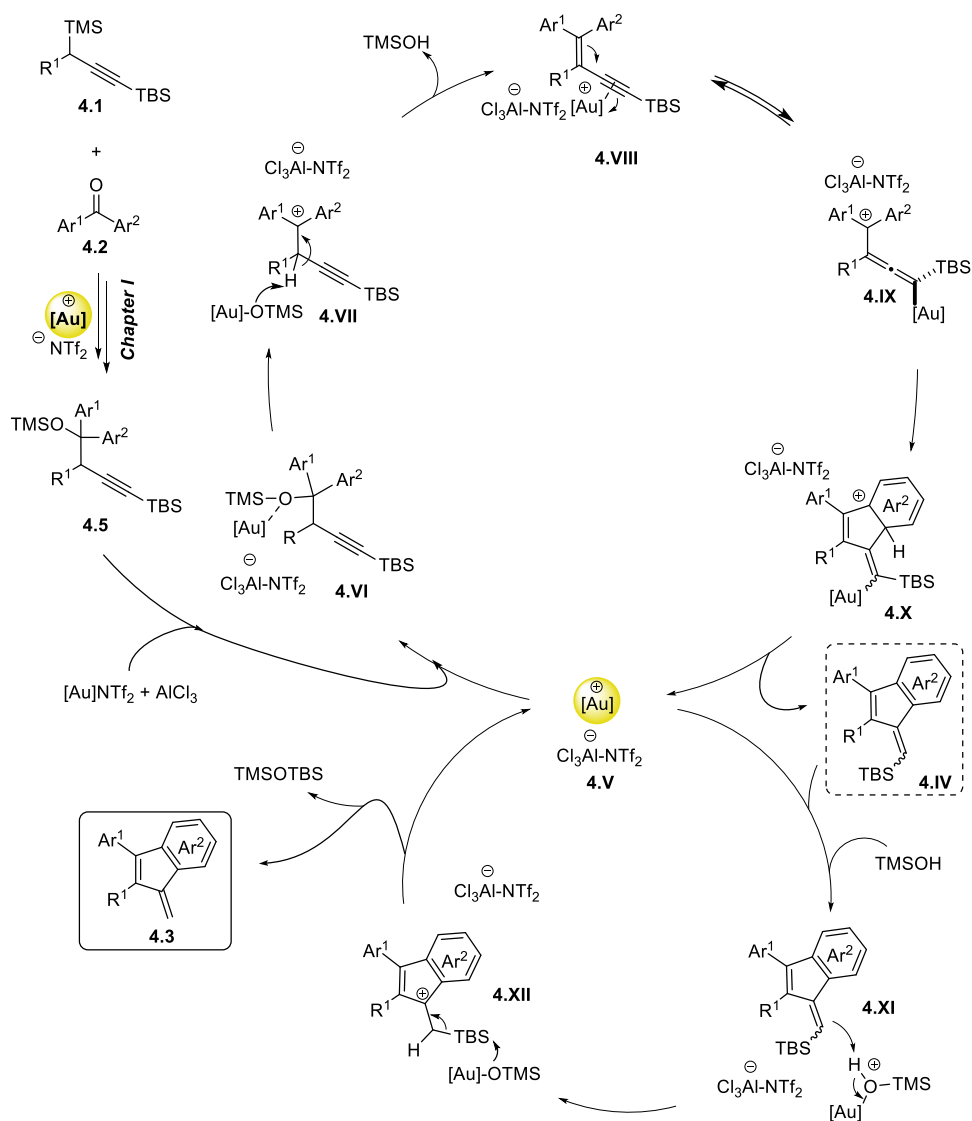


Figure 4.8: ^{19}F -spectra of gold coordination low temperature NMR-experiments.

Therefore, these outcomes support an interaction between the gold(I) catalyst and the Lewis acid cocatalyst, producing a more electrophilic species with enhanced activity. This most plausible explanation points out to a coordination of the triflimidate, with presumable generation of an aluminate anion, increasing the electrophilicity of the gold centre without significant changes in the stability of the complex.

Taking all the bibliographic background and these control experiments results into account, a catalytic cycle, including the proposed more electrophilic gold

catalyst **V**, can be envisioned to justify this transformation, and it is depicted in Scheme 4.25.



Scheme 4.25: Mechanistic proposal for the formation of benzofulvenes **4.3**.

Thus, after formation of homopropargyltrimethylsilyl ether **4.5**, through a synergistic gold-catalyzed propargylation of benzophenone derivative (see *Chapter I*), aluminum trichloride is added and the new highly electrophilic gold complex **4.V** would be generated. Next, coordination of this more electrophilic species **4.V** to the oxygen atom of the homopropargyl silyl ether **4.5a** (intermediate **4.VI**) could

facilitate the dehydration step, through a carbocationic intermediate **4.VII**, generating trimethylsilanol. Then, coordination of the gold complex **4.V** to the generated 1,3-enyne **4.4** would lead to enyne intermediate **4.VIII**. At this point, an equilibrium between π -1,3-enynegold(I) **4.VIII** and σ -allenylgold(I) **4.IX** cationic intermediates could take place,²⁹ allowing free rotation along the new C-C single bond, explaining the regioselectivity of the reaction in terms of the different nucleophilicity of the two arene rings. Cationic σ -allenylgold(I) intermediate **4.IX** could next evolve through a Nazarov-type ring-closure reaction,²¹ to form benzofulvene skeleton **4.X**. From intermediate **4.X**, consecutive rearomatization and protodeauration steps would give rise to silylbenzofulvene **4.IVa**. Finally, coordination to the previously released trimethylsilylmethanol molecule could generate an acidic species capable to react with silylbenzofulvene **4.IVa**. Following the usual reactivity pattern of vinylsilanes (see *General background, Figure 2*), formation of intermediate **4.XI** and carbon-silicon bond cleavage would furnish the observed benzofulvenes **4.3**.

As a summary, a one-pot gold-Lewis-acid-catalyzed synthesis of benzofulvene derivatives has been described. Several control experiments indicated that the enhancement of the gold(I) complex performance could be attributed to an interaction between both cocatalysts to generate a more electrophilic species, presumably by coordination of the gold counterion. In addition, low temperature NMR experiments also pointed out to this hypothesis, as significant changes in the spectra were observed. To the best of our knowledge, this kind of behaviour has been only proposed in the bibliography, representing this process the first example of this reactivity to be reported and supported with experimental evidence.

²⁹ For a copper similar proposed mechanism, see: Sai, M.; Matsubara, S. *Adv. Synth. Catal.* **2019**, *361*, 39-43.

4 Conclusions

A one-pot gold(I)-Lewis-acid-catalyzed synthesis of benzofulvene derivatives have been developed. This protocol employs benzophenone derivatives and propargylsilanes, under gold(I) catalysis in combination with a Lewis acid.

Following this methodology, several examples of benzofulvene derivatives have been synthesized in high yield. The reaction tolerates a wide range of substituents with various electronic properties at different positions of both aromatic rings. For non-symmetric benzophenones a mixture of regioisomers was obtained, and the ratio between them strongly depended on the difference in the electronic nature of the rings, favouring the reaction through the most nucleophilic one.

This transformation is proposed to occur through the following steps: propargylation, dehydration of the homopropargyl silyl ether and formal hydroarylation of a 1,3-enyne through a Nazarov-type process. In fact, 1,3-enynes could be isolated, and their role as intermediates was also proved.

Aluminium trichloride is proposed to participate in the dehydration and hydroarylation steps. Several control experiments pointed out that the active catalyst is only generated upon combination of the gold(I) catalyst and AlCl_3 . Moreover, low temperature NMR studies allowed us to propose a coordination of the triflimidate anion as the key event, generating a more electrophilic phosphitegold(I) aluminate with enhanced activity.

General conclusions

The employment of gold(I) complexes has allowed to develop a new methodology for the catalytic propargylation of carbonyl compounds using propargylsilanes, through a synergistic gold-silylium catalysis.

The study of the mechanism of the propargylation reaction permitted to demonstrate the participation of a key σ -allenylgold(I) complex, formed after π -activation of the propargylsilane. This organometallic specie represented the first example of this kind of intermediates isolated and characterized with confirmed relevant catalytic activity.

Expanding the scope of the propargylation reaction to xanthone derivatives allowed to describe the first catalytic diastereoselective deoxygenative bispropargylation reaction, under gold(I) catalysis, leading to 9,9-bispropargylxanthone derivatives with no bibliographic precedents. Moreover, the process can be driven to selectively obtain monopropargyl xanthidols or non-symmetrically bispropargylated xanthone derivatives, among others.

A selective intermolecular gold-catalyzed synthesis of 2-silyl-4,5-dihydrofurans has been described, starting from benzaldehyde derivatives and propargylsilanes. Additionally, a gold-catalyzed *cis-to-trans* isomerization of these products was developed, enabling the access to *trans*-2-silyl-4,5-dihydrofurans, in a one-pot manner. Several deuterium labelled experiments and a Hammett plot support the mechanistical proposal, indicating that the key step would imply a carbon-carbon temporary cleavage, allowing free rotation to adopt the more stable *trans* configuration.

Finally, it has been developed a one-pot gold(I)-Lewis-acid cocatalyzed synthesis of benzofulvene scaffolds, starting from propargylsilanes and different benzophenones derivatives. This 3-steps methodology involves consecutives propargylation, elimination and Nazarov-type hydroarylation stages. The role of the Lewis acid is crucial in this transformation, due to its coordination to the counterion of the gold(I) complex increasing its electrophilicity and enhancing its catalytic activity. The performance of several low temperature NMR stoichiometric experiments supported, for the first time, this hypothesis.

Experimental section

1 General Aspects

Within this section, the experimental aspects of the transformations described in the present dissertation are detailed. First, a summary of the general considerations is given, related to the work conditions, reagents and analytical techniques employed in the isolation and characterization of the different compounds. Then, the experimental procedures for the synthesis of the starting materials and the final products are gathered, along with some control experiments. Similarly, this section contains the spectroscopic data of these compounds.

1.1 General Considerations

The reactions described in the 'Results and discussion' sections of this dissertation were carried out under inert argon (99.99%) or nitrogen atmosphere (99.99%). The glassware was dried and evacuated prior to use. For those transformations that took place at temperatures below 0 °C, acetone baths cooled with liquid nitrogen were used. In cases when maintaining low temperatures for a long time was necessary, a Cryocool apparatus (Neslab C-100II) was used. When heating was required, the reactions were arranged in mineral oil baths or in RR98030 Carrousel Reaction Station systems, from Radleys Discovery Technologies, controlling the temperature through heating plates equipped with contact thermometers.

Silica gel 60 (230-400 mesh) and deactivated aluminium oxide¹ were used as stationary phases for chromatographic purifications. Thin layer chromatographies (TLCs) were performed on aluminum plates, covered with silica gel 60 with F254 indicator, and revealed by exposure to ultraviolet light or with phosphomolybdic acid, potassium permanganate or vanillin dye solutions after subsequent heating. The solvents used for column chromatography and extractions were commercially purchased with an analytical purity grade and used without further purification. All the solvents employed in the reactions were dried by distillation over calcium hydride, sodium hydride or metallic sodium. Other reagents were purified following standard procedures prior to their use.

1.2 Instrumental Techniques

Nuclear Magnetic Resonance (NMR) experiments were performed on the Bruker AV-300, Bruker DPX-300, Bruker Nav-400 and AV-400 devices. The chemical shifts (δ) are expressed in ppm (parts per million) and referred to the residual signal of the solvent used in ¹H- and ¹³C-NMR spectra. The multiplicity of the ¹³C signals has been determined using DEPT-type experiments. Coupling constants (*J*) are expressed in Hertz (Hz). The abbreviations used to indicate the multiplicity of the signals are the following: s (singlet), d (doublet), t (triplet), q (quadruplet) and m (multiplet).

Mass spectra were determined at the scientific-technical services of the University of Oviedo and Vigo (CACTI) using a Finnigan-Matt 95, micro TOF focus (Bruker Daltonics, Bremen Germany) or Vg AutoSpec M spectrometers to obtain high resolution mass spectra (HRMS).

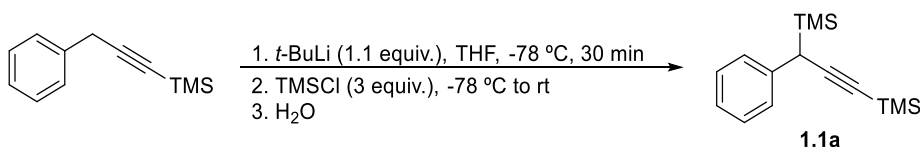
Melting points were measured after column chromatography purification on a Büchi-Tottoli apparatus and have not been corrected.

¹ To a flask containing 460 g of basic aluminum oxide, 50 mL of water (1 mL / 9.2 g) were added and it was vigorously shaken to obtain a free-floating solid, ready to be used.

2 Experimental Procedures

2.1 Synthesis of propargylsilanes

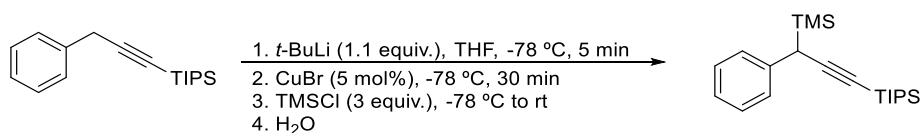
Procedure A:



Scheme 5.1: Synthesis of propargylsilane **1.1a**.

To a solution of the silylated alkyne (1.88 g, 10 mmol), at -78 °C, in anhydrous THF (20 mL), *tert*-butyllithium (6.3 mL, 1.7 M in pentane, 11 mmol) was added dropwise over 5 min. After 30 min of reaction, freshly distilled trimethylchlorosilane (TMSCl) (3.8 mL, 30 mmol) was added in one portion, and the mixture allowed to reach room temperature. When a white precipitate of LiCl appeared, the reaction mixture was quenched with water (50 mL), extracted with ethyl acetate (3 x 20 mL) and washed with brine (2 x 20 mL). The organic phase was dried over anhydrous Na₂SO₄, filtered and concentrated under vacuum. The obtained yellowish oil was purified by column chromatography through silica gel, giving rise to the pure propargylsilane.

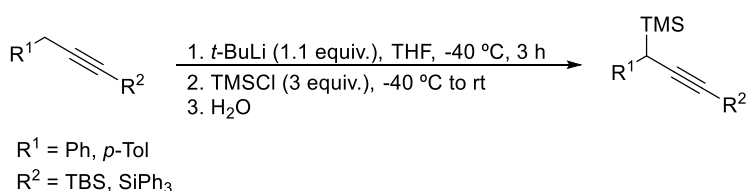
Procedure B:



Scheme 5.2: Synthesis of propargylsilane **1.1g**.

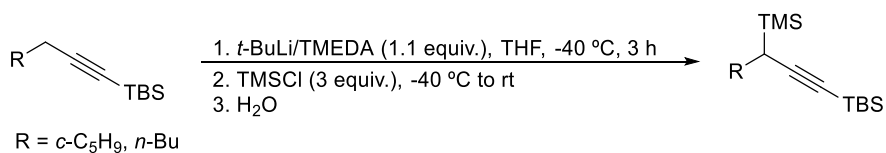
t-BuLi (6.3 mL, 1.7 M in pentane, 11 mmol) was added dropwise over 5 min to a solution, in THF (20 mL) at -78 °C, of the corresponding silylated alkyne (2.73 g, 10 mmol). Then, 5 mol% of CuBr (72 mg) was added. After 30 min, freshly distilled TMSCl (3.8 mL, 30 mmol) was added in one portion, and the mixture allowed to reach room temperature. When a white precipitate of LiCl appeared, the reaction mixture was quenched with water (50 mL), extracted with ethyl acetate (3 x 20 mL) and washed with brine (2 x 20 mL). The organic phase was dried over anhydrous Na₂SO₄, filtered and concentrated under vacuum. The obtained yellowish oil was purified through a chromatographic column on deactivated aluminum oxide, to give the corresponding pure propargylsilane.

Procedure C:



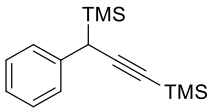
Scheme 5.3: Synthesis of propargylsilanes **1.1c,f**.

The experimental procedure for synthesizing these reagents follows *Procedure A*, but the formation of the anion and addition of TMSCl takes place at -40 °C for 3 hours. For R¹ = Ph, instead of the chromatographic purification, the extracted residue was dissolved in the minimal amount of dry MeOH and cooled down to -80 °C. The precipitate was filtered under argon atmosphere and washed with cool MeOH. Then, it was dissolved under argon in dry pentane and the solvents were removed under vacuum.

Procedure D:**Scheme 5.4:** Synthesis of propargylsilanes **1.d-e**.

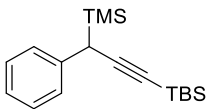
To a cooled solution of freshly distilled tetramethylethylenediamine (TMEDA) (1.65 mL, 11 mmol) at -40 °C in anhydrous THF (20 mL), *t*-BuLi (6.3 mL, 1.7 M in pentane, 11 mmol) was added dropwise over 5 min under nitrogen. After 15 min, the silylated alkyne (10 mmol) was added in one portion. From this point to the end, it follows *Procedure A*.

(3-Phenylprop-1-yne-1,3-diyl)bis(trimethylsilane) (1.1a, 4.1a)

	Yield = 88% Colorless oil. Slowly turns to pink on exposure to air.
---	--

Data are in agreement with scientific report.²

Tert-butyltrimethyl(3-phenyl-3-(trimethylsilyl)prop-1-yn-1-yl)silane (1.1b, 2.1a, 3.1a, 4.1b)

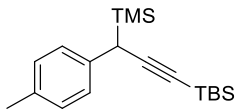
	Yield = 73% White solid, slowly turn to yellow in contact with air. mp = 49.5-52.0 °C R _f (SiO ₂) = 0.35 (Hexane). HRMS for C ₁₈ H ₃₁ Si ₂ [M+H]: Calc.: 303.1964; found: 303.1959.
---	---

¹H-NMR (300 MHz, CDCl₃, 25 °C, TMS): δ (ppm) = 7.34-7.25 (m, 2H), 7.23-7.10 (m, 3H), 3.24 (s, 1H), 1.02 (s, 9H), 0.16 (s, 6H), 0.09 (s, 9H).

¹³C-NMR (75 MHz, CDCl₃, 25 °C): δ (ppm) = 139.1 (C), 128.3 (2 x CH), 127.2 (2 x CH), 125.2 (CH), 107.7 (C), 85.2 (C), 31.2 (CH), 26.4 (3 x CH₃), 16.8 (C), -3.1 (3 x CH₃), -4.1 (2 x CH₃).

² Rochat, R.; Yamamoto, K.; López, M. J.; Nagae, H.; Tsurugi, H.; Mashima, K. *Chem. Eur. J.* **2015**, *21*, 8112-8120.

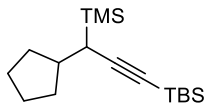
Tert-butyldimethyl(3-(*p*-tolyl)-3-(trimethylsilyl)prop-1-yn-1-yl)silane (1.1c, 2.1b, 3.1b, 4.1c)

	<p>Yield = 65%</p> <p>Colorless oil. Slowly turns to pink on exposure to air.</p> <p>R_f (SiO₂) = 0.36 (Hexane).</p> <p>HRMS for C₁₉H₃₃Si₂ [M+H]: Calc.: 317.2121; found: 317.2115.</p>
---	--

¹H-NMR (300 MHz, CDCl₃, 25 °C, TMS): δ (ppm) = 7.11-7.02 (m, 4H), 3.16 (s, 1H), 2.31 (s, 3H), 0.97 (s, 9H), 0.12 (s, 3H), 0.12 (s, 3H), 0.05 (s, 9H).

¹³C-NMR (75 MHz, CDCl₃, 25 °C): δ (ppm) = 135.8 (C), 135.4 (C), 128.8 (2 x CH), 126.9 (2 x CH), 107.8 (C), 84.8 (C), 30.5 (CH), 26.2 (3 x CH₃), 20.9 (CH₃), 16.7 (C), -3.3 (3 x CH₃), -4.3 (2 x CH₃).

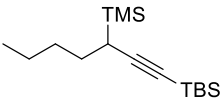
Tert-butyl(3-cyclopentyl-3-(trimethylsilyl)prop-1-yn-1-yl)dimethylsilane (1.1d, 2.1c, 3.1c, 4.1d)

	<p>Yield = 47%</p> <p>Colorless oil. Slowly turns to pink on exposure to air.</p> <p>R_f (SiO₂) = 0.60 (Hexane).</p> <p>HRMS for C₁₇H₃₅Si₂ [M+H]: Calc.: 295.2277; found: 295.2272.</p>
---	--

¹H-NMR (300 MHz, CDCl₃, 25 °C, TMS): δ (ppm) = 2.02-1.87 (m, 1H), 1.84 (d, *J*_(H,H) = 5.1 Hz, 1H), 1.78-1.35 (m, 8H), 0.92 (s, 9H), 0.09 (s, 9H), 0.06 (s, 6H).

¹³C-NMR (75 MHz, CDCl₃, 25 °C): δ (ppm) = 109.2 (C), 83.7 (C), 39.5 (CH), 33.6 (CH₂), 30.7 (CH₂), 26.9 (CH₃), 26.3 (3 x CH₃), 25.8 (CH₂), 25.7 (CH₂), 16.8 (C), -2.1 (3 x CH₃), -4.0 (2 x CH₃).

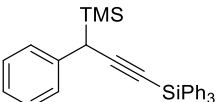
Tert-butyltrimethyl(3-(trimethylsilyl)hept-1-yn-1-yl)silane (1.1e, 2.1d, 3.1d, 4.1e)

	<p>Yield = 40%</p> <p>Colorless oil. Slowly turns to pink on exposure to air.</p> <p>R_f (SiO₂) = 0.59 (Hexane).</p> <p>HRMS for C₁₆H₃₅Si₂ [M+H]: Calc.: 283.2277; found: 283.2272.</p>
---	--

¹H-NMR (300 MHz, CDCl₃, 25 °C, TMS): δ (ppm) = 1.79-1.50 (m, 2H), 1.50-1.17 (m, 5H), 0.93 (s, 6H), 0.91 (t, $J_{(H,H)} = 7.2$ Hz, 3H), 0.08 (s, 9H), 0.07 (s, 6H).

¹³C-NMR (75 MHz, CDCl₃, 25 °C): δ (ppm) = 110.6 (C), 82.5 (C), 31.9 (CH₂), 29.0 (CH₂), 26.3 (3 x CH₃), 22.5 (CH₂), 21.5 (CH₃), 16.8 (C), 14.2 (CH), -3.0 (3 x CH₃), -4.0 (2 x CH₃).

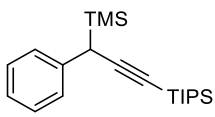
Trimethyl(1-phenyl-3-(triphenylsilyl)prop-2-yn-1-yl)silane (1.1g)

	<p>Yield = 89%</p> <p>White solid. Quickly turns to yellow oil in contact with air.</p> <p>R_f (SiO₂) = 0.24 (Hexane).</p> <p>HRMS for C₃₀H₃₁Si₂ [M+H]: Calc.: 447.1964; found: 447.1959.</p>
---	--

¹H-NMR (300 MHz, CDCl₃, 25 °C, TMS): δ (ppm) = 7.73 (dd, $J_{(H,H)} = 7.6, 1.7$ Hz, 6H), 7.50-7.37 (m, 9H), 7.37-7.24 (m, 4H), 7.24-7.15 (m, 1H), 3.43 (s, 1H), 0.13 (s, 3H).

¹³C-NMR (75 MHz, CDCl₃, 25 °C): δ (ppm) = 138.7 (C), 135.7 (6 x CH), 134.5 (3 x C), 129.8 (3 x CH), 128.4 (2 x CH), 128.0 (6 x CH), 127.3 (2 x CH), 125.4 (CH), 112.5 (C), 82.1 (C), 31.6 (CH), -3.0 (3 x CH₃).

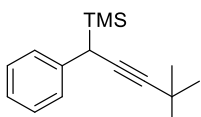
Triisopropyl(3-phenyl-3-(trimethylsilyl)prop-1-yn-1-yl)silane (1.1g, 2.1e, 3.1e, 4.1f)

	<p>Yield = 88%</p> <p>Colorless oil. Slowly turns to pink on exposure to air.</p> <p>R_f (SiO₂) = 0.38 (Hexane).</p> <p>HRMS for C₂₁H₃₇Si₂ [M+H]: Calc.: 345.2434; found: 345.2428.</p>
---	---

¹H-NMR (300 MHz, CDCl₃, 25 °C, TMS): δ (ppm) = 7.35-7.10 (m, 5H), 3.27 (s, 1H), 1.25-1.00 (m, 3H), 1.12 (s, 18H), 0.09 (s, 9H).

¹³C-NMR (75 MHz, CDCl₃, 25 °C): δ (ppm) = 139.4 (C), 128.2 (2 x CH), 127.2 (2 x CH), 125.1 (CH), 108.4 (C), 82.8 (C), 31.3 (CH), 18.9 (6 x CH₃), 11.7 (3 x CH₃), -3.1 (3 x CH₃).

(4,4-Dimethyl-1-phenylpent-2-yn-1-yl)trimethylsilane (1.1h, 2.1f, 3.1f, 4.1g)

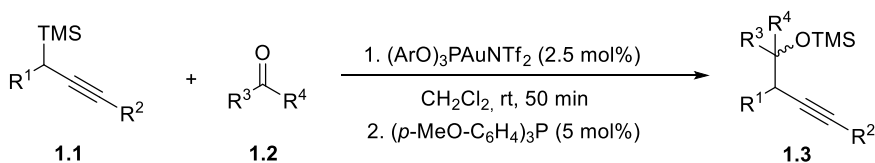
	<p>Yield = 35%</p> <p>Colorless oil. Quickly turns to yellow oil in contact with air.</p> <p>R_f (SiO₂) = 0.45 (Hexane).</p> <p>HRMS could not be obtained. Unstable compound.</p>
---	--

¹H-NMR (300 MHz, CDCl₃, 25 °C, TMS): δ (ppm) = 7.30-7.20 (m, 2H), 7.19-7.06 (m, 3H), 3.08 (s, 1H), 1.27 (s, 9H), 0.03 (s, 9H).

¹³C-NMR (75 MHz, CDCl₃, 25 °C): δ (ppm) = 140.3 (C), 128.1 (CH), 127.1 (CH), 125.0 (CH), 92.3 (C), 78.2 (C), 31.7 (CH₃), 29.3 (CH), 27.9 (C), -3.2 (CH₃).

2.2 Experimental procedures described in Chapter I

2.2.1 General procedure for the propargylation of carbonyl derivatives



Scheme 5.5: Gold(I)-catalyzed propargylation of carbonyl derivatives.

To a solution of 0.24 mmol of propargylsilane **1.1** (0.6 mmol for **1.3a-b,r-w**) in 1 mL of dichloromethane, at 25 °C (-20 °C for **1.3e-f,m-n**), 0.2 mmol of the corresponding carbonyl compound **1.2** and 5.6 mg (0.005 mmol, 2.5 mol %) (11.2 mg for **1.3a-b,h,s-w** (0.01 mmol, 5 mol %)) of the gold catalyst were added.³ The mixture was stirred for 50 min (3 h for **1.3b,e-f,m-q**; 16 h for **1.3u-v**). Upon completion, 3.3 mg of (*p*-MeO-C₆H₄)₃P (0.01 mmol, 5 mol %) (6.6 mg for **1.3a-b,h,s-w** (0.02 mmol, 10 mol%)) were added to the mixture and the solvents evaporated under vacuum. Finally, after purification of the residue by deactivated aluminum oxide flash chromatography, the corresponding homopropargyl silyl ethers **1.3a-u** were obtained as pure compounds.

The same procedure was employed for obtaining the homopropargyl methyl ether **1.8** and the homopropargyl dimethyl acetal **1.10**, using respectively benzaldehyde dimethyl acetal **1.7** and trimethyl orthobenzoate **1.9**.

³ For compounds **1.3u-w** the reaction was performed in a polypropylene tube inside the schlenck to avoid contact of the mixture with the glass walls.

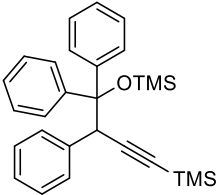
Trimethyl((2-phenyl-1-(*p*-tolyl)-4-(trimethylsilyl)but-3-yn-1-yl)oxy)silane (1.3a)

	<p>Yield = 80%, 61 mg. (Mixture of diastereoisomers; <i>dr</i> = 1:1)</p> <p>White solid.</p> <p>R_f (SiO₂) = 0.09 (Hexane : Ethyl acetate, 200:1).</p> <p>HRMS for C₂₃H₃₂NaOSi₂ [M+Na]: Calc.: 403.1889; found: 403.1884.</p>
--	--

¹H-NMR (300 MHz, CDCl₃, 25 °C, TMS): δ (ppm) = 7.36-7.05 (m, 14H), 6.99 (s, 4H), 4.74 (d, $J_{(H,H)}$ = 6.2 Hz, 1H), 4.67 (d, $J_{(H,H)}$ = 7.3 Hz, 1H), 3.86 (d, $J_{(H,H)}$ = 6.2 Hz, 1H), 3.76 (d, $J_{(H,H)}$ = 7.3 Hz, 1H), 2.35 (s, 3H), 2.31 (s, 3H), 0.20 (s, 9H), 0.12 (s, 9H), -0.04 (s, 9H), -0.19 (s, 9H).

¹³C-NMR (75 MHz, CDCl₃, 25 °C): δ (ppm) = 139.8 (C), 139.2 (C), 138.9 (C), 138.3 (C), 136.9 (C), 136.9 (C), 129.4 (2 x CH), 129.3 (2 x CH), 128.3 (2 x CH), 128.2 (2 x CH), 127.9 (4 x CH), 127.0 (2 x CH), 127.0 (CH), 126.9 (CH), 126.9 (2 x CH), 106.6 (C), 106.5 (C), 89.0 (C), 88.5 (C), 79.0 (CH), 78.9 (CH), 49.3 (CH), 49.1 (CH), 21.3 (CH₃), 21.3 (CH₃), 0.3 (3 x CH₃), 0.1 (3 x CH₃), 0.1 (3 x CH₃), -0.2 (3 x CH₃).

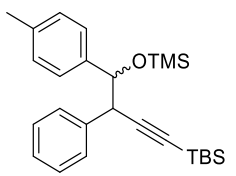
Trimethyl-4-((trimethylsilyl)oxy-3,4,4-triphenylbut-1-yn-1-yl)silane (1.3b)

	<p>Yield = 79%, 70 mg.</p> <p>White solid. mp = 104.0-107.1 °C.</p> <p>R_f (SiO₂) = 0.12 (Hexane : Ethyl acetate, 200:1).</p> <p>HRMS for C₂₈H₃₄NaOSi₂ [M+Na]: Calc.: 465.2046; found: 465.2044.</p>
---	--

¹H-NMR (300 MHz, CDCl₃, 25 °C, TMS): δ (ppm) = 7.46-7.35 (m, 2H), 7.35-7.00 (m, 11H), 6.88 (d, *J*_(H,H) = 7.0 Hz, 2H), 4.73 (s, 1H), 0.09 (s, 9H), -0.11 (s, 9H).

¹³C-NMR (75 MHz, CDCl₃, 25 °C): δ (ppm) = 144.8 (C), 143.4 (C), 137.5 (C), 130.7 (2 x CH), 129.3 (2 x CH), 129.2 (2 x CH), 127.5 (CH), 127.4 (2 x CH), 127.1 (CH), 126.7 (2 x CH), 126.6 (CH), 126.5 (2 x CH), 107.5 (C), 91.0 (C), 84.3 (C), 49.9 (CH), 2.0 (3 x CH₃), -0.1 (3 x CH₃).

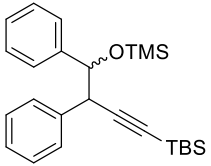
Tert-butyldimethyl(4-(trimethylsilyl)oxy-3-phenyl-4-(*p*-tolyl)but-1-yn-1-yl)silane (1.3c, 2.21)

	<p>Yield = 99%, 84 mg. (Mixture of diastereoisomers; <i>dr</i> = 1.2:1)</p> <p>White solid.</p> <p>R_f (SiO₂) = 0.08 (Hexane : Ethyl acetate, 200:1).</p> <p>HRMS for C₂₆H₃₈NaOSi₂ [M+Na]: Calc.: 445.2359; found: 445.2353.</p>
---	--

¹H-NMR (300 MHz, CDCl₃, 25 °C, TMS): δ (ppm) = 7.40-7.00 (m, 18H), 4.79 (d, $J_{(H,H)}$ = 5.2 Hz, 1H), 4.65 (d, $J_{(H,H)}$ = 7.6 Hz, 1H), 3.92 (d, $J_{(H,H)}$ = 5.2 Hz, 1H), 3.86 (d, $J_{(H,H)}$ = 7.6 Hz, 1H), 2.37 (s, 3H), 2.35 (s, 3H), 1.02 (s, 9H), 0.91 (s, 9H), 0.16 (s, 3H), 0.15 (s, 3H), 0.07 (s, 3H), 0.06 (s, 3H), -0.06 (s, 9H), -0.18 (s, 9H).

¹³C-NMR (75 MHz, CDCl₃, 25 °C): δ (ppm) = 139.8 (C), 139.4 (C), 139.3 (C), 138.7 (C), 136.8 (C), 136.7 (C), 129.4 (2 x CH), 129.2 (2 x CH), 128.3 (2 x CH), 128.3 (2 x CH), 127.9 (2 x CH), 127.9 (2 x CH), 127.1 (2 x CH), 126.9 (CH), 126.9 (CH), 126.8 (2 x CH), 106.8 (C), 106.6 (C), 87.2 (C), 86.9 (C), 79.3 (CH), 78.8 (CH), 49.4 (CH), 49.0 (CH), 26.3 (3 x CH₃), 26.2 (3 x CH₃), 21.3 (2 x CH₃), 16.9 (C), 16.7 (C), -0.1 (3 x CH₃), -0.2 (3 x CH₃), -4.3 (2 x CH₃), -4.4 (2 x CH₃).

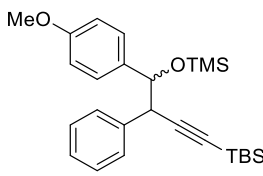
Tert-butyldimethyl(4-((trimethylsilyl)oxy)-3,4-diphenyl-but-1-yn-1-yl)silane (1.3d)

	<p>Yield = 98%, 80 mg. (Mixture of diastereoisomers; <i>dr</i> = 1.4:1)</p> <p>White solid.</p> <p>R_f (SiO₂) = 0.08 (Hexane : Ethyl acetate, 200:1).</p> <p>HRMS for C₂₅H₃₆NaOSi₂ [M+Na]: Calc.: 431.2202; found: 431.2216.</p>
---	---

¹H-NMR (300 MHz, CDCl₃, 25 °C, TMS): δ (ppm) = 7.43-7.14 (m, 20H), 4.82 (d, $J_{(H,H)} = 5.2$ Hz, 1H), 4.68 (d, $J_{(H,H)} = 7.6$ Hz, 1H), 3.95 (d, $J_{(H,H)} = 5.2$ Hz, 1H), 3.88 (d, $J_{(H,H)} = 7.6$ Hz, 1H), 1.02 (s, 9H), 0.91 (s, 9H), 0.16 (s, 3H), 0.15 (s, 3H), 0.07 (s, 3H), 0.06 (s, 3H), -0.06 (s, 9H), -0.17 (s, 9H).

¹³C-NMR (75 MHz, CDCl₃, 25 °C): δ (ppm) = 142.7 (C), 142.3 (C), 139.1 (C), 138.6 (C), 129.4 (2 x CH), 129.2 (2 x CH), 127.8 (2 x CH), 127.9 (2 x CH), 127.7 (2 x CH), 127.6 (2 x CH), 127.5 (CH), 127.4 (CH), 127.3 (2 x CH), 127.0 (CH), 126.9 (2 x CH), 126.9 (CH), 106.7 (C), 106.4 (C), 87.3 (C), 87.0 (C), 79.4 (CH), 78.9 (CH), 49.4 (CH), 48.9 (CH), 26.3 (3 x CH₃), 26.2 (3 x CH₃), 16.9 (C), 16.7 (C), -0.1 (3 x CH₃), -0.3 (3 x CH₃), -4.4 (2 x CH₃), -4.4 (2 x CH₃).

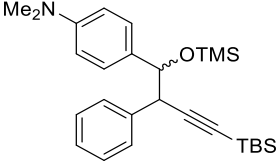
Tert-butyldimethyl(4-(*p*-methoxyphenyl)-4-((trimethylsilyl)oxy)-3-phenyl-but-1-yn-1-yl)silane (1.3e)

	<p>Yield = 98%, 86 mg. (Mixture of diastereoisomers; <i>dr</i> = 1.2:1)</p> <p>White solid.</p> <p>R_f (SiO₂) = 0.05 (Hexane : Ethyl acetate, 200:1).</p> <p>HRMS (EI) for C₂₆H₃₉O₂Si₂ [M+H]: Calc.: 439.2489; found: 439.2484.</p>
---	--

¹H-NMR (300 MHz, CDCl₃, 25 °C, TMS): δ (ppm) = 7.38-7.16 (m, 12H), 7.09 (d, $J_{(H,H)} = 8.6$ Hz, 2H), 6.83 (d, $J_{(H,H)} = 8.7$ Hz, 2H), 6.76 (d, $J_{(H,H)} = 8.7$ Hz, 2H), 4.76 (d, $J_{(H,H)} = 5.4$ Hz, 1H), 4.62 (d, $J_{(H,H)} = 7.6$ Hz, 1H), 3.89 (d, $J_{(H,H)} = 5.4$ Hz, 1H), 3.84 (d, $J_{(H,H)} = 7.5$ Hz, 1H), 3.83 (s, 3H), 3.80 (s, 3H), 1.00 (s, 9H), 0.90 (s, 9H), 0.15 (s, 3H), 0.13 (s, 3H), 0.06 (s, 3H), 0.05 (s, 3H) -0.06 (s, 9H), -0.19 (s, 9H).

¹³C-NMR (75 MHz, CDCl₃, 25 °C): δ (ppm) = 159.0 (C), 158.9 (C), 139.2 (C), 138.6 (C), 135.0 (C), 134.5 (C), 129.4 (2 x CH), 129.3 (2 x CH), 128.3 (2 x CH), 128.0 (2 x CH), 127.9 (2 x CH), 127.9 (2 x CH), 126.9 (CH), 126.9 (CH), 113.0 (2 x CH), 112.9 (2 x CH), 106.8 (C), 106.7 (C), 87.2 (C), 86.7 (C), 79.0 (CH), 78.5 (CH), 55.4 (CH₃), 55.3 (CH₃), 49.4 (CH), 49.1 (CH), 26.3 (3 x CH₃), 26.2 (3 x CH₃), 16.9 (C), 16.7 (C), -0.04 (3 x CH₃), -0.3 (3 x CH₃), -4.3 (2 x CH₃), -4.4 (2 x CH₃).

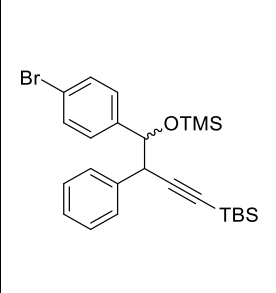
Tert-butyldimethyl(4-((trimethylsilyl)oxy)-4-(*p*-dimethylaminophenyl)-3-phenylbut-1-yn-1-yl)silane (1.3f)

	<p>Yield = 99%, 89 mg. (Mixture of diastereoisomers; <i>dr</i> = 2.3:1)</p> <p>White solid.</p> <p>R_f (SiO₂) = 0.04 (Hexane : Ethyl acetate, 200:1).</p> <p>HRMS (EI) for C₂₇H₄₂NOSi₂ [M+H]: Calc.: 452.2805; found: 452.2799.</p>
---	--

¹H-NMR (300 MHz, CDCl₃, 25 °C, TMS): δ (ppm) = 7.39-7.16 (m, 12H), 7.05 (d, $J_{(H,H)}$ = 8.7 Hz, 2H), 6.70 (d, $J_{(H,H)}$ = 8.7 Hz, 2H), 6.62 (d, $J_{(H,H)}$ = 8.7 Hz, 2H), 4.72 (d, $J_{(H,H)}$ = 5.5 Hz, 1H), 4.61 (d, $J_{(H,H)}$ = 7.6 Hz, 1H), 3.89 (d, $J_{(H,H)}$ = 5.5 Hz, 1H), 3.84 (d, $J_{(H,H)}$ = 7.6 Hz, 1H), 2.97 (s, 6H), 2.94 (s, 6H), 1.01 (s, 9H), 0.90 (s, 9H), 0.16 (s, 3H), 0.14 (s, 3H), 0.06 (s, 3H), 0.06 (s, 3H), -0.06 (s, 9H), -0.18 (s, 9H).

¹³C-NMR (75 MHz, CDCl₃, 25 °C): δ (ppm) = 150.0 (C), 149.9 (C), 139.5 (C), 139.0 (C), 130.8 (2 x C), 129.4 (2 x CH), 129.3 (2 x CH), 128.0 (2 x CH), 127.8 (2 x CH), 127.8 (2 x CH), 127.7 (2 x CH), 126.8 (CH), 126.7 (CH), 112.2 (2 x CH), 112.0 (2 x CH), 107.2 (C), 107.1 (C), 86.9 (C), 86.6 (C), 79.2 (CH), 78.8 (CH), 49.6 (CH), 49.2 (CH), 41.1 (2 x CH₃), 40.9 (2 x CH₃), 26.4 (3 x CH₃), 26.3 (3 x CH₃), 16.9 (C), 16.7 (C), 0.0 (3 x CH₃), -0.2 (3 x CH₃), -4.4 (2 x CH₃), -4.4 (2 x CH₃).

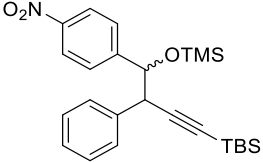
Tert-butyldimethyl(4-(*p*-bromophenyl)-4-((trimethylsilyl)oxy)-3-phenyl-but-1-yn-1-yl)silane (1.3g)

	<p>Yield = 99%, 97 mg. (Mixture of diastereoisomers; <i>dr</i> = 1.1:1)</p> <p>White solid.</p> <p>R_f (SiO₂) = 0.07 (Hexane : Ethyl acetate, 200:1).</p> <p>HRMS (EI) for C₂₅H₃₅BrOSi₂ [M]: Calc.: 486.1410; found: 486.1407.</p>
---	--

¹H-NMR (300 MHz, CDCl₃, 25 °C, TMS): δ (ppm) = 7.49-7.13 (m, 16H), 7.07 (d, $J_{(H,H)} = 8.4$ Hz, 2H), 4.80 (d, $J_{(H,H)} = 5.0$ Hz, 1H), 4.63 (d, $J_{(H,H)} = 7.5$ Hz, 1H), 3.91 (d, $J_{(H,H)} = 5.0$ Hz, 1H), 3.84 (d, $J_{(H,H)} = 7.5$ Hz, 1H), 1.00 (s, 9H), 0.91 (s, 9H), 0.15 (s, 3H), 0.14 (s, 3H), 0.07 (s, 6H), -0.06 (s, 9H), -0.17 (s, 9H).

¹³C-NMR (75 MHz, CDCl₃, 25 °C): δ (ppm) = 141.7 (C), 141.3 (C), 138.7 (C), 138.0 (C), 130.8 (2 x CH), 130.7 (2 x CH), 129.3 (2 x CH), 129.2 (2 x CH), 129.0 (2 x CH), 128.6 (2 x CH), 128.0 (2 x CH), 128.0 (2 x CH), 127.1 (CH), 127.1 (CH), 121.4 (C), 121.3 (C), 106.1 (C), 105.9 (C), 87.8 (C), 87.5 (C), 78.8 (CH), 78.1 (CH), 49.1 (CH), 48.9 (CH), 26.3 (3 x CH₃), 26.2 (3 x CH₃), 16.8 (C), 16.7 (C), -0.1 (3 x CH₃), -0.3 (3 x CH₃), -4.4 (2 x CH₃), -4.5 (2 x CH₃).

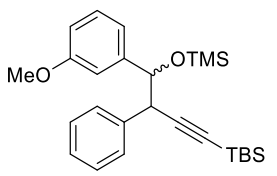
Tert-butyldimethyl(4-((trimethylsilyl)oxy)-4-(*p*-nitrophenyl)-3-phenyl-but-1-yn-1-yl)silane (1.3h)

	<p>Yield = 79%, 72 mg. (Mixture of diastereoisomers; <i>dr</i> = 1.2:1)</p> <p>Yellowish solid.</p> <p>R_f (SiO₂) = 0.06 (Hexane : Ethyl acetate, 200:1).</p> <p>HRMS (EI) for C₂₅H₃₅NNaO₃Si₂ [M+Na]: Calc.: 476.2053; found: 476.2043.</p>
---	---

¹H-NMR (300 MHz, CDCl₃, 25 °C, TMS): δ (ppm) = 8.15 (d, $J_{(H,H)} = 8.7$ Hz, 2H), 8.09 (d, $J_{(H,H)} = 8.7$ Hz, 2H), 7.47 (d, $J_{(H,H)} = 8.7$ Hz, 2H), 7.35 (d, $J_{(H,H)} = 8.7$ Hz, 2H), 7.32-7.16 (m, 10H), 4.94 (d, $J_{(H,H)} = 4.7$ Hz, 1H), 4.74 (d, $J_{(H,H)} = 7.4$ Hz, 1H), 3.96 (d, $J_{(H,H)} = 4.7$ Hz, 1H), 3.86 (d, $J_{(H,H)} = 7.4$ Hz, 1H), 0.96 (s, 9H), 0.87 (s, 9H), 0.12 (s, 3H), 0.11 (s, 3H), 0.04 (s, 6H), -0.07 (s, 9H), -0.17 (s, 9H).

¹³C-NMR (75 MHz, CDCl₃, 25 °C): δ (ppm) = 150.0 (C), 149.6 (C), 147.5 (C), 147.5 (C), 138.1 (C), 137.4 (C), 129.2 (2 x CH), 129.2 (2 x CH), 128.2 (2 x CH), 128.1 (2 x CH), 128.1 (2 x CH), 127.7 (2 x CH), 127.5 (CH), 127.4 (CH), 122.9 (2 x CH), 122.8 (2 x CH), 105.4 (C), 105.1 (C), 88.6 (C), 88.4 (C), 78.5 (CH), 77.7 (CH), 48.8 (CH), 48.7 (CH), 26.2 (3 x CH₃), 26.1 (3 x CH₃), 16.8 (C), 16.6 (C), -0.2 (3 x CH₃), -0.3 (3 x CH₃), -4.4 (CH₃), -4.4 (CH₃), -4.5 (CH₃), -4.5 (CH₃).

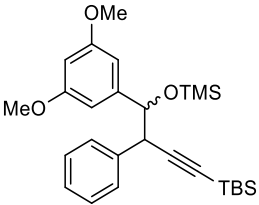
Tert-butyldimethyl(4-(*m*-methoxyphenyl)-4-((trimethylsilyl)oxy)-3-phenylbut-1-yn-1-yl)silane (1.3i)

	<p>Yield = 79%, 72 mg. (Mixture of diastereoisomers; <i>dr</i> = 1.0:1)</p> <p>White solid.</p> <p>R_f (SiO₂) = 0.05 (Hexane : Ethyl acetate, 200:1).</p> <p>HRMS (EI) for C₂₆H₃₈KO₂Si₂ [M+K]: Calc.: 477.2047; found: 477.2042.</p>
---	---

¹H-NMR (300 MHz, CDCl₃, 25 °C, TMS): δ (ppm) = 7.36-7.06 (m, 12H), 6.90 (d, $J_{(H,H)} = 7.6$ Hz, 1H), 6.85-6.67 (m, 5H), 4.75 (d, $J_{(H,H)} = 5.3$ Hz, 1H), 4.63 (d, $J_{(H,H)} = 7.5$ Hz, 1H), 3.90 (d, $J_{(H,H)} = 5.3$ Hz, 1H), 3.83 (d, $J_{(H,H)} = 7.5$ Hz, 1H), 3.76 (s, 3H), 3.69 (s, 3H), 0.97 (s, 9H), 0.87 (s, 9H), 0.11 (s, 3H), 0.10 (s, 3H), 0.03 (s, 3H), 0.02 (s, 3H), -0.08 (s, 9H), -0.20 (s, 9H).

¹³C-NMR (75 MHz, CDCl₃, 25 °C): δ (ppm) = 159.2 (C), 159.1 (C), 144.4 (C), 144.0 (C), 139.1 (C), 138.6 (C), 129.4 (2 x CH), 129.2 (2 x CH), 128.6 (CH), 128.5 (CH), 127.9 (2 x CH), 127.9 (2 x CH), 127.0 (2 x CH), 119.9 (CH), 119.4 (CH), 113.1 (CH), 113.0 (CH), 112.7 (CH), 112.2 (CH), 106.7 (C), 106.4 (C), 87.2 (C), 87.0 (C), 79.3 (CH), 78.9 (CH), 55.1 (CH₃), 55.2 (CH₃), 49.3 (C), 48.9 (C), 26.3 (3 x CH₃), 26.2 (3 x CH₃), 16.8 (C), 16.6 (C), -0.1 (3 x CH₃), -0.3 (3 x CH₃), -4.4 (2 x CH₃), -4.4 (2 x CH₃).

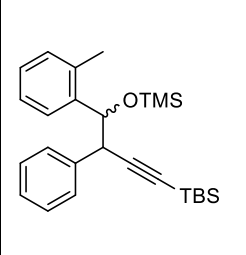
Tert-butyl dimethyl(4-(3,5-dimethoxyphenyl)-4-((trimethylsilyl)oxy)-3-phenylbut-1-yn-1-yl)silane (1.3j)

	<p>Yield = 99%, 93 mg. (Mixture of diastereoisomers; <i>dr</i> = 1.0:1)</p> <p>White solid.</p> <p>R_f (SiO₂) = 0.01 (Hexane : Ethyl acetate, 200:1).</p> <p>HRMS (EI) for C₂₇H₄₁O₃Si₂ [M+H]: Calc.: 469.2594; found: 469.2589.</p>
---	--

¹H-NMR (300 MHz, CDCl₃, 25 °C, TMS): δ (ppm) = 7.38-7.21 (m, 10H), 6.47 (d, $J_{(H,H)}$ = 2.3 Hz, 2H), 6.41-6.36 (m, 1H), 6.36-6.31 (m, 3H), 4.72 (d, $J_{(H,H)}$ = 5.5 Hz, 1H), 4.63 (d, $J_{(H,H)}$ = 7.3 Hz, 1H), 3.92 (d, $J_{(H,H)}$ = 5.5 Hz, 1H), 3.86 (d, $J_{(H,H)}$ = 7.3 Hz, 1H), 3.77 (s, 6H), 3.71 (s, 6H), 1.00 (s, 9H), 0.90 (s, 9H), 0.15 (s, 3H), 0.13 (s, 3H), 0.07 (s, 3H), 0.07 (s, 3H), -0.03 (s, 9H), -0.15 (s, 9H).

¹³C-NMR (75 MHz, CDCl₃, 25 °C): δ (ppm) = 160.2 (2 x C), 160.1 (2 x C), 145.2 (C), 144.8 (C), 139.0 (C), 138.7 (C), 129.5 (2 x CH), 129.1 (2 x CH), 127.9 (2 x CH), 127.8 (2 x CH), 127.0 (2 x CH), 106.7 (C), 106.5 (C), 105.3 (2 x CH), 104.9 (2 x CH), 99.6 (CH), 99.5 (CH), 87.1 (C), 86.9 (C), 79.4 (CH), 79.1 (CH), 55.3 (2 x CH₃), 55.3 (2 x CH₃), 49.3 (CH), 48.7 (CH), 26.3 (3 x CH₃), 26.2 (3 x CH₃), 16.8 (C), 16.6 (C), 0.0 (3 x CH₃), -0.2 (3 x CH₃), -4.3 (2 x CH₃), -4.4 (2 x CH₃).

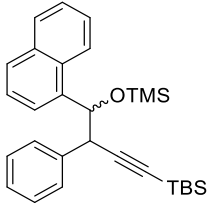
Tert-butyldimethyl(4-((trimethylsilyl)oxy)-3-phenyl-4-(*o*-tolyl)but-1-yn-1-yl)silane (1.3k)

	<p>Yield = 99%, 84 mg. (Mixture of diastereoisomers; <i>dr</i> = 1.8:1)</p> <p>White solid.</p> <p>R_f (SiO₂) = 0.08 (Hexane : Ethyl acetate, 200:1).</p> <p>HRMS (EI) for C₂₆H₃₉OSi₂ [M+H]: Calc.: 423.2539; found: 423.2534.</p>
---	--

¹H-NMR (300 MHz, CDCl₃, 25 °C, TMS): δ (ppm) = 7.62 (d, $J_{(H,H)}$ = 7.4 Hz, 1H), 7.47-7.06 (m, 16H), 7.01 (d, $J_{(H,H)}$ = 7.1 Hz, 1H), 4.96 (d, $J_{(H,H)}$ = 5.6 Hz, 1H), 4.96 (d, $J_{(H,H)}$ = 5.6 Hz, 1H), 3.92 (d, $J_{(H,H)}$ = 5.2 Hz, 1H), 2.39 (s, 3H), 2.10 (s, 3H), 1.03 (s, 9H), 0.86 (s, 9H), 0.16 (s, 3H), 0.14 (s, 3H), 0.03 (s, 3H), 0.02 (s, 3H), -0.12 (s, 9H), -0.21 (s, 9H).

¹³C-NMR (75 MHz, CDCl₃, 25 °C): δ (ppm) = 141.2 (C), 140.9 (C), 139.5 (C), 139.0 (C), 134.8 (C), 133.9 (C), 129.8 (CH), 129.6 (CH), 129.4 (2 x CH), 129.0 (2 x CH), 128.0 (2 x CH), 127.9 (2 x CH), 127.8 (CH), 127.4 (CH), 127.2 (CH), 127.1 (CH), 127.0 (CH), 127.0 (CH), 125.8 (CH), 125.7 (CH), 106.5 (C), 106.3 (C), 86.9 (C), 86.2 (C), 75.0 (CH), 75.0 (CH), 48.4 (CH), 48.1 (CH), 26.4 (3 x CH₃), 26.2 (3 x CH₃), 20.0 (CH₃), 19.1 (CH₃), 16.9 (C), 16.6 (C), -0.2 (3 x CH₃), -0.3 (3 x CH₃), -4.3 (2 x CH₃), -4.5 (2 x CH₃).

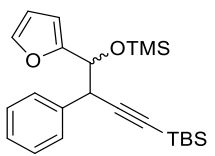
Tert-butyl dimethyl(4-((trimethylsilyl)oxy)-4-(1-naphthyl)-3-phenylbut-1-yn-1-yl)silane (1.3I)

	<p>Yield = 97%, 89 mg. (Mixture of diastereoisomers; <i>dr</i> = 1.5:1)</p> <p>White solid.</p> <p>R_f (SiO₂) = 0.09 (Hexane : Ethyl acetate, 200:1).</p> <p>HRMS (EI) for C₂₉H₃₈NaOSi₂ [M+Na]: Calc.: 481.2359; found: 481.2353.</p>
---	--

¹H-NMR (300 MHz, CDCl₃, 25 °C, TMS): δ (ppm) = δ 8.34 (s, 1H), 8.15 (d, $J_{(H,H)} = 7.9$ Hz, 1H), 7.98-7.86 (m, 2H), 7.80 (d, $J_{(H,H)} = 14.7$ and 7.7 Hz, 3H), 7.63-7.21 (m, 17H), 5.55 (d, $J_{(H,H)} = 3.7$ Hz, 2H), 4.28-4.15 (m, 2H), 1.04 (s, 9H), 0.81 (s, 9H), 0.12 (s, 3H), 0.12 (s, 3H), -0.08 (s, 3H), -0.09 (s, 3H), -0.14 (s, 9H), -0.15 (s, 9H).

¹³C-NMR (75 MHz, CDCl₃, 25 °C): δ (ppm) = 139.7 (C), 139.0 (C), 138.6 (C), 137.9 (C), 133.8 (C), 133.7 (C), 131.0 (C), 130.2 (C), 129.6 (2 x CH), 129.2 (CH), 128.9 (CH), 128.8 (2 x CH), 128.2 (2 x CH), 128.0 (CH), 128.0 (CH), 127.7 (2 x CH), 127.1 (CH), 127.0 (CH), 126.0 (CH), 125.9 (CH), 125.8 (CH), 125.2 (2 x CH), 125.2 (2 x CH), 125.2 (2 x CH), 122.6 (CH), 106.9 (C), 105.8 (C), 87.5 (2 x C), 48.1 (2 x CH), 26.3 (3 x CH₃), 26.2 (3 x CH₃), 16.9 (C), 16.6 (C), -0.2 (3 x CH₃), -0.3 (3 x CH₃), -4.4 (2 x CH₃), -4.6 (2 x CH₃).

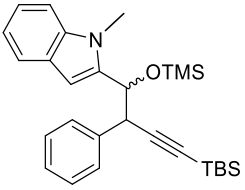
Tert-butyldimethyl(4-(2-furyl)-4-((trimethylsilyl)oxy)-3-phenylbut-1-yn-1-yl)silane (1.3m)

	<p>Yield = 65%, 52 mg. (Mixture of diastereoisomers; <i>dr</i> = 1.2:1)</p> <p>White solid.</p> <p>R_f (SiO₂) = 0.04 (Hexane : Ethyl acetate, 200:1).</p> <p>HRMS (EI) for C₂₃H₃₄NaO₂Si₂ [M+Na]: Calc.: 421.1995; found: 421.1990.</p>
---	---

¹H-NMR (300 MHz, CDCl₃, 25 °C, TMS): δ (ppm) = 7.61-7.03 (m, 12H), 6.35 (dd, $J_{(H,H)}$ = 3.2 and 1.8 Hz, 1H), 6.26 (d, $J_{(H,H)}$ = 3.1 Hz, 1H), 6.23 (dd, $J_{(H,H)}$ = 3.2 and 1.8 Hz, 1H), 6.06 (d, $J_{(H,H)}$ = 3.2 Hz, 1H), 4.76 (d, $J_{(H,H)}$ = 6.6 Hz, 1H), 4.69 (d, $J_{(H,H)}$ = 8.5 Hz, 1H), 4.18 (d, $J_{(H,H)}$ = 6.6 Hz, 1H), 4.12 (d, $J_{(H,H)}$ = 8.5 Hz, 1H), 1.00 (s, 9H), 0.90 (s, 9H), 0.14 (s, 6H), 0.07 (s, 3H), 0.05 (s, 3H), -0.01 (s, 9H), -0.17 (s, 9H).

¹³C-NMR (75 MHz, CDCl₃, 25 °C): δ (ppm) = 155.2 (C), 154.7 (C), 141.7 (CH), 141.4 (CH), 138.8 (C), 138.3 (C), 129.3 (2 x CH), 128.7 (2 x CH), 128.1 (2 x CH), 128.0 (2 x CH), 127.2 (CH), 127.1 (CH), 110.1 (2 x CH), 107.6 (CH), 107.6 (CH), 106.3 (C), 105.7 (C), 87.1 (C), 86.5 (C), 73.3 (CH), 73.0 (CH), 46.6 (CH), 45.8 (CH), 26.3 (3 x CH₃), 26.2 (3 x CH₃), 16.8 (C), 16.6 (C), -0.2 (3 x CH₃), -0.5 (3 x CH₃), -4.3 (2 x CH₃), -4.4 (2 x CH₃).

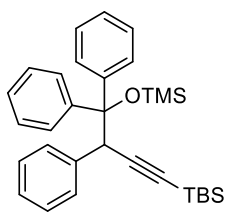
Tert-butyl dimethyl(4-(1-methylindol-2-yl)-4-((trimethylsilyl)oxy)-3-phenylbut-1-yn-1-yl)silane (1.3n)

	<p>Yield = 90%, 83 mg. (Mixture of diastereoisomers; <i>dr</i> = 2.9:1)</p> <p>Yellowish solid.</p> <p>R_f (SiO₂) = 0.02 (Hexane : Ethyl acetate, 200:1).</p> <p>HRMS for C₂₈H₄₀NOSi₂ [M+H]: Calc.: 462.2648; found: 462.2646.</p>
---	---

¹H-NMR (300 MHz, CDCl₃, 25 °C, TMS): δ (ppm) = 7.72 (d, $J_{(H,H)} = 7.7$ Hz, 1H), 7.66 (d, $J_{(H,H)} = 7.8$ Hz, 1H), 7.51- 7.38 (m, 10H), 7.38-7.17 (m, 6H), 6.62 (s, 1H), 6.47 (s, 1H), 5.14 (d, $J_{(H,H)} = 7.3$ Hz, 1H), 5.12 (d, $J_{(H,H)} = 7.3$ Hz, 1H), 4.27 (d, $J_{(H,H)} = 7.3$ Hz, 1H), 4.27 (d, $J_{(H,H)} = 7.3$ Hz, 1H), 3.85 (s, 3H), 3.53 (s, 3H), 1.16 (s, 9H), 0.93 (s, 9H), 0.33 (s, 3H), 0.30 (s, 3H), 0.17 (s, 9H), 0.11 (s, 3H), 0.09 (s, 3H), -0.03 (s, 9H).

¹³C-NMR (75 MHz, CDCl₃, 25 °C): δ (ppm) = 140.0 (C), 139.7 (C), 139.0 (C), 138.1 (C), 137.8 (C), 137.7 (C), 137.4 (C), 137.3 (C), 134.0 (CH), 133.7 (CH), 129.2 (CH), 128.9 (CH), 128.8 (CH), 128.6 (CH), 128.6 (CH), 128.1 (CH), 128.1 (CH), 127.6 (C), 127.5 (C), 127.3 (CH), 127.3 (CH), 121.2 (CH), 121.2 (CH), 120.7 (CH), 120.6 (CH), 119.4 (CH), 119.3 (CH), 109.0 (CH), 106.8 (C), 105.7 (C), 102.1 (CH), 101.7 (CH), 87.4 (C), 86.8 (C), 74.3 (CH), 74.0 (CH), 48.8 (CH), 48.0 (CH), 30.8 (CH₃), 30.4 (CH₃), 26.3 (3 x CH₃), 26.0 (3 x CH₃), 16.8 (C), 16.5 (C), 0.0 (3 x CH₃), -0.3 (3 x CH₃), -4.2 (CH₃), -4.3 (CH₃), -4.3 (CH₃), -4.5 (CH₃).

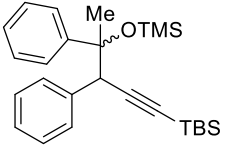
Tert-butyl dimethyl(4-((trimethylsilyl)oxy)-3,4,4-triphenylbut-1-yn-1-yl)silane (1.3o, 2.6, 4.6a)

	<p>Yield = 99%, 96 mg.</p> <p>White solid, mp = 96.5-98.3 °C</p> <p>R_f (SiO₂) = 0.10 (Hexane : Ethyl acetate, 200:1).</p> <p>HRMS (EI) for C₃₁H₄₀NaOSi₂ [M+Na]: Calc.: 507.2515; found: 511.2510.</p>
---	---

¹H-NMR (300 MHz, CDCl₃, 25 °C, TMS): δ (ppm) = 7.50 (m, 2H), 7.37-7.03 (m, 11H), 6.97-6.84 (m, 2H), 4.81 (s, 1H), 0.85 (s, 9H), 0.05 (s, 3H), 0.02 (s, 3H), -0.13 (s, 9H).

¹³C-NMR (75 MHz, CDCl₃): δ (ppm) = 144.3 (C), 142.9 (C), 137.5 (C), 130.7 (2 x CH), 129.8 (2 x CH), 129.1 (2 x CH), 127.7 (CH), 127.6 (2 x CH), 127.0 (CH), 126.7 (2 x CH), 126.6 (CH), 126.3 (2 x CH), 107.6 (C), 89.3 (C), 84.2 (C), 50.1 (CH), 26.2 (3 x CH₃), 16.8 (C), 1.9 (3 x CH₃), -4.6 (2 x CH₃).

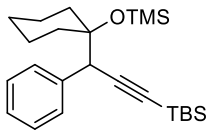
Tert-butyl dimethyl(4-((trimethylsilyl)oxy)-3,4-diphenylpent-1-yn-1-yl)silane (1.3p)

	<p>Yield = 99%, 84 mg. (Mixture of diastereoisomers; <i>dr</i> = 1.0:1) White solid. R_f (SiO₂) = 0.11 (Hexane : Ethyl acetate, 200:1). HRMS (EI) for C₂₆H₃₈NaOSi₂ [M+Na]: Calc.: 445.2359; found: 445.2353.</p>
---	--

¹H-NMR (300 MHz, CDCl₃, 25 °C, TMS): δ (ppm) = 7.47-6.99 (m, 20H), 3.99 (s, 1H), 3.93 (s, 1H), 1.84 (s, 3H), 1.74 (s, 3H), 1.01 (s, 9H), 0.97 (s, 9H), 0.15 (s, 3H), 0.14 (s, 3H), 0.11 (s, 6H), 0.08 (s, 9H), -0.02 (s, 9H).

¹³C-NMR (75 MHz, CDCl₃, 25 °C): δ (ppm) = 146.9 (C), 145.3 (C), 138.1 (C), 137.7 (C), 130.5 (2 x CH), 130.3 (2 x CH), 127.4 (2 x CH), 127.1 (2 x CH), 127.1 (2 x CH), 127.1 (2 x CH), 126.9 (2 x CH), 126.8 (2 x CH), 126.7 (2 x CH), 126.4 (2 x CH), 107.7 (C), 107.3 (C), 87.0 (C), 86.6 (C), 79.6 (C), 79.1 (C), 54.4 (CH), 54.1 (CH), 26.4 (3 x CH₃), 26.3 (3 x CH₃), 26.1 (CH₃), 24.4 (CH₃), 16.9 (C), 16.8 (C), 2.3 (3 x CH₃), 2.1 (3 x CH₃), -4.4 (2 x CH₃), -4.4 (2 x CH₃).

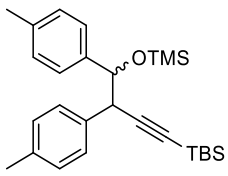
Tert-butyldimethyl(3-(1-((trimethylsilyl)oxy)cyclohexyl)-3-phenylprop-1-yn-1-yl)silane (1.3q)

	<p>Yield = 99%, 79 mg.</p> <p>Colorless oil.</p> <p>R_f (SiO₂) = 0.42 (Hexane).</p> <p>HRMS (EI) for C₂₄H₄₁OSi₂ [M+H]: Calc.: 401.2696; found: 401.2690.</p>
---	--

¹H-NMR (300 MHz, CDCl₃, 25 °C, TMS): δ (ppm) = 7.42-7.21 (m, 5H), 3.86 (s, 1H), 1.62-1.48 (m, 10H), 0.97 (s, 9H), 0.12 (s, 3H) 0.11 (s, 3H), 0.11 (s, 9H).

¹³C-NMR (75 MHz, CDCl₃, 25 °C): δ (ppm) = 138.8 (C), 130.4 (2 x CH), 127.6 (2 x CH), 126.9 (CH), 108.4 (C), 85.8 (C), 78.0 (CH), 49.0 (CH), 36.9 (CH₂), 35.6 (CH₂), 26.3 (3 x CH₃), 25.7 (CH₂), 22.9 (CH₂), 22.8 (CH₂), 16.9 (C), 2.9 (3 x CH₃), -4.3 (2 x CH₃).

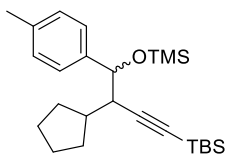
Tert-butyldimethyl(4-((trimethylsilyl)oxy)-3,4-di(*p*-tolyl)but-1-yn-1-yl)silane (1.3r)

	<p>Yield = 92%, 80 mg. (Mixture of diastereoisomers; <i>dr</i> = 1.0:1) Yellowish solid.</p> <p>R_f (SiO₂) = 0.09 (Hexane : Ethyl acetate, 200:1).</p> <p>HRMS (EI) for C₂₇H₄₀NaOSi₂ [M+Na]: Calc.: 459.2515; found: 459.2510.</p>
---	--

¹H-NMR (300 MHz, CDCl₃, 25 °C, TMS): δ (ppm) = 7.33-6.98 (m, 16H), 4.77 (d, $J_{(H,H)} = 5.2$ Hz, 1H), 4.66 (d, $J_{(H,H)} = 7.4$ Hz, 1H), 3.90 (d, $J_{(H,H)} = 5.3$ Hz, 1H), 3.84 (d, $J_{(H,H)} = 7.4$ Hz, 1H), 2.38 (s, 3H), 2.35 (s, 3H), 1.03 (s, 9H), 0.92 (s, 9H), 0.17 (s, 3H), 0.15 (s, 3H), 0.07 (s, 6H), -0.04 (s, 9H), -0.15 (s, 9H).

¹³C-NMR (75 MHz, CDCl₃, 25 °C): δ (ppm) = 139.9 (C), 139.5 (C), 136.9 (C), 136.8 (C), 136.8 (C), 136.4 (C), 136.2 (C), 135.7 (C), 129.3 (2 x CH), 129.1 (2 x CH), 128.5 (2 x CH), 128.5 (2 x CH), 128.3 (2 x CH), 128.3 (2 x CH), 127.2 (2 x CH), 126.9 (2 x CH), 107.1 (C), 107.0 (C), 86.9 (C), 86.6 (C), 79.2 (CH), 78.8 (CH), 49.0 (CH), 48.6 (CH), 26.3 (3 x CH₃), 26.2 (3 x CH₃), 21.3 (CH₃), 21.3 (CH₃), 21.2 (CH₃), 21.2 (CH₃), 16.9 (C), 16.7 (C), 0.0 (3 x CH₃), -0.2 (3 x CH₃), -4.3 (2 x CH₃), -4.4 (2 x CH₃).

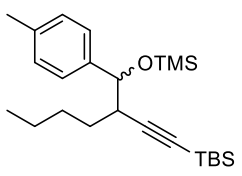
Tert-butyldimethyl(3-cyclopentyl-4-((trimethylsilyl)oxy)-4-(*p*-tolyl)but-1-yn-1-yl)silane (1.3s)

	<p>Yield = 99%, 82 mg. (Mixture of diastereoisomers; <i>dr</i> = 1.1:1) White solid. R_f (SiO₂) = 0.12 (Hexane : Ethyl acetate, 200:1). HRMS (EI) for C₂₅H₄₃OSi₂ [M+H]: Calc.: 415.2852; found: 415.2847.</p>
---	--

¹H-NMR (300 MHz, CDCl₃, 25 °C, TMS): δ (ppm) = 7.24 (d, $J_{(H,H)} = 7.8$ Hz, 2H), 7.24 (d, $J_{(H,H)} = 7.8$ Hz, 2H), 7.12 (d, $J_{(H,H)} = 7.8$ Hz, 2H), 7.10 (d, $J_{(H,H)} = 7.8$ Hz, 2H), 4.53 (d, $J_{(H,H)} = 8.3$ Hz, 1H), 4.53 (d, $J_{(H,H)} = 8.3$ Hz, 1H), 2.94-2.63 (m, 2H), 2.36 (s, 3H), 2.35 (s, 3H), 1.81-1.34 (m, 16H), 0.98 (s, 9H), 0.87 (s, 9H), 0.13 (s, 6H), 0.12 (s, 6H), 0.03 (s, 9H), 0.02 (s, 9H), 0.00 (s, 6H).

¹³C-NMR (75 MHz, CDCl₃, 25 °C): δ (ppm) = 140.7 (C), 140.4 (C), 137.0 (C), 136.7 (C), 128.7 (2 x CH), 128.4 (2 x CH), 127.1 (2 x CH), 126.8 (2 x CH), 108.1 (C), 107.1 (C), 86.4 (C), 85.0 (C), 76.7 (CH), 76.7 (CH), 47.9 (CH), 47.5 (CH), 39.5 (CH), 38.8 (CH), 31.7 (CH₂), 31.5 (CH₂), 28.3 (CH₂), 27.8 (CH₂), 26.3 (3 x CH₃), 26.2 (3 x CH₃), 26.0 (CH₂), 26.0 (CH₂), 25.9 (CH₂), 25.6 (CH₂), 21.3 (CH₃), 21.3 (CH₃), 16.7 (C), 16.6 (C), 0.3 (6 x CH₃), -4.3 (CH₃), -4.3 (CH₃), -4.4 (2 x CH₃).

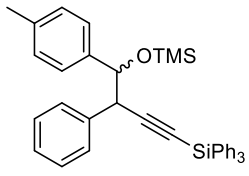
**Tert-butyl dimethyl(3-(*p*-tolyl((trimethylsilyl)oxy)methyl)hept-1-yn-1-yl)silane
(1.3t)**

	<p>Yield = 99%, 80 mg. (Mixture of diastereoisomers; <i>dr</i> = 1.0:1)</p> <p>White solid.</p> <p>R_f (SiO₂) = 0.12 (Hexane : Ethyl acetate, 200:1).</p> <p>HRMS (EI) for C₂₄H₄₃OSi₂ [M+H]: Calc.: 403.2852; found: 403.2847.</p>
---	---

¹H-NMR (300 MHz, CDCl₃, 25 °C, TMS): δ (ppm) = 7.25 (d, $J_{(H,H)} = 8.0$ Hz, 2H), 7.25 (d, $J_{(H,H)} = 8.0$ Hz, 2H), 7.11 (dd, $J_{(H,H)} = 8.0$ and 2.1 Hz, 2H), 7.11 (dd, $J_{(H,H)} = 8.0$ and 2.1 Hz, 2H), 4.63-4.54 (m, 2H), 2.70- 2.56 (m, 2H), 2.36 (s, 3H), 2.35 (s, 3H), 1.77-1.10 (m, 12H), 1.00-0.8 (m, 6H), 0.97 (s, 9H), 0.88 (s, 9H), 0.12 (s, 6H), 0.05 (s, 18H), 0.04 (s, 3H), 0.04 (s, 3H).

¹³C-NMR (75 MHz, CDCl₃, 25 °C): δ (ppm) = 140.5 (C), 139.9 (C), 136.9 (C), 136.7 (C), 128.6 (2 x CH), 128.4 (2 x CH), 126.9 (4 x CH), 109.3 (C), 108.9 (C), 85.5 (C), 84.9 (C), 77.1 (CH), 77.0 (CH), 42.7 (CH), 42.6 (CH), 30.3 (CH₂), 30.1 (CH₂), 29.6 (CH₂), 29.5 (CH₂), 26.3 (3 x CH₃), 26.2 (3 x CH₃), 22.7 (CH₂), 22.5 (CH₂), 21.3 (CH₃), 21.3 (CH₃), 16.8 (C), 16.6 (C), 14.2 (CH₃), 14.2 (CH₃), 0.3 (3 x CH₃), 0.3 (3 x CH₃), -4.3 (2 x CH₃), -4.4 (2 x CH₃).

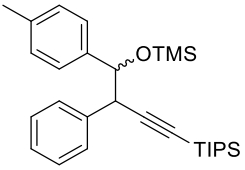
(4-((Trimethylsilyl)oxy)-3-phenyl-4-(*p*-tolyl)but-1-yn-1-yl)triphenylsilane (1.3u)

	<p>Yield = 99%, 112 mg. (Mixture of diastereoisomers; <i>dr</i> = 1.3:1)</p> <p>White solid.</p> <p>R_f (SiO₂) = 0.05 (Hexane : Ethyl acetate, 200:1).</p> <p>HRMS (EI) for C₃₈H₃₈NaOSi₂ [M+Na]: Calc.: 589.2359; found: 589.2353.</p>
---	---

¹H-NMR (300 MHz, CDCl₃, 25 °C, TMS): δ (ppm) = 7.76-7.65 (m, 6H), 7.62-7.54 (m, 4H), 7.50-7.11 (m, 35H), 7.02 (t, $J_{(H,H)} = 7.8$ Hz, 3H), 4.89 (d, $J_{(H,H)} = 4.4$ Hz, 1H), 4.72 (d, $J_{(H,H)} = 7.8$ Hz, 1H), 4.10 (d, $J_{(H,H)} = 4.5$ Hz, 1H), 4.06 (d, $J_{(H,H)} = 7.8$ Hz, 1H), 2.37 (s, 3H), 2.35 (s, 3H), -0.12 (m, 9H), -0.19 (m, 9H).

¹³C-NMR (75 MHz, CDCl₃, 25 °C): δ (ppm) = 139.5 (C), 139.4 (C), 138.9 (C), 138.5 (C), 137.0 (C), 136.8 (C), 135.7 (6 x CH), 135.7 (6 x CH), 134.2 (3 x C), 134.0 (3 x C), 129.8 (6 x CH), 129.4 (2 x CH), 129.2 (2 x CH), 128.5 (2 x CH), 128.5 (2 x CH), 128.1 (2 x CH), 128.0 (2 x CH), 127.9 (6 x CH), 127.9 (6 x CH), 127.2 (2 x CH), 127.1 (CH), 127.1 (CH), 126.7 (2 x CH), 111.1 (C), 110.8 (C), 84.2 (C), 83.9 (C), 79.3 (CH), 78.7 (CH), 49.8 (CH), 49.3 (CH), 21.4 (CH₃), 21.3 (CH₃), -0.2 (3 x CH₃), -0.3 (3 x CH₃).

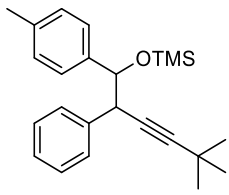
Triisopropyl(4-((trimethylsilyl)oxy)-3-phenyl-4-(*p*-tolyl)but-1-yn-1-yl)silane (1.3v)

	<p>Yield = 99%, 92 mg. (Mixture of diastereoisomers; <i>dr</i> = 1.2:1)</p> <p>White solid.</p> <p>R_f (SiO₂) = 0.06 (Hexane : Ethyl acetate, 200:1).</p> <p>HRMS (EI) for C₂₉H₄₄NaOSi₂ [M+Na]: Calc.: 487.2828; found: 487.2823.</p>
---	--

¹H-NMR (300 MHz, CDCl₃, 25 °C, TMS): δ (ppm) = 7.54-6.85 (m, 18H), 4.79 (d, $J_{(H,H)} = 4.2$ Hz, 1H), 4.59 (d, $J_{(H,H)} = 7.8$ Hz, 1H), 3.95 (d, $J_{(H,H)} = 4.3$ Hz, 1H), 3.91 (d, $J_{(H,H)} = 7.8$ Hz, 1H), 2.35 (s, 3H), 2.34 (s, 3H), 1.24-0.78 (m, 6H), 1.10 (s, 18H), 1.01 (s, 18H), -0.13 (s, 9H), -0.20 (s, 9H).

¹³C-NMR (75 MHz, CDCl₃, 25 °C): δ (ppm) = 139.8 (C), 139.7 (C), 139.6 (C), 139.3 (C), 137.0 (C), 136.7 (C), 129.4 (2 x CH), 129.2 (2 x CH), 128.4 (2 x CH), 128.3 (2 x CH), 127.8 (2 x CH), 127.8 (2 x CH), 127.2 (2 x CH), 126.9 (CH), 126.8 (CH), 126.7 (2 x CH), 107.5 (C), 107.1 (C), 85.0 (C), 84.9 (C), 79.5 (CH), 78.7 (CH), 49.5 (CH), 49.0 (CH), 21.3 (2 x CH₃), 18.8 (6 x CH₃), 18.7 (6 x CH₃), 11.5 (3 x CH), 11.4 (3 x CH), -0.2 (3 x CH₃), -0.3 (3 x CH₃).

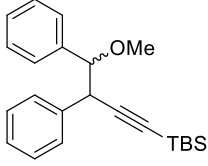
((5,5-Dimethyl-2-phenyl-1-(*p*-tolyl)hex-3-yn-1-yl)oxy)trimethylsilane (1.3w)

	<p>Yield = 84%, 61 mg. (Mixture of diastereoisomers; <i>dr</i> = 1.1:1)</p> <p>Yellowish solid.</p> <p>R_f (SiO₂) = 0.10 (Hexane : Ethyl acetate, 200:1).</p> <p>HRMS (EI) for C₂₄H₃₂NaOSi [M+Na]: Calc.: 387.2120; found: 387.2115.</p>
---	---

¹H-NMR (300 MHz, CDCl₃, 25 °C, TMS): δ (ppm) = 7.43-6.93 (m, 18H), 4.73 (d, $J_{(H,H)}$ = 5.7 Hz, 1H), 4.57 (d, $J_{(H,H)}$ = 7.7 Hz, 1H), 3.83 (d, $J_{(H,H)}$ = 5.7 Hz, 1H), 3.71 (d, $J_{(H,H)}$ = 7.7 Hz, 1H), 2.36 (s, 3H), 2.32 (s, 3H), 1.27 (s, 9H), 1.16 (s, 9H), -0.05 (s, 9H), -0.21 (s, 9H).

¹³C-NMR (75 MHz, CDCl₃, 25 °C): δ (ppm) = 140.3 (C), 140.3 (C), 139.5 (C), 139.4 (C), 136.7 (C), 136.6 (C), 129.4 (2 x CH), 129.3 (2 x CH), 128.2 (2 x CH), 128.1 (2 x CH), 127.7 (2 x CH), 127.7 (2 x CH), 127.2 (2 x CH), 127.0 (2 x CH), 126.7 (CH), 126.7 (CH), 93.4 (C), 93.0 (C), 79.5 (CH), 78.9 (CH), 78.4 (C), 78.1 (C), 48.1 (CH), 47.9 (CH), 31.4 (3 x CH₃), 31.2 (3 x CH₃), 27.7 (C), 27.5 (C), 21.3 (CH₃), 21.3 (CH₃), 0.0 (3 x CH₃), -0.3 (3 x CH₃).

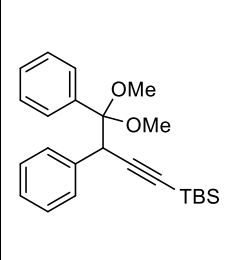
Tert-butyl(4-methoxy-3,4-diphenylbut-1-yn-1-yl)dimethylsilane (1.8)

	<p>Yield = 98%, 69 mg. (Mixture of diastereoisomers; <i>dr</i> = 1.1:1)</p> <p>Colorless oil.</p> <p>R_f (SiO₂) = 0.06 (Hexane : Ethyl acetate, 200:1).</p> <p>HRMS (EI) for C₂₃H₃₁O_{Si} [M+H]: Calc.: 351.2139; found: 351.2125.</p>
---	--

¹H-NMR (300 MHz, CDCl₃, 25 °C, TMS): δ (ppm) = 7.29-7.23 (m, 8H), 7.22-7.13 (m, 8H), 7.12-7.07 (m, 2H), 7.06-7.01 (m, 2H), 4.36 (d, $J_{(H,H)} = 5.9$ Hz, 1H), 4.24 (d, $J_{(H,H)} = 7.1$ Hz, 1H), 4.06 (d, $J_{(H,H)} = 7.0$ Hz, 1H), 4.01 (d, $J_{(H,H)} = 6.0$ Hz, 1H), 3.24 (s, 3H), 3.13 (s, 3H), 0.95 (s, 9H), 0.85 (s, 9H), 0.12 (s, 3H), 0.11 (s, 3H), 0.02 (s, 3H), 0.01 (s, 3H).

¹³C-NMR (75 MHz, CDCl₃, 25 °C): δ (ppm) = 138.9 (C), 138.8 (C), 138.7 (C), 137.6 (C), 129.2 (2 x CH), 129.0 (2 x CH), 128.1 (4 x CH), 128.0 (CH), 127.9 (2 x CH), 127.8 (3 x CH), 127.8 (2 x CH), 127.7 (2 x CH), 127.1 (CH), 127.0 (CH), 106.4 (C), 105.8 (C), 87.8 (C), 87.7 (CH), 87.4 (CH), 87.0 (C), 57.5 (CH₃), 57.3 (CH₃), 46.7 (CH), 46.6 (CH), 26.3 (3 x CH₃), 26.2 (3 x CH₃), 16.8 (C), 16.6 (C), -4.4 (2 x CH₃), -4.5 (2 x CH₃).

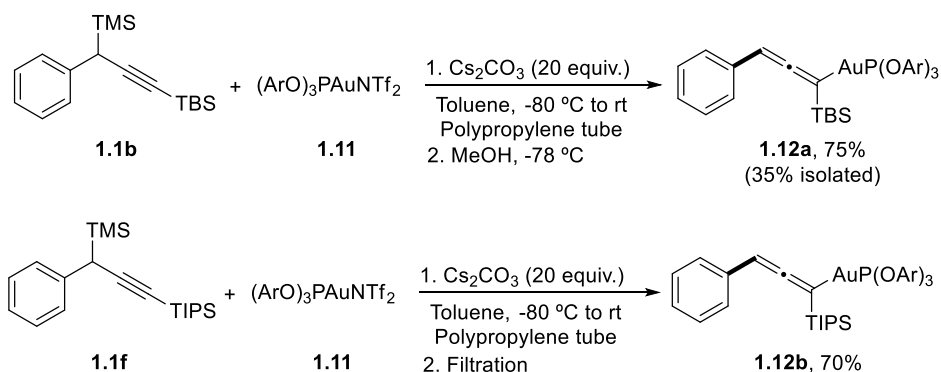
Tert-butyl(4,4-dimethoxy-3,4-diphenylbut-1-yn-1-yl)dimethylsilane (1.10)

	<p>Yield = 98%, 74 mg.</p> <p>Colorless oil.</p> <p>R_f (SiO₂) = 0.03 (Hexane : Ethyl acetate, 200:1).</p> <p>HRMS (EI) for C₂₄H₃₂O₂NaSi [M+Na]: Calc.: 403.2069; found: 403.2065.</p>
---	--

¹H-NMR (300 MHz, CDCl₃, 25 °C, TMS): δ (ppm) = 7.27-7.18 (m, 1H), 7.18-7.08 (m, 5H), 7.07-7.00 (m, 2H), 7.00-6.91 (m, 2H), 4.45 (s, 1H), 3.58 (s, 3H), 3.18 (s, 3H), 0.98 (s, 9H), 0.14 (s, 3H), 0.12 (s, 3H).

¹³C-NMR (75 MHz, CDCl₃, 25 °C): δ (ppm) = 136.7 (C), 136.6 (C), 130.3 (2 x CH), 128.8 (2 x CH), 127.9 (CH), 127.2 (2 x CH), 126.9 (CH), 126.7 (2 x CH), 105.2 (C), 104.7 (C), 87.5 (C), 49.9 (CH₃), 49.1 (CH₃), 46.9 (CH), 26.3 (3 x CH₃), 16.9 (C), -4.4 (2 x CH₃).

2.2.2 Procedure for the synthesis of σ -allenylgold(I) complexes **1.12**



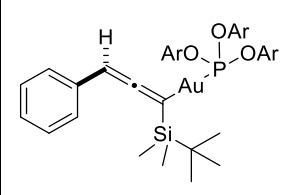
Scheme 5.6: Synthesis of σ -allenylgold(I) complexes **1.12**.

In a polypropylene tube inside the schlenck, a suspension of Cs_2CO_3 (163 mg, 0.5 mmol, 20 equiv.) in 0.5 mL of toluene-*d*8 at $-78 \text{ }^\circ\text{C}$, was prepared. The corresponding propargylsilane **1.1b** (1 equiv.) was added and the mixture was stirred for 30 min. Then, a solution of the phosphite gold complex (30 mg, 0.026 mmol, 1.05 equiv.) in 0.5 mL of toluene-*d*8 was added dropwise and the reaction was allowed to slowly reach room temperature.

The resultant slightly yellow mixture was then filtered through a short pad of Celite under argon and the solvent was removed under vacuum. The residue was then dissolved in dry pentane and filtered again under argon. The solvent was removed under vacuum to yield a foamy solid.

For compound **1.12a**, the product was precipitated from dry methanol by cooling down the mixture at $-78 \text{ }^\circ\text{C}$. After 16 h at that temperature, the supernatant was removed and the white solid dried under vacuum.

σ -Allenylgold(I) complex 1.12a

	<p>Yield = ca. 75% (Estimated prior to precipitation).</p> <p>White solid, mp = <60 °C (decomposition)</p> <p>HRMS (EI) for C₅₇H₈₅AuO₃PSi [M+H]: Calc.: 1073.5671; found: 1073.5684.</p>
---	---

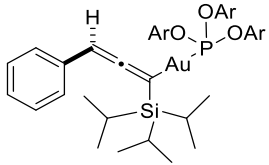
¹H-NMR (400 MHz, Toluene-*d*₈, 25 °C, TMS): δ (ppm) = 7.86 (d, $J_{(H,H)} = 8.3$ Hz, 3H), 7.52 (s, 3H), 7.41-6.86 (m, 5H), 7.03 (d, $J_{(H,H)} = 8.4$ Hz, 3H), 5.43 (d, $J_{(H,P)} = 8.4$ Hz, 1H), 1.51 (s, 27H), 1.21 (s, 27H), 1.09 (s, 9H), 0.22 (s, 6H).

¹³C-NMR (100 MHz, Toluene-*d*₈, 25 °C): δ (ppm) = 204.7 (C, $J_{(C,P)} = 10.8$ Hz), 148.6 (3 x C; $J_{(C,P)} = 4.6$ Hz), 148.4 (3 x C), 141.6 (C, $J_{(C,H)} = 6.1$ Hz), 139.9 (3 x C; $J_{(C,P)} = 5.7$ Hz), 128.9 (2 x CH), 125.7 (3 x CH), 125.7 (2 x CH), 125.0 (3 x CH), 123.6 (CH), 120.9 (3 x CH, $J_{(C,P)} = 9.6$ Hz), 108.0 (C, $J_{(C,P)} = 140.6$), 75.9 (CH, $J_{(C,P)} = 11.4$ Hz), 31.8 (9 x CH₃), 31.1 (9 x CH₃), 27.8 (3 x CH₃), 17.8 (6 x C), 17.5 (C), -2.8 (CH₃), -2.9 (CH₃).

³¹P-NMR (125 MHz, Toluene-*d*₈, 25 °C): δ (ppm) = 137.6.

IR (ATR): $\tilde{\nu}$ (cm⁻¹) = 2953, 2861, 1884, 1863, 1594, 1490, 1397, 1362, 1244, 1179, 1076, 918, 884, 816, 691, 643, 579, 507.

σ -Allenylgold(I) complex 1.12b

	<p>Yield = ca. 70% (Estimated).</p> <p>White solid.</p> <p>HRMS (EI) for C₆₀H₉₁AuO₃PSi [M+H]: Calc.: 1115.6141; found: 1115.6135.</p>
---	--

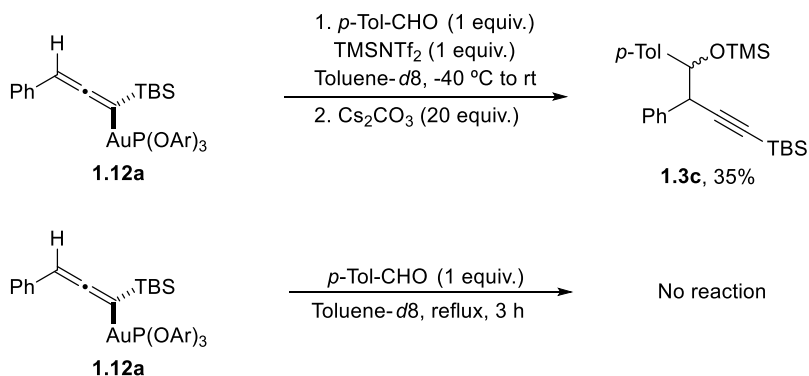
¹H-NMR (400 MHz, Toluene-*d*8, 25 °C, TMS): δ (ppm) = 7.86 (d, $J_{(H,H)} = 8.3$ Hz, 3H), 7.52 (s, 3H), 7.42-6.93 (m, 8H), 5.38 (d, $J_{(H,P)} = 8.4$ Hz, 1H), 1.51 (s, 27H), 1.24 (s, 18H), 1.21 (s, 27H).

¹³C-NMR (100 MHz, Toluene-*d*8, 25 °C): δ (ppm) (Selected signals) = 203.8 (C, $J_{(C,P)} = 10.8$ Hz), 148.6 (3 x C; $J_{(C,P)} = 4.4$ Hz), 148.4 (3 x C), 141.8 (C, $J_{(C,H)} = 18.5$ Hz), 139.9 (3 x C; $J_{(C,P)} = 5.6$ Hz), 125.7 (2 x CH), 125. (3 x CH), 123.4 (CH), 120.1 (3 x CH, $J_{(C,P)} = 9.5$ Hz), 104.0 (C, $J_{(C,P)} = 132.8$), 75.0 (CH, $J_{(C,P)} = 11.1$ Hz), 31.8 (9 x CH₃), 31.1 (9 x CH₃), 20.0 (3 x CH₃), 19.9 (3 x CH₃), 13.6 (3 x CH).

³¹P-NMR (125 MHz, Toluene-*d*8, 25 °C): δ (ppm) = 136.5.

IR (ATR): $\tilde{\nu}$ (cm⁻¹) = 2955, 2865, 1884, 1824, 1595, 1490, 1461, 1397, 1362, 1247, 1180, 1077, 1018, 922, 885, 818, 693, 672, 645, 604, 494.

2.2.3 Stoichiometric reaction from σ -allenylgold(I) intermediate **1.12a**

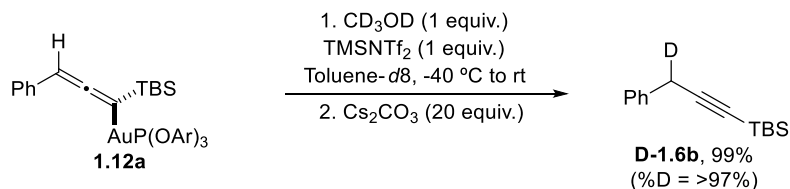


Scheme 5.7: Studies of the synergistic activation of the carbonyl derivative.

p-Tolualdehyde (3 μL , 0.025 mmol, 1 equiv.) was dissolved in 0.25 mL of toluene-*d*8, in a polypropylene tube inside the schlenck, under Ar. The solution was cooled down to $-40\text{ }^\circ\text{C}$ and, after 1 hour, a solution of freshly distilled TMSNTf₂ (4.2 μL , 0.025 mmol, 1 equiv.) 0.25 mL of toluene-*d*8 (0.25 mL) was dropped. After 30 min the mixture became deep red, and a solution of the σ -allenyl gold complex **1.12a** (27 mg, 0.025 mmol, 1 equiv.) in 0.5 mL of toluene-*d*8, was added. The reaction was allowed to reach room temperature and stirred for an additional period of 30 min. Finally, the reaction was quenched adding Cs₂CO₃ (8 mg, 0.025 mmol, 1 equiv.). The crude mixture was directly analyzed by ¹H and ³¹P-NMR experiments, showing the formation of the diastereoisomeric homopropargyl silyl ethers **1.3c** in a 35% yield.

The same procedure was followed for the stoichiometric reaction between *p*-tolualdehyde **1.2a** and complex **1.12a** without TMSNTf₂ activation, but refluxing the mixture for 3 h. The direct NMR analysis of the crude mixture revealed no reaction at all.

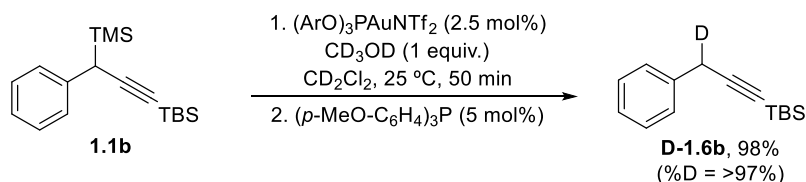
2.2.4 Deuteration reaction of σ -allenylgold(I) intermediate **1.12a**.



Scheme 5.8: Stoichiometric deuteration of complex **1.12a**.

In a polypropylene tube inside the schlenck under Ar, to a solution of freshly distilled TMSNTf₂ (4.2 μL , 0.025 mmol) in toluene-*d*8 (1 mL) at -40 °C, CD₃OD (20 μL ; 17.5 mg; 20 equiv.) was dropped. After 10 min of stirring, σ -allenylgold complex **1.12a** (27 mg, 0.025 mmol) was added and the mixture was allowed to reach room temperature and stirred for an additional 30 min. Finally, the reaction was quenched adding Cs₂CO₃ (8 mg, 0.025 mmol) and filtered through a celite pad. After removal of the solvents, under reduced pressure, and chromatographic purification, 5.8 mg of silane **D-1.6b** were obtained.

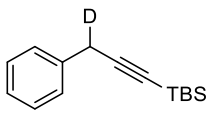
2.2.5 Catalytic deuterosilylation of propargylsilane **1.1b**.



Scheme 5.9: Catalytic deuterosilylation of propargylsilane **1.1b**.

To a solution of 0.20 mmol of propargylsilane **1.1b** in 1 mL of dichloromethane, at 25 °C, 0.2 mmol of methanol-*d*4 (8 μL , 1 equiv.) and 5.6 mg (0.005 mmol, 2.5 mol %) of the gold catalyst were subsequently added. The mixture was stirred for 50 min. Upon completion, 3.3 mg of (*p*-MeO-C₆H₄)₃P (0.01 mmol, 5 mol %) were added to the mixture and the solvents evaporated under vacuum. Finally, after purification of the residue by silica gel flash chromatography, the corresponding alkynylsilane **D-1.6b** was obtained as a pure compound.

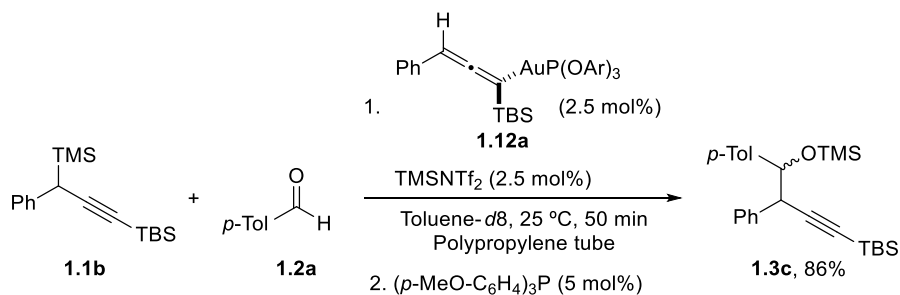
Tert-butyldimethyl(3-phenylprop-1-yn-1-yl-3-d)silane (D-1.6b)

	<p>Yield = 99%, 6 mg (starting from complex 1.12a). 98%, 45 mg (starting from propargylsilane 1.1a).</p> <p>Colorless oil.</p> <p>R_f (SiO₂) = 0.60 (Hexane).</p> <p>HRMS for C₁₅H₂₁DNaSi [M+Na]: Calc.: 254.1451; found: 254.1446.</p>
---	---

¹H-NMR (300 MHz, CDCl₃, 25 °C, TMS): δ (ppm) = 7.49-7.20 (m, 5H), 3.70 (m, 1H), 0.98 (s, 9H), 0.15 (s, 6H).

¹³C-NMR (75 MHz, CDCl₃, 25 °C): δ (ppm) = 136.6 (C), 128.6 (2 x CH), 128.0 (2 x CH), 126.7 (CH), 104.9 (C), 85.2 (C), 26.3 (3 x CH₃), 26.1 (t, $J_{(C,D)}$ = 19.9 Hz, CDH), 16.7 (C), -4.3 (2 x CH₃).

2.2.6 Catalytic reaction using σ -allenylgold(I) intermediate **1.12a**



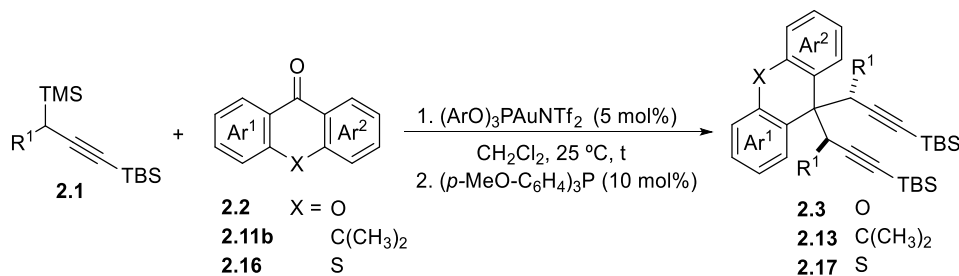
Scheme 5.10: Gold-catalyzed propargylation using complex **1.12a** and TMSNTf₂ as catalysts.

In a polypropylene tube inside the schlenk, under Ar, *p*-tolaldehyde **1.2a** (24 μ L, 0.2 mmol, 1 equiv.), propargylsilane **1.1b** (72.5 mg, 0.24 mmol, 1.2 equiv.) and σ -allenylgold complex **1.12a** (5.4 mg, 2.5 mol%) were dissolved in 0.75 mL of dichloromethane. Then, a solution of freshly distilled TMSNTf₂ (0.5 μ L, 2.5 mol%) in 0.25 mL of dichloromethane was dropped. After 50 min the reaction was quenched adding (*p*-MeO-C₆H₄)₃P (4 mg, 5 mol%) and the solvents removed under vacuo.

The reaction was analyzed by ¹H using CH₂Br₂ as internal standard, showing the formation of the diastereoisomeric homopropargyl silyl ethers **1.3c** in a 86% yield.

2.3 Experimental procedures described in Chapter II

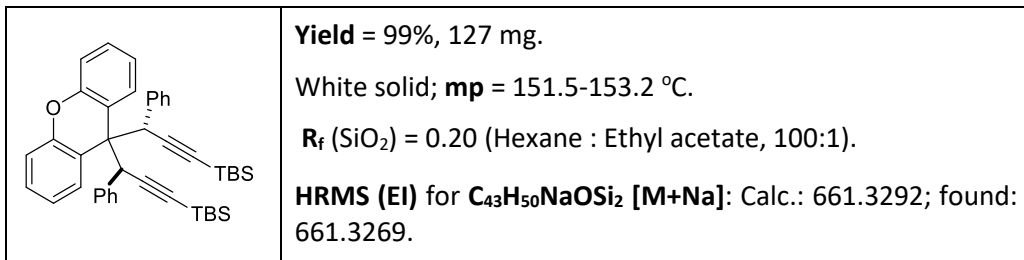
2.3.1 Experimental procedure for the gold(I)-catalyzed bispropargylation reaction of xanthone, anthrone and thioxanthone derivatives.



Scheme 5.11: Gold(I)-catalyzed bispropargylation reaction of xanthone derivatives.

To a solution of 0.20 mmol of the corresponding xanthone **2.2**, anthrone **2.11** or thioxanthone **2.16**, in 1 mL of dry dichloromethane at 25 °C under argon atmosphere, were sequentially added 0.6 mmol of the propargylsilane **2.1** and 11.2 mg of the gold catalyst (5 mol%). The reaction mixture was stirred for 3 h for xanthenes **2.2** and anthrone **2.11b** (6 h for products **2.3d-e,h,k,m,n** or 16 h for **2.3r-s**) and 8 h for thioxanthenes **2.16** (16 h for products **2.17c,h**), at 25 °C (60 °C for products **2.3k** and **2.17h**), upon starting material disappearance. Finally, 8.2 mg (0.02 mmol, 10 mol%) of (p-MeO-C₆H₄)₃P were added for catalyst deactivation, and the solvent was removed under vacuum. Flash column chromatography through silica gel of the residue afforded the corresponding 9,9-bispropargylxanthenes **2.3a-s**, 9,9-bispropargylanthrene **2.13** or 9,9-bispropargylthioxanthenes **2.17a-h**. No relevant differences were observed for a reaction performed at 3 mmol scale, obtaining compound **2.3a** in 97% yield.

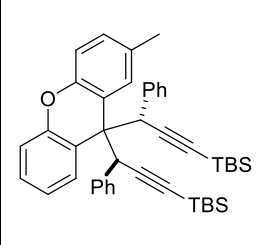
((3*S,3'*S*'*)-(9*H*-Xanthene-9,9-diyl)bis(3-phenylprop-1-yne-3,1-diyl))bis(*tert*-butyldimethylsilane) (2.3a)**



¹H-NMR (300 MHz, CDCl₃, 25 °C, TMS): δ (ppm) = 8.83-8.68 (m, 2H), 7.20-7.07 (m, 4H), 7.02-6.92 (m, 2H), 6.86 (tt, $J_{(H,H)} = 6.4, 1.6$ Hz, 4H), 6.67-6.60 (m, 4H), 6.56-6.49 (m, 2H), 5.19 (s, 2H), 1.11 (s, 18H), 0.27 (s, 6H), 0.26 (s, 6H).

¹³C-NMR (75 MHz, CDCl₃, 25 °C): δ (ppm) = 151.3 (2 x C), 137.9 (2 x C), 129.8 (4 x CH), 128.7 (4 x CH), 127.2 (4 x CH), 126.7 (2 x CH), 121.7 (2 x CH), 120.7 (2 x C), 116.2 (2 x CH), 108.3 (2 x C), 89.3 (2 x C), 50.3 (2 x CH), 50.1 (C), 26.5 (6 x CH₃), 17.1(2 x C), -4.4 (4 x CH₃).

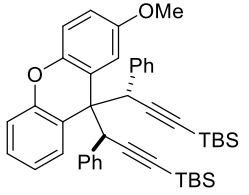
((3*S,3'*S*'*)-(2-Methyl-9*H*-xanthene-9,9-diyl)bis(3-phenylprop-1-yne-3,1-diyl))bis(*tert*-butyldimethylsilane) (2.3b)**

	<p>Yield = 98%, 128 mg.</p> <p>White solid, mp = 120.3-122.4 °C.</p> <p>R_f (SiO₂) = 0.22 (Hexane : Ethyl acetate, 100:1).</p> <p>HRMS (EI) for C₄₄H₅₃OSi₂ [M+H]: Calc.: 653.3635; found: 653.3630.</p>
---	--

¹H-NMR (300 MHz, CDCl₃, 25 °C, TMS): δ (ppm) = 8.75 (dd, $J_{(H,H)} = 7.5, 2.6$ Hz, 1H), 8.56 (s, 1H), 7.13 (td, $J_{(H,H)} = 8.4, 7.8, 3.6$ Hz, 2H), 6.96 (q, $J_{(H,H)} = 6.7, 6.2$ Hz, 3H), 6.87 (td, $J_{(H,H)} = 7.5, 7.1, 2.0$ Hz, 4H), 6.64 (dd, $J_{(H,H)} = 13.7, 7.6$ Hz, 5H), 6.56-6.48 (m, 1H), 6.42 (d, $J_{(H,H)} = 8.4$ Hz, 1H), 5.22 (s, 1H), 5.18 (s, 1H), 2.48 (s, 3H), 1.11 (s, 18H), 0.30 (s, 3H), 0.27 (s, 9H).

¹³C-NMR (75 MHz, CDCl₃, 25 °C): δ (ppm) = 151.5 (C), 149.2 (C), 138.0 (2 x C), 130.9 (C), 129.9 (2 x CH), 129.8 (2 x CH), 129.4 (CH), 128.7 (CH), 128.6 (CH), 128.6 (CH), 127.2 (2 x CH), 127.1 (2 x CH), 126.6 (CH), 126.6 (CH), 121.4 (CH), 120.7 (C), 120.3 (C), 116.1 (CH), 115.8 (CH), 108.4 (C), 108.3 (C), 89.2 (C), 88.9 (C), 50.4 (2 x CH), 50.0 (C), 26.6 (3 x CH₃), 26.5 (3 x CH₃), 21.3 (CH₃), 17.1 (C), 17.0 (C), -4.2 (CH₃), -4.3 (CH₃), -4.4 (2 x CH₃).

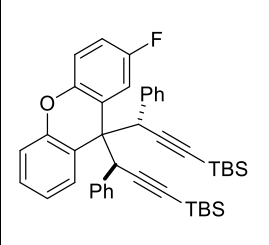
((3*S,3'*S*'*)-(2-Methoxy-9*H*-xanthene-9,9-diyl)bis(3-phenylprop-1-yne-3,1-diyl))bis(*tert*-butyldimethylsilane) (2.3c)**

	<p>Yield = 97%, 130 mg.</p> <p>White solid, mp = 140.0-142.0 °C.</p> <p>R_f (SiO₂) = 0.23 (Hexane : Ethyl acetate, 40:1).</p> <p>HRMS (EI) for C₄₄H₅₂NaO₂Si₂ [M+Na]: Calc.: 691.3398; found: 691.3383.</p>
---	---

¹H-NMR (300 MHz, CDCl₃, 25 °C, TMS): δ (ppm) = 8.70 (dd, $J_{(H,H)} = 7.8, 2.1$ Hz, 1H), 8.31 (d, $J_{(H,H)} = 2.9$ Hz, 1H), 7.19-7.06 (m, 2H), 7.02-6.93 (m, 2H), 6.93-6.82 (m, 4H), 6.79-6.67 (m, 3H), 6.64-6.57 (m, 2H), 6.52 (dd, $J_{(H,H)} = 7.8, 1.7$ Hz, 1H), 6.44 (d, $J_{(H,H)} = 8.9$ Hz, 1H), 5.27 (s, 1H), 5.13 (s, 1H), 3.93 (s, 3H), 1.09 (s, 9H), 1.08 (s, 9H), 0.27 (s, 3H), 0.25 (s, 3H), 0.24 (s, 3H), 0.23 (s, 3H).

¹³C-NMR (75 MHz, CDCl₃, 25 °C): δ (ppm) = 154.5 (C), 151.6 (C), 145.6 (C), 137.9 (2 x C), 129.7 (5 x CH), 128.8 (CH), 128.7 (CH), 127.2 (2 x CH), 127.1 (2 x CH), 126.7 (CH), 121.4 (CH), 119.8 (2 x C), 116.7 (CH), 116.0 (CH), 114.9 (CH), 113.4 (CH), 108.3 (2 x C), 89.3 (C), 89.2 (C), 56.3 (CH₃), 50.8 (CH), 50.4 (C), 49.5 (CH), 26.5 (3 x CH₃), 26.4 (3 x CH₃), 17.1 (2 x C), -4.3 (2 x CH₃), -4.4 (2 x CH₃).

((3*S,3'*S*'*)-(2-Fluoro-9*H*-xanthene-9,9-diyl)bis(3-phenylprop-1-yne-3,1-diyl))bis(*tert*-butyldimethylsilane) (2.3d)**

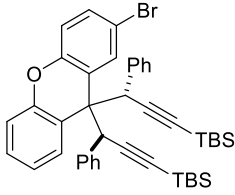
	<p>Yield = 95%, 125 mg.</p> <p>White solid, mp = 137.9-139.0 °C.</p> <p>R_f (SiO₂) = 0.19 (Hexane : Ethyl acetate, 100:1).</p> <p>HRMS (EI) for C₄₃H₄₉FNaOSi₂ [M+Na]: Calc.: 679.3198; found: 679.3200.</p>
---	--

¹H-NMR (300 MHz, CDCl₃, 25 °C, TMS): δ (ppm) = 8.86-8.74 (m, 1H), 8.57 (dt, $J_{(H,H,F)}$ = 8.1, 1.6 Hz, 1H), 7.27-7.15 (m, 2H), 7.12-6.97 (m, 4H), 6.91 (dd, $J_{(H,H,F)}$ = 8.3, 6.6 Hz, 4H), 6.65 (ddt, $J_{(H,H,F)}$ = 9.7, 7.1, 1.3 Hz, 5H), 5.24 (s, 1H), 5.19 (s, 1H), 1.13 (s, 18H), 0.30 (s, 6H), 0.29 (s, 6H).

¹³C-NMR (75 MHz, CDCl₃, 25 °C): δ (ppm) = 150.7 (d, $J_{(C,F)}$ = 247.4 Hz, C), 150.6 (C), 140.4 (d, $J_{(C,F)}$ = 11.1 Hz, C), 137.6 (C), 137.5 (C), 129.7 (4 x CH), 129.0 (CH), 128.7 (CH), 127.3 (4 x CH), 126.9 (2 x CH), 123.7 (d, $J_{(C,F)}$ = 3.9 Hz, CH), 123.4 (C), 122.3 (CH), 120.7 (d, $J_{(C,F)}$ = 7.2 Hz, CH), 120.4 (C), 116.5 (CH), 115.0 (d, $J_{(C,F)}$ = 17.4 Hz, CH), 108.1 (C), 108.0 (C), 89.6 (C), 89.5 (C), 50.5 (C), 50.2 (2 x CH), 26.5 (6 x CH₃), 17.1 (2 x C), -4.4 (4 x CH₃).

¹⁹F-NMR (282 MHz, CDCl₃, 25 °C): δ (ppm) = -136.2.

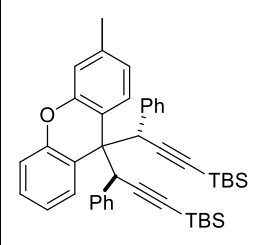
((3*S,3'*S*'*)-(2-Bromo-9*H*-xanthene-9,9-diyl)bis(3-phenylprop-1-yne-3,1-diyl))bis(*tert*-butyldimethylsilane) (2.3e)**

	<p>Yield = 98%, 141 mg.</p> <p>Colorless oil.</p> <p>R_f (SiO₂) = 0.22 (Hexane : Ethyl acetate, 100:1).</p> <p>HRMS (EI) for C₄₃H₄₉BrNaOSi₂ [M+Na]: Calc.: 739.2398; found: 739.2399.</p>
---	--

¹H-NMR (300 MHz, CDCl₃, 25 °C, TMS): δ (ppm) = 8.92 (d, $J_{(H,H)} = 2.4$ Hz, 1H), 8.73 (dd, $J_{(H,H)} = 7.7, 2.0$ Hz, 1H), 7.21 (dd, $J_{(H,H)} = 8.7, 2.3$ Hz, 1H), 7.18-7.09 (m, 2H), 7.02-6.94 (m, 2H), 6.93-6.83 (m, 4H), 6.71-6.65 (m, 2H), 6.63-6.55 (m, 2H), 6.55-6.49 (m, 1H), 6.38 (d, $J_{(H,H)} = 8.7$ Hz, 1H), 5.21 (s, 1H), 5.07 (s, 1H), 1.10 (s, 9H), 1.08 (s, 9H), 0.34 (s, 3H), 0.27 (s, 3H), 0.24 (s, 6H).

¹³C-NMR (75 MHz, CDCl₃, 25 °C): δ (ppm) = 151.1 (C), 150.3 (C), 137.6 (C), 137.6 (C), 131.7 (CH), 131.1 (CH), 129.8 (4 x CH), 129.0 (CH), 128.8 (CH), 127.4 (2 x CH), 127.3 (2 x CH), 126.9 (CH), 126.8 (CH), 123.1 (C), 122.0 (CH), 120.1 (C), 117.9 (CH), 116.2 (CH), 114.1 (C), 107.9 (C), 107.3 (C), 90.1 (C), 89.6 (C), 51.0 (CH), 50.0 (C), 49.8 (CH), 26.6 (3 x CH₃), 26.5 (3 x CH₃), 17.1 (2 x C), -4.2 (CH₃), -4.3 (CH₃), -4.4 (2 x CH₃).

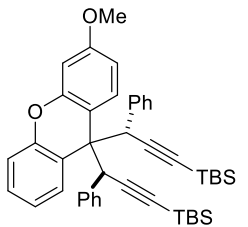
((3*S,3'*S*'*)-(3-Methyl-9*H*-xanthene-9,9-diyl)bis(3-phenylprop-1-yne-3,1-diyl))bis(*tert*-butyldimethylsilane) (2.3f)**

	<p>Yield = 98%, 128 mg.</p> <p>White solid; mp = 116.7-118.4 °C.</p> <p>R_f (SiO₂) = 0.23 (Hexane : Ethyl acetate, 100:1).</p> <p>HRMS (EI) for C₄₄H₅₃OSi₂ [M+H]: Calc.: 653.3635; found: 653.3629.</p>
---	--

¹H-NMR (300 MHz, CDCl₃, 25 °C, TMS): δ (ppm) = 8.80-8.70 (m, 1H), 8.61 (d, $J_{(H,H)}$ = 8.2 Hz, 1H), 7.19-7.05 (m, 2H), 7.03-6.92 (m, 3H), 6.87 (dd, $J_{(H,H)}$ = 8.4, 6.7 Hz, 4H), 6.70-6.60 (m, 4H), 6.57-6.46 (m, 1H), 6.35 (t, $J_{(H,H)}$ = 1.3 Hz, 1H), 5.18 (s, 1H), 5.17 (s, 1H), 2.28 (s, 3H), 1.11 (s, 17H), 0.27 (s, 6H), 0.25 (s, 6H).

¹³C-NMR (75 MHz, CDCl₃, 25 °C): δ (ppm) = 151.4 (C), 151.1 (C), 138.7 (C), 138.1 (C), 138.0 (C), 129.8 (3 x CH), 128.7 (CH), 128.6 (CH), 128.5 (CH), 127.1 (5 x CH), 126.6 (2 x CH), 122.8 (CH), 121.5 (CH), 120.8 (C), 117.6 (C), 116.4 (CH), 116.1 (CH), 108.5 (2 x C), 89.2 (C), 89.1 (C), 50.3 (2 x CH), 49.9 (C), 26.6 (3 x CH₃), 26.5 (3 x CH₃), 21.1 (CH₃), 17.1 (2 x C), -4.4 (4 x CH₃).

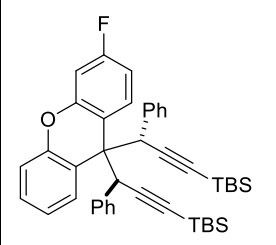
((3*S,3'*S*'*)-(3-Methoxy-9*H*-xanthene-9,9-diyl)bis(3-phenylprop-1-yne-3,1-diyl))bis(*tert*-butyldimethylsilane) (2.3g)**

	<p>Yield = 99%, 133 mg.</p> <p>White solid; mp = decomp. >138.0 °C.</p> <p>R_f (SiO₂) = 0.19 (Hexane : Ethyl acetate, 40:1).</p> <p>HRMS (EI) for C₄₄H₅₂NaO₂Si₂ [M+Na]: Calc.: 691.3398; found: 691.3382.</p>
---	---

¹H-NMR (300 MHz, CDCl₃, 25 °C, TMS): δ (ppm) = 8.84-8.75 (m, 1H), 8.67 (d, $J_{(H,H)}$ = 9.1 Hz, 1H), 7.21-7.11 (m, 2H), 7.05-6.96 (m, 2H), 6.96-6.87 (m, 4H), 6.75 (dd, $J_{(H,H)}$ = 8.9, 2.7 Hz, 1H), 6.73-6.64 (m, 4H), 6.57-6.47 (m, 1H), 6.10 (d, $J_{(H,H)}$ = 2.7 Hz, 1H), 5.21 (s, 1H), 5.18 (s, 1H), 3.78 (s, 3H), 1.14 (s, 9H), 1.13 (s, 9H), 0.31 (s, 3H), 0.30 (s, 3H), 0.29 (s, 3H), 0.29 (s, 3H).

¹³C-NMR (75 MHz, CDCl₃, 25 °C): δ (ppm) = 159.7 (C), 152.2 (C), 151.3 (C), 138.1 (C), 138.0 (C), 129.8 (4 x CH), 129.5 (CH), 128.7 (CH), 128.6 (CH), 127.2 (4 x CH), 126.6 (2 x CH), 121.7 (CH), 120.9 (C), 116.0 (CH), 112.8 (C), 109.4 (CH), 108.4 (2 x C), 99.8 (C), 89.1 (2 x C), 55.3 (CH₃), 50.3 (CH), 50.2 (CH), 49.8 (C), 26.5 (6 x CH₃), 17.1 (2 x C), -4.4 (4 x CH₃).

((3*S,3'*S*'*)-(3-Fluoro-9*H*-xanthene-9,9-diyl)bis(3-phenylprop-1-yne-3,1-diyl))bis(*tert*-butyldimethylsilane) (2.3h)**

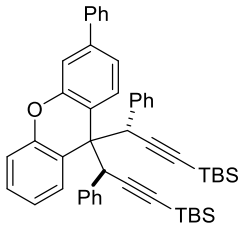
	<p>Yield = 96%, 126 mg.</p> <p>White solid, mp = >178.1 °C decomp.</p> <p>R_f (SiO₂) = 0.21 (Hexane : Ethyl acetate, 100:1).</p> <p>HRMS (EI) for C₄₃H₄₉FNaOSi₂ [M+Na]: Calc.: 679.3198; found: 679.3194.</p>
---	--

¹H-NMR (300 MHz, CDCl₃, 25 °C, TMS): δ (ppm) = 8.86-8.68 (m, 2H), 7.19 (dt, $J_{(H,H,F)}$ = 6.1, 3.9 Hz, 2H), 7.02 (t, $J_{(H,H,F)}$ = 7.3 Hz, 2H), 6.92 (t, $J_{(H,H,F)}$ = 7.5 Hz, 5H), 6.72-6.61 (m, 4H), 6.55 (dd, $J_{(H,H,F)}$ = 6.2, 3.4 Hz, 1H), 6.29 (dd, J = 9.7, 2.8 Hz, 1H), 5.23 (s, 1H), 5.16 (s, 1H), 1.14 (s, 18H), 0.31 (s, 6H), 0.29 (s, 6H).

¹³C-NMR (75 MHz, CDCl₃, 25 °C): δ (ppm) = 162.4 (d, $J_{(C,F)}$ = 246.8 Hz, C), 152.2 (d, $J_{(C,F)}$ = 12.1 Hz, C), 151.0 (C), 137.7 (2 x C), 130.0 (d, $J_{(C,F)}$ = 9.3 Hz, C), 129.7 (4 x CH), 128.9 (CH), 128.7 (CH), 127.3 (4 x CH), 126.8 (2 x CH), 122.1 (CH), 120.5 (C), 116.9 (d, J = 3.3 Hz, C), 116.2 (CH), 109.1 (d, $J_{(C,F)}$ = 21.2 Hz, CH), 108.1 (C), 108.0 (C), 103.1 (d, $J_{(C,F)}$ = 24.1 Hz, CH), 89.6 (C), 89.4 (C), 50.5 (CH), 50.1 (CH), 49.9 (C), 26.5 (6 x CH₃), 17.1 (2 x C), -4.4 (4 x CH₃).

¹⁹F-NMR (282 MHz, CDCl₃, 25 °C): δ (ppm) = -112.9.

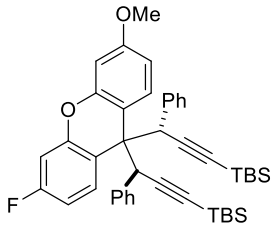
((3*S,3'*S*'*)-(3-Phenyl-9*H*-xanthene-9,9-diyl)bis(3-phenylprop-1-yne-3,1-diyl)bis(*tert*-butyldimethylsilane) (2.3i)**

	<p>Yield = 98%, 140 mg.</p> <p>White solid, mp = 178.2-178.1 °C.</p> <p>R_f (SiO₂) = 0.21 (Hexane : Ethyl acetate, 100:1).</p> <p>HRMS (EI) for C₄₉H₅₄NaOSi₂ [M+Na]: Calc.: 737.3611; found: 737.3607.</p>
---	---

¹H-NMR (300 MHz, CDCl₃, 25 °C, TMS): δ (ppm) = 8.85 (d, $J_{(H,H)} = 8.5$ Hz, 1H), 8.82-8.73 (m, 1H), 7.73-7.63 (m, 2H), 7.55-7.36 (m, 4H), 7.24-7.12 (m, 2H), 7.06-6.97 (m, 2H), 6.96-6.87 (m, 4H), 6.86 (d, $J_{(H,H)} = 2.0$ Hz, 1H), 6.72 (ddq, $J_{(H,H)} = 6.8, 3.2, 1.9, 1.5$ Hz, 4H), 6.63-6.55 (m, 1H), 5.26 (s, 2H), 1.16 (s, 9H), 1.15 (s, 9H), 0.33 (s, 3H), 0.32 (s, 3H), 0.31 (s, 3H), 0.31 (s, 3H).

¹³C-NMR (75 MHz, CDCl₃, 25 °C): δ (ppm) = 151.7 (C), 151.4 (C), 141.3 (C), 139.9 (C), 137.9 (2 x C), 129.8 (4 x CH), 129.1 (CH), 128.9 (2 x CH), 128.8 (CH), 128.7 (CH), 127.8 (CH), 127.2 (4 x CH), 126.9 (2 x CH), 126.7 (2 x CH), 121.8 (CH), 120.7 (C), 120.2 (CH), 119.9 (C), 116.2 (CH), 114.2 (CH), 108.3 (C), 108.2 (C), 89.4 (2 x C), 50.3 (2 x CH), 50.1 (C), 26.5 (6 x CH₃), 17.1 (2 x C), -4.4 (4 x CH₃).

((3*S,3'*S*'*)-(3-Fluoro-6-methoxy-9*H*-xanthene-9,9-diyl)bis(3-phenylprop-1-yne-3,1-diyl))bis(*tert*-butyldimethylsilane) (2.3j)**

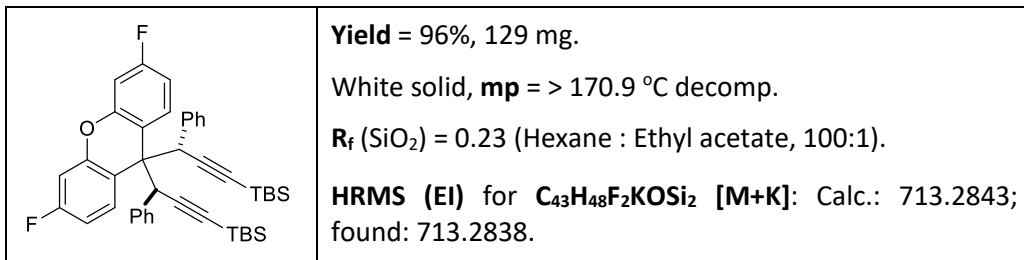
	<p>Yield = 99%, 136 mg.</p> <p>White solid, mp = 145.0-146.0 °C.</p> <p>R_f (SiO₂) = 0.21 (Hexane : Ethyl acetate, 40:1).</p> <p>HRMS (EI) for C₄₄H₅₁FN₁O₂Si₂ [M+Na]: Calc.: 709.3304; found: 709.3304.</p>
---	--

¹H-NMR (300 MHz, CDCl₃, 25 °C, TMS): δ (ppm) = 8.74 (dd, $J_{(H,H,F)}$ = 9.1, 6.3 Hz, 1H), 8.65 (d, $J_{(H,H,F)}$ = 9.0 Hz, 1H), 7.01 (t, $J_{(H,H,F)}$ = 7.2 Hz, 2H), 6.98-6.80 (m, 5H), 6.75 (dd, $J_{(H,H,F)}$ = 8.9, 2.8 Hz, 1H), 6.66 (dd, $J_{(H,H,F)}$ = 12.9, 7.4 Hz, 4H), 6.24 (dd, $J_{(H,H,F)}$ = 9.7, 2.8 Hz, 1H), 6.08 (d, $J_{(H,H,F)}$ = 2.8 Hz, 1H), 5.16 (s, 1H), 5.11 (s, 1H), 3.77 (s, 3H), 1.12 (s, 9H), 1.11 (s, 9H), 0.27 (s, 12H).

¹³C-NMR (75 MHz, CDCl₃, 25 °C): δ (ppm) = 162.4 (d, $J_{(C,F)}$ = 246.8 Hz, C), 159.9 (C), 152.3 (d, $J_{(C,F)}$ = 12.3 Hz, C), 152.0 (C), 137.8 (d, $J_{(C,F)}$ = 6.9 Hz, C), 130.0 (CH), 129.9 (CH), 129.8 (2 x CH), 129.7 (2 x CH), 129.5 (CH), 127.3 (4 x CH), 126.7 (2 x CH), 117.1 (d, $J_{(C,F)}$ = 3.6 Hz, C), 112.7 (C), 109.7 (CH), 109.1 (d, $J_{(C,F)}$ = 21.2 Hz, CH), 108.3 (C), 108.2 (C), 103.02 (d, $J_{(C,F)}$ = 24.5 Hz, CH), 99.93 (CH), 89.5 (C), 89.3 (C), 55.4 (CH₃), 50.6 (CH), 50.0 (C), 49.6 (CH), 26.5 (6 x CH₃), 17.1 (2 x C), -4.4 (4 x CH₃).

¹⁹F-NMR (282 MHz, CDCl₃, 25 °C): δ (ppm) = -113.1.

((3*S,3'*S*'*)-(3,6-Difluoro-9*H*-xanthene-9,9-diyl)bis(3-phenylprop-1-yne-3,1-diyl))bis(*tert*-butyldimethylsilane) (2.3k)**

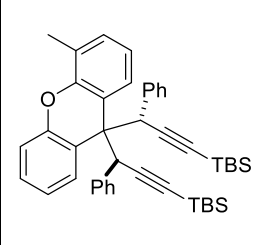


¹H-NMR (300 MHz, CDCl₃, 25 °C, TMS): δ (ppm) = 8.73 (dd, $J_{(H,H,F)} = 9.1, 6.3$ Hz, 2H), 7.06-6.96 (m, 2H), 6.95-6.81 (m, 6H), 6.69-6.55 (m, 4H), 6.25 (dd, $J_{(H,H,F)} = 9.5, 2.7$ Hz, 2H), 5.12 (s, 2H), 1.09 (s, 18H), 0.26 (s, 6H), 0.25 (s, 6H).

¹³C-NMR (75 MHz, CDCl₃, 25 °C): δ (ppm) = 162.5 (d, $J_{(C,F)} = 247.4$ Hz, 2 x C), 152.0 (d, $J_{(C,F)} = 12.0$ Hz, 2 x C), 137.5 (2 x C), 130.0 (d, $J_{(C,F)} = 9.1$ Hz, 2 x CH), 129.7 (4 x CH), 127.4 (4 x CH), 126.9 (2 x CH), 116.8 (d, $J_{(C,F)} = 3.3$ Hz, 2 x C), 109.6 (d, $J_{(C,F)} = 21.2$ Hz, 2 x CH), 107.8 (2 x C), 103.2 (d, $J_{(C,F)} = 24.6$ Hz, 2 x CH), 89.8 (2 x C), 50.4 (2 x CH), 49.7 (C), 26.4 (6 x CH₃), 17.1 (2 x C), -4.4 (4 x CH₃).

¹⁹F-NMR (282 MHz, CDCl₃, 25 °C): δ (ppm) = -112.6.

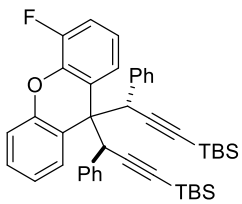
((3*S,3'*S*'*)-(4-Methyl-9*H*-xanthene-9,9-diyl)bis(3-phenylprop-1-yne-3,1-diyl))bis(*tert*-butyldimethylsilane) (2.3I)**

	<p>Yield = 99%, 130 mg.</p> <p>White solid; mp = 125.1-127.4 °C.</p> <p>R_f (SiO₂) = 0.20 (Hexane : Ethyl acetate, 100:1).</p> <p>HRMS (EI) for C₄₄H₅₃OSi₂ [M+H]: Calc.: 653.3635; found: 653.3631.</p>
---	--

¹H-NMR (300 MHz, CDCl₃, 25 °C, TMS): δ (ppm) = 8.73 (dd, $J_{(H,H)} = 7.4, 2.4$ Hz, 1H), 8.65-8.47 (m, 1H), 7.12 (ddt, $J_{(H,H)} = 10.5, 7.3, 3.7$ Hz, 2H), 7.04-6.94 (m, 4H), 6.87 (t, $J_{(H,H)} = 7.6$ Hz, 4H), 6.65 (d, $J_{(H,H)} = 7.6$ Hz, 4H), 6.56 (dd, $J_{(H,H)} = 7.3, 2.3$ Hz, 1H), 5.19 (s, 2H), 1.93 (s, 3H), 1.11 (s, 9H), 1.10 (s, 9H), 0.27 (s, 3H), 0.26 (s, 6H), 0.25 (s, 3H).

¹³C-NMR (75 MHz, CDCl₃, 25 °C): δ (ppm) = 151.3 (C), 149.7 (C), 138.0 (C), 137.9 (C), 129.8 (4 x CH), 129.7 (CH), 128.6 (2 x CH), 127.1 (4 x CH), 126.6 (2 x CH), 126.2 (CH), 125.0 (C), 121.5 (CH), 120.9 (CH), 120.6 (C), 119.9 (C), 116.2 (CH), 108.4 (2 x C), 89.1 (C), 89.0 (C), 50.2 (2 x CH), 50.1 (C), 26.5 (6 x CH₃), 17.1 (2 x C), 16.1 (CH₃), -4.4 (4 x CH₃).

((3*S,3'*S*'*)-(4-Fluoro-9*H*-xanthene-9,9-diyl)bis(3-phenylprop-1-yne-3,1-diyl))bis(*tert*-butyldimethylsilane) (2.3m)**

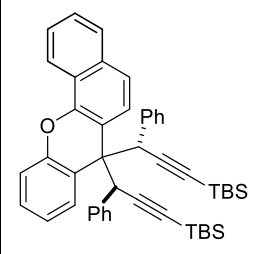
	<p>Yield = 97%, 128 mg.</p> <p>White solid, mp = >185.5 decomp.</p> <p>R_f (SiO₂) = 0.22 (Hexane : Ethyl acetate, 100:1).</p> <p>HRMS (EI) for C₄₃H₄₉FN₂OSi₂ [M+Na]: Calc.: 679.3198; found: 679.3192.</p>
---	--

¹H-NMR (300 MHz, CDCl₃, 25 °C, TMS): δ (ppm) = 8.85-8.72 (m, 1H), 8.57 (dd, $J_{(H,H,F)}$ = 10.9, 3.0 Hz, 1H), 7.17 (tt, $J_{(H,H,F)}$ = 7.2, 5.1 Hz, 2H), 7.06-6.97 (m, 2H), 6.95-6.83 (m, 5H), 6.75-6.68 (m, 2H), 6.68-6.61 (m, 2H), 6.57-6.47 (m, 2H), 5.23 (s, 1H), 5.13 (s, 1H), 1.13 (s, 9H), 1.12 (s, 9H), 0.33 (s, 3H), 0.29 (s, 3H), 0.29 (s, 3H), 0.28 (s, 3H).

¹³C-NMR (75 MHz, CDCl₃, 25 °C): δ (ppm) = 157.61 (d, $J_{(C,F)}$ = 238.8 Hz, C), 151.2 (2 x C), 147.5 (2 x C), 137.6 (d, $J_{(C,F)}$ = 5.6 Hz, C), 129.7 (3 x CH), 128.9 (CH), 128.6 (CH), 127.3 (2 x CH), 127.2 (2 x CH), 126.8 (CH), 126.7 (CH), 122.0 (d, $J_{(C,F)}$ = 7.4 Hz, C), 121.8 (CH), 119.6 (CH), 117.2 (d, $J_{(C,F)}$ = 7.9 Hz, CH), 116.1 (CH), 115.8 (d, $J_{(C,F)}$ = 23.4 Hz, CH), 114.6 (d, $J_{(C,F)}$ = 25.2 Hz, CH), 107.8 (C), 107.7 (C), 90.0 (C), 89.5 (C), 50.6 (CH), 50.2 (C), 49.9 (CH), 26.5 (6 x CH₃), 17.1 (2 x C), -4.4 (2 x CH₃), -4.5 (2 x CH₃).

¹⁹F-NMR (282 MHz, CDCl₃, 25 °C): δ (ppm) = -120.7.

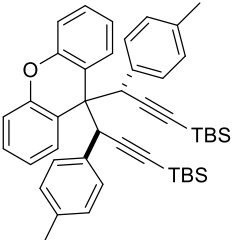
((3*S,3'*S*'*)-(7*H*-benzo[*c*]xanthene-7,7-diyl)bis(3-phenylprop-1-yne-3,1-diyl))bis(*tert*-butyldimethylsilane) (2.3n)**

	<p>Yield = 97%, 134 mg.</p> <p>Ywllowish solid, mp = >170.5 °C decomp.</p> <p>R_f (SiO₂) = 0.20 (Hexane : Ethyl acetate, 100:1).</p> <p>HRMS (EI) for C₄₇H₅₂NaOSi₂ [M+Na]: Calc.: 711.34544; found: 711.34547.</p>
---	---

¹H-NMR (300 MHz, CDCl₃, 25 °C, TMS): δ (ppm) = 8.90 (d, $J_{(H,H)} = 8.9$ Hz, 1H), 8.80 (dd, $J_{(H,H)} = 7.2, 2.4$ Hz, 1H), 7.92 (d, $J = 8.4$ Hz, 1H), 7.81 (d, $J = 8.1$ Hz, 1H), 7.61 (d, $J_{(H,H)} = 8.9$ Hz, 1H), 7.53-7.41 (m, 1H), 7.37 (t, $J_{(H,H)} = 7.3$ Hz, 1H), 7.27-7.08 (m, 2H), 6.89 (t, $J = 6.9$ Hz, 2H), 6.83-6.68 (m, 5H), 6.67 (d, $J_{(H,H)} = 7.4$ Hz, 2H), 6.60 (d, $J_{(H,H)} = 7.2$ Hz, 2H), 5.29 (s, 2H), 1.14 (s, 9H), 1.13 (s, 9H), 0.31 (s, 3H), 0.29 (s, 6H), 0.28 (s, 3H).

¹³C-NMR (75 MHz, CDCl₃, 25 °C): δ (ppm) = 151.1 (C), 146.7 (C), 138.0 (C), 137.9 (C), 133.4 (C), 129.7 (2 x CH), 129.6 (2 x CH), 128.7 (CH), 128.6 (CH), 127.2 (2 x CH), 127.1 (3 x CH), 126.6 (3 x CH), 125.8 (CH), 125.5 (CH), 123.5 (CH), 122.1 (CH), 122.0 (CH), 121.0 (C), 120.8 (CH), 116.3 (CH), 114.4 (C), 108.4 (C), 108.3 (C), 89.3 (C), 89.1 (C), 50.6 (C), 50.1 (CH), 49.9 (CH), 26.5 (6 x CH₃), 17.1 (2 x C), -4.4 (4 x CH₃).

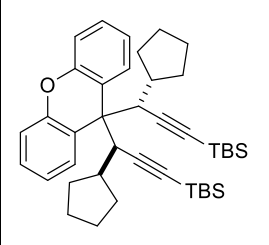
((3*S,3'*S*'*)-(9*H*-Xanthene-9,9-diyl)bis(3-(*p*-tolyl)prop-1-yne-3,1-diyl))bis(*tert*-butyldimethylsilane) (2.3q)**

	<p>Yield = 98%, 131 mg.</p> <p>White solid, mp = >172.3 decomp.</p> <p>R_f (SiO₂) = 0.22 (Hexane : Ethyl acetate, 100:1).</p> <p>HRMS (EI) for C₄₅H₅₄NaOSi₂ [M+Na]: Calc.: 689.3605; found: 689.3588.</p>
---	---

¹H-NMR (300 MHz, CDCl₃, 25 °C, TMS): δ (ppm) = 8.89-8.74 (m, 2H), 7.17 (hept, *J*_(H,H) = 5.1 Hz, 4H), 6.71 (d, *J*_(H,H) = 8.1 Hz, 4H), 6.57 (ddd, *J*_(H,H) = 8.3, 6.6, 2.1 Hz, 6H), 5.21 (s, 2H), 2.15 (s, 6H), 1.16 (d, *J*_(H,H) = 1.9 Hz, 18H), 0.32 (s, 6H), 0.30 (s, 6H).

¹³C-NMR (75 MHz, CDCl₃, 25 °C): δ (ppm) = 151.3 (2 x C), 136.1 (2 x C), 134.9 (2 x C), 129.6 (4 x CH), 128.8 (2 x CH), 128.6 (2 x CH), 128.0 (4 x CH), 121.6 (2 x CH), 121.0 (2 x C), 116.1 (2 x CH), 108.7 (2 x C), 88.9 (2 x C), 50.0 (2 x CH), 49.9 (C), 26.5 (6 x CH₃), 21.1 (2 x CH₃), 17.1 (2 x C), -4.4 (4 x CH₃).

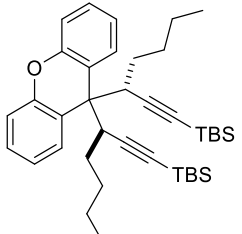
((3*S,3'*S*'*)-(9*H*-Xanthene-9,9-diyl)bis(3-cyclopentylprop-1-yne-3,1-diyl))bis(*tert*-butyldimethylsilane) (2.3r)**

	<p>Yield = 99%, 123 mg.</p> <p>Colorless oil.</p> <p>R_f (SiO₂) = 0.30 (Hexane : Ethyl acetate, 100:1).</p> <p>HRMS (EI) for C₄₁H₅₉OSi₂ [M+H]: Calc.: 623.4099; found: 623.4108.</p>
---	--

¹H-NMR (300 MHz, CDCl₃, 25 °C, TMS): δ (ppm) = 8.25 (dd, $J_{(H,H)}$ = 8.5, 1.6 Hz, 2H), 7.25-7.16 (m, 2H), 6.95 (ddd, $J_{(H,H)}$ = 7.0, 6.1, 1.5 Hz, 4H), 3.83 (s, 1H), 3.82 (s, 1H), 1.53 (d, $J_{(H,H)}$ = 9.9 Hz, 2H), 1.45-1.07 (m, 14H), 1.02 (s, 18H), 0.69 (dtd, $J_{(H,H)}$ = 11.6, 7.6, 3.8 Hz, 2H), 0.18 (s, 12H).

¹³C-NMR (75 MHz, CDCl₃, 25 °C): δ (ppm) = 151.4 (2 x C), 128.5 (2 x CH), 128.3 (2 x CH), 123.2 (2 x C), 122.1 (2 x CH), 116.1 (2 x CH), 108.6 (2 x C), 88.3 (2 x C), 50.2 (2 x CH), 45.4 (C), 40.2 (2 x CH), 33.2 (2 x CH₂), 28.0 (2 x CH₂), 26.4 (6 x CH₃), 25.8 (2 x CH₂), 24.7 (2 x CH₂), 17.0 (2 x C), -4.3 (2 x CH₃), -4.4 (2 x CH₃).

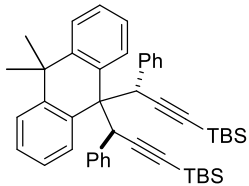
((3*S,3'*S*'*)-(9*H*-Xanthene-9,9-diyl)bis(hept-1-yne-3,1-diyl))bis(*tert*-butyldimethylsilane) (2.3s)**

	<p>Yield = 99%, 119 mg. Colorless oil. R_f (SiO₂) = 0.29 (Hexane : Ethyl acetate, 100:1). HRMS (EI) for C₃₉H₅₈NaOSi₂ [M+Na]: Calc.: 621.3918; found: 621.3911.</p>
---	--

¹H-NMR (300 MHz, CDCl₃, 25 °C, TMS): δ (ppm) = 8.42 (dd, $J_{(H,H)} = 8.1, 1.6$ Hz, 1H), 7.31 (dd, $J_{(H,H)} = 8.4, 1.6$ Hz, 1H), 7.21 (dddd, $J_{(H,H)} = 8.8, 7.3, 5.9, 1.6$ Hz, 2H), 7.08-6.89 (m, 4H), 3.39 (d, $J_{(H,H)} = 2.5$ Hz, 1H), 3.35 (d, $J_{(H,H)} = 2.6$ Hz, 1H), 1.67-1.47 (m, 4H), 1.40-1.14 (m, 8H), 0.83 (s, 18H), 0.82 (m, 6H), 0.02 (s, 6H), 0.00 (s, 6H).

¹³C-NMR (75 MHz, CDCl₃, 25 °C): δ (ppm) = 152.6 (C), 151.3 (C), 128.1 (CH), 127.9 (CH), 127.8 (CH), 127.1 (CH), 125.3 (C), 122.4 (CH), 121.9 (CH), 121.7 (C), 116.9 (CH), 116.1 (CH), 108.9 (2 x C), 86.3 (2 x C), 47.4 (C), 44.5 (2 x CH), 31.1 (2 x CH₂), 30.7 (2 x CH₂), 26.2 (6 x CH₃), 22.5 (2 x CH₂), 16.6 (2 x C), 14.2 (2 x CH₃), -4.5 (2 x CH₃), -4.6 (2 x CH₃).

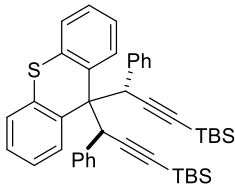
((3*S,3'*S*'*)-(10,10-Dimethyl-9,10-dihydroanthracene-9,9-diyl)bis(3-phenylprop-1-yne-3,1-diyl))bis(*tert*-butyldimethylsilane) (2.13)**

	<p>Yield = 99%, 132 mg.</p> <p>White solid, mp = 101.8-103.5 °C.</p> <p>R_f (SiO₂) = 0.21 (Hexane : Ethyl acetate, 100:1).</p> <p>HRMS (EI) for C₄₆H₅₇Si₂ [M+H]: Calc.: 665.3999; found: 665.3994.</p>
---	--

¹H-NMR (300 MHz, CDCl₃, 25 °C, TMS): δ (ppm) = 9.05 (d, $J_{(H,H)}$ = 8.3 Hz, 2H), 7.27 (dt, $J_{(H,H)}$ = 28.1, 7.1 Hz, 4H), 7.03 (d, $J_{(H,H)}$ = 7.2 Hz, 2H), 6.84 (d, $J_{(H,H)}$ = 7.4 Hz, 2H), 6.75 (t, $J_{(H,H)}$ = 7.5 Hz, 4H), 6.44 (d, $J_{(H,H)}$ = 7.5 Hz, 4H), 5.27 (s, 2H), 1.13 (s, 18H), 0.57 (s, 6H), 0.28 (s, 12H).

¹³C-NMR (75 MHz, CDCl₃, 25 °C): δ (ppm) = 145.1 (2 x C), 138.3 (2 x C), 133.8 (2 x C), 129.8 (5 x CH), 128.1 (2 x CH), 127.1 (2 x CH), 126.8 (5 x CH), 126.2 (2 x CH), 124.6 (2 x CH), 109.3 (2 x C), 88.8 (2 x C), 52.9 (C), 50.9 (2 x CH), 36.0 (C), 33.9 (2 x CH₃), 26.5 (6 x CH₃), 17.2 (2 x C), -4.3 (4 x CH₃).

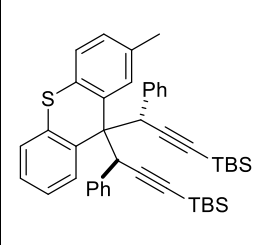
((3*S,3'*S*'*)-(9*H*-Thioxanthene-9,9-diyl)bis(3-phenylprop-1-yne-3,1-diyl))bis(*tert*-butyldimethylsilane) (2.17a)**

	<p>Yield = 99%, 130 mg.</p> <p>White solid, mp = 140.3-141.8 °C.</p> <p>R_f (SiO₂) = 0.20 (Hexane : Ethyl acetate, 100:1).</p> <p>HRMS (EI) for C₄₃H₅₀NaSSi₂ [M+Na]: Calc.: 677.3064; found: 677.3050.</p>
---	---

¹H-NMR (300 MHz, CDCl₃, 25 °C, TMS): δ (ppm) = 8.95 (dd, $J_{(H,H)} = 8.3, 1.5$ Hz, 2H), 7.18 (ddd, $J_{(H,H)} = 8.4, 7.1, 1.6$ Hz, 2H), 7.12-6.98 (m, 4H), 6.89 (dd, $J_{(H,H)} = 8.3, 6.8$ Hz, 4H), 6.70 (dd, $J_{(H,H)} = 7.8, 1.6$ Hz, 2H), 6.63 (dt, $J_{(H,H)} = 7.1, 1.3$ Hz, 4H), 5.30 (s, 2H), 1.10 (s, 18H), 0.26 (s, 6H), 0.26 (s, 6H).

¹³C-NMR (75 MHz, CDCl₃, 25 °C): δ (ppm) = 137.9 (2 x C), 132.2 (2 x C), 131.9 (2 x C), 130.3 (2 x CH), 129.8 (4 x CH), 127.3 (6 x CH), 126.6 (2 x CH), 124.6 (2 x CH), 124.5 (2 x CH), 108.8 (2 x C), 89.9 (2 x C), 54.9 (C), 51.2 (2 x CH), 26.5 (6 x CH₃), 17.1 (2 x C), -4.4 (4 x CH₃).

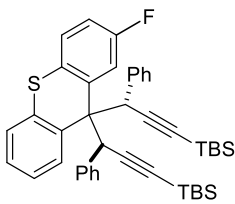
((3*S,3'*S*'*)-(2-Methyl-9*H*-thioxanthene-9,9-diyl)bis(3-phenylprop-1-yne-3,1-diyl))bis(*tert*-butyldimethylsilane) (2.17b)**

	<p>Yield = 98%, 131 mg.</p> <p>White solid, mp = 119.6-121.4 °C.</p> <p>R_f (SiO₂) = 0.21 (Hexane : Ethyl acetate, 100:1).</p> <p>HRMS (EI) for C₄₄H₅₂NaSSi₂ [M+Na]: Calc.: 691.3220; found: 691.3215.</p>
---	---

¹H-NMR (300 MHz, CDCl₃, 25 °C, TMS): δ (ppm) = 8.94 (d, $J_{(H,H)} = 8.2$ Hz, 1H), 8.79 (s, 1H), 7.24-7.15 (m, 1H), 7.10 (t, $J_{(H,H)} = 7.8$ Hz, 1H), 7.02 (t, $J_{(H,H)} = 6.9$ Hz, 2H), 6.91 (td, $J_{(H,H)} = 7.6, 3.5$ Hz, 5H), 6.72 (td, $J_{(H,H)} = 5.4, 2.6$ Hz, 3H), 6.60 (dd, $J_{(H,H)} = 7.9, 4.4$ Hz, 3H), 5.39 (s, 1H), 5.27 (s, 1H), 2.46 (s, 3H), 1.10 (s, 18H), 0.31 (s, 3H), 0.28 (s, 6H), 0.26 (s, 3H).

¹³C-NMR (75 MHz, CDCl₃, 25 °C): δ (ppm) = 138.0 (C), 137.9 (C), 134.0 (C), 132.6 (C), 131.7 (C), 131.6 (C), 130.4 (CH), 130.3 (CH), 129.9 (2 x CH), 129.7 (2 x CH), 128.4 (C), 128.2 (CH), 127.2 (2 x CH), 127.1 (3 x CH), 126.6 (CH), 126.5 (CH), 124.6 (CH), 124.5 (CH), 124.3 (CH), 108.8 (C), 108.6 (C), 89.8 (C), 89.5 (C), 54.7 (C), 51.6 (CH), 50.6 (CH), 26.6 (3 x CH₃), 26.5 (3 x CH₃), 21.7 (CH₃), 17.2 (C), 17.1 (C), -4.1 (CH₃), -4.2 (CH₃), -4.3 (CH₃), -4.4 (CH₃).

((3*S,3'*S*'*)-(2-Fluoro-9*H*-thioxanthene-9,9-diyl)bis(3-phenylprop-1-yne-3,1-diyl))bis(*tert*-butyldimethylsilane) (2.17c)**

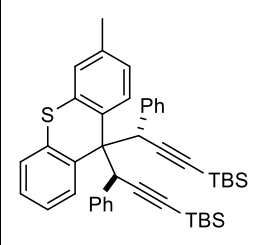
	<p>Yield = 94%, 127 mg.</p> <p>White solid; mp = >158.0 °C decomp.</p> <p>R_f (SiO₂) = 0.20 (Hexane : Ethyl acetate, 100:1).</p> <p>HRMS (EI) for C₄₃H₅₀FSSi₂ [M+H]: Calc.: 673.3150; found: 673.3148.</p>
---	---

¹H-NMR (300 MHz, CDCl₃, 25 °C, TMS): δ (ppm) = 9.00-8.86 (m, 2H), 7.24-7.16 (m, 2H), 7.10 (m, 1H), 7.07-6.99 (m, 2H), 6.97-6.87 (m, 4H), 6.69 (dd, $J_{(H,H,F)}$ = 7.8, 1.6 Hz, 1H), 6.62 (m, 4H), 6.42 (dd, $J_{(H,H,F)}$ = 8.9, 2.8 Hz, 1H), 5.31 (s, 1H), 5.20 (s, 1H), 1.09 (s, 9H), 1.09 (s, 9H), 0.26 (s, 3H), 0.25 (s, 6H), 0.25 (s, 3H).

¹³C-NMR (75 MHz, CDCl₃, 25 °C): δ (ppm) = 161.2 (d, $J_{(C,F)}$ = 248.7 Hz, C), 137.6 (C), 137.5 (C), 134.4 (d, $J_{(C,F)}$ = 8.1 Hz, C), 131.9 (d, $J_{(C,F)}$ = 8.1 Hz, CH), 131.6 (C), 131.3 (C), 130.3 (CH), 129.8 (2 x CH), 129.7 (2 x CH), 127.8 (d, $J_{(C,F)}$ = 3.3 Hz, C), 127.5 (CH), 127.4 (2 x CH), 127.3 (2 x CH), 126.7 (CH), 126.6 (CH), 124.8 (CH), 124.6 (CH), 111.8 (d, $J_{(C,F)}$ = 20.6 Hz, CH), 110.7 (d, $J_{(C,F)}$ = 23.4 Hz, CH), 108.5 (C), 108.4 (C), 90.2 (C), 90.0 (C), 54.5 (C), 51.6 (CH), 51.0 (CH), 26.5 (6 x CH₃), 17.1 (2 x C), -4.4 (4 x CH₃).

¹⁹F-NMR (282 MHz, CDCl₃, 25 °C): δ (ppm) = -115.2.

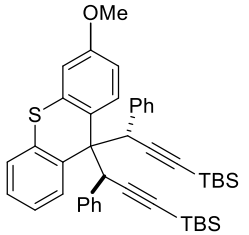
((3*S,3'*S*'*)-(3-Methyl-9*H*-thioxanthene-9,9-diyl)bis(3-phenylprop-1-yne-3,1-diyl))bis(*tert*-butyldimethylsilane) (2.17d)**

	<p>Yield = 95%, 127 mg.</p> <p>White solid, mp = 115.2-117.4 °C.</p> <p>R_f (SiO₂) = 0.17 (Hexane : Ethyl acetate, 100:1).</p> <p>HRMS (EI) for C₄₄H₅₂NaSSi₂ [M+Na]: Calc.: 691.3220; found: 691.3216.</p>
---	--

¹H-NMR (300 MHz, CDCl₃, 25 °C, TMS): δ (ppm) = 8.88 (d, *J*_(H,H) = 7.6 Hz, 1H), 8.79 (d, *J*_(H,H) = 8.5 Hz, 1H), 7.24-7.13 (m, 1H), 7.08 (td, *J*_(H,H) = 7.5, 2.0 Hz, 2H), 7.05-6.94 (m, 3H), 6.88 (td, *J*_(H,H) = 7.7, 2.1 Hz, 4H), 6.77 (dd, *J*_(H,H) = 7.7, 1.8 Hz, 1H), 6.63 (dd, *J*_(H,H) = 10.7, 7.5 Hz, 4H), 5.31 (s, 1H), 5.27 (s, 1H), 1.98 (s, 3H), 1.08 (s, 18H), 0.24 (s, 6H), 0.23 (s, 6H).

¹³C-NMR (75 MHz, CDCl₃, 25 °C): δ (ppm) = 137.9 (C), 137.8 (C), 132.1 (C), 132.0 (2 x C), 131.7 (C), 131.6 (C), 130.1 (CH), 129.9 (5 x CH), 128.5 (CH), 127.6 (CH), 127.2 (2 x CH), 127.1 (2 x CH), 126.6 (2 x CH), 125.0 (CH), 124.6 (CH), 123.6 (CH), 108.8 (2 x C), 89.7 (2 x C), 55.1 (C), 51.6 (CH), 51.1 (CH), 26.5 (6 x CH₃), 20.1 (CH₃), 17.1 (2 x C), -4.4 (4 x CH₃).

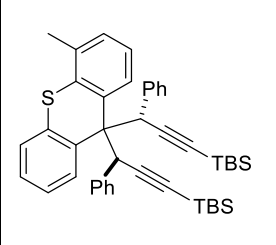
((3*S,3'*S*'*)-(3-Methoxy-9*H*-thioxanthene-9,9-diyl)bis(3-phenylprop-1-yne-3,1-diyl))bis(*tert*-butyldimethylsilane) (2.17e)**

	<p>Yield = 97%, 133 mg.</p> <p>White solid; mp = >132.3 decomp.</p> <p>R_f (SiO₂) = 0.22 (Hexane : Ethyl acetate, 40:1).</p> <p>HRMS (EI) for C₄₄H₅₂NaOSSi₂ [M+Na]: Calc.: 707.3170; found: 707.3175.</p>
---	--

¹H-NMR (300 MHz, CDCl₃, 25 °C, TMS): δ (ppm) = 8.94 (dd, $J_{(H,H)} = 8.4, 1.4$ Hz, 1H), 8.84 (d, $J_{(H,H)} = 9.2$ Hz, 1H), 7.16 (ddd, $J_{(H,H)} = 8.4, 7.1, 1.6$ Hz, 1H), 7.10-6.97 (m, 3H), 6.90 (ddd, $J_{(H,H)} = 8.0, 6.5, 1.3$ Hz, 4H), 6.75 (dd, $J_{(H,H)} = 9.1, 2.9$ Hz, 1H), 6.64 (m, 5H), 6.21 (d, $J_{(H,H)} = 2.8$ Hz, 1H), 5.26 (s, 1H), 5.25 (s, 1H), 3.76 (s, 3H), 1.09 (s, 9H), 1.08 (s, 9H), 0.25 (s, 3H), 0.24 (s, 6H), 0.24 (s, 3H).

¹³C-NMR (75 MHz, CDCl₃, 25 °C): δ (ppm) = 158.1 (C), 138.0 (C), 137.9 (C), 133.4 (C), 132.1 (C), 132.0 (C), 131.5 (CH), 130.2 (CH), 129.9 (2 x CH), 129.8 (2 x CH), 127.3 (5 x CH), 127.2 (CH), 126.6 (CH), 124.6 (CH), 124.5 (CH), 124.1 (C), 111.9 (CH), 108.9 (C), 108.8 (C), 107.9 (CH), 89.7 (2 x C), 55.3 (CH₃), 54.5 (C), 51.3 (CH), 51.1 (CH), 26.5 (6 x CH₃), 17.1 (2 x C), -4.4 (4 x CH₃).

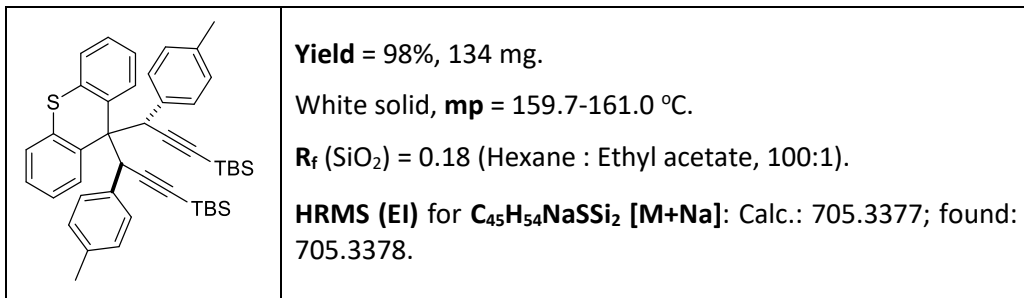
((3*S,3'*S*'*)-(4-Methyl-9*H*-thioxanthene-9,9-diyl)bis(3-phenylprop-1-yne-3,1-diyl))bis(*tert*-butyldimethylsilane) (2.17f)**

	<p>Yield = 97%, 130 mg.</p> <p>White solid; mp = 112.4-113.9 °C.</p> <p>R_f (SiO₂) = 0.19 (Hexane : Ethyl acetate, 100:1).</p> <p>HRMS (EI) for C₄₄H₅₂NaSSi₂ [M+Na]: Calc.: 691.3220; found: 691.3214.</p>
---	---

¹H-NMR (300 MHz, CDCl₃, 25 °C, TMS): δ (ppm) = 8.90 (d, $J_{(H,H)} = 8.3$ Hz, 1H), 8.80 (d, $J_{(H,H)} = 8.1$ Hz, 1H), 7.24-7.12 (m, 1H), 7.15-7.04 (m, 2H), 7.05-6.94 (m, 3H), 6.89 (td, $J_{(H,H)} = 7.7, 2.0$ Hz, 4H), 6.78 (dd, $J_{(H,H)} = 7.8, 1.7$ Hz, 1H), 6.64 (dd, $J_{(H,H)} = 10.1, 7.9$ Hz, 4H), 5.33 (s, 1H), 5.29 (s, 1H), 1.99 (s, 3H), 1.10 (s, 18H), 0.26 (s, 12H).

¹³C-NMR (75 MHz, CDCl₃, 25 °C): δ (ppm) = 138.0 (C), 137.9 (C), 132.1 (C), 132.0 (C), 131.8 (C), 131.7 (C), 130.1 (CH), 129.9 (4 x CH), 128.5 (CH), 127.7 (CH), 127.2 (3 x CH), 127.1 (3 x CH), 126.6 (CH), 126.5 (CH), 125.0 (CH), 124.6 (CH), 123.6 (CH), 108.8 (2 x C), 89.9 (C), 89.8 (C), 55.2 (C), 51.6 (CH), 51.2 (CH), 26.5 (3 x CH₃), 26.4 (3 x CH₃), 20.0 (CH₃), 17.1 (2 x C), -4.4 (4 x CH₃).

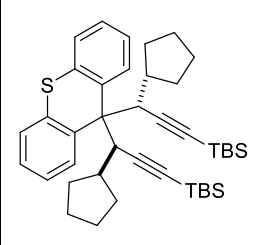
((3*S,3'*S*'*)-(9*H*-Thioxanthene-9,9-diyl)bis(3-(*p*-tolyl)prop-1-yne-3,1-diyl))bis(*tert*-butyldimethylsilane) (2.17g)**



¹H-NMR (300 MHz, CDCl₃, 25 °C, TMS): δ (ppm) = 8.94 (dd, *J*_(H,H) = 8.3, 1.5 Hz, 2H), 7.17 (ddd, *J*_(H,H) = 8.3, 7.1, 1.6 Hz, 2H), 7.08 (td, *J*_(H,H) = 7.5, 1.4 Hz, 2H), 6.77-6.65 (m, 6H), 6.57-6.46 (m, 4H), 5.26 (s, 2H), 2.16 (s, 6H), 1.09 (s, 18H), 0.25 (s, 6H), 0.25 (s, 6H).

¹³C-NMR (75 MHz, CDCl₃, 25 °C): δ (ppm) = 136.1 (2 x C), 134.8 (2 x C), 132.2 (2 x C), 132.0 (2 x C), 130.2 (2 x CH), 129.6 (4 x CH), 128.0 (4 x CH), 127.1 (2 x CH), 124.6 (2 x CH), 124.4 (2 x C), 109.1(2 x C), 89.4 (2 x C), 54.7 (C), 50.8 (2 x C), 26.5 (6 x CH₃), 21.1 (2 x CH₃), 17.1 (2 x C), -4.4 (4 x CH₃).

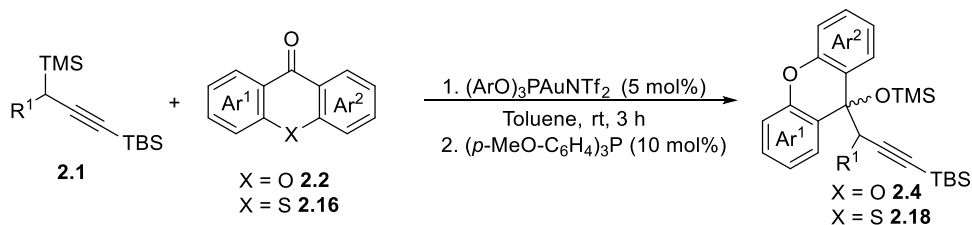
((3*S,3'*S*'*)-(9*H*-Thioxanthene-9,9-diyl)bis(3-cyclopentylprop-1-yne-3,1-diyl))bis(*tert*-butyldimethylsilane) (2.17h)**

	<p>Yield = 80%, 102 mg.</p> <p>White solid; mp = 111.4-113.2 °C.</p> <p>R_f (SiO₂) = 0.32 (Hexane : Ethyl acetate, 100:1).</p> <p>HRMS (EI) for C₄₁H₅₉SSi₂ [M+H]: Calc.: 639.3871; found: 639.3850.</p>
---	--

¹H-NMR (300 MHz, CDCl₃, 25 °C, TMS): δ (ppm) = 8.55 (dd, $J_{(H,H)} = 7.7, 2.6$ Hz, 2H), 7.13 (ddd, $J_{(H,H)} = 8.0, 6.7, 1.4$ Hz, 2H), 7.07-6.99 (m, 4H), 3.85 (s, 1H), 3.84 (s, 1H), 1.65 (m, 2H), 1.45-1.08 (m, 12H), 1.02 (s, 18H), 0.99-0.79 (m, 4H), 0.19 (s, 6H), 0.18 (s, 6H).

¹³C-NMR (75 MHz, CDCl₃, 25 °C): δ (ppm) = 134.1 (2 x C), 130.6 (2 x C), 130.0 (2 x CH), 127.0 (2 x CH), 124.8 (4 x CH), 109.3 (2 x C), 88.5 (2 x C), 51.8 (2 x CH), 50.9 (C), 40.8 (2 x CH), 33.1 (2 x CH₂), 28.7 (2 x CH₂), 26.4 (6 x CH₃), 25.7 (2 x CH₂), 24.9 (2 x CH₂), 17.0 (2 x C), -4.2 (2 x CH₃), -4.3 (2 x CH₃).

2.3.2 General protocol for the selective monopropargylation reaction of xanthone derivatives

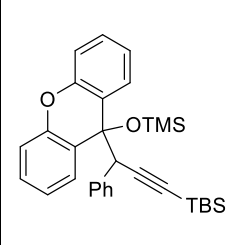


Scheme 5.12: Gold(I)-catalyzed selective monopropargylation of xanthone derivatives.

To a solution of 0.20 mmol of the corresponding xanthone **2.2**, or thioxanthone **2.16**, in 1 mL of dry toluene at 25 °C under argon atmosphere, were sequentially added 0.24 mmol of the propargylsilane **2.1** (1.2 equiv.) and 11.2 mg of the gold catalyst (5 mol%). The reaction mixture was stirred for 3 h at that temperature. Finally, 8.2 mg (0.02 mmol, 10 mol%) of (*p*-MeO-C₆H₄)₃P were added for catalyst deactivation, and the solvent was removed under vacuum. Flash column chromatography through deactivated aluminium oxide of the residue afforded the corresponding 9-propargylxanthidrols **2.4a,c,e,q**, 9-propargylthioxanthidrol **2.18a**. No relevant differences were observed for a reaction performed at 3 mmol scale, obtaining compound **2.4a** in 98% yield.

For compounds **2.4o-p**, **2.10**, **2.15** and **2.18i-j** the reaction was performed following the bispropargylation reaction conditions previously described.

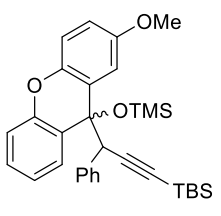
Tert-butyldimethyl(3-phenyl-3-(9-((trimethylsilyl)oxy)-9H-xanthen-9-yl)prop-1-yn-1-yl)silane (2.4a)

	<p>Yield = 98%, 98 mg.</p> <p>White solid, mp = 70.5-72.1 °C.</p> <p>R_f (SiO₂) = 0.06 (Hexane : Ethyl acetate, 200:1).</p> <p>HRMS (EI) for C₃₁H₃₈NaO₂Si₂ [M+Na]: Calc.: 521.2303; found: 521.2288.</p>
---	--

¹H-NMR (300 MHz, CDCl₃, 25 °C, TMS): δ (ppm) = 8.00 (dd, $J_{(H,H)} = 7.8, 1.7$ Hz, 1H), 7.36-7.19 (m, 2H), 7.19-7.12 (m, 2H), 7.10-6.84 (m, 6H), 6.76-6.66 (m, 2H), 4.24 (s, 1H), 0.89 (s, 9H), 0.08 (s, 3H), 0.05 (s, 3H), -0.18 (s, 9H).

¹³C-NMR (75 MHz, CDCl₃, 25 °C): δ (ppm) = 150.6 (C), 150.4 (C), 136.3 (C), 130.3 (2 x CH), 129.1 (2 x CH), 128.5 (2 x CH), 127.1 (CH), 127.0 (2 x CH), 124.9 (C), 124.2 (C), 122.3 (CH), 122.0 (CH), 115.7 (CH), 115.5 (CH), 105.9 (C), 87.6 (C), 74.1 (C), 56.9 (CH), 26.3 (3 x CH₃), 16.7 (C), 1.8 (3 x CH₃), -4.6 (CH₃), -4.7 (CH₃).

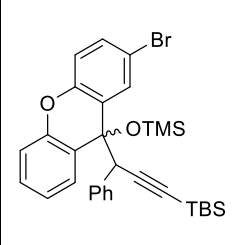
Tert-butyl(3-(2-methoxy-9-((trimethylsilyl)oxy)-9H-xanthen-9-yl)-3-phenylprop-1-yn-1-yl)dimethylsilane (2.4c)

	<p>Yield = 95%, 100 mg. (Mixture of diastereoisomers; <i>dr</i> = 1.1:1)</p> <p>Colorless oil.</p> <p>R_f (SiO₂) = 0.05 (Hexane : Ethyl acetate, 100:1).</p> <p>HRMS (EI) for C₃₂H₄₀NaO₂Si₂ [M+Na]: Calc.: 551.2408; found: 551.2409.</p>
---	--

¹H-NMR (300 MHz, CDCl₃, 25 °C, TMS): δ (ppm) = 8.14 (dd, $J_{(H,H)} = 7.8, 1.7$ Hz, 1H), 7.69 (dd, $J_{(H,H)} = 8.1, 1.5$ Hz, 1H), 7.46-6.84 (m, 20H), 6.82-6.67 (m, 2H), 4.36 (s, 1H), 4.35 (s, 1H), 3.97 (s, 3H), 3.93 (s, 3H), 1.02 (s, 9H), 0.99 (s, 9H), 0.22 (s, 3H), 0.18 (s, 6H), 0.15 (s, 3H), -0.05 (s, 9H), -0.07 (s, 9H).

¹³C-NMR (75 MHz, CDCl₃, 25 °C): δ (ppm) 150.3 (C), 150.2 (C), 147.1 (C), 147.0 (C), 140.7 (C), 140.5 (C), 136.3 (C), 136.3 (C), 130.3 (2 x CH), 130.0 (2 x CH), 129.1 (CH), 129.0 (CH), 128.6 (CH), 128.5 (CH), 127.2 (CH), 127.1 (CH), 127.0 (4 x CH), 125.8 (C), 125.3 (C), 124.3 (C), 123.8 (C), 122.3 (CH), 122.0 (CH), 121.6 (CH), 121.5 (CH), 120.2 (CH), 120.0 (CH), 116.0 (CH), 115.8 (CH), 111.1 (CH), 111.0 (CH), 106.3 (C), 105.9 (C), 87.6 (C), 87.5 (C), 74.2 (C), 74.1 (C), 56.8 (2 x CH), 56.2 (CH₃), 56.1 (CH₃), 26.3 (3 x CH₃), 26.2 (3 x CH₃), 16.7 (C), 16.6 (C), 1.9 (3 x CH₃), 1.8 (3 x CH₃), -4.5 (2 x CH₃), -4.6 (2 x CH₃).

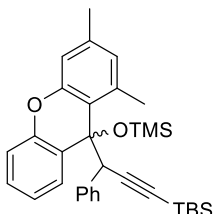
(3-(2-Bromo-9-((trimethylsilyl)oxy)-9H-xanthen-9-yl)-3-phenylprop-1-yn-1-yl)(tert-butyl)dimethylsilane (2.4e)

	<p>Yield = 99%, 115 mg. (Mixture of diastereoisomers, <i>dr</i> = 1.8:1)</p> <p>Colorless oil.</p> <p>R_f (SiO₂) = 0.04 (Hexane : Ethyl acetate, 200:1).</p> <p>HRMS (EI) for C₃₁H₃₇BrNaO₂Si₂ [M+Na]: Calc.: 599.1408; found: 599.1410.</p>
---	---

¹H-NMR (300 MHz, CDCl₃, 25 °C, TMS): δ (ppm) = 8.16 (d, $J_{(H,H)} = 2.5$ Hz, 1H), 7.93 (dd, $J_{(H,H)} = 7.8, 1.7$ Hz, 1H), 7.44 (dd, $J_{(H,H)} = 8.7, 2.5$ Hz, 1H), 7.40-6.81 (m, 20H), 6.79-6.71 (m, 2H), 4.27 (s, 1H), 4.25 (s, 1H), 0.95 (s, 9H), 0.90 (s, 9H), 0.16 (s, 3H), 0.15 (s, 3H), 0.09 (s, 3H), 0.06 (s, 3H), -0.11 (s, 9H), -0.13 (s, 9H).

¹³C-NMR (75 MHz, CDCl₃, 25 °C): δ (ppm) = 150.3 (C), 150.2 (C), 149.7 (C), 149.6 (C), 136.0 (C), 135.8 (C), 132.1 (CH), 131.9 (CH), 131.7 (CH), 131.2 (CH), 130.5 (2 x CH), 130.4 (CH), 130.3 (2 x CH), 129.3 (2 x CH), 128.4 (CH), 128.1 (CH), 127.5 (CH), 127.3 (CH), 127.2 (2 x CH), 127.1 (CH), 127.0 (C), 126.0 (C), 124.9 (C), 123.9 (C), 122.8 (CH), 122.4 (CH), 117.5 (2 x CH), 115.7 (2 x CH), 114.7 (C), 114.0 (C), 105.3 (C), 105.1 (C), 88.2 (C), 88.1 (C), 74.0 (C), 73.9 (C), 56.9 (CH), 56.8 (CH), 26.4 (3 x CH₃), 26.3 (3 x CH₃), 16.7 (C), 16.6 (C), 1.8 (3 x CH₃), 1.7 (3 x CH₃), -4.4 (CH₃), -4.5 (2 x CH₃), -4.6 (CH₃).

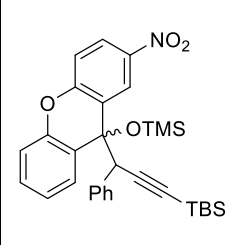
Tert-butyl(3-(1,3-dimethyl-9-((trimethylsilyl)oxy)-9H-xanthen-9-yl)-3-phenylprop-1-yn-1-yl)dimethylsilane (2.4o)

	<p>Yield = 96%, 101 mg. (Mixture of diastereoisomers, <i>dr</i> = 3.0:1) White solid. R_f (SiO₂) = 0.07 (Hexane : Ethyl acetate, 200:1). HRMS (EI) for C₃₃H₄₂NaO₂Si₂ [M+Na]: Calc.: 549.2616; found: 549.2605.</p>
---	---

¹H-NMR (300 MHz, CDCl₃, 25 °C, TMS): δ (ppm) = 8.4 (dd, $J_{(H,H)} = 7.9, 1.7$ Hz, 1H), 7.4 (dd, $J_{(H,H)} = 7.6, 2.1$ Hz, 2H), 7.4-7.2 (m, 4H), 7.1 (td, $J_{(H,H)} = 7.6, 7.2, 1.3$ Hz, 1H), 7.0-6.9 (m, 2H), 6.9-6.8 (m, 6H), 6.7 (dd, $J_{(H,H)} = 8.2, 1.2$ Hz, 1H), 6.6 (td, $J_{(H,H)} = 7.6, 7.1, 1.3$ Hz, 1H), 6.5-6.4 (m, 1H), 6.4-6.2 (m, 2H), 6.1 (dd, $J_{(H,H)} = 8.0, 1.6$ Hz, 1H), 4.8 (s, 1H), 4.7 (s, 1H), 2.9 (s, 3H), 2.9 (s, 3H), 2.4 (s, 3H), 2.3 (s, 3H), 1.1 (s, 9H), 0.7 (s, 9H), 0.2 (s, 3H), 0.2 (s, 3H), -0.1 (s, 3H), -0.1 (s, 3H), -0.1 (s, 9H), -0.3 (s, 9H).

¹³C-NMR (75 MHz, CDCl₃, 25 °C): δ (ppm) = 151.1 (C), 150.9 (C), 150.1 (C), 149.5 (C), 138.7 (C), 138.4 (C), 137.6 (C), 137.1 (C), 137.0 (C), 136.5 (C), 131.6 (CH), 130.5 (CH), 130.2 (CH), 129.3 (3 x CH), 129.2 (CH), 128.8 (CH), 128.4 (CH), 128.3 (CH), 127.3 (CH), 127.0 (4 x CH), 126.8 (CH), 123.4 (C), 122.7 (C), 121.7 (C), 121.0 (CH), 120.2 (C), 120.0 (CH), 115.1 (CH), 114.9 (CH), 114.7 (CH), 114.4 (CH), 107.6 (C), 104.5 (C), 88.1 (C), 87.4 (C), 75.0 (C), 74.5 (C), 52.5 (CH), 51.7 (CH), 26.4 (3 x CH₃), 26.1 (3 x CH₃), 21.8 (CH₃), 21.5 (CH₃), 21.0 (2 x CH₃), 17.0 (C), 16.4 (C), 1.8 (3 x CH₃), 1.5 (3 x CH₃), -4.3 (CH₃), -4.4 (CH₃), -4.8 (2 x CH₃).

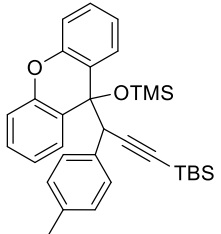
Tert-butyldimethyl(3-(2-nitro-9-((trimethylsilyl)oxy)-9H-xanthen-9-yl)-3-phenylprop-1-yn-1-yl)silane (2.4p)

	<p>Yield = 97%, 106 mg. (Mixture of diastereoisomers; <i>dr</i> = 2.1:1) Colorless oil. R_f (SiO₂) = 0.04 (Hexane : Ethyl acetate, 100:1). HRMS (EI) for C₃₁H₃₇NNaO₄Si₂ [M+Na]: Calc.: 566.2153; found: 566.2156.</p>
---	---

¹H-NMR (300 MHz, CDCl₃, 25 °C, TMS): δ (ppm) = 8.91 (d, $J_{(H,H)}$ = 2.7 Hz, 1H), 8.22 (dd, $J_{(H,H)}$ = 9.0, 2.7 Hz, 1H), 8.15 (dd, $J_{(H,H)}$ = 9.0, 2.8 Hz, 1H), 7.88 (dd, $J_{(H,H)}$ = 7.8, 1.7 Hz, 1H), 7.61 (d, $J_{(H,H)}$ = 2.7 Hz, 1H), 7.38 (ddd, $J_{(H,H)}$ = 8.1, 7.3, 1.7 Hz, 2H), 7.37-7.19 (m, 4H), 7.23-7.11 (m, 4H), 7.13-7.00 (m, 5H), 6.95 (ddd, J = 8.6, 4.1, 1.4 Hz, 3H), 6.75 (d, $J_{(H,H)}$ = 7.0 Hz, 1H), 4.26 (s, 1H), 4.25 (s, 1H), 0.86 (s, 9H), 0.83 (s, 9H), 0.09 (s, 6H), 0.02 (s, 3H), -0.01 (s, 3H), -0.13 (s, 9H), -0.17 (s, 9H).

¹³C-NMR (75 MHz, CDCl₃, 25 °C): δ (ppm) = 155.1 (C), 155.0 (C), 149.7 (2 x C), 143.0 (C), 142.1 (C), 135.5 (C), 135.1 (C), 130.5 (2 x CH), 130.3 (CH), 129.7 (2 x CH), 129.7 (CH), 128.5 (CH), 128.0 (CH), 127.9 (CH), 127.6 (CH), 127.5 (2 x CH), 127.3 (2 x CH), 126.4 (C), 125.8 (CH), 125.1 (C), 125.0 (CH), 124.8 (CH), 124.7 (CH), 124.6 (2 x C), 124.0 (CH), 123.4 (CH), 116.7 (2 x CH), 116.0 (CH), 116.0 (CH), 104.3 (2 x C), 89.1 (C), 88.6 (C), 74.0 (2 x C), 57.1 (CH), 56.9 (CH), 26.2 (6 x CH₃), 16.6 (C), 16.6 (C), 1.8 (3 x CH₃), 1.8 (3 x CH₃), -4.6 (CH₃), -4.7 (3 x CH₃).

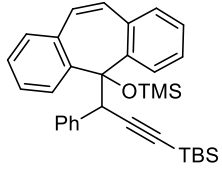
Tert-butyl dimethyl(3-(*p*-tolyl)-3-(9-((trimethylsilyl)oxy)-9H-xanthen-9-yl)prop-1-yn-1-yl)silane (2.4q)

	<p>Yield = 98%, 100 mg.</p> <p>Colorless oil.</p> <p>R_f (SiO₂) = 0.06 (Hexane : Ethyl acetate, 200:1).</p> <p>HRMS (EI) for C₃₂H₄₀O₂NaSi₂ [M+Na]: Calc.: 535.2465; found: 535.2462.</p>
---	---

¹H-NMR (300 MHz, CDCl₃, 25 °C, TMS): δ (ppm) = 8.06 (dd, $J_{(H,H)} = 7.8, 1.7$ Hz, 1H), 7.40-7.24 (m, 2H), 7.24-7.09 (m, 2H), 7.09-6.82 (m, 5H), 6.66 (d, $J_{(H,H)} = 7.7$ Hz, 2H), 4.27 (s, 1H), 2.31 (s, 3H), 0.94 (s, 9H), 0.13 (s, 3H), 0.09 (s, 3H), -0.12 (s, 9H).

¹³C-NMR (75 MHz, CDCl₃, 25 °C): δ (ppm) = 150.5 (C), 150.4 (C), 136.6 (C), 133.2 (C), 130.1 (3 x CH), 129.0 (CH), 128.5 (CH), 127.8 (3 x CH), 124.9 (C), 124.3 (C), 122.2 (CH), 121.9 (CH), 115.6 (CH), 115.5 (CH), 106.2 (C), 87.4 (C), 74.0 (C), 56.5 (CH), 26.3 (3 x CH₃), 21.3 (CH₃), 16.7 (C), 1.8 (3 x CH₃), -4.6 (2 x CH₃).

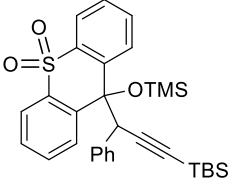
Tert-butyl dimethyl(3-phenyl-3-(5-((trimethylsilyl)oxy)-5H-dibenzo[*a,d*][7]annulen-5-yl)prop-1-yn-1-yl)silane (2.10)

	<p>Yield = 99%, 101 mg.</p> <p>White solid; mp = 96.6-98.0 °C.</p> <p>R_f (SiO₂) = 0.10 (Hexane : Ethyl acetate, 200:1).</p> <p>HRMS (EI) for C₃₃H₄₀OSi₂ [M+K]: Calc.: 477.2047; found: 477.2042.</p>
---	---

¹H-NMR (300 MHz, CDCl₃, 25 °C, TMS): δ (ppm) = 7.92 (d, $J_{(H,H)}$ = 8.1 Hz, 1H), 7.55-7.40 (m, 4H), 7.39-7.26 (m, 4H), 7.26-7.02 (m, 5H), 6.84 (dd, $J_{(H,H)}$ = 8.0, 1.8 Hz, 2H), 5.16 (s, 1H), 0.81 (s, 9H), 0.27 (s, 9H), -0.03 (s, 3H), -0.04 (s, 3H).

¹³C-NMR (75 MHz, CDCl₃, 25 °C): δ (ppm) = 143.1 (C), 141.4 (C), 137.3 (C), 133.2 (CH), 132.6 (C), 132.3 (C), 131.2 (CH), 130.0 (2 x CH), 129.6 (CH), 129.5 (CH), 128.3 (CH), 128.1 (CH), 127.2 (2 x CH), 127.0 (CH), 126.7 (CH), 126.6 (CH), 126.4 (CH), 126.1 (CH), 106.4 (C), 88.3 (C), 87.2 (C), 41.8 (CH), 26.2 (3 x CH₃), 16.4 (C), 3.7 (3 x CH₃), -4.3 (CH₃), -4.4 (CH₃).

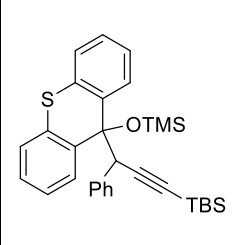
9-(3-(*Tert*-butyldimethylsilyl)-1-phenylprop-2-yn-1-yl)-9-((trimethylsilyl)oxy)-9H-thioxanthene 10,10-dioxide (2.15)

	<p>Yield = 98%, 107 mg.</p> <p>White solid; mp = 71.7-73.0 °C.</p> <p>R_f (SiO₂) = 0.15 (Hexane : Ethyl acetate, 40:1).</p> <p>HRMS (EI) for C₃₁H₃₈NaO₃SSi₂ [M+Na]: Calc.: 569.1972; found: 569.1953.</p>
---	---

¹H-NMR (300 MHz, CDCl₃, 25 °C, TMS): δ (ppm) = 8.34-8.24 (m, 1H), 8.16 (dd, J = 7.6, 1.6 Hz, 1H), 8.09 (dd, J = 7.9, 1.5 Hz, 1H), 7.72-7.55 (m, 2H), 7.42 (td, J = 7.6, 1.2 Hz, 1H), 7.22-7.03 (m, 4H), 7.02-6.95 (m, 2H), 6.82 (dd, J = 8.1, 1.2 Hz, 1H), 4.38 (s, 1H), 0.97 (s, 9H), 0.12 (s, 3H), 0.08 (s, 3H), -0.07 (s, 9H).

¹³C-NMR (75 MHz, CDCl₃, 25 °C): δ (ppm) = 142.6 (C), 141.7 (C), 137.4 (C), 135.0 (C), 134.7 (C), 131.4 (CH), 130.9 (CH), 130.3 (3 x CH), 129.5 (CH), 129.0 (CH), 128.7 (CH), 127.4 (3 x CH), 123.2 (CH), 122.7 (CH), 105.7 (C), 88.3 (C), 78.3 (C), 53.1 (CH), 26.3 (3 x CH₃), 16.8 (C), 2.2 (3 x CH₃), -4.4 (CH₃), -4.5 (CH₃).

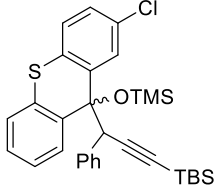
Tert-butyldimethyl(3-phenyl-3-(9-((trimethylsilyl)oxy)-9H-thioxanthen-9-yl)prop-1-yn-1-yl)silane (2.18a)

	<p>Yield = 98%, 102 mg.</p> <p>Colorless oil.</p> <p>R_f (SiO₂) = 0.05 (Hexane : Ethyl acetate, 200:1).</p> <p>HRMS (EI) for C₃₁H₃₈NaOSSi₂ [M+Na]: Calc.: 537.2074; found: 537.2068.</p>
---	--

¹H-NMR (300 MHz, CDCl₃, 25 °C, TMS): δ (ppm) = 7.91-7.77 (m, 1H), 7.69 (dd, $J_{(H,H)}$ = 8.0, 1.5 Hz, 1H), 7.32-7.23 (m, 2H), 7.23-7.14 (m, 4H), 7.13-7.08 (m, 1H), 7.03 (dd, $J_{(H,H)}$ = 8.3, 7.0 Hz, 2H), 6.76-6.66 (m, 2H), 4.21 (s, 1H), 0.99 (s, 9H), 0.17 (s, 3H), 0.12 (s, 3H), 0.00 (s, 9H).

¹³C-NMR (75 MHz, CDCl₃, 25 °C): δ (ppm) = 136.7 (C), 136.6 (2 x C), 135.2 (C), 130.3 (2 x CH), 130.1 (C), 130.0 (CH), 129.7 (CH), 127.7 (CH), 127.6 (CH), 127.1 (2 x CH), 127.0 (CH), 125.0 (CH), 124.7 (CH), 124.6 (CH), 124.4 (CH), 106.6 (C), 87.3 (C), 79.7 (C), 53.7 (CH), 26.4 (3 x CH₃), 16.9 (C), 2.2 (3 x CH₃), -4.4 (CH₃), -4.5 (CH₃).

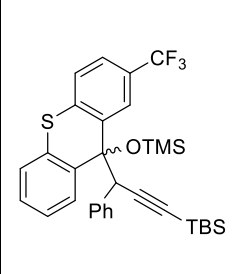
Tert-butyl(3-(2-chloro-9-((trimethylsilyl)oxy)-9H-thioxanthen-9-yl)-3-phenylprop-1-yn-1-yl)dimethylsilane (2.18i)

	<p>Yield = 97%, 107 mg. (Mixture of diastereoisomers; <i>dr</i> = 1.3:1)</p> <p>Colorless oil.</p> <p>R_f (SiO₂) = 0.03 (Hexane : Ethyl acetate, 200:1).</p> <p>HRMS (EI) for C₃₁H₃₇ClNaOSSi₂ [M+Na]: Calc.: 571.1684; found: 571.1686.</p>
---	--

¹H-NMR (300 MHz, CDCl₃, 25 °C, TMS): δ (ppm) = 7.9-7.7 (m, 3H), 7.5 (d, $J_{(H,H)} = 8.0$ Hz, 1H), 7.3-7.1 (m, 10H), 7.1-7.0 (m, 6H), 6.8 (d, $J_{(H,H)} = 7.4$ Hz, 2H), 6.7 (d, $J_{(H,H)} = 7.5$ Hz, 2H), 4.2 (s, 1H), 4.1 (s, 1H), 1.0 (s, 9H), 1.0 (s, 9H), 0.2 (s, 3H), 0.2 (s, 3H), 0.1 (s, 3H), 0.1 (s, 3H), 0.0 (s, 9H), -0.1 (s, 9H).

¹³C-NMR (75 MHz, CDCl₃, 25 °C): δ (ppm) = 138.7 (C), 136.9 (C), 136.4 (C), 136.1 (C), 136.0 (C), 135.2 (C), 131.0 (C), 130.7 (C), 130.3 (2 x CH), 130.2 (2 x CH), 130.1 (CH), 129.9 (C), 129.8 (CH), 129.7 (2 x CH), 129.5 (C), 128.9 (C), 128.7 (C), 128.0 (CH), 127.8 (2 x CH), 127.8 (CH), 127.3 (CH), 127.2 (3 x CH), 127.1 (2 x CH), 126.1 (CH), 125.6 (CH), 125.4 (CH), 125.0 (CH), 124.7 (CH), 124.6 (CH), 105.9 (C), 105.8 (C), 87.9 (C), 87.7 (C), 80.0 (C), 79.4 (C), 54.2 (CH), 52.3 (CH), 26.4 (3 x CH₃), 26.3 (3 x CH₃), 16.8 (2 x C), 2.3 (3 x CH₃), 2.2 (3 x CH₃), -4.4 (3 x CH₃), -4.5 (CH₃).

Tert-butyldimethyl(3-phenyl-3-(2-(trifluoromethyl)-9-((trimethylsilyl)oxy)-9H-thioxanthen-9-yl)prop-1-yn-1-yl)silane (2.18j)

	<p>Yield = 99%, 116 mg. (Mixture of diastereoisomers; <i>dr</i> = 1.3:1).</p> <p>Colorless oil.</p> <p>R_f (SiO₂) = 0.04 (Hexane : Ethyl acetate, 200:1).</p> <p>HRMS (EI) for C₃₂H₃₇F₃NaOSSi₂ [M+Na]: Calc.: 605.1948; found: 605.1952.</p>
---	---

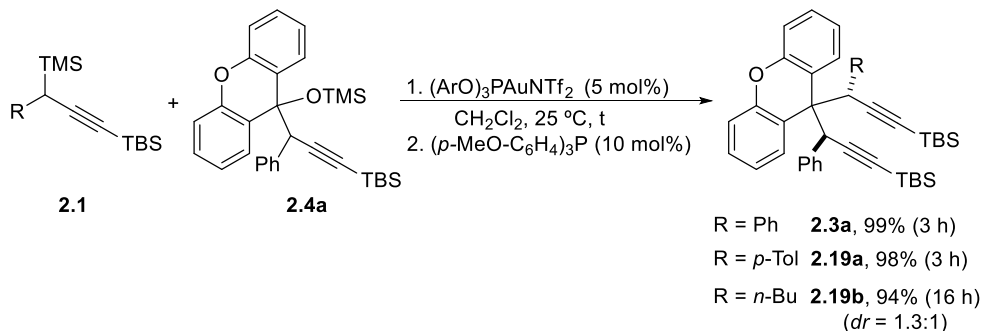
¹H-NMR (300 MHz, CDCl₃, 25 °C, TMS): δ (ppm) = 7.9-7.8 (m, 2H), 7.8-7.7 (m, 1H), 7.7 (dd, $J_{(H,H)} = 7.9, 1.6$ Hz, 1H), 7.5 (dd, $J_{(H,H)} = 8.5, 2.4$ Hz, 1H), 7.4 (dd, $J_{(H,H)} = 8.4, 2.3$ Hz, 1H), 7.3 (dd, $J_{(H,H)} = 3.8, 2.1$ Hz, 3H), 7.3-7.1 (m, 7H), 7.1 (dt, $J_{(H,H)} = 8.5, 7.1$ Hz, 4H), 6.8-6.7 (m, 2H), 6.7-6.6 (m, 2H), 4.2 (s, 1H), 4.2 (s, 1H), 1.0 (s, 9H), 0.9 (s, 9H), 0.1 (s, 3H), 0.1 (s, 3H), 0.1 (s, 3H), 0.1 (s, 3H), 0.0 (s, 9H), -0.1 (s, 9H).

¹³C-NMR (75 MHz, CDCl₃, 25 °C): δ (ppm) = 136.8 (C), 136.5 (C), 136.4 (C), 136.3 (2 x C), 136.2 (C), 135.2 (C), 134.8 (C), 130.4 (2 x CH), 130.1 (2 x CH), 130.0 (CH), 129.8 (CH), 129.1 (C), 128.8 (C), 128.1 (CH), 128.0 (CH), 127.4 (2 x CH), 127.3 (4 x CH), 127.1 (q, $J_{(C,F)} = 97.3$ Hz, C), 127.0 (q, $J_{(C,F)} = 97.3$ Hz, C), 126.8 (m, 2 x CH), 125.6 (CH), 125.4 (CH), 125.2 (CH), 125.1 (CH), 124.9 (CH), 124.6 (CH), 124.4 (q, $J_{(C,F)} = 271.7$ Hz, C), 124.3 (q, $J_{(C,F)} = 272.3$ Hz, C), 124.2 (q, $J_{(C,F)} = 3.6$ Hz, CH), 124.1 (q, $J_{(C,F)} = 3.6$ Hz, CH), 105.5 (C), 105.4 (C), 88.1 (C), 87.8 (C), 79.8 (C), 79.5 (C), 54.0 (CH), 52.7 (CH), 26.3 (3 x CH₃), 26.2 (3 x CH₃), 16.8 (2 x C), 2.1 (3 x CH₃), 2.0 (3 x CH₃), -4.5 (2 x CH₃), -4.6 (2 x CH₃).

¹⁹F-NMR (282 MHz, CDCl₃, 25 °C): δ (ppm) = -62.1, -62.2.

2.3.3 Experimental procedure for the synthesis of non-symmetrical 9,9-bispropargylxanthenes **2.19**

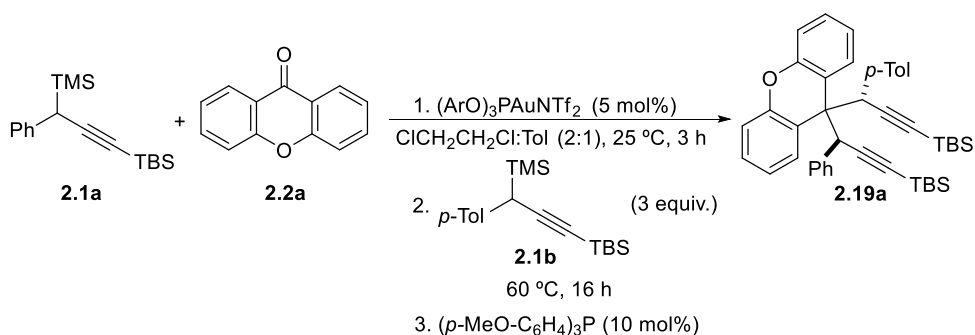
A. Stepwise procedure



Scheme 5.13: Gold-catalyzed propargylation of isolated xanthrydrol **2.4a**.

To a solution in 1 mL of dry dichloromethane of 0.20 mmol of the xanthrydrol silyl ether **2.4a** (100 mg), synthesized following the previously described methodology, 0.60 mmol of the corresponding propargylsilane **2.1** (3 equiv.) and 11.2 mg of the gold catalyst (5 mol%) were sequentially added at 25 °C under argon atmosphere. The reaction mixture was stirred for 3 h for derivatives **2.3a** and **2.19a**, and 16 h for derivative **2.19b**. Afterwards, 8.2 mg (0.02 mmol, 10 mol%) of $(p\text{-MeO-C}_6\text{H}_4)_3\text{P}$ were added for deactivating the catalyst, and the solvent was removed under vacuum. Flash column chromatography of the residue through silica gel afforded the corresponding non-symmetrical 9,9-bispropargylxanthenes **2.3a** and **2.19a-b**.

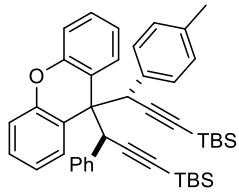
B. One-pot procedure



Scheme 5.14: One-pot non-symmetrical bispropargylation of xanthone **2.2a**.

In a Schlenk tube under argon atmosphere, xanthone **2.2a** (39.2 mg, 0.20 mmol) and propargylsilane **2.1a** (72.5 mg, 0.24 mmol, 1.2 equiv) were dissolved in a mixture of 0.7 mL of dry 1,2-dichloroethane and 0.3 mL of toluene, at 25 °C. Then, 11.2 mg of the gold catalyst (5 mol%) were added, and the reaction mixture was stirred for 3 h. After that time, propargylsilane **2.1b** (190 mg, 0.6 mmol, 3 equiv.) was added in one portion, and the reaction was set at 60 °C for 16 h. Finally, 8.2 mg (0.02 mmol, 10 mol%) of (*p*-MeO-C₆H₄)₃P were added for catalyst deactivation, and the solvent was removed under vacuum. The crude mixture was directly analyzed by ¹H-NMR, using dibromomethane as internal standard. The corresponding 9,9-bispropargylxanthene **2.19a** was generated in 80% yield.

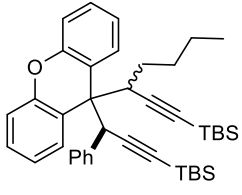
***Tert*-butyl((*S*^{*})-3-(9-((*S*^{*})-3-(*tert*-butyldimethylsilyl)-1-(*p*-tolyl)prop-2-yn-1-yl)-9*H*-xanthen-9-yl)-3-phenylprop-1-yn-1-yl)dimethylsilane (**2.19a**)**

	<p>Yield = 98%, 128 mg. White solid; mp = 113.1-115.0 °C. R_f (SiO₂) = 0.21 (Hexane : Ethyl acetate, 100:1). HRMS (EI) for C₄₄H₅₂NaOSi₂ [M+Na]: Calc.: 675.3454; found: 675.3450.</p>
--	--

¹H-NMR (300 MHz, CDCl₃, 25 °C, TMS): δ (ppm) = 8.78 (dd, *J*_(H,H) = 7.2, 2.6 Hz, 1H), 8.71 (dd, *J*_(H,H) = 7.2, 2.6 Hz, 1H), 7.12 (ddt, *J*_(H,H) = 10.2, 7.2, 3.8 Hz, 4H), 6.96 (t, *J*_(H,H) = 7.3 Hz, 1H), 6.85 (dd, *J*_(H,H) = 8.3, 6.6 Hz, 2H), 6.67 (d, *J*_(H,H) = 8.2 Hz, 2H), 6.62-6.57 (m, 2H), 6.53 (dd, *J*_(H,H) = 7.7, 2.5 Hz, 4H), 5.18 (s, 1H), 5.16 (s, 1H), 2.11 (s, 3H), 1.10 (s, 9H), 1.09 (s, 9H) 0.26 (s, 6H), 0.25 (s, 6H).

¹³C-NMR (75 MHz, CDCl₃, 25 °C): δ (ppm) = 151.3 (C), 138.0 (C), 136.1 (C), 134.9 (C), 129.8 (2 x CH), 129.7 (2 x CH), 128.7 (CH), 128.6 (CH), 128.6 (CH), 128.5 (CH), 128.0 (3 x CH), 127.1 (2 x CH), 126.6 (CH), 121.7 (CH), 121.6 (CH), 120.9 (C), 120.8 (C), 116.1 (CH), 116.0 (C), 108.7 (C), 108.3 (C), 89.2 (C), 89.0 (C), 50.6 (CH), 50.0 (C), 49.6 (CH), 26.5 (6 x CH₃), 21.0 (CH₃), 17.1 (2 x C), -4.4 (4 x CH₃).

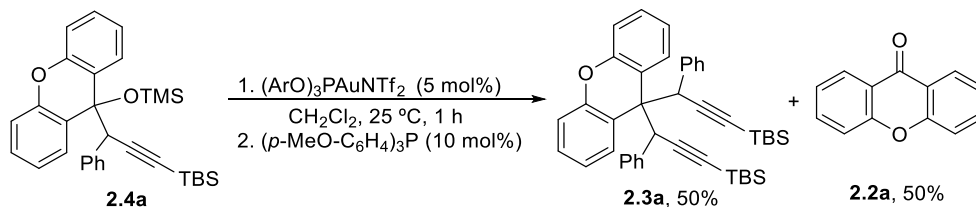
Tert-butyl(3-(9-(3-(tert-butyl(dimethylsilyl)-1-phenylprop-2-yn-1-yl)-9H-xanthen-9-yl)hept-1-yn-1-yl)dimethylsilane (2.19b)

	<p>Yield = 98%, 116 mg. (Mixture of diastereoisomers; <i>dr</i> = 1.3:1)</p> <p>Colorless oil.</p> <p>R_f (SiO₂) = 0.25 (Hexane : Ethyl acetate, 100:1).</p> <p>HRMS (EI) for C₄₁H₅₄NaOSi₂ [M+Na]: Calc.: 641.3611; found: 641.3604.</p>
---	--

¹H-NMR (300 MHz, CDCl₃, 25 °C, TMS): δ (ppm) = 8.81 (dd, $J_{(H,H)} = 8.1, 1.7$ Hz, 1H), 8.75 (dd, $J_{(H,H)} = 8.1, 1.6$ Hz, 1H), 8.10 (dd, $J_{(H,H)} = 8.1, 1.6$ Hz, 1H), 7.48 (d, $J_{(H,H)} = 7.8$ Hz, 2H), 7.35-7.15 (m, 6H), 7.14-7.03 (m, 4H), 7.00 (ddd, $J_{(H,H)} = 8.1, 4.3, 1.5$ Hz, 3H), 6.85 (t, $J_{(H,H)} = 7.7$ Hz, 2H), 6.70 (tt, $J_{(H,H)} = 8.1, 1.8$ Hz, 3H), 6.32-6.23 (m, 2H), 6.17 (d, $J_{(H,H)} = 7.7$ Hz, 1H), 4.95 (s, 1H), 4.73 (s, 1H), 4.00 (dd, $J_{(H,H)} = 11.0, 3.6$ Hz, 1H), 3.12 (m, 1H), 1.64-1.43 (m, 4H), 1.38-1.13 (m, 8H), 1.09 (s, 9H), 1.07 (s, 9H), 1.04 (s, 9H), 1.00-0.87 (m, 2H), 0.80 (t, $J_{(H,H)} = 7.3$ Hz, 3H), 0.79 (s, 9H), 0.74 (t, $J_{(H,H)} = 7.2$ Hz, 3H), 0.26 (s, 6H), 0.24 (s, 6H), 0.22 (s, 3H), 0.21 (s, 3H), -0.04 (s, 3H), -0.07 (s, 3H).

¹³C-NMR (75 MHz, CDCl₃, 25 °C): δ (ppm) = 152.5 (C), 152.2 (C), 151.9 (C), 151.6 (C), 137.6 (C), 137.2 (C), 131.1 (2 x CH), 129.5 (2 x CH), 128.6 (CH), 128.5 (CH), 128.4 (CH), 128.3 (CH), 128.2 (CH), 128.1 (CH), 128.0 (CH), 127.5 (2 x CH), 127.4 (CH), 127.3 (CH), 126.9 (2 x CH), 126.8 (CH), 124.5 (C), 122.6 (C), 122.4 (2 x CH), 122.0 (CH), 121.0 (CH), 120.7 (C), 119.9 (C), 116.4 (CH), 116.3 (CH), 116.1 (CH), 116.0 (CH), 110.9 (C), 110.0 (C), 107.6 (C), 107.0 (C), 88.4 (2 x C), 87.0 (2 x C), 52.7 (CH), 51.1 (CH), 49.7 (C), 48.5 (C), 41.7 (CH), 41.6 (CH), 31.6 (CH₂), 31.2 (CH₂), 30.5 (CH₂), 30.3 (CH₂), 26.4 (6 x CH₃), 26.3 (3 x CH₃), 26.2 (3 x CH₃), 22.2 (CH₂), 22.0 (CH₂), 17.1 (C), 17.0 (C), 16.9 (C), 16.5 (C), 14.1 (2 x CH₃), -4.3 (CH₃), -4.4 (4 x CH₃), -4.7 (3 x CH₃).

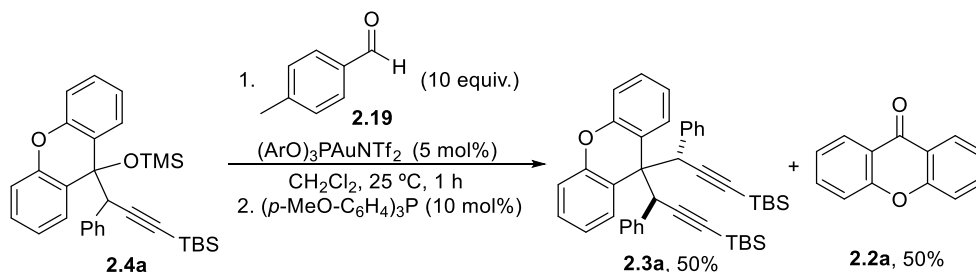
2.3.4 Experimental procedure for the disproportionation reaction of xanthidrol silyl ether **2.4a**



Scheme 5.15: Desproportionation reaction of xanthidrol **2.4a**.

Xanthidrol silyl ether **2.4a** (100 mg, 0.20 mmol) was dissolved in 1 mL of dry dichloromethane, under argon atmosphere, at 25 °C. Then, 11.2 mg of the gold catalyst (5 mol%) were added, and the mixture was stirred for 1 h at that temperature. Finally, the gold catalyst was deactivated by adding 8.2 mg (0.02 mmol, 10 mol%) of $(p\text{-MeO-C}_6\text{H}_4)_3\text{P}$, and the solvents was removed under vacuum. The crude mixture was directly analyzed by $^1\text{H-NMR}$, and the yields were determined using dibromomethane as internal standard.

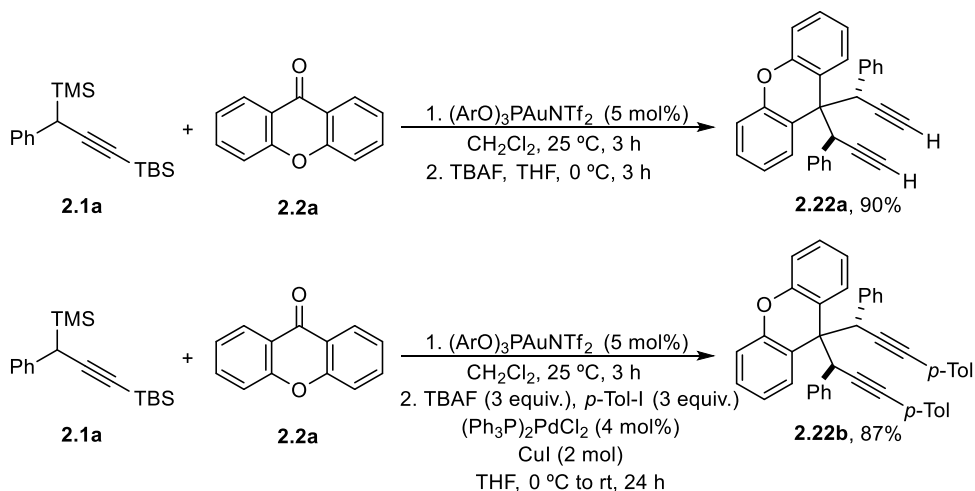
- Control experiment for mechanism determination



Scheme 5.16: Disproportionation of xanthidrol **2.4a** in the presence of *p*-tolualdehyde.

A solution of xanthidrol silyl ether **2.4a** (100 mg, 0.20 mmol) and *p*-tolualdehyde (237 μL , 2 mmol) in 1 mL of dry dichloromethane was prepared in a Schlenk tube, under argon atmosphere, at 25 °C. Then, the mixture was treated as described in the previous procedure.

2.3.5 Experimental procedure for the one-pot synthesis of 9,9-propargylxanthene derivatives **2.22**

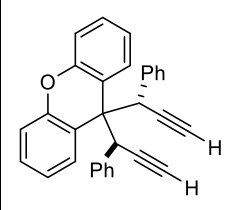


Scheme 5.17: One-pot propargylation-deprotection/Sonogashira reaction of xanthone **2.2a**.

Following the described methodology for the bispropargylation reaction, after 3 h of reaction the mixture was cooled down to 0 °C, and 1 mL of THF was added. Then, 0.5 mmol of TBAF (0.5 mL, 1M in THF) were added dropwise. After complete addition, the cooling bath was removed and the mixture stirred at room temperature for an additional period of 3 h. The crude was diluted with EtOAc, washed with water, dried over Na₂SO₄, filtered and the solvents were removed under vacuum. Flash column chromatography over silica gel afforded pure compound **2.22a** in a 90% yield.

For the in-situ Sonogashira reaction, 4-iodotoluene (131 mg, 0.6 mmol, 3 equiv), Pd(PPh₃)₂Cl₂ (5.6 mg, 4 mol %) and Cul (1 mg, 2 mol %) were added before dropping the TBAF solution. After complete addition, the cooling bath was removed and the mixture stirred at room temperature for an additional period of 6 h. The crude was diluted with EtOAc, washed with water, dried over Na₂SO₄, filtered and the solvents were removed under vacuum. Flash column chromatography over silica gel afforded pure compound **2.22b** in a 87% yield.

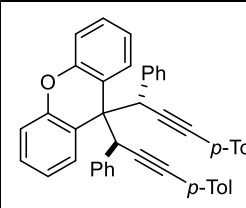
9,9-Bis((S*)-1-phenylprop-2-yn-1-yl)-9H-xanthene (2.22a)

	<p>Yield = 98%, 74 mg.</p> <p>White solid, mp = >174.0 °C decomp.</p> <p>R_f (SiO₂) = 0.18 (Hexane : Ethyl acetate, 40:1).</p> <p>HRMS could not be obtained. Unstable compound.</p>
---	--

¹H-NMR (300 MHz, CDCl₃, 25 °C, TMS): δ (ppm) = 8.81-8.51 (m, 2H), 7.18 (q, $J_{(H,H)}$ = 5.1, 4.7 Hz, 4H), 6.98 (t, $J_{(H,H)}$ = 7.3 Hz, 2H), 6.87 (t, $J_{(H,H)}$ = 7.6 Hz, 4H), 6.63 (d, $J_{(H,H)}$ = 7.8 Hz, 4H), 6.59-6.50 (m, 2H), 5.19 (d, $J_{(H,H)}$ = 2.8 Hz, 2H), 2.71 (d, $J_{(H,H)}$ = 2.8 Hz, 2H).

¹³C-NMR (75 MHz, CDCl₃, 25 °C): δ (ppm) = 151.3 (2 x C), 137.5 (2 x C), 129.7 (4 x CH), 128.9 (2 x CH), 128.6 (2 x CH), 127.3 (4 x CH), 126.8 (2 x CH), 122.0 (2 x CH), 120.5 (2 x C), 116.3 (2 x CH), 85.5 (2 x C), 74.4 (2 x CH), 49.6 (C), 48.8 (2 x CH).

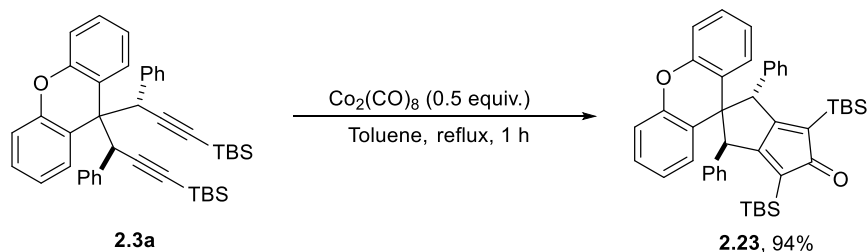
9,9-bis((S*)-1-phenyl-3-(p-tolyl)prop-2-yn-1-yl)-9H-xanthene (2.22b)

	<p>Yield = 87%, 103 mg.</p> <p>Yellowish oil.</p> <p>R_f (SiO₂) = 0.25 (Hexane : Ethyl acetate, 20:1).</p> <p>HRMS could not be obtained. Unstable compound.</p>
---	--

¹H-NMR (300 MHz, CDCl₃, 25 °C, TMS): δ (ppm) = 8.77-8.60 (m, 2H), 7.54 (d, $J_{(H,H)}$ = 8.0 Hz, 4H), 7.25-7.09 (m, 8H), 7.03-6.92 (m, 2H), 6.87 (t, $J_{(H,H)}$ = 7.5 Hz, 4H), 6.75-6.64 (m, 4H), 6.60-6.49 (m, 2H), 5.41 (s, 2H), 2.40 (s, 6H).

¹³C-NMR (75 MHz, CDCl₃, 25 °C): δ (ppm) = 151.3 (2 x C), 138.3 (2 x C), 138.2 (2 x C), 131.7 (5 x CH), 129.8 (3 x CH), 129.3 (5 x CH), 128.7 (2 x CH), 128.6 (2 x CH), 127.2 (3 x CH), 126.7 (2 x CH), 122.0 (2 x CH), 121.0 (2 x C), 120.9 (2 x C), 116.1 (2 x CH), 90.5 (2 x C), 85.9 (2 x C), 51.0 (C), 50.0 (2 x CH), 21.7 (2 x CH₃).

2.3.6 Experimental procedure for the synthesis of spirocyclopentadienone derivative 2.23

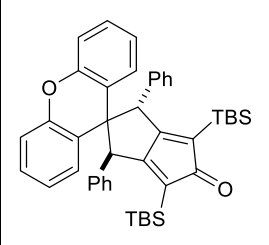


Scheme 5.18: Carbonylative [2+2+1] intramolecular cyclization of product **2.3a**.

This protocol was adapted from a previously reported methodology.⁴ To a refluxing toluene solution (30 mL, 0.005 M) of 9,9-bispropargylxanthene **2.3a** (96 mg, 0.15 mmol) under nitrogen atmosphere, a toluene solution (20 ml) of freshly sublimated dicobalt octacarbonyl (69 mg, 0.20 mmol) was added dropwisely over 30 min. The resulting mixture was refluxed for an additional period of 1 h. Then, the black precipitate formed was removed by filtration through a small pad of silica gel, using hexane as eluent. After solvent removal under reduced pressure, the residue was purified by flash silica gel column chromatography to afford spirocyclopentadienone derivative **2.23**.

⁴ Shibata, T.; Yamashita, K.; Takagi, K.; Ohta, T.; Soai, K. *Tetrahedron* **2000**, *56*, 9259-9267.

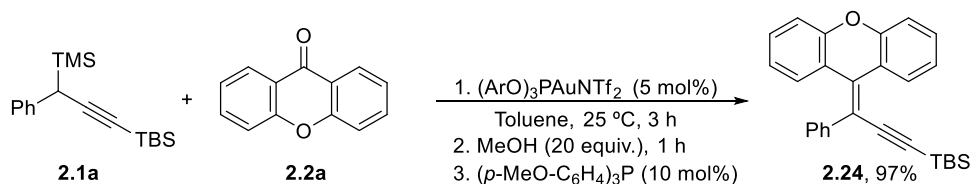
(1*S,3*S**)-4,6-Bis(*tert*-butyldimethylsilyl)-1,3-diphenyl-1*H*-spiro[pentalene-2,9'-xanthen]-5(3*H*)-one (2.23)**

	<p>Yield = 94%, 94 mg.</p> <p>Bright yellow solid, mp = >200.0 °C decomp.</p> <p>R_f (SiO₂) = 0.20 (Hexane : Ethyl acetate, 20:1).</p> <p>HRMS (EI) for C₄₄H₅₀NaO₂Si₂ [M+Na]: Calc.: 689.3242; found: 689.3239.</p>
---	---

¹H-NMR (300 MHz, CDCl₃, 25 °C, TMS): δ (ppm) = 7.16-6.99 (m, 10H), 6.84 (dd, $J_{(H,H)}$ = 8.2, 1.4 Hz, 2H), 6.81-6.72 (m, 6H), 4.66 (s, 2H), 0.85 (s, 18H), -0.12 (s, 6H), -0.28 (s, 6H).

¹³C-NMR (75 MHz, CDCl₃, 25 °C): δ (ppm) = 212.2 (C), 180.8 (2 x C), 150.5 (2 x C), 139.0 (2 x C), 130.3 (4 x CH), 129.0 (2 x CH), 128.2 (2 x CH), 128.1 (4 x CH), 127.3 (2 x CH), 125.8 (2 x C), 123.0 (2 x C), 122.0 (2 x CH), 116.5 (2 x CH), 61.4 (2 x CH), 58.9 (C), 27.6 (6 x CH₃), 18.3 (2 x C), -4.3 (2 x CH₃), -4.7 (2 x CH₃).

2.3.7 One-pot procedure for the synthesis of xanthyldene derivative 2.24



Scheme 5.19: One-pot synthesis of xanthyldene derivative **2.24**.

Following the procedure described for the selective monopropargylation of xanthone derivatives, a 0.20 mmol solution of xanthidrol silyl ether **2.4a** in toluene (1 mL) was prepared reacting propargylsilane **2.1a** and xanthone **2.2a** in the presence of the gold catalyst. Then, before deactivation of the complex, 162 μL (4 mmol, 20 equiv.) of MeOH were added in one portion, and the mixture was stirred for an additional period of 1 h. Finally, 8.2 mg (0.02 mmol, 10 mol%) were used as deactivating agent and the solvent was removed under vacuum. Flash column chromatography of the residue through silica gel afforded the corresponding xanthyldene derivative **2.24** in a 97% yield.

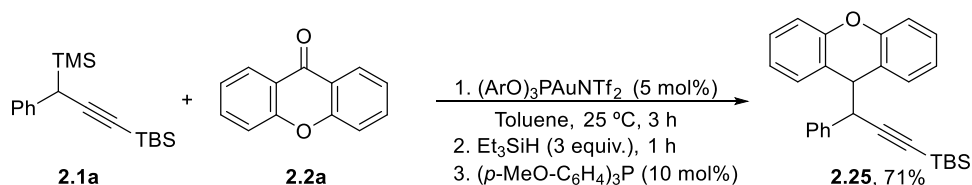
***Tert*-butyldimethyl(3-phenyl-3-(9*H*-xanthen-9-ylidene)prop-1-yn-1-yl)silane (2.24)**

	<p>Yield = 97%, 79 mg.</p> <p>White solid, mp = 127.1-129.0 °C.</p> <p>R_f (SiO₂) = 0.21 (Hexane : Ethyl acetate, 100:1).</p> <p>HRMS (EI) for C₂₈H₂₈NaOSi [M+Na]: Calc.: 431.1802; found: 431.1803.</p>
--	---

¹H-NMR (300 MHz, CDCl₃, 25 °C, TMS): δ (ppm) = 8.77 (dd, $J_{(\text{H,H})}$ = 8.0, 1.6 Hz, 1H), 7.42-7.22 (m, 7H), 7.17 (tdd, $J_{(\text{H,H})}$ = 4.1, 3.4, 1.4 Hz, 3H), 6.69 (dd, $J_{(\text{H,H})}$ = 4.2, 2.9 Hz, 2H), 1.00 (s, 9H), 0.16 (s, 6H).

¹³C-NMR (75 MHz, CDCl₃, 25 °C): δ (ppm) = 153.5 (C), 153.1 (C), 140.4 (C), 132.4 (C), 130.0 (2x CH), 129.8 (CH), 129.4 (CH), 128.9 (CH), 128.5 (2 x CH), 127.8 (CH), 127.4 (CH), 124.2 (C), 123.0 (C), 122.4 (CH), 122.3 (CH), 117.4 (C), 116.7 (CH), 116.3 (CH), 108.1 (C), 101.3 (C), 26.4 (3 x CH₃), 17.1 (C), -4.6 (2 x CH₃).

2.3.8 One-pot procedure for the synthesis of 9-propargylxanthene derivative **2.25**



Scheme 5.20: One-pot synthesis of 9-propargylxanthene derivative **2.25**.

Following the procedure described for the selective monopropargylation of xanthone derivatives, a 0.20 mmol solution of xanthidrol silyl ether **2.4a** in toluene (1 mL) was prepared from propargylsilane **2.1a** and xanthone **2.2a**. Then, 96 μL (0.6 mmol, 3 equiv.) of Et_3SiH were added in one portion, and the mixture was stirred for an additional period of 1 h. Finally, 8.2 mg (0.02 mmol, 10 mol%) were used as deactivating agent and the solvent was removed under vacuum. Flash column chromatography of the residue through silica gel afforded the corresponding 9-propargylxanthene derivative **2.25** in a 71% yield.

Tert-butyldimethyl(3-phenyl-3-(9H-xanthen-9-yl)prop-1-yn-1-yl)silane (2.25)

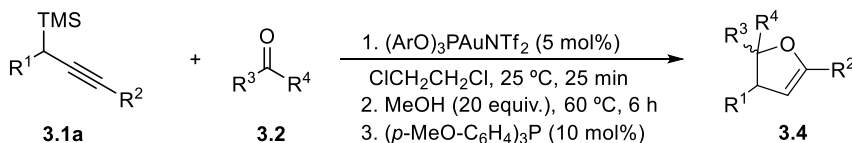
	<p>Yield = 71%, 58 mg.</p> <p>White solid, mp = 87.7-89.4 $^\circ\text{C}$.</p> <p>R_f (SiO_2) = 0.30 (Hexane : Ethyl acetate, 100:1).</p> <p>HRMS (EI) for $\text{C}_{28}\text{H}_{31}\text{OSi}$ [M+H]: Calc.: 411.2144; found: 411.2140.</p>
--	--

$^1\text{H-NMR}$ (300 MHz, CDCl_3 , 25 $^\circ\text{C}$, TMS): δ (ppm) = 7.32 (dd, $J_{(\text{H,H})}$ = 7.6, 1.7 Hz, 1H), 7.21 (ddt, $J_{(\text{H,H})}$ = 7.0, 5.3, 1.7 Hz, 3H), 7.17-7.09 (m, 2H), 7.07-6.87 (m, 5H), 6.77 (dt, $J_{(\text{H,H})}$ = 7.0, 1.5 Hz, 2H), 4.37 (d, $J_{(\text{H,H})}$ = 4.8 Hz, 1H), 4.00 (d, $J_{(\text{H,H})}$ = 4.7 Hz, 1H), 0.93 (s, 9H), 0.14 (s, 3H), 0.10 (s, 3H).

$^{13}\text{C-NMR}$ (75 MHz, CDCl_3 , 25 $^\circ\text{C}$): δ (ppm) = 153.0 (C), 152.9 (C), 137.5 (CH), 129.7 (CH), 129.5 (CH), 128.9 (2 x CH), 128.2 (2 x CH), 127.8 (2 x CH), 127.2 (CH), 122.6 (2 x CH), 121.9 (C), 121.8 (C), 116.2 (CH), 116.1 (CH), 106.5 (C), 88.0 (C), 49.2 (CH), 46.8 (CH), 26.3 (3 x CH_3), 16.7 (C), -4.5 (2 x CH_3).

2.4 Experimental procedures described in Chapter III

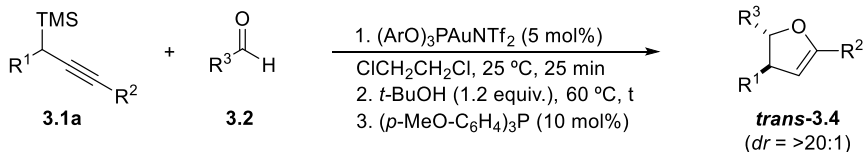
2.4.1 Experimental procedure for the synthesis of diastereomeric mixtures of *trans-cis*-2-silyl-4,5-dihydrofurans 3/4.



Scheme 5.21: Gold(I)-catalyzed one-pot synthesis of dihydrofurans **3.4**.

To a solution 0.24 mmol of propargylsilane **2.1** (1.2 equiv.) (0.6 mmol for compounds **3.4t-w**, 3equiv.) in 1 mL of dry 1,2-dichloroethane at 25 °C were sequentially added 0.2 mmol of the corresponding aldehyde **2.2** and 11.2 mg of the gold catalyst (5 mol%). The reaction was then stirred for 25 min. Upon starting material disappearance, 161 μ L (128 mg; 4 mmol; 20 equivalents) of dry methyl alcohol was added and the reaction heated at 60 °C for 6 hours. Then, 8.2 mg (0.02 mmol; 10 mol%) of (*p*-MeO-C₆H₄)₃P were added for catalyst deactivation. After cooling down, the solvents were removed under vacuum and the residue analyzed by NMR using CH₂Br₂ as internal standard. *Trans/cis* diastereomeric ratios are represented in brackets. No relevant differences were observed for a reaction performed at 1 mmol scale, obtaining dihydrofurans **3.4a** in a 98% yield.

2.4.2 General procedure for the synthesis and isomerization of 2-silyl-4,5-dihydrofurans 3.4 and naphthalene 3.5.

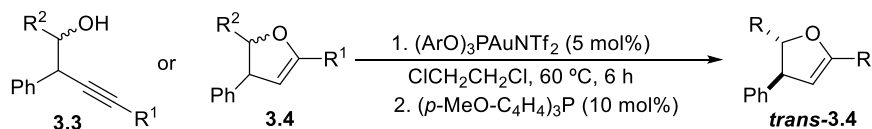


Scheme 5.22: Gold(I)-catalyzed one-pot synthesis of *trans*-dihydrofurans **trans-3.4**.

To a reaction prepared in a similar manner to the mixture of the previous section, 23 μ L of dry *tert*-butyl alcohol (18.8 mg; 0.24 mmol, 1.2 equiv.) (58 μ L for compounds **trans-3.4t-w**, 0.6 mmol, 3 equiv.) was added instead of methanol and

the reaction heated at 60 °C for the period reported in the text. After that period, 8.2 mg (0.02 mmol; 10 mol%) of (*p*-MeO-C₆H₄)₃P were added to inactivate the gold catalyst. After cooling down, solvents were removed under vacuum and the residue purified under deactivated aluminium oxide flash chromatography to obtain the corresponding *trans*-2-silyl-4,5-dihydrofurans **trans-3.4** or naphthalene **3.5** for 3,5-dimethoxybenzaldehyde.

2.4.3 Experimental procedure for the formation of *trans*-2-silyl-4,5-dihydrofurans from a *cis/trans* mixture of isomers or from a *syn/anti* mixture or corresponding alkynols 5.

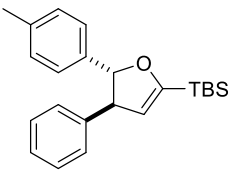


Scheme 5.23: Synthesis of **trans-3.4** starting from alkynols **3.3** or dihydrofurans **3.4**.

To a solution of 0.2 mmol of dihydrofurans mixture **3/4** in 1 mL of dry 1,2-dichloroethane, 11.2 mg of the gold catalyst (5 mol%) were added and the reaction stirred at 60 °C for 6 hours. Then, 8.2 mg (0.02 mmol; 10 mol%) of (*p*-MeO-C₆H₄)₃P were added for catalyst deactivation. After cooling down, the solvents were removed under vacuum and the residue purified by chromatographic column through deactivated aluminium oxide yielding pure *trans*-2-silyl-4,5-dihydrofurans **trans-3.4**.

Identical procedure was followed starting from a mixture of alkynols **3.3**.

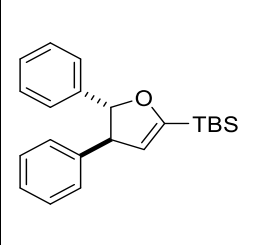
***Trans-tert*-butyldimethyl(4-phenyl-5-(*p*-tolyl)-4,5-dihydrofuran-2-yl)silane (*trans*-3.4a)**

	<p>Yield = 99%, 70 mg.</p> <p>Colorless oil.</p> <p>R_f (SiO₂) = 0.24 (Hexane : Ethyl acetate, 200:1).</p> <p>HRMS (EI) for C₂₃H₃₁OSi [M+H]: Calc.: 351.2127; found: 351.2139.</p>
---	--

¹H-NMR (300 MHz, CDCl₃, 25 °C, TMS): δ (ppm) = 7.39-7.31 (m, 2H), 7.30-7.13 (m, 7H), 5.28 (d, $J_{(H,H)} = 1.1$ Hz, 1H), 5.26 (d, $J_{(H,H)} = 3.5$ Hz, 1H), 4.01 (dd, $J_{(H,H)} = 7.2, 2.4$ Hz, 1H), 2.36 (s, 3H), 1.04 (s, 9H), 0.23 (s, 3H), 0.21 (s, 3H).

¹³C-NMR (75 MHz, CDCl₃, 25 °C): δ (ppm) = 161.9 (C), 144.6 (C), 140.6 (C), 137.3 (C), 129.3 (2 x CH), 128.8 (2 x CH), 127.7 (2 x CH), 126.8 (CH), 125.5 (2 x CH), 116.2 (CH), 92.0 (CH), 59.5 (CH), 26.8 (3 x CH₃), 21.3 (CH₃), 16.7 (C), -6.2 (CH₃), -6.3 (CH₃).

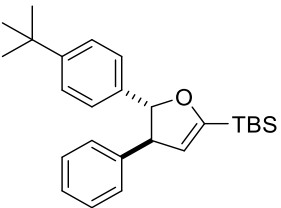
**Trans-tert-butyl(dimethyl-4,5-diphenyl-4,5-dihydrofuran-2-yl)dimethylsilane
(trans-3.4b)**

	<p>Yield = 99%, 67 mg.</p> <p>Colorless oil.</p> <p>R_f (SiO₂) = 0.22 (Hexane : Ethyl acetate, 200:1).</p> <p>HRMS (EI) for C₂₂H₂₉OSi [M+H]: Calc.: 337.2139; found: 337.2127.</p>
---	--

¹H-NMR (300 MHz, CDCl₃, 25 °C, TMS): δ (ppm) = 7.44-7.23 (m, 10H), 5.35 (d, $J_{(H,H)} = 7.1$ Hz, 1H), 5.31 (d, $J_{(H,H)} = 2.4$ Hz, 1H), 4.06 (dd, $J_{(H,H)} = 7.2$ and 2.5 Hz, 1H), 1.09 (s, 9H), 0.28 (s, 3H), 0.26 (s, 3H).

¹³C-NMR (75 MHz, CDCl₃, 25 °C): δ (ppm) = 162.0 (C), 144.5 (C), 143.6 (C), 128.8 (2 x CH), 128.6 (2 x CH), 127.8 (2 x CH), 127.6 (CH), 126.9 (CH), 125.4 (2 x CH), 116.3 (CH), 92.1 (CH), 59.6 (CH), 26.8 (3 x CH₃), 16.7 (C), -6.2 (CH₃), -6.3 (CH₃).

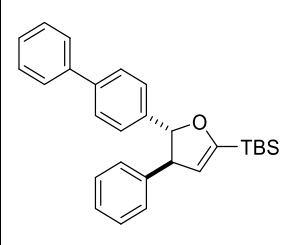
Trans-tert-butyl(5-(4-(tert-butyl)phenyl)-4-phenyl-4,5-dihydrofuran-2-yl)dimethylsilane (trans-3.4aa).

	<p>Yield = 98%, 77 mg.</p> <p>Colorless oil.</p> <p>R_f (SiO₂) = 0.24 (Hexane : Ethyl acetate, 200:1).</p> <p>HRMS (EI) for C₂₆H₃₇OSi [M+H]: Calc.: 393.2608; found: 393.2611.</p>
---	--

¹H-NMR (300 MHz, CDCl₃, 25 °C, TMS): δ (ppm) = 7.52-7.32 (m, 5H), 7.31-7.19 (m, 4H), 5.37-5.24 (m, 2H), 4.05 (dd, $J_{(H,H)} = 7.0$ and 2.5 Hz, 1H), 1.36 (s, 9H), 1.07 (s, 9H), 0.25 (d, $J_{(H,H)} = 8.9$ Hz, 6H).

¹³C-NMR (75 MHz, CDCl₃, 25 °C): δ (ppm) = 161.9 (C), 150.4 (C), 144.7 (C), 140.6 (C), 128.8 (2 x CH), 127.8 (2 x CH), 126.8 (CH), 125.5 (2 x CH), 125.1 (2 x CH), 116.2 (CH), 91.9 (CH), 59.4 (CH), 34.7 (C), 31.5 (3 x CH₃), 26.8 (3 x CH₃), 16.7 (C), -6.3 (2 x CH₃).

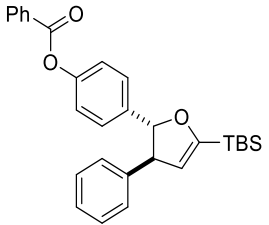
Trans-(5-([1,1'-biphenyl]-4-yl)-4-phenyl-4,5-dihydrofuran-2-yl)(tert-butyl)dimethylsilane (*trans*-3.4c).

	<p>Yield = 97%, 80 mg.</p> <p>Colorless oil.</p> <p>R_f (SiO₂) = 0.16 (Hexane : Ethyl acetate, 200:1).</p> <p>HRMS (EI) for C₂₈H₃₃OSi [M+H]: Calc.: 413.2295; found: 413.2284.</p>
---	--

¹H-NMR (300 MHz, CDCl₃, 25 °C, TMS): δ (ppm) = 7.68-7.57 (m, 4H), 7.48 (t, $J_{(H,H)}$ = 7.4 Hz, 2H), 7.44-7.36 (m, 5H), 7.34-7.26 (m, 3H), 5.38 (d, $J_{(H,H)}$ = 7.1 Hz, 1H), 5.33 (d, $J_{(H,H)}$ = 2.4 Hz, 1H), 4.10 (dd, $J_{(H,H)}$ = 7.1, 2.4 Hz, 1H), 1.09 (s, 9H), 0.29 (3H), 0.26 (3H).

¹³C-NMR (75 MHz, CDCl₃, 25 °C): δ (ppm) = 162.3 (C), 148.8 (C), 142.9 (C), 141.4 (C), 140.8 (C), 129.2 (4 x CH), 128.1 (2 x CH), 127.7 (2 x CH), 127.7 (CH), 127.5 (2 x CH), 127.2 (CH), 126.2 (CH), 116.6 (CH), 92.1 (CH), 59.9 (CH), 27.1 (3 x CH₃), 17.0 (C), -6.0 (2 x CH₃).

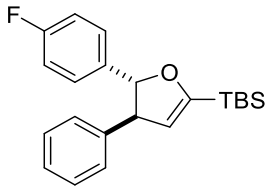
***Trans*-4-(5-(*tert*-butyldimethylsilyl)-3-phenyl-2,3-dihydrofuran-2-yl)phenyl benzoate (*trans*-3.4d).**

	<p>Yield = 99%, 90 mg.</p> <p>Colorless oil.</p> <p>R_f (SiO₂) = 0.15 (Hexane : Ethyl acetate, 10:1).</p> <p>HRMS (EI) for C₂₉H₃₃O₃Si [M+H]: Calc.: 457.2193; found: 457.2198.</p>
---	--

¹H-NMR (300 MHz, CDCl₃, 25 °C, TMS): δ (ppm) = 8.31-8.18 (m, 2H), 7.73-7.62 (m, 1H), 7.55 (t, $J_{(H,H)} = 7.5$ Hz, 2H), 7.43-7.35 (m, 4H), 7.343-7.20 (m, 5H), 5.36 (d, $J_{(H,H)} = 7.1$ Hz, 1H), 5.31 (d, $J_{(H,H)} = 2.5$ Hz, 1H), 4.07 (dd, $J_{(H,H)} = 7.1$ and 2.4 Hz, 1H), 1.07 (s, 9H), 0.27 (s, 3H), 0.24 (s, 3H).

¹³C-NMR (75 MHz, CDCl₃, 25 °C): δ (ppm) = 165.3 (C), 161.8 (C), 150.2 (C), 144.2 (C), 141.1 (C), 133.6 (CH), 130.2 (2 x CH), 129.6 (C), 128.8 (2 x CH), 128.6 (2 x CH), 127.6 (2 x CH), 126.9 (CH), 126.5 (2 x CH), 121.7 (2 x CH), 116.2 (CH), 91.4 (CH), 59.4 (CH), 26.6 (3 x CH₃), 16.6 (C), -6.4 (CH₃), -6.4 (CH₃).

Trans-tert-butyl(5-(4-fluorophenyl)-4-phenyl-4,5-dihydrofuran-2-yl)dimethylsilane (trans-3.4e).

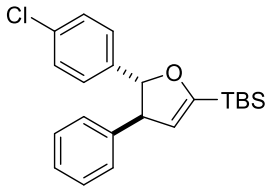
	<p>Yield = 97%, 69 mg.</p> <p>Colorless oil.</p> <p>R_f (SiO₂) = 0.31 (Hexane : Ethyl acetate, 200:1).</p> <p>HRMS (EI) for C₂₂H₂₈FOSi [M+H]: Calc.: 355.1888; found: 355.1889.</p>
---	---

¹H-NMR (300 MHz, CDCl₃, 25 °C, TMS): δ (ppm) = 7.42- 7.31 (m, 2H), 7.33- 7.18 (m, 5H), 7.12- 6.99 (m, 2H), 5.35-5.21 (m, 2H), 4.00 (q, $J_{(H,H)} = 2.5$ Hz, 1H), 1.06 (s, 9H), 0.25 (s, 3H), 0.23 (s, 3H).

¹³C-NMR (75 MHz, CDCl₃, 25 °C): δ (ppm) = 162.2 (CF, d, $J_{(H,H)} = 265.2$ Hz), 161.8 (C), 144.1 (C), 139.2 (C), 128.8 (2 x CH), 127.6 (2 x CH), 127.1 (CH), 126.9 (2 x CH, d, $J_{(H,H)} = 6.9$ Hz), 116.2 (CH), 115.3 (2 x CH, d, $J_{(H,H)} = 21.4$ Hz), 91.4 (CH), 59.5 (CH), 26.6 (3 x CH₃), 16.5 (C), -6.5 (CH₃), -6.5 (CH₃).

¹⁹F-NMR (282 MHz, CDCl₃, 25 °C): δ (ppm) = -115.2.

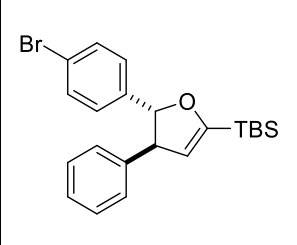
Trans-tert-butyl(5-(4-chlorophenyl)-4-phenyl-4,5-dihydrofuran-2-yl)dimethylsilane (trans-3.4f)

	<p>Yield = 99%, 73 mg.</p> <p>Colorless oil.</p> <p>R_f (SiO₂) = 0.20 (Hexane : Ethyl acetate, 200:1).</p> <p>HRMS (EI) for C₂₂H₂₈ClOSi [M+H]: Calc.: 371.1591; found: 371.1594.</p>
---	--

¹H-NMR (300 MHz, CDCl₃, 25 °C, TMS): δ (ppm) = 7.45-7.18 (m, 9H), 5.37-5.21 (m, 2H), 4.06-3.96 (m, 1H), 1.06 (s, 9H), 0.26 (s, 3H), 0.24 (s, 3H).

¹³C-NMR (75 MHz, CDCl₃, 25 °C): δ (ppm) = 162.0 (C), 144.1 (C), 142.0 (C), 133.3 (C), 128.9 (2 x CH), 128.8 (2 x CH), 127.7 (2 x CH), 127.1 (CH), 126.9 (2 x CH), 116.3 (CH), 91.4 (CH), 59.6 (CH), 26.7 (3 x CH₃), 16.7 (C), -6.2 (CH₃), -6.3 (CH₃).

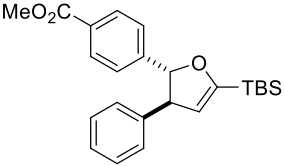
Trans-tert-butyltrimethyl(5-(*p*-bromophenyl)-4-phenyl-4,5-dihydrofuran-2-yl)silane (trans-3.4g).

	<p>Yield = 99%, 82 mg.</p> <p>Colorless oil.</p> <p>R_f (SiO₂) = 0.21 (Hexane : Ethyl acetate, 200:1).</p> <p>HRMS (EI) for C₂₂H₂₈BrOSi [M+H]: Calc.: 415.1093; found: 415.1087.</p>
---	--

¹H-NMR (300 MHz, CDCl₃, 25 °C, TMS): δ (ppm) = 7.54-7.43 (m, 2H), 7.42-7.15 (m, 7H), 5.38-5.15 (m, 2H), 3.99 (dd, $J_{(H,H)}$ = 7.2 and 2.5 Hz, 1H), 1.06 (s, 9H), 0.25 (s, 3H), 0.23 (s, 3H).

¹³C-NMR (75 MHz, CDCl₃, 25 °C): δ (ppm) = 162.0 (C), 144.1 (C), 142.6 (C), 131.7 (2 x CH), 128.9 (2 x CH), 127.7 (2 x CH), 127.2 (2 x CH), 127.1 (CH), 121.4 (C), 116.3 (CH), 91.4 (CH), 59.6 (CH), 26.7 (3 x CH₃), 16.7 (C), - 6.3 (CH₃), - 6.3 (CH₃).

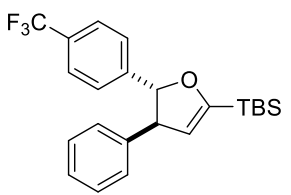
Methyl 4-(*trans*-5-(*tert*-butyldimethylsilyl)-3-phenyl-2,3-dihydrofuran-2-yl)benzoate (*trans*-3.4h).

	<p>Yield = 98%, 77 mg.</p> <p>Colorless oil.</p> <p>R_f (SiO₂) = 0.23 (Hexane : Ethyl acetate, 10:1).</p> <p>HRMS (EI) for C₂₄H₃₁O₃Si [M+H]: Calc.: 395.2037; found: 395.2038.</p>
---	---

¹H-NMR (300 MHz, CDCl₃, 25 °C, TMS): δ (ppm) = 7.93 (d, $J_{(H,H)} = 8.0$ Hz, 2H), 7.33-7.07 (m, 7H), 5.25 (d, $J_{(H,H)} = 7.1$ Hz, 1H), 5.17 (d, $J_{(H,H)} = 2.5$ Hz, 1H), 3.89 (dd, $J_{(H,H)} = 7.0, 2.5$ Hz, 1H), 3.82 (s, 3H), 0.95 (s, 10H), 0.15 (s, 3H), 0.12 (s, 3H).

¹³C-NMR (75 MHz, CDCl₃, 25 °C): δ (ppm) = 167.1 (C), 162.0 (C), 148.6 (C), 144.0 (C), 130.0 (2 x CH), 129.4 (C), 128.9 (2 x CH), 127.7 (2 x CH), 127.1 (CH), 125.3 (2 x CH), 116.3 (CH), 91.5 (CH), 59.6 (CH), 52.2 (CH₃), 26.7 (3 x CH₃), 16.7 (C), -6.3 (CH₃), -6.3 (CH₃).

***Trans*-tert-butyl dimethyl(4-phenyl-5-(4-(trifluoromethyl)phenyl)-4,5-dihydrofuran-2-yl)silane (*trans*-3.4i)**

	<p>Yield = 99%, 80 mg. (Mixture of diastereoisomers, <i>dr</i> = 3.0:1)</p> <p>Colorless oil.</p> <p>R_f (SiO₂) = 0.24 (Hexane : Ethyl acetate, 200:1).</p> <p>HRMS (EI) for C₂₃H₂₇F₃NaOSi [M+Na]: Calc.: 427.1675; found: 427.1664.</p>
---	--

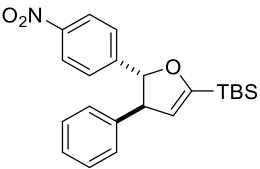
Data for pure *trans*-isomer synthesized from alkynol *anti*-3.3i.

¹H-NMR (300 MHz, CDCl₃, 25 °C, TMS): δ (ppm) = 7.68 – 7.59 (m, 2H), 7.47 – 7.21 (m, 7H), 5.37 (d, $J_{(H,H)} = 7.1$ Hz, 1H), 5.30 (d, $J_{(H,H)} = 2.5$ Hz, 1H), 4.00 (dd, $J_{(H,H)} = 7.2, 2.5$ Hz, 1H), 1.07 (s, 9H), 0.27 (s, 3H), 0.25 (s, 3H).

¹³C-NMR (75 MHz, CDCl₃, 25 °C): δ (ppm) = 162.1 (C), 147.5 (C), 143.9 (C), 129.0 (2 x CH), 127.8 (2 x CH), 125.7 (2 x CH), 125.7 (2 x CH), 125.7 (CH), 127.2 (C), 116.3 (CH), 91.3 (CH), 59.7 (CH), 26.7 (3 x CH₃), 16.7 (C), -6.3 (CH₃), -6.3 (CH₃).

¹⁹F-NMR (282 MHz, CDCl₃, 25 °C): δ (ppm) = -62.4.

***Trans-tert*-butyldimethyl(5-(4-nitrophenyl)-4-phenyl-4,5-dihydrofuran-2-yl)silane (*trans*-3.4j).**

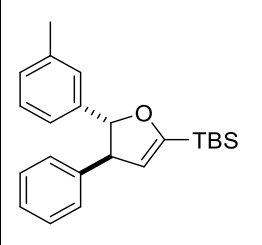
	<p>Yield = 77%, 59 mg. (Mixture of diastereoisomers, <i>dr</i> = 1.5:1)</p> <p>Yellowish oil.</p> <p>R_f (SiO₂) = 0.07 (Hexane : Ethyl acetate, 200:1).</p> <p>HRMS (EI) for C₂₂H₂₈NO₃Si [M+H]: Calc.: 382.1833; found: 382.1835.</p>
---	--

Data for pure *trans*-isomer synthesized from alkynol ***anti*-3.3J**. Yellowish oil

¹H-NMR (300 MHz, CDCl₃, 25 °C, TMS): δ (ppm) = 8.23- 8.15 (m, 2H), 7.46- 7.14 (m, 7H), 5.36 (d, $J_{(H,H)}$ = 7.2 Hz, 1H), 5.25 (d, $J_{(H,H)}$ = 2.5 Hz, 1H), 3.94 (dd, $J_{(H,H)}$ = 7.3 and 2.5 Hz, 1H), 1.02 (s, 9H), 0.23 (s, 3H), 0.20 (s, 3H).

¹³C-NMR (75 MHz, CDCl₃, 25 °C): δ (ppm) = 162.1 (C), 150.7 (C), 147.5 (C), 143.5 (C), 129.1 (2 x CH), 127.7 (2 x CH), 127.3 (CH), 126.1 (2 x CH), 124.0 (2 x CH), 116.4 (CH), 90.9 (CH), 59.6 (CH), 26.7 (3 x CH₃), 16.6 (C), -6.3 (2 x CH₃).

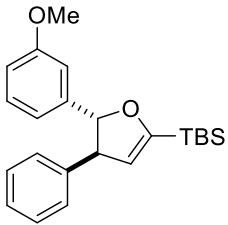
Trans-tert-butyl(dimethyl(4-phenyl-5-(*m*-tolyl)-4,5-dihydrofuran-2-yl)silane (trans-3.4k).

	<p>Yield = 77%, 59 mg.</p> <p>Colorless oil.</p> <p>R_f (SiO₂) = 0.23 (Hexane : Ethyl acetate, 200:1).</p> <p>HRMS (EI) for C₂₃H₃₁OSi [M+H]: Calc.: 351.2139; found: 351.2143.</p>
---	--

¹H-NMR (300 MHz, CDCl₃, 25 °C, TMS): δ (ppm) = 7.46-7.33 (m, 2H), 7.33-7.21 (m, 4H), 7.19-7.08 (m, 3H), 5.33-5.25 (m, 2H), 4.04 (dd, $J_{(H,H)} = 6.9$ and 2.4 Hz, 1H), 2.38 (s, 3H), 1.07 (s, 10H), 0.27 (s, 3H), 0.24 (s, 3H).

¹³C-NMR (75 MHz, CDCl₃, 25 °C): δ (ppm) = 161.8 (C), 144.5 (C), 143.5 (C), 138.1 (s), 128.7 (2 x CH), 128.4 (CH), 128.2 (CH), 127.6 (2 x CH), 126.7 (CH), 126.0 (CH), 122.4 (CH), 116.2 (CH), 91.9 (CH), 59.4 (CH), 26.6 (CH₃), 21.5 (3 x CH₃), 16.6 (C), -6.4 (2 x CH₃).

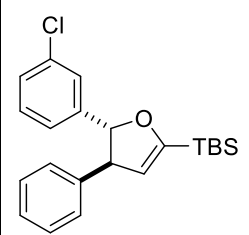
Trans-tert-butyl(5-(3-methoxyphenyl)-4-phenyl-4,5-dihydrofuran-2-yl)dimethylsilane (trans-3.4I).

	<p>Yield = 98%, 72 mg.</p> <p>Colorless oil.</p> <p>R_f (SiO₂) = 0.18 (Hexane : Ethyl acetate, 200:1).</p> <p>HRMS (EI) for C₂₃H₃₁O₂Si [M+H]: Calc.: 367.2091; found: 367.2088.</p>
---	--

¹H-NMR (300 MHz, CDCl₃, 25 °C, TMS): δ (ppm) = 7.54-7.14 (m, 6H), 6.98-6.73 (m, 3H), 5.40-5.21 (m, 2H), 4.03 (d, $J_{(H,H)} = 6.8$ Hz, 1H), 3.82 (s, 3H), 1.07 (s, 9H), 0.26 (s, 3H) 0.26 (s, 3H).

¹³C-NMR (75 MHz, CDCl₃, 25 °C): δ (ppm) = 161.9 (C), 159.9 (C), 145.3 (C), 144.5 (C), 129.7 (CH), 128.8 (2 x CH), 127.7 (2 x CH), 126.9 (CH), 117.7 (CH), 116.3 (CH), 113.3 (CH), 110.5 (CH), 91.9 (CH), 59.6 (CH), 55.3 (CH₃), 26.8 (3 x CH₃), 16.7 (C), -6.3 (2 x CH₃).

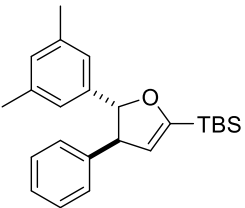
Trans-tert-butyl(5-(3-chlorophenyl)-4-phenyl-4,5-dihydrofuran-2-yl)dimethylsilane (trans-3.4m).

	<p>Yield = 99%, 73 mg.</p> <p>Colorless oil.</p> <p>R_f (SiO₂) = 0.27 (Hexane : Ethyl acetate, 200:1).</p> <p>HRMS (EI) for C₂₂H₂₈ClOSi [M+H]: Calc.: 371.1592; found: 371.1584.</p>
---	--

¹H-NMR (300 MHz, CDCl₃, 25 °C, TMS): δ (ppm) = 7.45- 7.21 (m, 8H), 7.19- 7.14 (m, 1H), 5.30 (d, $J_{(H,H)} = 1.4$ Hz, 1H), 5.28 (d, $J_{(H,H)} = 2.9$ Hz, 1H), 4.00 (dd, $J_{(H,H)} = 6.9, 2.5$ Hz, 1H), 1.07 (s, 9H), 0.27 (s, 3H), 0.24 (s, 3H).

¹³C-NMR (75 MHz, CDCl₃, 25 °C): δ (ppm) = 162.0 (C), 145.6 (C), 144.1 (C), 134.5 (C), 130.0 (CH), 128.9 (2 x CH), 127.7 (CH), 127.6 (2 x CH), 127.1 (CH), 125.6 (CH), 123.6 (CH), 116.3 (CH), 91.2 (CH), 59.5 (CH), 26.7 (3 x CH₃), 16.7 (C), -6.3 (2 x CH₃).

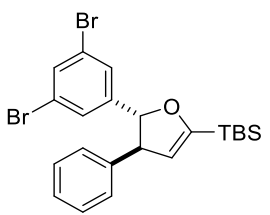
Trans-tert-butyl(5-(3,5-dimethylphenyl)-4-phenyl-4,5-dihydrofuran-2-yl)dimethylsilane (trans-3.4n).

	<p>Yield = 97%, 71 mg.</p> <p>Colorless oil.</p> <p>R_f (SiO₂) = 0.31 (Hexane : Ethyl acetate, 200:1).</p> <p>HRMS (EI) for C₂₄H₃₃OSi [M+H]: Calc.: 365.2295; found: 365.2297.</p>
---	---

¹H-NMR (300 MHz, CDCl₃, 25 °C, TMS): δ (ppm) = 7.44-7.33 (m, 2H), 7.33-7.23 (m, 3H), 6.96 (d, $J_{(H,H)} = 1.1$ Hz, 3H), 5.31 (d, $J_{(H,H)} = 2.5$ Hz, 1H), 5.28 (d, $J_{(H,H)} = 6.7$ Hz, 1H), 4.04 (dd, $J_{(H,H)} = 6.7, 2.5$ Hz, 1H), 2.35 (s, 6H), 1.09 (s, 9H), 0.28 (s, 3H), 0.25 (s, 3H).

¹³C-NMR (75 MHz, CDCl₃, 25 °C): δ (ppm) = 161.9 (C), 144.8 (C), 143.6 (C), 138.1 (2 x C), 129.2 (CH), 128.8 (2 x CH), 127.7 (2 x CH), 126.8 (CH), 123.3 (2 x CH), 116.3 (CH), 92.1 (CH), 59.4 (CH), 26.8 (3 x CH₃), 21.5 (2 x CH₃), 16.7 (C), -6.3 (2 x CH₃).

***Trans*-tert-butyl(5-(3,5-dibromophenyl)-4-phenyl-4,5-dihydrofuran-2-yl)dimethylsilane (*trans*-3.4p).**

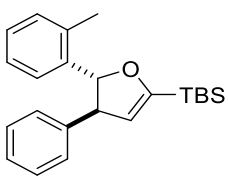
	<p>Yield = 99%, 97 mg. (Mixture of diastereoisomers, <i>dr</i> = 2.0:1)</p> <p>Colorless oil.</p> <p>R_f (SiO₂) = 0.26 (Hexane : Ethyl acetate, 200:1).</p> <p>HRMS (EI) for C₂₂H₂₇Br₂OSi [M+H]: Calc.: 493.0192; found: 493.0173.</p>
---	--

Data for pure *trans*-isomer synthesized from alkynol ***anti*-3.3p**.

¹H-NMR (300 MHz, CDCl₃, 25 °C, TMS): δ (ppm) = 7.60 (t, $J_{(H,H)} = 1.8$ Hz, 1H), 7.44-7.19 (m, 7H), 5.29 (d, $J_{(H,H)} = 2.5$ Hz, 1H), 5.24 (d, $J_{(H,H)} = 6.3$ Hz, 1H), 3.96 (dd, $J_{(H,H)} = 6.4, 2.6$ Hz, 1H), 1.06 (s, 9H), 0.27 (s, 3H), 0.24 (s, 3H).

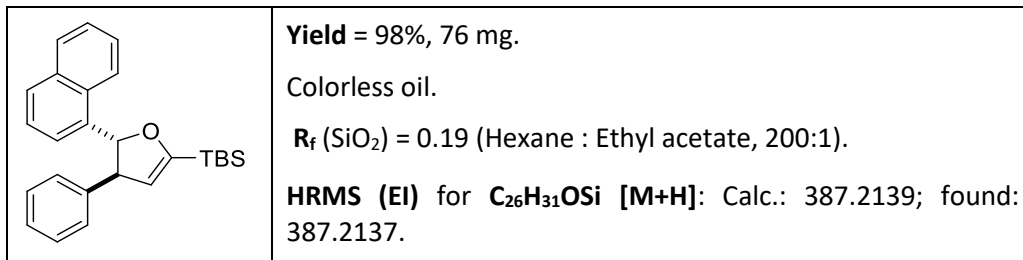
¹³C-NMR (75 MHz, CDCl₃, 25 °C): δ (ppm) = 161.9 (C), 147.5 (C), 143.6 (C), 133.1 (CH), 129.0 (2 x CH), 127.6 (2 x CH), 127.3 (3 x CH), 123.2 (2 x C), 116.4 (CH), 90.2 (CH), 59.4 (CH), 26.7 (3 x CH₃), 16.6 (C), -6.3 (CH₃), -6.3 (CH₃).

***Trans-tert*-butyldimethyl(4-phenyl-5-(*o*-tolyl)-4,5-dihydrofuran-2-yl)silane (*trans*-3.4q).**

	<p>Yield = 99%, 68 mg.</p> <p>Colorless oil.</p> <p>R_f (SiO₂) = 0.24 (Hexane : Ethyl acetate, 200:1).</p> <p>HRMS (EI) for C₂₃H₃₁OSi [M+H]: Calc.: 351.2134; found: 351.2139.</p>
---	--

¹H-NMR (300 MHz, CDCl₃, 25 °C, TMS): δ (ppm) = 7.44-7.33 (m, 3H), 7.33-7.13 (m, 6H), 5.61 (d, $J_{(H,H)} = 6.9$ Hz, 1H), 5.30 (d, $J_{(H,H)} = 2.5$ Hz, 1H), 3.97 (dd, $J_{(H,H)} = 6.9$ and 2.5 Hz, 1H), 2.11 (s, 3H), 1.10 (s, 9H), 0.31 (s, 3H), 0.25 (s, 3H).

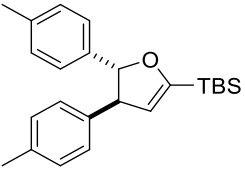
¹³C-NMR (75 MHz, CDCl₃, 25 °C): δ (ppm) = 161.4 (C), 144.7 (C), 113.3 (C), 134.7 (C), 130.6 (CH), 128.8, (2 x CH) 127.7 (2 x CH), 127.3 (CH), 126.9 (CH), 126.2 (CH), 125.3 (CH), 116.8 (CH), 89.7 (CH), 59.0 (CH), 26.8 (3 x CH₃), 19.7 (CH₃), 16.7 (C), -6.3 (2 x CH₃).

Trans-tert-butyltrimethyl(5-(naphthalen-1-yl)-4-phenyl-4,5-dihydrofuran-2-yl)silane (trans-3.4r).

¹H-NMR (300 MHz, CDCl₃, 25 °C, TMS): δ (ppm) = 7.91 (d, $J_{(H,H)} = 8.2$ Hz, 1H), 7.82 (dd, $J_{(H,H)} = 7.3$ and 1.9 Hz, 1H), 7.73 (d, $J_{(H,H)} = 8.5$ Hz, 1H), 7.55-7.22 (m, 9H), 6.03 (d, $J_{(H,H)} = 6.5$ Hz, 1H), 5.36 (d, $J_{(H,H)} = 2.5$ Hz, 1H), 4.11 (dd, $J_{(H,H)} = 6.5$ and 2.5 Hz, 1H), 1.11 (s, 9H), 0.35 (s, 3H), 0.27 (s, 3H).

¹³C-NMR (75 MHz, CDCl₃, 25 °C): δ (ppm) = 161.3 (C), 144.5 (C), 138.3 (C), 134.1 (C), 130.2 (C), 128.8 (CH), 128.7 (2 x CH), 128.0 (CH), 127.9 (2 x CH), 126.9 (CH), 125.7 (CH), 125.5 (CH), 125.4 (CH), 124.3 (CH), 122.9 (CH), 117.1 (CH), 90.6 (CH), 58.8 (CH), 26.7 (3 x CH₃), 16.6 (C), -6.3 (CH₃), -6.3 (CH₃).

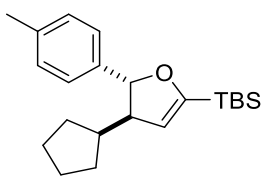
Trans-tert-butyl(-4,5-di-*p*-tolyl-4,5-dihydrofuran-2-yl)dimethylsilane (trans-3.4s).

	<p>Yield = 98%, 72 mg.</p> <p>Colorless oil.</p> <p>R_f (SiO₂) = 0.24 (Hexane : Ethyl acetate, 200:1).</p> <p>HRMS (EI) for C₂₄H₃₃OSi [M+H]: Calc.: Not obtained. Unstable compound.</p>
---	--

¹H-NMR (300 MHz, CDCl₃, 25 °C, TMS): δ (ppm) = 7.26-7.12 (m, 8H), 5.28 (d, $J_{(H,H)} = 2.5$ Hz, 1H), 5.28 (d, $J_{(H,H)} = 7.1$ Hz, 1H), 4.01 (dd, $J_{(H,H)} = 7.2$ and 2.5 Hz, 1H), 2.39 (s, 6H), 1.07 (s, 9H), 0.26 (s, 3H), 0.24 (s, 3H).

¹³C-NMR (75 MHz, CDCl₃, 25 °C): δ (ppm) = 161.7 (C), 141.7 (C), 140.8 (C), 137.2 (C), 136.4 (C), 129.5 (2 x CH), 129.3 (2 x CH), 127.6 (2 x CH), 125.5 (2 x CH), 116.5 (CH), 92.1 (CH), 59.1 (CH), 26.8 (3 x CH₃), 21.3 (CH₃), 21.2 (CH₃), 16.7 (C), -6.2 (CH₃), -6.3 (CH₃).

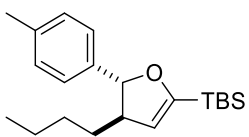
Trans-tert-butyl(4-cyclopentyl-5-(*p*-tolyl)-4,5-dihydrofuran-2-yl)dimethylsilane (trans-3.4u).

	<p>Yield = 97%, 66 mg.</p> <p>Colorless oil.</p> <p>R_f (SiO₂) = 0.29 (Hexane : Ethyl acetate, 200:1).</p> <p>HRMS (EI) for C₂₂H₃₄OSi [M+H]: Not obtained. Unstable compound.</p>
---	---

¹H-NMR (300 MHz, CDCl₃, 25 °C, TMS): δ (ppm) = 7.22 (d, $J_{(H,H)} = 8.0$ Hz, 2H), 7.15 (d, $J_{(H,H)} = 8.0$ Hz, 2H), 5.15 (d, $J_{(H,H)} = 2.5$ Hz, 1H), 5.10 (d, $J_{(H,H)} = 6.2$ Hz, 1H), 2.79 (ddd, $J_{(H,H)} = 7.6, 6.3$ and 2.5 Hz, 1H), 2.47-2.26 (m, 1H), 2.34 (s, 3H), 1.99- 1.49 (m, 8H), 0.97 (s, 9H), 0.17 (s, 3H), 0.14(s, 3H).

¹³C-NMR (75 MHz, CDCl₃, 25 °C): δ (ppm) = 160.7 (C), 141.7 (C), 136.9 (C), 129.2 (2 x CH), 125.7 (2 x CH), 115.4 (CH), 88.0 (CH), 58.5 (CH), 45.5 (CH), 30.6 (CH₂), 30.0 (CH₂), 26.7 (3 x CH₃), 25.5 (2 x CH₂), 21.3 (CH₃), 16.6 (C), -6.3 (CH₃), -6.4 (CH₃).

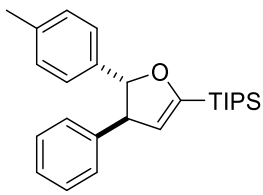
Trans-tert-butyl(4-butyl-5-(*p*-tolyl)-4,5-dihydrofuran-2-yl)dimethylsilane (trans-3.4v).

	<p>Yield = 98%, 65 mg.</p> <p>Colorless oil.</p> <p>R_f (SiO₂) = 0.30 (Hexane : Ethyl acetate, 200:1).</p> <p>HRMS (EI) for C₂₁H₃₅OSi [M+H]: Not obtained. Unstable compound.</p>
---	--

¹H-NMR (300 MHz, CDCl₃, 25 °C, TMS): δ (ppm) = 7.37-7.05 (m, 4H), 5.21 (d, $J_{(H,H)} = 2.4$ Hz, 1H), 5.01 (d, $J_{(H,H)} = 7.0$ Hz, 1H), 2.83 (qt, $J_{(H,H)} = 12.3$ and 6.1 Hz, 1H), 2.37 (s, 3H), 1.69-1.13 (m, 6H), 1.00 (s, 9H), 0.93 (t, $J_{(H,H)} = 6.5$ Hz), 0.19 (s, 3H), 0.17 (s, 3H).

¹³C-NMR (75 MHz, CDCl₃, 25 °C): δ (ppm) = 160.4 (C), 141.1 (C), 136.9 (C), 129.0 (2 x CH), 125.6 (2 x CH), 116.4 (CH), 89.1 (CH), 53.3 (CH), 35.7 (CH₂), 29.5 (CH₂), 26.6 (3 x CH₃), 22.8 (CH₂), 21.1 (CH₃), 16.4 (C), 14.1 (CH₃), -6.5 (2 x CH₃).

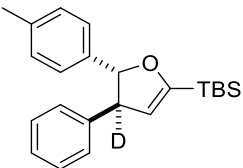
Trans-triisopropyl(4-phenyl-5-(*p*-tolyl)-4,5-dihydrofuran-2-yl)silane (*trans*-3.4w).

	<p>Yield = 99%, 78 mg.</p> <p>Colorless oil.</p> <p>R_f (SiO₂) = 0.19 (Hexane : Ethyl acetate, 200:1).</p> <p>HRMS (EI) for C₂₆H₃₇OSi [M+H]: Calc.: 393.3608; found: 393.2609.</p>
---	---

¹H-NMR (300 MHz, CDCl₃, 25 °C, TMS): δ (ppm) = 7.40-7.12 (m, 9H), 5.31 (d, $J_{(H,H)}$ = 2.4 Hz, 1H), 5.22 (d, $J_{(H,H)}$ = 8.1 Hz, 1H), 4.08 (dd, $J_{(H,H)}$ = 7.9, 2.4 Hz, 1H), 2.37 (s, 3H), 1.35-1.13 (m, 21H).

¹³C-NMR (75 MHz, CDCl₃, 25 °C): δ (ppm) = 160.0 (C), 145.0 (C), 140.8 (C), 137.5 (C), 129.5 (2 x CH), 129.1 (2 x CH), 128.1 (2 x CH), 127.1 (CH), 126.0 (2 x CH), 117.2 (CH), 92.2 (CH), 59.9 (CH), 21.6 (CH₃), 19.1 (3 x CH₃), 19.1 (3 x CH₃), 11.3 (3 x CH).

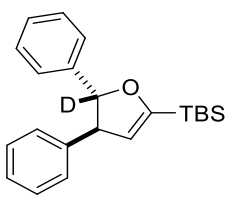
**(E)-tert-butyl(dimethyl(4-deutero-4-phenyl-5-(p-tolyl)-4,5-dihydrofuran-2-yl)silane
(4D-trans-3.4a)**

	<p>Yield = 94%, 66 mg.</p> <p>Colorless oil.</p> <p>R_f (SiO₂) = 0.24 (Hexane : Ethyl acetate, 200:1).</p> <p>HRMS (EI) for C₂₃H₃₀DOSi [M+H]: Calc.: 352.2201; found: 352.2199.</p>
---	---

¹H-NMR (300 MHz, CDCl₃, 25 °C, TMS): δ (ppm) = 7.41-7.32 (m, 2H), 7.32-7.15 (m, 7H), 5.29 (s, 2H), 2.38 (s, 3H), 1.06 (s, 9H), 0.26 (s, 3H), 0.23 (s, 3H).

¹³C-NMR (75 MHz, CDCl₃, 25 °C): δ (ppm) = 161.8 (C), 144.4 (C), 140.5 (C), 137.1 (C), 129.1 (2 x CH), 128.7 (2 x CH), 127.6 (2 x CH), 126.7 (CH), 125.3 (2 x CH), 116.0 (CH), 91.8 (CH), 59.2 (t, $J_{(C,D)}$ = 19.5 Hz, CD), 26.6 (3 x CH₃), 21.2 (CH₃), 16.6 (C), -6.4 (2 x CH₃).

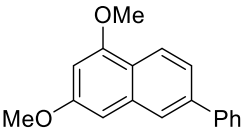
(E)-tert-butyl(dimethyl(5-deutero-4,5-diphenyl-4,5-dihydrofuran-2-yl)silane (5D-trans-3.4b)

	<p>Yield = 98%, 66 mg.</p> <p>Colorless oil.</p> <p>R_f (SiO₂) = 0.22 (Hexane : Ethyl acetate, 200:1).</p> <p>HRMS (EI) for C₂₂H₂₈DOSi [M+H]: Calc.: 338.22045; found: 338.2055.</p>
---	--

¹H-NMR (300 MHz, CDCl₃, 25 °C, TMS): δ (ppm) = 7.47-7.19 (m, 11H), 5.31 (d, $J_{(H,H)}$ = 2.4 Hz, 1H), 4.05 (d, $J_{(H,H)}$ = 2.3 Hz, 1H), 1.08 (s, 10H), 0.28 (s, 3H), 0.25 (s, 3H).

¹³C-NMR (75 MHz, CDCl₃, 25 °C): δ (ppm) = 162.2 (C), 144.8 (C), 143.8 (C), 129.1 (2 x CH), 128.9 (2 x CH), 128.0 (2 x CH), 127.9 (CH), 127.2 (CH), 125.7 (2 x CH), 116.5 (CH), 91.9 (t, $J_{(C,D)}$ = 21.3 Hz, CD), 59.8 (CH), 27.0 (3 x CH₃), 17.0 (C), -6.0 (2 x CH₃).

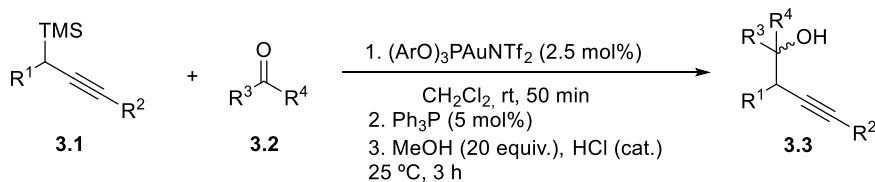
1,3-dimethoxy-6-phenylnaphthalene (3.5)

 <p>The chemical structure shows a naphthalene ring system. The left ring has methoxy groups (-OMe) at positions 1 and 3. The right ring has a phenyl group (-Ph) at position 6.</p>	<p>Yield = 88%, 46 mg.</p> <p>Colorless oil.</p> <p>R_f (SiO₂) = 0.31 (Hexane : Ethyl acetate, 20:1).</p> <p>HRMS (EI) for C₁₈H₁₇O₂ [M+H]: Calc.: 265.1223; found: 265.1218.</p>
---	---

¹H-NMR (300 MHz, CDCl₃, 25 °C, TMS): δ (ppm) = 8.23 (d, $J_{(H,H)} = 8.6$ Hz, 1H), 7.92 (d, $J_{(H,H)} = 1.8$ Hz, 1H), 7.74 (dt, $J_{(H,H)} = 8.3, 1.8$ Hz, 2H), 7.61 (dd, $J_{(H,H)} = 8.6, 1.8$ Hz, 1H), 7.55-7.46 (m, 2H), 7.44-7.36 (m, 1H), 6.82 (d, $J_{(H,H)} = 2.1$ Hz, 1H), 6.53 (d, $J_{(H,H)} = 2.2$ Hz, 1H), 4.02 (s, 3H), 3.96 (s, 3H).

¹³C-NMR (75 MHz, CDCl₃, 25 °C): δ (ppm) = 158.6 (C), 156.6 (C), 141.3 (C), 139.7 (C), 135.4 (C), 128.8 (2 x CH), 128.4 (2 x CH), 127.3 (CH), 124.5 (CH), 122.6 (CH), 122.6 (CH), 120.9 (C), 98.2 (CH), 97.7 (CH), 55.6 (CH₃), 55.3 (CH₃).

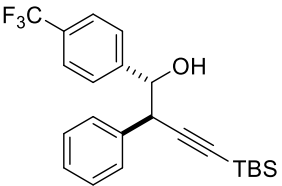
2.4.4 *Experimental procedure for the synthesis of homopropargyl alcohols syn-3.3 for Hammett plot and anti-3.3 for the synthesis of pure trans-dihydrofurans 3.4i, 3.4j and 3.4p.*



Scheme 5.24: Synthesis of alkynol derivatives **3.3**.

To a mixture of 0.48 mmol of propargylsilane **3.1** and 0.4 mmol of carbonyl compound **3.2** in dry dichloromethane (2 mL) at $25\text{ }^\circ\text{C}$, were added 11.2 mg of the gold catalyst (2.5 mol%) and the reaction was then stirred for 50 min. After that time, they were sequentially added 2.6 mg (0.01 mmol, 5 mol%) of PPh_3 to deactivate the catalyst, 360 μL of dry methanol (250 mg; 8 mmol; 20 equivalents) and concentrated HCl (25 μL) to deprotect the silylether. The mixture was stirred for 3 h and then solvents were removed under vacuum. The residue was purified under flash chromatography to separately obtain the corresponding *syn* or *anti* homopropargyl alcohols **3.3**.

**Anti-4-(tert-butyldimethylsilyl)-1-(4-trifluoromethylphenyl)-2-phenylbut-3-yn-1-ol
(anti-3.3i)**

	<p>Yield = 55%, 89 mg. White solid, mp = 76.0-77.5 °C. R_f (SiO₂) = 0.05 (Hexane : Ethyl acetate, 20:1). HRMS (EI) for C₂₃H₂₇F₃NaOSi [M+Na]: Calc.: 427.1675; found: 427.1682.</p>
---	--

¹H-NMR (300 MHz, CDCl₃, 25 °C, TMS): δ (ppm) = 7.55 (d, $J_{(H,H)}$ = 8.1 Hz, 2H), 7.38-7.26 (m, 5H), 7.24-7.07 (m, 2H), 4.94-4.77 (m, 1H), 4.01 (d, $J_{(H,H)}$ = 6.0 Hz, 1H), 2.78 (d, $J_{(H,H)}$ = 3.6 Hz, 1H), 0.98 (s, 9H), 0.17 (s, 6H).

¹³C-NMR (75 MHz, CDCl₃, 25 °C): δ (ppm) = 145.0 (C), 137.2 (C), 128.9 (4 x CH), 128.0 (CH), 127.4 (2 x CH), 125.2 (d, $J_{(H,H)}$ = 3.4 Hz, 2 x CH), 104.6 (C), 90.0 (C), 77.8 (CH), 49.4 (CH), 26.5 (3 x CH₃), 17.0 (C), -4.2 (2 x CH₃).

¹⁹F-NMR (282 MHz, CDCl₃, 25 °C): δ (ppm) = -62.4.

Anti-4-(tert-butyldimethylsilyl)-1-(4-nitrophenyl)-2-phenylbut-3-yn-1-ol (anti-3.3j)

	<p>Yield = 42%, 64 mg.</p> <p>White solid, mp = 104.5-105.7 °C.</p> <p>R_f (SiO₂) = 0.10 (Hexane : Ethyl acetate, 10:1).</p> <p>HRMS (EI) for C₂₂H₂₇NNaO₃Si [M+Na]: Calc.: 404.1652; found: 404.1652.</p>
--	---

¹H-NMR (300 MHz, CDCl₃, 25 °C, TMS): δ (ppm) = 8.12 (d, $J_{(H,H)} = 8.8$ Hz, 2H), 7.36 (d, $J_{(H,H)} = 8.7$ Hz, 2H), 7.30 (dt, $J_{(H,H)} = 4.6$ and 2.2 Hz, 3H), 7.20 (dd, $J_{(H,H)} = 6.9$, 2.6 Hz, 2H), 4.93 (dd, $J_{(H,H)} = 5.8$, 3.2 Hz, 1H), 4.01 (d, $J_{(H,H)} = 6.0$ Hz, 1H), 2.88 (d, $J_{(H,H)} = 3.4$ Hz, 1H), 0.97 (s, 9H), 0.16 (s, 6H).

¹³C-NMR (75 MHz, CDCl₃, 25 °C): δ (ppm) = 147.9 (C), 147.4 (C), 136.4 (C), 128.6 (2 x CH), 128.5 (2 x CH), 127.8 (CH), 127.5 (2 x CH), 123.0 (2 x CH), 103.9 (C), 89.8 (C), 77.1 (CH), 48.8 (CH), 26.1 (3 x CH₃), 16.5 (C), -4.6 (2 x CH₃).

Anti-4-(tert-butyltrimethylsilyloxy)-1-(3,5-dibromophenyl)-2-phenylbut-3-yn-1-ol
(anti-3.3p)

	<p>Yield = 54%, 106 mg.</p> <p>Colorless oil.</p> <p>R_f (SiO₂) = 0.07 (Hexane : Ethyl acetate, 20:1).</p> <p>HRMS (EI) for C₂₂H₂₇Br₂OSi [M+H]: Calc.: 493.0192; found: 493.0164.</p>
--	--

¹H-NMR (300 MHz, CDCl₃, 25 °C, TMS): δ (ppm) = 7.59 (t, $J_{(H,H)} = 1.7$ Hz, 1H), 7.42-7.22 (m, 7H), 4.75 (d, $J_{(H,H)} = 3.6$ Hz, 1H), 3.98 (d, $J_{(H,H)} = 5.1$ Hz, 1H), 2.65 (bs, 1H), 0.99 (s, 9H), 0.19 (s, 3H), 0.18 (s, 3H).

¹³C-NMR (75 MHz, CDCl₃, 25 °C): δ (ppm) = 144.7 (C), 136.7 (C), 133.3 (CH), 128.6 (2 x CH), 128.5 (4 x CH), 127.8 (CH), 122.4 (2 x C), 103.4 (C), 90.1 (C), 76.4 (CH), 48.6 (CH), 26.1 (3 x CH₃), 16.5 (C), -4.4 (CH₃), -4.5 (CH₃).

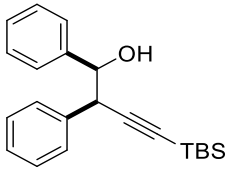
Syn-4-(tert-butyldimethylsilyl)-2-phenyl-1-(p-tolyl)but-3-yn-1-ol (syn-3.3a)

	<p>Yield = 45%, 63 mg.</p> <p>White solid, mp = 78.6-80.0 °C.</p> <p>R_f (SiO₂) = 0.08 (Hexane : Ethyl acetate, 20:1).</p> <p>HRMS (EI) for C₂₃H₃₀NaOSi [M+Na]: Calc.: 373.1958; found: 359.1946.</p>
--	--

¹H-NMR (300 MHz, CDCl₃, 25 °C, TMS): δ (ppm) = 7.30 (d, $J_{(H,H)} = 3.4$ Hz, 5H), 7.16 (d, $J_{(H,H)} = 8.1$ Hz, 2H), 7.08 (d, $J_{(H,H)} = 7.9$ Hz, 2H), 4.76 (dd, $J_{(H,H)} = 7.2$ and 3.5 Hz, 1H), 3.98 (d, $J_{(H,H)} = 7.2$ Hz, 1H), 2.33 (s, 3H), 2.17 (d, $J_{(H,H)} = 3.7$ Hz, 1H), 0.87 (s, 9H), 0.05 (s, 6H).

¹³C-NMR (75 MHz, CDCl₃, 25 °C): δ (ppm) = 137.9 (C), 137.5 (C), 128.9 (C), 128.5 (2 x CH), 128.4 (2 x CH), 127.4 (CH), 126.9 (2 x CH), 105.5 (C), 88.1 (C), 78.0 (CH), 48.2 (CH), 26.1 (3 x CH₃), 21.2 (CH₃), 16.5 (C), -4.6 (2 x CH₃).

Syn-4-(tert-butyldimethylsilyl)-1,2-diphenylbut-3-yn-1-ol (syn-3.3b)

	<p>Yield = 47%, 63 mg.</p> <p>Colorless oil.</p> <p>R_f (SiO₂) = 0.05 (Hexane : Ethyl acetate, 20:1).</p> <p>HRMS (EI) for C₂₂H₂₈NaOSi [M+Na]: Calc.: 359.1802; found: 359.1792.</p>
---	--

¹H-NMR (300 MHz, CDCl₃, 25 °C, TMS): δ (ppm) = 7.37-7.17 (m, 10H), 4.83 (dd, $J_{(H,H)}$ = 7.1 and 2.9 Hz, 1H), 4.04 (d, $J_{(H,H)}$ = 7.2 Hz, 1H), 2.31 (d, $J_{(H,H)}$ = 3.2 Hz, 1H), 0.93 (s, 9H), 0.11 (s, 6H).

¹³C-NMR (75 MHz, CDCl₃, 25 °C): δ (ppm) = 140.8 (C), 137.8 (C), 129.0 (2 x CH), 128.5 (2 x CH), 128.0 (CH), 127.9 (2 x CH), 127.6 (CH), 127.2 (2 x CH), 105.5 (C), 88.4 (C), 78.2 (CH), 48.3 (CH), 26.2 (3 x CH₃), 16.6 (C), -4.5 (2 x CH₃).

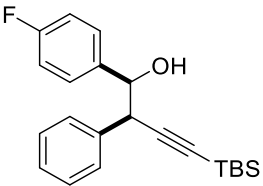
Syn-1-([1,1'-biphenyl]-4-yl)-4-(tert-butyldimethylsilyl)-2-phenylbut-3-yn-1-ol (syn-3.3c)

	<p>Yield = 44%, 71 mg.</p> <p>Colorless oil.</p> <p>R_f (SiO₂) = 0.04 (Hexane : Ethyl acetate, 20:1).</p> <p>HRMS (EI) for C₂₈H₃₂NaOSi [M+Na]: Calc: 435.2115; found: 425.2114.</p>
--	---

¹H-NMR (300 MHz, CDCl₃, 25 °C, TMS): δ (ppm) = 7.60 (d, $J_{(H,H)}$ = 6.9 Hz, 2H), 7.54 (d, $J_{(H,H)}$ = 8.2 Hz, 2H), 7.46 (t, $J_{(H,H)}$ = 7.4 Hz, 2H), 7.35 (td, $J_{(H,H)}$ = 8.7, 5.2 Hz, 8H), 4.95-4.73 (m, 1H), 4.05 (d, $J_{(H,H)}$ = 7.3 Hz, 1H), 2.28 (d, $J_{(H,H)}$ = 3.5 Hz, 1H), 0.89 (s, 9H), 0.08 (s, 6H).

¹³C-NMR (75 MHz, CDCl₃, 25 °C): δ (ppm) = 141.1 (C), 140.9 (C), 139.9 (C), 137.8 (C), 129.0 (2 x CH), 128.9 (2 x CH), 128.6 (2 x CH), 127.7 (CH), 127.6 (2 x CH), 127.4 (CH), 127.2 (2 x CH), 126.7 (2 x CH), 105.5 (C), 88.5 (C), 78.1 (CH), 48.3 (CH), 26.2 (3 x CH₃), 16.6 (C), -4.5 (2 x CH₃).

Syn-4-(tert-butyltrimethylsilyl)-1-(4-fluorophenyl)-2-phenylbut-3-yn-1-ol (syn-3.3e)

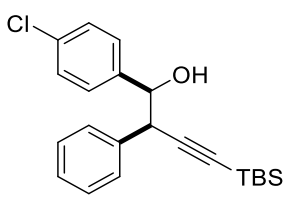
	<p>Yield = 44%, 62 mg.</p> <p>White solid, mp = 66.3-67.3 °C.</p> <p>R_f (SiO₂) = 0.08 (Hexane : Ethyl acetate, 20:1).</p> <p>HRMS (EI) for C₂₂H₂₇FNaOSi [M+Na]: Calc.: 377.1707; found: 377.1721.</p>
---	---

¹H-NMR (300 MHz, CDCl₃, 25 °C, TMS): δ (ppm) = 7.44-7.10 (m, 7H), 6.98 (td, $J_{(H,H)} = 9.0, 2.3$ Hz, 2H), 4.79 (d, $J_{(H,H)} = 7.2$ Hz, 1H), 3.99 (d, $J_{(H,H)} = 7.1$ Hz, 1H), 2.39 (s, 1H), 0.92 (s, 9H), 0.10 (s, 6H).

¹³C-NMR (75 MHz, CDCl₃, 25 °C): δ (ppm) = 162.6 (d, $J_{(H,H)} = 245.7$ Hz, C), 137.5 (C), 136.5 (C), 128.9 (2 x CH), 128.8 (d, $J_{(H,H)} = 8.1$ Hz, 2 x CH), 128.6 (2 x CH), 127.7 (CH), 114.7 (d, $J_{(H,H)} = 21.4$ Hz, 2 x CH), 105.2 (C), 88.7 (C), 77.6 (CH), 48.4 (CH), 26.2 (3 x CH₃), 16.6 (C), -4.5 (2 x CH₃).

¹⁹F-NMR (282 MHz, CDCl₃, 25 °C): δ (ppm) = -114.5.

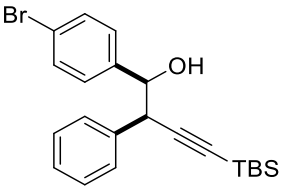
Syn-4-(tert-butyldimethylsilyl)-1-(4-chlorophenyl)-2-phenylbut-3-yn-1-ol (syn-3.3f)

	<p>Yield = 47%, 70 mg.</p> <p>White solid, mp = 74.8-76.0 °C.</p> <p>R_f (SiO₂) = 0.07 (Hexane : Ethyl acetate, 20:1).</p> <p>HRMS (EI) for C₂₂H₂₇NaOSi [M+Na]: Calc.: 393.1412; found: 393.1405.</p>
---	---

¹H-NMR (300 MHz, CDCl₃, 25 °C, TMS): δ (ppm) = 7.45-7.25 (m, 7H), 7.21 (d, $J_{(H,H)}$ = 8.5 Hz, 2H), 4.78 (d, $J_{(H,H)}$ = 7.1 Hz, 1H), 4.00 (d, $J_{(H,H)}$ = 7.1 Hz, 1H), 2.34 (s, 1H), 0.92 (s, 9H), 0.10 (s, 6H).

¹³C-NMR (75 MHz, CDCl₃, 25 °C): δ (ppm) = 139.1 (C), 137.2 (C), 133.6 (C), 128.8 (2 x CH), 128.5 (2 x CH), 128.4 (2 x CH), 127.9 (2 x CH), 127.6 (CH), 104.9 (C), 88.8 (C), 77.4 (C), 48.2 (CH), 26.0 (3 x CH₃), 16.5 (C), -4.6 (2 x CH₃).

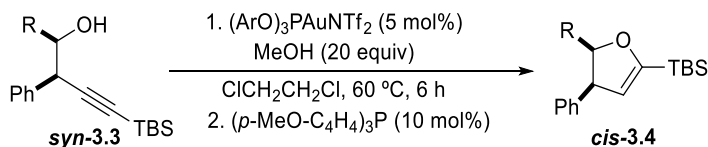
Syn-1-(4-Bromophenyl)-4-(tert-butyldimethylsilyl)-2-phenylbut-3-yn-1-ol (syn-3.3g)

	<p>Yield = 45%, 75 mg.</p> <p>White solid, mp = 73.9-75.3 °C.</p> <p>R_f (SiO₂) = 0.22 (Hexane : Ethyl acetate, 20:1).</p> <p>HRMS (EI) for C₂₂H₂₇BrNaOSi [M+Na]: Calc.: 437.0912; found: 437.0906.</p>
---	--

¹H-NMR (300 MHz, CDCl₃, 25 °C, TMS): δ (ppm) = 7.40 (d, $J_{(H,H)} = 8.3$ Hz, 2H), 7.34-7.19 (m, 5H), 7.13 (d, $J_{(H,H)} = 8.3$ Hz, 2H), 4.74 (d, $J_{(H,H)} = 6.8$ Hz, 1H), 3.97 (d, $J_{(H,H)} = 7.1$ Hz, 1H), 2.30 (s, 1H), 0.90 (s, 9H), 0.08 (s, 6H).

¹³C-NMR (75 MHz, CDCl₃, 25 °C): δ (ppm) = 139.7 (C), 137.3 (C), 131.0 (2 x CH), 128.9 (2 x CH), 128.9 (2 x CH), 128.6 (2 x CH), 127.8 (CH), 121.9 (C), 105.0 (C), 88.9 (C), 77.6 (CH), 48.2 (CH), 26.2 (3 x CH₃), 16.6 (C), -4.5 (2 x CH₃).

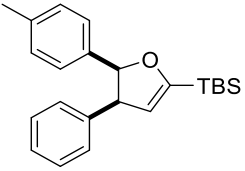
2.4.5 General procedure for the synthesis of *cis*-2-silyl-4,5-dihydrofurans *cis*-3.4



Scheme 5.25: Gold(I)-catalyzed synthesis of *cis*-dihydrofurans **cis-3.4**.

To a solution of 0.2 mmol of the corresponding *syn*-homopropargyl alcohol **syn-3.3** in 1 mL dry 1,2-dichloroethane were added 161 μL (128 mg; 4 mmol; 20 equivalents) of methanol followed by 11.2 mg of the gold catalyst (5 mol%). The reaction was heated at 60 °C for 6 hours. Then, 8.2 mg (0.02 mmol; 10 mol%) of $(p\text{-MeO-C}_6\text{H}_4)_3\text{P}$ was added. After cooling down, solvents were removed under vacuum. The residue was purified under deactivated aluminium oxide flash chromatography to obtain the corresponding *cis*-2-silyl-4,5-dihydrofurans **cis-3.4**.

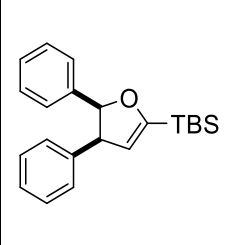
***Cis-tert*-butyldimethyl(4-phenyl-5-(*p*-tolyl)-4,5-dihydrofuran-2-yl)silane (*cis*-3.4a)**

	<p>Yield = 99%, 69 mg.</p> <p>Colorless oil.</p> <p>R_f (SiO₂) = 0.24 (Hexane : Ethyl acetate, 200:1).</p> <p>HRMS (EI) for C₂₃H₃₁OSi [M+H]: Calc.: 351.2139; found: 351.2127.</p>
---	---

¹H-NMR (300 MHz, CDCl₃, 25 °C, TMS): δ (ppm) = 7.30-6.95 (m, 2H), 6.93-6.78 (m, 7H), 5.76 (d, $J_{(H,H)} = 10.0$ Hz, 1H), 5.47 (d, $J_{(H,H)} = 2.6$ Hz, 1H), 4.29 (dd, $J_{(H,H)} = 10.0$ and 2.6 Hz, 1H), 2.20 (s, 3H), 1.10 (s, 9H), 0.26 (s, 3H), 0.24 (s, 3H).

¹³C-NMR (75 MHz, CDCl₃, 25 °C): δ (ppm) = 162.6 (C), 140.0 (C), 136.2 (C), 135.5 (C), 129.1 (2 x CH), 128.2 (2 x CH), 127.7 (2 x CH), 126.7 (2 x CH), 126.3 (CH), 117.6 (CH), 88.2 (CH), 54.4 (CH), 26.8 (3 x CH₃), 21.3 (CH₃), 16.7 (C), - 6.30 (2 x CH₃).

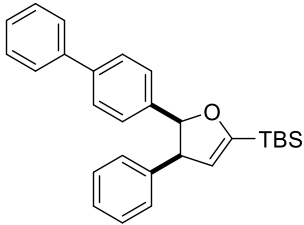
Cis-tert-butyl-dimethyl-4,5-diphenyl-4,5-dihydrofuran-2-yl)dimethylsilane (cis-3.4b)

	<p>Yield = 99%, 67 mg.</p> <p>Colorless oil.</p> <p>R_f (SiO₂) = 0.22 (Hexane : Ethyl acetate, 200:1).</p> <p>HRMS (EI) for C₂₂H₂₉OSi [M+H]: Calc.: 337.2139; found: 337.2127.</p>
---	---

¹H-NMR (300 MHz, CDCl₃, 25 °C, TMS): δ (ppm) = 7.11 – 6.94 (m, 8H), 6.92-6.83 (m, 2H), 5.79 (d, $J_{(H,H)} = 10.1$ Hz, 1H), 5.46 (d, $J_{(H,H)} = 2.7$ Hz, 1H), 4.30 (dd, $J_{(H,H)} = 10.1$ and 2.7 Hz, 1H), 1.08 (s, 9H), 0.27 (s, 3H), 0.24 (s, 3H).

¹³C-NMR (75 MHz, CDCl₃, 25 °C): δ (ppm) = 162.7 (C), 139.8 (C), 138.7 (C), 129.1 (2 x CH), 127.7 (2 x CH), 127.5 (2 x CH), 126.7 (3 x CH), 126.3 (CH), 117.6 (CH), 88.1 (CH), 54.6 (CH), 26.8 (3 x CH₃), 16.7 (C), -6.2 (CH₃), -6.3 (CH₃).

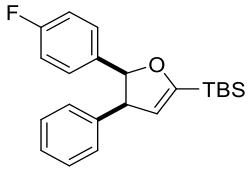
***Cis*-(5-([1,1'-biphenyl]-4-yl)-4-phenyl-4,5-dihydrofuran-2-yl)(*tert*-butyl)dimethylsilane (*cis*-3.4c)**

	<p>Yield = 96%, 79 mg. Colorless oil. R_f (SiO₂) = 0.16 (Hexane : Ethyl acetate, 200:1). HRMS (EI) for C₂₈H₃₃OSi [M+H]: Calc.: 413.2295; found: 413.2301.</p>
---	---

¹H-NMR (300 MHz, CDCl₃, 25 °C, TMS): δ (ppm) = 7.56-7.44 (m, 2H), 7.44-.28 (m, 5H), 7.15-.88 (m, 7H), 5.82 (d, $J_{(H,H)} = 10.0$ Hz, 1H), 5.48 (d, $J_{(H,H)} = 2.7$ Hz, 1H), 4.33 (dd, $J_{(H,H)} = 10.0$ and 2.7 Hz, 1H), 1.10 (s, 9H), 0.29 (s, 3H), 0.26 (s, 3H).

¹³C-NMR (75 MHz, CDCl₃, 25 °C): δ (ppm) = 162.7 (C), 141.1 (C), 139.7 (C), 139.4 (C), 137.9 (C), 129.1 (2 x CH), 128.7 (2 x CH), 127.8 (2 x CH), 127.2 (2 x CH), 127.1 (CH), 127.0 (2 x CH), 126.4 (CH), 126.2 (2 x CH), 117.6 (CH), 88.0 (CH), 54.6 (CH), 26.8 (3 x CH₃), 16.7 (C), -6.2 (CH₃), -6.3 (CH₃).

Cis-tert-butyl(5-(4-fluorophenyl)-4-phenyl-4,5-dihydrofuran-2-yl)dimethylsilane
(*cis-3.4e*)

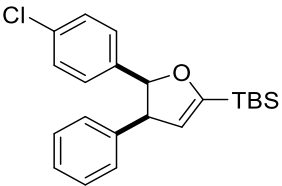
	<p>Yield = 98%, 69 mg.</p> <p>Colorless oil.</p> <p>R_f (SiO₂) = 0.31 (Hexane : Ethyl acetate, 200:1).</p> <p>HRMS (EI) for C₂₂H₂₈FOSi [M+H]: Calc.: 355.1888; found: 355.1889.</p>
---	---

¹H-NMR (300 MHz, CDCl₃, 25 °C, TMS): δ (ppm) = 7.13-6.96 (m, 5H), 6.92-6.85 (m, 2H), 6.83-6.71 (m, 2H), 5.78 (d, $J_{(H,H)} = 10.1$ Hz, 1H), 5.47 (d, $J_{(H,H)} = 2.7$, 1H), 4.30 (dd, $J_{(H,H)} = 10.1, 2.7$ Hz, 1H), 1.10 (s, 9H), 0.29 (s, 3H), 0.26 (s, 3H).

¹³C-NMR (75 MHz, CDCl₃, 25 °C): δ (ppm) = 162.7 (C), 161.7 (d, $J_{(H,H)} = 244.4$ Hz, C), 139.6 (C), 134.5 (d, $J_{(H,H)} = 3.2$ Hz, C), 129.0 (2 x CH), 128.3 (d, $J_{(H,H)} = 3.2$ Hz, 2x CH), 127.9 (2 x CH), 126.5 (CH), 117.5 (CH), 114.4 (d, $J_{(H,H)} = 21.3$ Hz, 2 x CH), 87.5 (CH), 54.5 (CH), 26.8 (3 x CH₃), 16.7 (C), -6.3 (CH₃), -6.3 (CH₃).

¹⁹F-NMR (282 MHz, CDCl₃, 25 °C): δ (ppm) = -116.0.

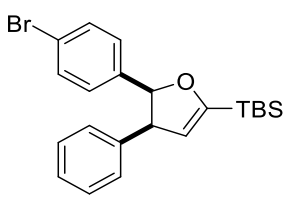
Cis-tert-butyl(5-(4-chlorophenyl)-4-phenyl-4,5-dihydrofuran-2-yl)dimethylsilane
(*cis*-3.4f)

	<p>Yield = 98%, 73 mg.</p> <p>Colorless oil.</p> <p>R_f (SiO₂) = 0.20 (Hexane : Ethyl acetate, 200:1).</p> <p>HRMS (EI) for C₂₂H₂₈ClOSi [M+H]: Calc.: 371.1592; found: 371.1595.</p>
---	--

¹H-NMR (300 MHz, CDCl₃, 25 °C, TMS): δ (ppm) = 7.11-7.00 (m, 5H), 6.99-6.91 (m, 2H), 6.89-6.82 (m, 2H), 5.73 (dd, $J_{(H,H)} = 10.1$ and 0.8 Hz, 1H), 5.45 (dd, $J_{(H,H)} = 2.7$ and 0.6 Hz, 1H), 4.29 (dd, $J_{(H,H)} = 10.1$ and 2.7 Hz, 1H), 1.07 (s, 9H), 0.26 (s, 3H), 0.24 (s, 3H).

¹³C-NMR (75 MHz, CDCl₃, 25 °C): δ (ppm) = 162.6 (C), 139.4 (C), 137.3 (C), 132.4 (C), 129.0 (2 x CH), 128.1 (2 x CH), 127.9 (2 x CH), 127.7 (2 x CH), 126.6 (CH), 117.6 (CH), 87.4 (CH), 54.5 (CH), 26.8 (3 x CH₃), 16.7 (C), -6.3 (CH₃), -6.3 (CH₃).

Cis-tert-butyl(dimethyl(5-(*p*-bromophenyl)-4-phenyl-4,5-dihydrofuran-2-yl)silane (cis-3.4g)

	<p>Yield = 99%, 82 mg.</p> <p>Colorless oil.</p> <p>R_f (SiO₂) = 0.21 (Hexane : Ethyl acetate, 200:1).</p> <p>HRMS (EI) for C₂₂H₂₈BrOSi [M+H]: Calc.: 415.1093; found: 415.1087.</p>
---	--

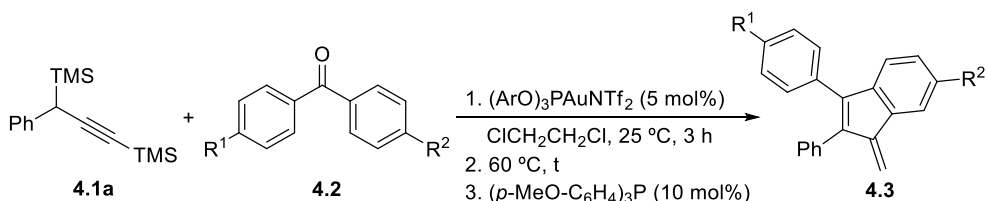
¹H-NMR (300 MHz, CDCl₃, 25 °C, TMS): δ (ppm) = 7.21 (d, $J_{(H,H)}$ = 8.5 Hz, 2H), 7.14-7.00 (m, 3H), 6.99-6.81 (m, 4H), 5.73 (d, $J_{(H,H)}$ = 10.1 Hz, 1H), 5.46 (dd, $J_{(H,H)}$ = 2.7 and 0.5 Hz, 1H), 2H), 4.30 (dd, $J_{(H,H)}$ = 10.1 and 2.7 Hz, 1H), 1.08 (s, 9H), 0.27 (s, 3H), 0.25 (s, 3H).

¹³C-NMR (75 MHz, CDCl₃, 25 °C): δ (ppm) = 162.6 (C), 139.4 (C), 137.8 (C), 130.6 (2 x CH), 129.0 (2 x CH), 128.5 (2 x CH), 127.9 (2 x CH), 126.7 (CH), 120.5 (C), 117.7 (CH), 87.4 (CH), 54.4 (CH), 26.8 (3 x CH₃), 16.7 (C), - 6.3 (CH₃), - 6.3 (CH₃).

2.5 Experimental procedures described in Chapter IV

2.5.1 Experimental procedure for the synthesis of benzofulvenes **3** or **9** from benzophenones **2**.

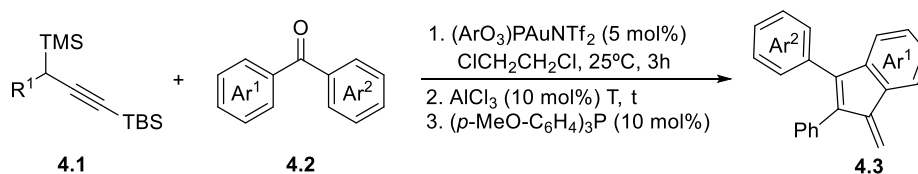
- In absence of aluminium trichloride.



Scheme 5.26: Gold-catalyzed one-pot synthesis of benzofulvene derivatives **4.3**.

To a mixture of 0.60 mmol of propargylsilane **4.1a** and 0.20 mmol of benzophenone **4.2**, prepared in dry 1,2-dichloroethane (1 mL) at 25 °C and under argon atmosphere, 11.2 mg (0,01 mmol, 5 mol%) of tris(2,4-di-*t*-butylphenyl)phosphitegold(I) triflimidate were added and the reaction stirred at 60 °C for the period described in Scheme 4.14. Finally, 7.0 mg of $(p\text{-MeO-C}_6\text{H}_4)_3\text{P}$ (0.02 mmol, 10 mol%) were added to deactivate gold catalyst and the solvent was removed under vacuum. The residue was purified under flash chromatography yielding the corresponding benzofulvenes **4.3**.

- Cocatalyzed by gold(I) and aluminium chloride.

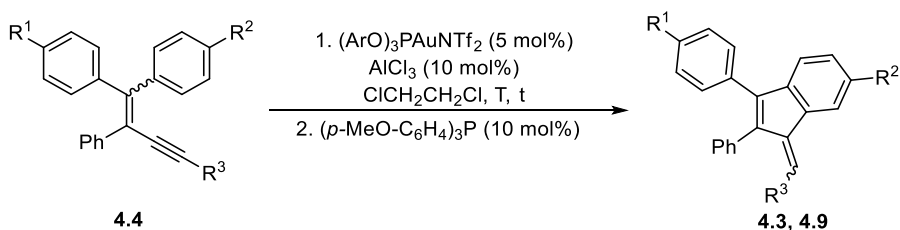


Scheme 5.27: Gold-aluminium-catalyzed one-pot synthesis of benzofulvene derivatives **4.3**.

To a dry 1,2-dichloroethane solution (1 mL), under argon atmosphere at 25 °C, 0.24 mmol (0,72 mmol for **3c**) of propargylsilane **4.1**, 0.20 mmol of benzophenone **4.2** and 11.2 mg (0,01 mmol, 5 mol%) of gold catalyst were added. The mixture was stirred for 3 hours at 25 °C (60 °C for compounds **4.3p-r**). Next, 2.6 mg (0.02 mmol,

10 mol%) of aluminum trichloride were added and the mixture stirred under the conditions described in Schemes 4.18-4.19. Finally, 7.0 mg of (*p*-MeO-C₆H₄)₃P (0.02 mmol, 10 mol%) were added and the solvent was removed under vacuum. After purification through a chromatographic column, corresponding benzofulvenes **4.3** were obtained.

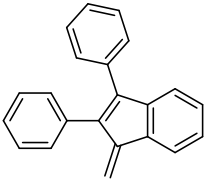
- From 1,3-enynes 5.



Scheme 5.28: Gold-aluminum-catalyzed cyclization of enynes **4.4**.

To a mixture of 0.20 mmol of 1,3-enyne **4.4** in dry 1,2-dichloroethane (1 mL) 11.2 mg (0.01 mmol, 5 mol%) of the gold catalyst were added and the reaction stirred under the conditions described in Schemes 4.23-4.24. Next, 7.0 mg of (*p*-MeO-C₆H₄)₃P (0.02 mmol, 10 mol%) were added and the solvent was removed under vacuum. The residue was purified under flash chromatography yielding the corresponding benzofulvenes **4.3** or **4.9**.

1-Methylene-2,3-diphenyl-1H-indene (4.3a)

	<p>Yield = 99%, 55 mg.</p> <p>Bright yellow solid. Slightly decomposes on exposure to air and no mp can be measured.</p> <p>R_f (SiO₂) = 0.22 (Hexane).</p>
---	---

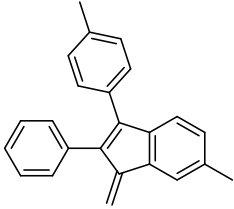
¹H-NMR (300 MHz, CDCl₃, 25 °C, TMS): δ (ppm) = 7.77 (m, 1H), 7.47-7.19 (m, 13H), 6.31 (s, 1H), 5.78 (s, 1H).

¹³C-NMR (75 MHz, CDCl₃, 25 °C): δ (ppm) = 147.6 (C), 142.7 (C), 141.9 (C), 137.5 (C), 136.2 (C), 134.6 (C), 134.6 (C), 130.8 (2 x CH), 129.5 (2 x CH), 128.3 (2 x CH), 128.2 (CH), 128.0 (2 x CH), 127.5 (CH), 127.0 (CH), 125.7 (CH), 120.8 (CH), 119.9 (CH), 114.2 (CH₂).

Experimental data in agreement with scientific literature⁵

⁵ Patureau, F. W.; Besset, T.; Kuhl, N.; Glorius, F. *J. Am. Chem. Soc.*, **2011**, *133*, 2154–2156

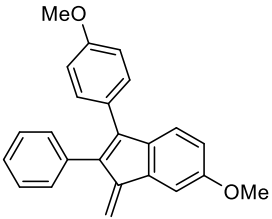
6-Methyl-1-methylene-2-phenyl-3-(*p*-tolyl)-1*H*-indene (4.3b)

	<p>Yield = 97%, 60 mg.</p> <p>Bright yellow solid. Slightly decomposes on exposure to air and no mp can be measured.</p> <p>R_f (SiO₂) = 0.21 (Hexane).</p> <p>HRMS for C₂₄H₂₀ [M]: Calc.: 308.1560; found: 308.1559.</p>
---	---

¹H-NMR (300 MHz, CDCl₃, 25 °C, TMS): δ (ppm) = 7.55 (d $J_{(H,H)} = 1.7$ Hz, 1H), 7.42-7.19 (m, 8H), 7.19-7.07 (m, 3H), 6.21 (s, 1H), 5.68 (s, 1H), 2.46 (s, 3H), 2.36 (s, 3H).

¹³C-NMR (75 MHz, CDCl₃, 25 °C): δ (ppm) = 147.8 (C), 141.9 (C), 140.4 (C), 137.2 (C), 136.7 (C), 136.5 (C), 135.6 (C), 135.1 (C), 131.8 (C), 130.9 (2 x CH), 129.4 (2 x CH), 129.1 (2 x CH), 128.9 (CH), 128.1 (2 x CH), 126.9 (CH), 120.8 (CH), 120.0 (CH), 113.4 (CH₂), 21.7 (CH₃), 21.5 (CH₃).

6-Methoxy-3-(4-methoxyphenyl)-1-methylene-2-phenyl-1*H*-indene (4.3c)

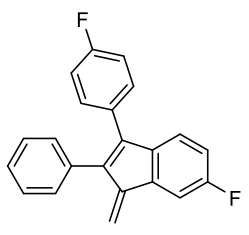
	<p>Yield = 78%, 53 mg.</p> <p>Bright yellow solid. Slightly decomposes on exposure to air and no mp can be measured.</p> <p>R_f (SiO₂) = 0.36 (Hexane : Ethyl acetate, 10:1).</p>
---	---

¹H-NMR (300 MHz, CDCl₃, 25 °C, TMS): δ (ppm) = 7.38-7.10 (m, 9H), 6.95-6.80(m, 3H), 6.19 (s, 1H), 5.69 (s, 1H), 3.91 (s, 3H), 3.83 (s, 3H).

¹³C-NMR (75 MHz, CDCl₃, 25 °C): δ (ppm) = 159.0 (C), 158.9 (C), 147.7 (C), 141.5 (C), 138.4 (C), 136.1 (C), 135.3 (C), 135.2 (C), 130.9 (2 x CH), 130.7 (2 x CH), 128.2 (2 x CH), 127.1 (C), 126.8 (CH), 120.8 (CH), 113.8 (2 x CH), 113.1 (CH), 113.1 (CH₂), 106.8 (CH), 55.9 (CH₃), 55.3 (CH₃).

Experimental data in agreement with scientific literature. ⁵

6-Fluoro-3-(4-fluorophenyl)-1-methylene-2-phenyl-1H-indene (4.3d)

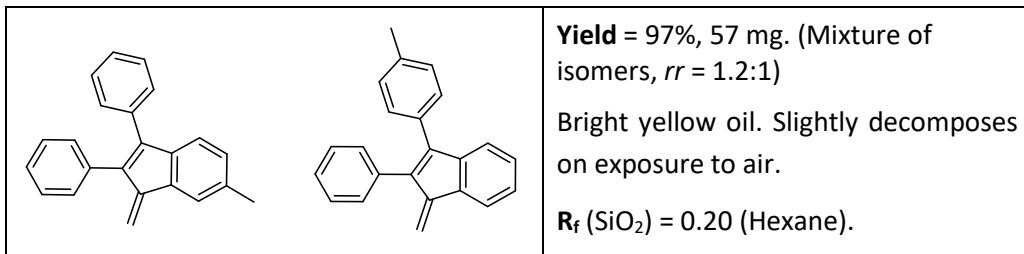
	<p>Yield = 96%, 61 mg.</p> <p>Bright yellow solid. Slightly decomposes on exposure to air and no mp can be measured.</p> <p>R_f (SiO₂) = 0.20 (Hexane).</p> <p>HRMS for C₂₂H₁₄F₂ [M]: Calc.: 316.1058; found: 316.1060.</p>
---	---

¹H-NMR (300 MHz, CDCl₃, 25 °C, TMS): δ (ppm) = 7.42 (dd, $J_{(H,H)}$ = 8.6 and 2.5 Hz, 1H), 7.38-7.14 (m, 8H), 7.14-6.90 (m, 3H), 6.25 (s, 1H), 5.78 (s, 1H).

¹³C-NMR (75 MHz, CDCl₃, 25 °C): δ (ppm) = 162.2 (d, $J(C-F)$ = 247 Hz, C), 162.1 (d, $J(C-F)$ = 244 Hz, C), 146.8 (d, $J(C-F)$ = 2 Hz, C), 140.3 (d, $J(C-F)$ = 1 Hz, C), 138.4 (d, $J(C-F)$ = 2 Hz, C), 138.2 (d, $J(C-F)$ = 9 Hz, C), 137.5 (d, $J(C-F)$ = 4 Hz, C), 134.2 (C), 131.1 (d, $J(C-F)$ = 6 Hz, 2 x CH), 130.6 (2 x CH), 130.2 (d, $J(C-F)$ = 3 Hz, C), 128.2 (2 x CH), 127.2 (CH), 120.6 (d, $J(C-F)$ = 8 Hz, CH), 115.4 (d, $J(C-F)$ = 22 Hz, 2 x CH), 115.2 (CH₂), 114.3 (d, $J(C-F)$ = 17 Hz, CH), 107.7 (d, $J(C-F)$ = 14 Hz, CH).

¹⁹F-NMR (282 MHz, CDCl₃, 25 °C): δ (ppm) = -113.7, -116.9.

6-Methyl-1-methylene-2,3-diphenyl-1H-indene or 1-Methylene-2-phenyl-3-(p-tolyl)-1H-indene (4.3e)



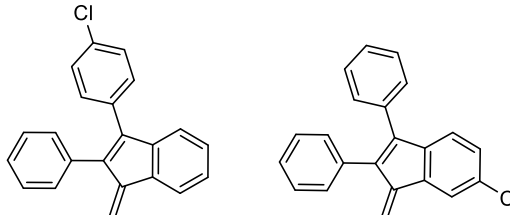
¹H-NMR (300 MHz, CDCl₃, 25 °C, TMS): δ (ppm) = 7.75 (m, 1H), 7.57 (m, 1H), 7.49-7.20 (m, 21H), 7.18-7.11 (m, 3H), 6.27 (s, 1H), 6.25 (s, 1H), 5.74 (s, 1H), 5.72 (s, 1H), 2.48 (s, 3H), 2.38 (s, 3H).

¹³C-NMR (75 MHz, CDCl₃, 25 °C): δ (ppm) = 147.8 (C), 147.8 (C), 142.9 (C), 142.0 (C), 140.3 (C), 137.3 (C), 137.2 (C), 136.8 (C), 136.7 (C), 136.4 (C), 135.6 (C), 135.6 (C), 135.0 (C), 134.9 (C), 134.8 (C), 131.6 (C), 130.9 (2 x CH), 130.9 (2 x CH), 129.6 (2 x CH), 129.5 (2 x CH), 129.1 (2 x CH), 128.9 (CH), 128.3 (2 x CH), 128.3 (CH), 128.1 (2 x CH), 128.1 (2 x CH), 127.5 (CH), 127.0 (CH), 127.0 (CH), 125.7 (CH), 120.9 (CH), 120.3 (CH), 120.0 (CH), 119.9 (CH), 113.9 (CH₂), 113.7 (CH₂), 21.7 (CH₃), 21.5 (CH₃).

Experimental data in agreement with scientific literature.⁶

⁶ Zhou, B.; Wu, Z.; Qi, W.; Sun, X.; Zhang, Y. *Adv. Synth. Catal.* **2018**, *360*, 4480-4484.

3-(4-Chlorophenyl)-1-methylene-2-phenyl-1H-indene or 6-Chloro-1-methylene-2,3-diphenyl-1H-indene (4.3f)

	<p>Yield = 99%, 62 mg. (Mixture of isomers, <i>rr</i> = 1.6:1)</p> <p>Bright yellow oil. Slightly decomposes on exposure to air.</p> <p>R_f (SiO₂) = 0.21 (Hexane).</p>
---	--

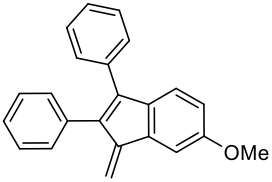
¹H-NMR (300 MHz, CDCl₃, 25 °C, TMS): δ (ppm) = 7.80 (m, 1H), 7.72 (t, $J_{(H,H)} = 1.4$ Hz, 1H), 7.42-7.19 (m, 24H), 6.33 (s, 1H), 6.29 (s, 1H), 5.83 (s, 1H), 5.80 (s, 1H).

¹³C-NMR (75 MHz, CDCl₃, 25 °C): δ (ppm) = 147.6 (C), 146.9 (C), 142.4 (C), 141.4 (C), 141.2 (C), 140.7 (C), 138.1 (C), 138.0 (C), 137.8 (C), 136.3 (C), 134.4 (C), 134.3 (C), 134.2 (C), 133.4 (C), 133.2 (C), 131.7 (C), 130.9 (2 x CH), 130.8 (2 x CH), 130.9 (2 x CH), 130.8 (2 x CH), 129.5 (CH), 128.7 (CH), 128.5 (CH), 128.4 (CH), 128.3 (2 x CH), 128.2 (2 x CH), 128.1 (CH), 127.8 (CH), 127.3 (CH), 127.3 (CH), 126.0 (CH), 121.1 (CH), 120.5 (CH), 120.1 (2 x CH), 120.0 (2 x CH), 115.5 (CH₂), 114.7 (CH₂).

Experimental data in agreement with scientific literature.⁷

⁷ Yu, Y.; Wu, Q.; Liu, D.; Hu, L.; Yu, L.; Ze Tan, L.; Zhu, G. *J. Org. Chem.* **2019**, *84*, 7449-7458.

6-Methoxy-1-methylene 2,3-diphenyl-1H-indene (4.3g)

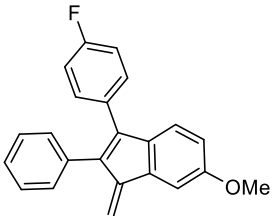
	<p>Yield = 96%, 61 mg. (Mixture of isomers, <i>rr</i> = 6.0:1)</p> <p>Bright yellow solid. Slightly decomposes on exposure to air.</p> <p>R_f (SiO₂) = 0.34 (Hexane : Ethyl acetate, 20:1).</p> <p>HRMS for C₂₂H₁₄F₂ [M]: Calc.: 316.1058; found: 316.1060.</p>
---	---

¹H-NMR (300 MHz, CDCl₃, 25 °C, TMS): δ (ppm) (*Major isomer*) = 7.45-7.15 (m, 11H), 6.86 (dd, $J_{(H,H)} = 8.2$ and 2.6 Hz, 2H), 6.24 (s, 1H), 5.73 (s, 1H), 3.90 (s, 3H).

¹³C-NMR (75 MHz, CDCl₃, 25 °C): δ (ppm) (*Major isomer*) = 158.9 (C), 147.7 (C), 141.9 (C), 138.2 (C), 136.0 (C), 136.0 (CH), 134.9 (C), 134.8 (C), 130.8 (2 x CH), 129.5 (2 x CH), 128.3 (2 x CH), 128.1 (2 x CH), 127.5 (CH), 126.9 (CH), 120.8 (CH), 113.7 (CH), 113.2 (CH), 106.9 (CH), 55.9 (CH₃).

Experimental data in agreement with scientific literature^[1]

3-(4-Fluorophenyl)-6-methoxy-1-methylene-2-phenyl-1H-indene (4.3h)

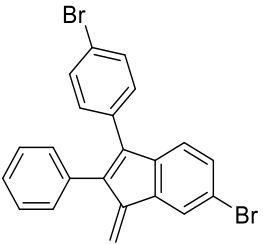
	<p>Yield = 95%, 62 mg.</p> <p>Bright yellow solid. Slightly decomposes on exposure to air and no mp can be measured.</p> <p>R_f (SiO₂) = 0.32 (Hexane : Ethyl acetate, 20:1).</p> <p>HRMS for C₂₃H₁₇FO [M]: Calc.: 328.1258; found: 328.1253.</p>
---	--

¹H-NMR (300 MHz, CDCl₃, 25 °C, TMS): δ (ppm) = 7.35-7.22 (m, 6H), 7.21-7.14 (m, 2H), 7.05-6.94 (m, 2H), 6.85 (dd, $J_{(H,H)} = 8.3$ and 2.4 Hz, 2H), 6.21 (s, 1H), 5.70 (s, 1H), 3.89 (s, 3H).

¹³C-NMR (75 MHz, CDCl₃, 25 °C): δ (ppm) = 162.2 (d, $J_{(C,F)} = 247$ Hz, C), 159.0 (C), 147.6 (C), 140.8 (C), 138.2 (C), 136.2 (C), 135.8 (C), 134.7 (C), 131.2 (d, $J_{(C,F)} = 8$ Hz, 2 x CH), 130.8 (C), 130.8 (2 x CH), 128.2 (2 x CH), 127.0 (CH), 120.6 (CH), 115.4 (d, $J_{(C,F)} = 21$ Hz, 2 x CH), 113.9 (CH₂), 113.2 (CH), 106.9 (CH), 55.9 (CH₃).

¹⁹F-NMR (282 MHz, CDCl₃, 25 °C): δ (ppm) = -113.9.

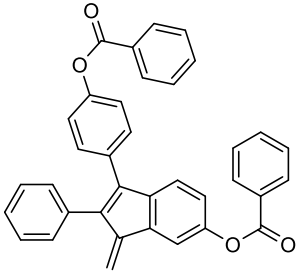
6-Bromo-3-(4-bromophenyl)-1-methylene-2-phenyl-1H-indene (4.3i)

	<p>Yield = 98%, 86 mg.</p> <p>Bright yellow solid. Slightly decomposes on exposure to air and no mp can be measured.</p> <p>R_f (SiO₂) = 0.21 (Hexane).</p> <p>HRMS for C₂₂H₁₄Br₂ [M]: Calc.: 435.9457; found: 435.9458.</p>
---	--

¹H-NMR (300 MHz, CDCl₃, 25 °C, TMS): δ (ppm) = 7.83 (d, $J_{(H,H)} = 1.8$ Hz, 1H), 7.50-7.40 (m, 3H), 7.39-7.28 (m, 3H), 7.23-7.09 (m, 5H), 6.28 (s, 1H), 5.81 (s, 1H).

¹³C-NMR (75 MHz, CDCl₃, 25 °C): δ (ppm) = 146.7 (C), 141.1 (C), 140.2 (C), 138.3 (C), 138.2 (C), 133.9 (C), 133.1 (C), 131.8 (2 x CH), 131.1 (2 x CH), 131.1 (CH), 130.7 (2 x CH), 128.4 (2 x CH), 127.5 (CH), 123.5 (CH), 121.9 (C), 121.2 (CH), 119.8 (C), 116.1 (CH₂).

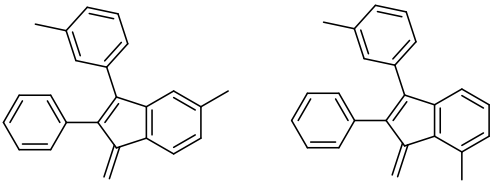
4-(6-(Benzoyloxy)-1-methylene-2-phenyl-1H-inden-3-yl)phenyl benzoate (4.3j)

	<p>Yield = 97%, 101 mg.</p> <p>Bright yellow solid. Slightly decomposes on exposure to air and no mp can be measured.</p> <p>R_f (SiO₂) = 0.18 (Hexane : Ethyl acetate, 10:1).</p> <p>HRMS for C₃₆H₂₅O₄ [M+H]: Calc.: 521.1747; found: 521.1749.</p>
---	--

¹H-NMR (300 MHz, CDCl₃, 25 °C, TMS): δ (ppm) = 8.27-8.11 (m, 4H), 7.64-7.05 (m, 18H), 6.20 (s, 1H), 5.73 (s, 1H).

¹³C-NMR (75 MHz, CDCl₃, 25 °C): δ (ppm) = 165.6 (C), 165.1 (C), 150.4 (C), 149.7 (C), 147.1 (C), 140.6 (C), 140.3 (C), 138.2 (C), 137.7 (C), 134.3 (C), 133.7 (CH), 133.7 (CH), 132.1 (C), 130.8 (2 x CH), 130.6 (2 x CH), 130.3 (2 x CH), 130.2 (2 x CH), 129.7 (C), 129.6 (C), 128.7 (4 x CH), 128.3 (2 x CH), 127.3 (CH), 121.8 (2 x CH), 121.4 (CH), 120.6 (CH), 115.4 (CH₂), 114.1 (CH).

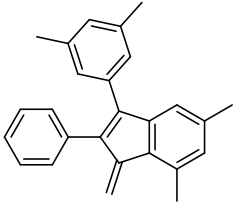
5-Methyl-1-methylene-2-phenyl-3-(*m*-tolyl)-1*H*-indene or 7-methyl-1-methylene-2-phenyl-3-(*m*-tolyl)-1*H*-indene(4.3k)

	<p>Yield = 96%, 59 mg. (Mixture of isomers, <i>rr</i> = 2.8:1)</p> <p>Bright yellow solid. Slightly decomposes on exposure to air and no mp can be measured.</p> <p>R_f (SiO₂) = 0.21 (Hexane).</p> <p>HRMS for C₂₄H₂₁ [M+H]: Calc.: 309.1638; found: 309.1636.</p>
---	--

¹H-NMR (300 MHz, CDCl₃, 25 °C, TMS): δ (ppm) (*Major isomer*) = 7.40-6.95 (m, 12H), 6.29 (s, 1H), 5.69 (s, 1H), 2.67 (s, 3H), 2.32 (s, 3H).

¹³C-NMR (75 MHz, CDCl₃, 25 °C): δ (ppm) (*Major isomer*) = 149.2 (C), 143.4 (C), 141.4 (C), 138.5 (C), 137.7 (C), 135.0 (C), 134.7 (C), 133.8 (C), 132.7 (C), 131.1 (CH), 131.1 (CH), 130.3 (CH), 129.1 (CH), 128.1 (2 x CH), 128.1 (CH), 128.0 (2 x CH), 127.8 (CH), 127.0 (CH), 126.9 (CH), 118.6 (CH₂), 21.6 (CH₃), 21.2 (CH₃).

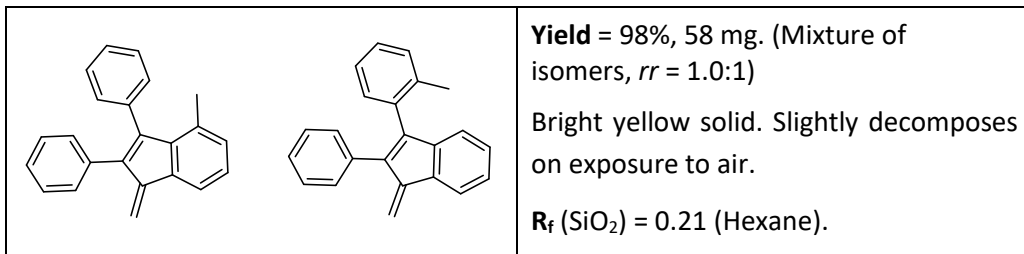
5,7-Dimethyl-1-methylene-3-(3,5-dimethylphenyl)-2-phenyl-1H-indene (4.3I)

	<p>Yield = 98%, 66 mg.</p> <p>Bright yellow solid. Slightly decomposes on exposure to air and no mp can be measured.</p> <p>R_f (SiO₂) = 0.23 (Hexane).</p> <p>HRMS for C₂₆H₂₄ [M]: Calc.: 336.1873; found: 336.1875.</p>
---	---

¹H-NMR (300 MHz, CDCl₃, 25 °C, TMS): δ (ppm) = 7.36-7.17 (m, 5H), 7.04 (s, 1H), 6.92 (s, 2H), 6.89 (s, 2H), 6.21 (s, 1H), 5.76 (s, 1H), 2.62 (s, 3H), 2.38 (s, 3H), 2.26 (s, 6H).

¹³C-NMR (75 MHz, CDCl₃, 25 °C): δ (ppm) = 149.0 (C), 144.1 (C), 141.5 (C), 138.7 (C), 137.8 (C), 137.6 (2 x C), 135.1 (C), 134.8 (C), 133.5 (C), 131.1 (2 x CH), 130.2 (C), 129.7 (CH), 129.1 (CH), 127.9 (2 x CH), 127.5 (2 x CH), 126.8 (CH), 119.4 (CH), 117.5 (CH₂), 21.7 (CH₃), 21.5 (2 x CH₃), 21.0 (CH₃).

4-Methyl-1-methylene-2,3-diphenyl-1H-indene or 1-methylene-2-phenyl-3-(o-tolyl)-1H-indene (4.3m)

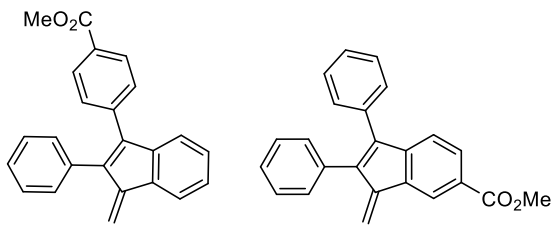


¹H-NMR (300 MHz, CDCl₃, 25 °C, TMS): δ (ppm) = 7.81-7.72 (m, 1H), 7.64 (d, $J_{(H,H)}$ = 7.4 Hz, 1H), 7.38-7.17 (m, 1H), 7.08 (d, $J_{(H,H)}$ = 7.4 Hz, 1H), 7.08 (m, 1H), 6.32 (s, 1H), 6.28 (s, 1H), 5.87 (s, 1H), 5.71 (s, 1H), 2.05 (s, 3H), 1.95 (s, 3H).

¹³C-NMR (75 MHz, CDCl₃, 25 °C): δ (ppm) = 147.6 (C), 147.3 (C), 144.1 (C), 143.6 (C), 142.7 (C), 140.6 (C), 138.7 (C), 137.9 (C), 137.6 (C), 136.8 (C), 136.3 (C), 136.1 (C), 134.9 (C), 134.6 (C), 134.4 (C), 131.7 (CH), 131.6 (C), 130.8 (2 x CH), 130.3 (CH), 130.2 (2 x CH), 130.0 (CH), 129.8 (2 x CH), 128.4 (CH), 128.1 (2 x CH), 128.0 (2 x CH), 127.8 (2 x CH), 127.7 (CH), 127.2 (CH), 127.0 (CH), 126.8 (CH), 125.7 (2 x CH), 125.6 (CH), 120.3 (CH), 119.8 (CH), 117.7 (CH), 114.1 (CH₂), 114.1 (CH₂), 20.2 (CH₃), 20.1 (CH₃).

Experimental data in accordance with literature.⁵

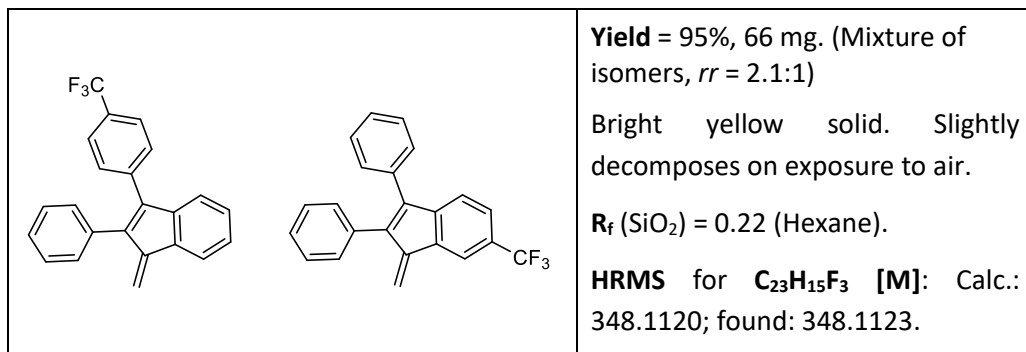
Methyl 4-(1-methylene-2-phenyl-1*H*-inden-3-yl)benzoate or methyl 1-methylene-2,3-diphenyl-1*H*-indene-6-carboxylate (4.3n)

	<p>Yield = 93%, 63 mg. (Mixture of isomers, <i>rr</i> = 2.5:1)</p> <p>Bright yellow solid. Slightly decomposes on exposure to air.</p> <p>R_f (SiO₂) = 0.10 (Hexane : Ethyl acetate, 40:1).</p> <p>HRMS for C₂₄H₁₉O₂ [M+H]: Calc.: 339.185; found: 339.1378.</p>
---	--

¹H-NMR (300 MHz, CDCl₃, 25 °C, TMS): δ (ppm) (*Major isomer*) = 7.94 (d, $J_{(H,H)} = 1.9$ Hz, 2H), 7.70 (m, 1H), 7.43-7.07 (m, 10H), 6.26 (s, 1H), 5.73 (s, 1H), 3.87 (s, 3H).

¹³C-NMR (75 MHz, CDCl₃, 25 °C): δ (ppm) (*Major isomer*) = 167.1 (C), 147.6 (C), 142.2 (C), 139.7 (C), 138.8 (C), 136.2 (C), 136.2 (C), 134.3 (C), 130.8 (2 x CH), 129.7 (2 x CH), 129.6 (2 x CH), 129.1 (C), 128.5 (CH), 128.3 (2 x CH), 127.4 (CH), 126.0 (CH), 120.1 (CH), 120.0 (CH), 115.2 (CH₂), 52.2 (CH₃).

1-Methylene-2,3-diphenyl-6-(trifluoromethyl)-1H-indene or 1-methylene-2-phenyl-3-(4-(trifluoromethyl)phenyl)-1H-indene (4.3o)

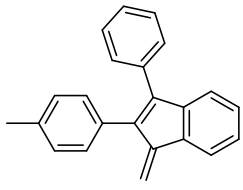


¹H-NMR (300 MHz, CDCl₃, 25 °C, TMS): δ (ppm) (*Major isomer*) = 7.77 (m, 1H), 7.59 (d, $J_{(H,H)} = 8.3$ Hz, 2H), 7.43 (d, $J_{(H,H)} = 8.3$ Hz, 2H), 7.40-7.17 (m, 8H), 6.34 (s, 1H), 5.79 (s, 1H).

¹³C-NMR (75 MHz, CDCl₃, 25 °C): δ (ppm) (*Major isomer – selected signals*) = 147.4 (C), 142.1 (C), 140.3 (C), 138.7 (C), 138.4 (C), 136.0 (C), 134.0 (C), 130.8 (2 x CH), 129.7 (2 x CH), 128.4 (CH), 128.2 (2 x CH), 127.3 (CH), 126.0 (CH), 125.2 (q, $J(C-F) = 4$ Hz, 2 x CH), 120.0 (CH), 119.8 (CH), 115.3 (CH₂).

¹⁹F-NMR (282 MHz, CDCl₃, 25 °C): δ (ppm) (*Major isomer*) = -62.5.

1-Methylene-3-phenyl-2-(*p*-tolyl)-1*H*-indene (4.3p)

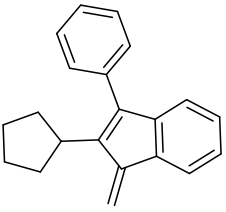
	<p>Yield = 95%, 56 mg.</p> <p>Bright yellow solid. Slightly decomposes on exposure to air and no mp can be measured.</p> <p>R_f (SiO₂) = 0.21 (Hexane).</p> <p>HRMS for C₂₃H₁₅F₃ [M]: Calc.: 348.1120; found: 348.1123.</p>
---	--

¹H-NMR (300 MHz, CDCl₃, 25 °C, TMS): δ (ppm) = 7.84-7.67 (m, 1H), 7.49-7.23 (m, 8H), 7.14 (s, 4H), 6.29 (s, 1H), 5.78 (s, 1H), 2.38 (s, 3H).

¹³C-NMR (75 MHz, CDCl₃, 25 °C): δ (ppm) = 147.7 (C), 142.9 (C), 141.6 (C), 137.5 (C), 136.7 (C), 136.3 (C), 134.8 (C), 131.6 (C), 130.7 (2 x CH), 129.6 (2 x CH), 128.9 (2 x CH), 128.4 (2 x CH), 128.3 (CH), 127.5 (CH), 125.7 (CH), 120.1 (CH), 119.9 (CH), 114.3 (CH₂), 21.4 (CH₃).

Experimental data in agreement with scientific literature.⁵

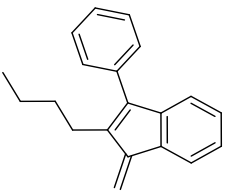
2-Cyclopentyl-1-methylene-3-phenyl-1H-indene (4.3q)

	<p>Yield = 90%, 50 mg.</p> <p>Bright yellow oil. Slightly decomposes on exposure to air.</p> <p>R_f (SiO₂) = 0.45 (Hexane).</p> <p>HRMS for C₂₁H₂₁ [M+H]: Calc.: 273.1638; found: 273.1638.</p>
---	---

¹H-NMR (300 MHz, CDCl₃, 25 °C, TMS): δ (ppm) = 7.0 (m, 1H), 7.53-7.44 (m, 2H), 7.39 (m, 3H), 7.25-7.09 (m, 2H), 7.01 (m, 1H), 6.18 (s, 1H), 5.88 (s, 1H), 3.18 (p, $J_{(H,H)}$ = 9.3 Hz, 1H), 2.03-1.73 (m, 6H), 1.72-1.57 (m, 2H).

¹³C-NMR (75 MHz, CDCl₃, 25 °C): δ (ppm) = 145.6 (C), 143.5 (C), 142.6 (C), 140.2 (C), 136.8 (C), 135.6 (C), 129.2 (2 x CH), 128.5 (2 x CH), 128.1 (CH), 127.6 (CH), 125.1 (CH), 119.4 (CH), 119.2 (CH), 112.4 (CH₂), 38.1(CH), 34.2 (2 x CH₂), 27.0 (2 x CH₂).

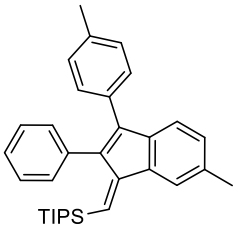
2-Butyl-1-methylene-3-phenyl-1H-indene (4.3r)

	<p>Yield = 93%, 48 mg.</p> <p>Bright yellow oil. Slightly decomposes on exposure to air.</p> <p>R_f (SiO₂) = 0.44 (Hexane).</p> <p>HRMS for C₂₀H₂₁ [M+H]: Calc.: 261.1638; found: 261.1628.</p>
---	---

¹H-NMR (300 MHz, CDCl₃, 25 °C, TMS): δ (ppm) = 7.68 (m, 1H), 7.60-7.40 (m, 5H), 7.33-7.14 (m, 3H), 6.18 (s, 1H), 5.85 (s, 1H), 2.70-2.57 (m, 2H), 1.71-1.52 (m, 2H), 1.44-1.31 (m, 2H), 0.92 (t, $J_{(H,H)}$ = 7.3 Hz, 3H).

¹³C-NMR (75 MHz, CDCl₃, 25 °C): δ (ppm) = 147.6 (C), 143.7 (C), 141.6 (C), 138.0 (C), 136.2 (C), 135.2 (C), 128.9 (2 x CH), 128.6 (2 x CH), 128.1 (CH), 127.5 (CH), 125.0 (CH), 119.5 (CH), 119.4 (CH), 111.1 (CH₂), 33.9 (CH₂), 24.9 (CH₂), 23.0 (CH₂), 14.0 (CH₃).

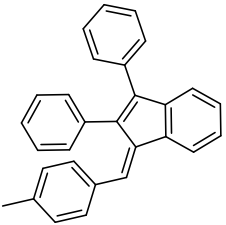
(E)-1-(4-triisopropylsilylmethylidene)-2,3-diphenyl-1H-indene (4.9a)

	<p>Yield = 97%, 90 mg.</p> <p>Bright yellow solid. Slightly decomposes on exposure to air. mp = 155.8-157.5 °C.</p> <p>R_f (SiO₂) = 0.50 (Hexane : Ethyl acetate, 40:1).</p> <p>HRMS for C₃₃H₄₀NaSi [M+Na]: Calc.: 487.2791; found: 487.27984.</p>
---	---

¹H-NMR (300 MHz, CDCl₃, 25 °C, TMS): δ (ppm) = 7.53 (s, 1H), 7.33-7.03 (m, 11H), 6.98 (s, 1H), 2.51 (s, 3H), 2.34 (s, 3H), 1.03 (s, 9H), 1.00 (s, 9H), 0.55 (dq, $J_{(H,H)} = 15.1$ and 7.5 Hz, 3H).

¹³C-NMR (75 MHz, CDCl₃, 25 °C): δ (ppm) = 156.0 (C), 145.4 (C), 139.3 (C), 138.8 (C), 138.0 (C), 137.2 (C), 136.8 (C), 135.8 (C), 132.2 (C), 131.9 (2 x CH), 129.6 (2 x CH), 129.1 (2 x CH), 128.7 (CH), 128.6 (CH), 128.0 (2 x CH), 127.4 (CH), 120.3 (CH), 120.0 (CH), 22.1 (CH₃), 21.8 (CH₃), 20.0 (6 x CH₃), 13.4 (3 x CH).

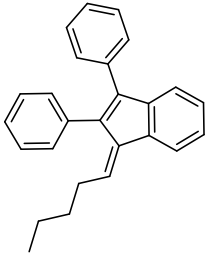
(E)-1-(4-methylbenzylidene)-2,3-diphenyl-1H-indene (4.9b)

	<p>Yield = 95%, 70 mg.</p> <p>Bright yellow solid. Slightly decomposes on exposure to air.</p> <p>mp = 194.0-195.2 °C.</p> <p>R_f (SiO₂) = 0.05 (Hexane).</p> <p>HRMS for C₂₉H₂₂ [M]: Calc.: 370.1716; found: 370.1719.</p>
---	--

¹H-NMR (300 MHz, CDCl₃, 25 °C, TMS): δ (ppm) = 7.71 (d, $J_{(H,H)}$ = 7.6 Hz, 1H), 7.50 (d, $J_{(H,H)}$ = 8.1 Hz, 2H), 7.41 (d, $J_{(H,H)}$ = 7.5 Hz, 1H), 7.38-7.24 (m, 13H), 7.19 (s, 1H), 7.09 (td, $J_{(H,H)}$ = 7.5 and 1.3 Hz, 1H), 2.46 (s, 3H).

¹³C-NMR (75 MHz, CDCl₃, 25 °C): δ (ppm) = 143.9 (C), 141.1 (C), 140.2 (C), 140.0 (C), 138.3 (C), 135.3 (C), 135.0 (CH), 135.0 (C), 134.6 (C), 134.2 (C), 131.4 (2 x CH), 129.7 (2 x CH), 129.5 (2 x CH), 129.3 (2 x CH), 128.3 (2 x CH), 128.1 (2 x CH), 128.0 (CH), 127.3 (CH), 127.1 (CH), 125.3 (CH), 123.4 (CH), 120.2 (CH), 21.6 (CH₃).

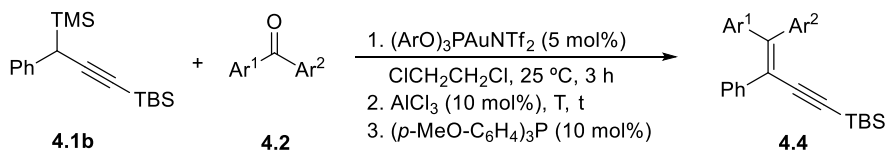
1-Pentylidene-2,3-diphenyl-1H-indene (4.9c)

	<p>Yield = 96%, 65 mg. (Mixture of diastereoisomers, <i>dr</i> = 3.3:1)</p> <p>Bright yellow oil. Slightly decomposes on exposure to air.</p> <p>R_f (SiO₂) = 0.10 (Hexane : Ethyl acetate, 100:1).</p> <p>HRMS for C₂₆H₂₄ [M]: Calc.: 336.1873; found: 336.1874.</p>
---	--

¹H-NMR (300 MHz, CDCl₃, 25 °C, TMS): δ (ppm) (*Major diastereoisomer*) = 7.91 (m, 1H), 7.53-6.96 (m, 13H), 6.34 (t, $J_{(H,H)} = 7.5$ Hz, 1H), 2.91 (q, $J_{(H,H)} = 7.5$ Hz, 2H), 1.77-1.56 (m, 2H), 1.56-1.42 (m, 2H), 1.01 (t, $J_{(H,H)} = 7.2$ Hz, 3H).

¹³C-NMR (75 MHz, CDCl₃, 25 °C): δ (ppm) (*Major diastereoisomer*) = 143.5 (C), 140.4 (C), 139.6 (C), 139.2 (CH), 138.7 (C), 135.4 (C), 135.2 (C), 135.0 (C), 131.2 (2 x CH), 129.6 (2 x CH), 128.1 (2 x CH), 127.8 (2 x CH), 127.2 (CH), 127.0 (CH), 126.8 (CH), 125.3 (CH), 123.7 (CH), 120.2 (CH), 31.7 (CH₂), 29.7 (CH₂), 22.8 (CH₂), 14.0 (CH₃).

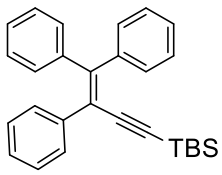
2.5.2 Experimental procedure for the synthesis of 1,3-enynes **4.4 starting from propargylsilanes **4.1a** and benzophenones **4.2**.**



Scheme 5.29: Synthesis of 1,3-enyne derivatives **4.4**.

To a mixture of 0.24 mmol of propargylsilane **4.1b** and 0.2 mmol of benzophenone **2** in dry dichloromethane (1 mL) at 25 °C, were added 11.2 mg of the gold catalyst (2.5 mol%) and the reaction was then stirred for 3 hours. After that time, the mixture was cooled to -40 °C (for **4.4a,g,h**) and 2.6 mg (0.02 mmol, 10 mol%) of aluminum trichloride were added. The mixture was stirred for 3 h (for **4.4i**), 6 h (for **4.4g,h**) or 16 h (for **4.4a**). Finally, 7.0 mg of $(p\text{-MeO-C}_6\text{H}_4)_3\text{P}$ (0.02 mmol, 10 mol%) and the solvent was removed under vacuum. The residue was purified under flash chromatography furnishing the corresponding enynes **4.4**.

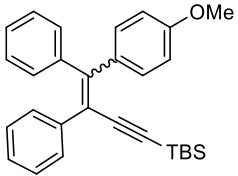
Tert-butyldimethyl(3,4,4-triphenylbut-3-en-1-yn-1-yl)silane (4.4a)

	<p>Yield = 93%, 73 mg.</p> <p>White solid, mp = 83.4-85.4 °C.</p> <p>R_f (SiO₂) = 0.19 (Hexane : Ethyl acetate, 200:1).</p> <p>HRMS for C₂₈H₃₁Si [M+H]: Calc.: 395.2190; found: 395.2195.</p>
---	--

¹H-NMR (300 MHz, CD₂Cl₂, 25 °C, TMS): δ (ppm) = 7.56-7.48 (m, 2H), 7.42-7.27 (m, 5H), 7.23-7.12 (m, 6H), 7.04-6.96 (m, 2H), 0.88 (s, 9H), 0.04 (s, 6H).

¹³C-NMR (75 MHz, CD₂Cl₂, 25 °C): δ (ppm) = 150.3 (C), 143.0 (C), 141.8 (C), 139.9 (C), 131.3 (2 x CH), 130.6 (2 x CH), 130.4 (2 x CH), 128.3 (2 x CH), 128.2 (2 x CH), 128.1 (CH), 128.1 (2 x CH), 127.7 (CH), 127.4 (CH), 122.0 (C), 108.1 (C), 97.4 (C), 26.2 (3 x CH₃), 17.0 (C), -4.7 (2 x CH₃).

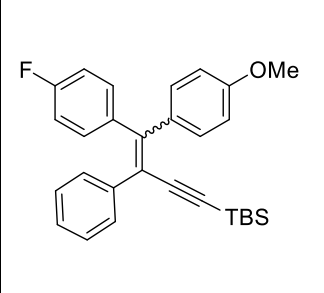
Tert-butyl(4-(4-methoxyphenyl)-3,4-diphenylbut-3-en-1-yn-1-yl)dimethylsilane (4.4g).

	<p>Yield = 92%, 78 mg. (Mixture of diastereoisomers, <i>dr</i> = 1.2:1).</p> <p>Yellowish solid.</p> <p>R_f (SiO₂) = 0.55 (Hexane : Ethyl acetate, 20:1).</p> <p>HRMS for C₂₉H₃₃OSi [M+H]: Calc.: 425.2295; found: 425.2297.</p>
---	--

¹H-NMR (300 MHz, CDCl₃, 25 °C, TMS): δ (ppm) = 7.64-7.53 (m, 4H), 7.46-7.33 (m, 8H), 7.31-7.14 (m, 9H), 7.07 (m, 1H), 7.02-6.87 (m, 4H), 6.78-6.65 (m, 2H), 3.88 (s, 3H), 3.77 (s, 3H), 0.98 (s, 9H), 0.94 (s, 9H), 0.18 (s, 6H), 0.13 (s, 6H).

¹³C-NMR (75 MHz, CDCl₃, 25 °C): δ (ppm) = 159.4 (C), 158.9 (C), 149.7 (C), 149.5 (C), 143.0 (C), 141.7 (C), 139.7 (C), 139.7 (C), 135.1 (C), 133.6 (C), 132.5 (2 x CH), 132.0 (2 x CH), 131.3 (2 x CH), 130.6 (2 x CH), 130.2 (2 x CH), 130.1 (CH), 130.1 (2 x CH), 128.0 (2 x CH), 127.9 (4 x CH), 127.8 (2 x CH), 127.3 (CH), 126.9 (CH), 126.8 (CH), 120.6 (C), 120.5 (C), 113.2 (2 x CH), 113.0 (2 x CH), 108.4 (C), 108.2 (C), 96.3 (C), 96.2 (C), 55.3 (CH₃), 55.1 (CH₃), 26.2 (3 x CH₃), 26.2 (3 x CH₃), 16.9 (C), 16.8 (C), -4.5 (2 x CH₃), -4.6 (2 x CH₃).

Tert-butyl(4-(4-fluorophenyl)-4-(4-methoxyphenyl)-3-phenylbut-3-en-1-yn-1-yl)dimethylsilane (4.4h).

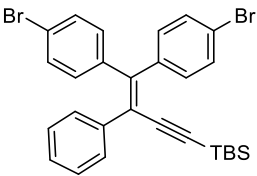
	<p>Yield = 95%, 84 mg. (Mixture of diastereoisomers, <i>dr</i> = 1.2:1).</p> <p>Yellowish solid.</p> <p>R_f (SiO₂) = 0.54 (Hexane : Ethyl acetate, 20:1).</p> <p>HRMS for C₂₉H₃₁FNaoSi [M+Na]: Calc.: 465.2020; found: 465.2027.</p>
---	--

¹H-NMR (300 MHz, CDCl₃, 25 °C, TMS): δ (ppm) = 7.56-7.40 (m, 4H), 7.37-7.24 (m, 4H), 7.23-7.10 (m, 6H), 7.08-6.92 (m, 4H), 6.92-6.78 (m, 6H), 6.74-6.60 (m, 2H), 3.83 (s, 3H), 3.74 (s, 3H), 0.85 (s, 9H), 0.83 (s, 9H), 0.05 (s, 6H), 0.03 (s, 6H).

¹³C-NMR (75 MHz, CDCl₃, 25 °C): δ (ppm) = 163.7 (d, $J_{(C,F)}$ = 247.6 Hz, C), 160.5 (d, $J_{(C,F)}$ = 248.6 Hz, C), 159.4 (C), 158.9 (C), 148.3 (C), 148.2 (C), 139.5 (C), 139.4 (C), 139.0 (d, $J_{(C,F)}$ = 3.3 Hz, C), 137.5 (d, $J_{(C,F)}$ = 2.5 Hz, C), 134.8 (C), 133.4 (C), 132.9 (d, $J_{(C,F)}$ = 8.0 Hz, 2 x CH), 132.3 (d, $J_{(C,F)}$ = 7.6 Hz, 2 x CH), 132.4 (2 x CH), 131.9 (2 x CH), 130.0 (2 x CH), 129.9 (2 x CH), 127.8 (2 x CH), 127.8 (2 x CH), 126.8 (CH), 126.8 (CH), 120.8 (C), 120.8 (C), 114.7 (d, $J_{(C,F)}$ = 21.3 Hz, 2 x CH), 114.5 (d, $J_{(C,F)}$ = 21.4 Hz, 2 x CH), 113.4 (2 x CH), 113.2 (2 x CH), 108.1 (C), 108.1 (C), 96.7 (C), 96.7 (C), 55.4 (CH₃), 55.3 (CH₃), 26.2 (3 x CH₃), 26.2 (3 x CH₃), 16.9 (C), 16.8 (C), -4.6 (2 x CH₃), -4.6 (2 x CH₃).

¹⁹F-NMR (282 MHz, CDCl₃, 25 °C): δ = -114.1, -114.3.

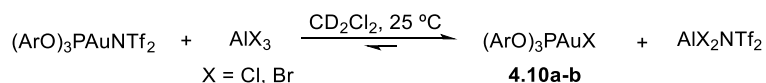
(4,4-Bis(4-bromophenyl)-3-phenylbut-3-en-1-yn-1-yl)(tert-butyl)dimethylsilane (4.4i).

	<p>Yield = 99%, 109 mg.</p> <p>White solid, mp = 116.7-118.7 °C.</p> <p>R_f (SiO₂) = 0.20 (Hexane : Ethyl acetate, 100:1).</p> <p>HRMS (EI) for C₂₈H₂₉Br₂Si [M+H]: Calc.: 551.0400; found: 551.0404.</p>
---	--

¹H-NMR (300 MHz, CDCl₃, 25 °C, TMS): δ (ppm) = 7.49-7.42 (m, 2H), 7.38-7.31 (m, 2H), 7.30-7.21 (m, 4H), 7.21-7.14 (m, 3H), 6.88-6.74 (m, 2H), 0.83 (s, 9H), 0.04 (s, 6H).

¹³C-NMR (75 MHz, CDCl₃, 25 °C): δ (ppm) = 147.0 (C), 141.2 (C), 139.8 (C), 138.8 (C), 132.8 (2 x CH), 132.2 (2 x CH), 131.2 (2 x CH), 131.1 (2 x CH), 130.0 (2 x CH), 128.2 (2 x CH), 127.6 (CH), 122.8 (C), 122.2 (C), 121.8 (C), 107.2 (C), 98.5 (C), 26.1 (3 x CH₃), 16.8 (C), -4.7 (2 x CH₃).

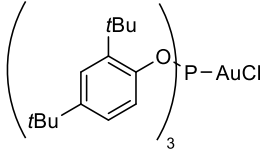
2.5.3 Experimental procedure for the reaction of [Tris(2,4-di-*tert*-butylphenyl)]phosphite gold(I) bistriflimidate with the corresponding aluminium halide



Scheme 5.30: Anion shuffling between gold(I) triflimidate and AlX₃.

To a solution of 0.05 mmol of triflimide gold complex in 0.5 mL of dry CD₂Cl₂, at 25 °C and under Argon atmosphere, 0.1 mmol of the corresponding aluminum halide (AlCl₃ or AlBr₃) were added. Three equivalents of acetonitrile were added to the mixture containing AlBr₃ to increase stability. The mixture was stirred for 30 minutes, and the sample was directly analyzed by NMR techniques under argon atmosphere. The results were in agreement to the NMR spectra of respective chloride or bromide [Tris(2,4-di-*tert*-butylphenyl)]phosphite gold(I) complexes.

[Tris(2,4-di-*tert*-butylphenyl)]phosphite gold(I) chloride (4.10a)

	<p>Yield = 99% (Estimated by NMR)</p> <p>White solid, mp = >250 °C.</p>
---	--

*(From [Tris(2,4-di-*tert*-butylphenyl)]phosphite gold(I) bistriflimidate + AlCl₃).*

¹H-NMR (300 MHz, CD₂Cl₂, 25 °C, TMS): δ (ppm) = 7.48 (dd, $J_{(H,H)}$ = 2.5 and 1.6 Hz, 3H), 7.44 (dd, $J_{(H,H)}$ = 8.6 and 1.6 Hz, 3H), 7.18 (dd, $J_{(H,H)}$ = 8.6 and 2.5 Hz, 3H), 1.47 (s, 27H), 1.29 (s, 27H).

¹³C-NMR (75 MHz, CD₂Cl₂, 25 °C): δ (ppm) = 148.8 (3 x C), 147.7 (d, $J_{(C,P)}$ = 6.0 Hz, 3 x C), 139.6 (d, $J(C, P)$ = 6.9 Hz, 3 x C), 126.0 (3 x CH), 124.5 (3 x CH), 119.4 (d, $J_{(C,P)}$ = 9.0 Hz, 3 x CH), 35.5 (3 x C), 35.0 (3 x C), 31.5 (9 x CH₃), 30.7 (9 x CH₃).

³¹P-NMR (121 MHz, CD₂Cl₂, 25 °C): δ (ppm) = 101.0.

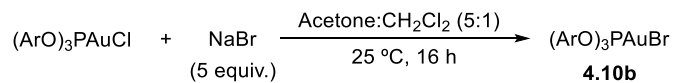
*(from a [Tris(2,4-di-*tert*-butylphenyl)]phosphite gold(I) chloride sample)*

¹H-NMR (300 MHz, CD₂Cl₂, 25 °C, TMS): δ (ppm) = 7.48 (dd, $J_{(H,H)}$ = 2.5 and 1.6 Hz, 3H), 7.44 (dd, $J_{(H,H)}$ = 8.6 and 1.6 Hz, 3H), 7.18 (dd, $J_{(H,H)}$ = 8.6 and 2.5 Hz, 3H), 1.46 (s, 27H), 1.29 (s, 27H).

¹³C-NMR (75 MHz, CD₂Cl₂, 25 °C): δ (ppm) = 148.8 (3 x C), 147.7 (d, $J_{(C,P)}$ = 6.0 Hz, 3 x C), 139.6 (d, $J(C, P)$ = 6.9 Hz, 3 x C), 126.0 (3 x CH), 124.5 (3 x CH), 119.4 (d, $J_{(C,P)}$ = 9.0 Hz, 3 x CH), 35.5 (3 x C), 35.0 (3 x C), 31.5 (9 x CH₃), 30.7 (9 x CH₃).

³¹P-NMR (121 MHz, CD₂Cl₂, 25 °C): δ (ppm) = 100.7.

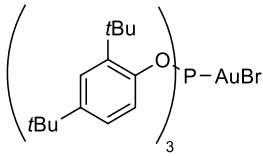
2.5.4 Experimental procedure for the synthesis of [Tris(2,4-di-*tert*-butylphenyl)]phosphite gold(I) bromide **4.10b**.



Scheme 5.31: Synthesis of gold(I) bromide complex **4.10b**.

Under argon atmosphere, to a suspension of 0.5 mmol of the corresponding gold chloride complex, in 1 mL of dry CH₂Cl₂ and 5 mL of acetone at 25 °C, and, 515 mg (5 mmol) of sodium bromide were added, and the mixture stirred for 15 h. After that period, the solvents were removed under vacuum, and the white residue was washed (3 x 5 mL) with dry CH₂Cl₂. The organic layers were collected, dried over anhydrous Na₂SO₄ and filtrated. Finally, the solvents were removed under vacuum, affording [Tris(2,4-di-*tert*-butylphenyl)]phosphite gold(I) bromide, as a white solid in a 94% yield.

[Tris(2,4-di-*tert*-butylphenyl)]phosphite gold(I) bromide (4.10b)

	<p>Yield = 94%, 434 mg.</p> <p>White solid, mp = >250 °C.</p> <p>HRMS for C₄₂H₆₃AuBrNaO₃P [M+Na]: Calc.: 945.3256; found: 945.3232.</p>
---	--

(From [Tris(2,4-di-*tert*-butylphenyl)]phosphite gold(I) chloride, synthesized as described above)

¹H-NMR (300 MHz, CD₂Cl₂, 25 °C, TMS): δ (ppm) = 7.47 (dd, $J_{(H,H)}$ = 2.5 and 1.6 Hz, 3H), 7.44 (dd, $J_{(H,H)}$ = 8.6 and 1.6 Hz, 3H), 7.18 (dd, $J_{(H,H)}$ = 8.6 and 2.5 Hz, 3H), 1.47 (s, 27H), 1.29 (s, 27H).

¹³C-NMR (75 MHz, CD₂Cl₂, 25 °C): δ (ppm) = 148.7 (3 x C), 147.5 (d, $J_{(C,P)}$ = 6.0 Hz, 3 x C), 139.4 (d, $J_{(C,P)}$ = 6.9 Hz, 3 x C), 126.0 (3 x CH), 124.5 (3 x CH), 119.2 (d, $J_{(C,P)}$ = 9.2 Hz, 3 x CH), 35.4 (3 x C), 34.9 (3 x C), 31.5 (9 x CH₃), 30.6 (9 x CH₃).

³¹P-NMR (121 MHz, CD₂Cl₂, 25 °C): δ (ppm) = 105.0.

(From [Tris(2,4-di-*tert*-butylphenyl)]phosphite gold(I) bistriflimidate + AlBr₃)

¹H-NMR (300 MHz, CD₂Cl₂, 25 °C, TMS): δ (ppm) = 7.47 (dd, $J_{(H,H)}$ = 2.5 and 1.4 Hz, 3H), 7.44 (dd, $J_{(H,H)}$ = 8.6 and 1.6 Hz, 3H), 7.18 (dd, $J_{(H,H)}$ = 8.6 and 2.5 Hz, 3H), 1.49 (s, 27H), 1.32 (s, 27H).

³¹P-NMR (121 MHz, CD₂Cl₂, 25 °C): δ (ppm) = 104.8.

2.5.5 **Experimental procedure for the low temperature NMR experiments of [Tris(2,4-di-tert-butylphenyl)]phosphite gold(I) triflimidate and chloride with the corresponding aluminum species**

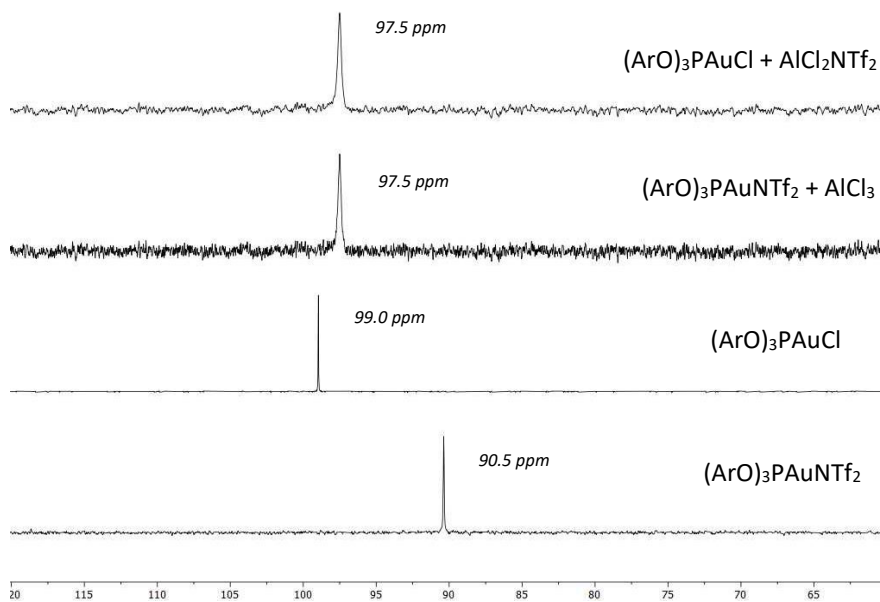
(from [Tris(2,4-di-tert-butylphenyl)]phosphite gold(I) bistriflimidate + AlCl₃)

Following the previously described procedure, to a solution of 0.05 mmol of triflimide gold complex in 0.5 mL of dry CD₂Cl₂, at 25 °C and under Argon atmosphere, 0.05 mmol of AlCl₃ (7 mg, 1 equiv.) were added. The mixture was stirred for 30 minutes and analyzed by NMR techniques, under argon atmosphere at -85 °C. The results are shown below for comparison with the one obtained starting from [Tris(2,4-di-tert-butylphenyl)]phosphite gold(I) chloride and AlCl₂NTf₂.

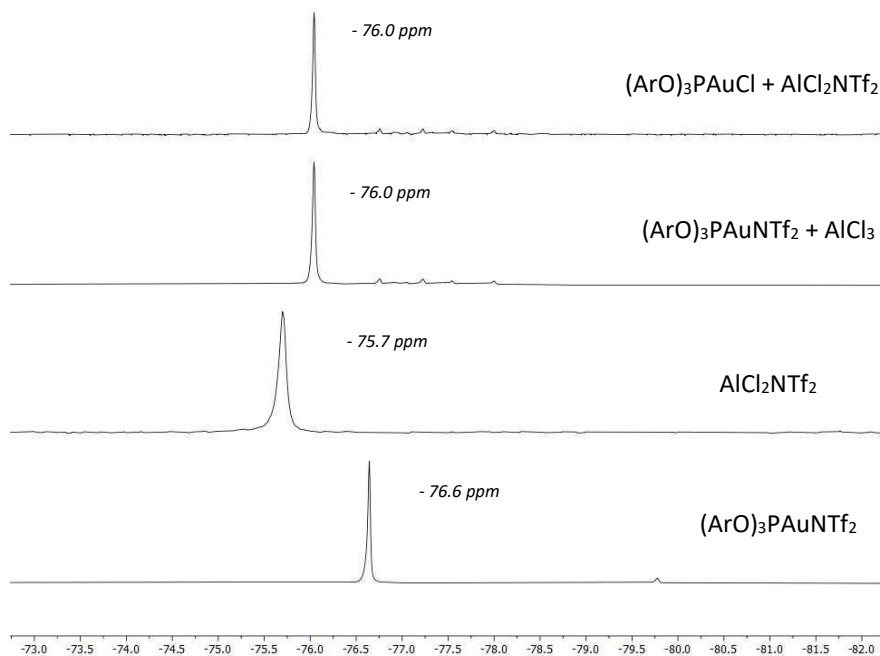
(from [Tris(2,4-di-tert-butylphenyl)]phosphite gold(I) chloride + AlCl₂NTf₂)

Under argon atmosphere, to a solution of 0.5 mmol of EtAlCl₂ (1 M in hexane), a solution of 0.5 mmol of freshly distilled triflimide (141 mg) in 1 mL of dry CD₂Cl₂ was added dropwise at 0 °C. The cooling bath was removed after complete addition, and the mixture was stirred for 30 min at room temperature, affording a 0.3 M solution of AlCl₂NTf₂. In a separate Schlenck under argon atmosphere, 0.05 mmol of the corresponding gold chloride complex (44 mg) was dissolved in 0.5 mL of dry CH₂Cl₂, and then 1 equivalent of the previously prepared AlCl₂NTf₂ solution of (165 μL, 0.05 mmol) was added. Finally, the sample was analyzed by NMR techniques, under argon atmosphere at -85 °C. The results corresponding to the ³¹P and ¹⁹F-NMR spectra are shown below for comparison with the one obtained starting from [Tris(2,4-di-tert-butylphenyl)]phosphite gold(I) bistriflimidate and AlCl₃ and also in absence of any aluminium species.

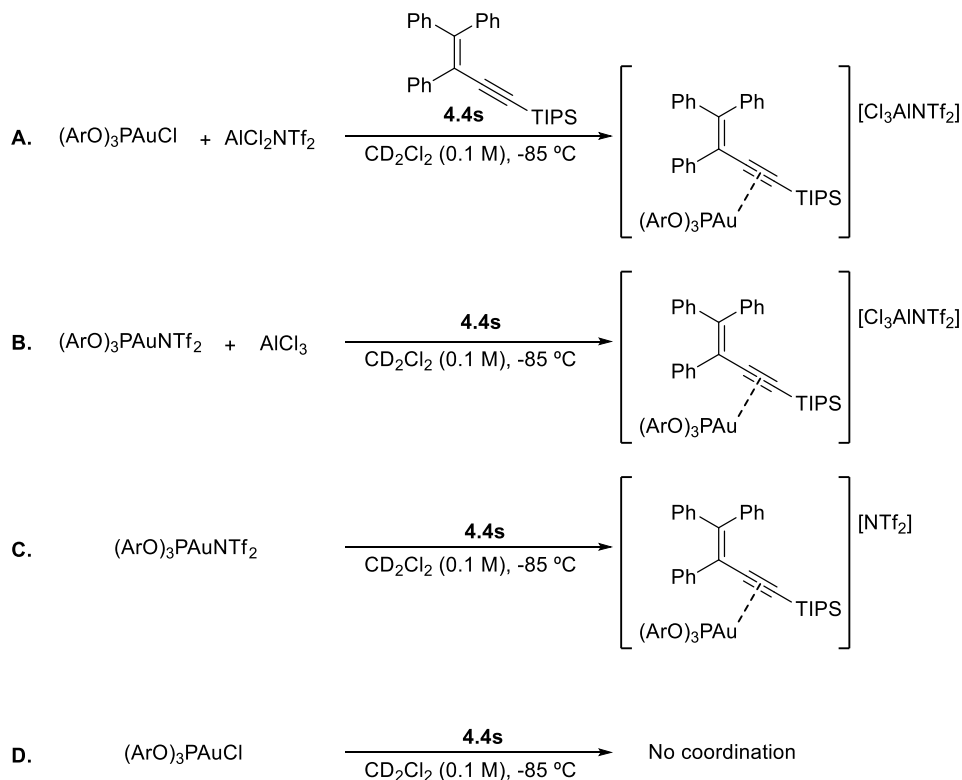
³¹P-NMR spectra (162 MHz, CD₂Cl₂, -85 °C)



¹⁹F-NMR spectra (376 MHz, CD₂Cl₂, -85 °C)



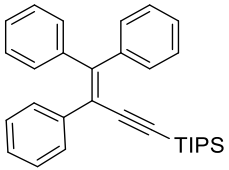
2.5.6 Experimental procedure for the low temperature NMR experiments of the different gold(I) species and 1,3-enyne 4.4s.



Scheme 5.32: Low temperature NMR coordination experiments to enyne **4.4s**.

Following the previously described procedure, different solutions of 0.05 mmol of each of the gold-aluminum mixtures in 0.5 mL of dry CD_2Cl_2 , at 25°C and under Argon atmosphere, were prepared and cooled down to -85°C . Then, 0.05 mmol of 1,3-enyne **4.4s** (22 mg, 1 equiv.) were added, and the mixture was transferred under argon atmosphere and measured by NMR techniques at -85°C . Similarly, different solutions of 0.05 mmol of the gold(I) triflimide (56 mg) or chloride (44 mg) and 0.05 mmol of enyne **4.4s** (22 mg, 1 equiv.) were prepared. NMR spectra of the different solutions are shown below for comparison.

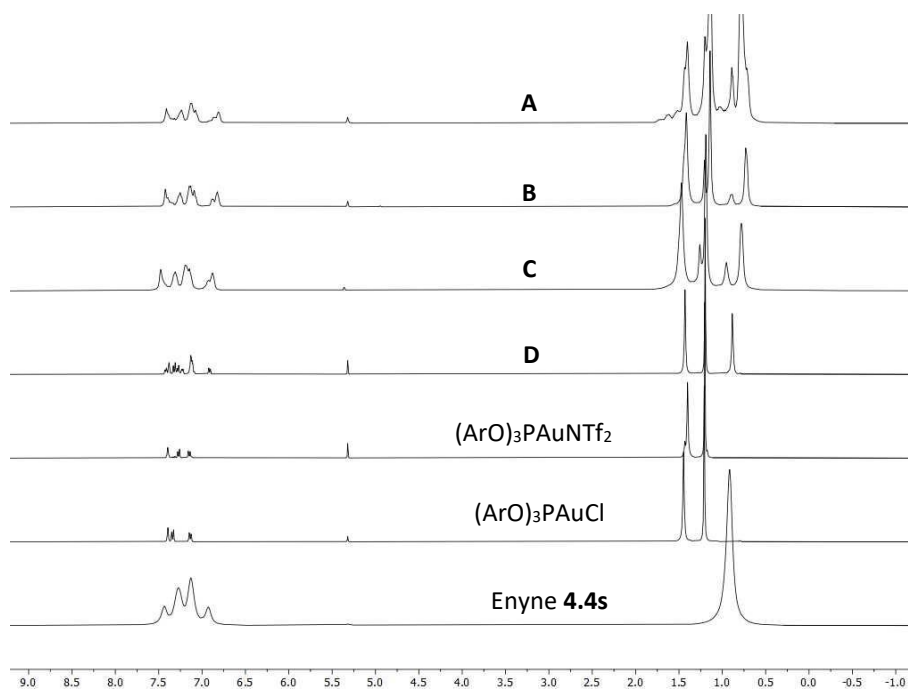
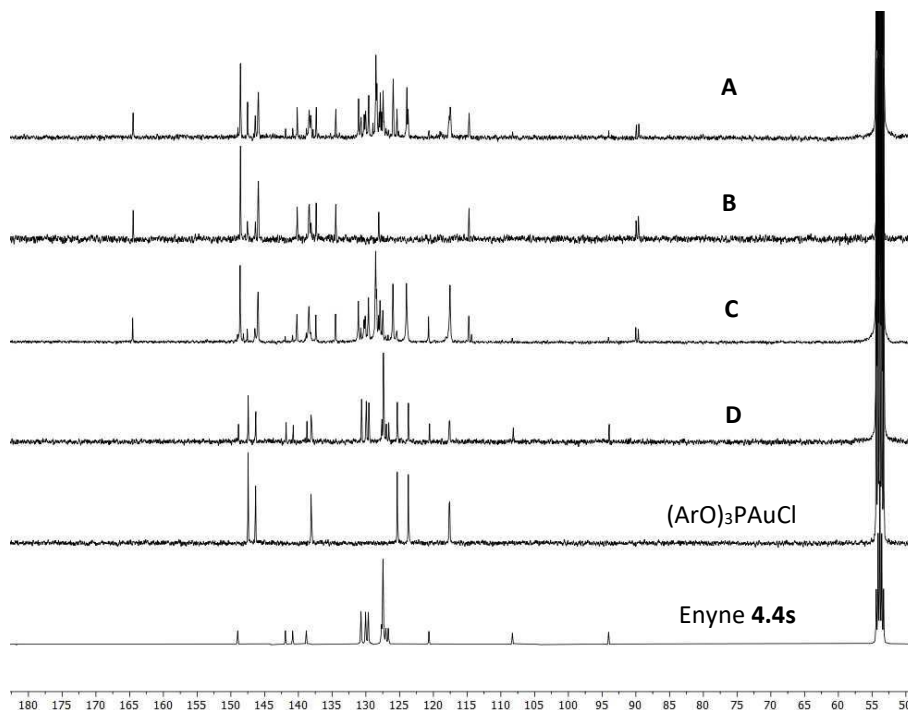
Triisopropyl(3,4,4-triphenylbut-3-en-1-yn-1-yl)silane (4.4s)

	<p>Yield = 42%, 1.83 g (synthesized following a reported procedure for TMS derivative).⁸</p> <p>White solid, mp = 64.1-66.0 °C.</p> <p>R_f (SiO₂) = 0.19 (Hexane/ Ethyl acetate, (100:1)).</p> <p>HRMS for C₃₁H₃₇Si [M+H]: Calc. 437.2665; found: 437.2660.</p>
---	---

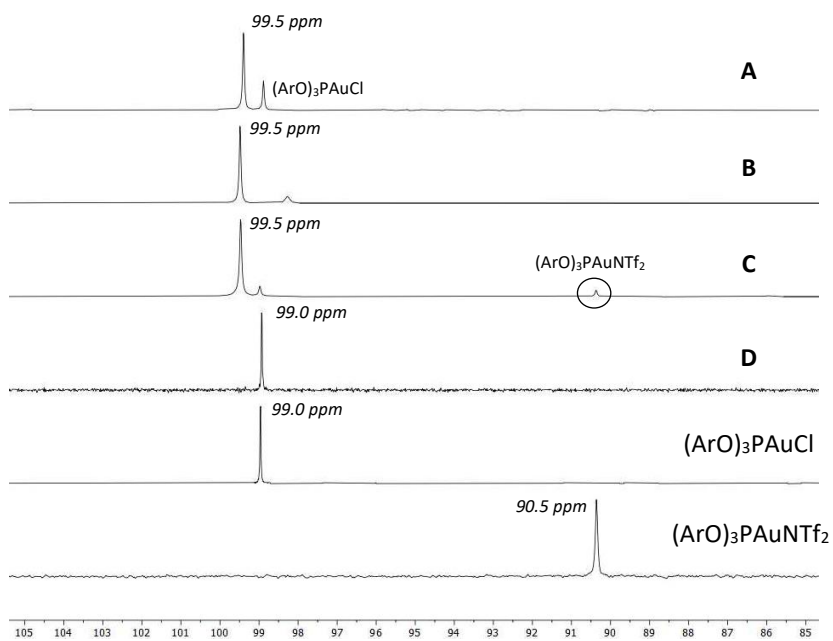
¹H-NMR (400 MHz, CD₂Cl₂, -85 °C, TMS): δ (ppm) = 7.53-7.39 (m, 2H), 7.37-7.23 (m, 5H), 7.22-7.02 (m, 6H), 7.02-6.86 (m, 2H), 0.93 (s, 21H).

¹³C-NMR (100 MHz, CD₂Cl₂, -85 °C): δ (ppm) = 149.0 (C), 141.9 (C), 140.8 (C), 138.8 (C), 130.7 (2 x CH), 130.0 (2 x CH), 129.6 (2 x CH), 127.7 (CH), 127.5 (6 x CH), 127.0 (CH), 126.7 (CH), 120.7 (C), 108.3 (C), 94.0 (C), 17.9 (6 x CH₃), 10.6 (3 x CH).

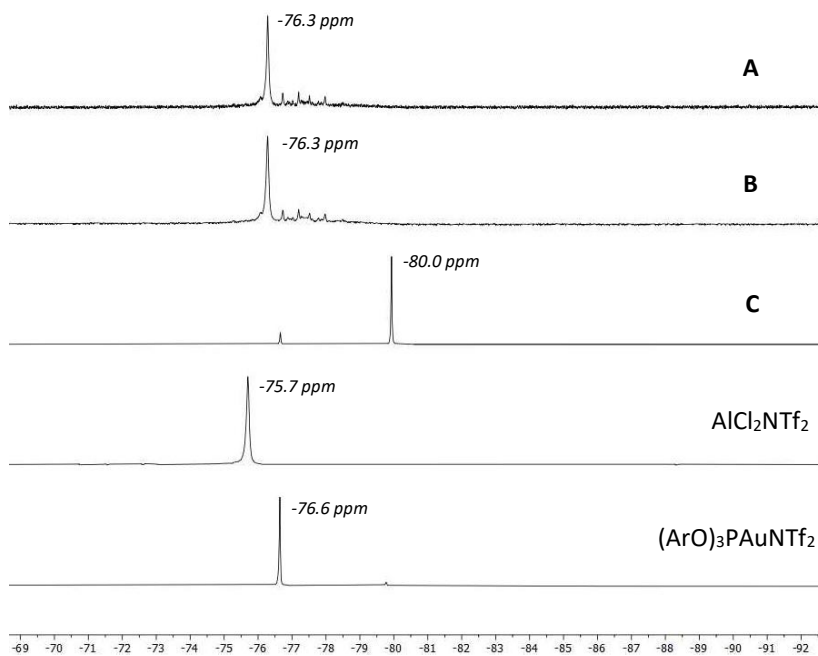
⁸ Miguel-Ávila, J.; Tomás-Gamasa, M.; Mascareñas, J. L. *Ang. Chem. Int. Ed.* **2020**, *59*, 17628-17633.

¹H-NMR spectra (400 MHz, CD₂Cl₂, -85 °C)**¹³C-NMR spectra (100 MHz, CD₂Cl₂, -85 °C) (only key aromatic area)**

^{31}P -NMR spectra (162 MHz, CD_2Cl_2 , $-85\text{ }^\circ\text{C}$)



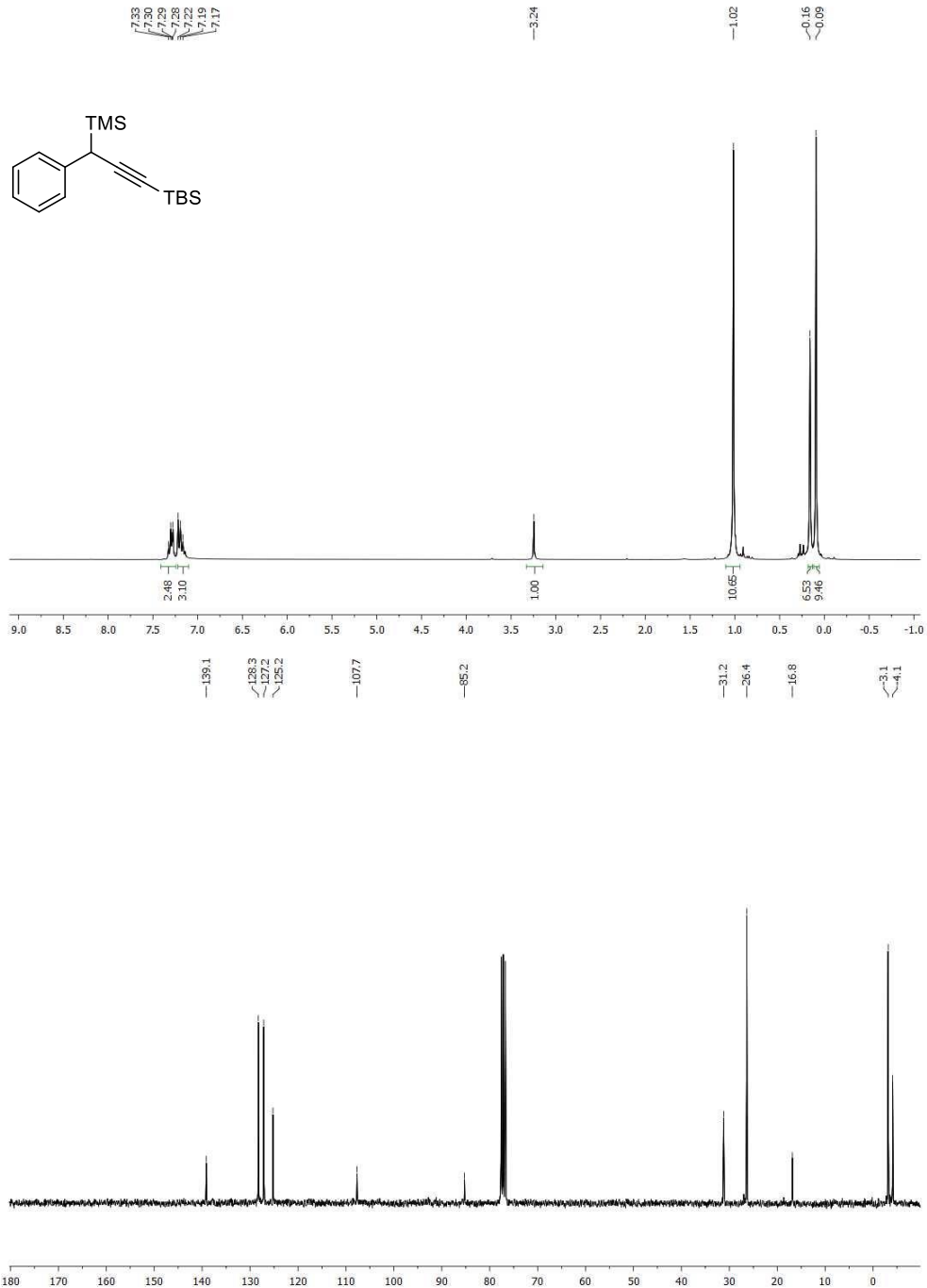
^{19}F -NMR spectra (376 MHz, CD_2Cl_2 , $-85\text{ }^\circ\text{C}$)



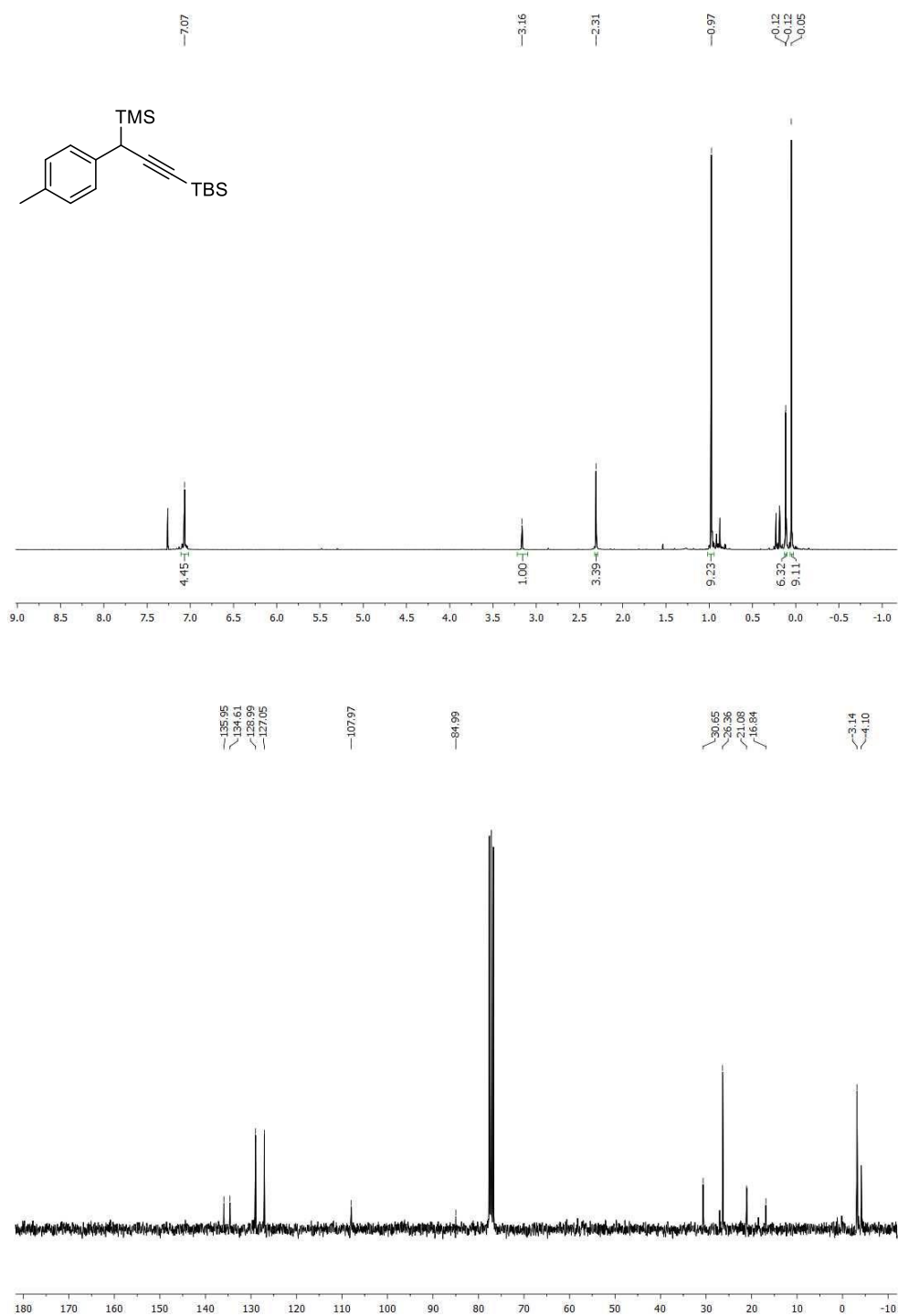
Annex I:
Nuclear Magnetic Resonance (NMR) spectra

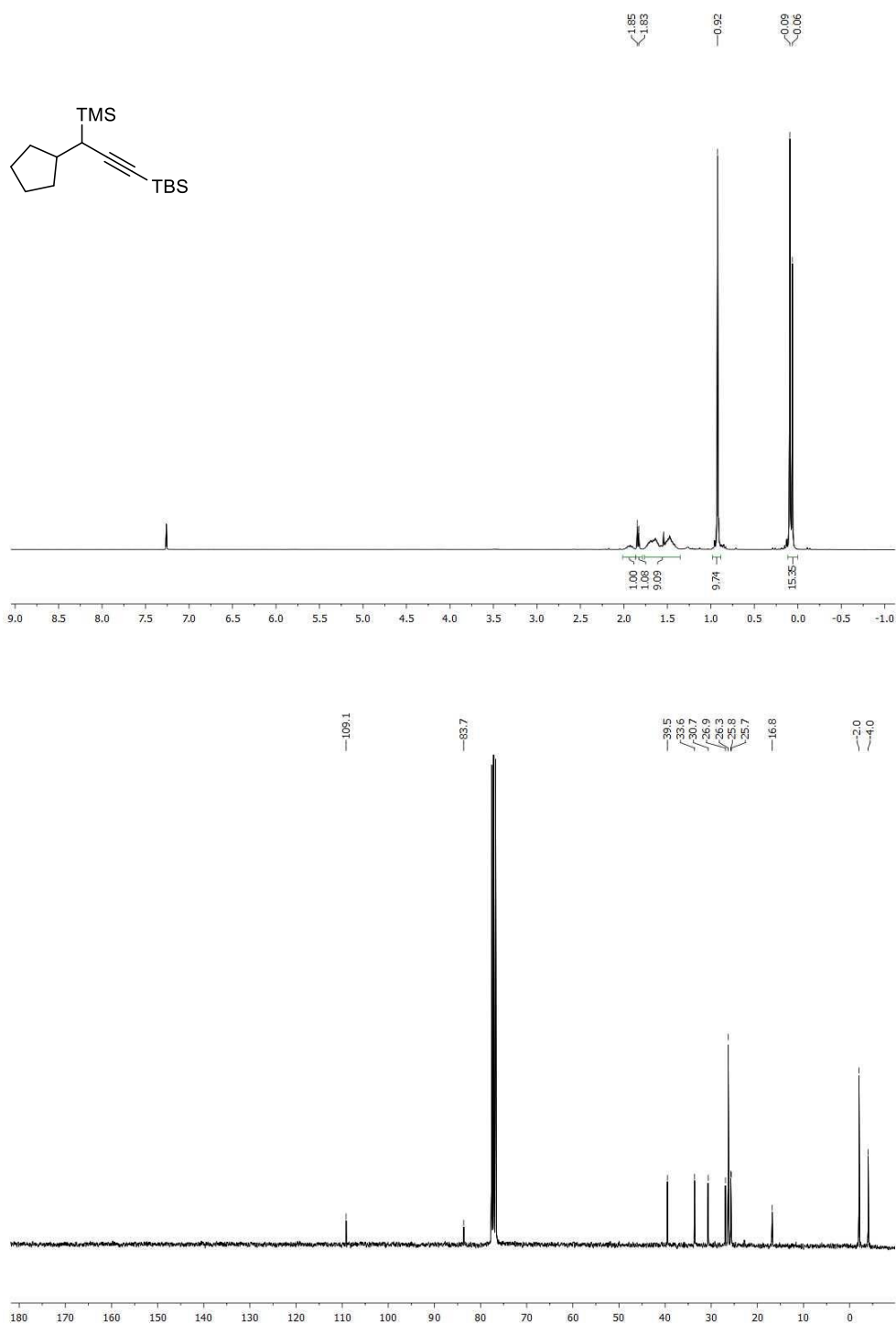
1 Chapter I

Tert-butyl dimethyl(3-phenyl-3-(trimethylsilyl)prop-1-yn-1-yl)silane (1.1b, 2.1a, 3.1a, 4.1a)

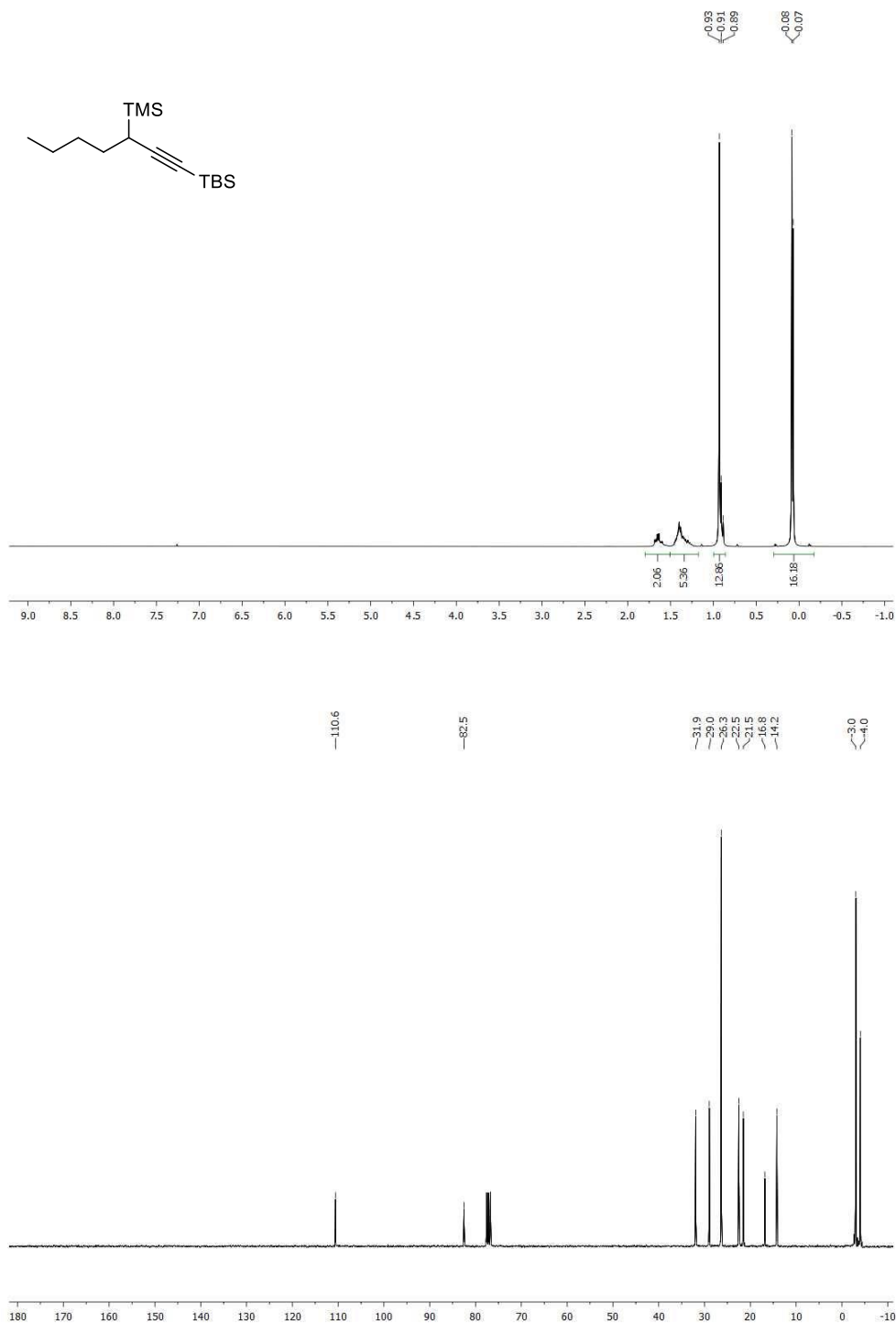


Tert-butyl dimethyl(3-(*p*-tolyl)-3-(trimethylsilyl)prop-1-yn-1-yl)silane (1.1c, 2.1b, 3.1b, 4.1b)

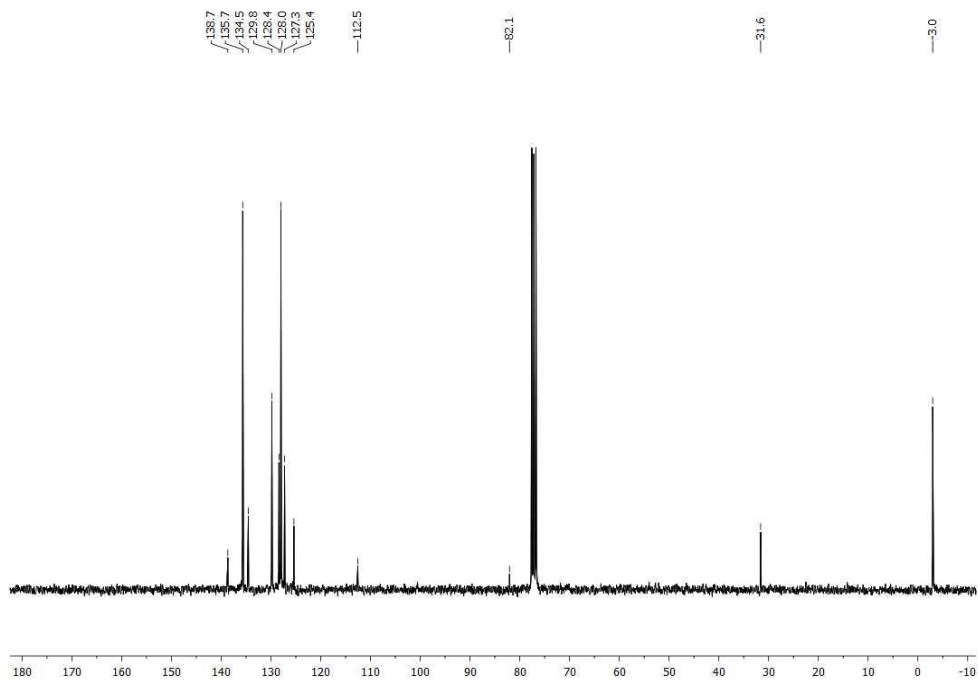
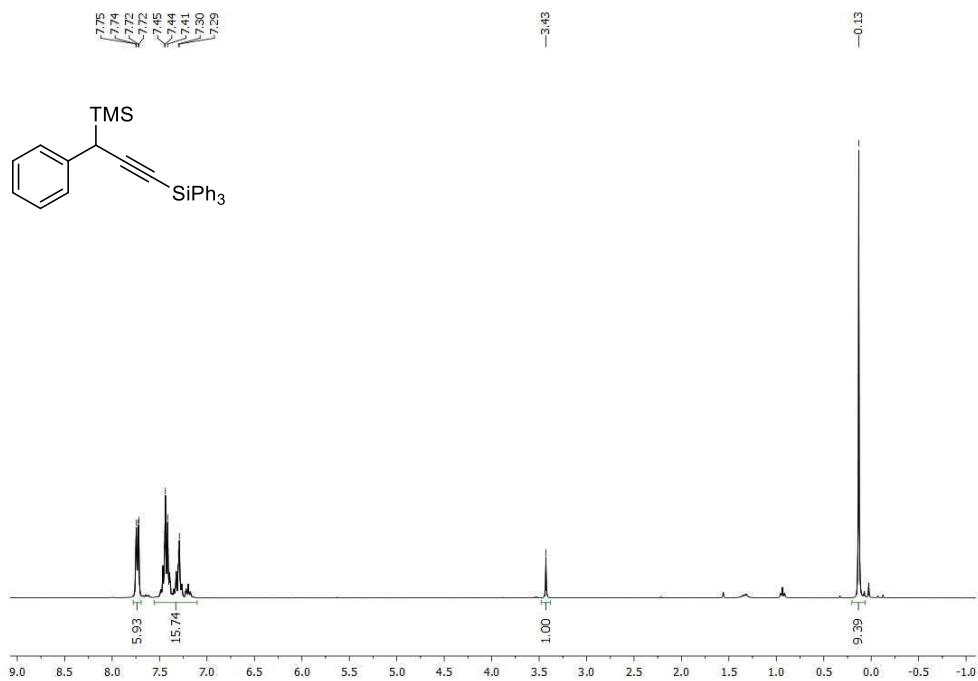


Tert-butyl(3-cyclopentyl-3-(trimethylsilyl)prop-1-yn-1-yl)dimethylsilane (1.1d, 2.1c, 3.1c, 4.1d)

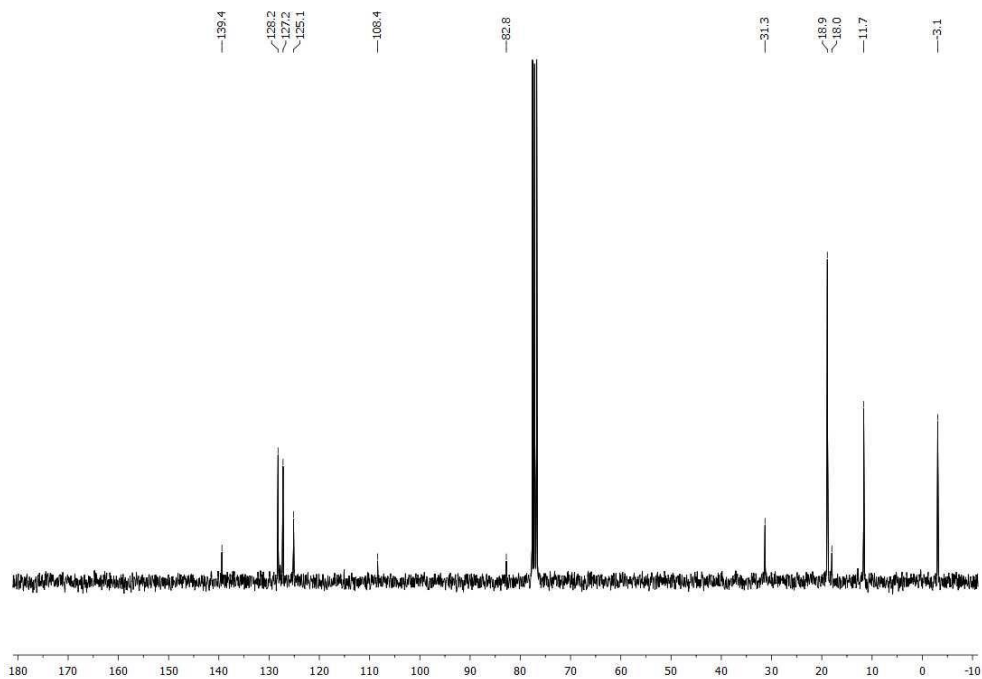
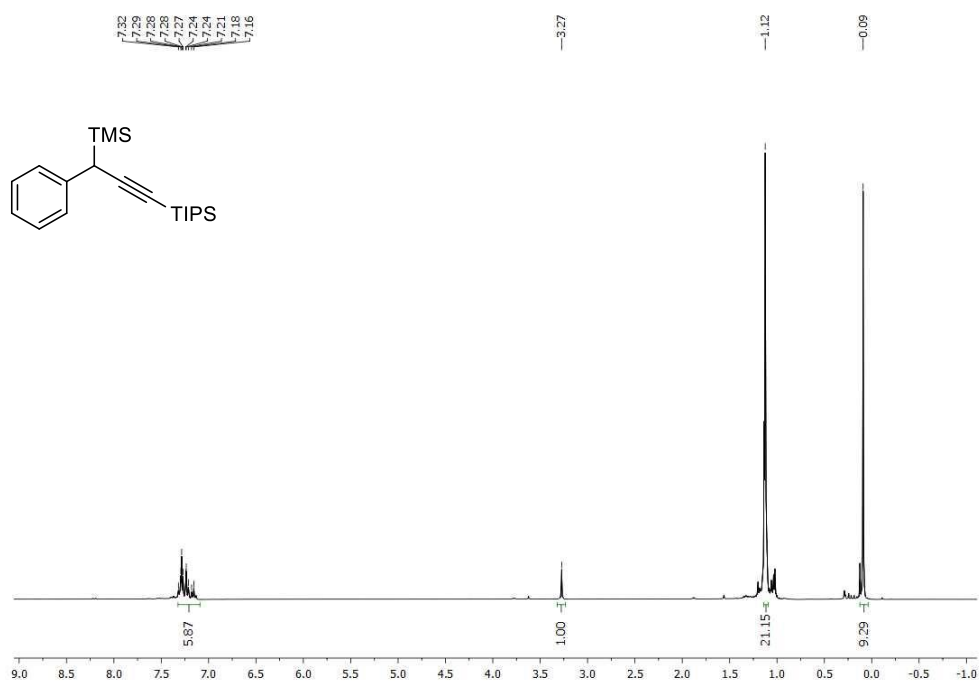
Tert-butyl dimethyl(3-(trimethylsilyl)hept-1-yn-1-yl)silane (1.1e, 2.1d, 3.1d, 4.1e)

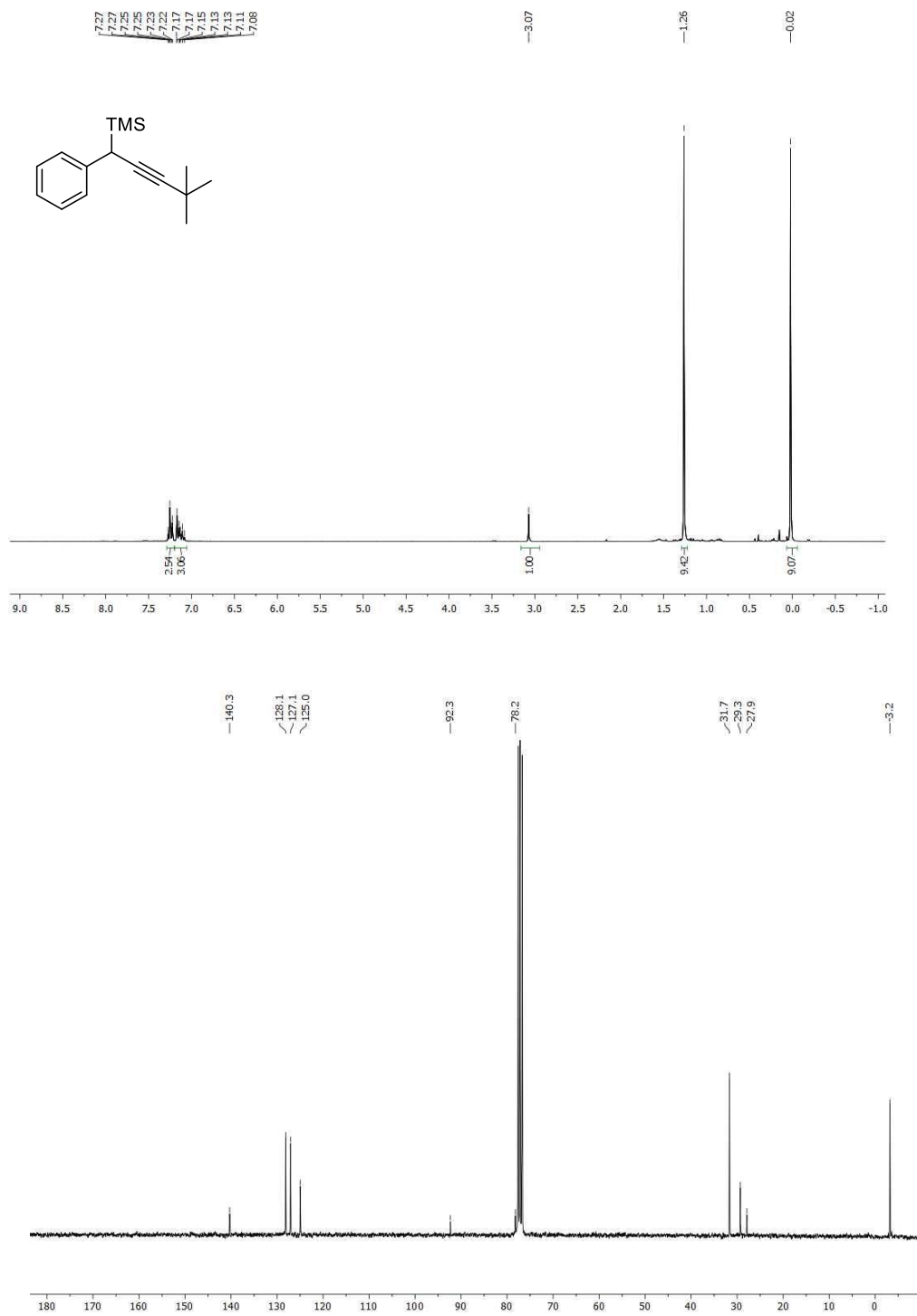


Trimethyl(1-phenyl-3-(triphenylsilyl)prop-2-yn-1-yl)silane (1.1g)

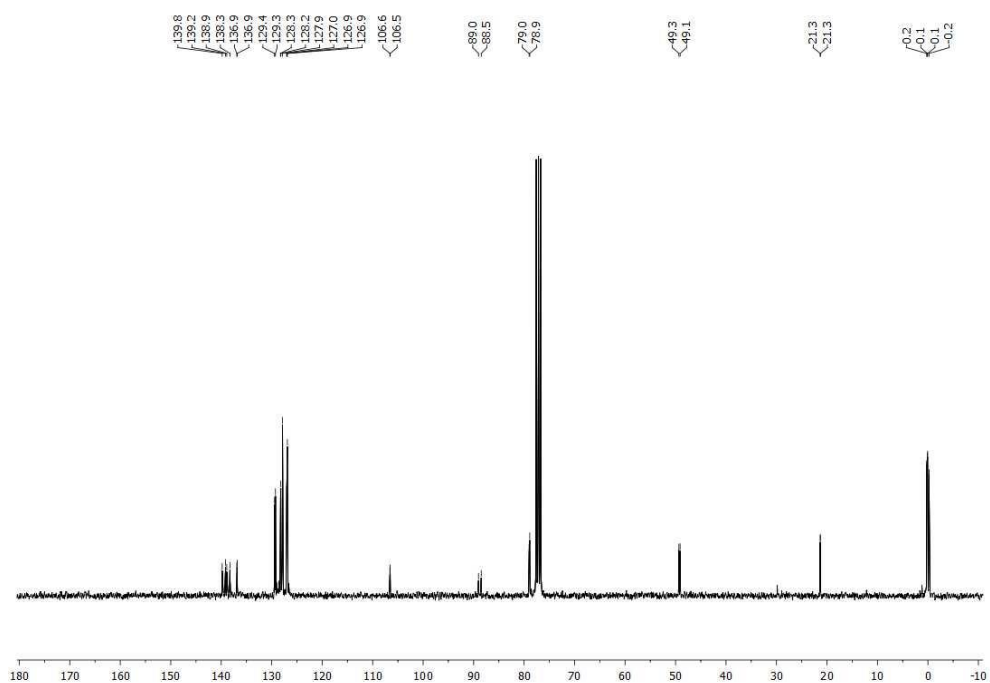
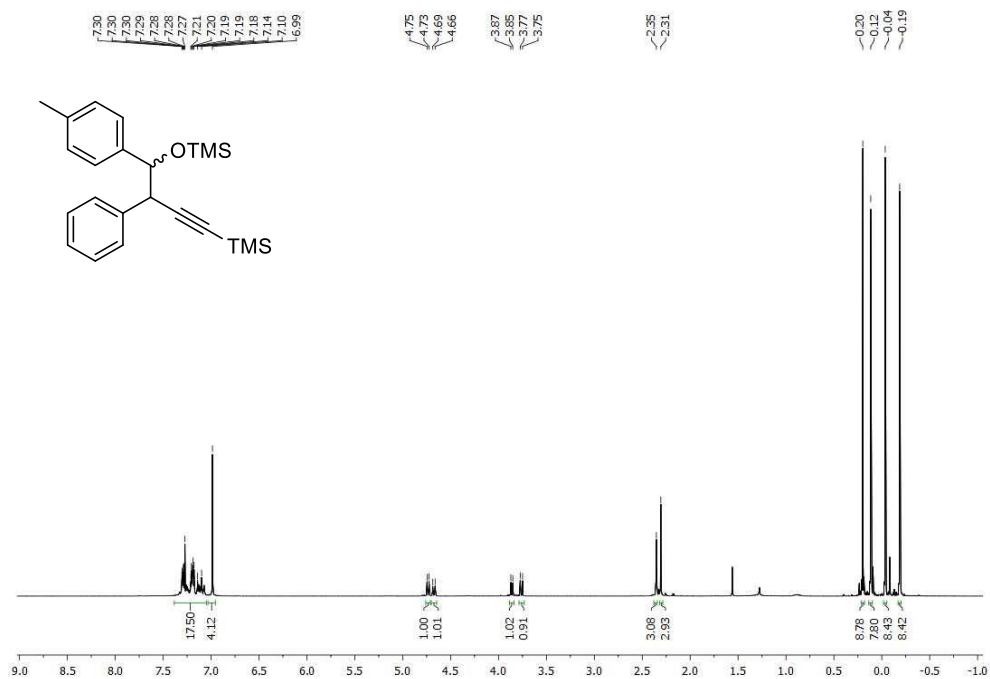


Triisopropyl(3-phenyl-3-(trimethylsilyl)prop-1-yn-1-yl)silane (1.1g, 2.1e, 3.1e, 4.1f)

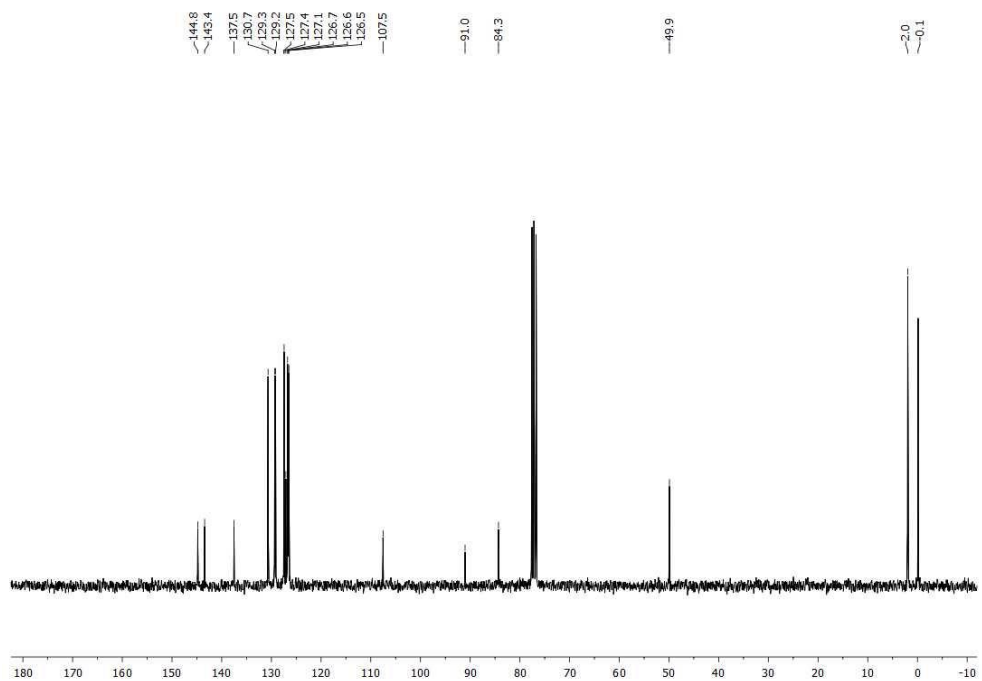
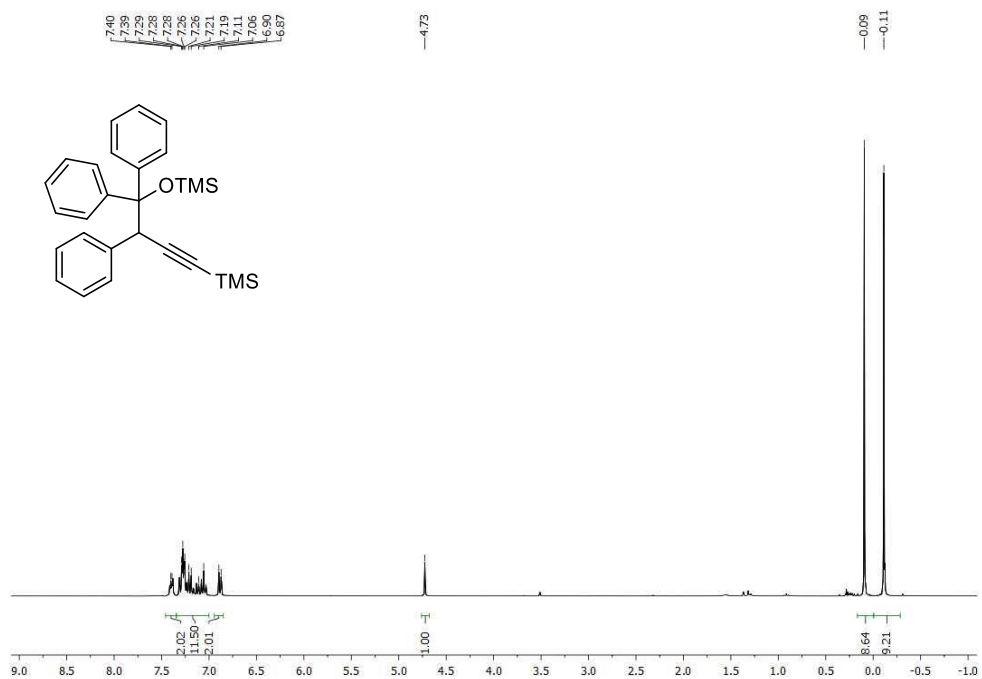


(4,4-Dimethyl-1-phenylpent-2-yn-1-yl)trimethylsilane (1.1h, 2.1f, 3.1f, 4.1g)

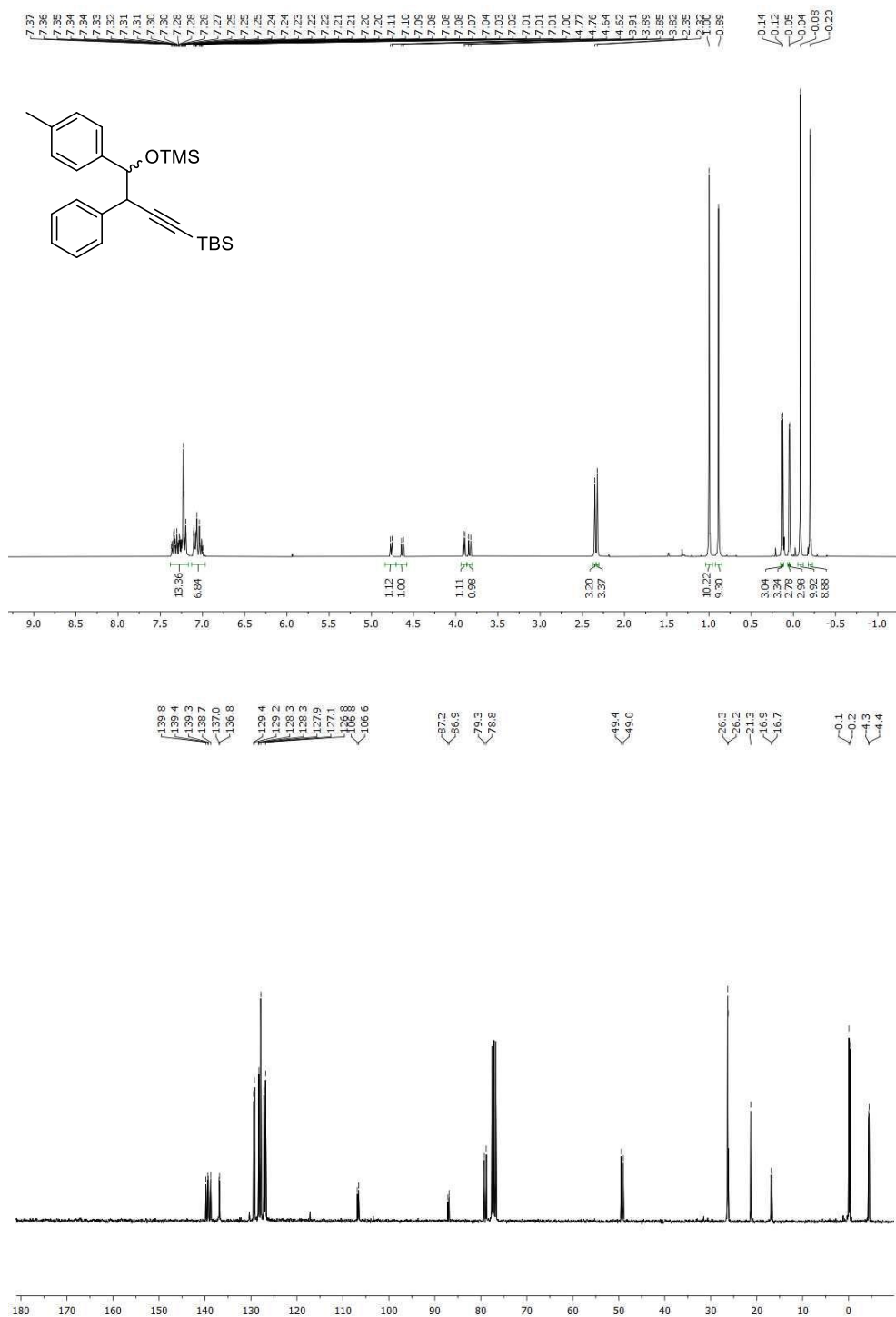
Trimethyl((2-phenyl-1-(*p*-tolyl)-4-(trimethylsilyl)but-3-yn-1-yl)oxy)silane (1.3a)

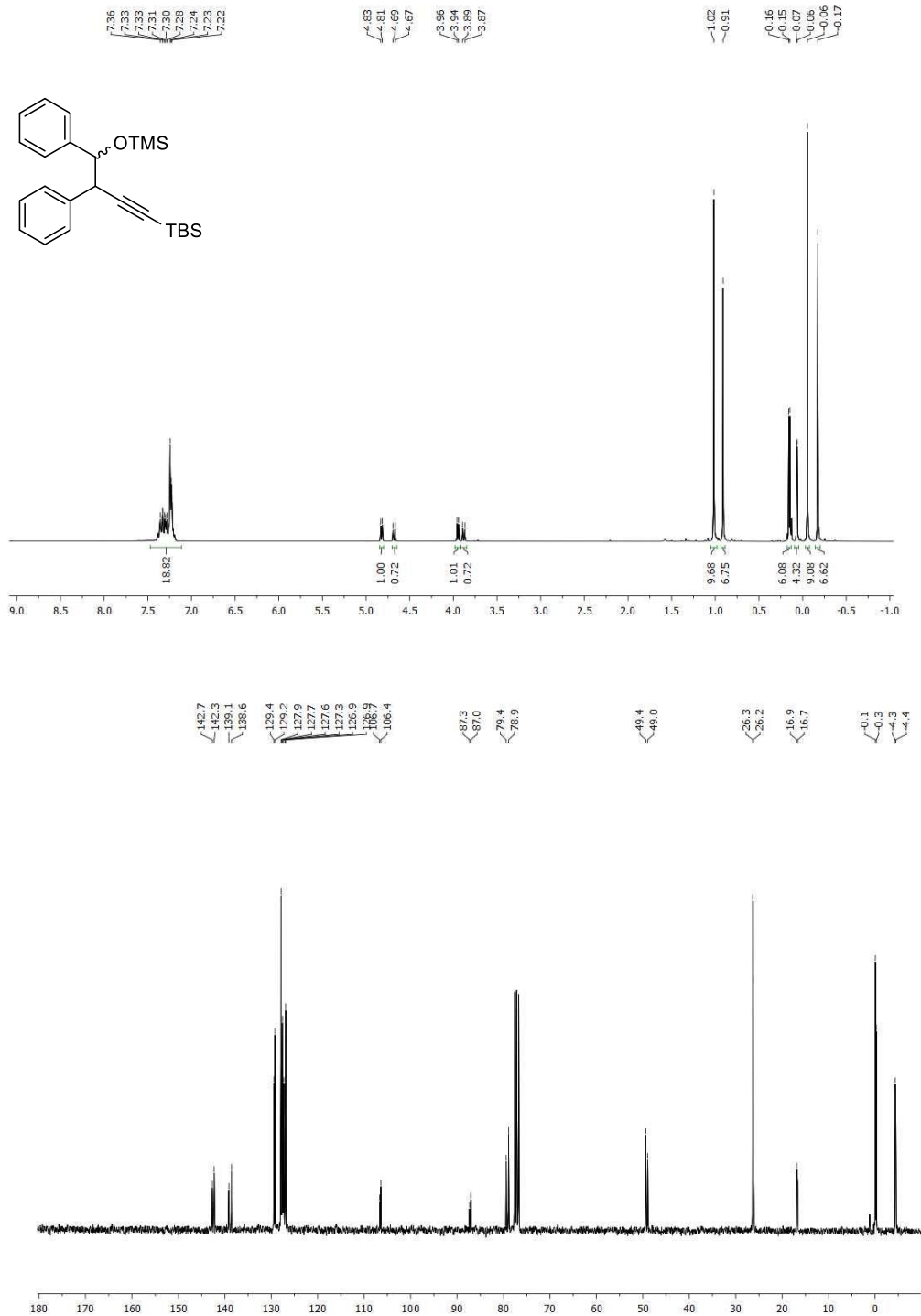


Trimethyl-4-((trimethylsilyl)oxy-3,4,4-triphenylbut-1-yn-1-yl)silane (1.3b)

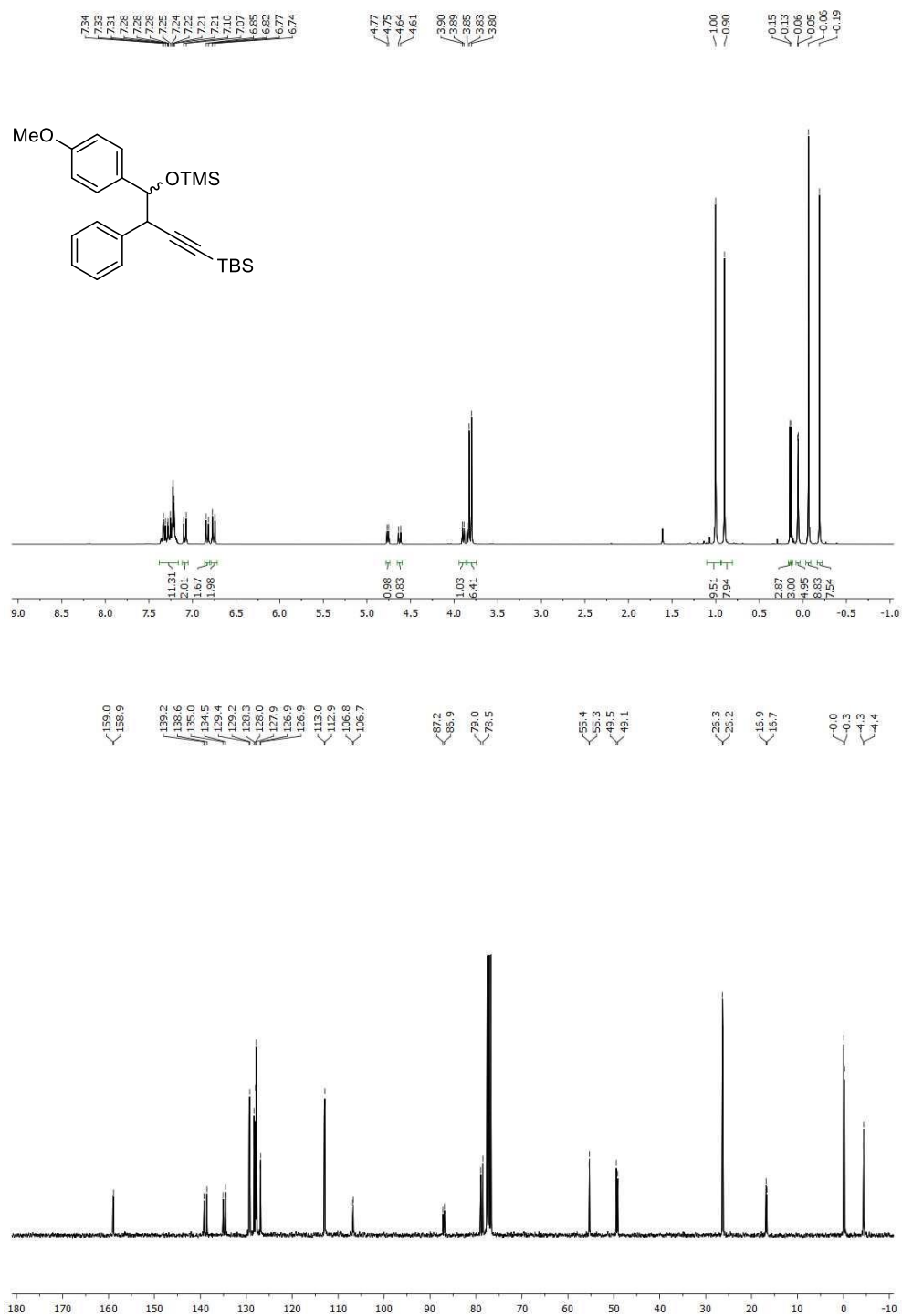


Tert-butyl dimethyl(4-(trimethylsilyloxy)-3-phenyl-4-(p-tolyl)but-1-yn-1-yl)silane (1.3c, 2.19)

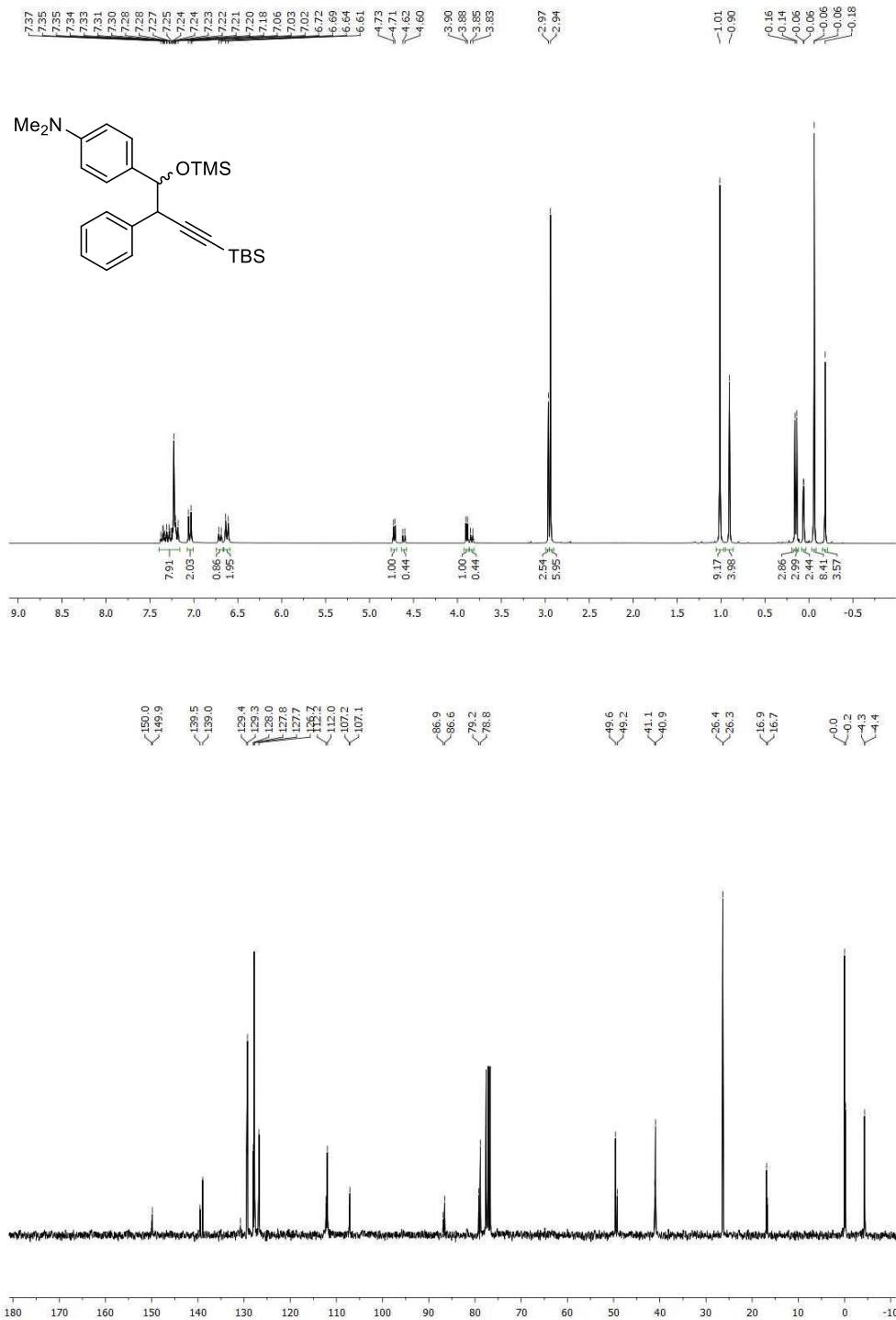


Tert-butyldimethyl(4-((trimethylsilyloxy)-3,4-diphenyl-but-1-yn-1-yl)silane (1.3d)

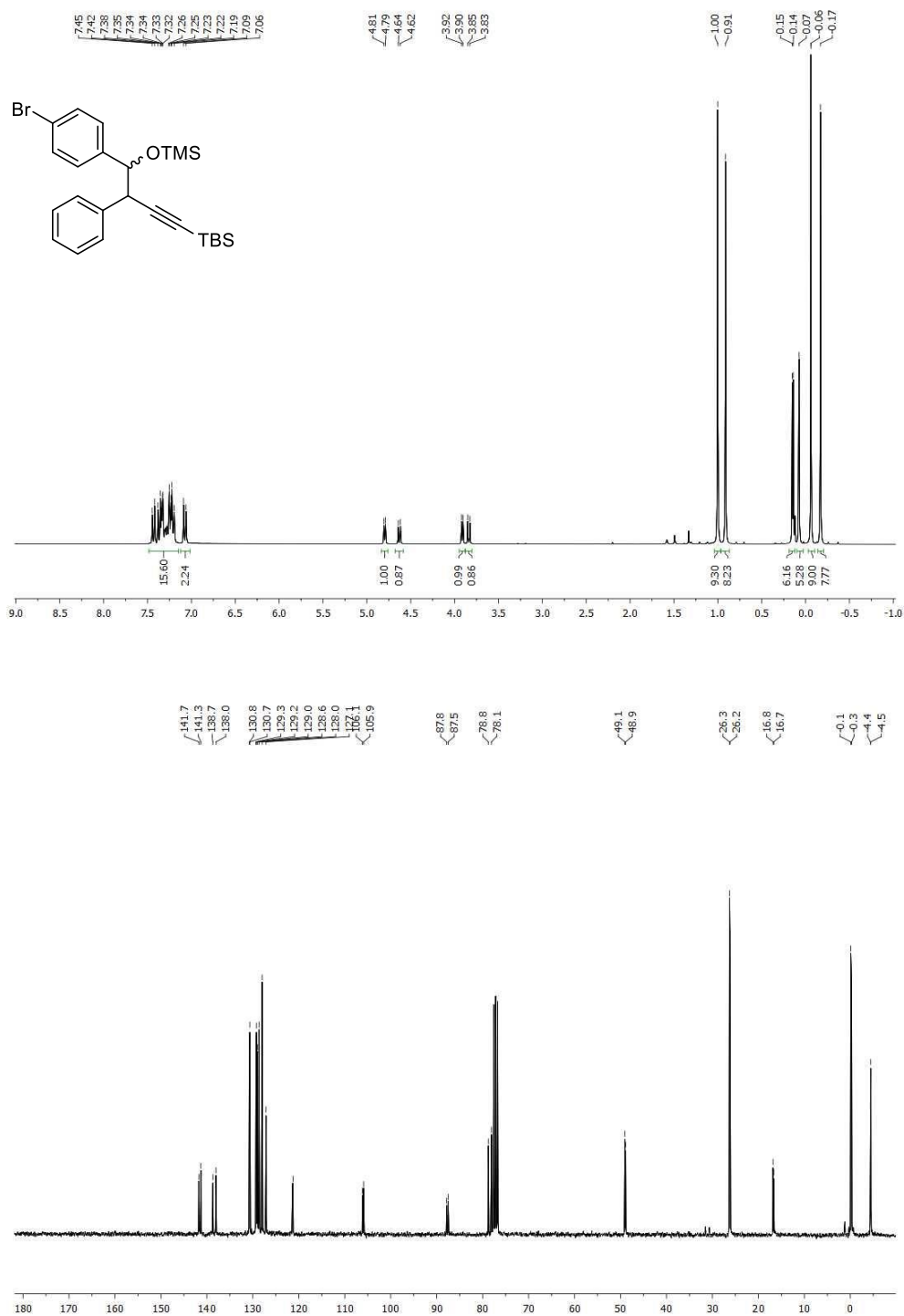
Tert-butyl dimethyl(4-(*p*-methoxyphenyl)-4-((trimethylsilyl)oxy)-3-phenyl-but-1-yn-1-yl)silane (1.3e)



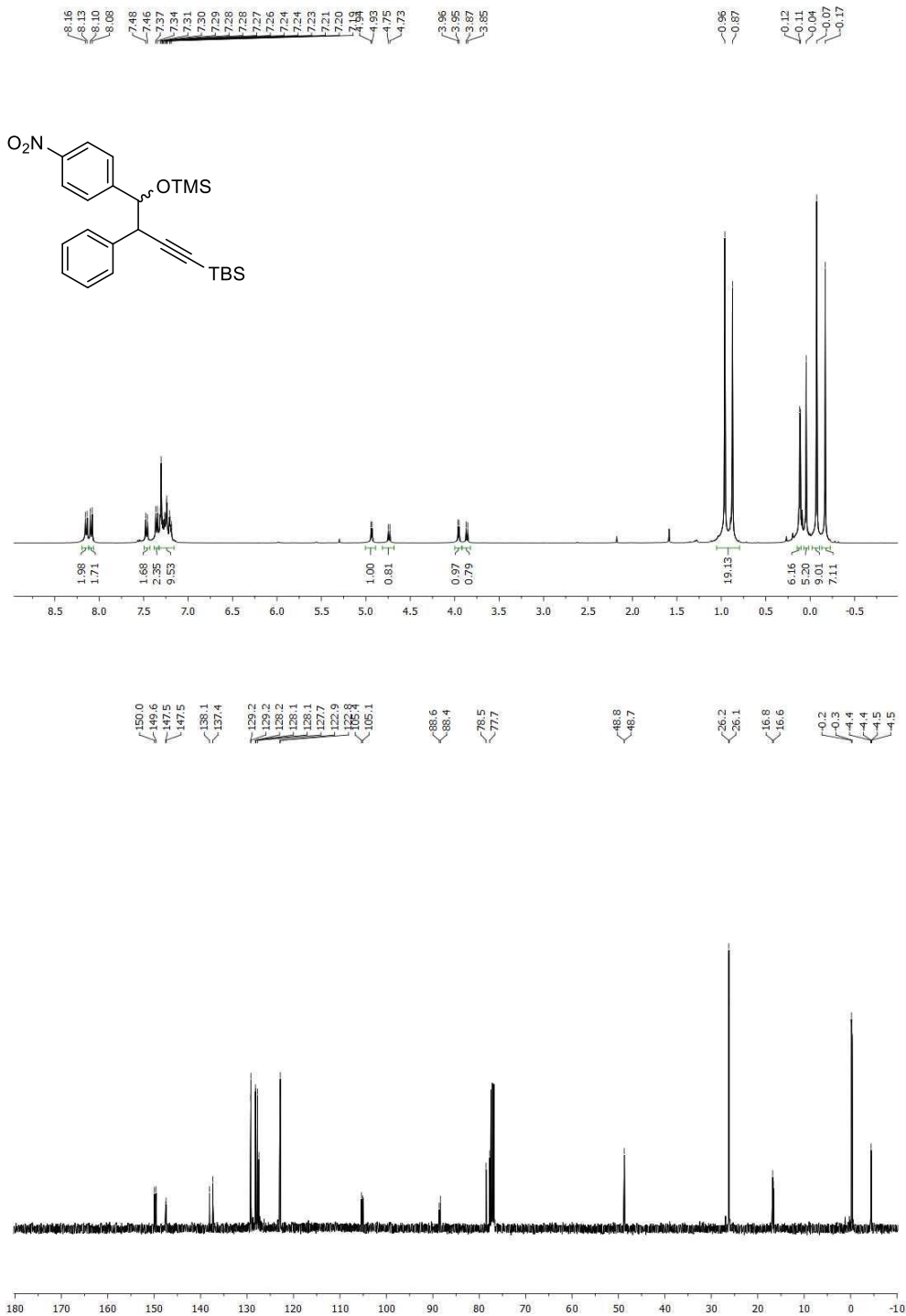
Tert-butyldimethyl(4-((trimethylsilyl)oxy)-4-(*p*-dimethylaminophenyl)-3-phenylbut-1-yn-1-yl)silane (1.3f)



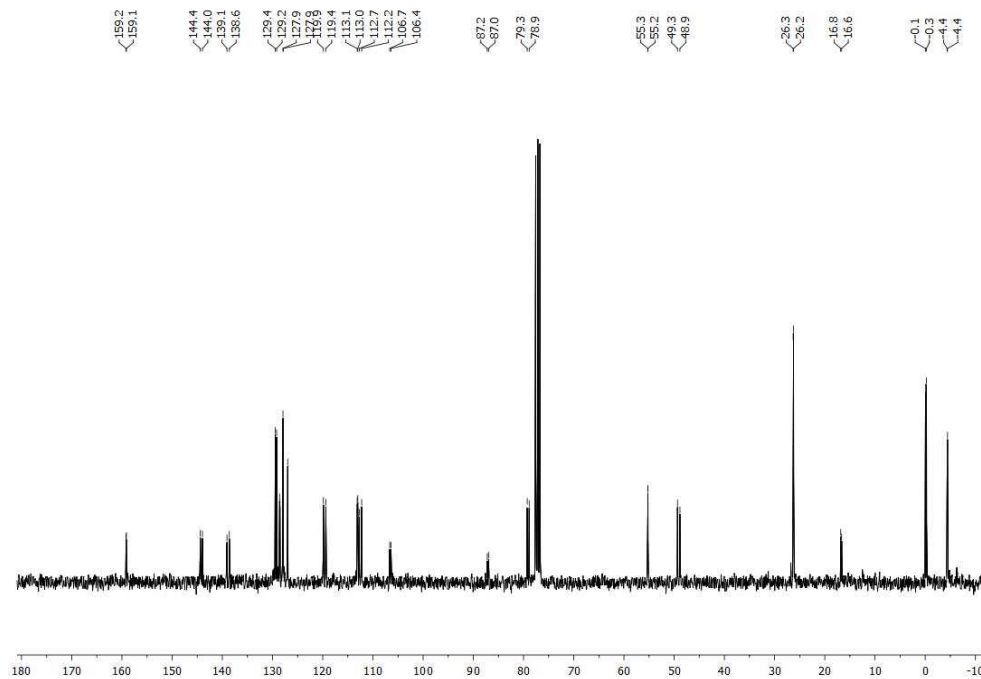
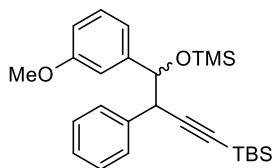
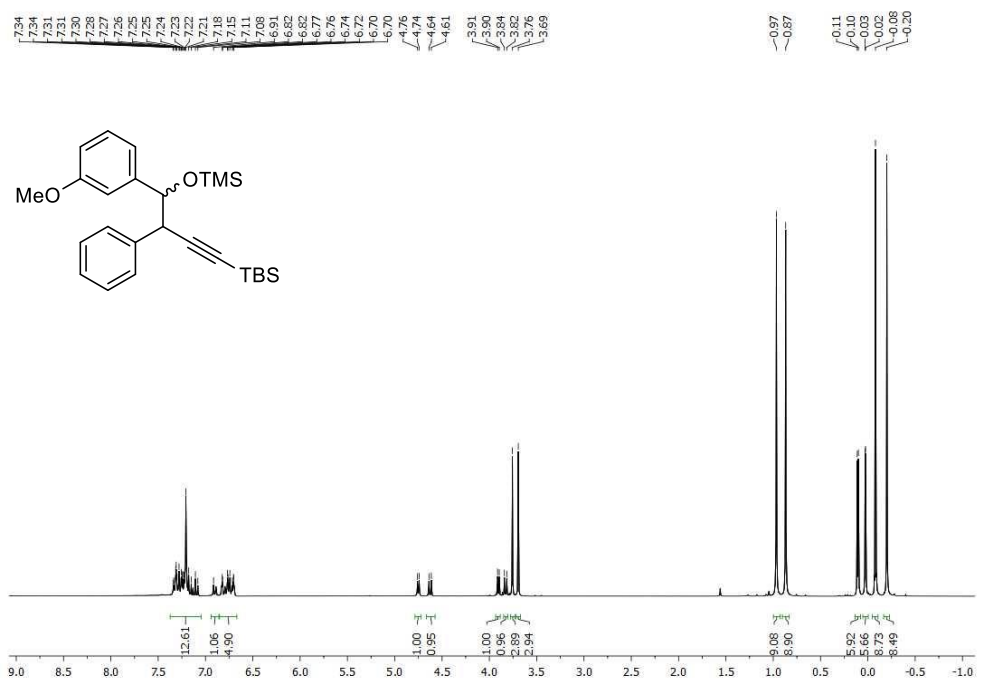
Tert-butyl dimethyl(4-(*p*-bromophenyl)-4-((trimethylsilyl)oxy)-3-phenyl-but-1-yn-1-yl)silane (1.3g)



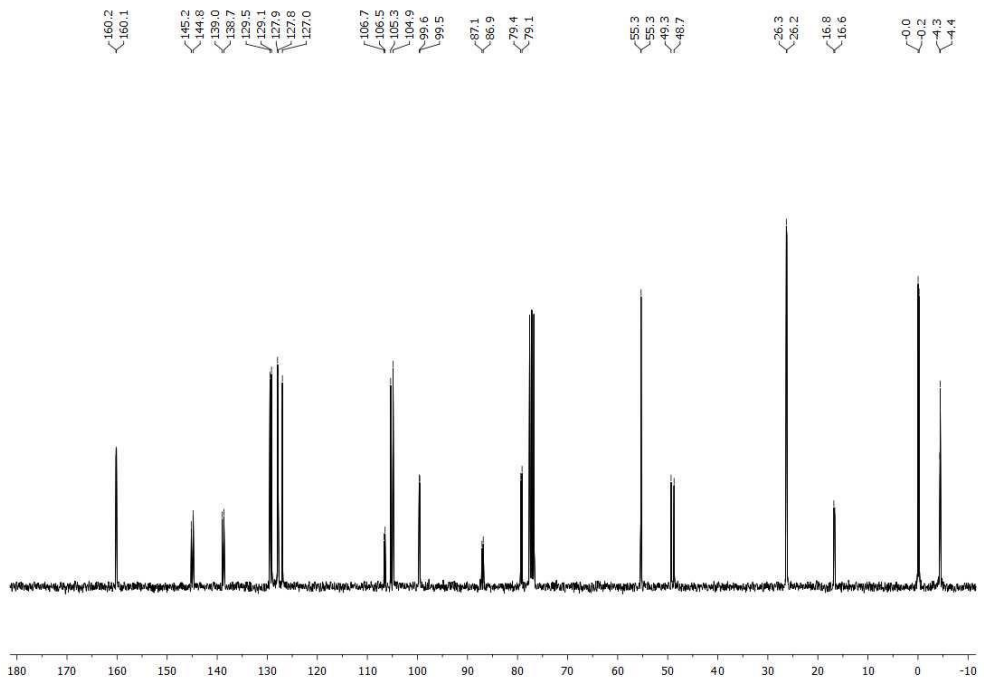
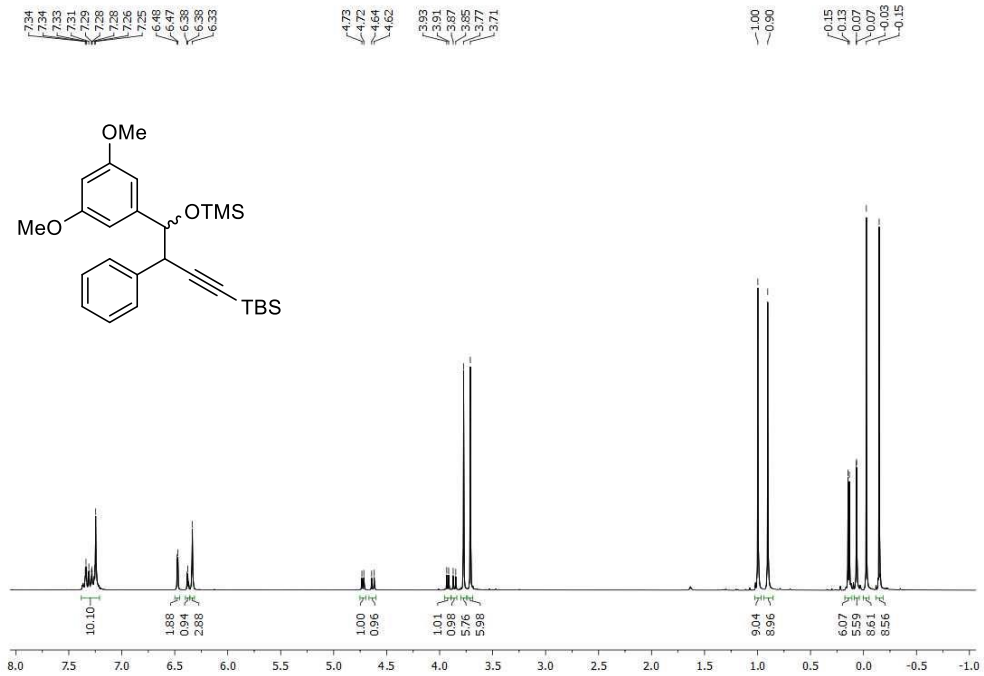
Tert-butyldimethyl(4-((trimethylsilyl)oxy)-4-(*p*-nitrophenyl)-3-phenyl-but-1-yn-1-yl)silane (1.3h)



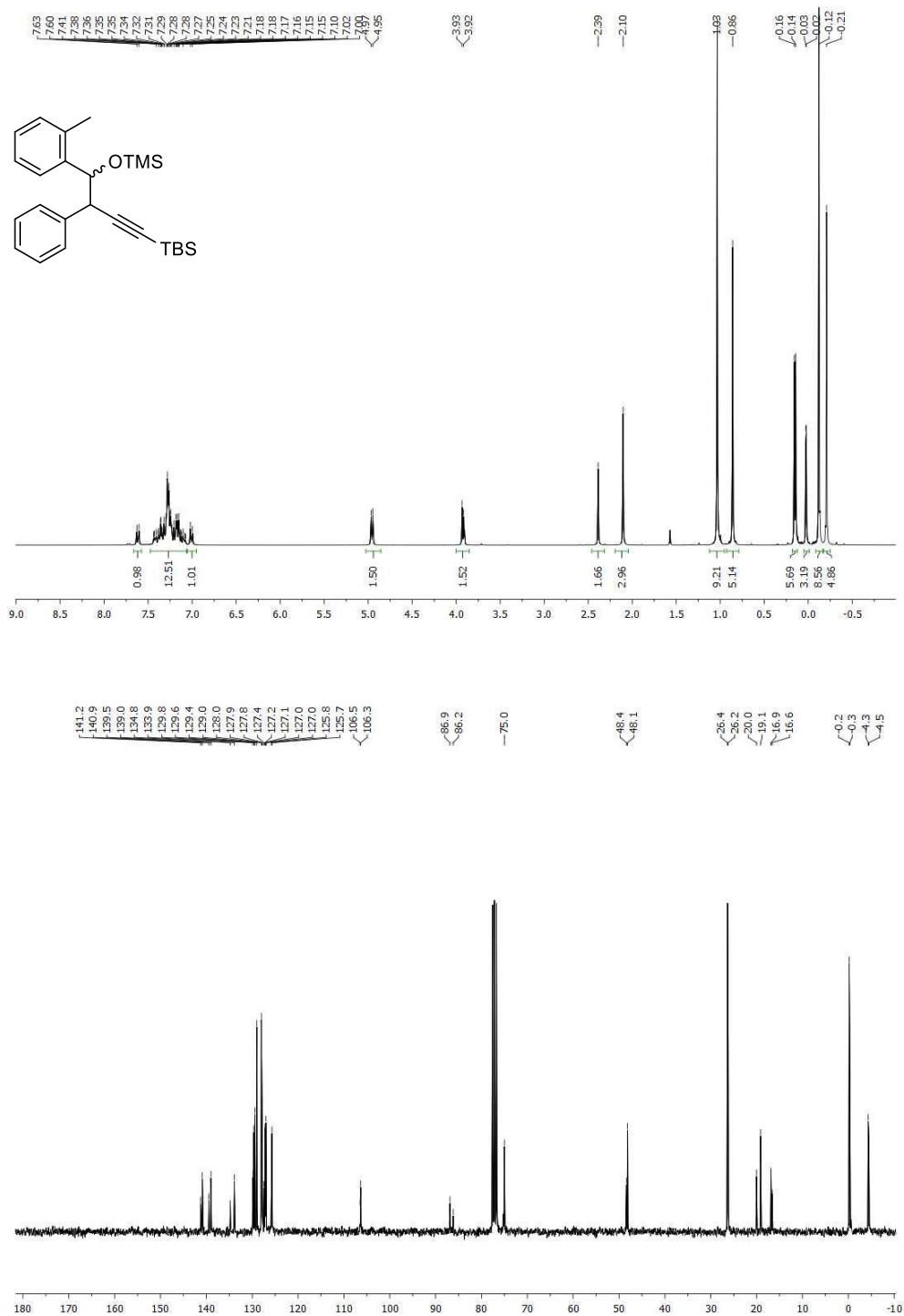
Tert-butyl dimethyl(4-(*m*-methoxyphenyl)-4-((trimethylsilyl)oxy)-3-phenylbut-1-yn-1-yl)silane (1.3i)



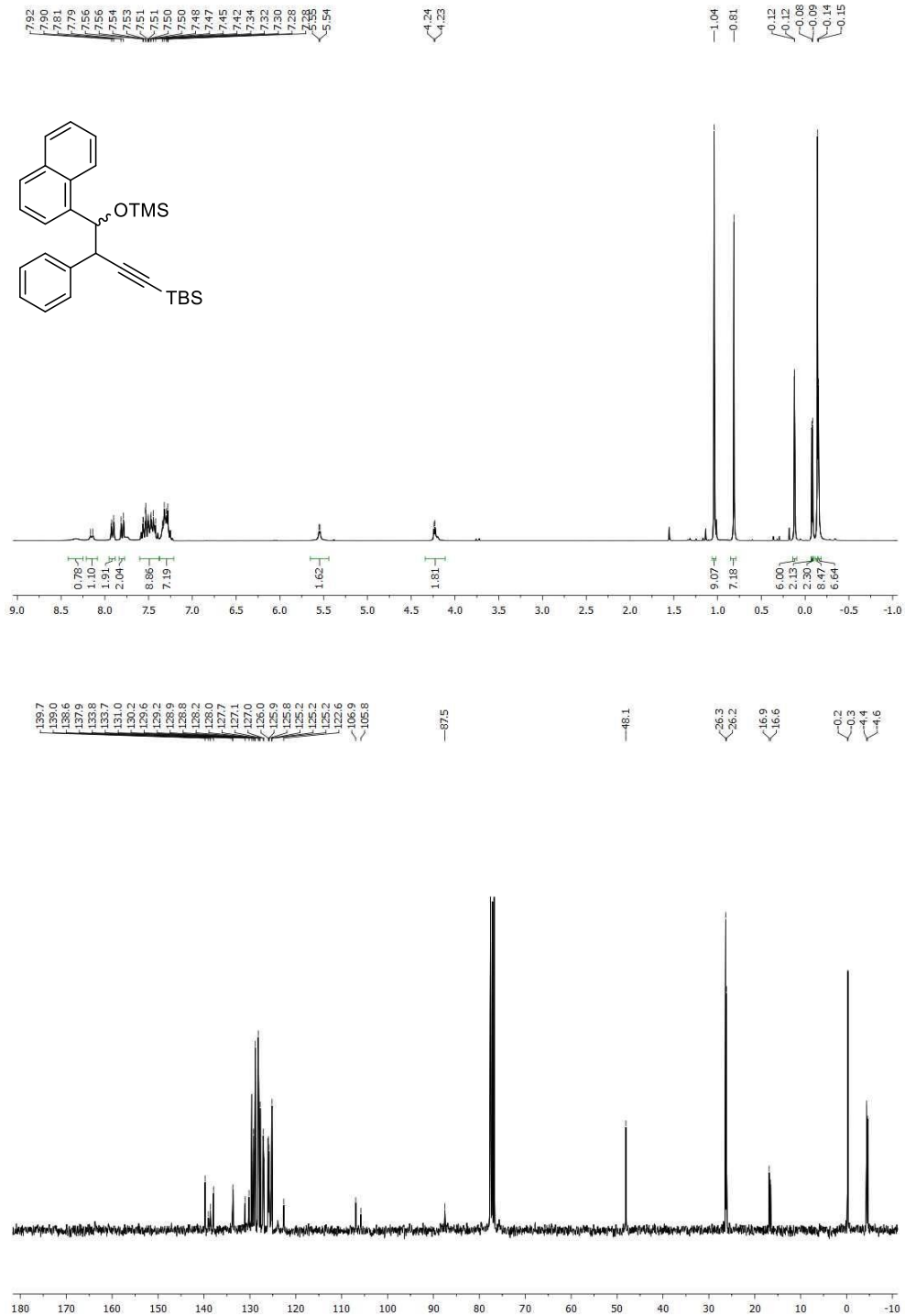
Tert-butyldimethyl(4-(3,5-dimethoxyphenyl)-4-((trimethylsilyloxy)-3-phenylbut-1-yn-1-yl)silane (1.3j)



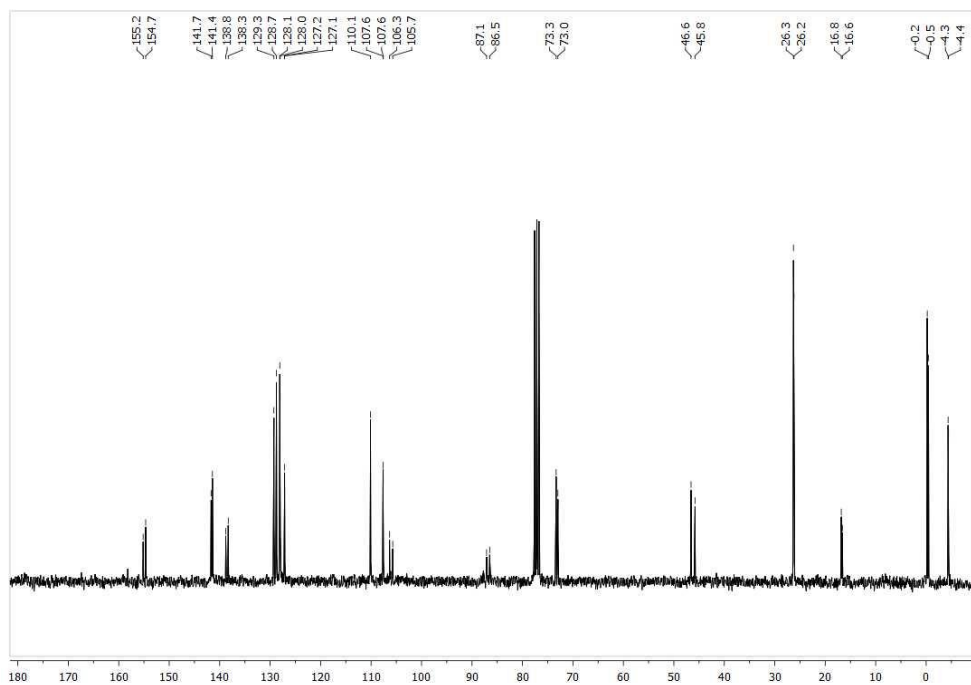
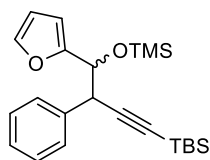
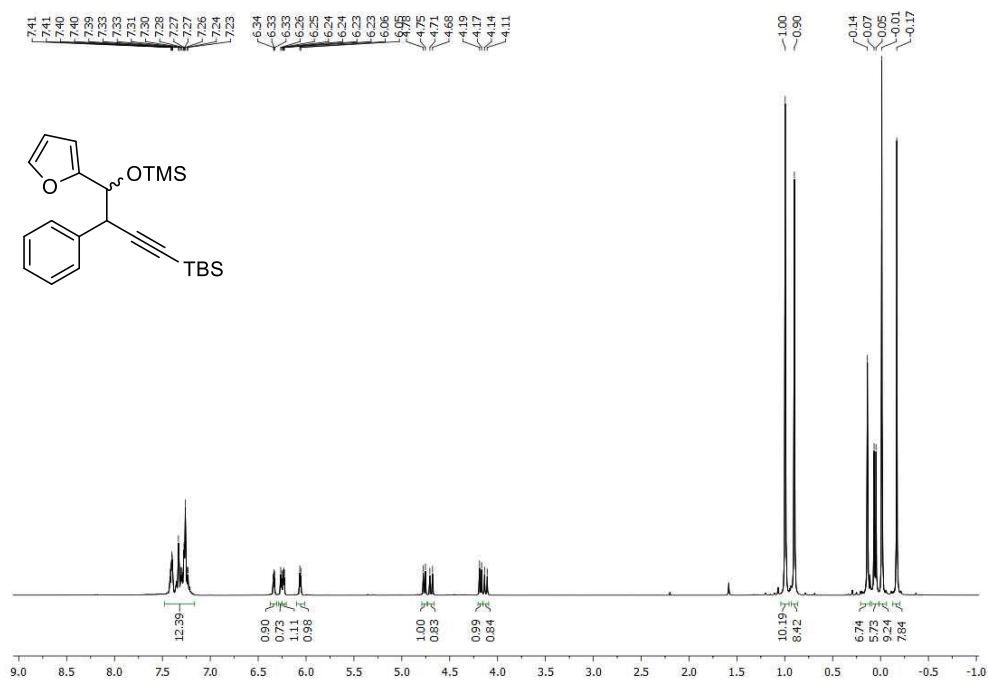
Tert-butyl dimethyl(4-((trimethylsilyl)oxy)-3-phenyl-4-(o-tolyl)but-1-yn-1-yl)silane (1.3k)



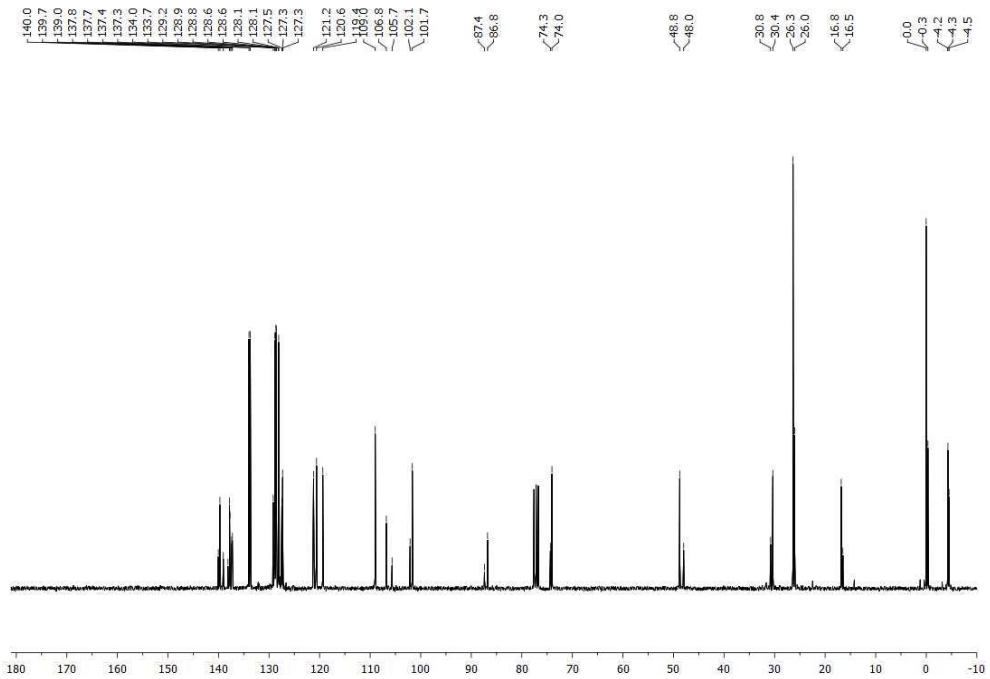
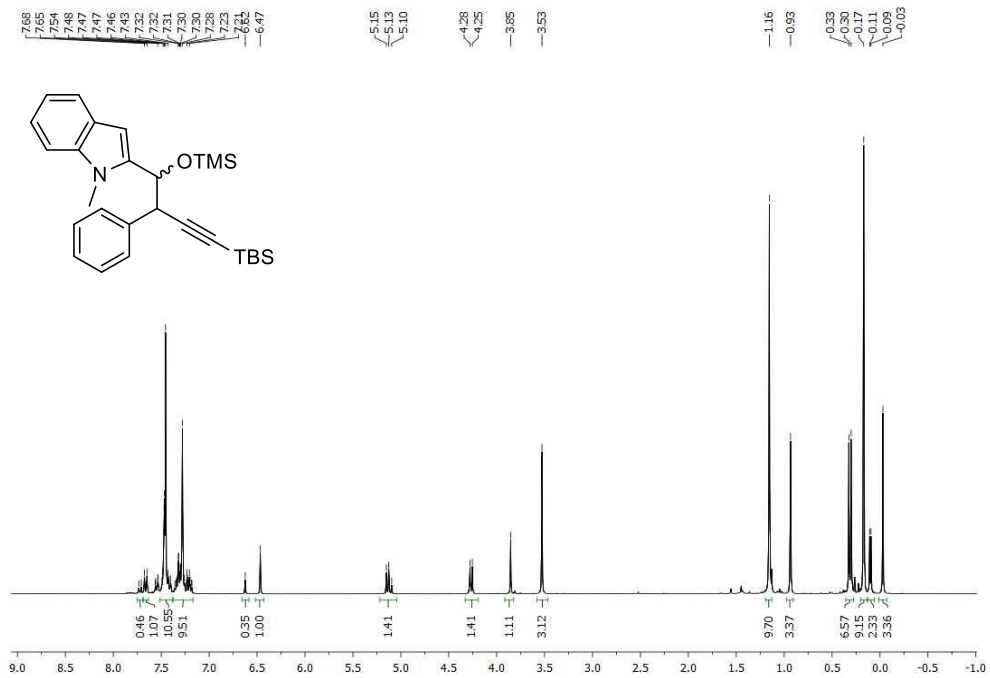
Tert-butyldimethyl(4-((trimethylsilyl)oxy)-4-(1-naphthyl)-3-phenylbut-1-yn-1-yl)silane (1.3l)



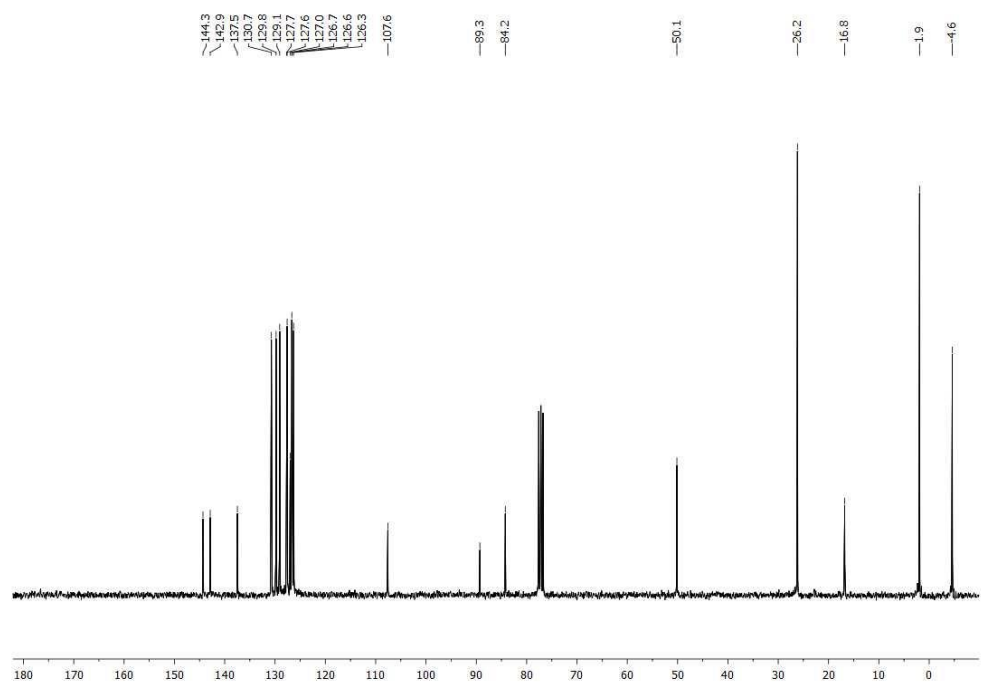
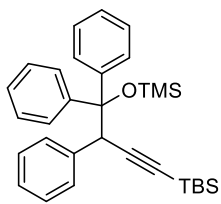
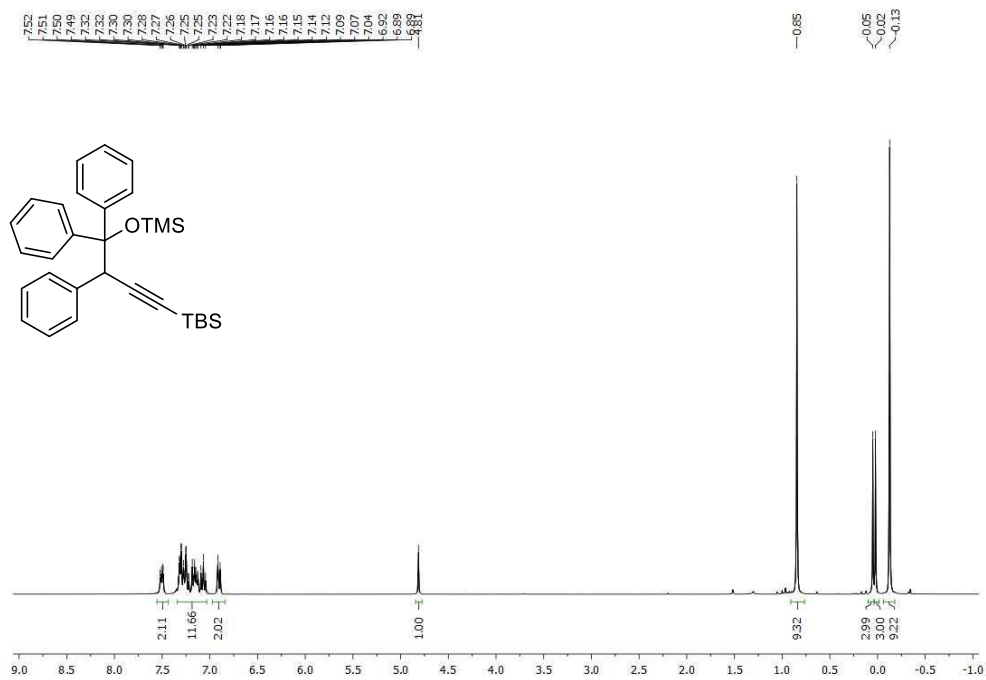
Tert-butyl dimethyl(4-(2-furyl)-4-((trimethylsilyl)oxy)-3-phenylbut-1-yn-1-yl)silane (1.3m)

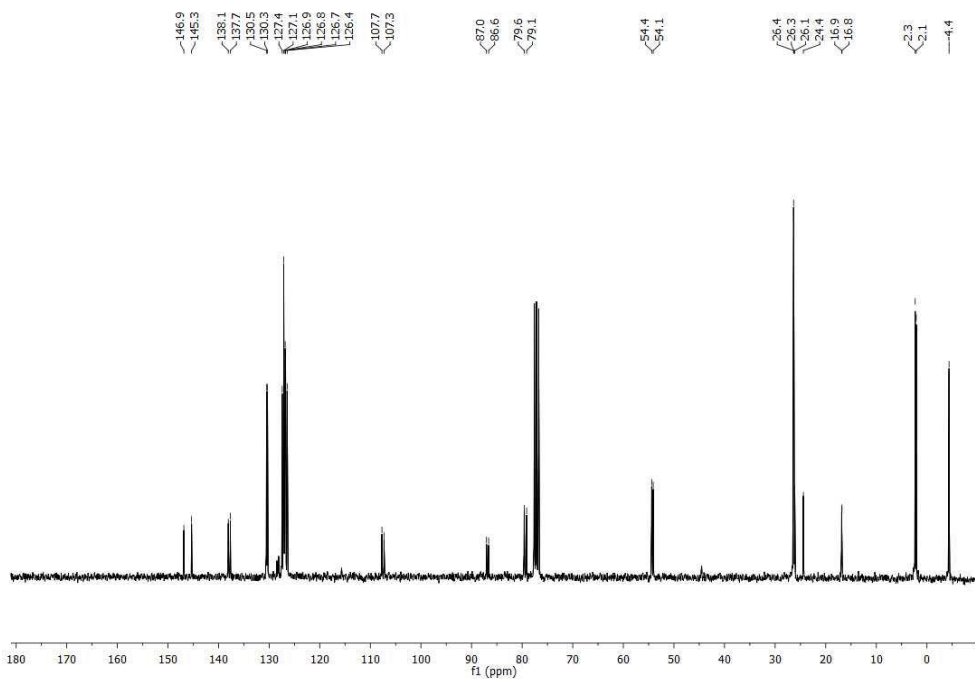
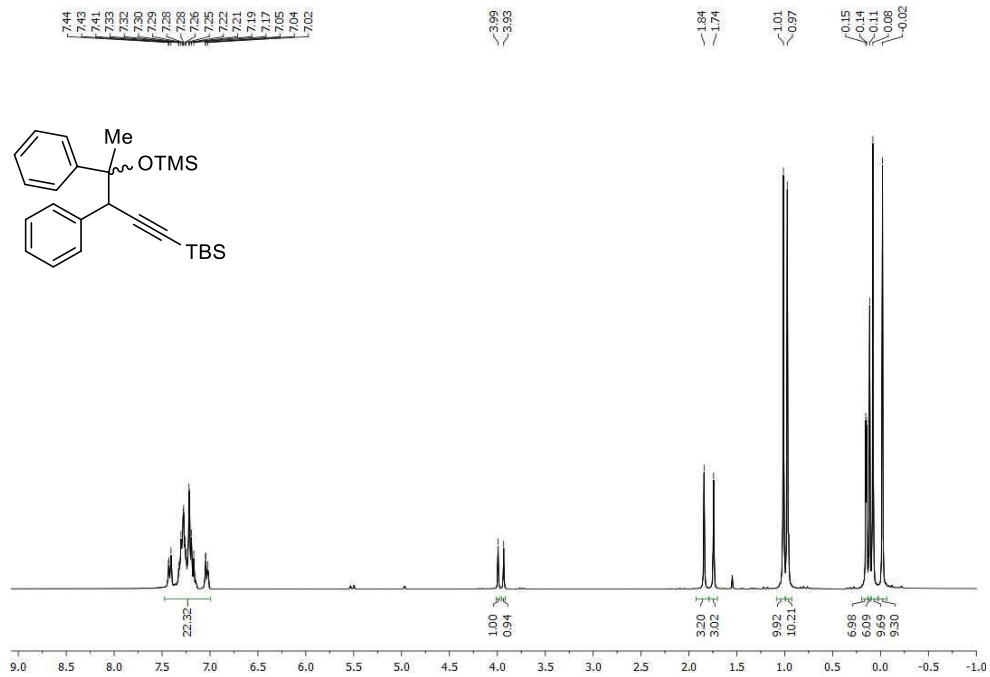


Tert-butyldimethyl(4-(1-methylindol-2-yl)-4-((trimethylsilyl)oxy)-3-phenylbut-1-yn-1-yl)silane (1.3n)

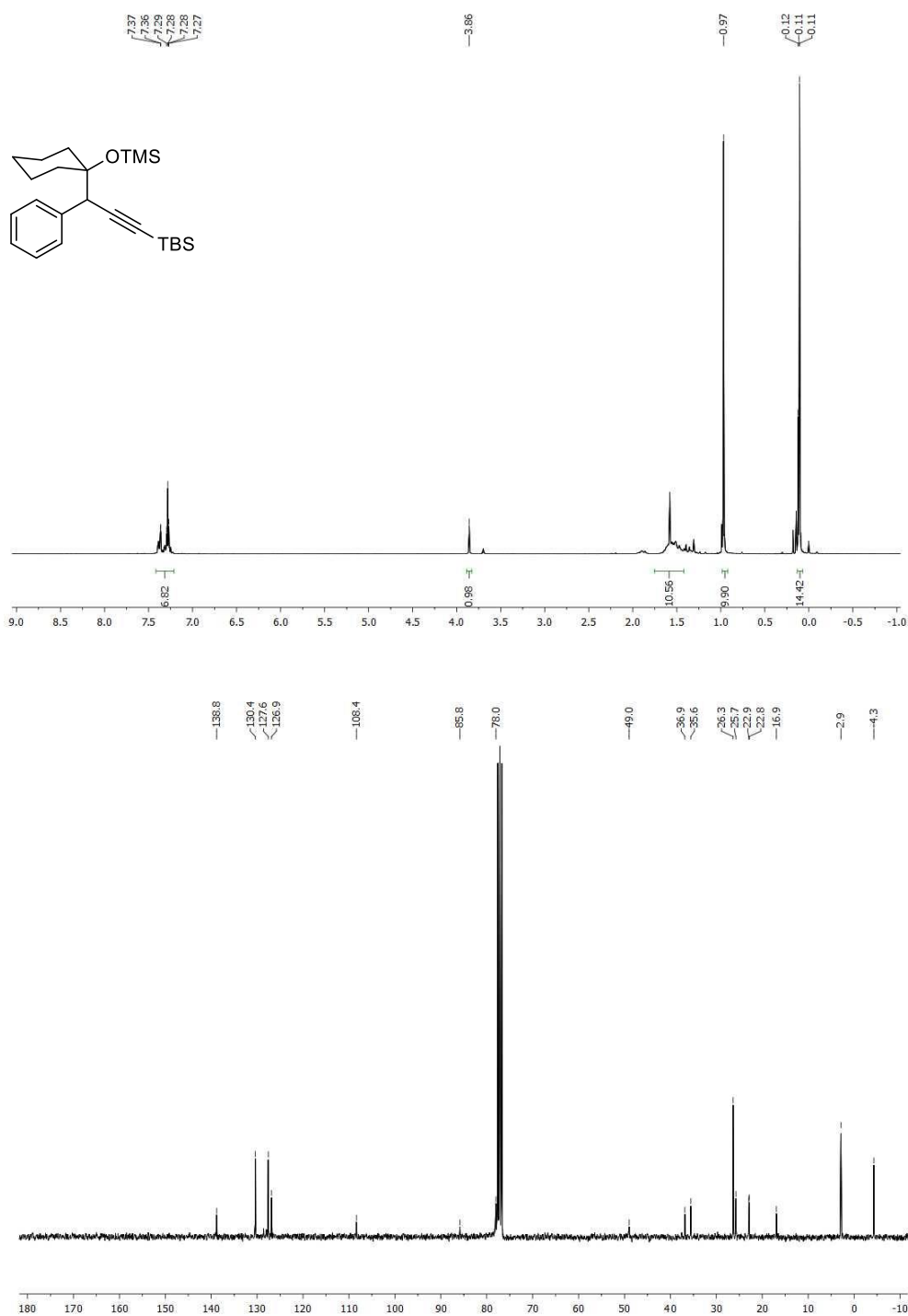


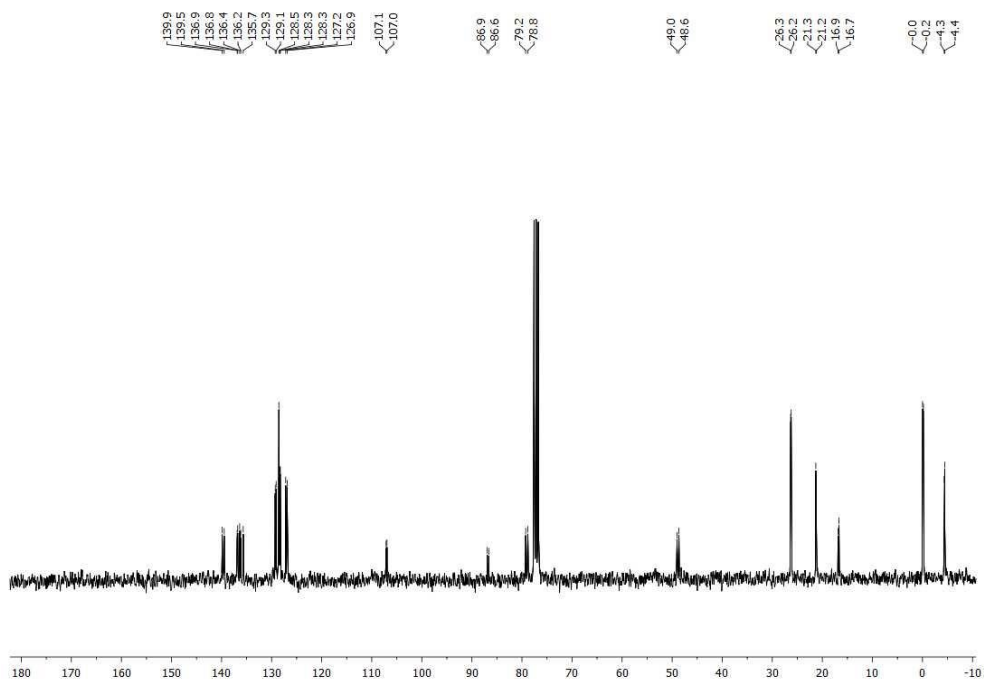
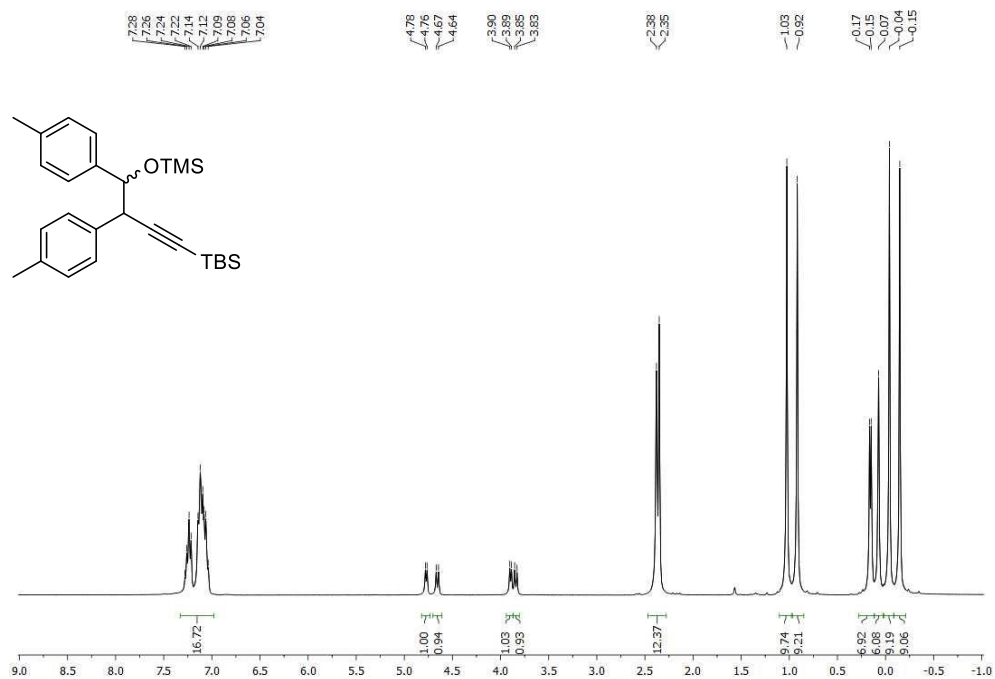
Tert-butyl dimethyl(4-((trimethylsilyloxy)-3,4,4-triphenylbut-1-yn-1-yl)silane (1.3o)



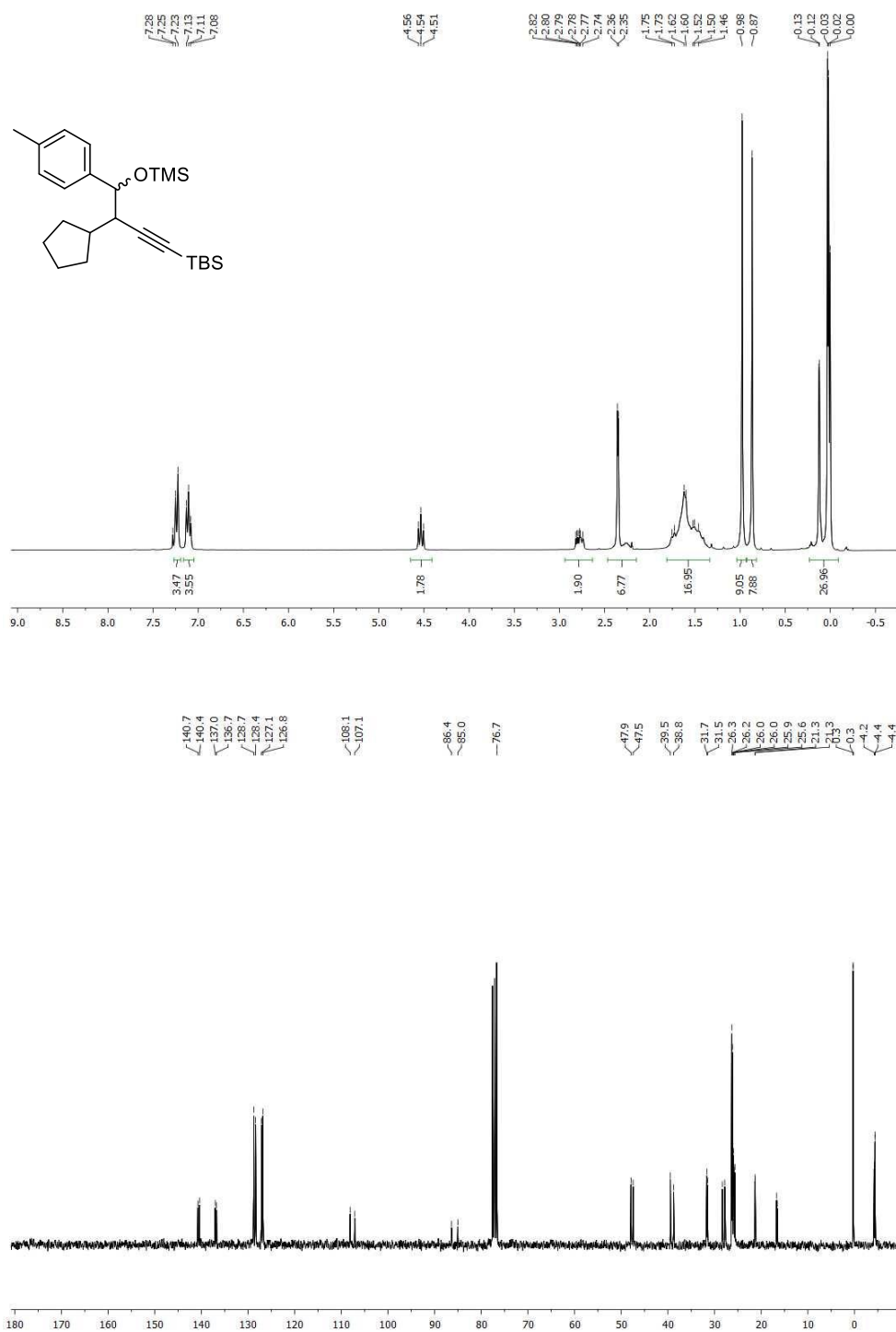
Tert-butyldimethyl(4-((trimethylsilyl)oxy)-3,4-diphenylpent-1-yn-1-yl)silane (1.3p)

Tert-butyl dimethyl(3-(1-((trimethylsilyl)oxy)cyclohexyl)-3-phenylprop-1-yn-1-yl)silane (1.3q)

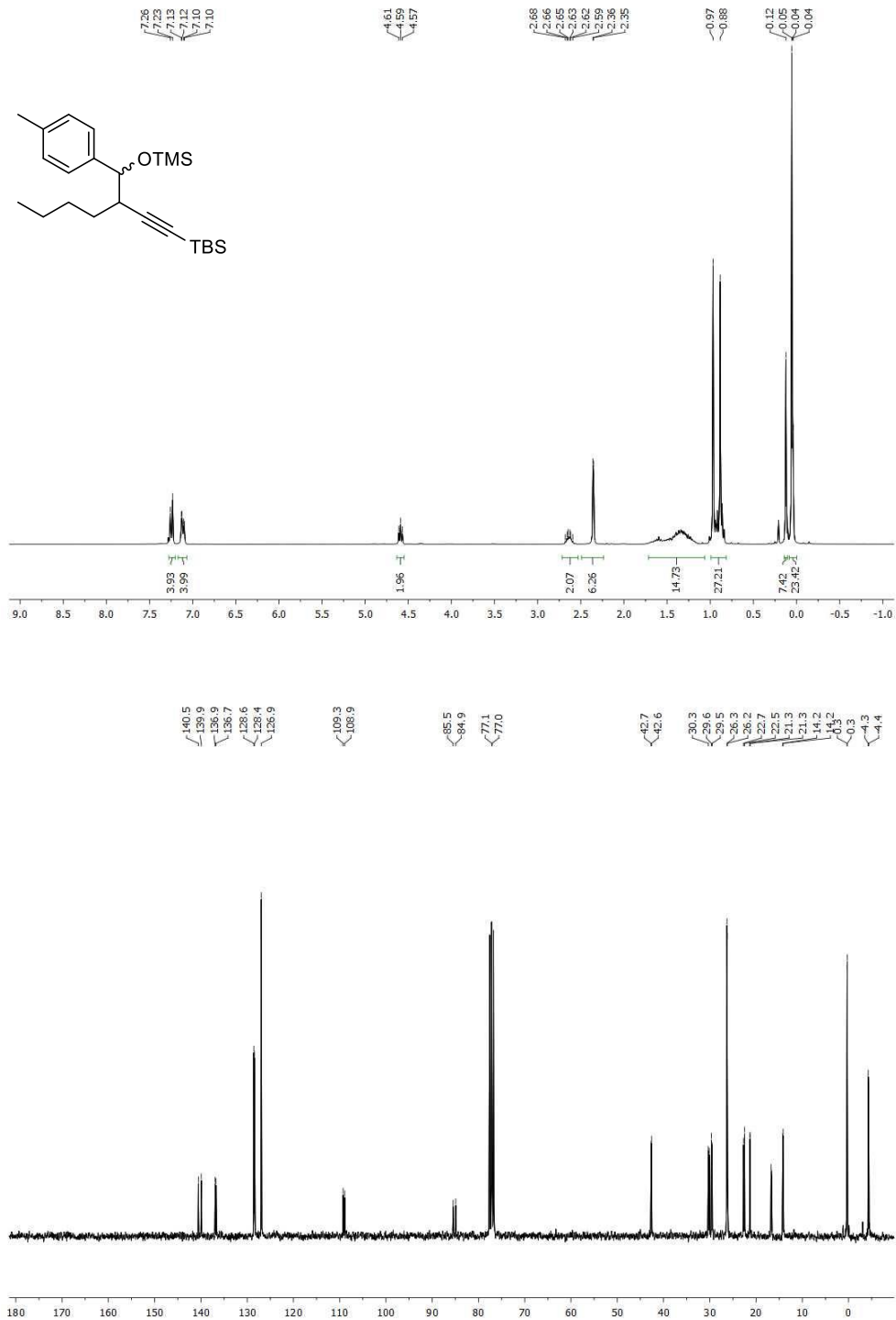


Tert-butyldimethyl(4-((trimethylsilyl)oxy)-3,4-di(*p*-tolyl)but-1-yn-1-yl)silane (1.3r)

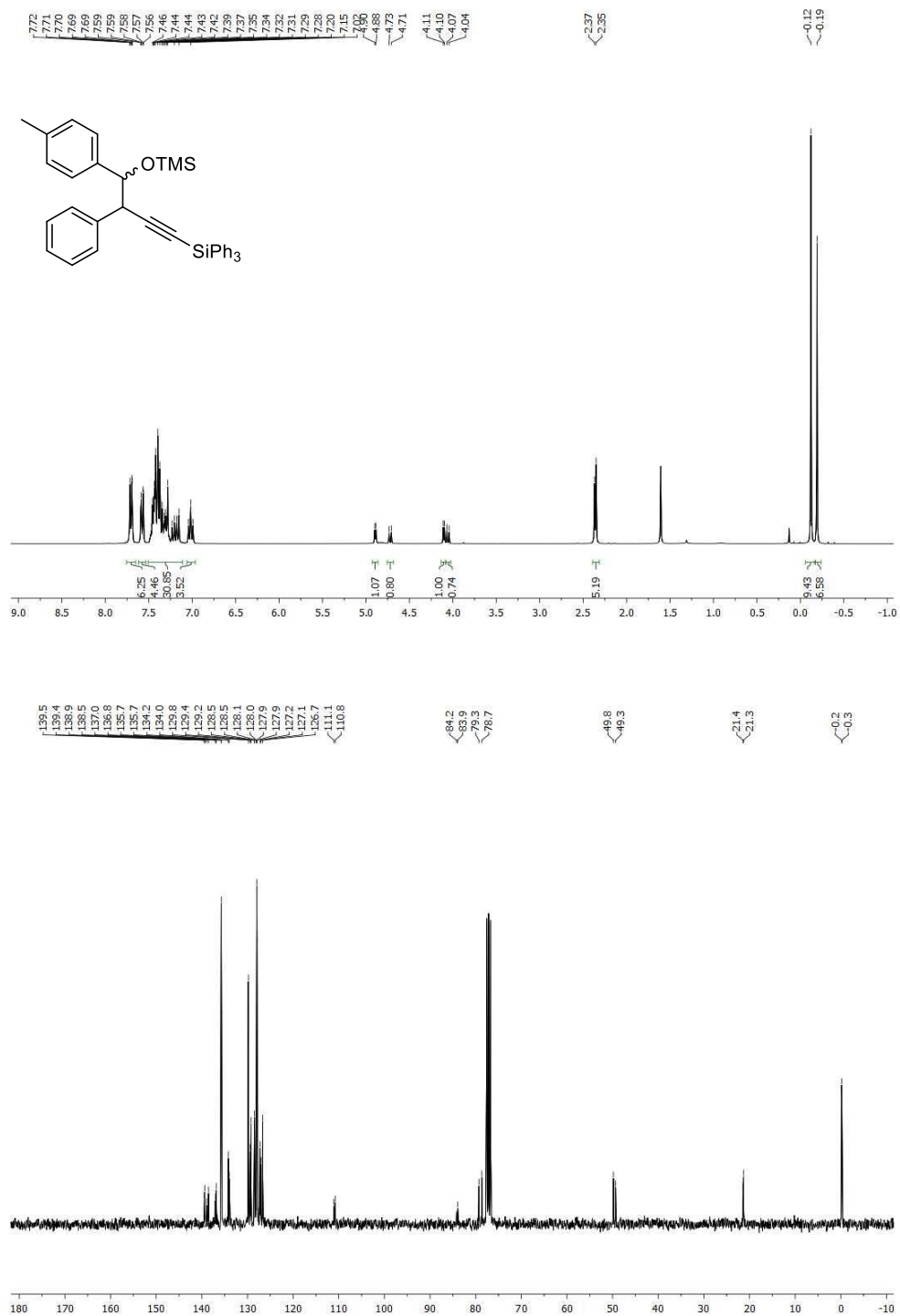
Tert-butyl dimethyl(3-cyclopentyl-4-((trimethylsilyl)oxy)-4-(*p*-tolyl)but-1-yn-1-yl)silane (1.3s)

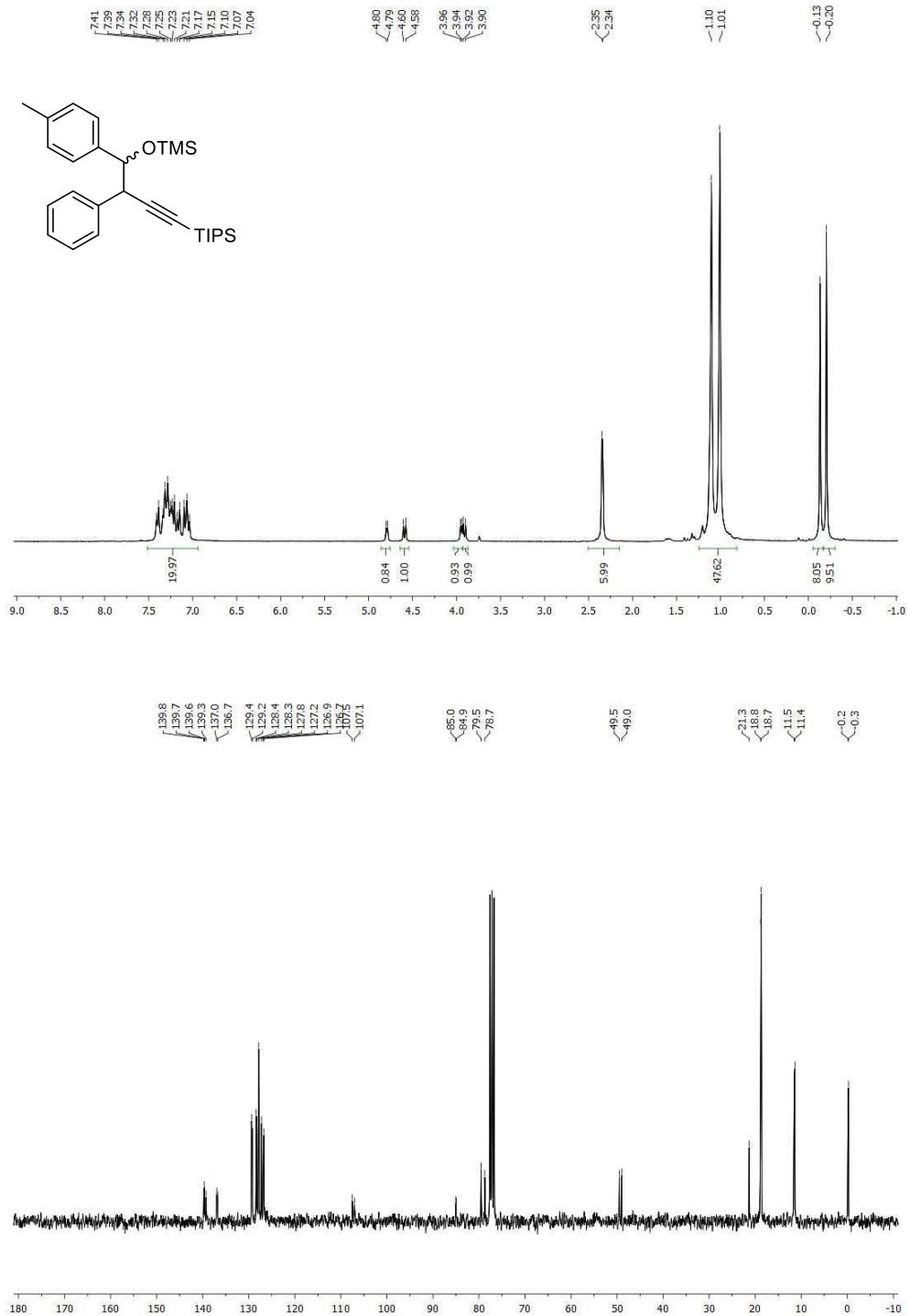


**Tert-butyldimethyl(3-(*p*-tolyl((trimethylsilyl)oxy)methyl)hept-1-yn-1-yl)silane
(1.3t)**

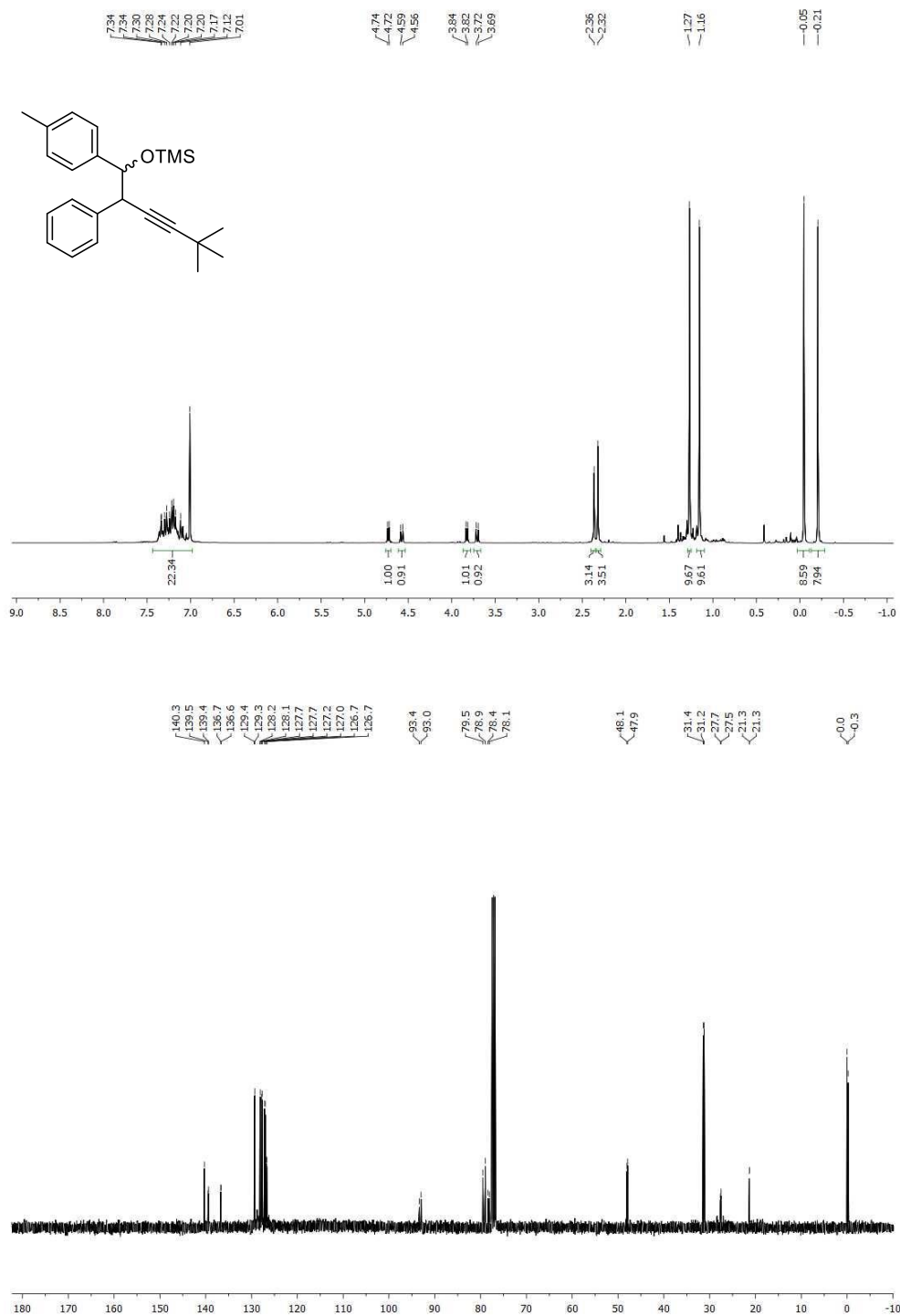


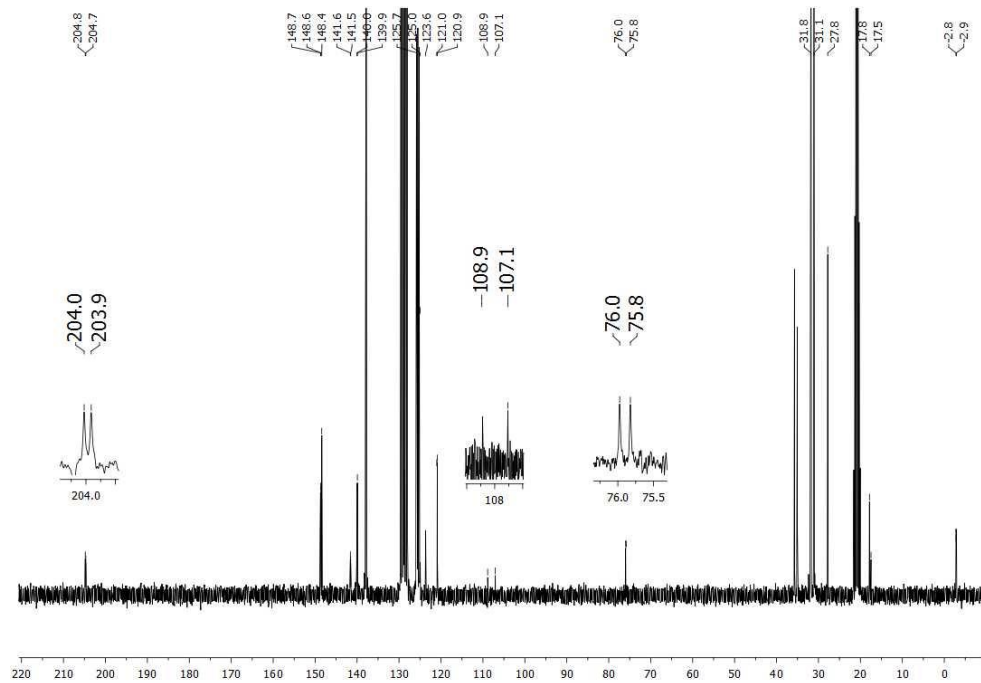
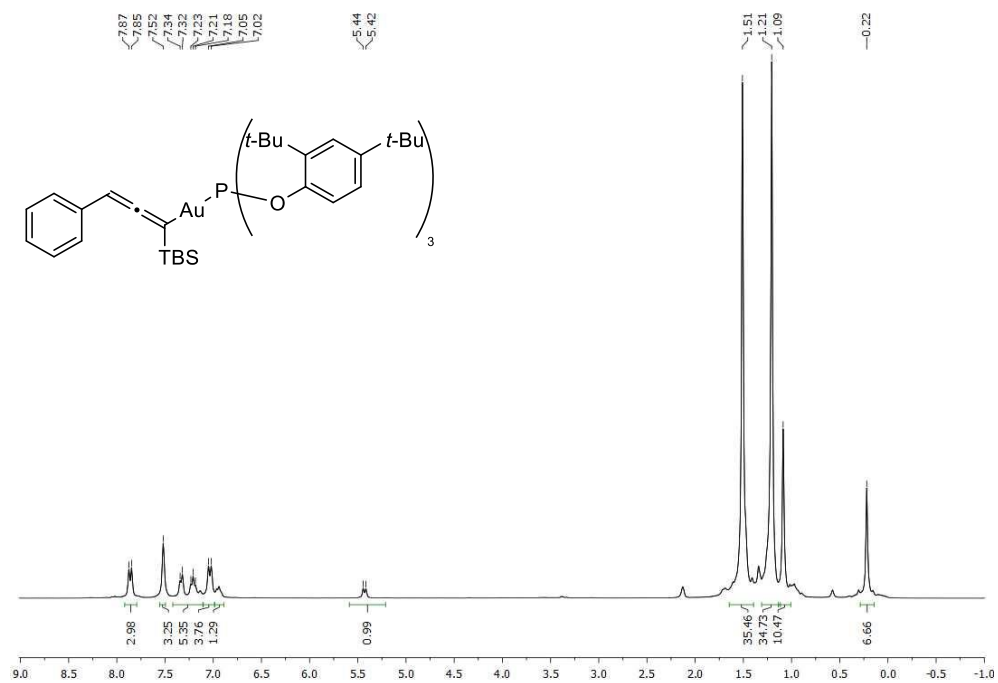
(4-((Trimethylsilyl)oxy)-3-phenyl-4-(*p*-tolyl)but-1-yn-1-yl)triphenylsilane (1.3u)



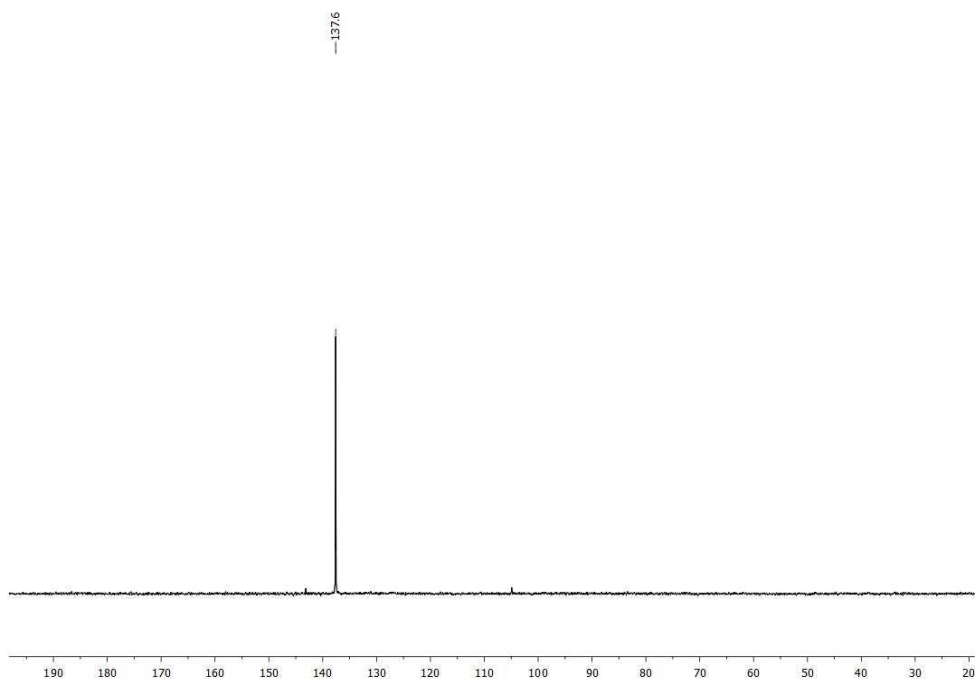
Triisopropyl(4-((trimethylsilyl)oxy)-3-phenyl-4-(*p*-tolyl)but-1-yn-1-yl)silane (1.3v)

((5,5-Dimethyl-2-phenyl-1-(*p*-tolyl)hex-3-yn-1-yl)oxy)trimethylsilane (1.3w)

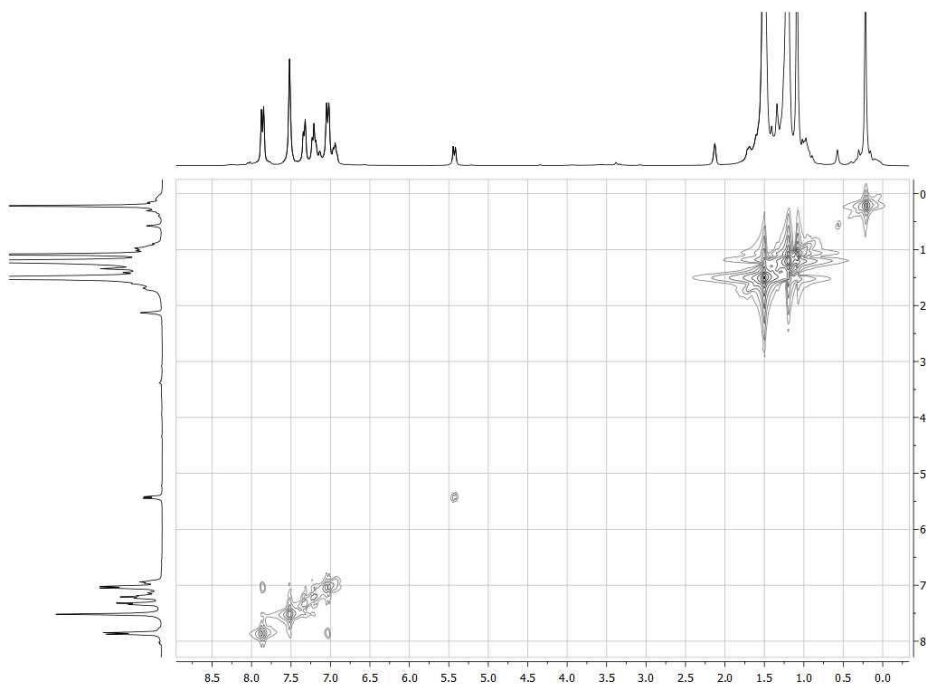


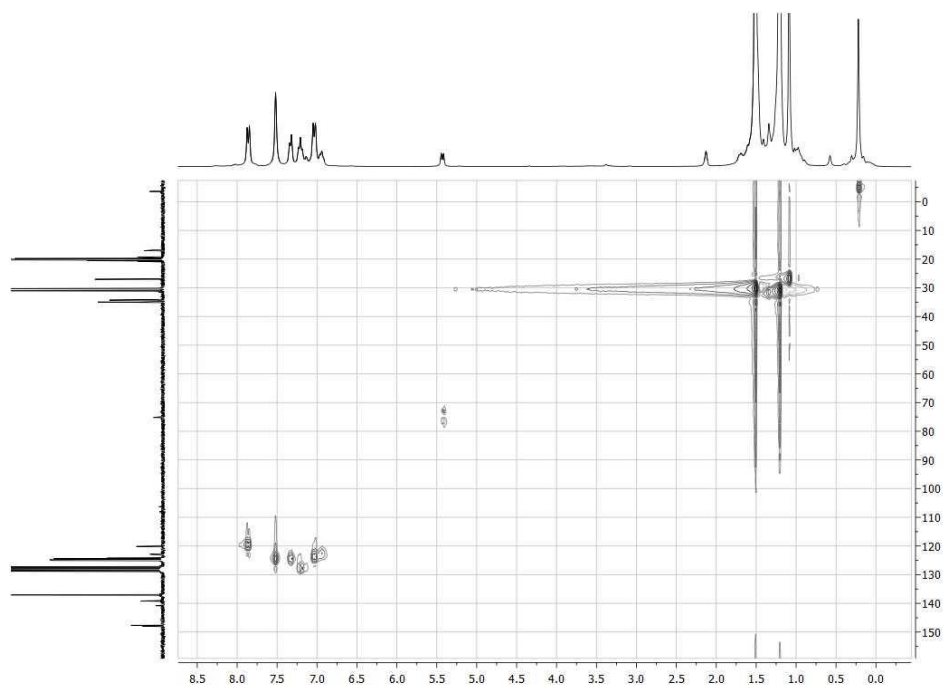
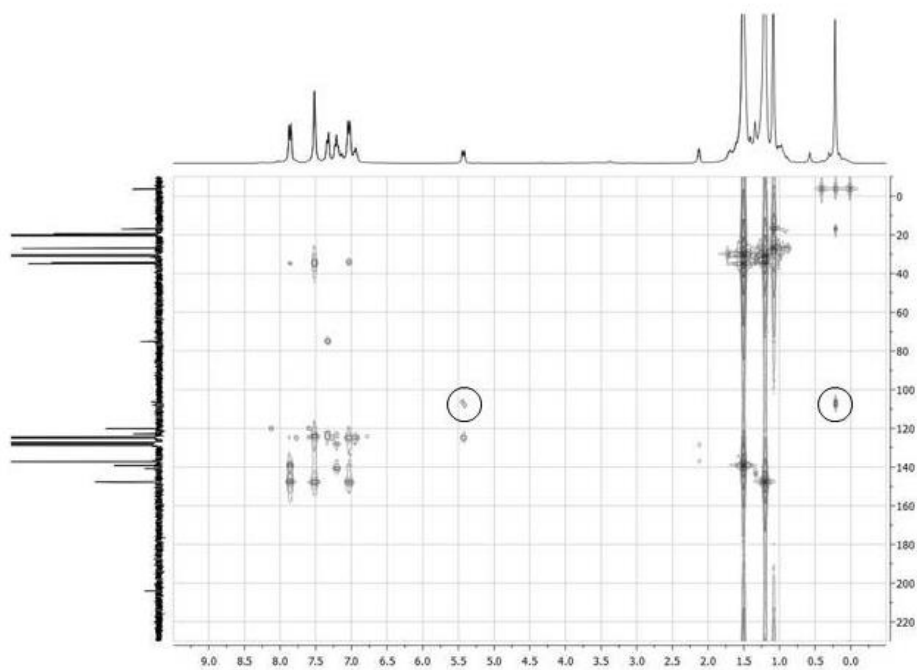
σ -allenylgold(I) complex 1.12a

^{31}P -NMR

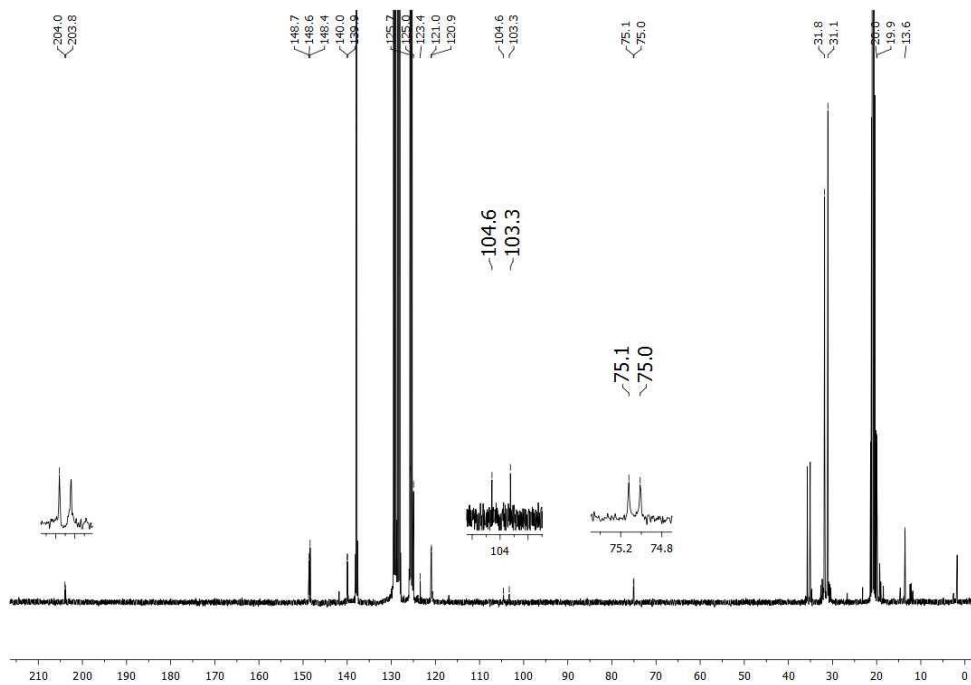
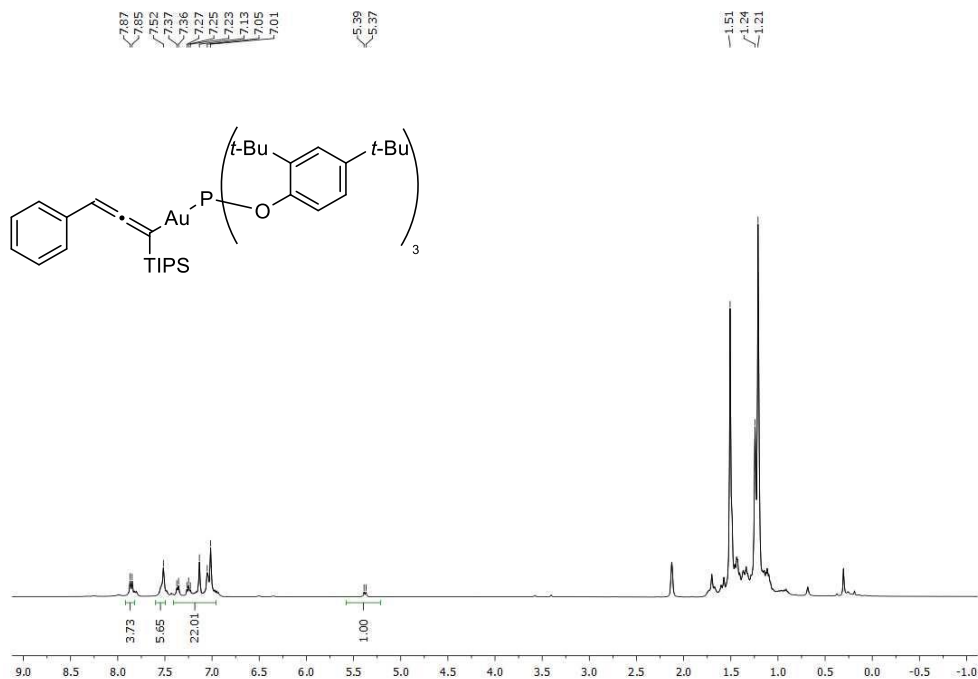


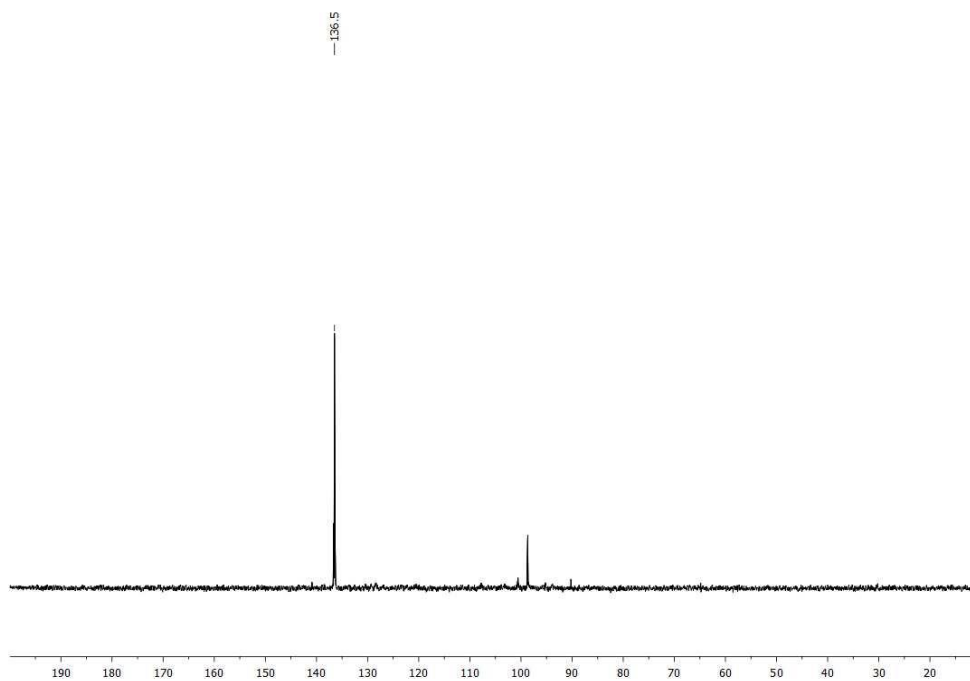
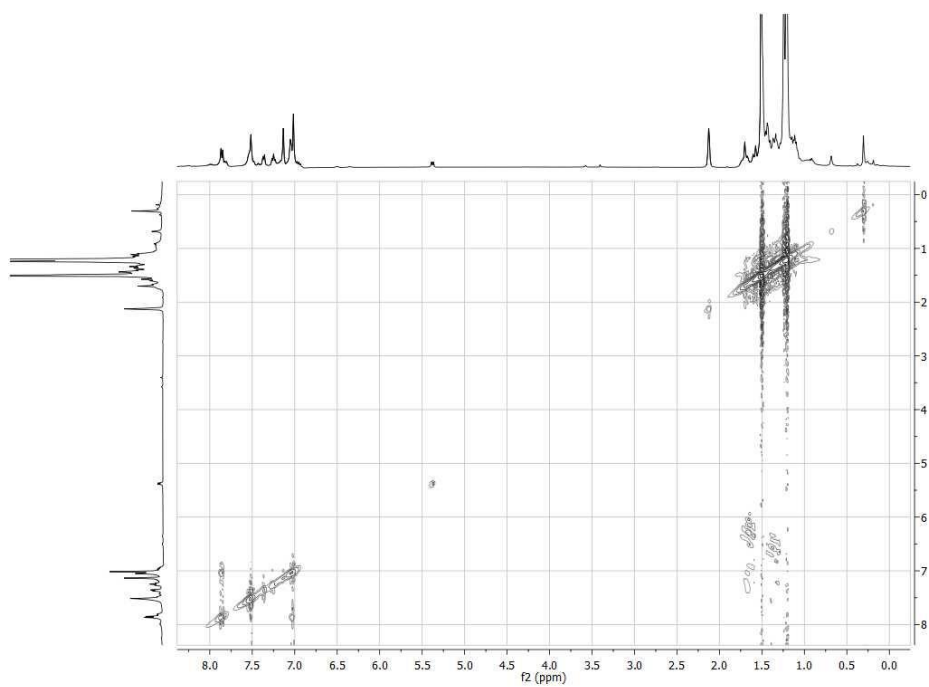
COSY (^1H - ^1H)



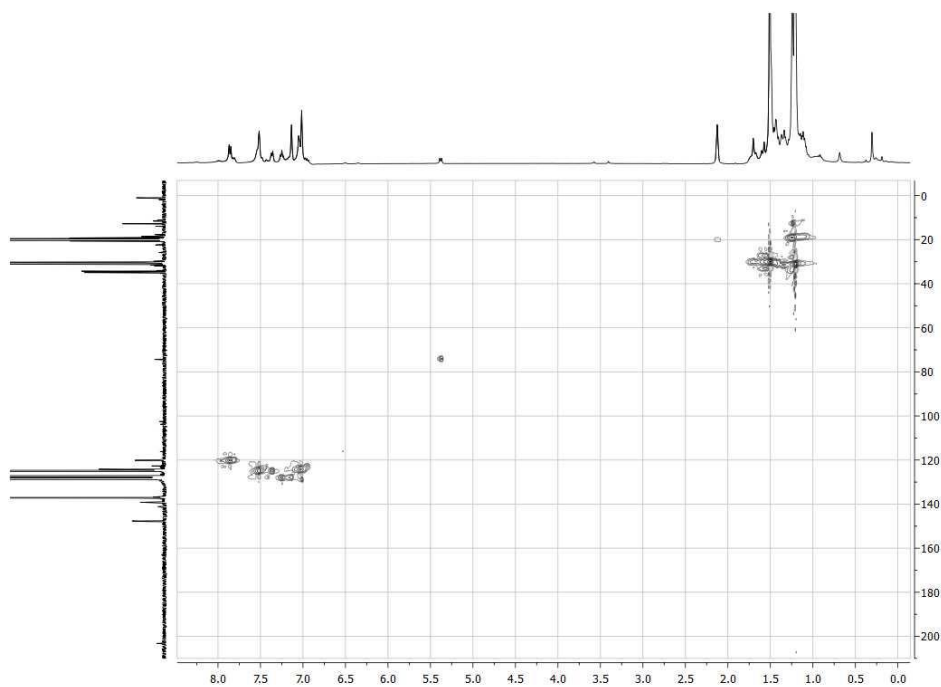
HSQC (^1H - ^{13}C)HMBC (^1H - ^{13}C)

σ -Allenylgold(I) complex (1.12b)

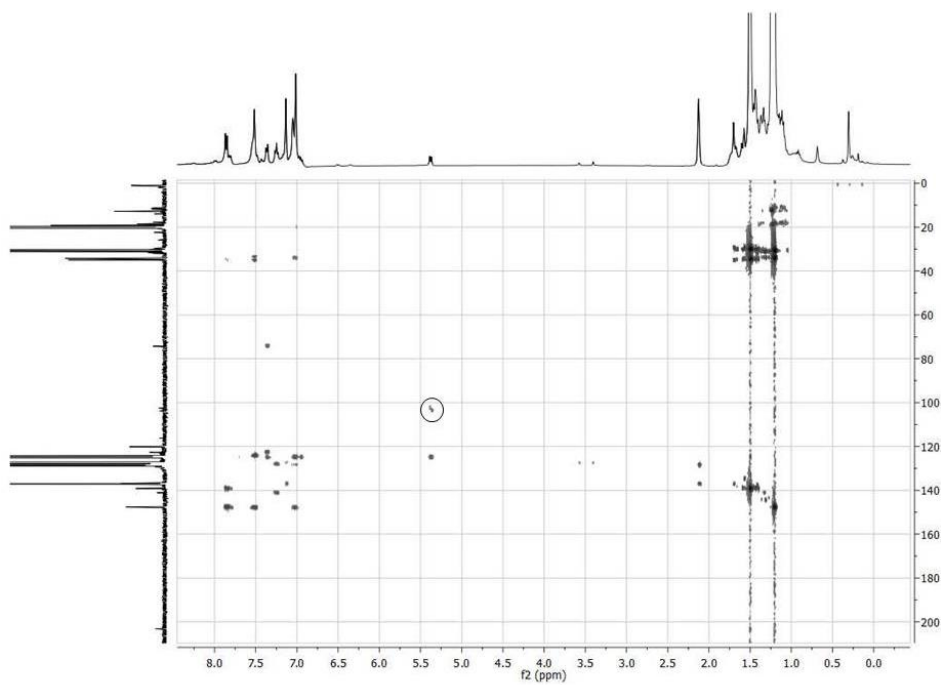


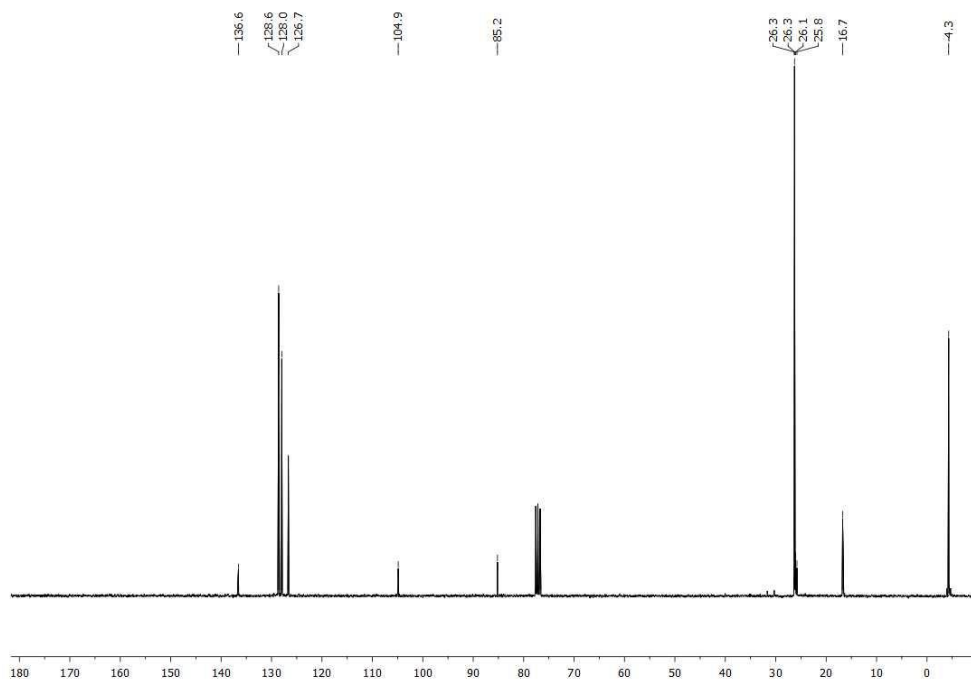
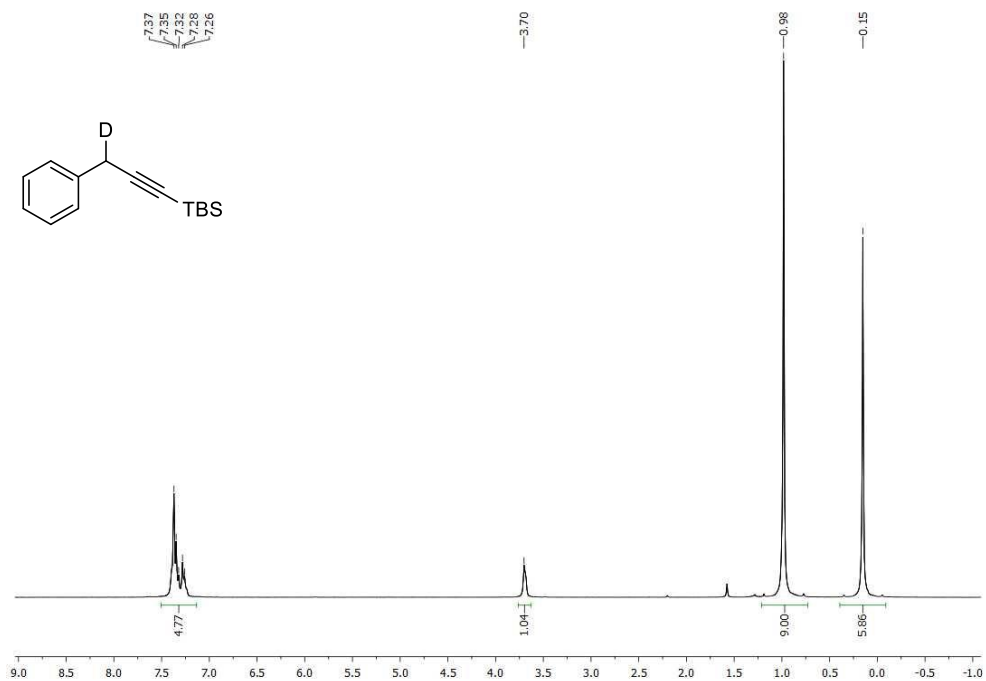
^{31}P -NMR**COSY (^1H - ^1H)**

HSQC (^1H - ^{13}C)



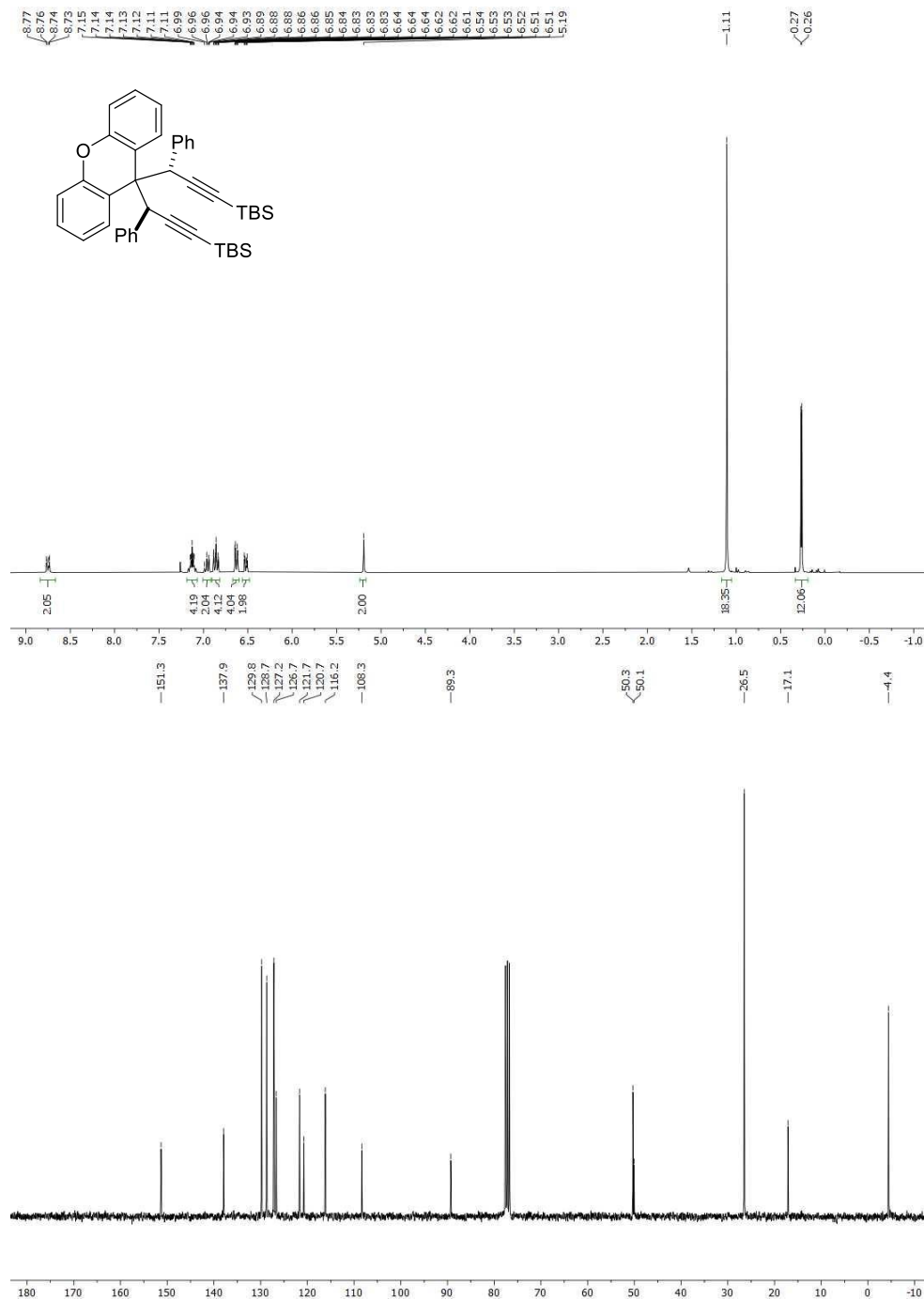
HMBC (^1H - ^{13}C)



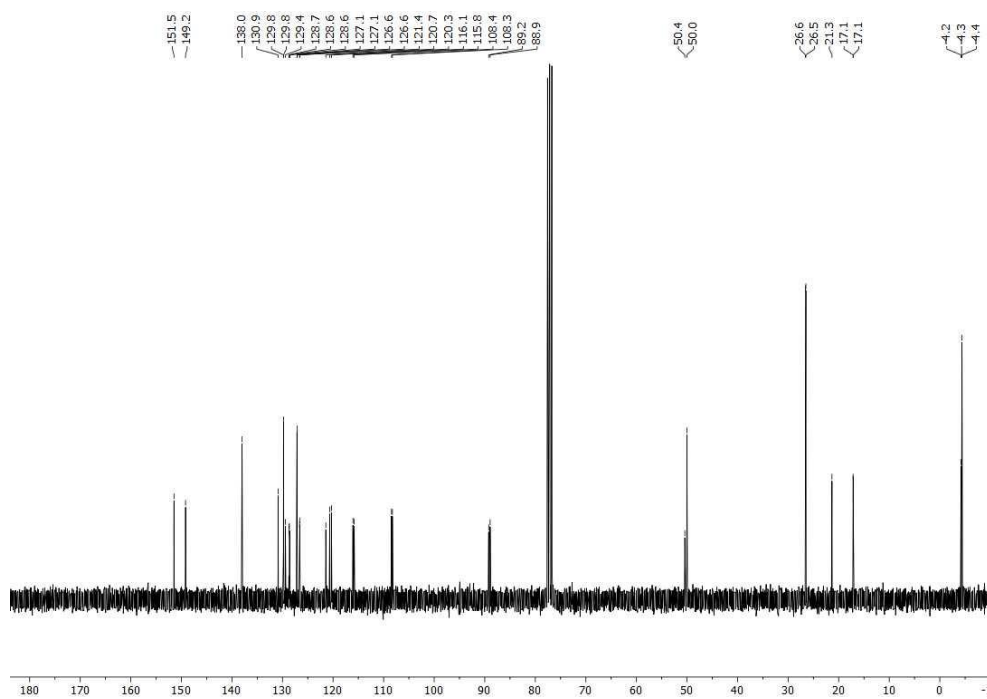
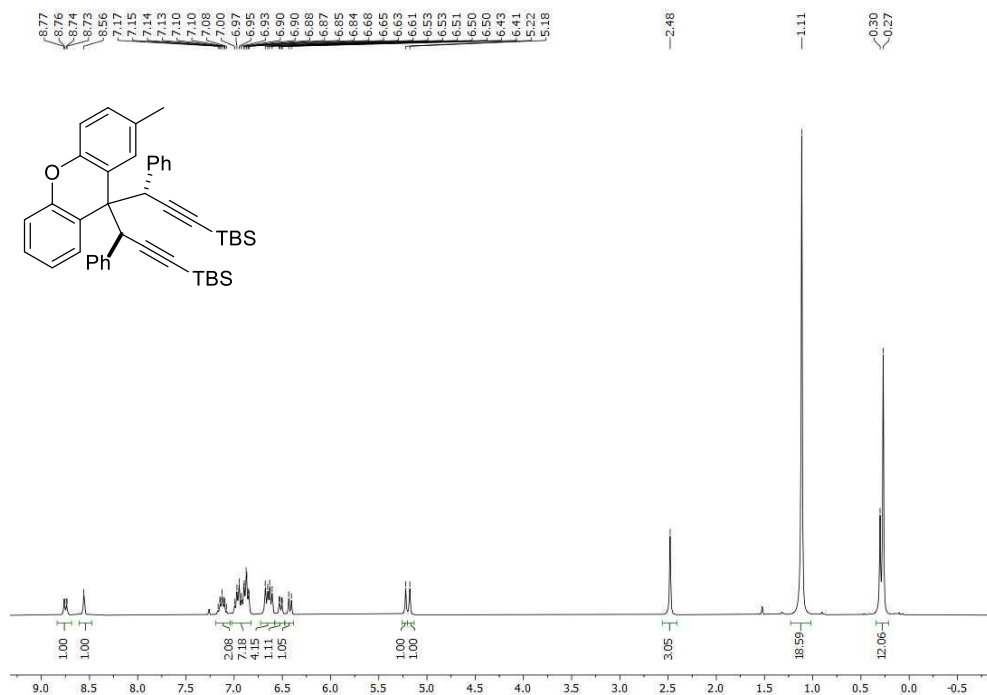
Tert-butyldimethyl(3-deutero-3-phenylprop-1-yn-1-yl)silane (7a)

2 Chapter II

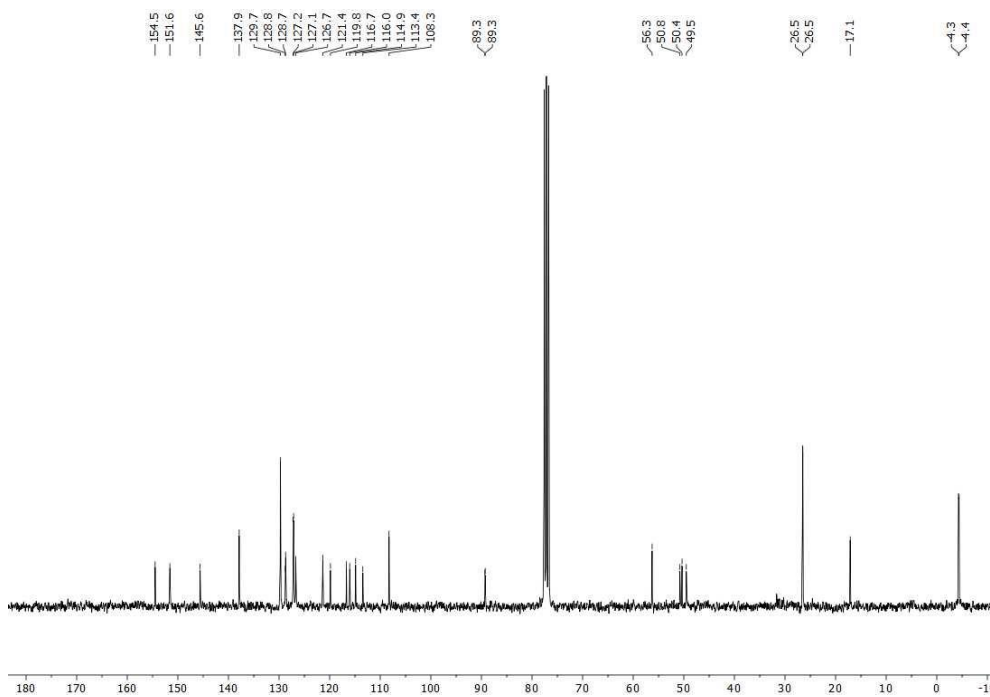
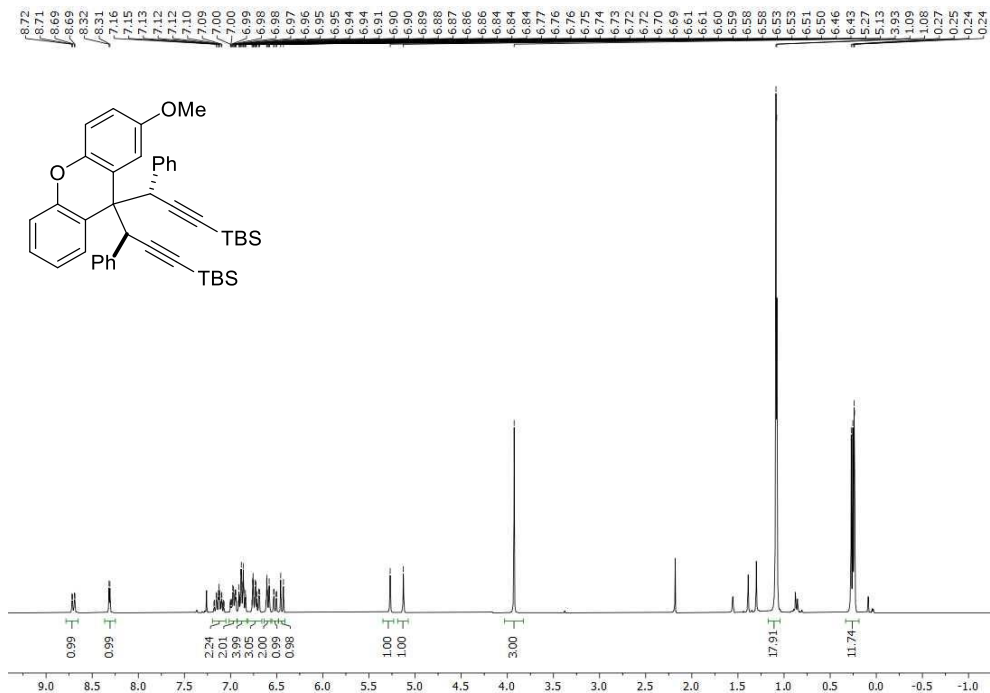
((3*S**,3'*S*')-(9*H*-Xanthene-9,9-diyl)bis(3-phenylprop-1-yne-3,1-diyl))bis(*tert*-butyldimethylsilane) (2.3a)



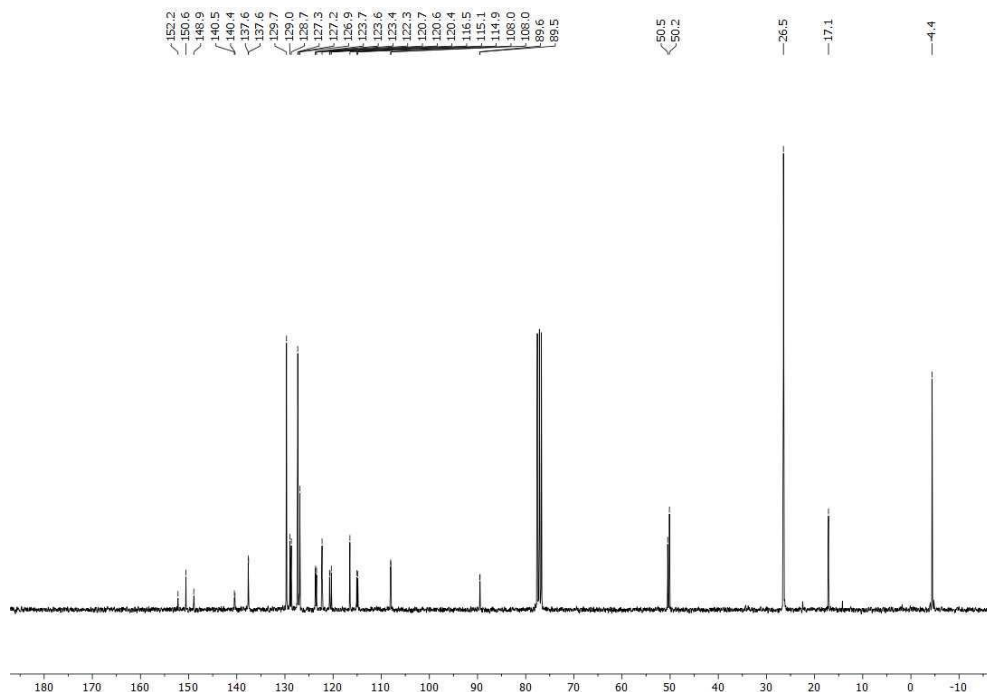
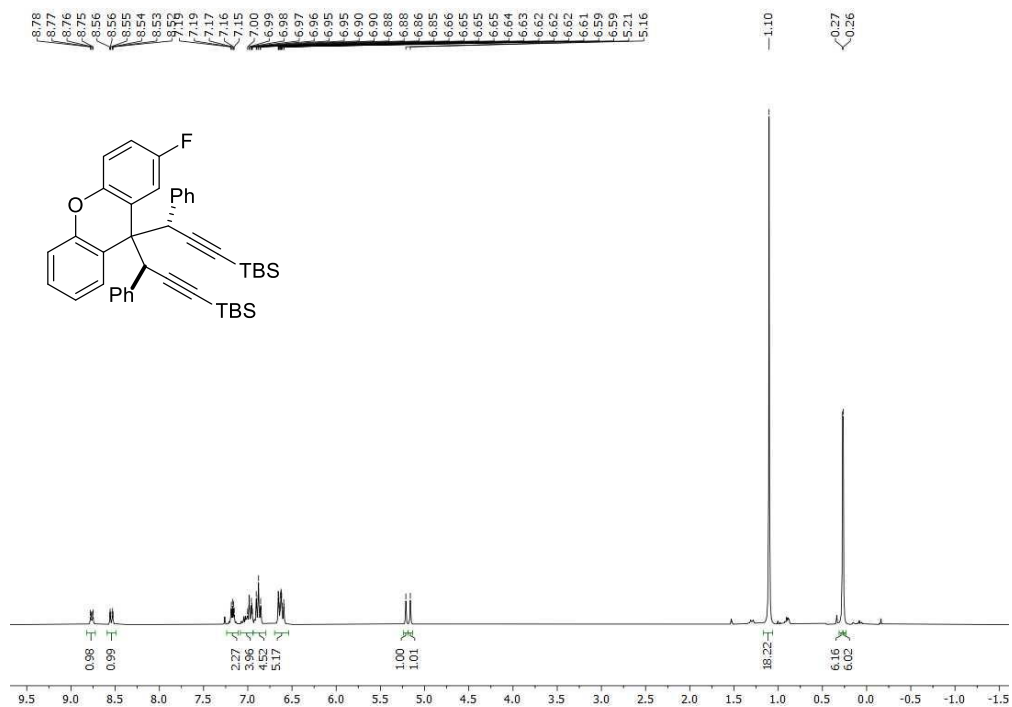
((3*S,3'*S*'*)-(2-Methyl-9*H*-xanthene-9,9-diyl)bis(3-phenylprop-1-yne-3,1-diyl))bis(*tert*-butyldimethylsilane) (2.3b).**



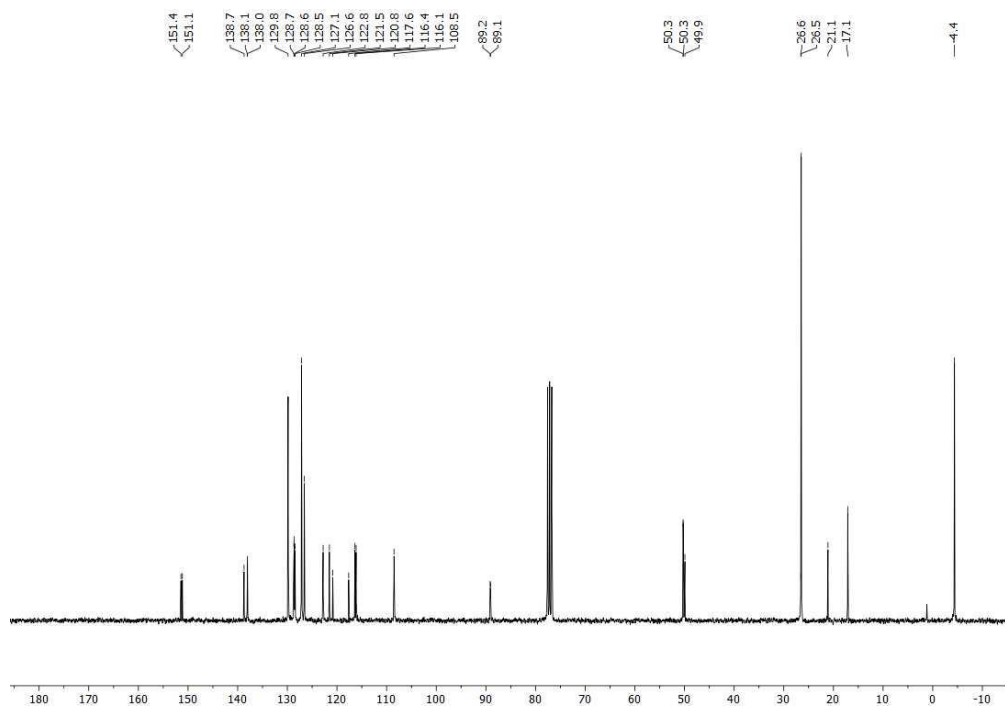
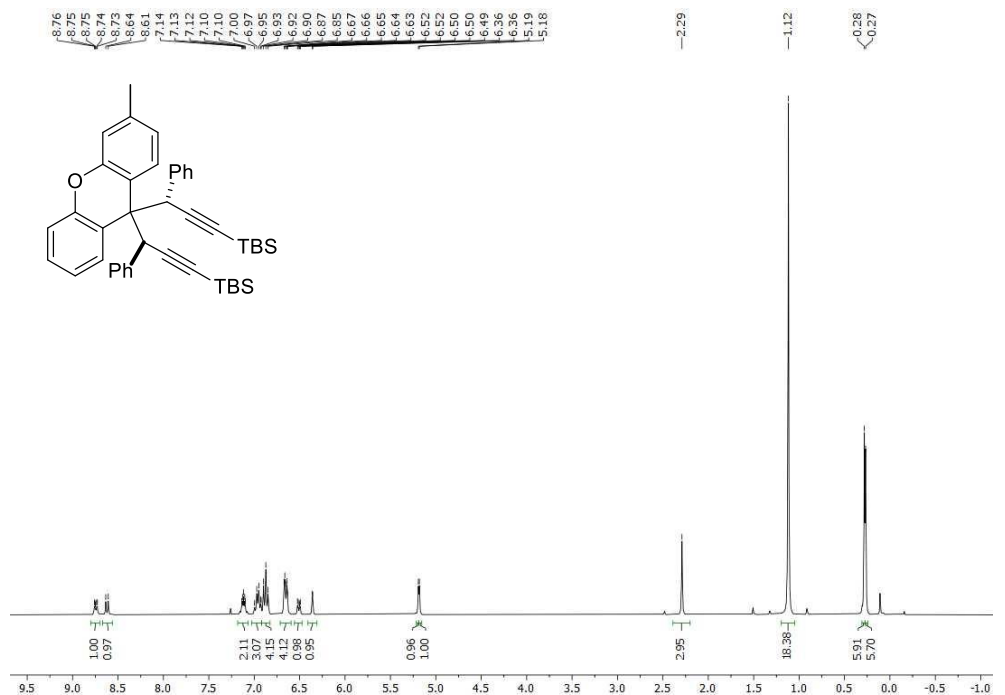
((3S*,3'S*)-(2-Methoxy-9H-xanthene-9,9-diyl)bis(3-phenylprop-1-yne-3,1-diyl))bis(tert-butylidimethylsilane) (2.3c)



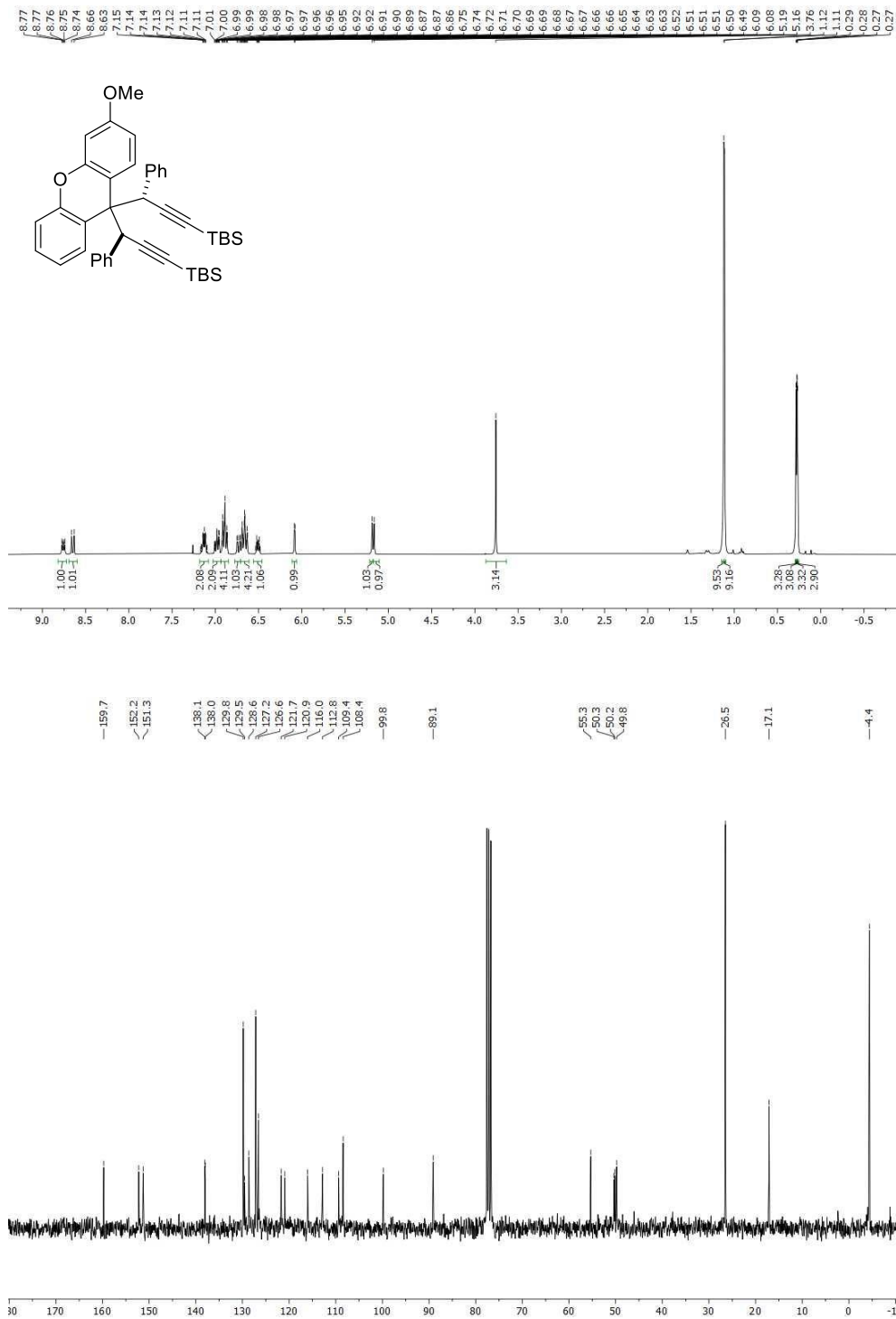
((3*S,3'*S*'*)-(2-Fluoro-9*H*-xanthene-9,9-diyl)bis(3-phenylprop-1-yne-3,1-diyl))bis(*tert*-butyldimethylsilane) (2.3d).**



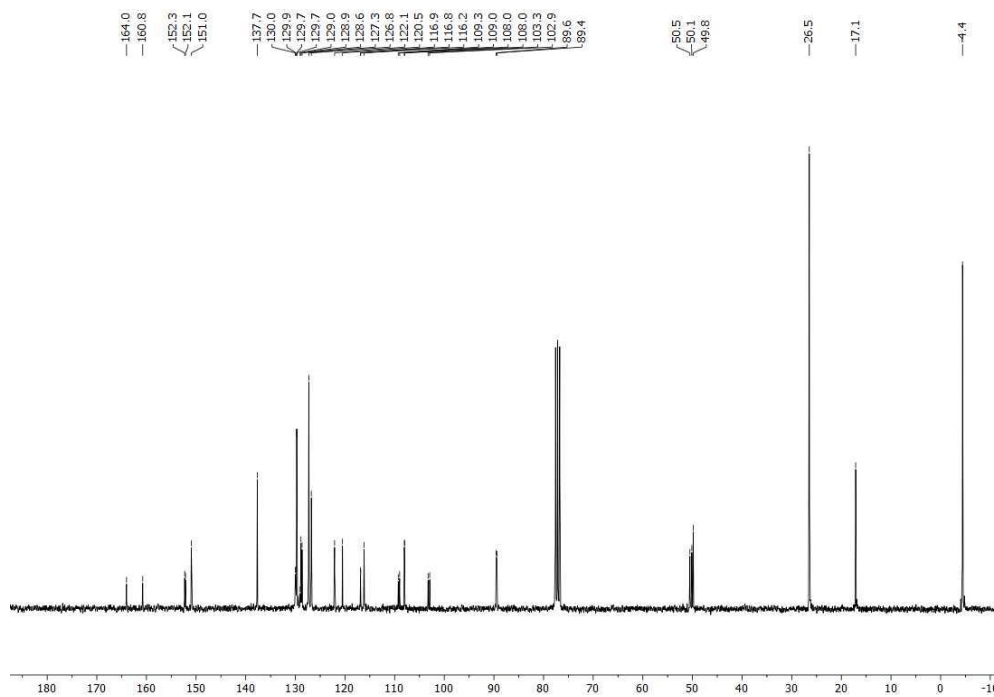
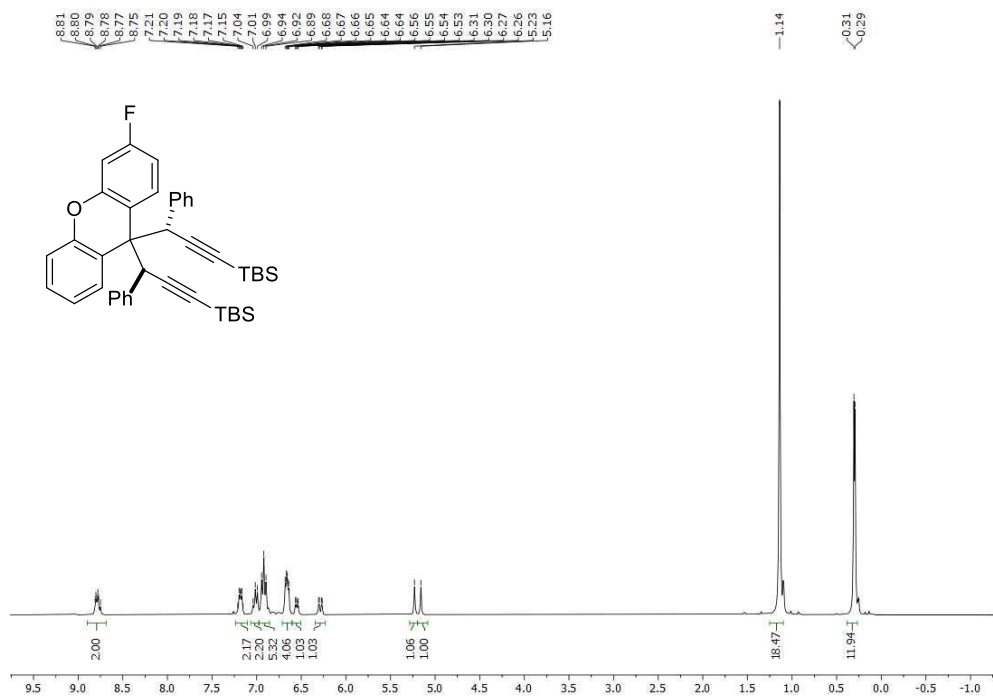
((3*S,3'*S*')-(3-Methyl-9*H*-xanthene-9,9-diyl)bis(3-phenylprop-1-yne-3,1-diyl))bis(*tert*-butyldimethylsilane) (2.3f)**



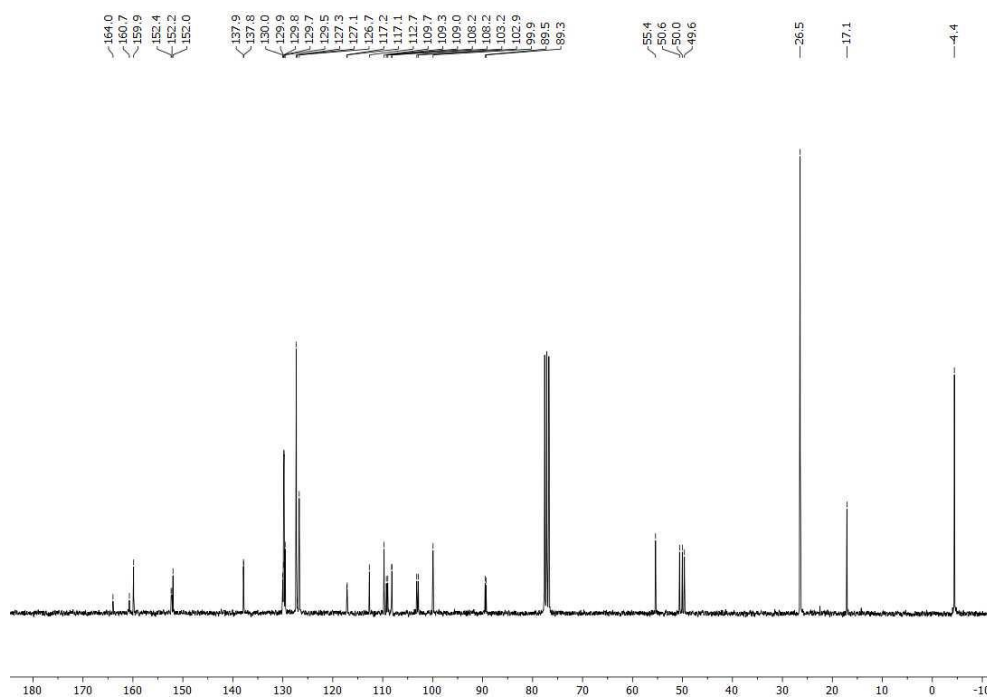
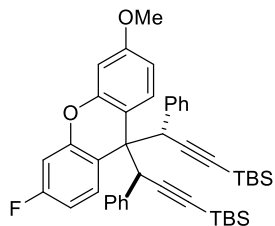
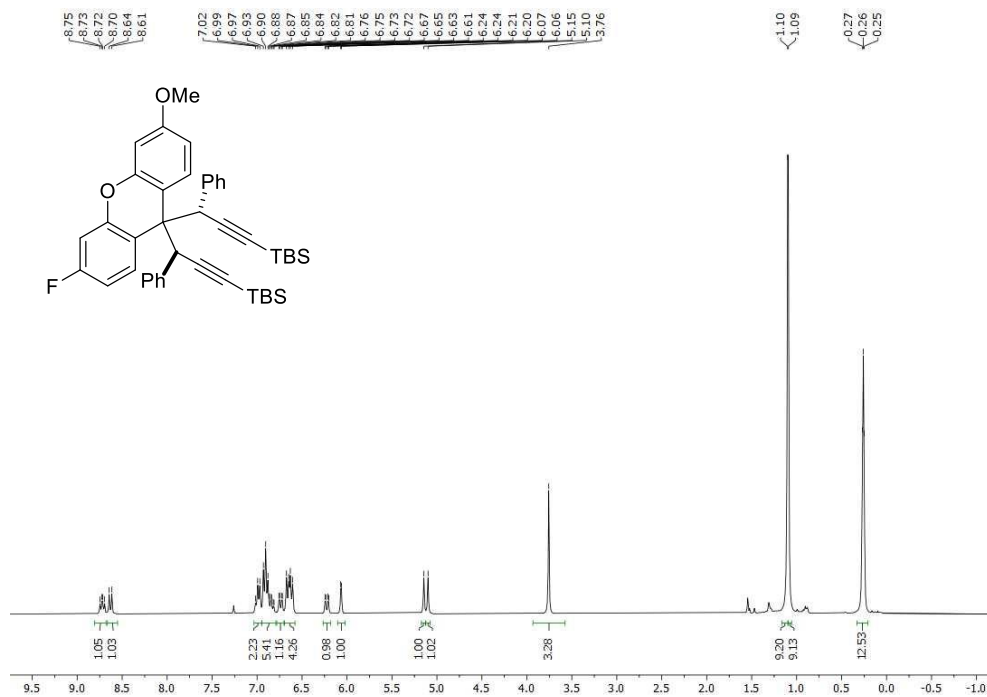
((3*S,3'*S*'*)-(3-Methoxy-9*H*-xanthene-9,9-diyl)bis(3-phenylprop-1-yne-3,1-diyl))bis(*tert*-butyldimethylsilane) (2.3g)**



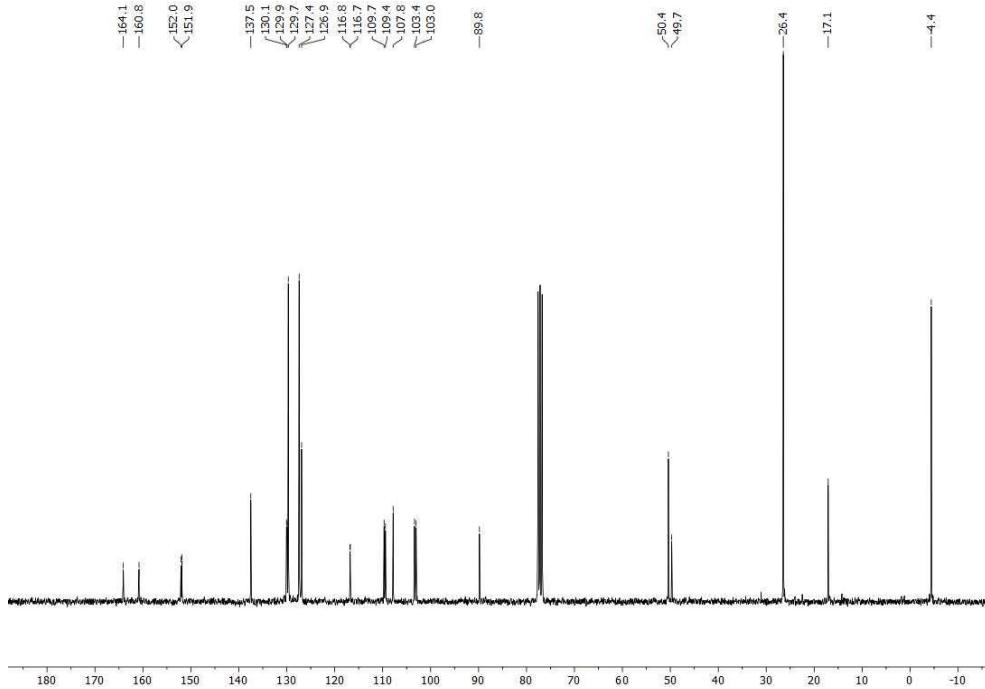
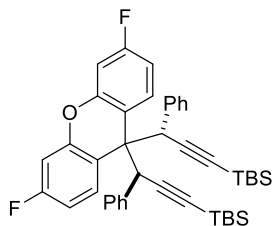
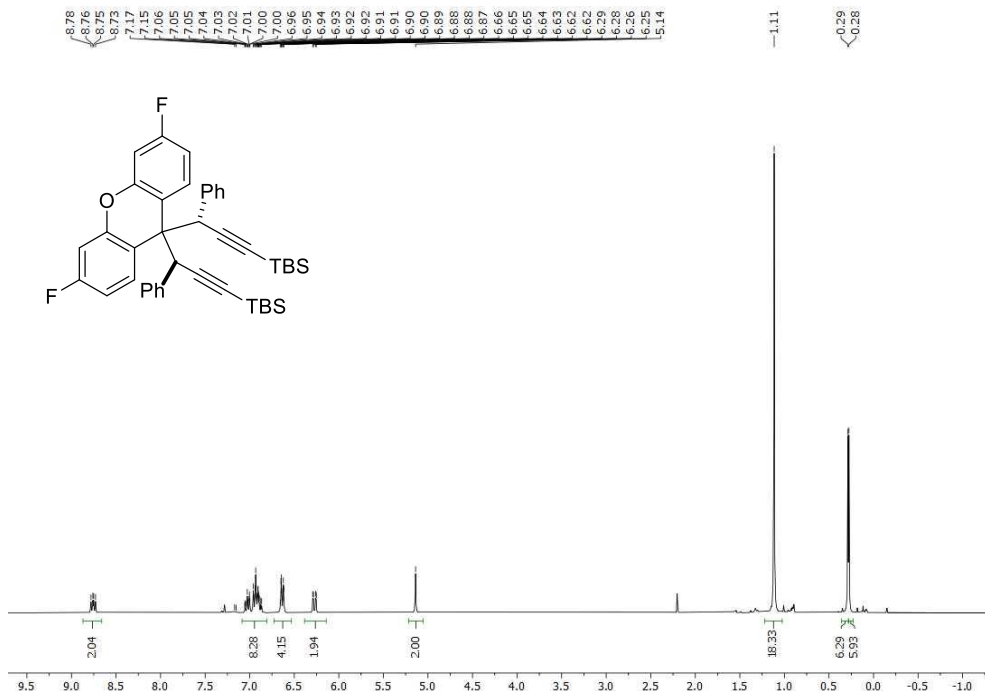
((3*S,3'*S*'*)-(3-Fluoro-9*H*-xanthene-9,9-diyl)bis(3-phenylprop-1-yne-3,1-diyl))bis(*tert*-butyldimethylsilane) (2.3h)**



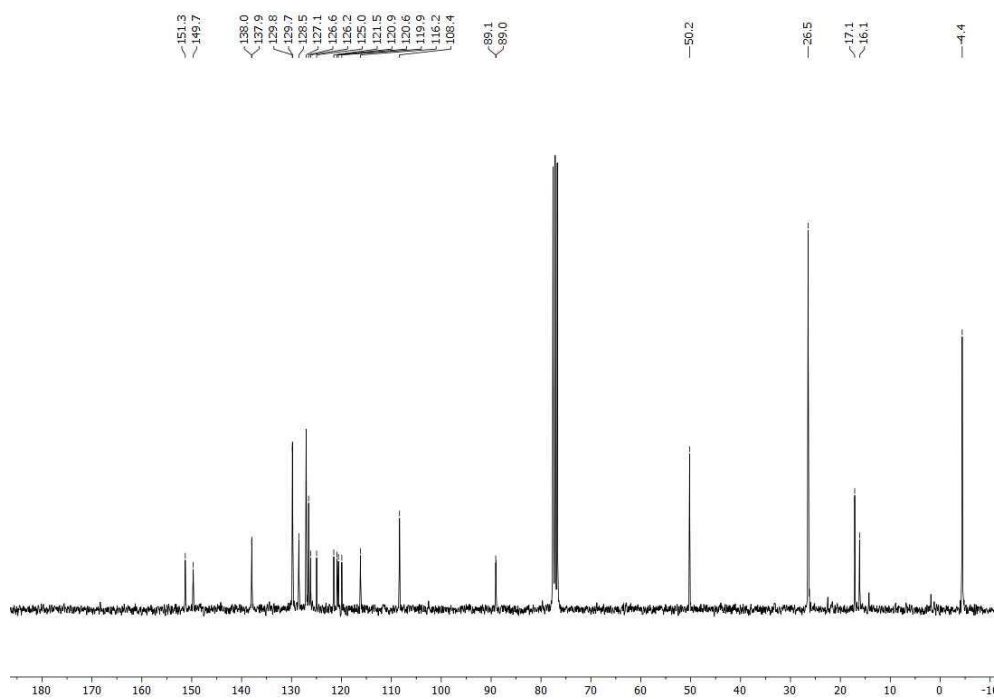
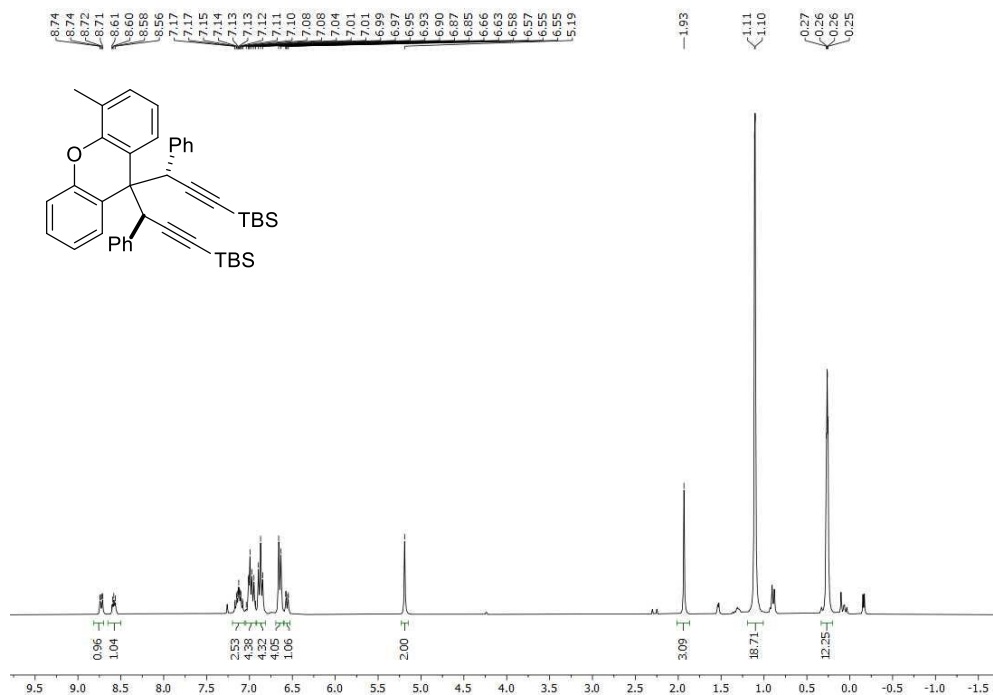
((3*S,3'*S*'*)-(3-Fluoro-6-methoxy-9*H*-xanthene-9,9-diyl)bis(3-phenylprop-1-yne-3,1-diyl))bis(*tert*-butyldimethylsilane) (2.3j)**



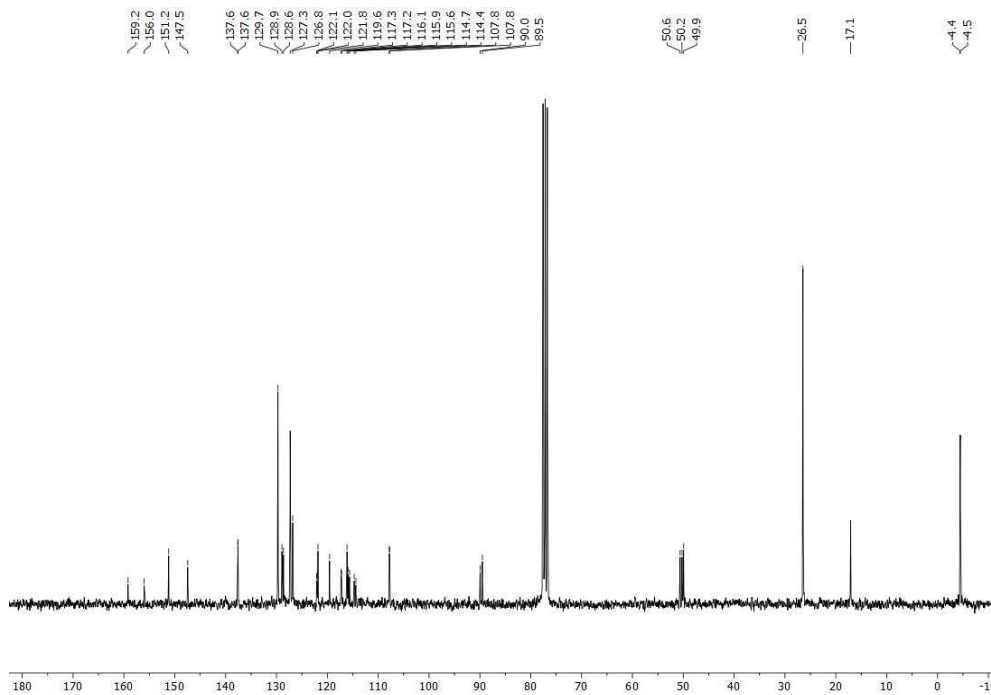
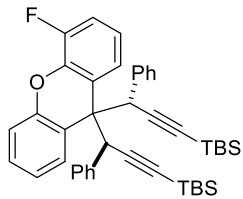
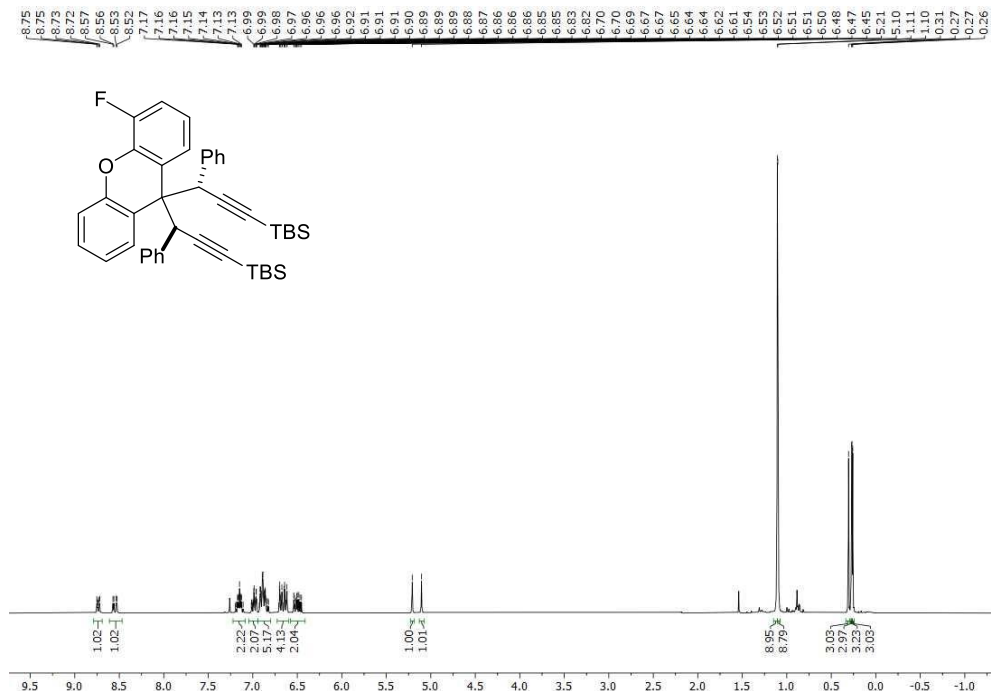
((3*S,3'*S*'*)-(3,6-Difluoro-9*H*-xanthene-9,9-diyl)bis(3-phenylprop-1-yne-3,1-diyl)bis(*tert*-butyldimethylsilane) (2.3k)**



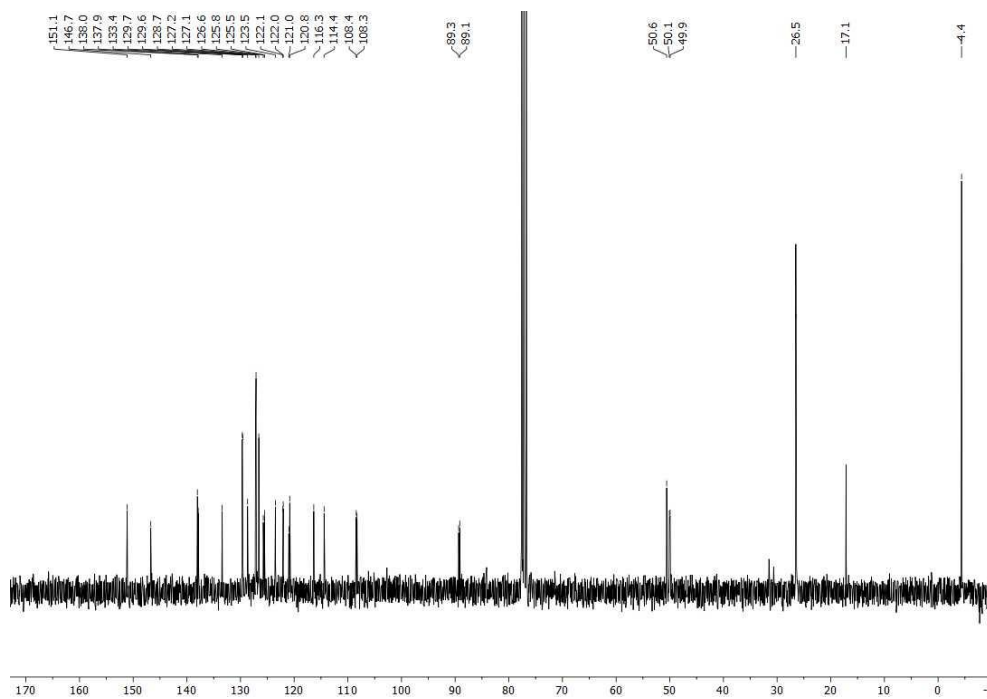
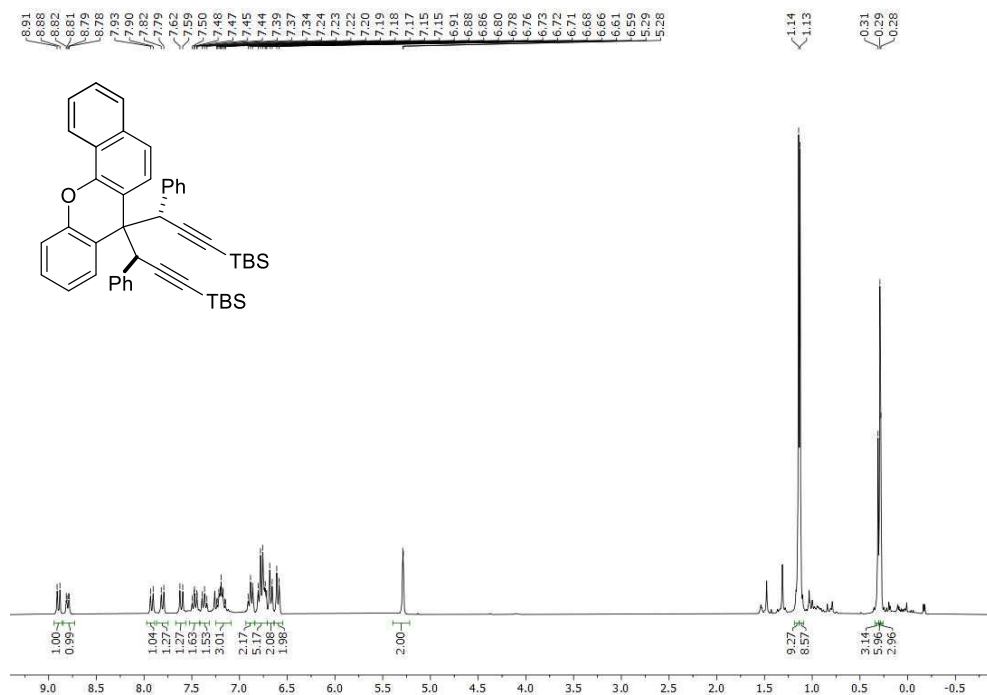
((3*S,3'*S*')-(4-Methyl-9H-xanthene-9,9-diyl)bis(3-phenylprop-1-yne-3,1-diyl))bis(*tert*-butyldimethylsilane) (2.3I)**



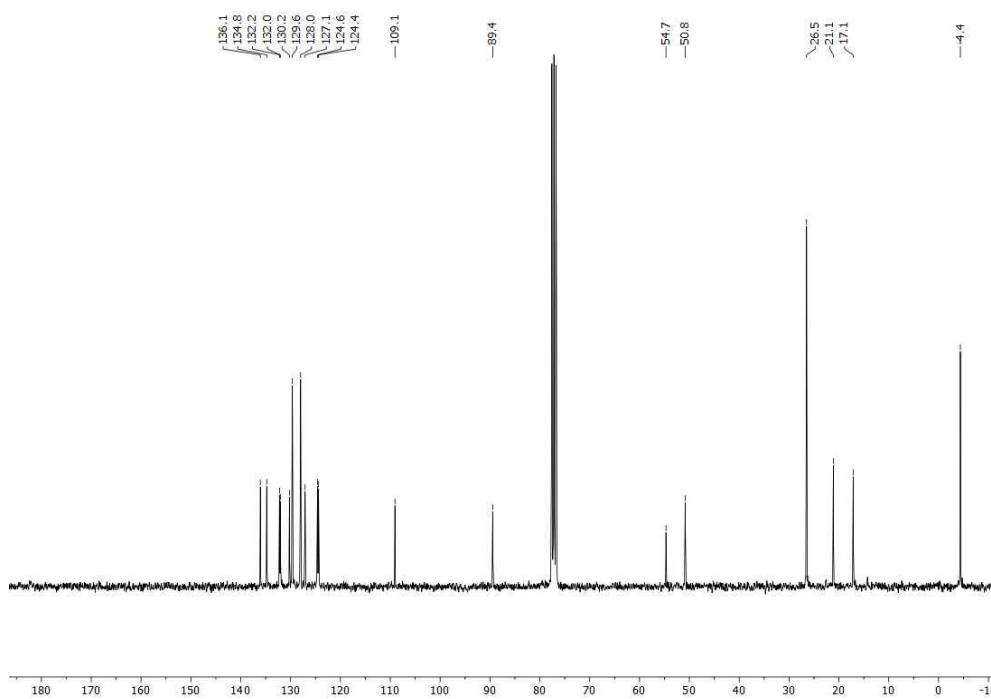
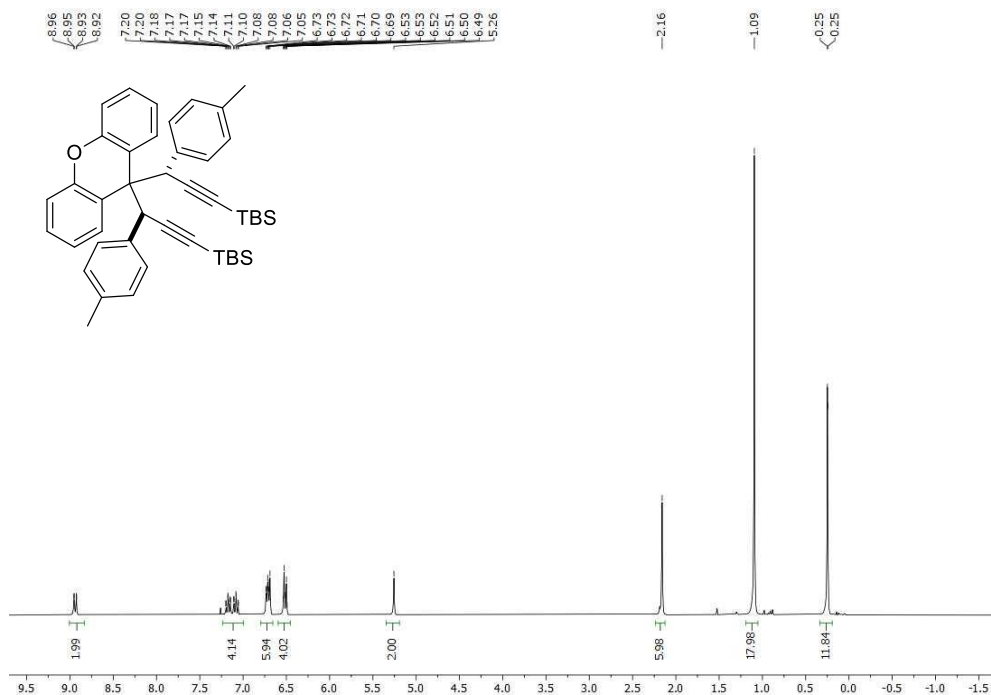
((3*S,3'*S*'*)-(4-Fluoro-9*H*-xanthene-9,9-diyl)bis(3-phenylprop-1-yne-3,1-diyl))bis(*tert*-butyldimethylsilane) (2.3m)**



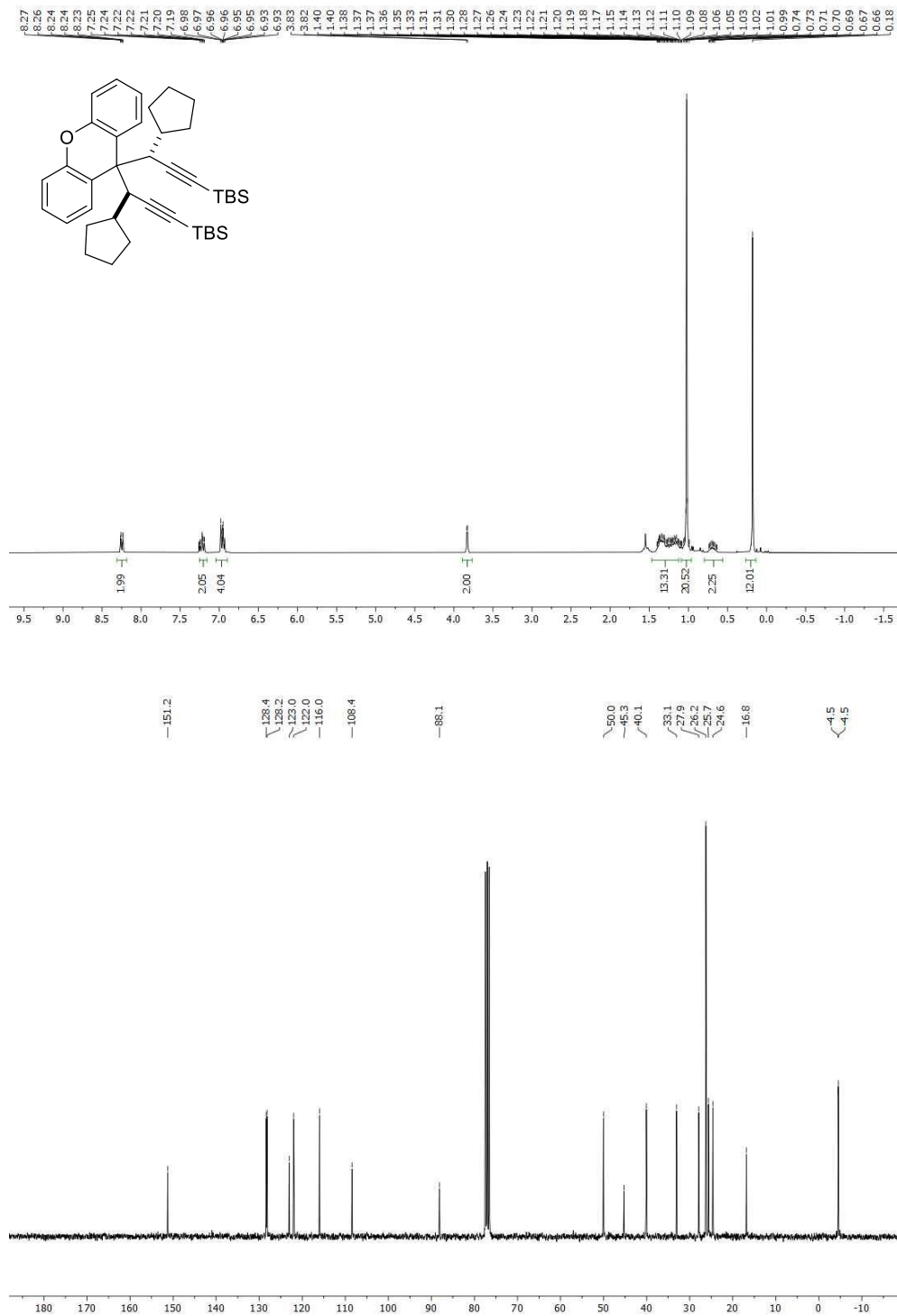
((3S*,3'S*)-(7H-benzo[c]xanthene-7,7-diyl)bis(3-phenylprop-1-yne-3,1-diyl))bis(*tert*-butyldimethylsilane) (2.3n)



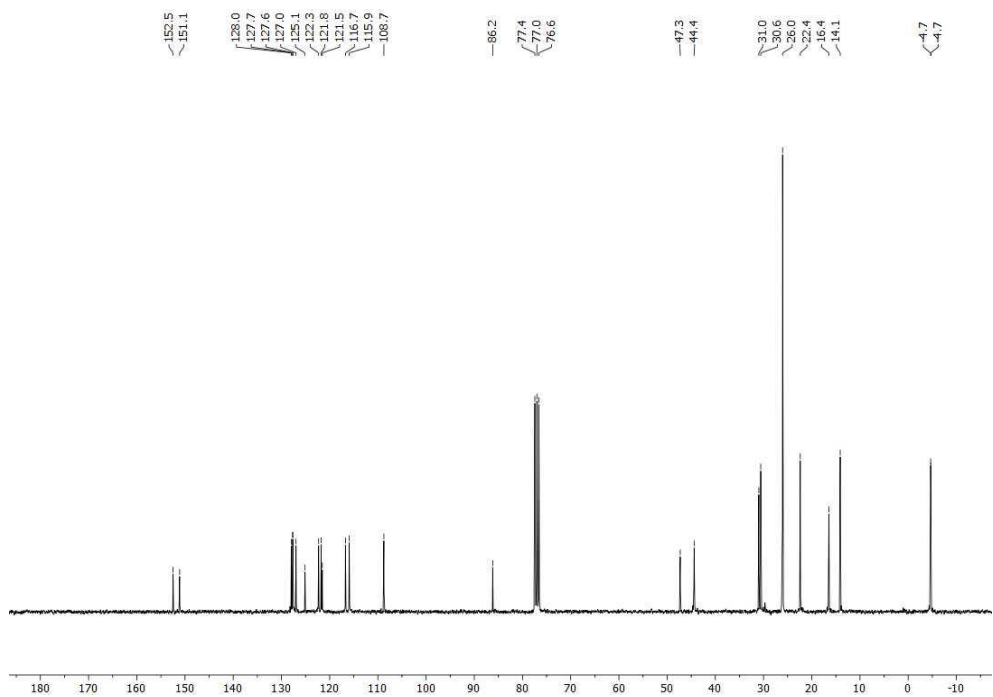
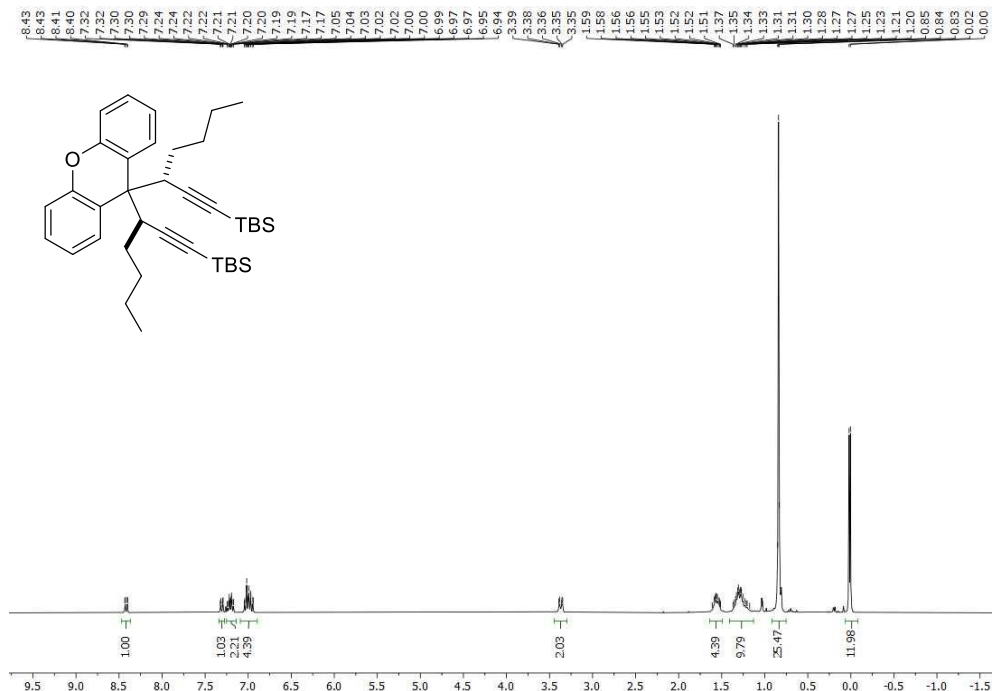
((3*S,3'*S*'*)-(9*H*-Xanthene-9,9-diyl)bis(3-(*p*-tolyl)prop-1-yne-3,1-diyl))bis(*tert*-butyldimethylsilane) (2.3q)**



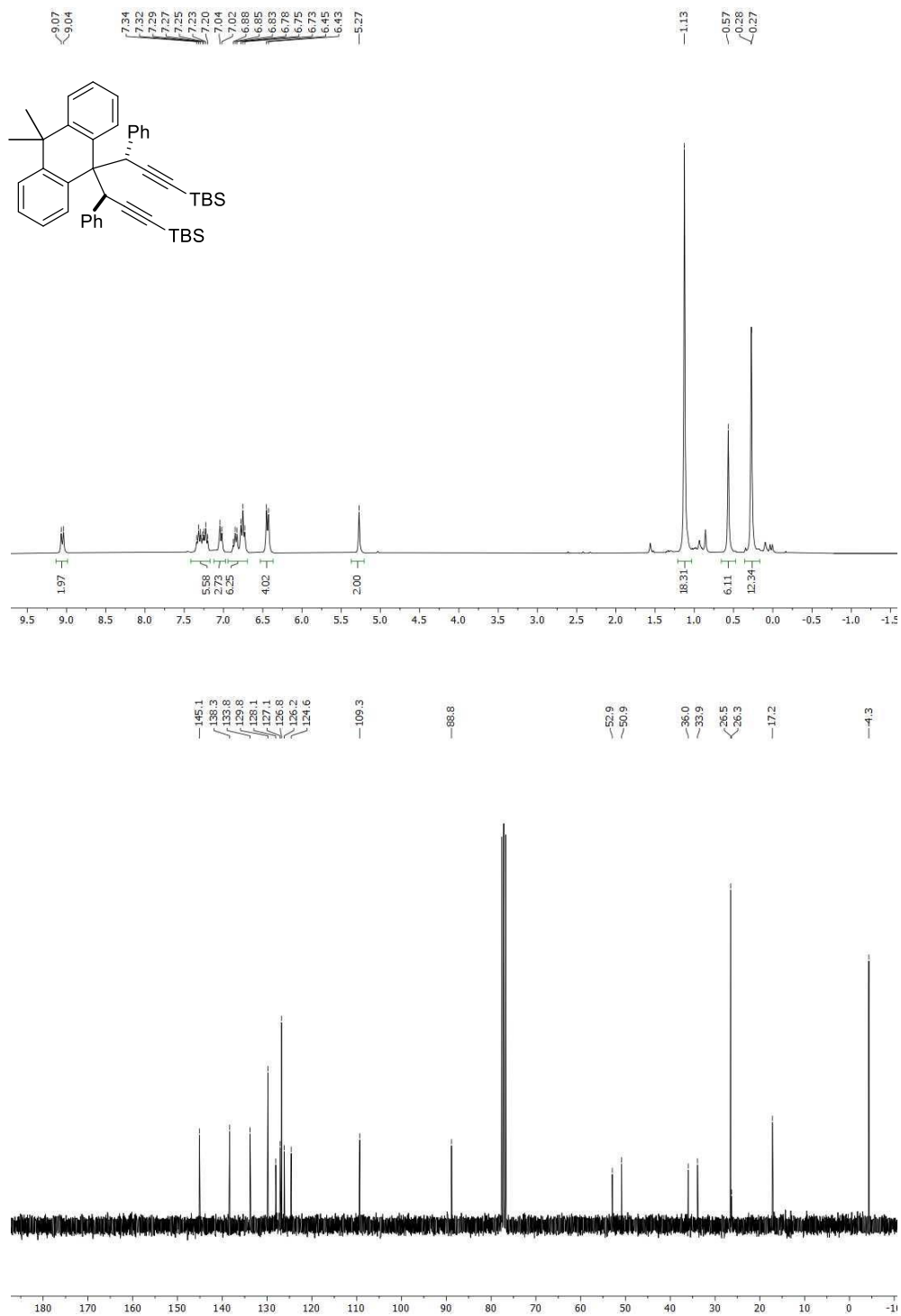
((3*S,3'*S*')-(9*H*-Xanthene-9,9-diyl)bis(3-cyclopentylprop-1-yne-3,1-diyl))bis(*tert*-butyldimethylsilane) (2.3r)**



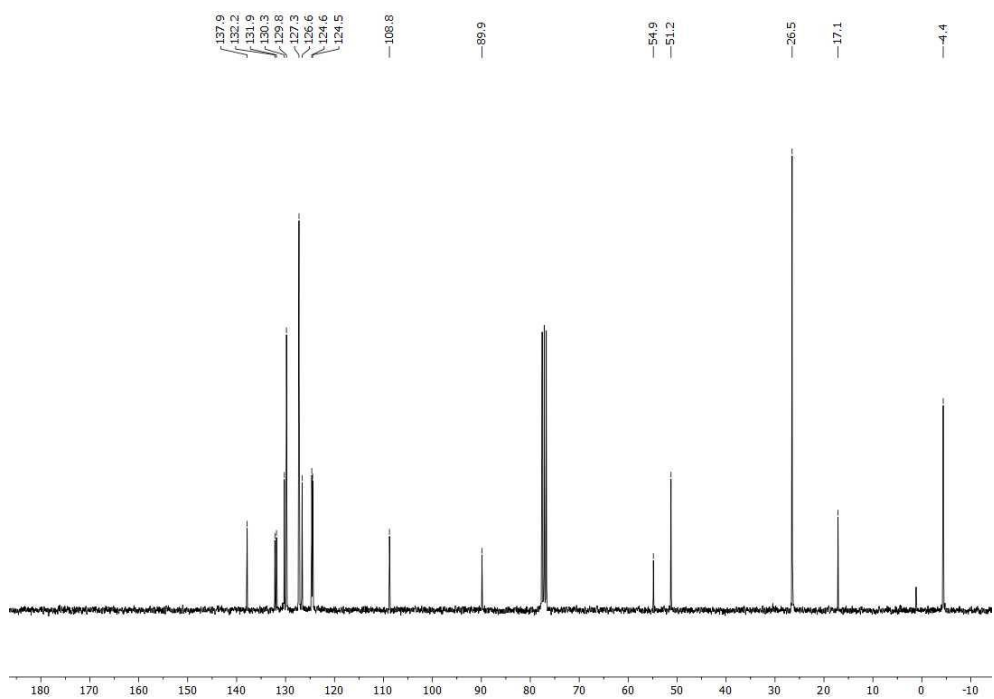
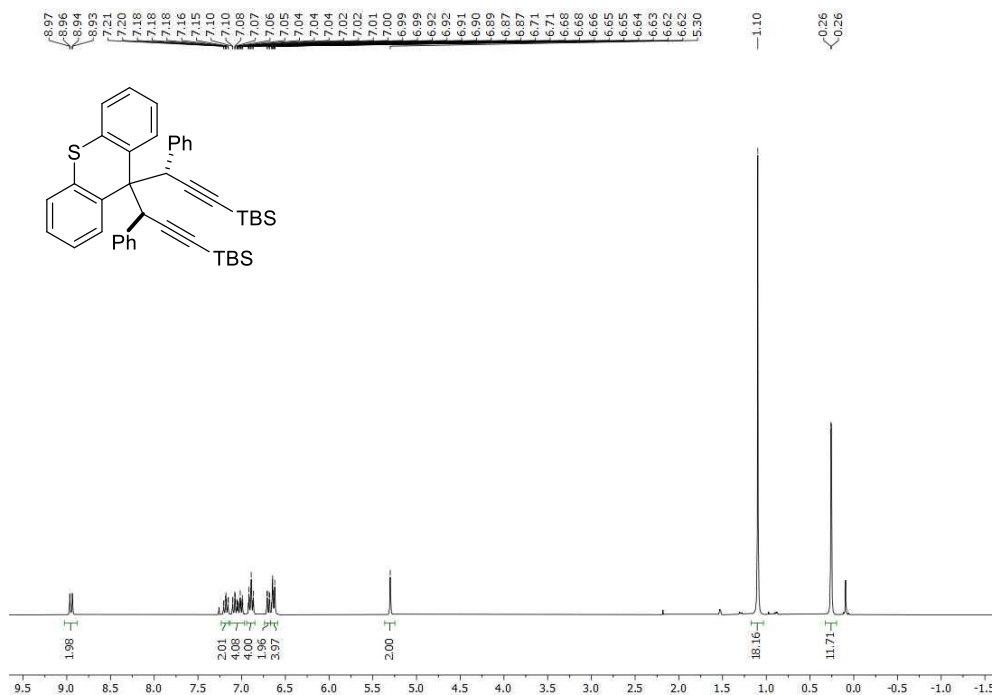
((3*S,3'*S*'*)-(9*H*-Xanthene-9,9-diyl)bis(hept-1-yne-3,1-diyl))bis(*tert*-butyldimethylsilane) (2.3s)**



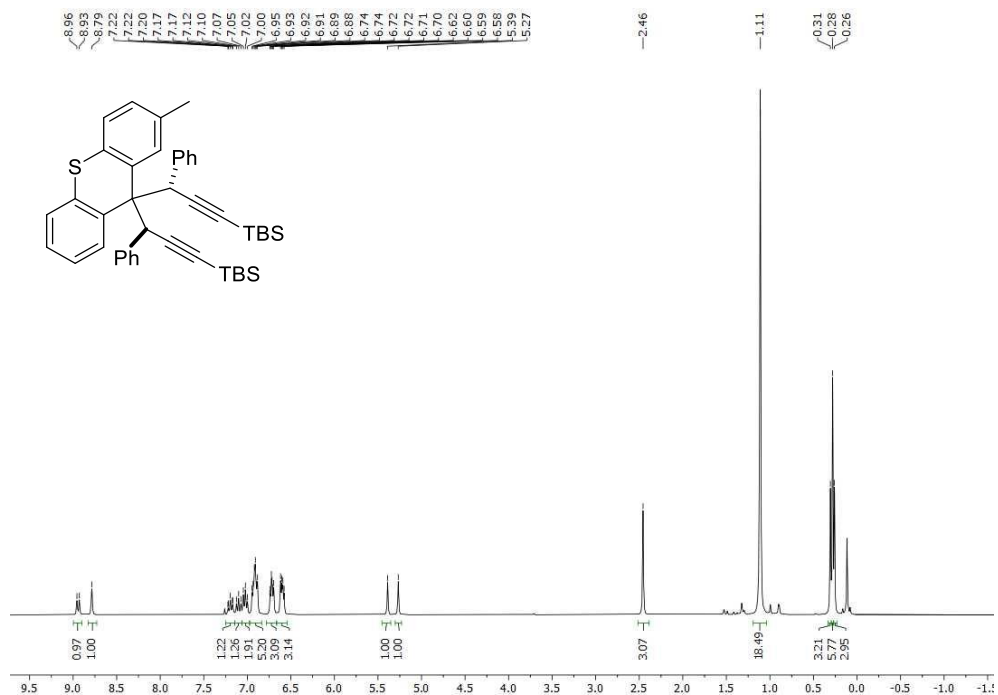
((3*S,3'*S*'*)-(10,10-Dimethyl-9,10-dihydroanthracene-9,9-diyl)bis(3-phenylprop-1-yne-3,1-diyl))bis(*tert*-butyldimethylsilane) (2.13)**



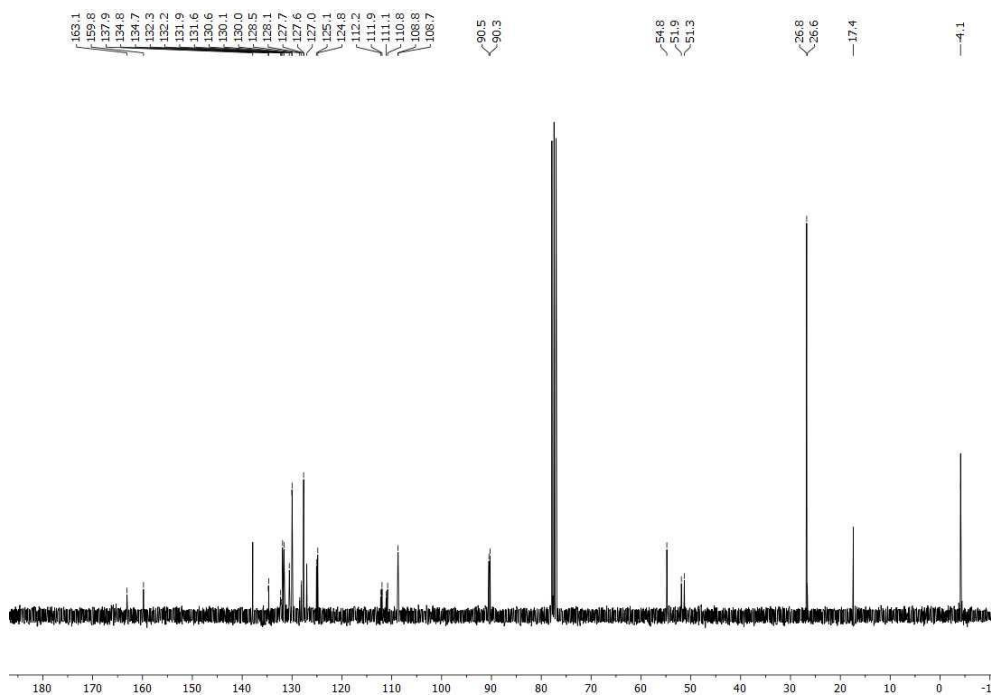
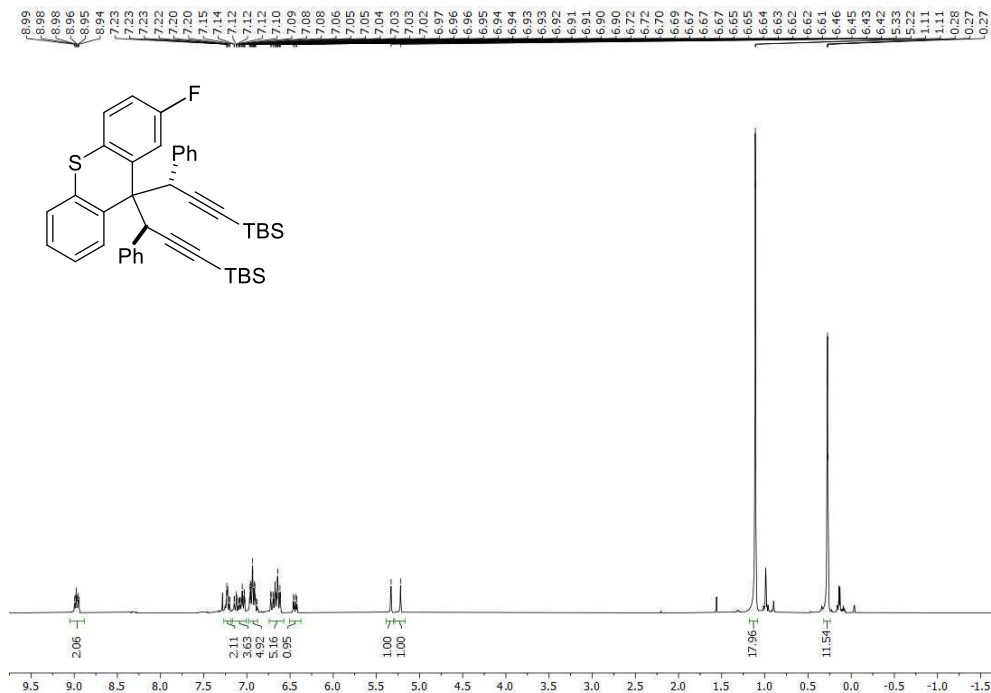
((3*S,3'*S*'*)-(9*H*-Thioxanthene-9,9-diyl)bis(3-phenylprop-1-yne-3,1-diyl))bis(*tert*-butyldimethylsilane) (2.17a)**



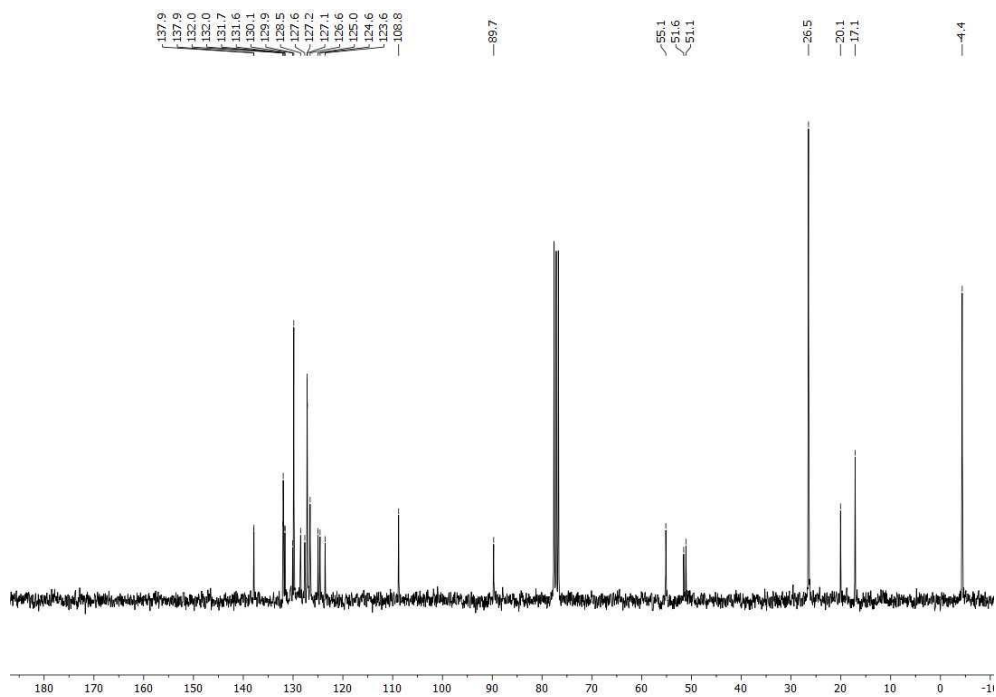
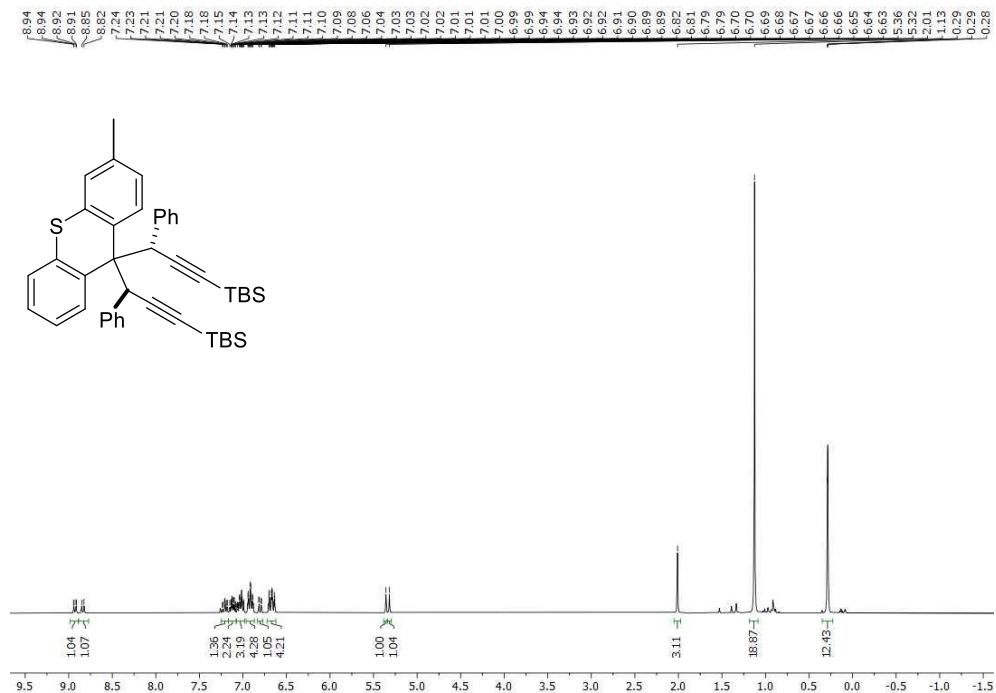
((3*S,3'*S*'*)-(2-Methyl-9*H*-thioxanthene-9,9-diyl)bis(3-phenylprop-1-yne-3,1-diyl))bis(*tert*-butyldimethylsilane) (2.17b)**



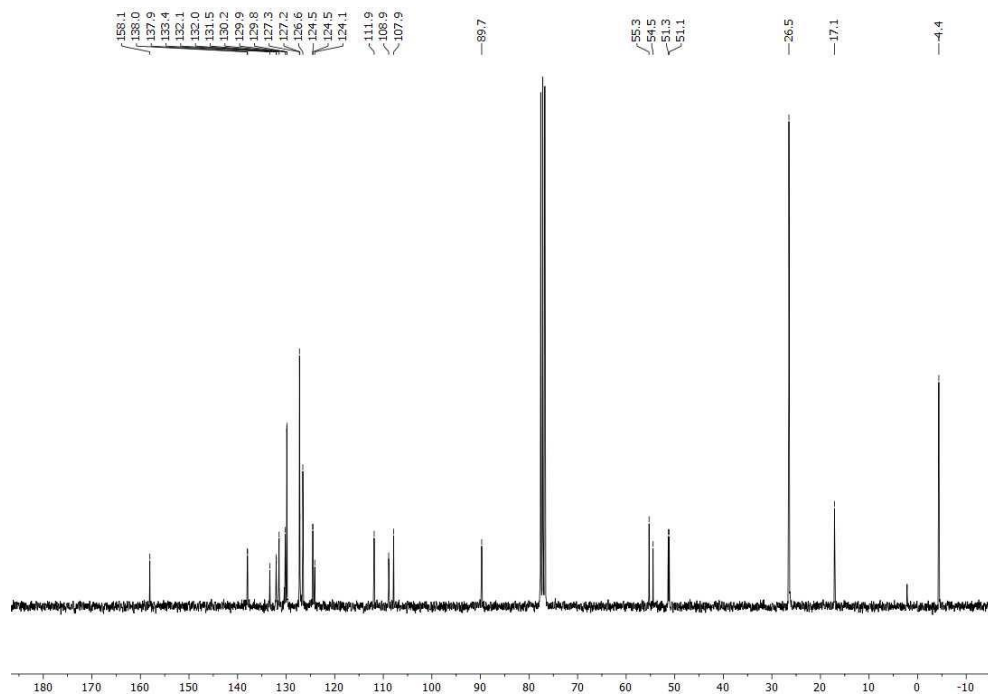
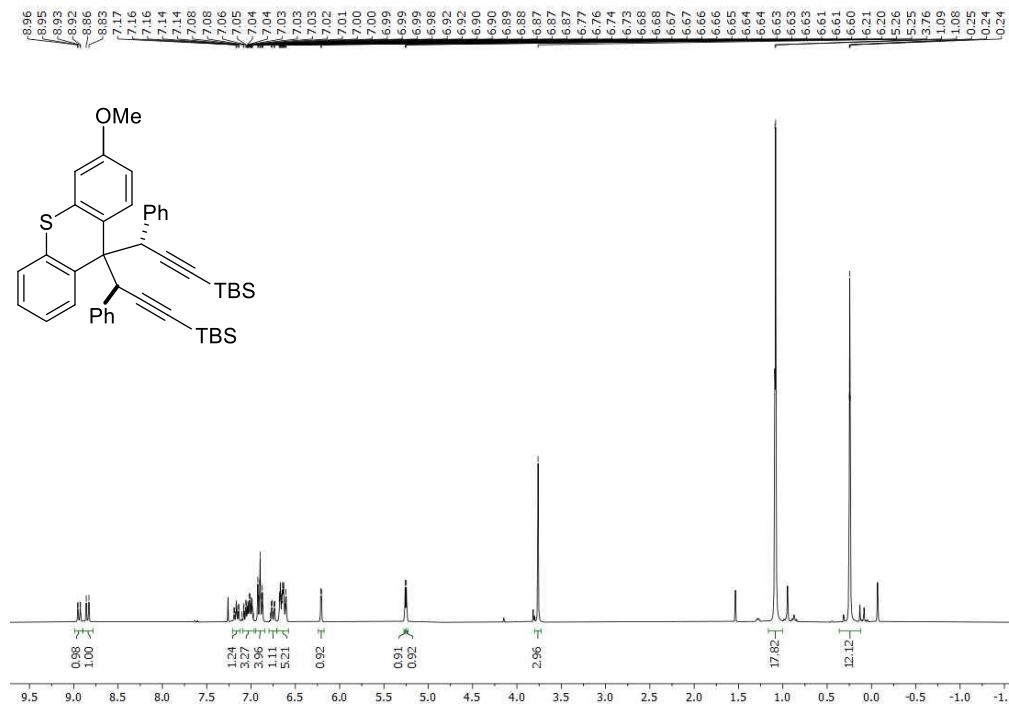
((3*S,3'*S*'*)-(2-Fluoro-9*H*-thioxanthene-9,9-diyl)bis(3-phenylprop-1-yne-3,1-diyl)bis(*tert*-butyldimethylsilane) (2.17c)**



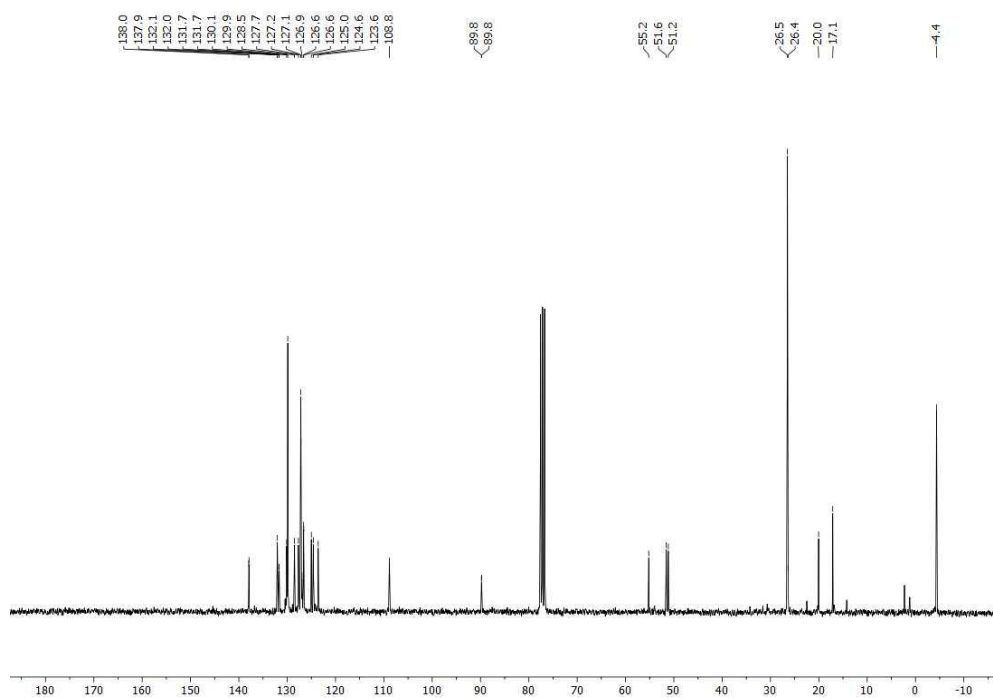
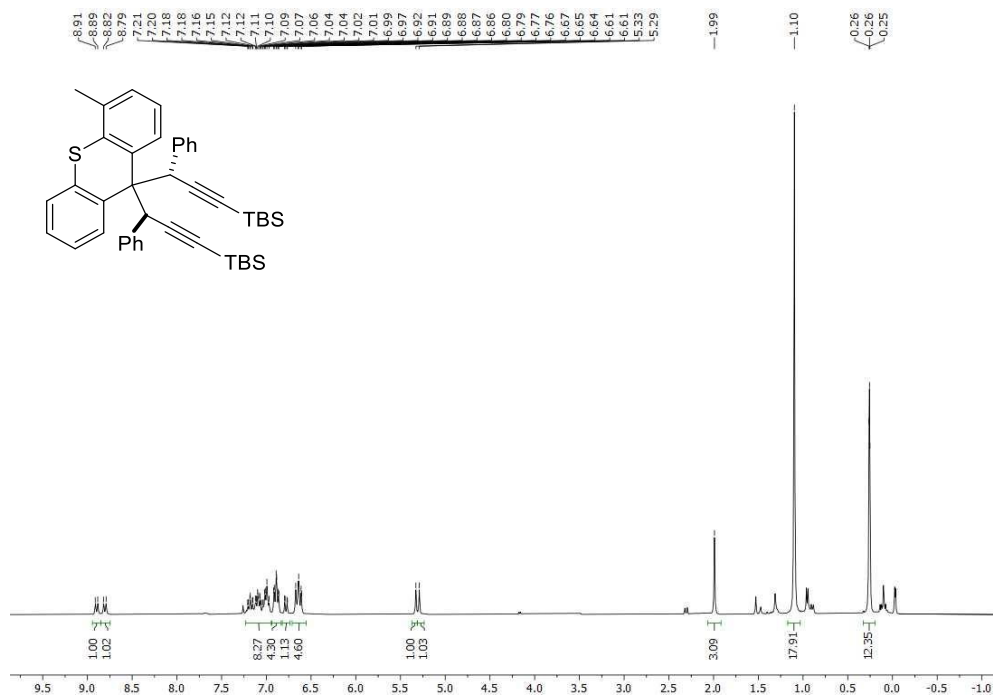
((3*S,3'*S*'*)-(3-Methyl-9*H*-thioxanthene-9,9-diyl)bis(3-phenylprop-1-yne-3,1-diyl))bis(*tert*-butyldimethylsilane) (2.17d)**



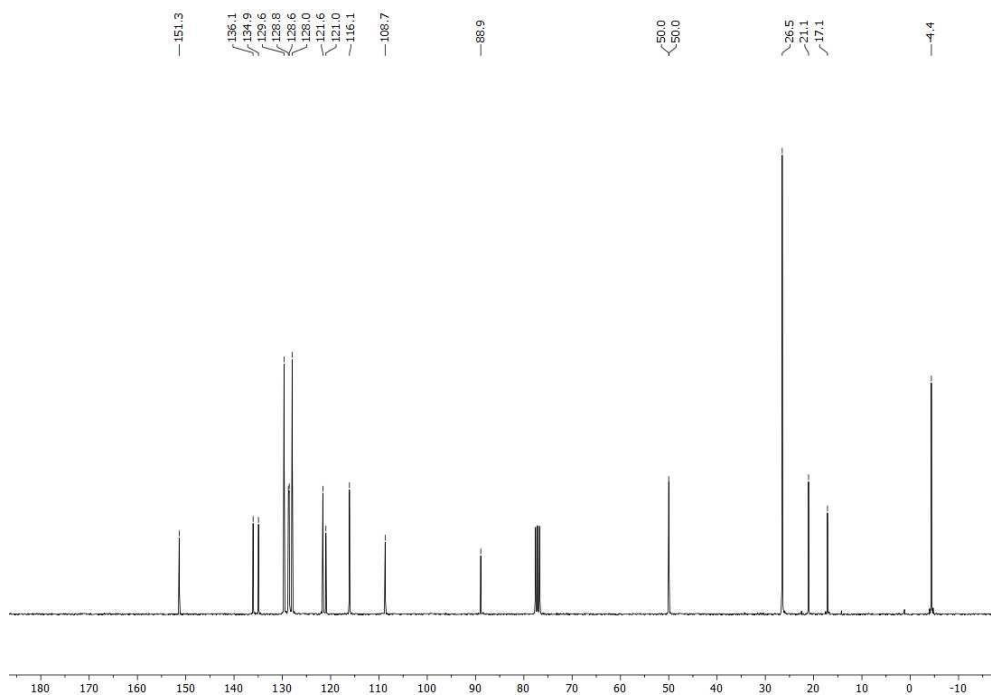
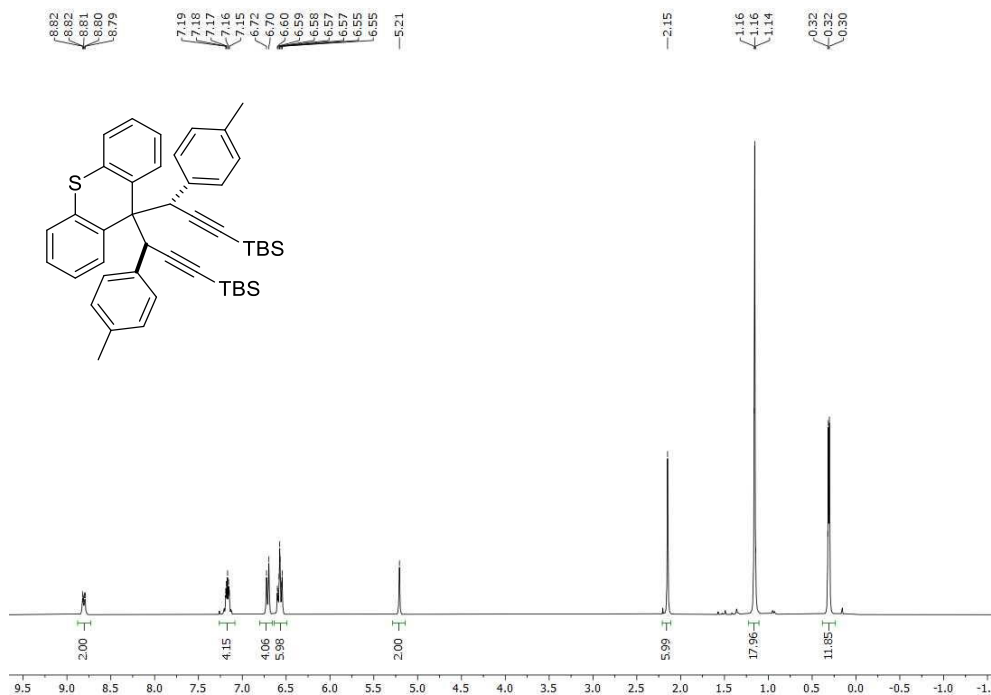
((3*S,3'*S*'*)-(3-Methoxy-9*H*-thioxanthene-9,9-diyl)bis(3-phenylprop-1-yne-3,1-diyl))bis(*tert*-butyldimethylsilane) (2.17e)**



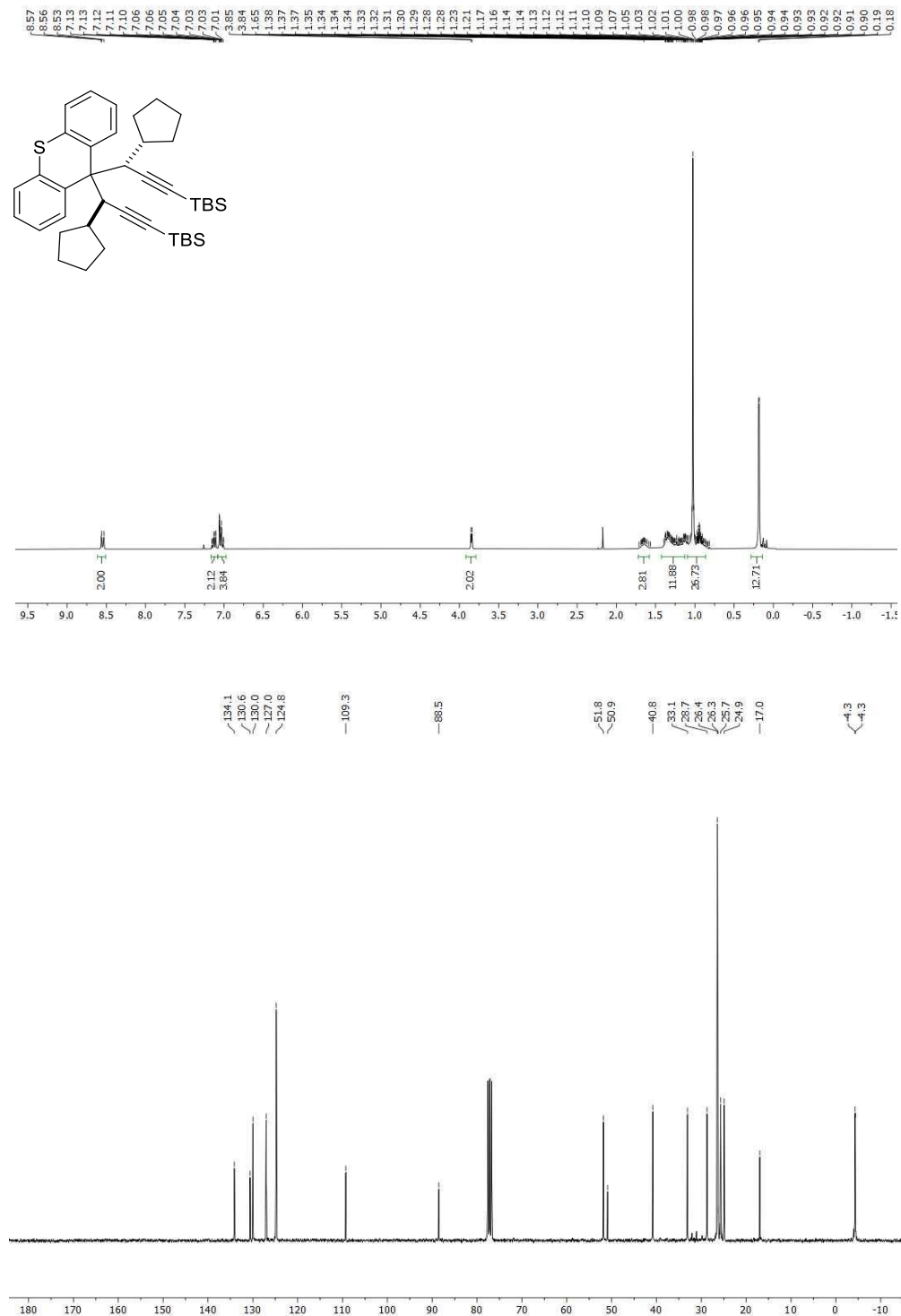
((3*S,3'*S*'*)-(4-Methyl-9*H*-thioxanthene-9,9-diyl)bis(3-phenylprop-1-yne-3,1-diyl))bis(*tert*-butyldimethylsilane) (2.17f)**



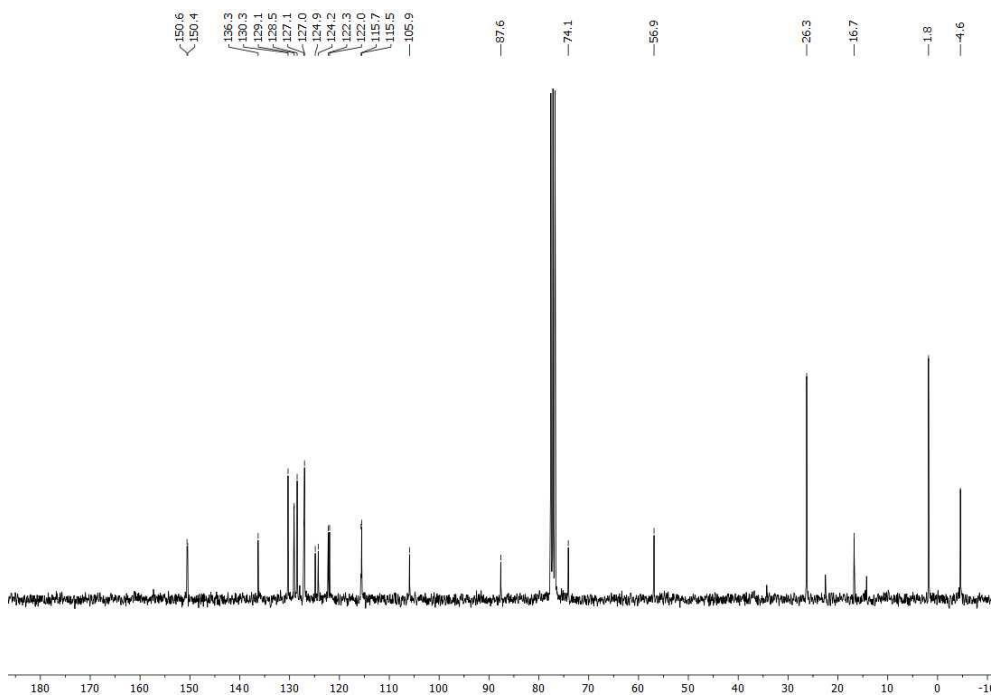
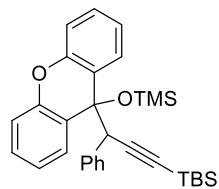
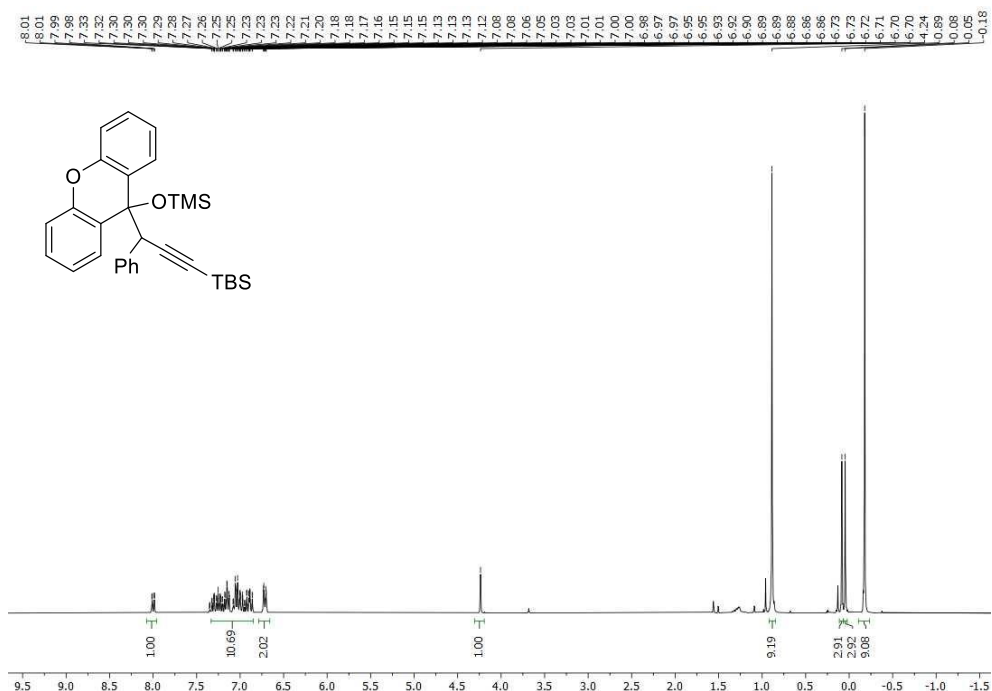
((3*S,3'*S*'*)-(9*H*-Thioxanthene-9,9-diyl)bis(3-(*p*-tolyl)prop-1-yne-3,1-diyl))bis(*tert*-butyldimethylsilane) (2.17g)**



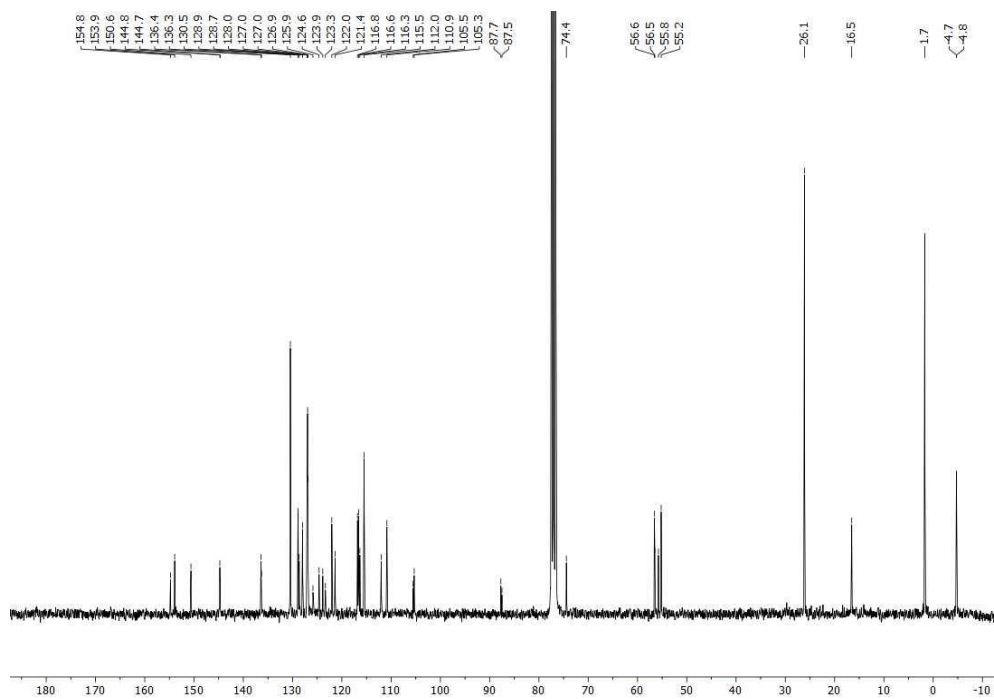
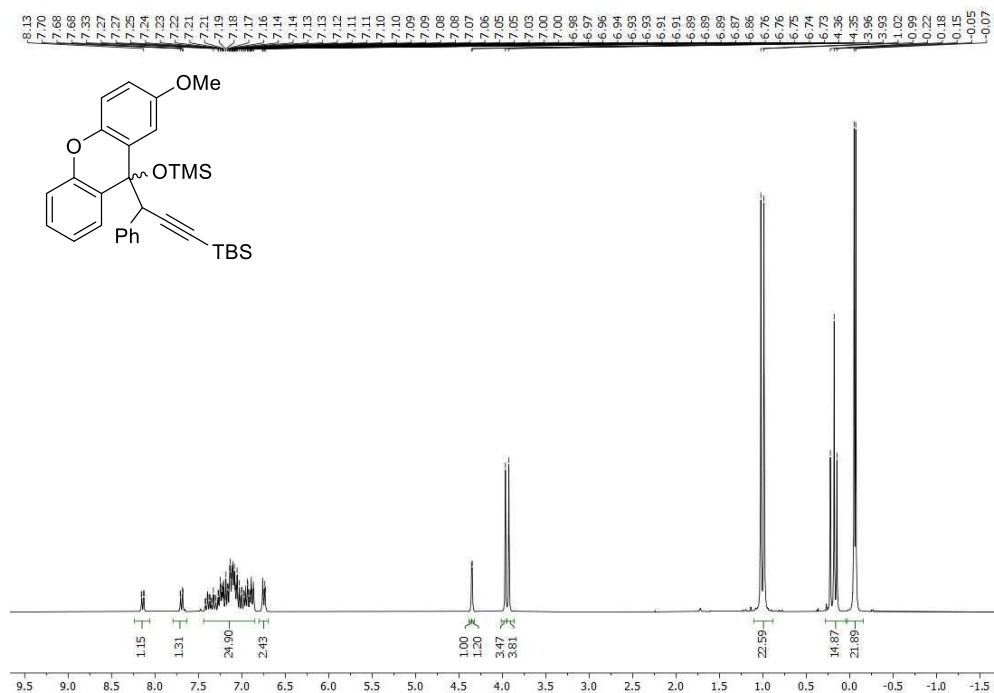
((3*S,3'*S*'*)-(9*H*-Thioxanthene-9,9-diyl)bis(3-cyclopentylprop-1-yne-3,1-diyl))bis(*tert*-butyldimethylsilane) (2.17h)**



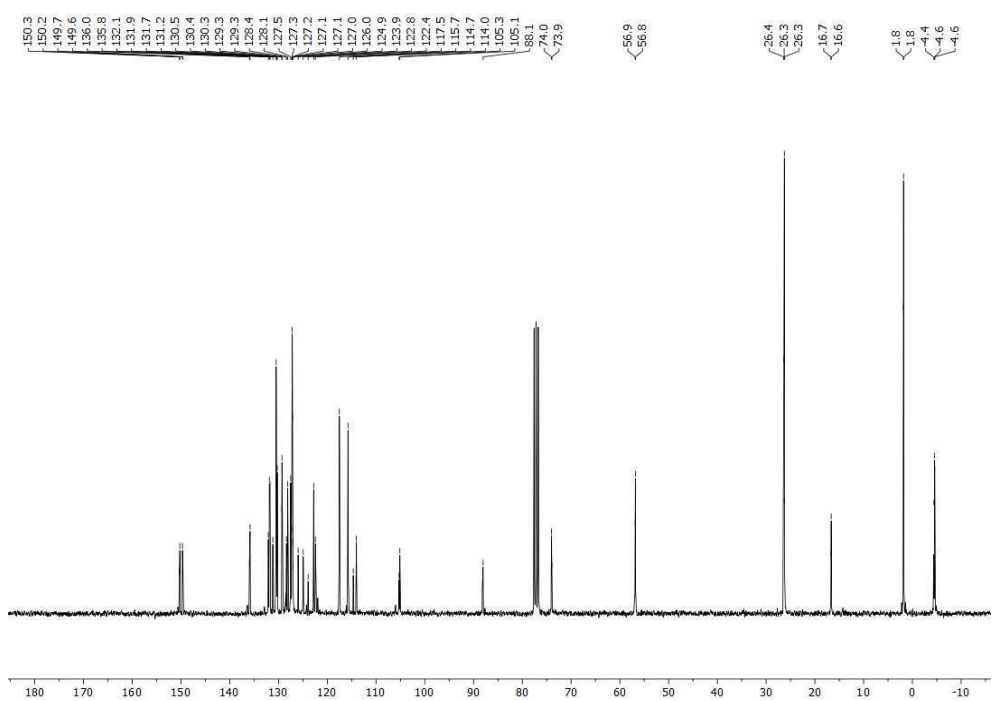
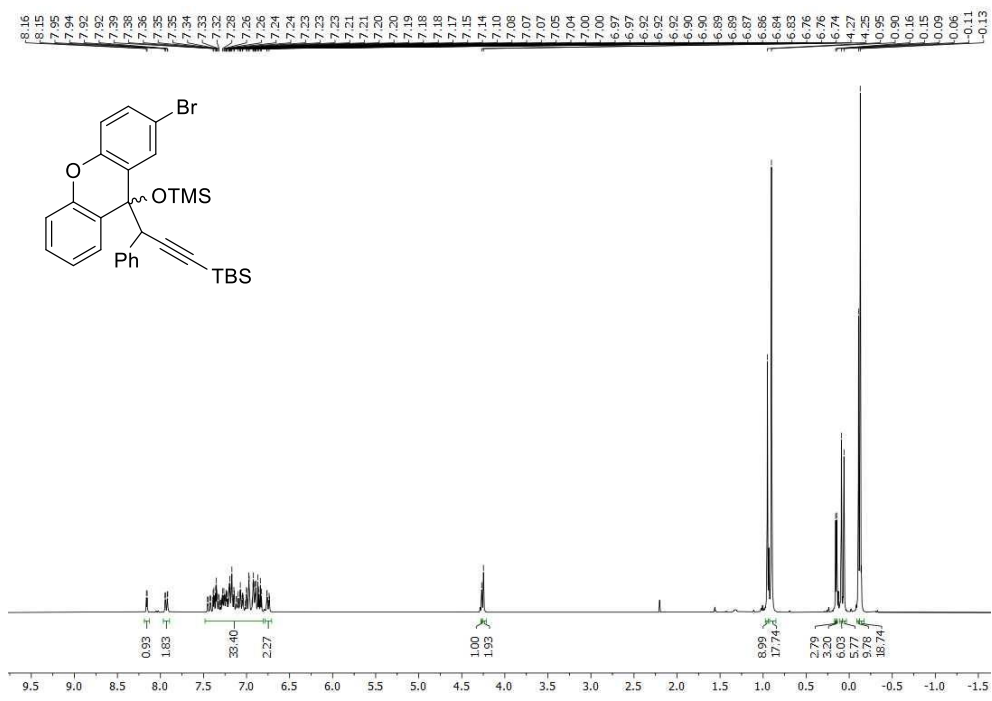
Tert-butyl dimethyl(3-phenyl-3-(9-((trimethylsilyl)oxy)-9H-xanthen-9-yl)prop-1-yn-1-yl)silane (2.4a)



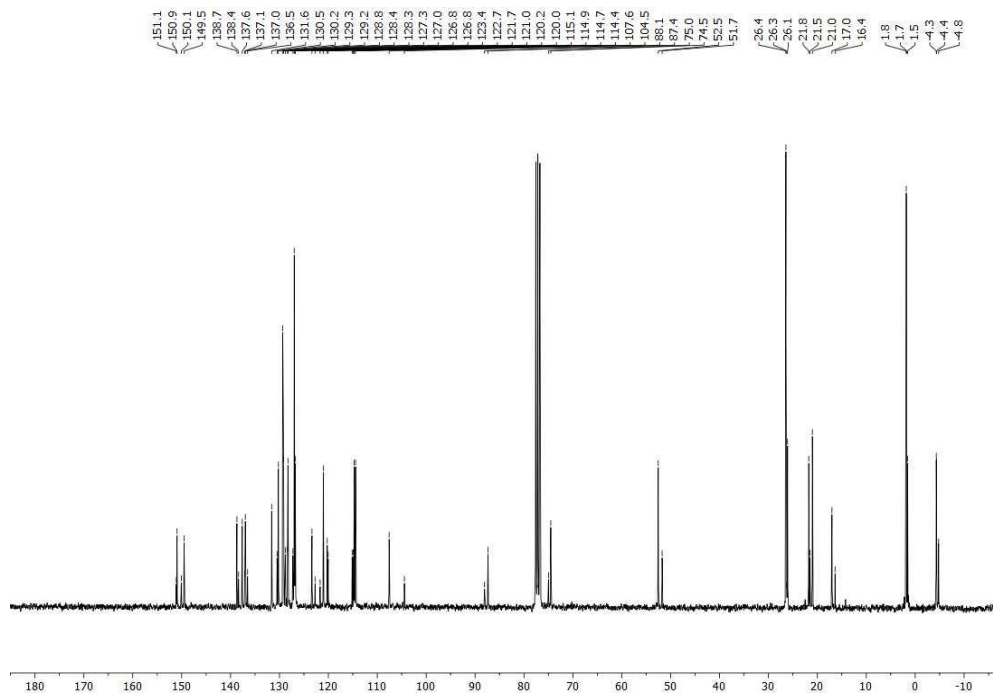
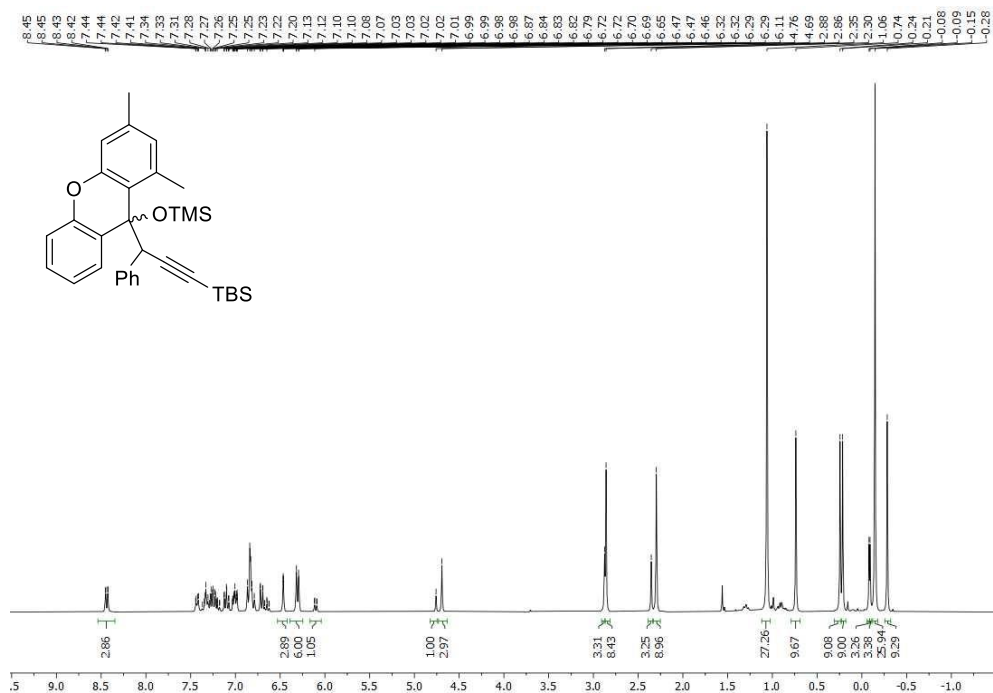
Tert-butyl(3-(2-methoxy-9-((trimethylsilyl)oxy)-9H-xanthen-9-yl)-3-phenylprop-1-yn-1-yl)dimethylsilane (2.4c)



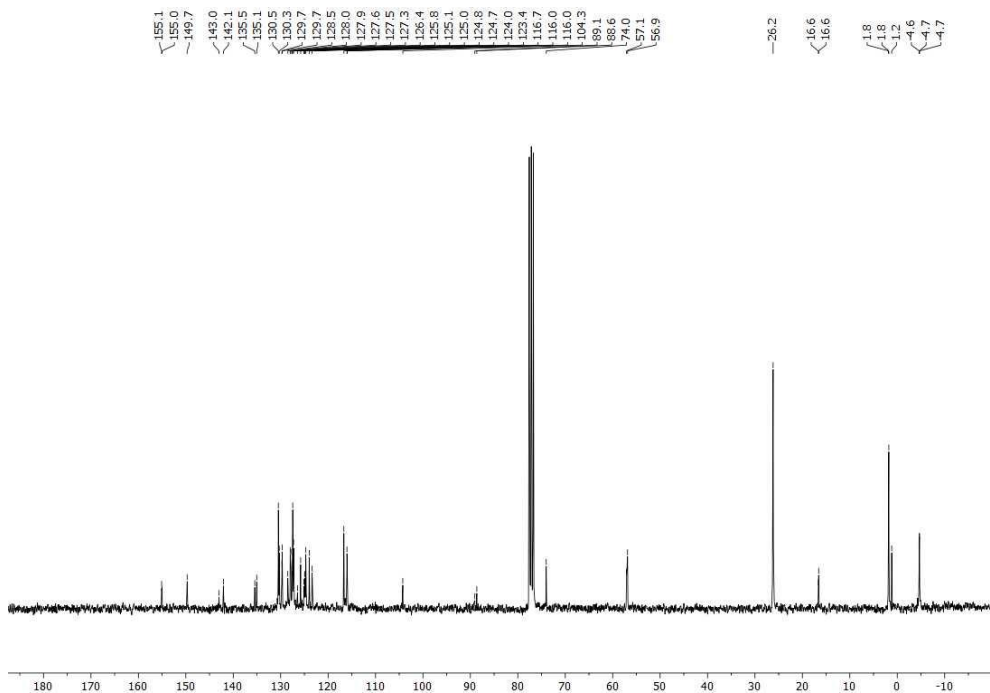
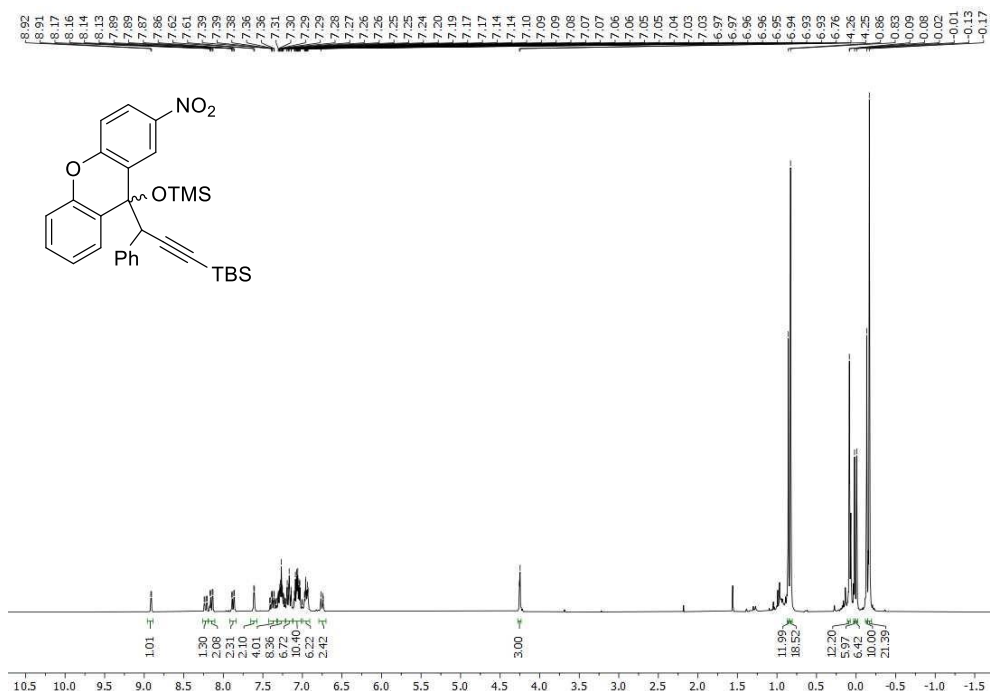
(3-(2-Bromo-9-((trimethylsilyl)oxy)-9H-xanthen-9-yl)-3-phenylprop-1-yn-1-yl)(tert-butyl)dimethylsilane (2.4e)



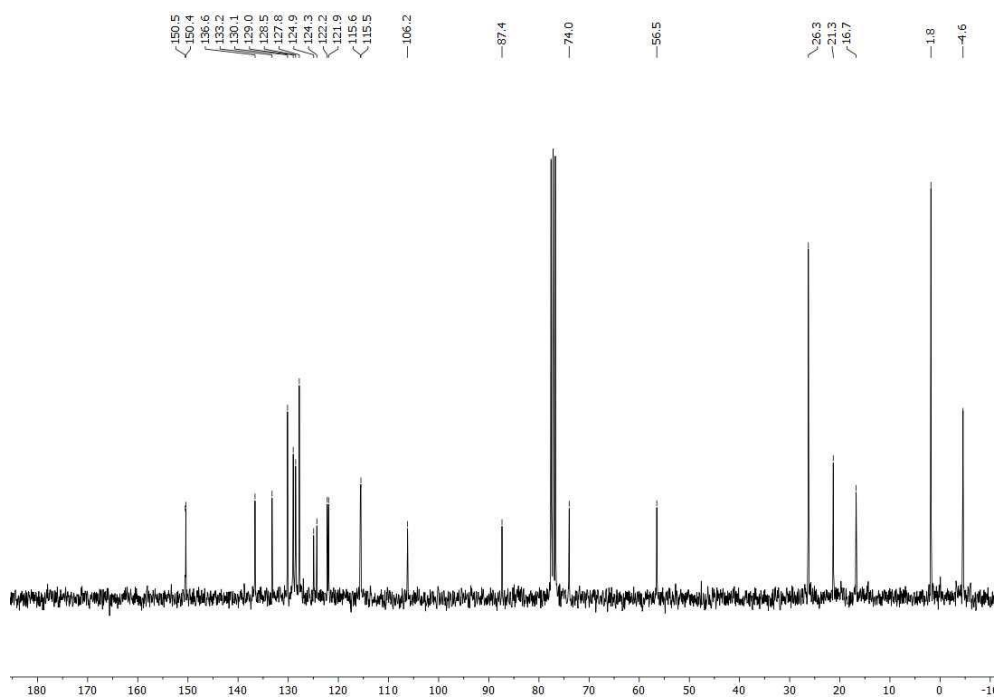
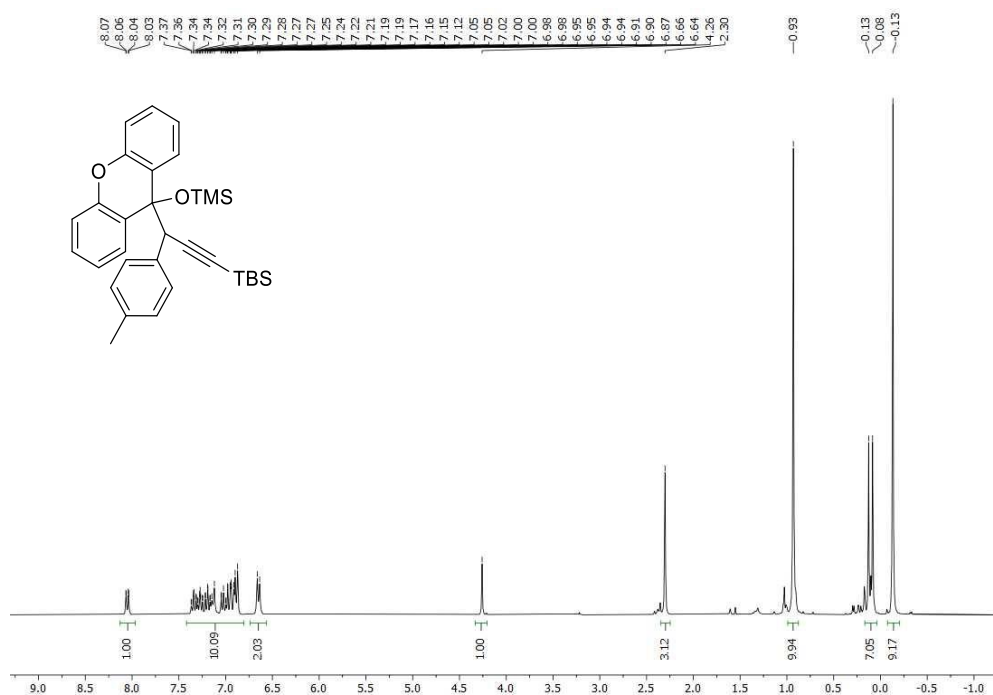
Tert-butyl(3-(1,3-dimethyl-9-((trimethylsilyl)oxy)-9H-xanthen-9-yl)-3-phenylprop-1-yn-1-yl)dimethylsilane (2.4o)



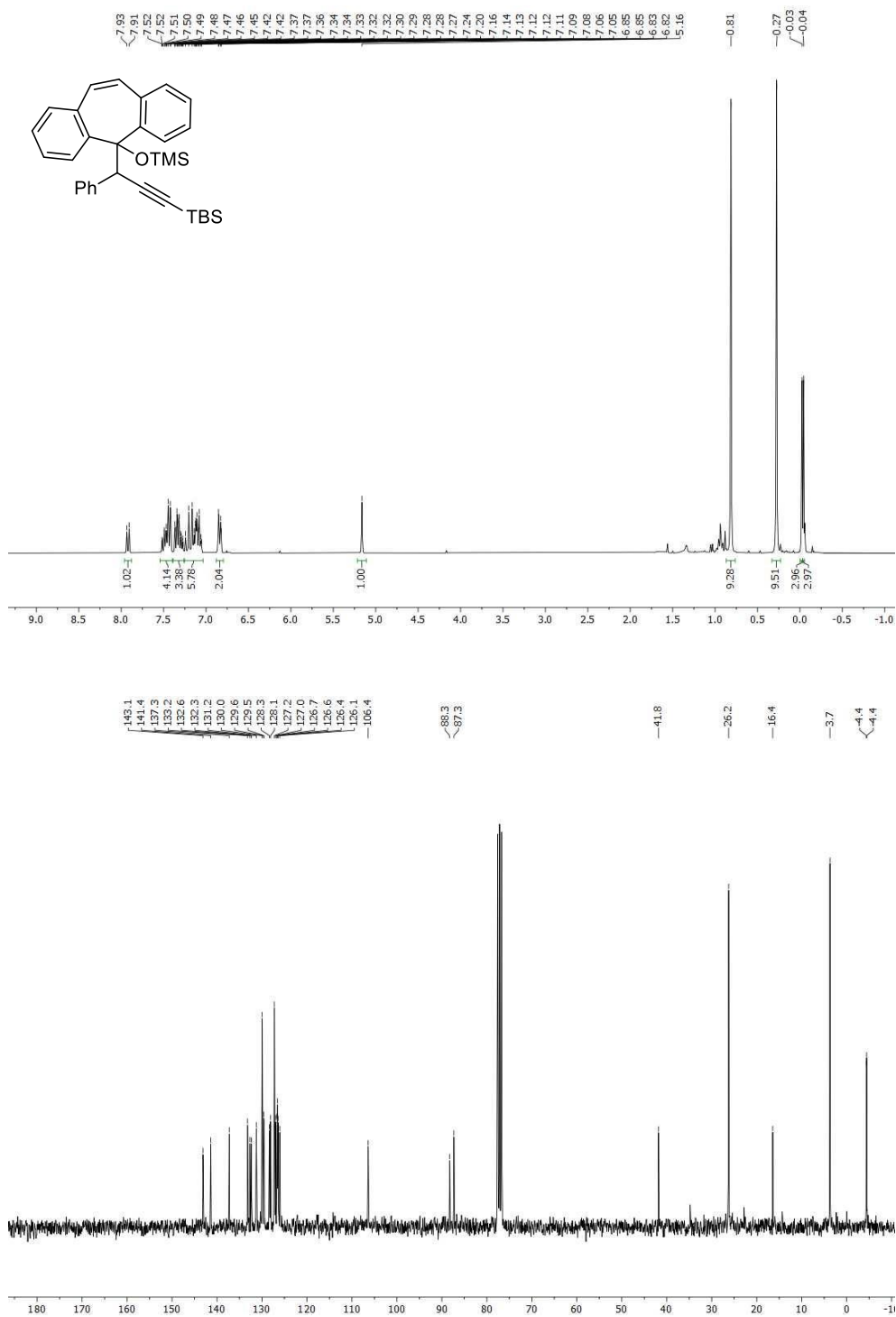
Tert-butyl dimethyl(3-(2-nitro-9-((trimethylsilyl)oxy)-9H-xanthen-9-yl)-3-phenylprop-1-yn-1-yl)silane (2.4p)



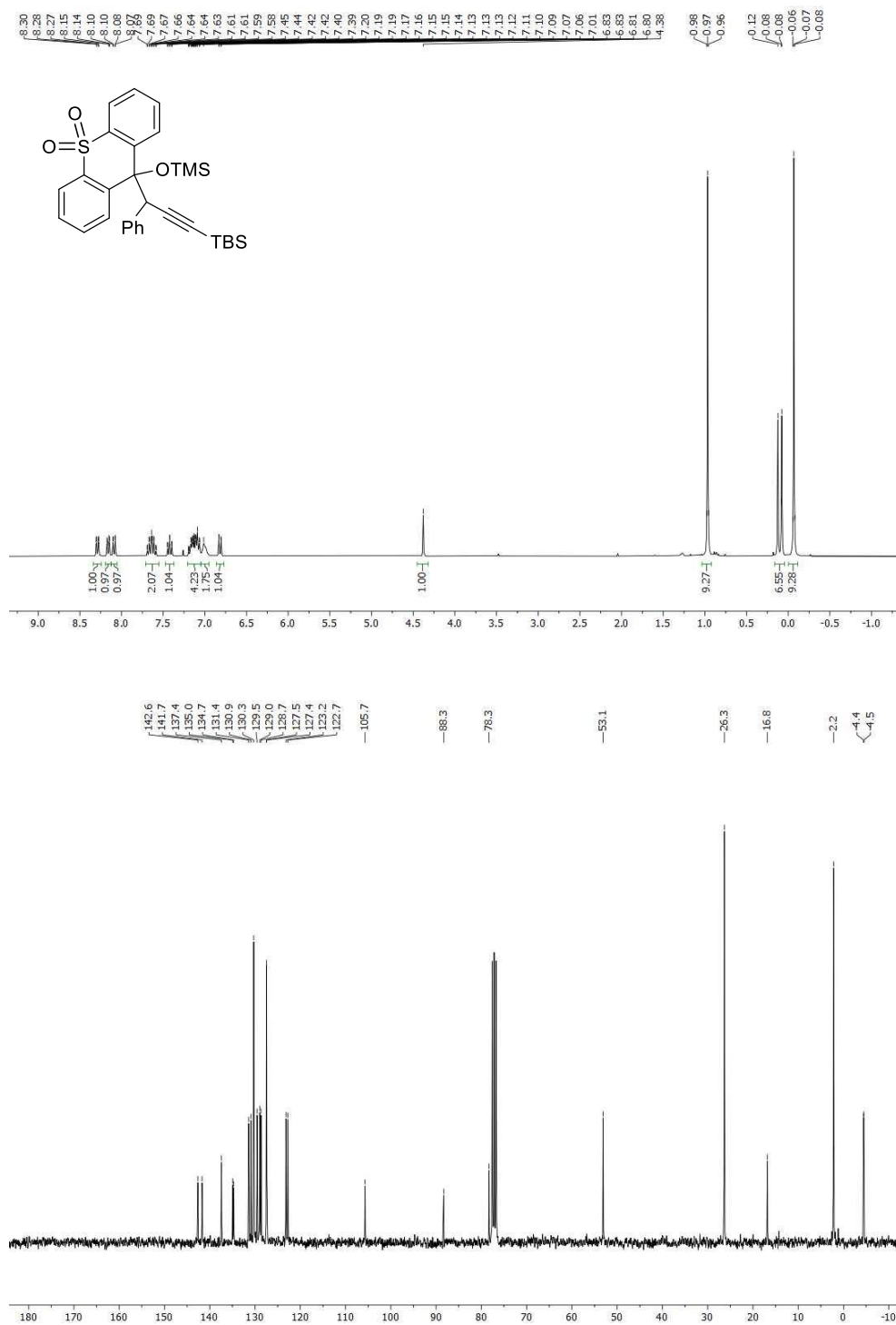
Tert-butyl dimethyl(3-(*p*-tolyl)-3-(9-((trimethylsilyloxy)-9H-xanthen-9-yl)prop-1-yn-1-yl)silane (2.4q)



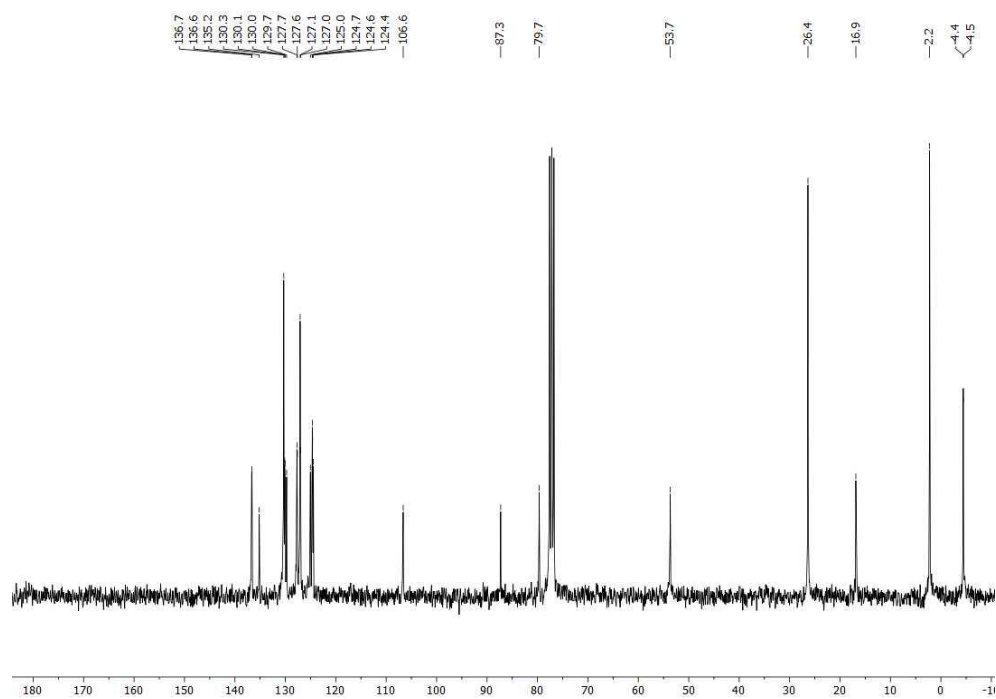
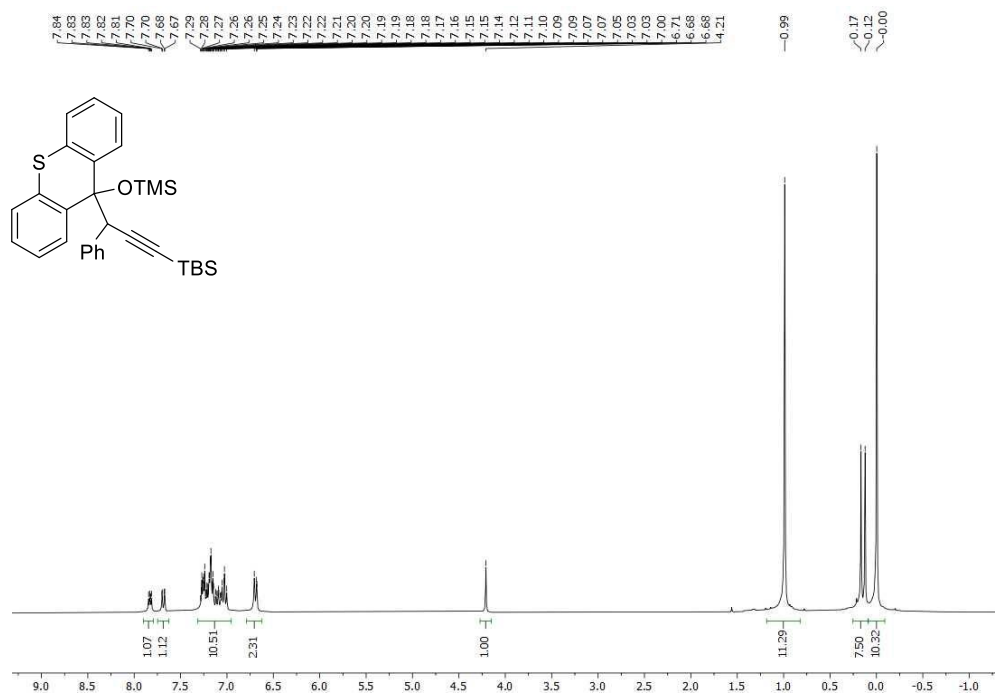
Tert-butyl dimethyl(3-phenyl-3-(5-((trimethylsilyl)oxy)-5H-dibenzo[*a,d*][7]annulen-5-yl)prop-1-yn-1-yl)silane (1.10)



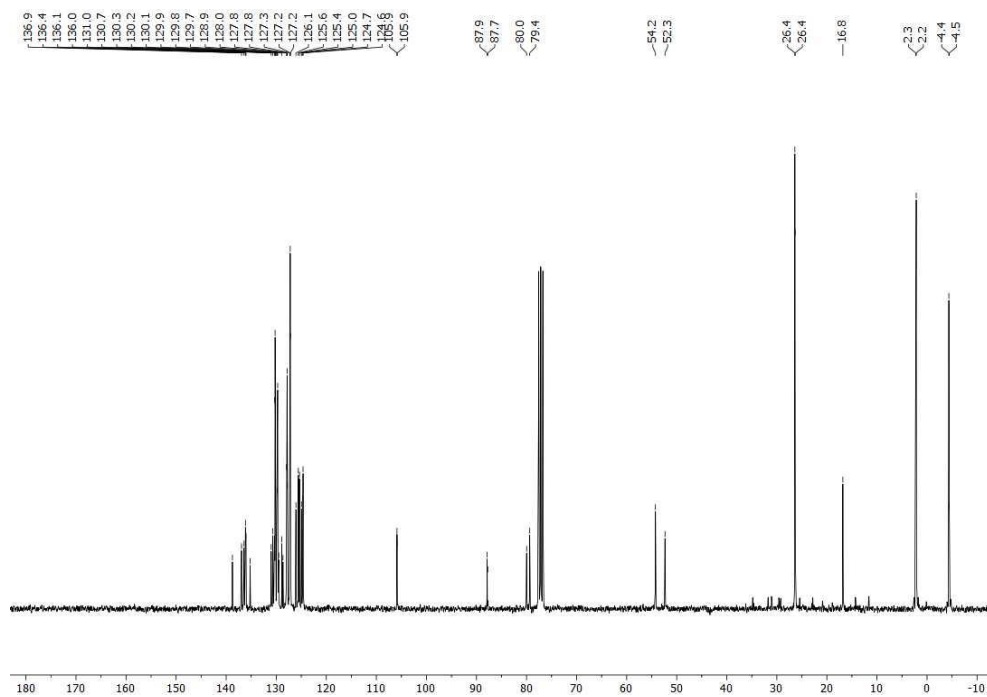
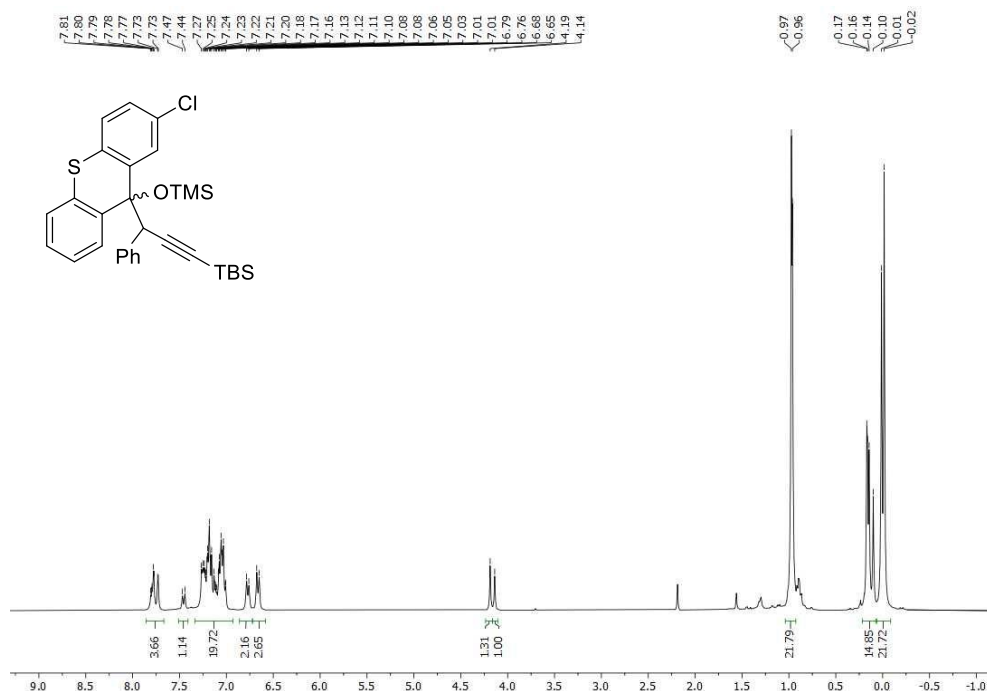
9-(3-(*Tert*-butyldimethylsilyl)-1-phenylprop-2-yn-1-yl)-9-((trimethylsilyl)oxy)-9H-thioxanthene 10,10-dioxide (2.15)



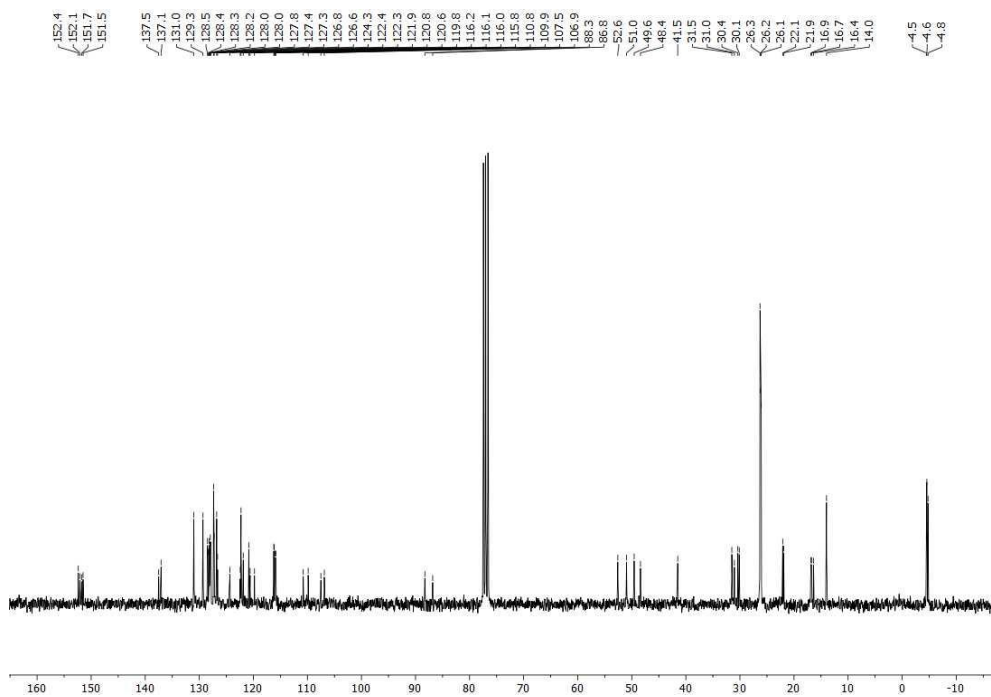
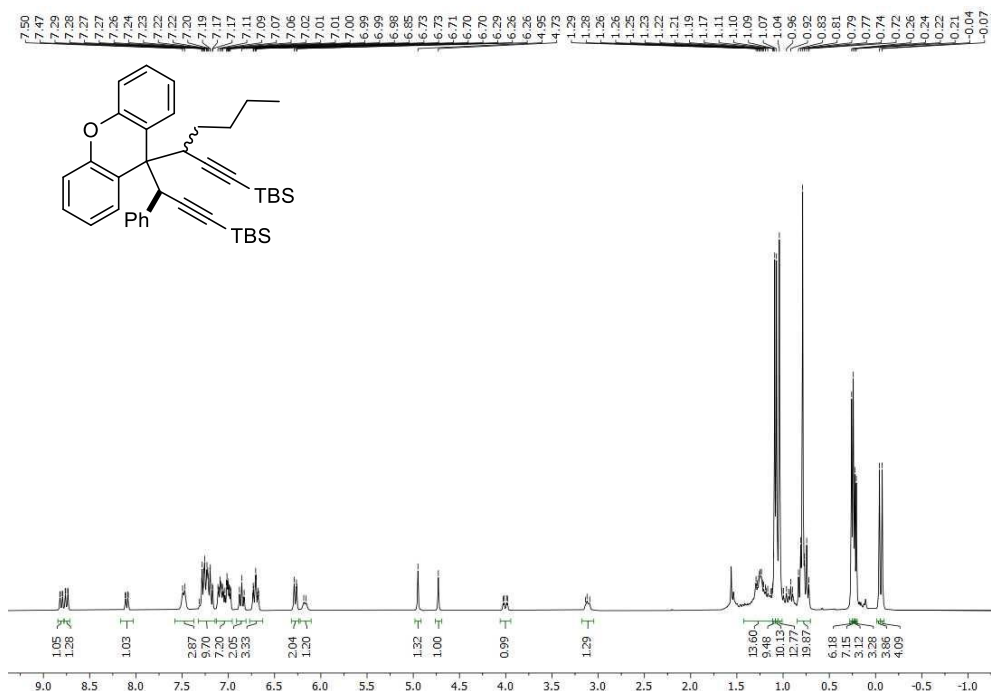
Tert-butyl dimethyl(3-phenyl-3-(9-((trimethylsilyl)oxy)-9H-thioxanthen-9-yl)prop-1-yn-1-yl)silane (2.18a)

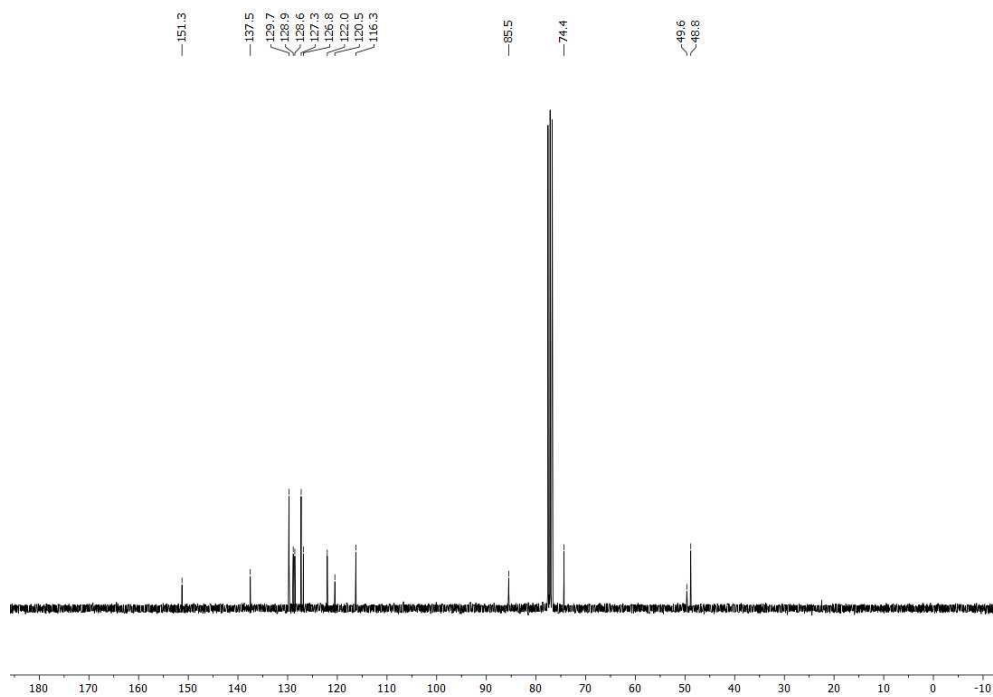
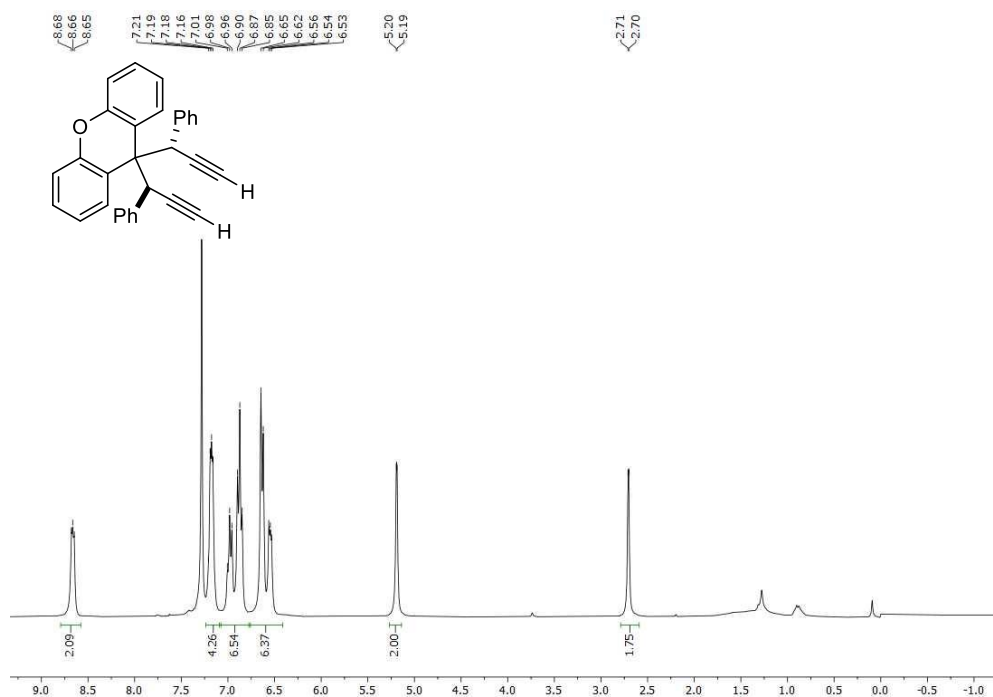


Tert-butyl(3-(2-chloro-9-((trimethylsilyl)oxy)-9H-thioxanthen-9-yl)-3-phenylprop-1-yn-1-yl)dimethylsilane (2.18i)

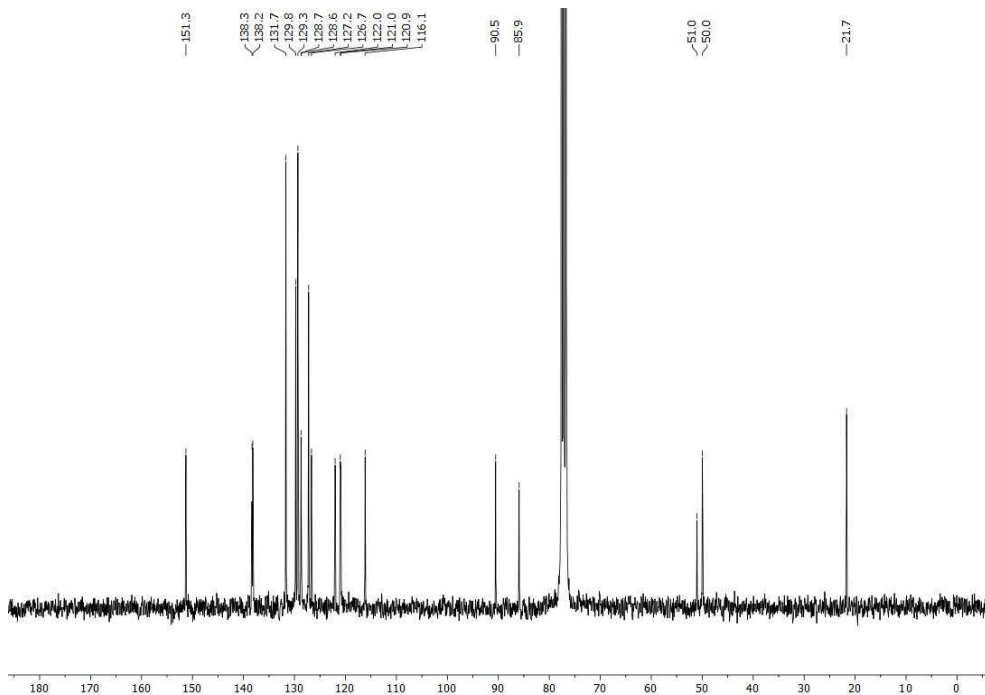
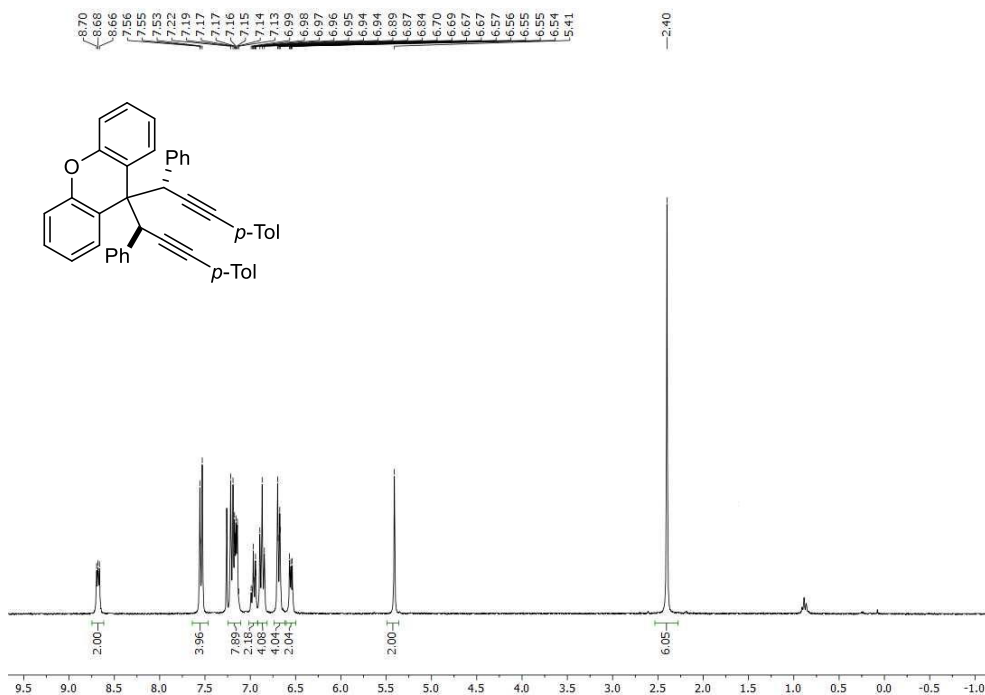


Tert-butyl(3-(9-(3-(tert-butyl dimethylsilyl)-1-phenylprop-2-yn-1-yl)-9H-xanthen-9-yl)hept-1-yn-1-yl)dimethylsilane (2.19b)

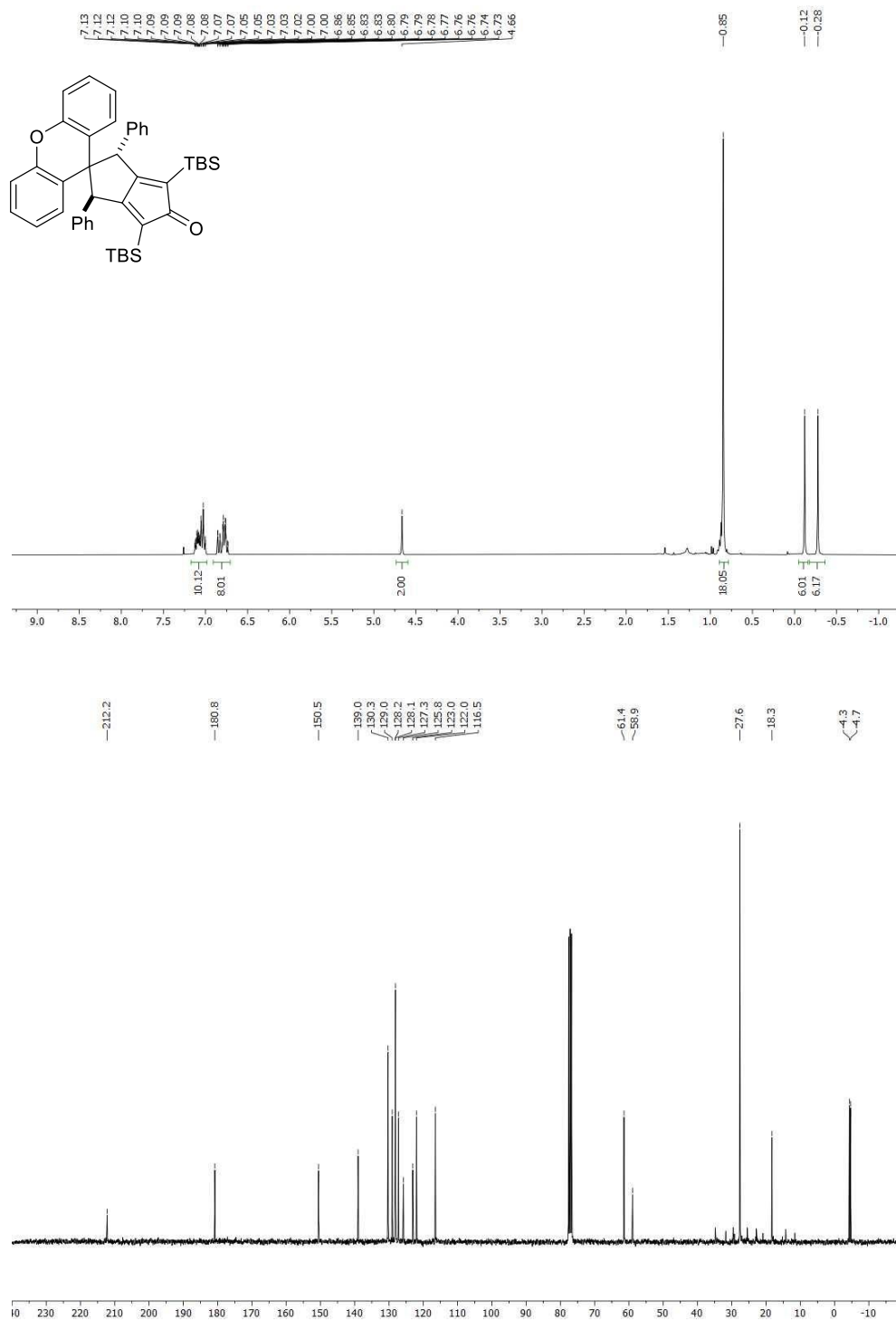


9,9-Bis((S*)-1-phenylprop-2-yn-1-yl)-9H-xanthene (2.22a)

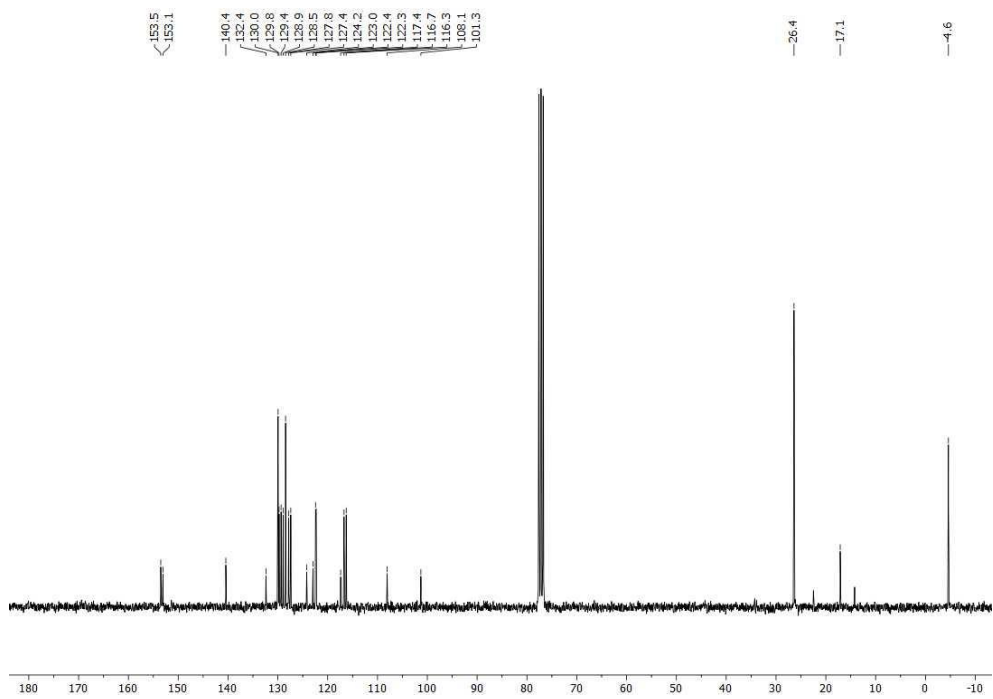
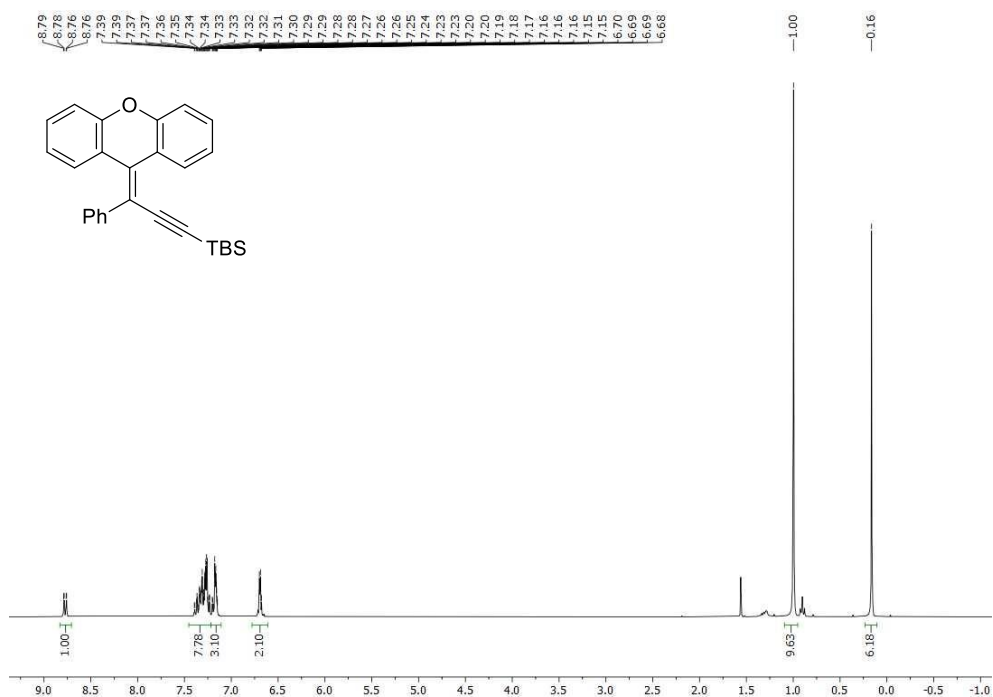
9,9-bis((*S*^{*})-1-phenyl-3-(*p*-tolyl)prop-2-yn-1-yl)-9*H*-xanthene (2.22b)

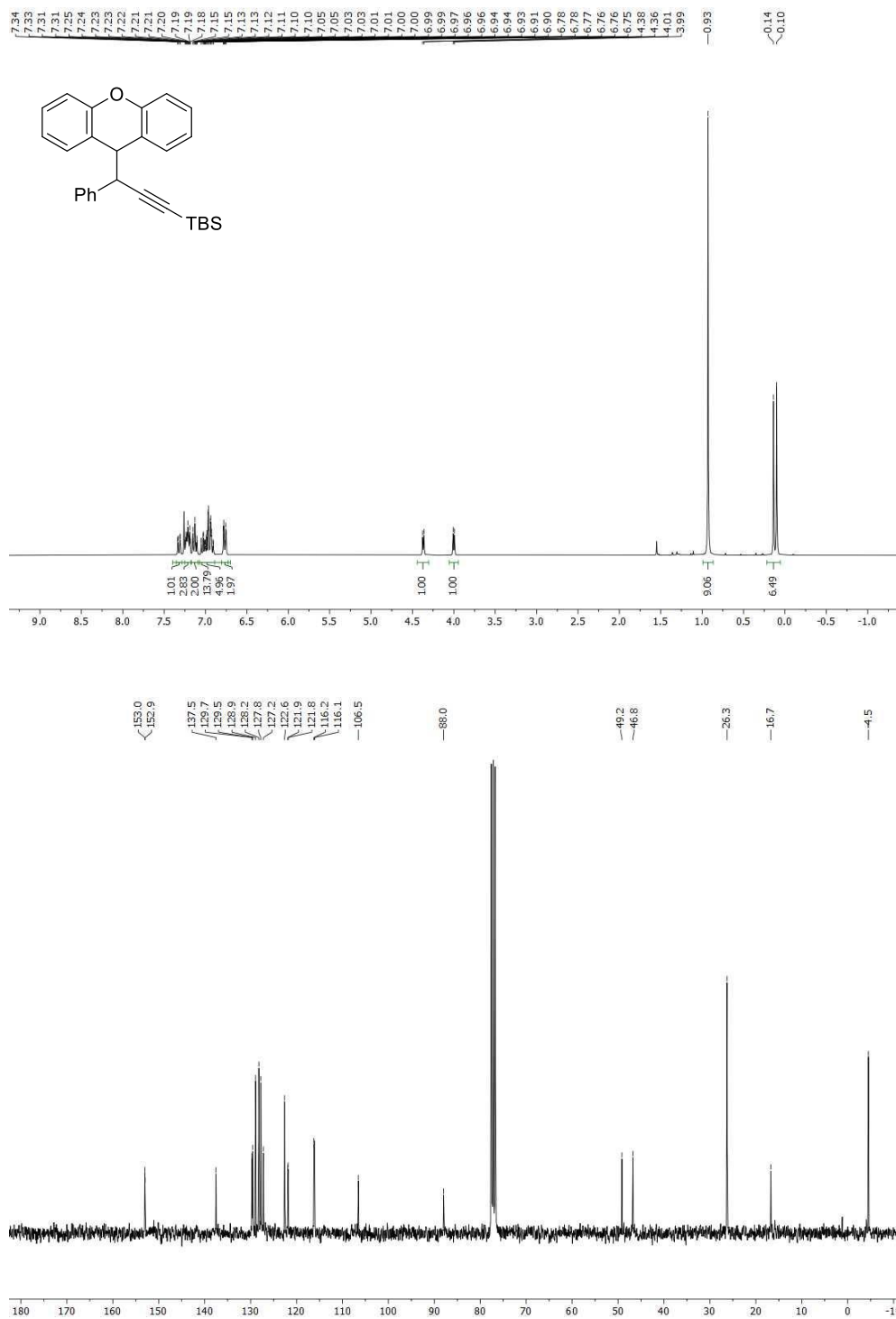


(1*S,3*S**)-4,6-Bis(*tert*-butyldimethylsilyl)-1,3-diphenyl-1*H*-spiro[pentalene-2,9'-xanthen]-5(3*H*)-one (2.23)**



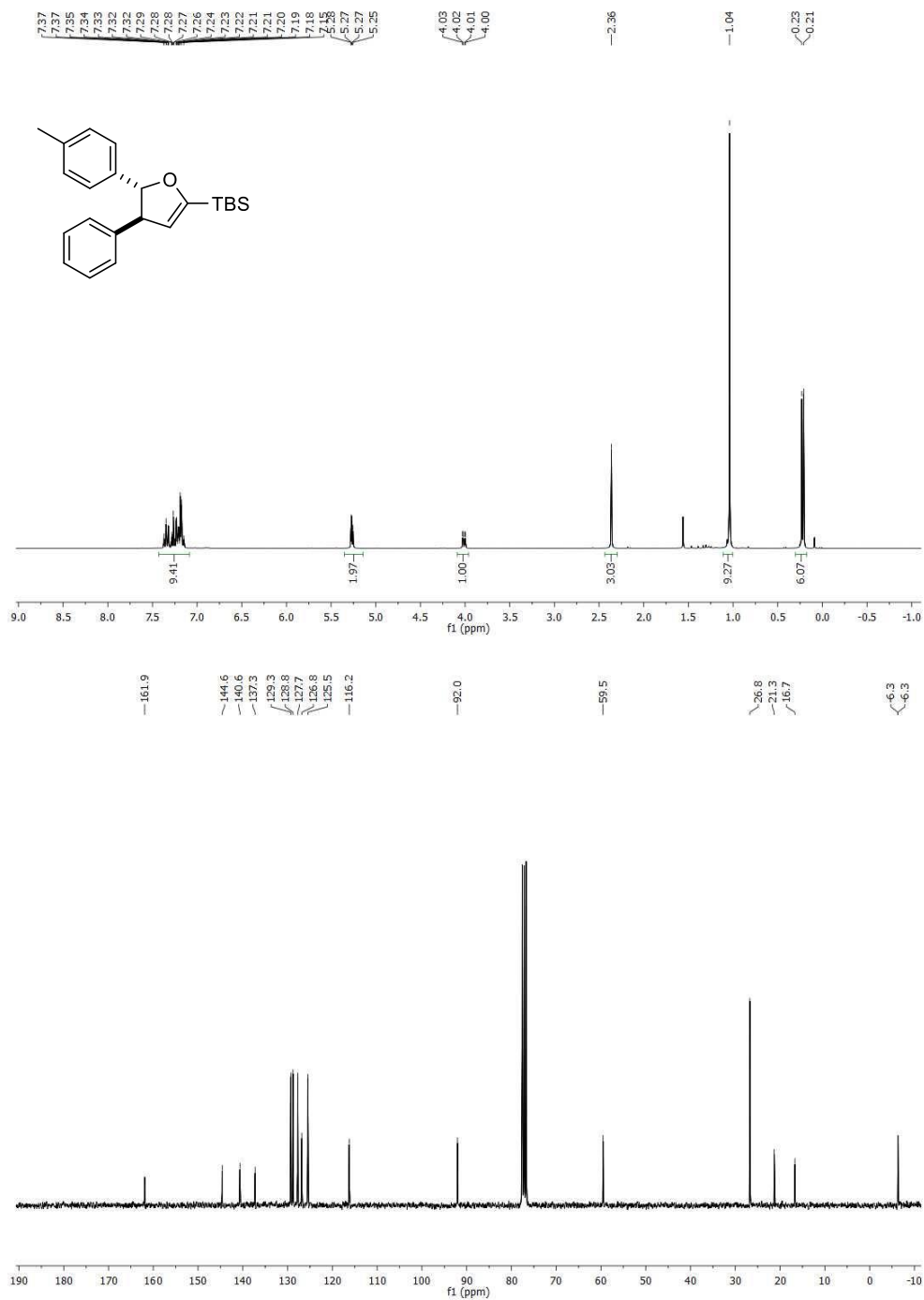
Tert-butyl dimethyl(3-phenyl-3-(9H-xanthen-9-ylidene)prop-1-yn-1-yl)silane (2.24)

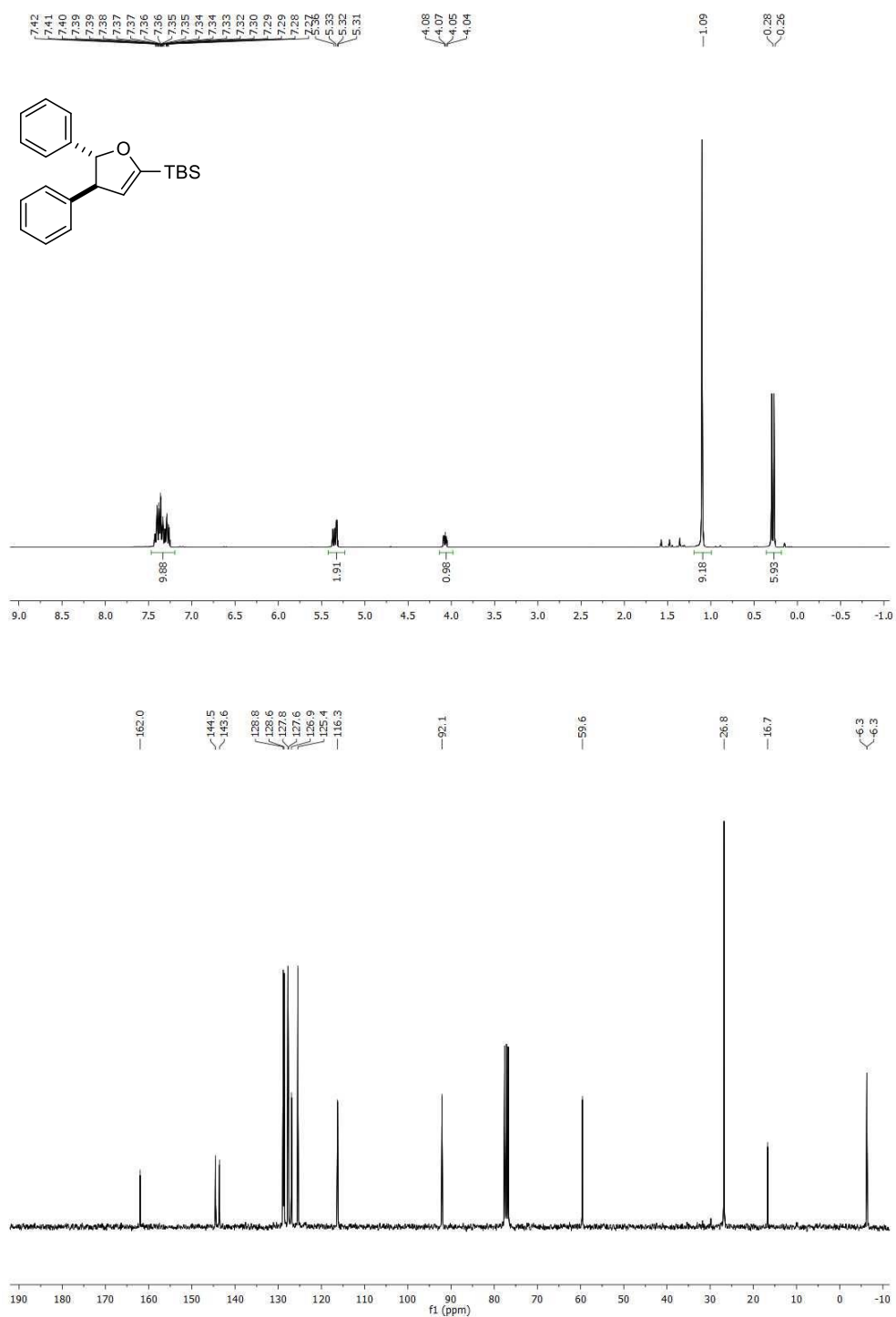


Tert-butyldimethyl(3-phenyl-3-(9H-xanthen-9-yl)prop-1-yn-1-yl)silane (2.25)

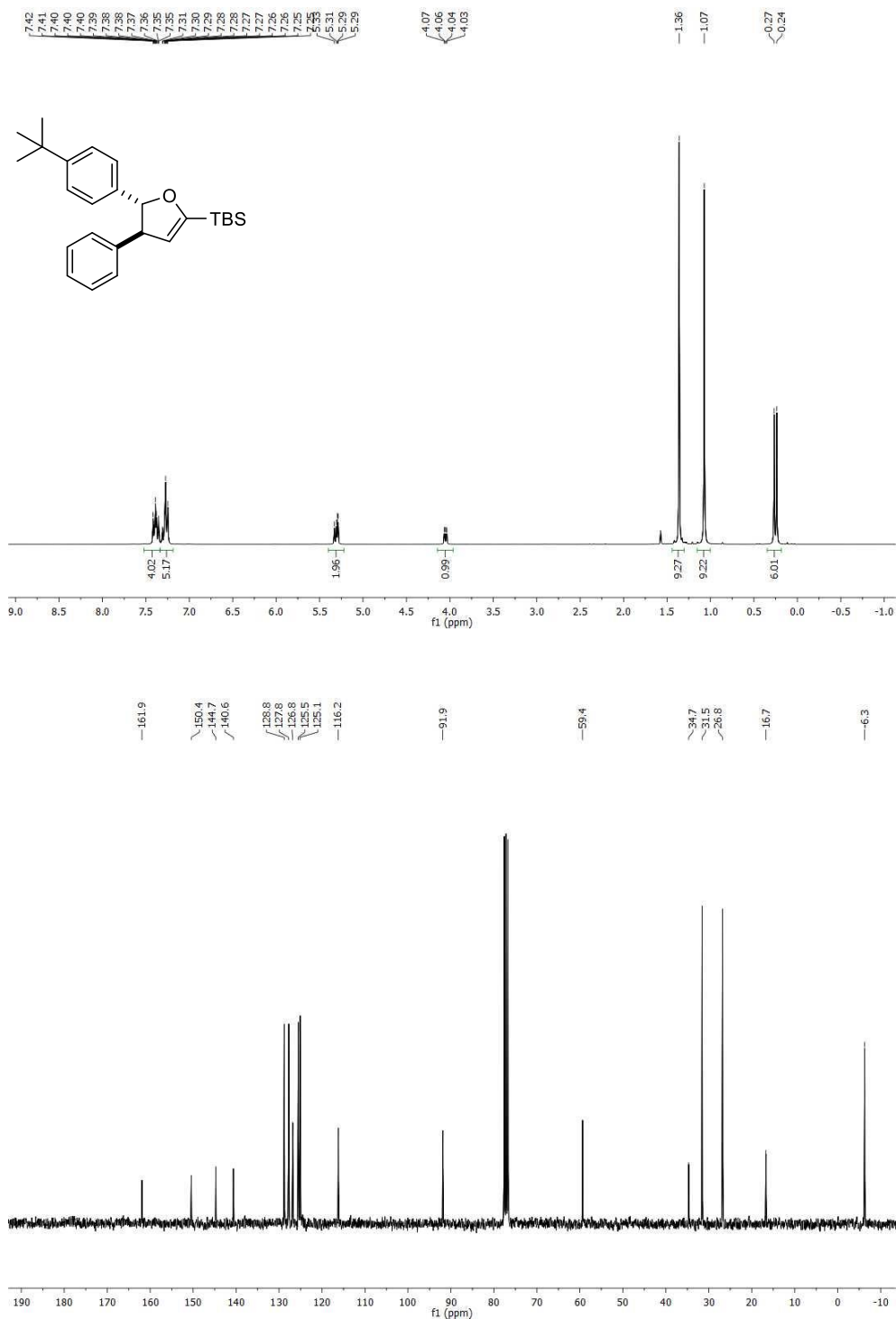
3 Chapter III

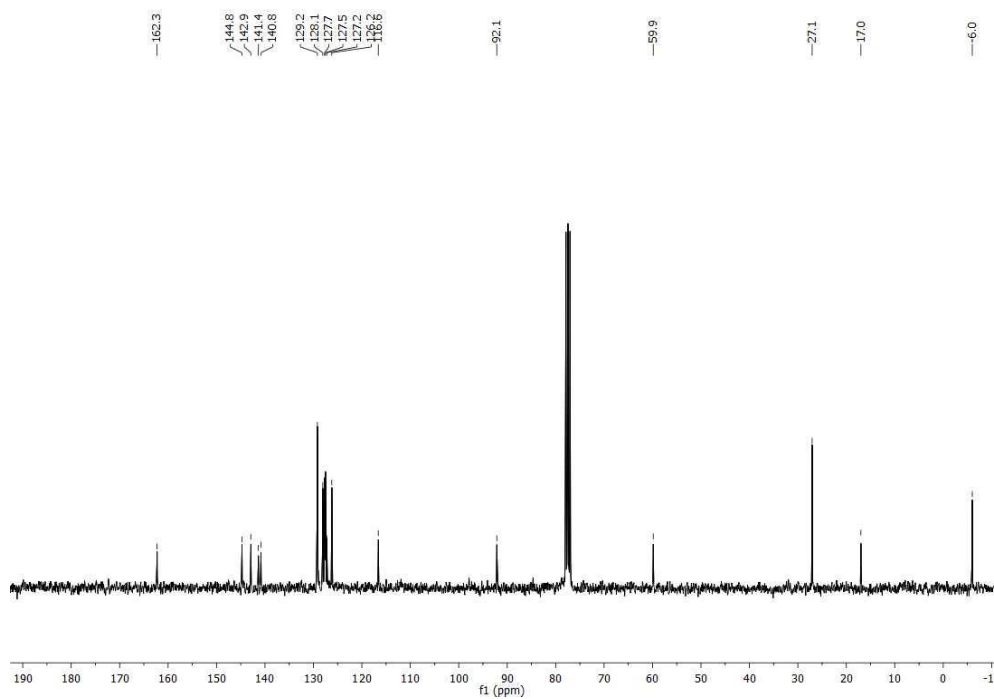
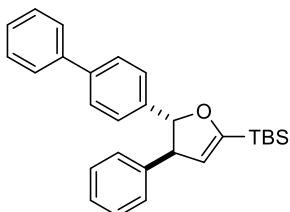
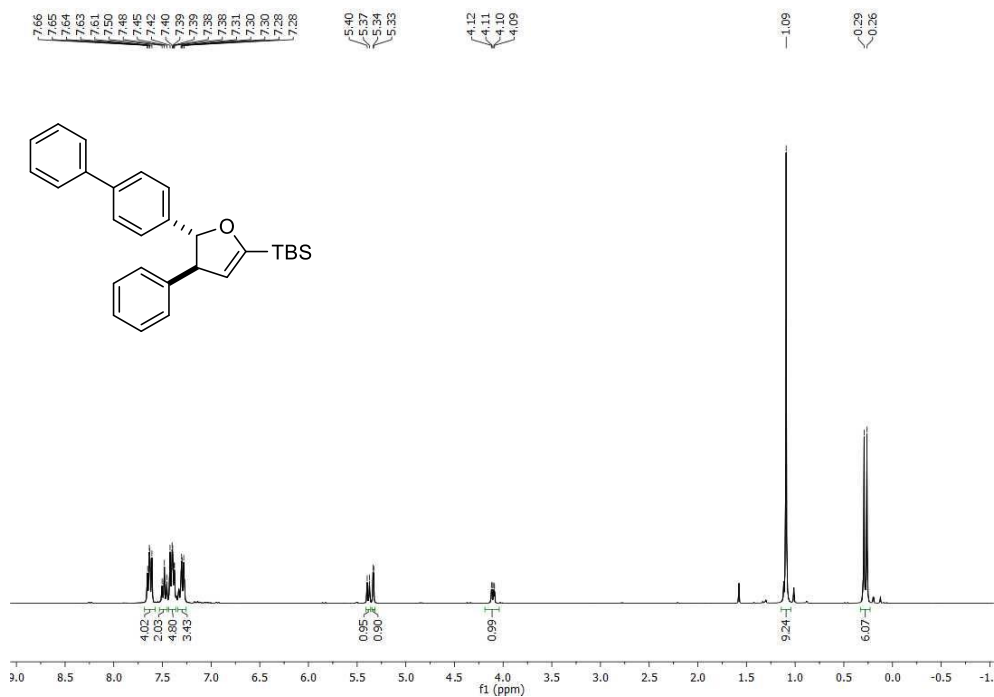
Trans-tert-butyldimethyl(4-phenyl-5-(*p*-tolyl)-4,5-dihydrofuran-2-yl)silane (*trans*-3.4a)



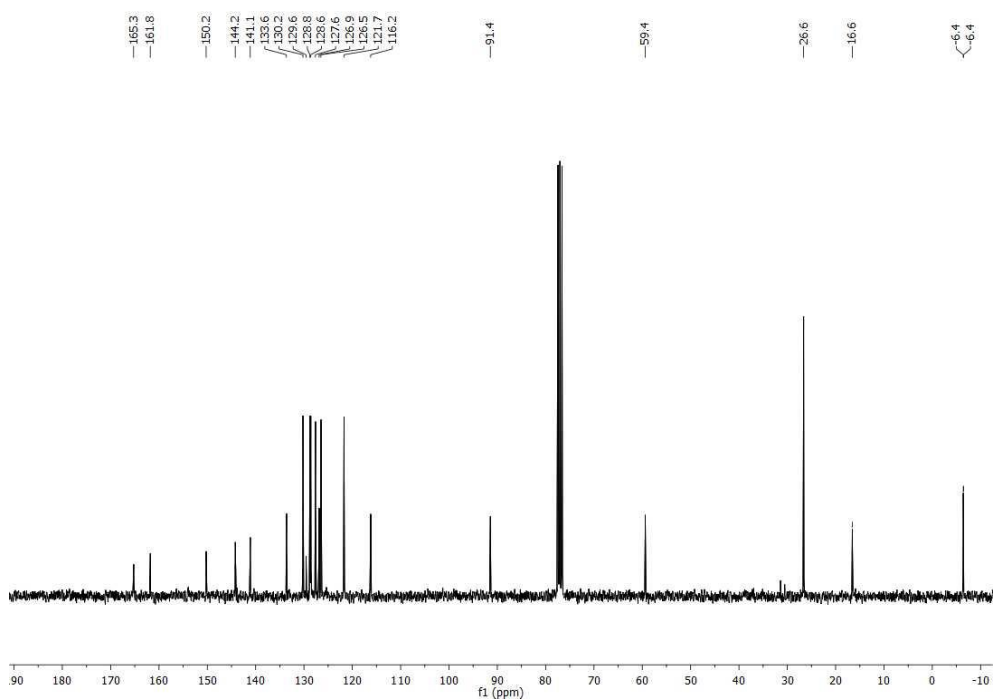
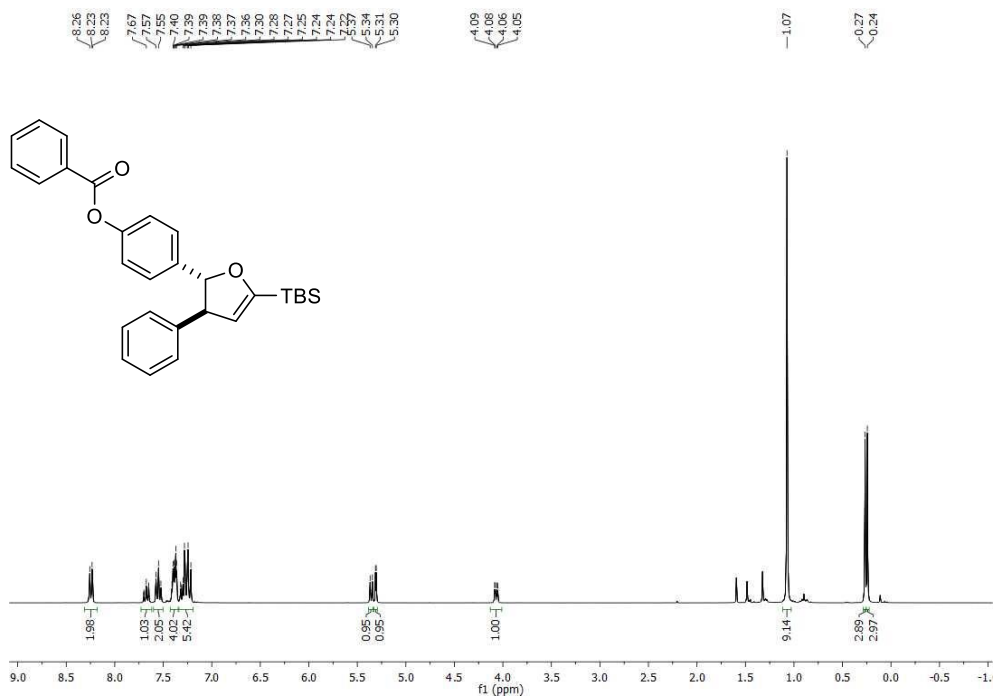
**Trans-tert-butyl(dimethyl-4,5-diphenyl-4,5-dihydrofuran-2-yl)dimethylsilane
(trans-3.4b)**

Trans-tert-butyl(5-(4-(tert-butyl)phenyl)-4-phenyl-4,5-dihydrofuran-2-yl)dimethylsilane (trans-4aa).

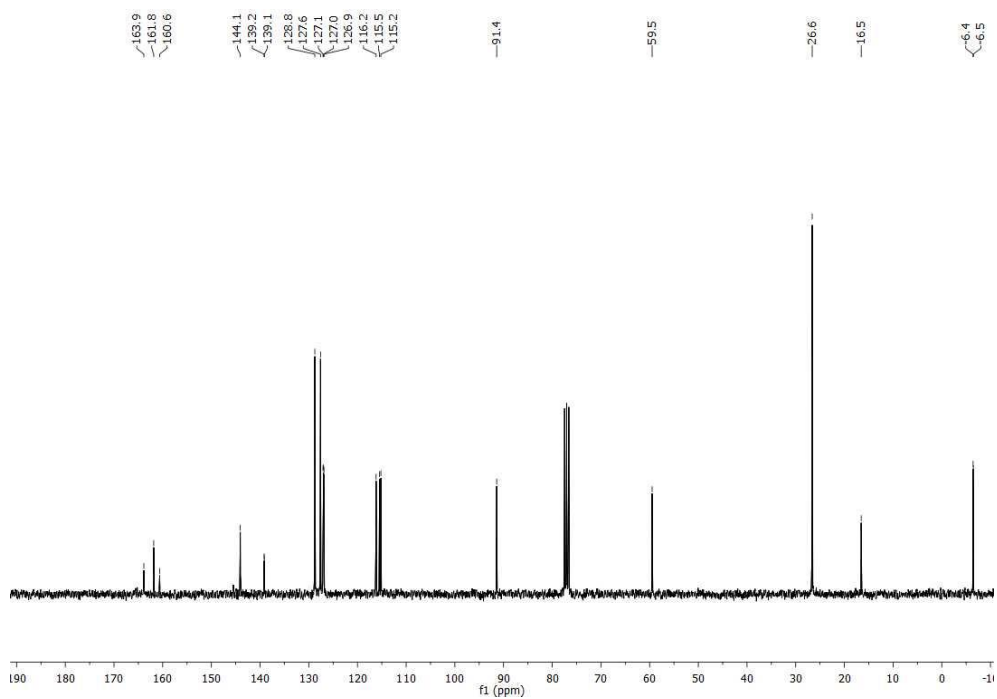
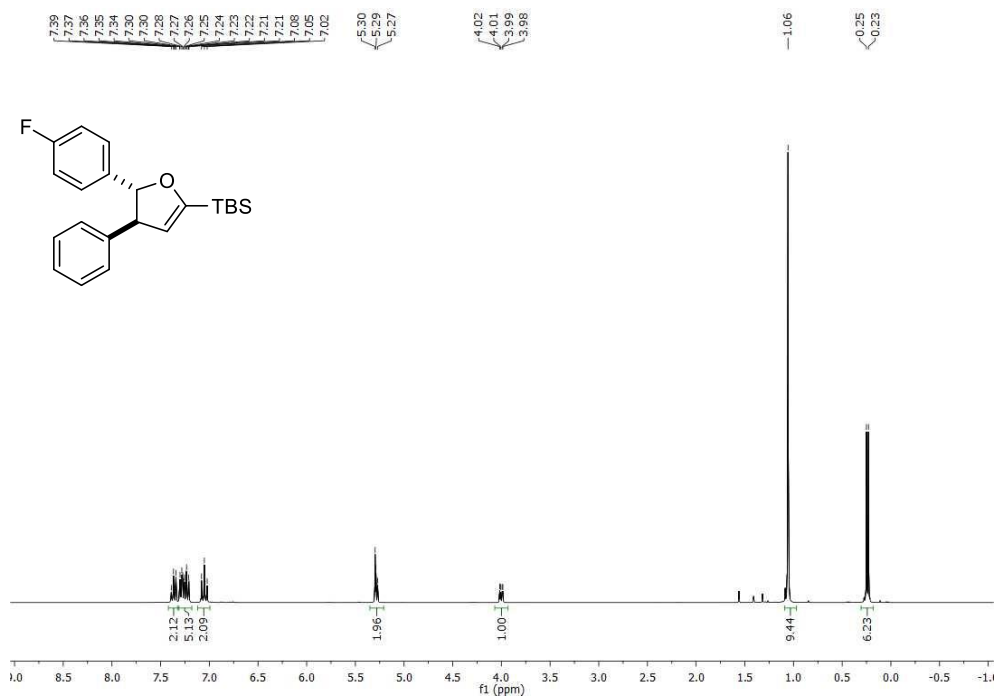


Trans-(5-([1,1'-biphenyl]-4-yl)-4-phenyl-4,5-dihydrofuran-2-yl)(tert-butyl)dimethylsilane (*trans*-4c).

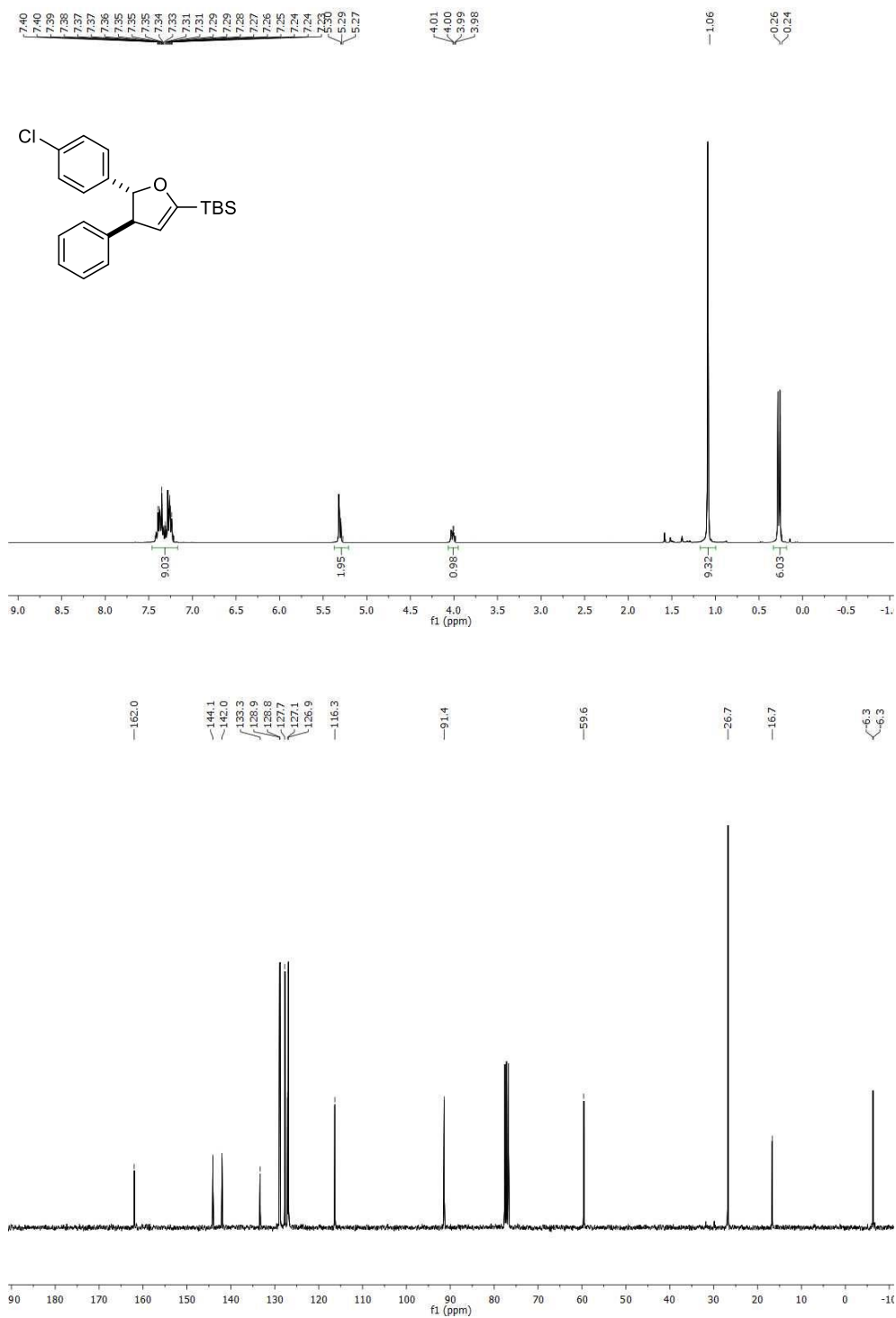
Trans-4-(5-(*tert*-butyldimethylsilyl)-3-phenyl-2,3-dihydrofuran-2-yl)phenyl benzoate (*trans*-3.4d).



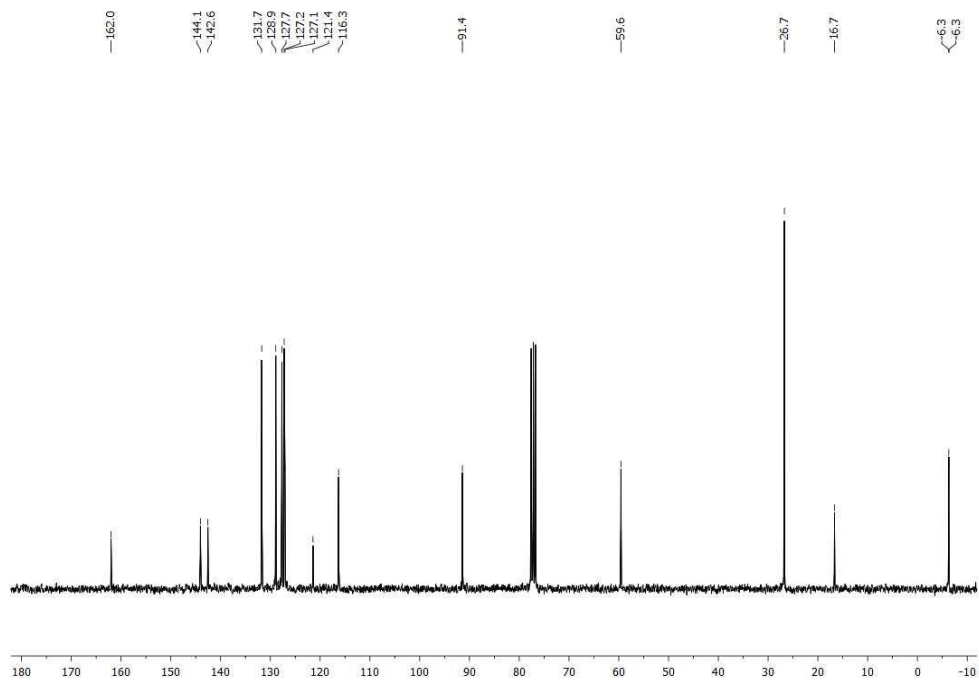
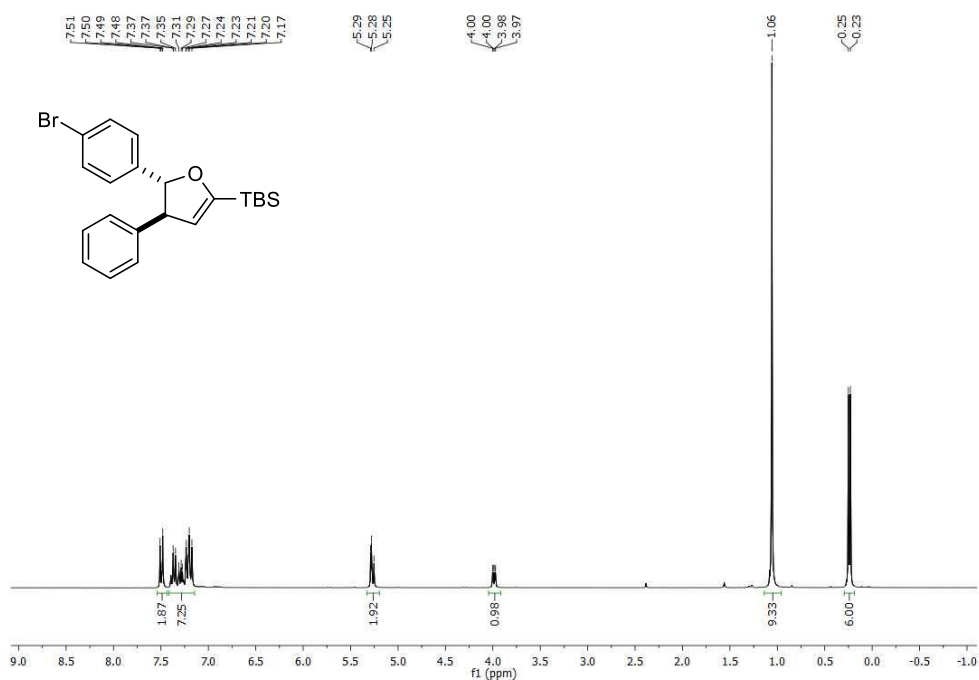
Trans-tert-butyl(5-(4-fluorophenyl)-4-phenyl-4,5-dihydrofuran-2-yl)dimethylsilane (*trans*-3.4e).



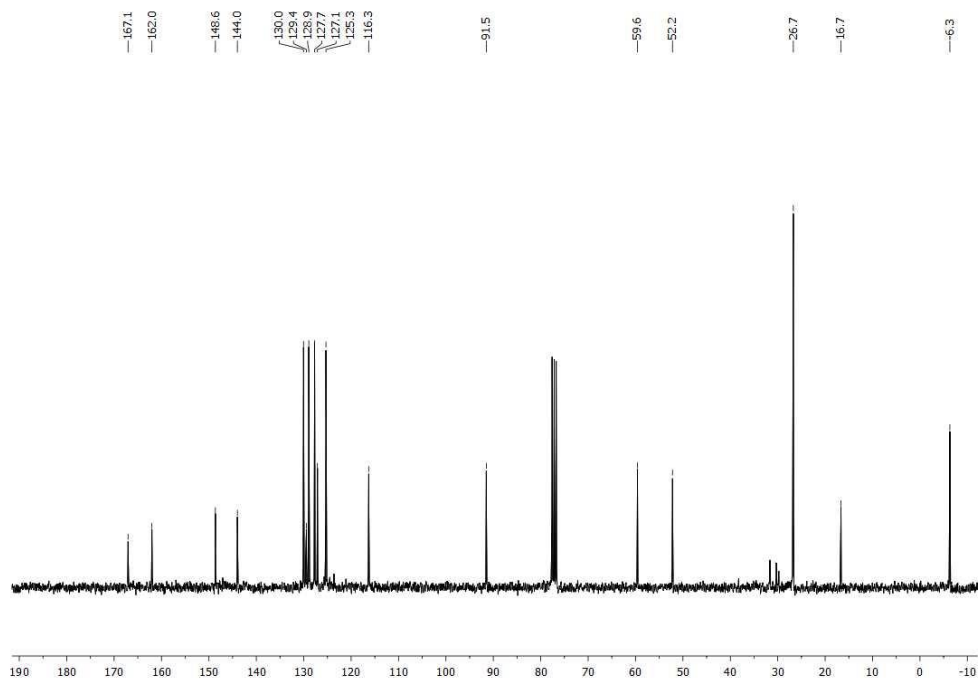
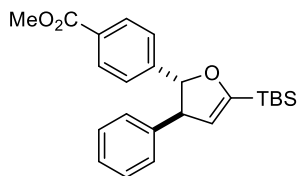
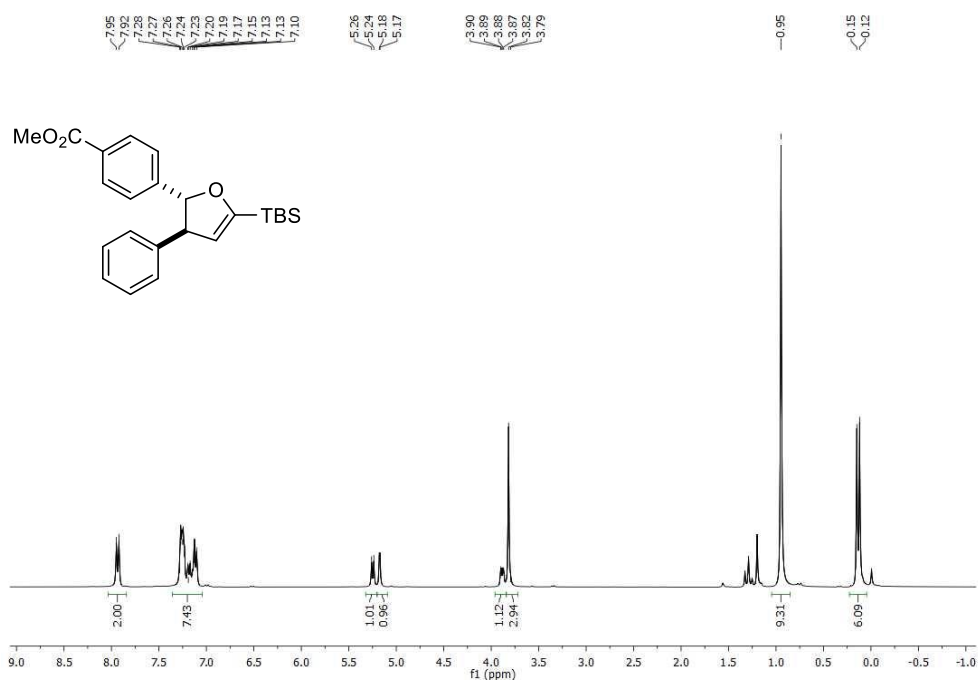
***Trans*-*tert*-butyl(5-(4-chlorophenyl)-4-phenyl-4,5-dihydrofuran-2-yl)dimethylsilane (*trans*-3.4f)**

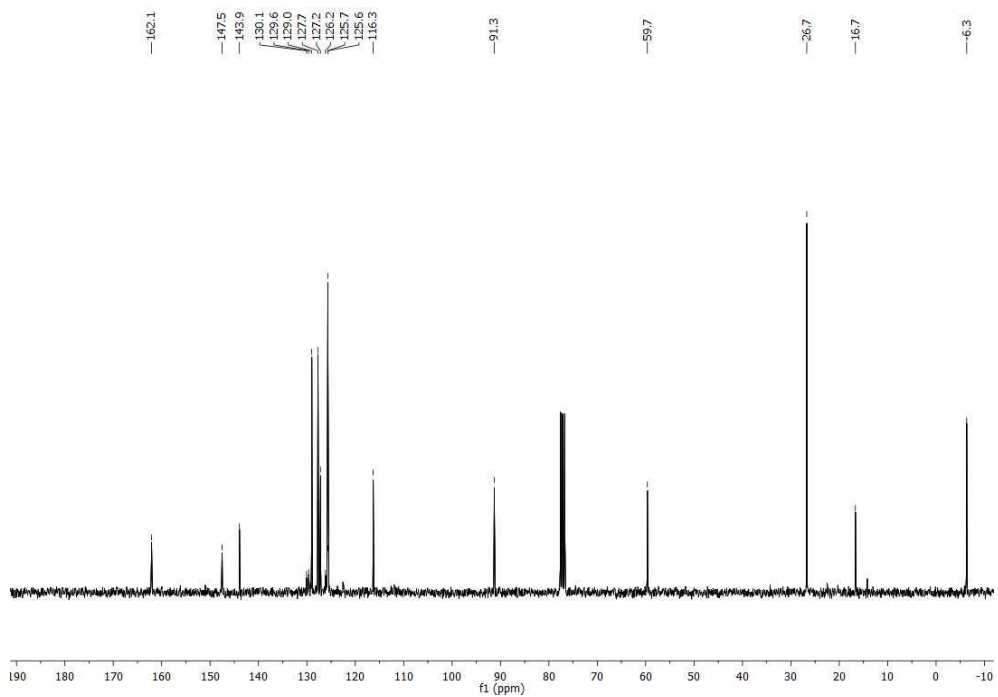
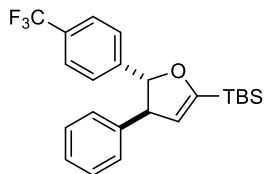
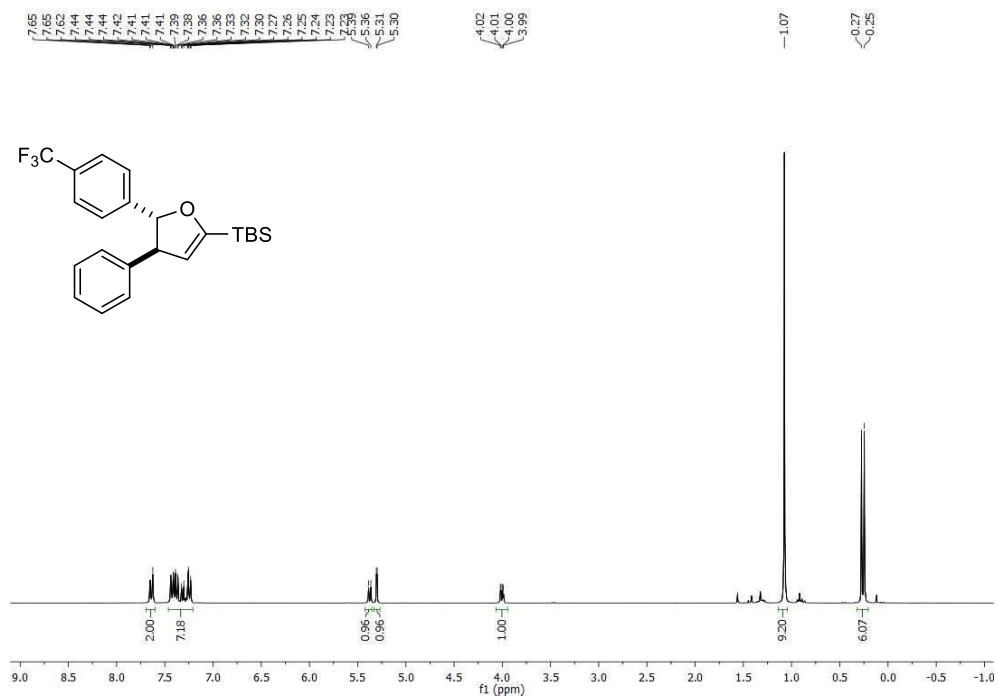


***Trans*-*tert*-butyldimethyl(5-(*p*-bromophenyl)-4-phenyl-4,5-dihydrofuran-2-yl)silane (*trans*-3.4g).**

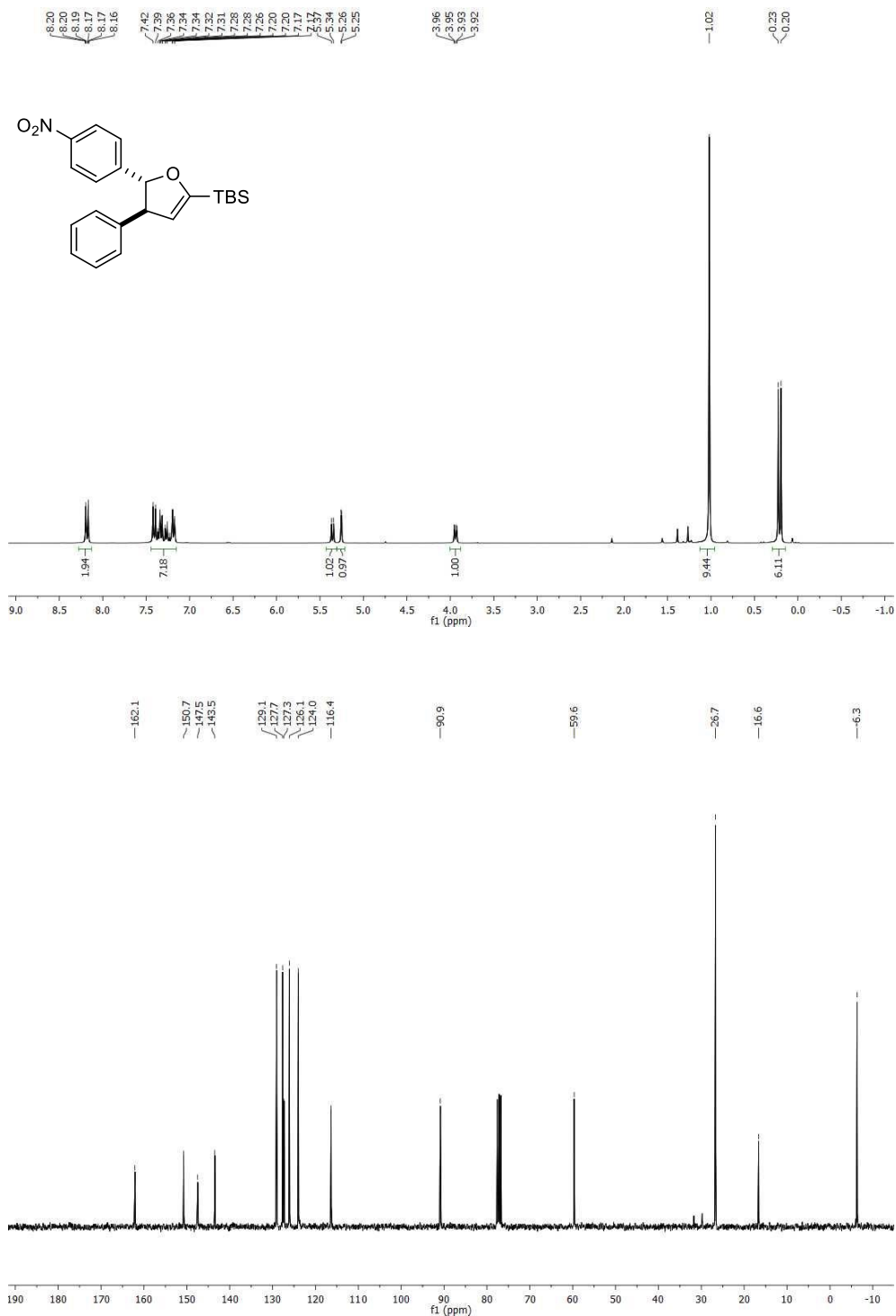


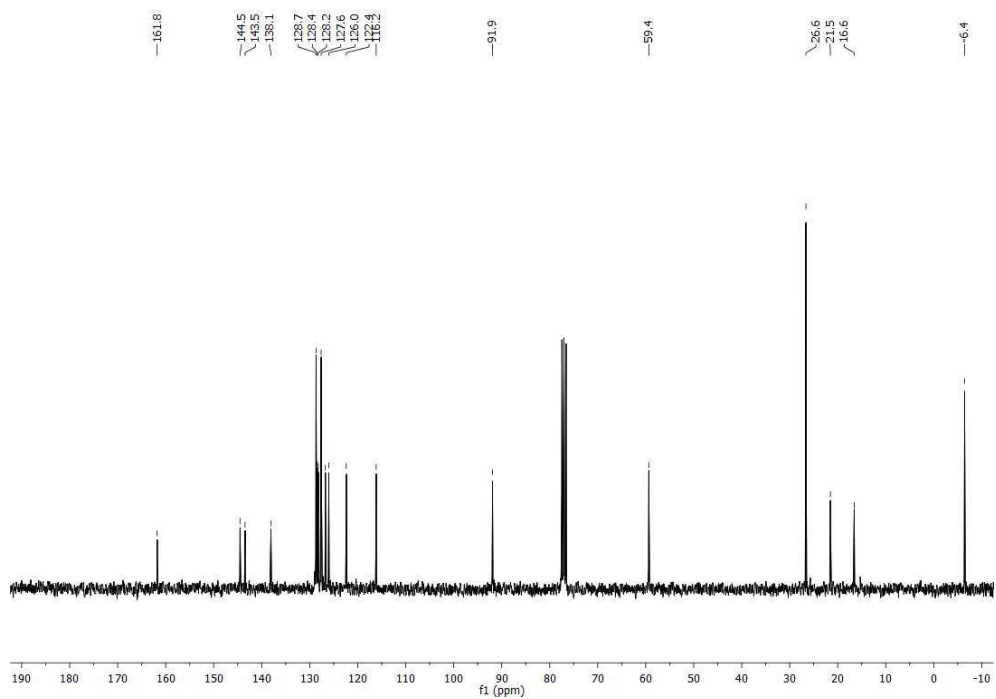
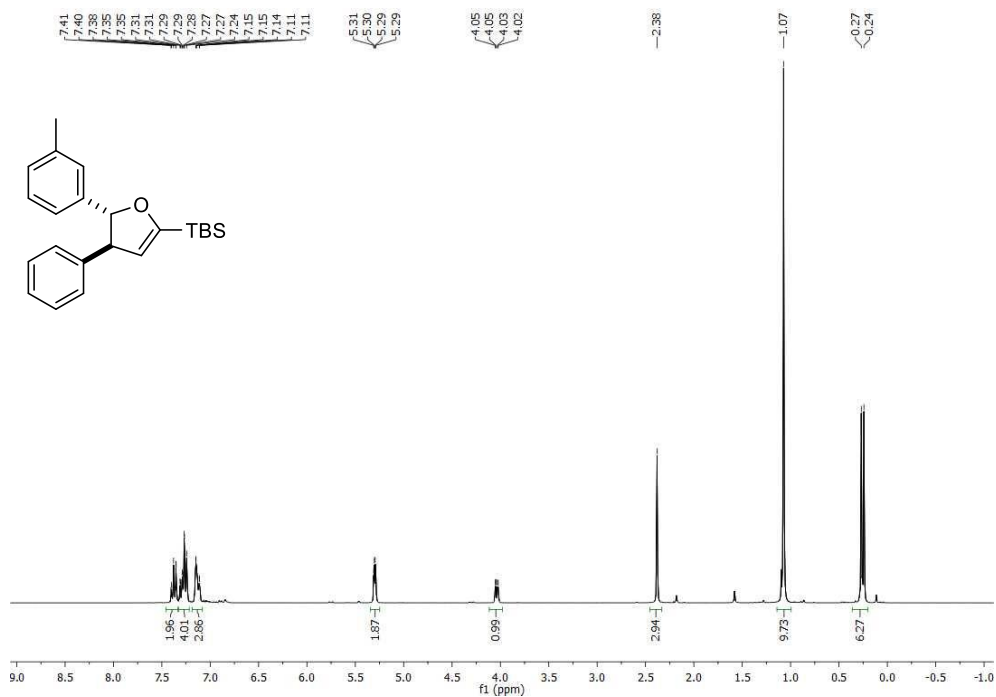
Methyl 4-(*trans*-5-(*tert*-butyldimethylsilyl)-3-phenyl-2,3-dihydrofuran-2-yl)benzoate (*trans*-3.4h).



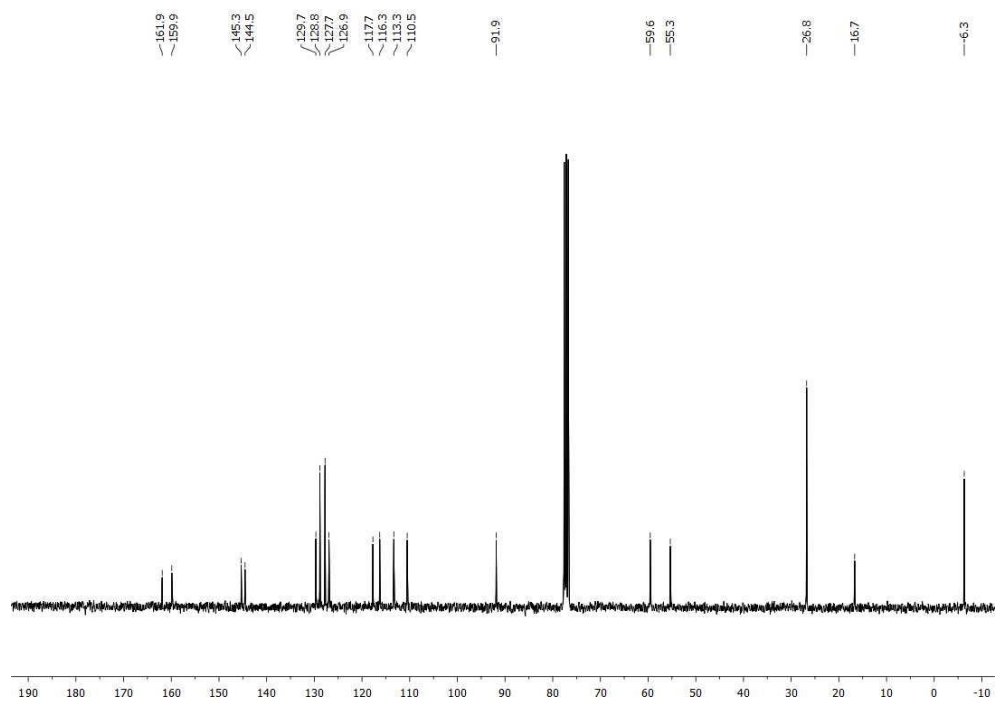
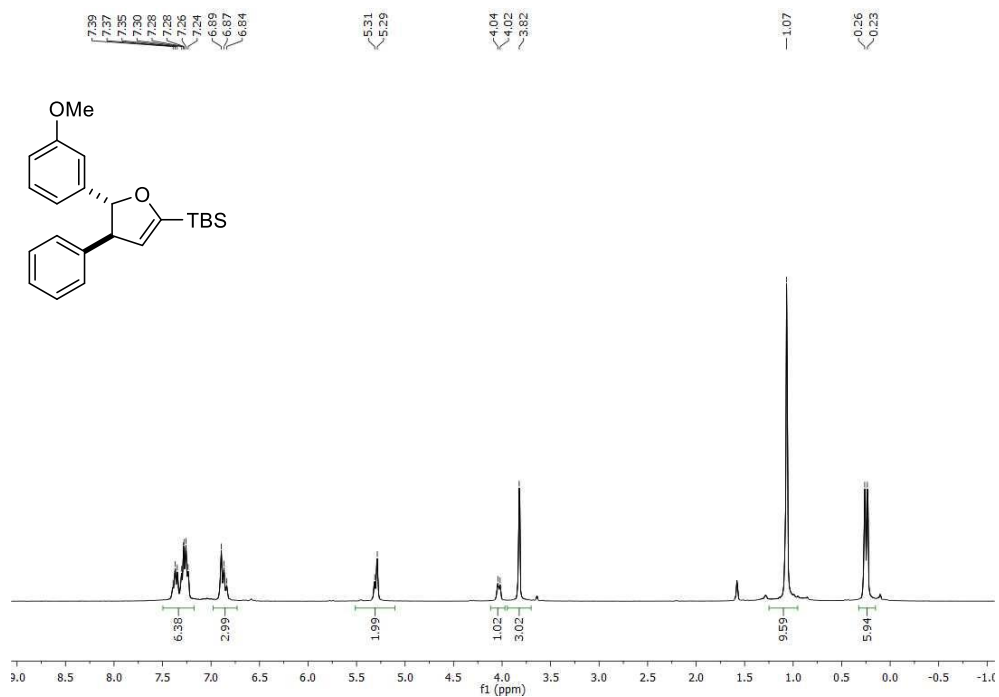
Trans-tert-butyl dimethyl(4-phenyl-5-(4-(trifluoromethyl)phenyl)-4,5-dihydrofuran-2-yl)silane (trans-3.4i)

***Trans-tert*-butyldimethyl(5-(4-nitrophenyl)-4-phenyl-4,5-dihydrofuran-2-yl)silane (*trans*-3.4j).**

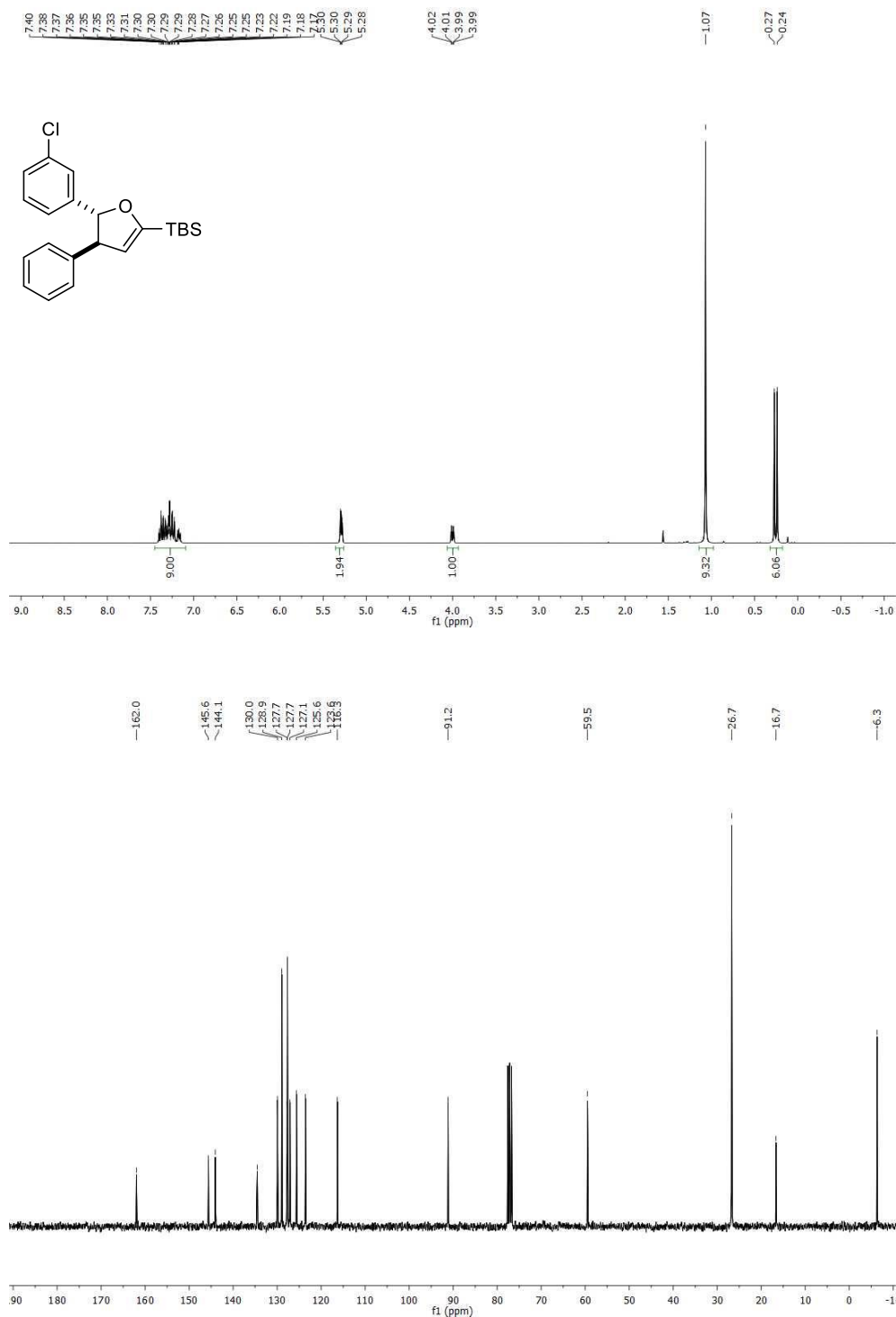


Trans-tert-butyltrimethylsilyl(4-phenyl-5-(*m*-tolyl)-4,5-dihydrofuran-2-yl)silane (*trans*-3.4k).

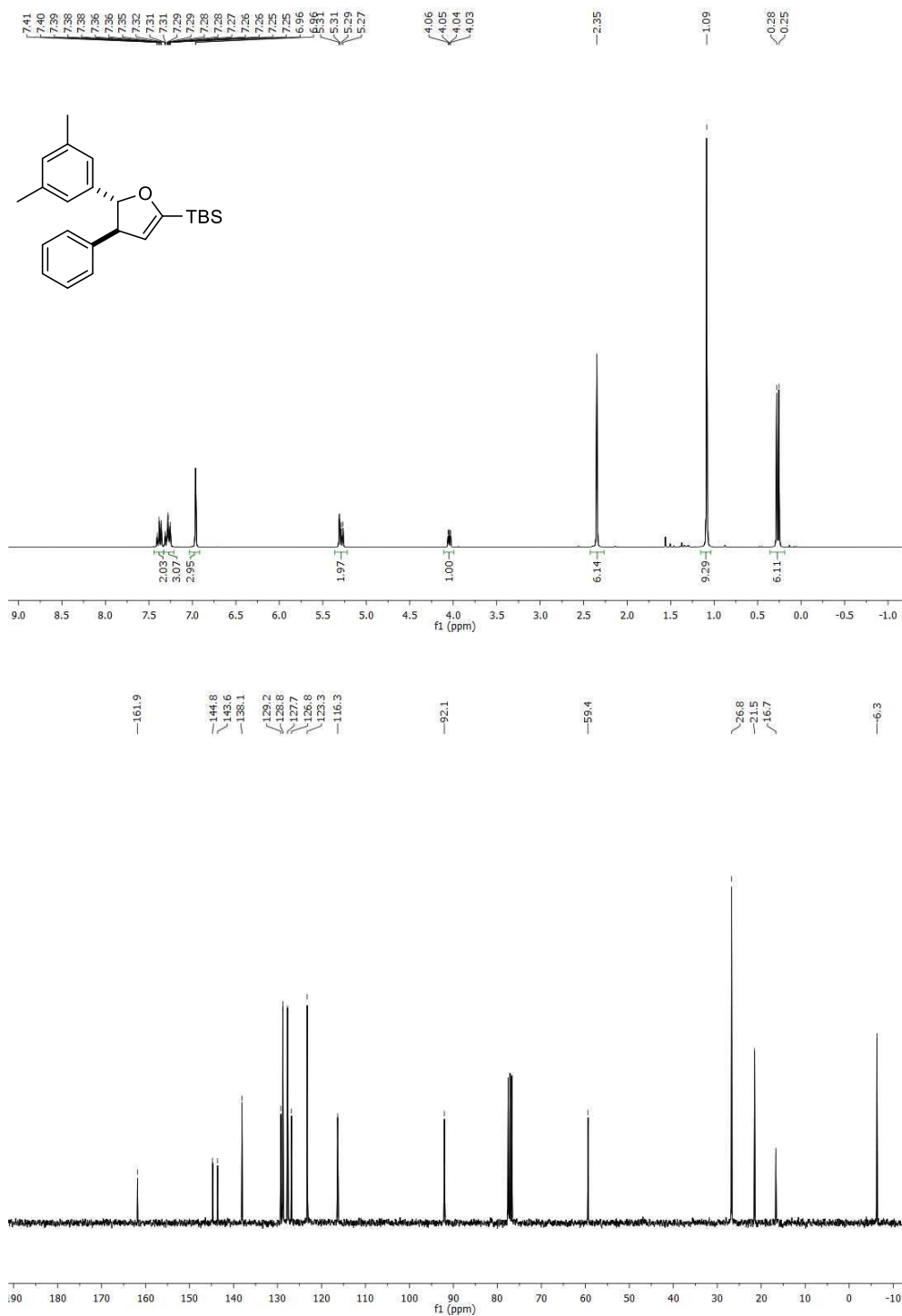
***Trans*-*tert*-butyl(5-(3-methoxyphenyl)-4-phenyl-4,5-dihydrofuran-2-yl)dimethylsilane (*trans*-3.4I).**

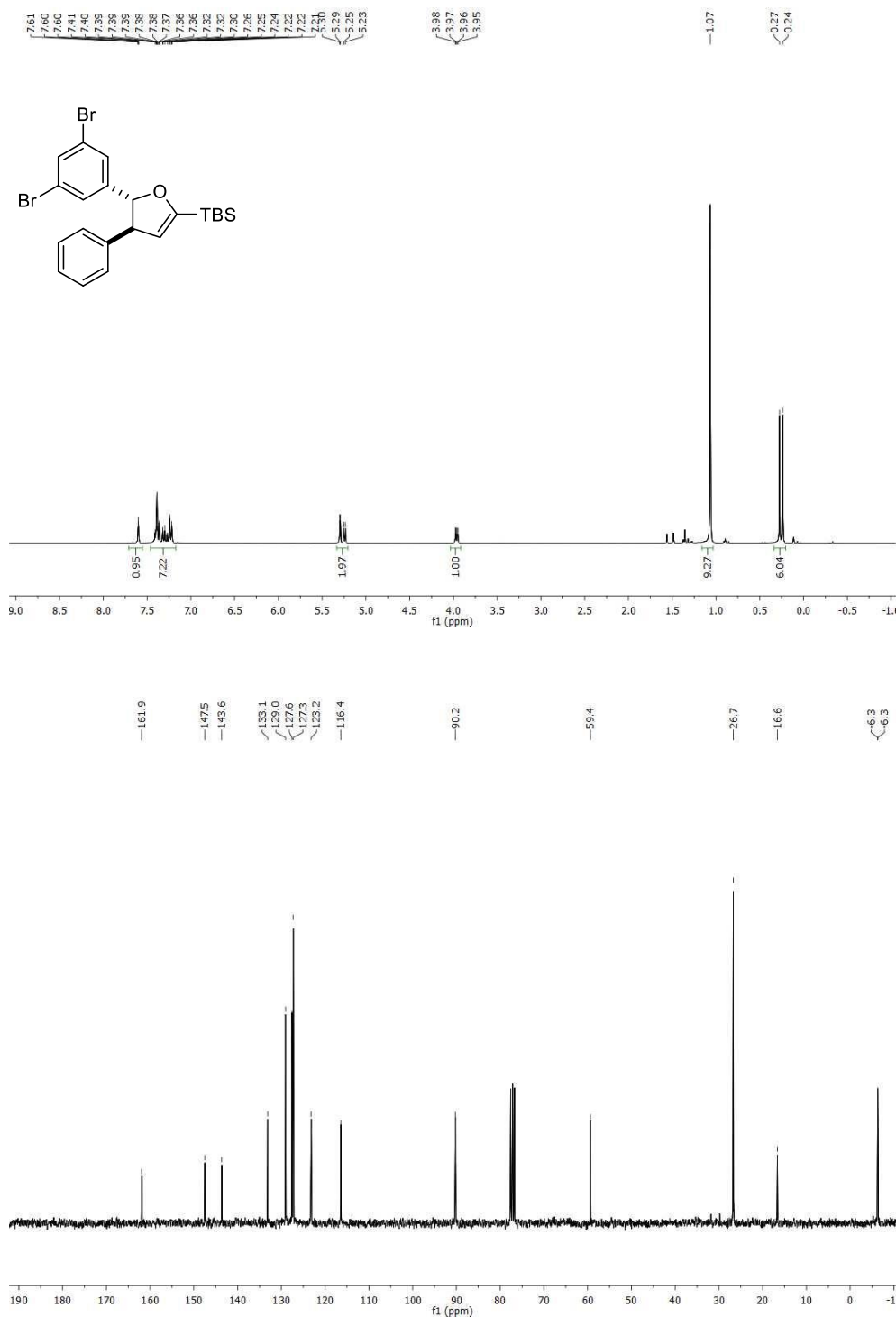


***Trans*-tert-butyl(5-(3-chlorophenyl)-4-phenyl-4,5-dihydrofuran-2-yl)dimethylsilane (*trans*-3.4m).**

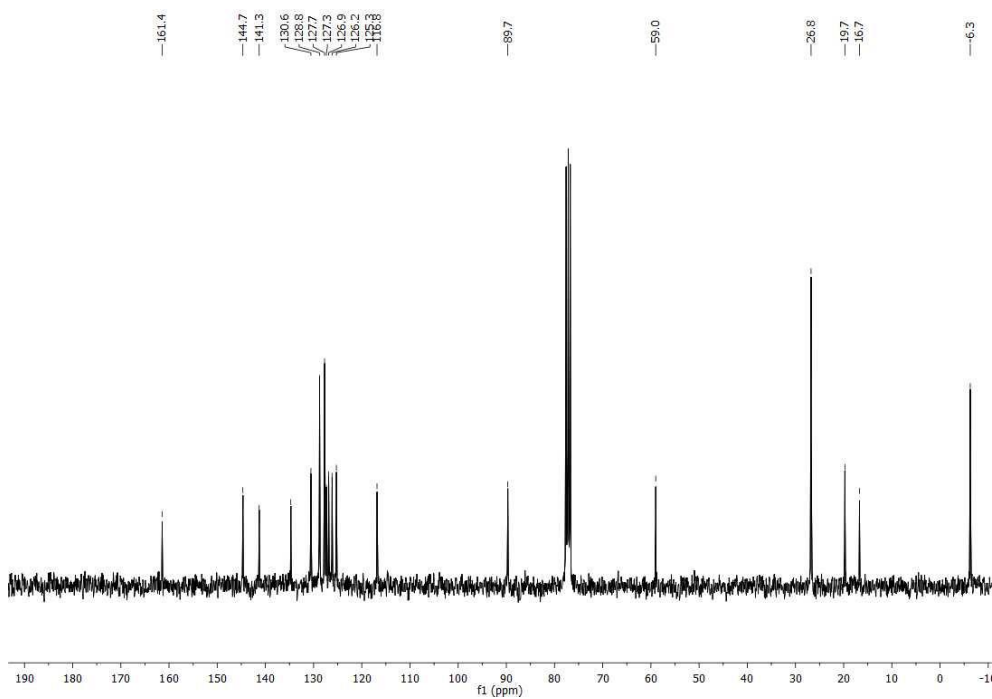
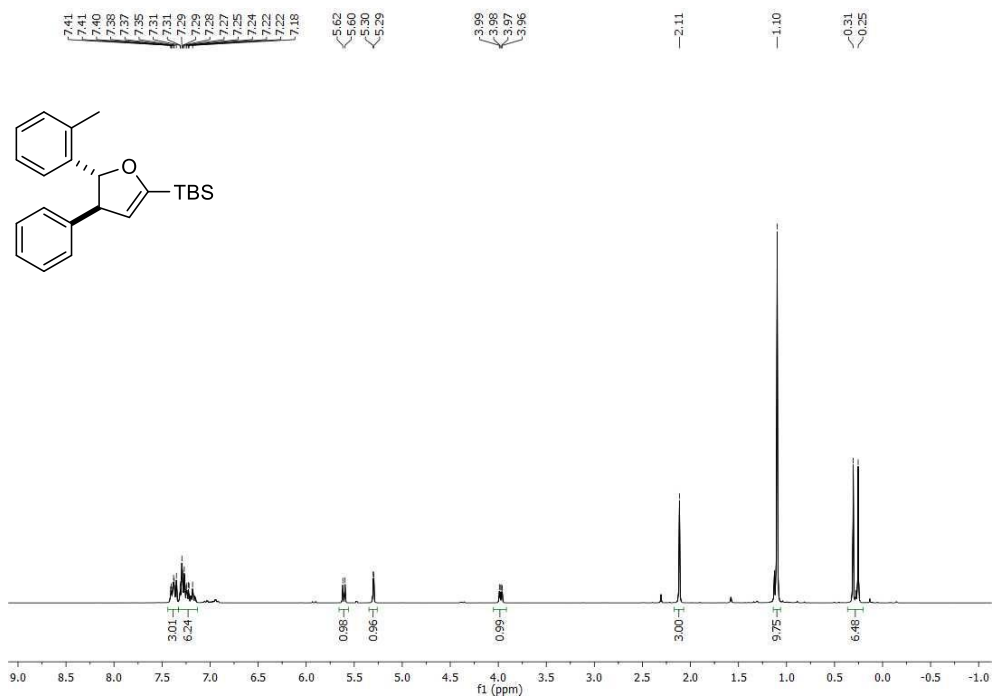


Trans-tert-butyl(5-(3,5-dimethylphenyl)-4-phenyl-4,5-dihydrofuran-2-yl)dimethylsilane (trans-3.4n).

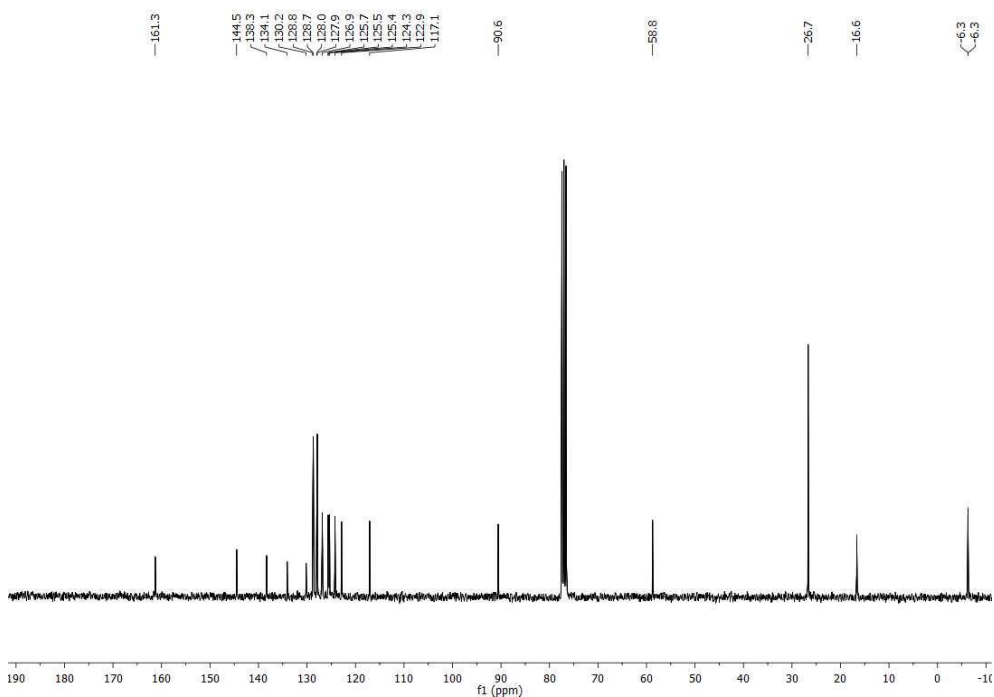
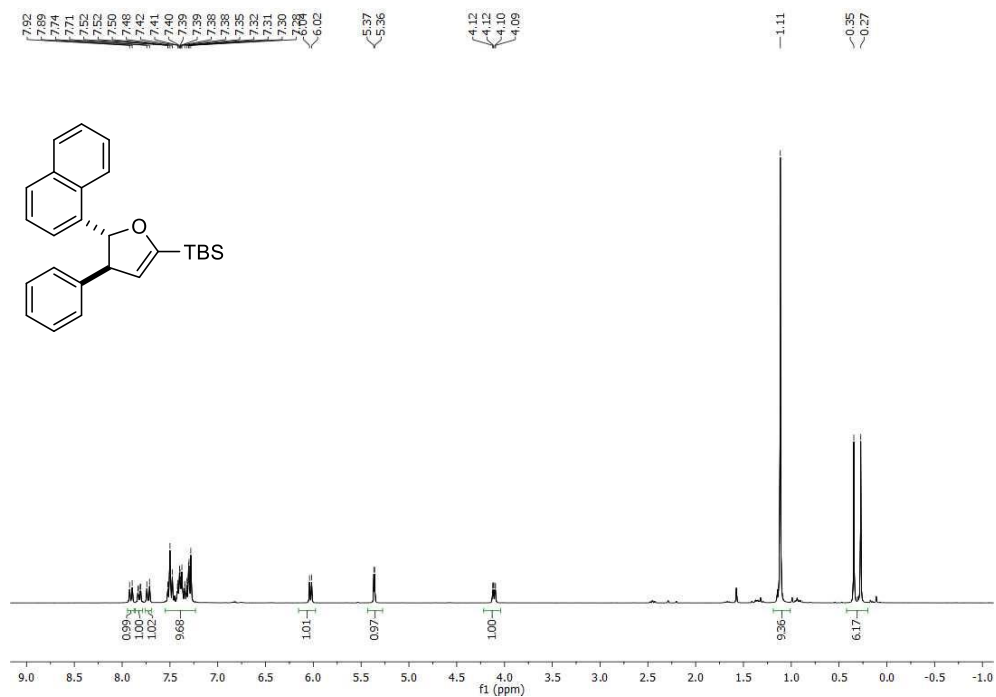


Trans-tert-butyl(5-(3,5-dibromophenyl)-4-phenyl-4,5-dihydrofuran-2-yl)dimethylsilane (trans-3.4p).

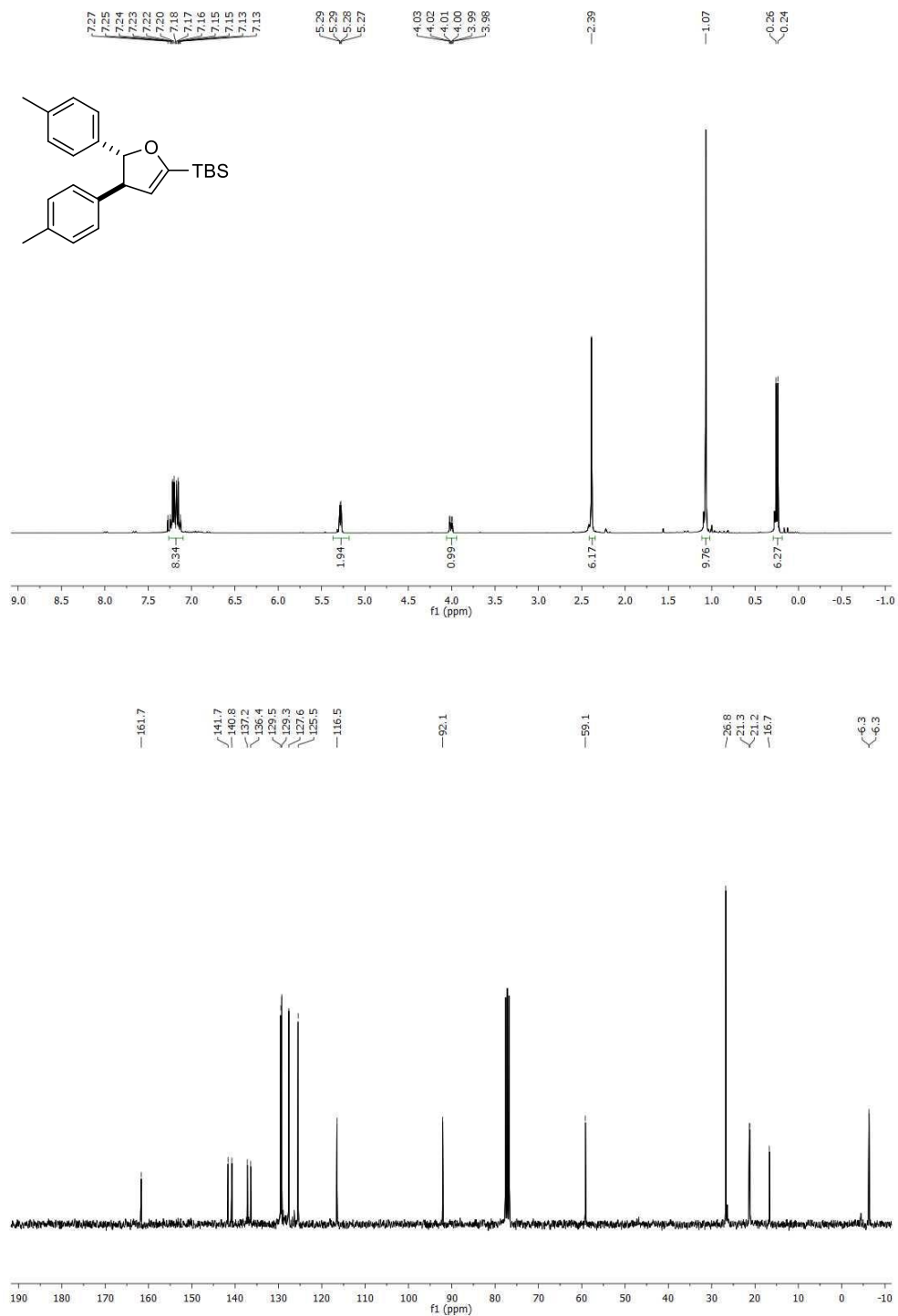
Trans-tert-butyltrimethylsilyloxydimethyl(4-phenyl-5-(*o*-tolyl)-4,5-dihydrofuran-2-yl)silane (*trans*-3.4q).

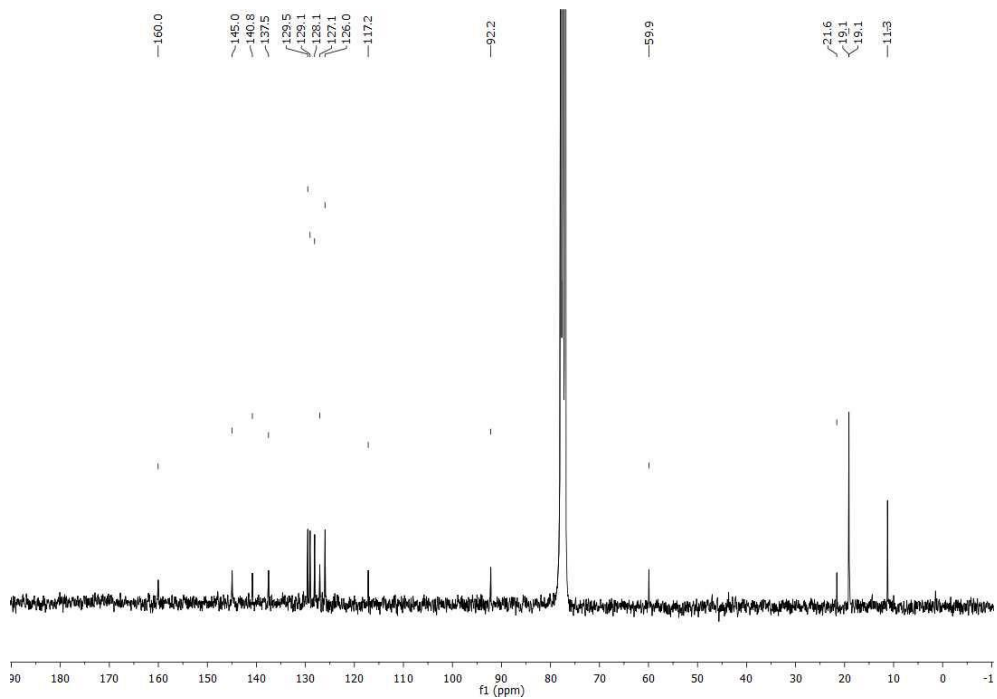
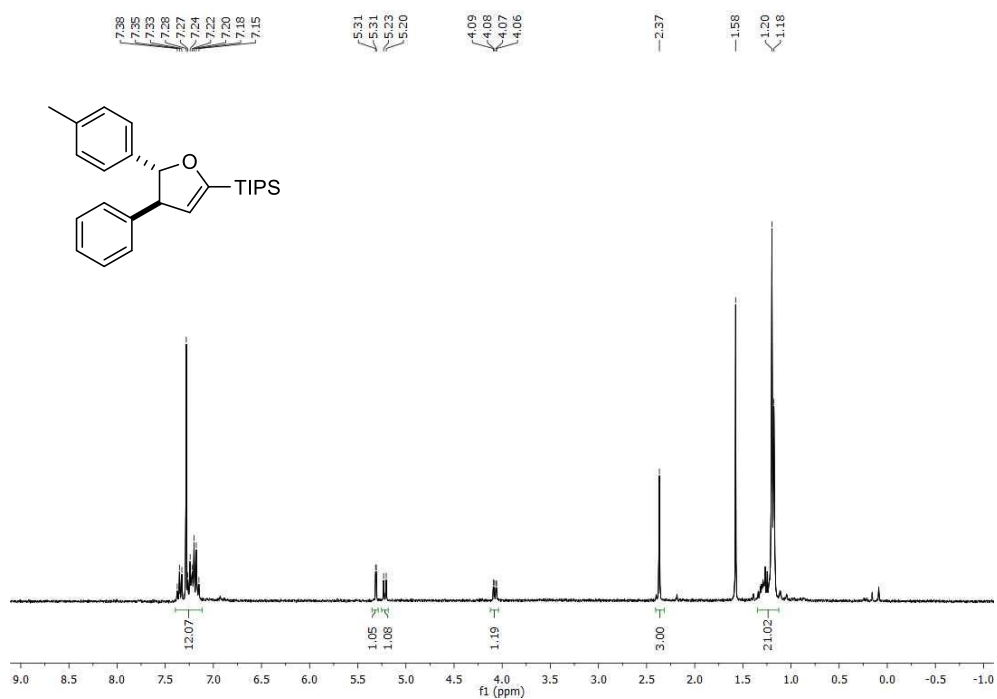


***Trans*-tert-butyltrimethylsilyl(5-(naphthalen-1-yl)-4-phenyl-4,5-dihydrofuran-2-yl)silane (*trans*-3.4r).**

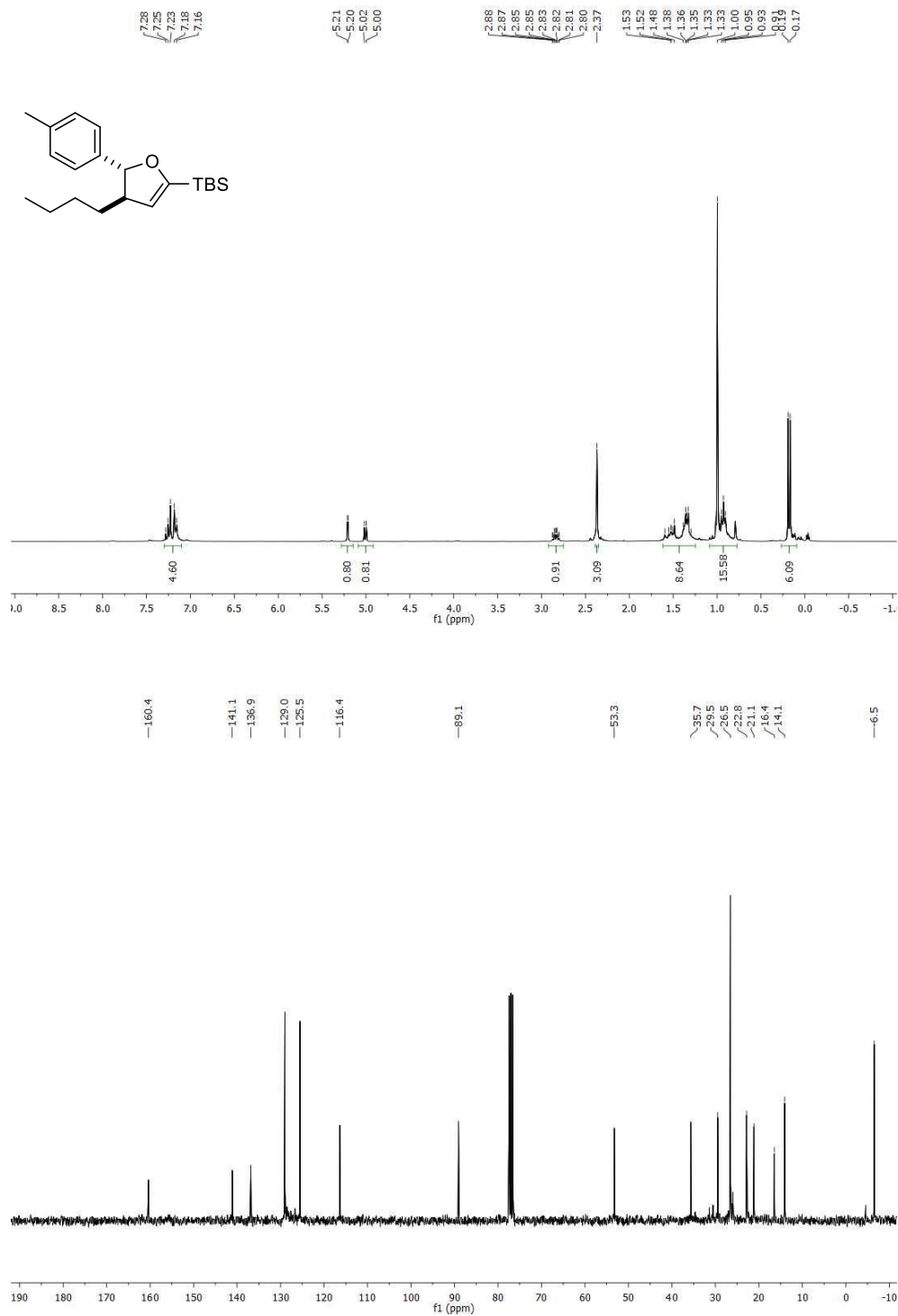


Trans-tert-butyl(-4,5-di-*p*-tolyl-4,5-dihydrofuran-2-yl)dimethylsilane (trans-3.4s).

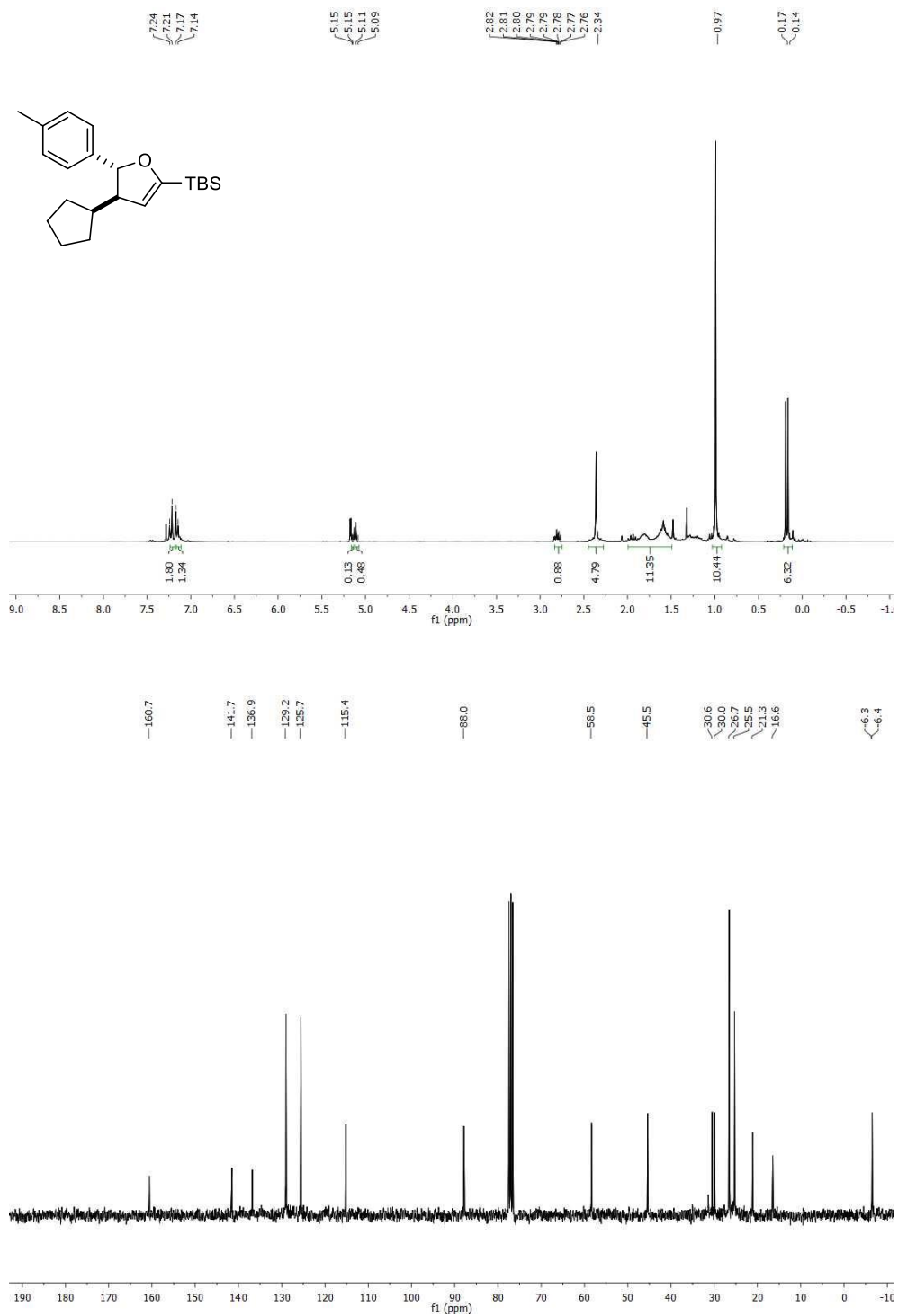


Trans-triisopropyl(4-phenyl-5-(*p*-tolyl)-4,5-dihydrofuran-2-yl)silane (*trans*-3.4t).

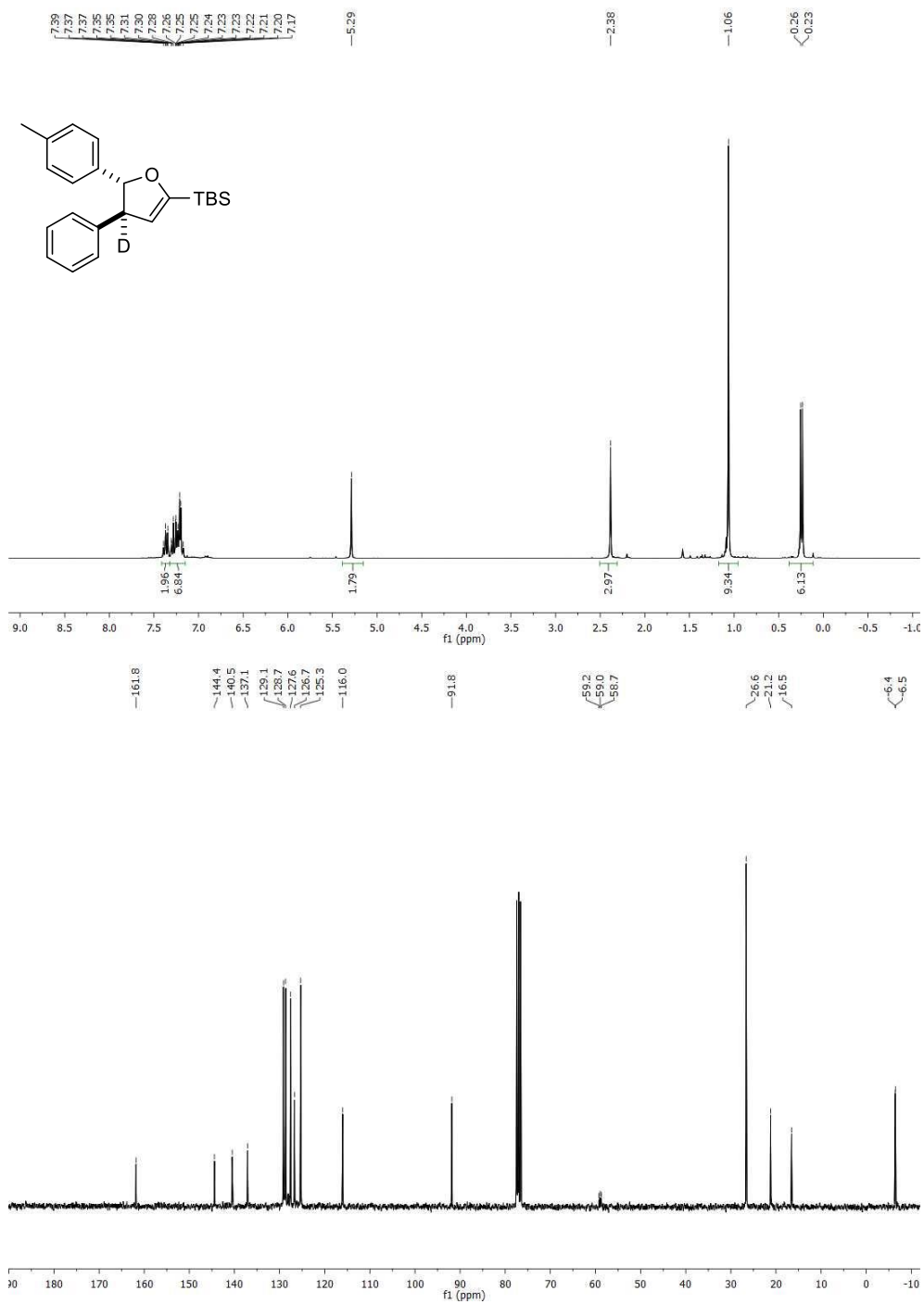
Trans-tert-butyl(4-butyl-5-(*p*-tolyl)-4,5-dihydrofuran-2-yl)dimethylsilane (*trans*-3.4u).

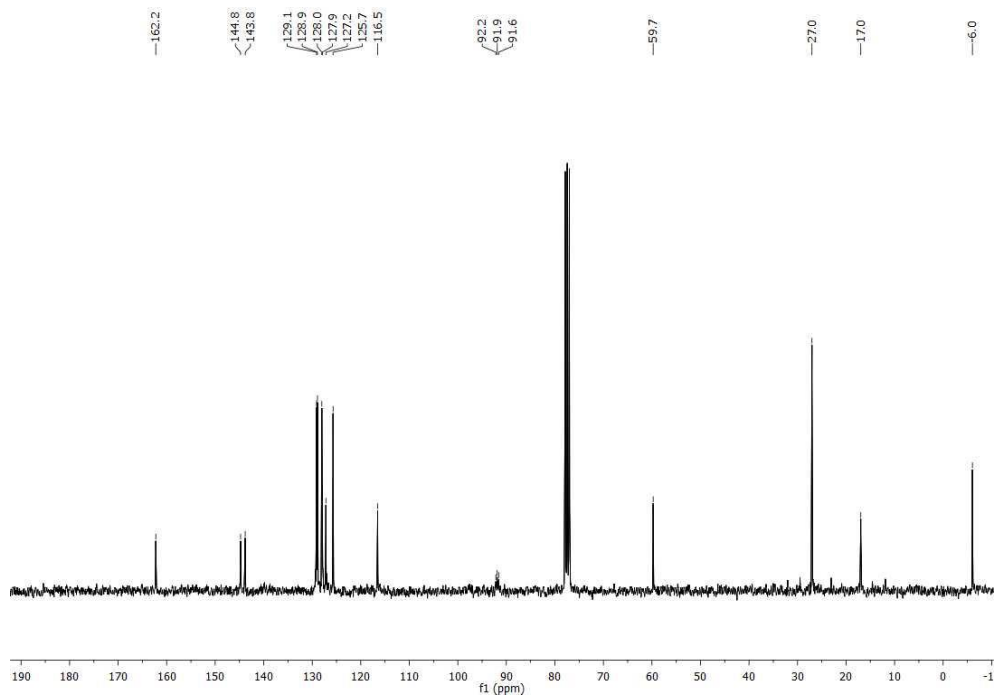
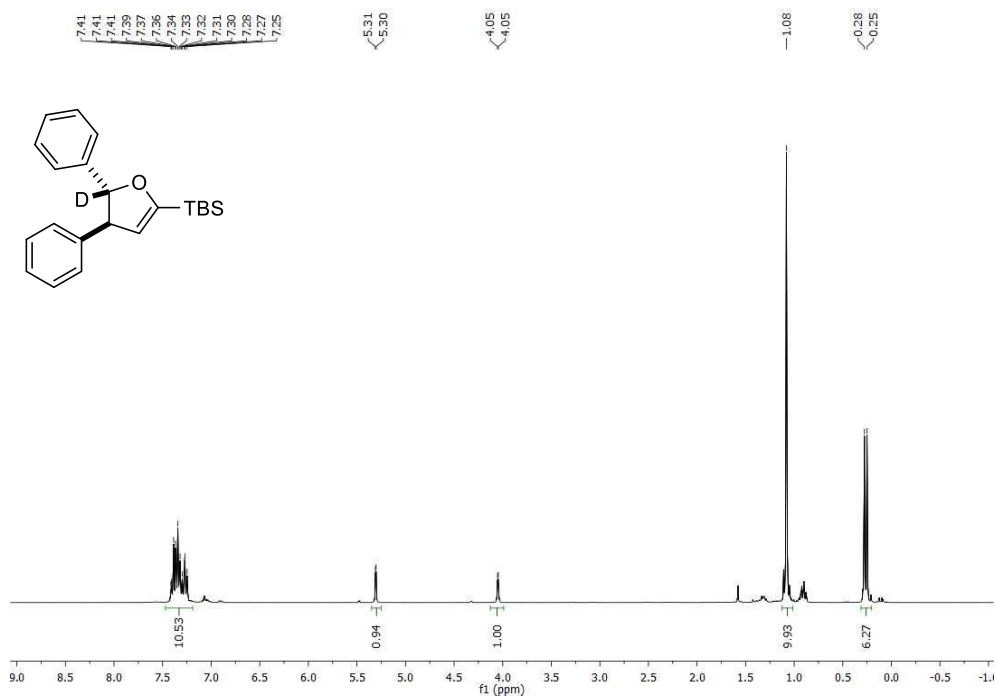


**Trans-tert-butyl(4-cyclopentyl-5-(p-tolyl)-4,5-dihydrofuran-2-yl)dimethylsilane
(trans-3.4v).**

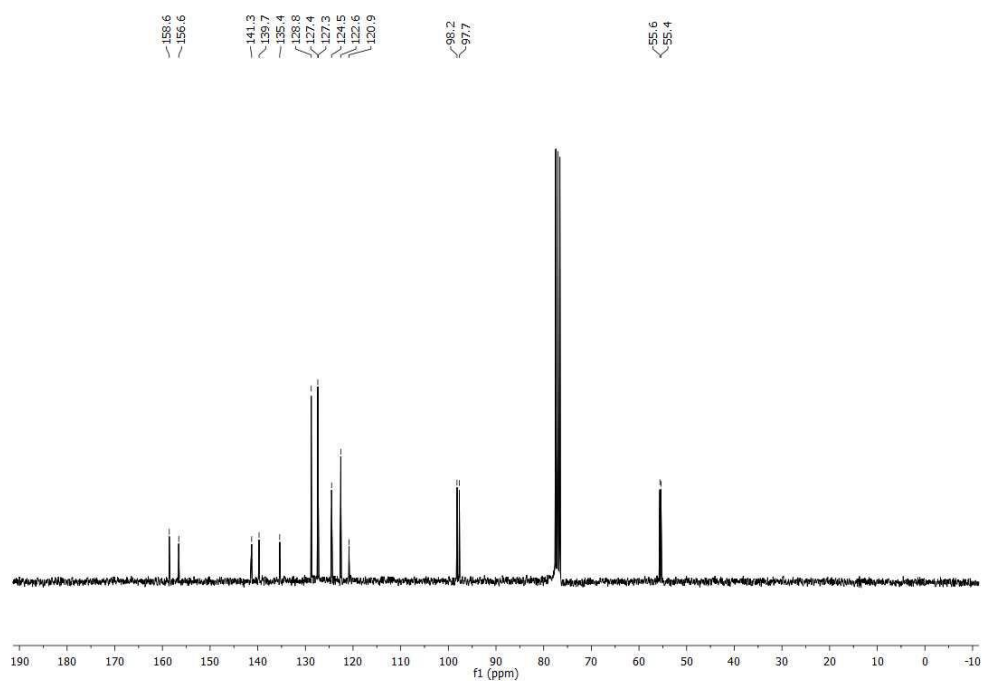
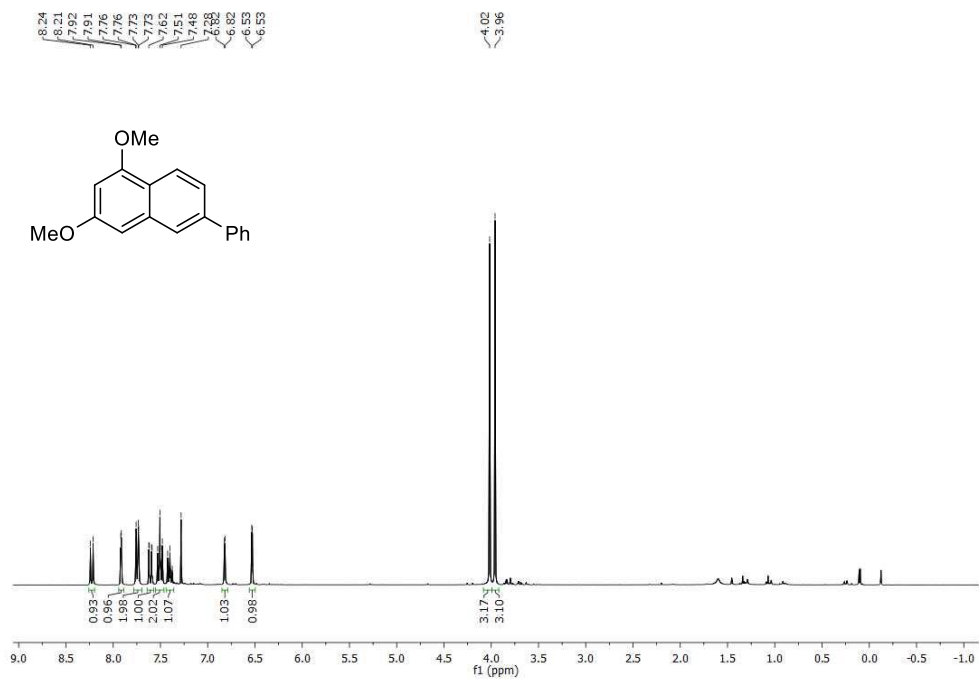


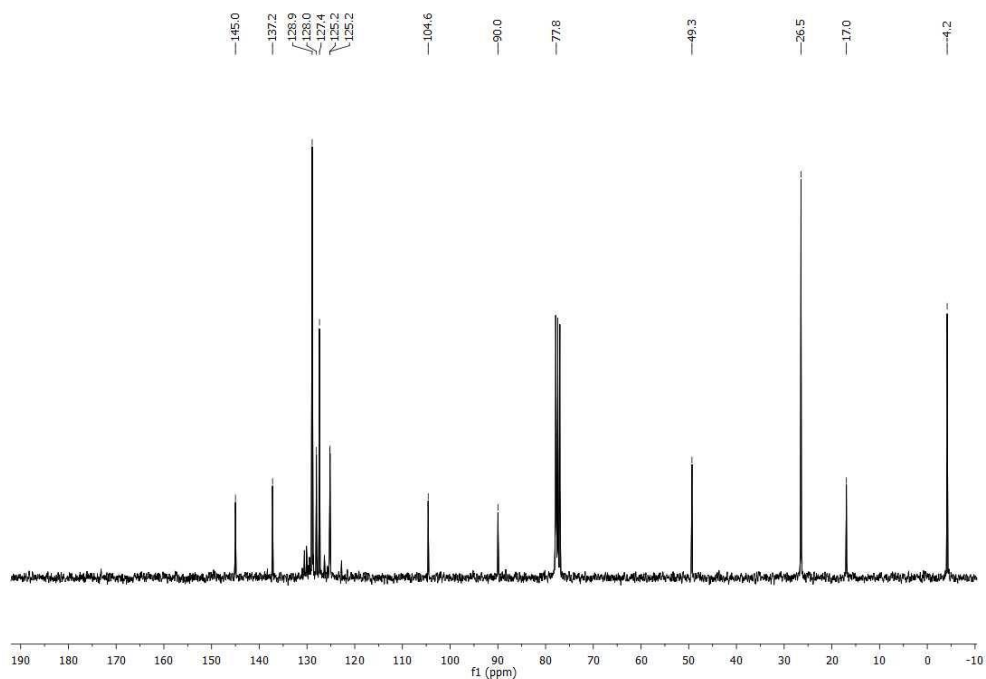
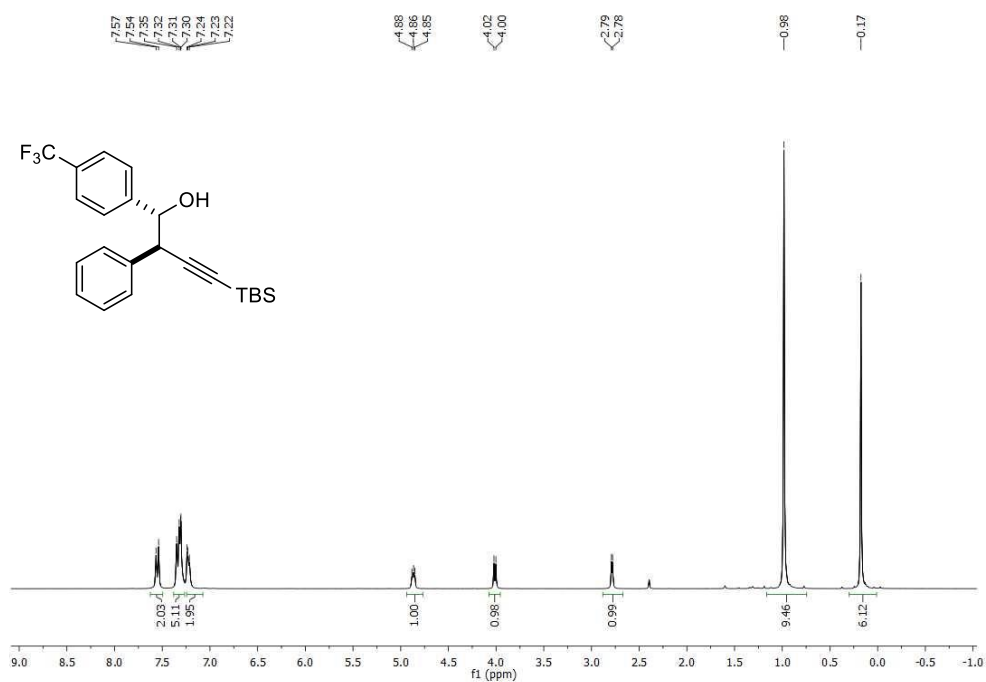
(E)-tert-butyl dimethyl(4-deutero-4-phenyl-5-(p-tolyl)-4,5-dihydrofuran-2-yl)silane (4D-trans-3.4a)



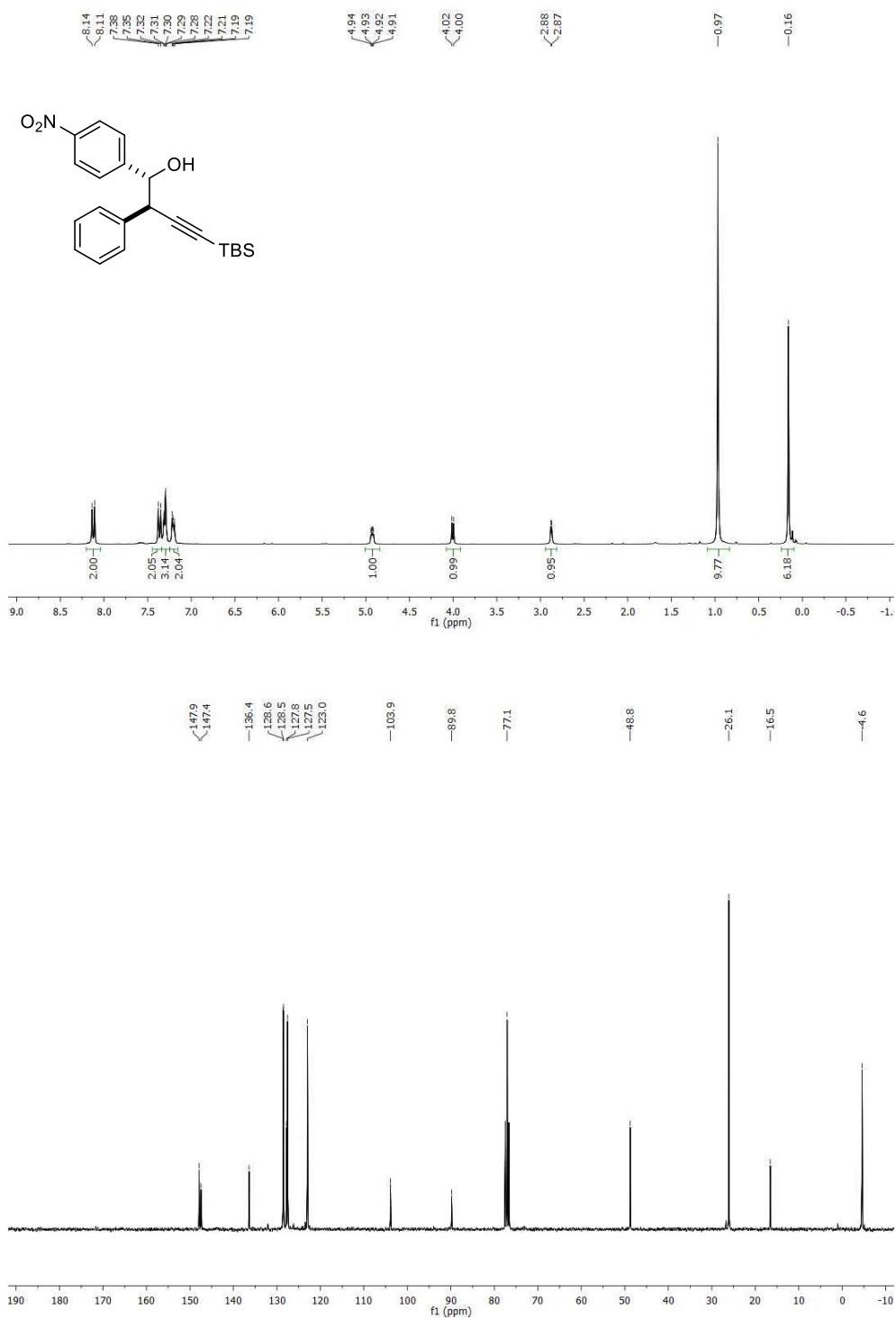
(E)-tert-butyl dimethyl(5-deutero-4,5-diphenyl-4,5-dihydrofuran-2-yl)silane (5D-trans-3.4b)

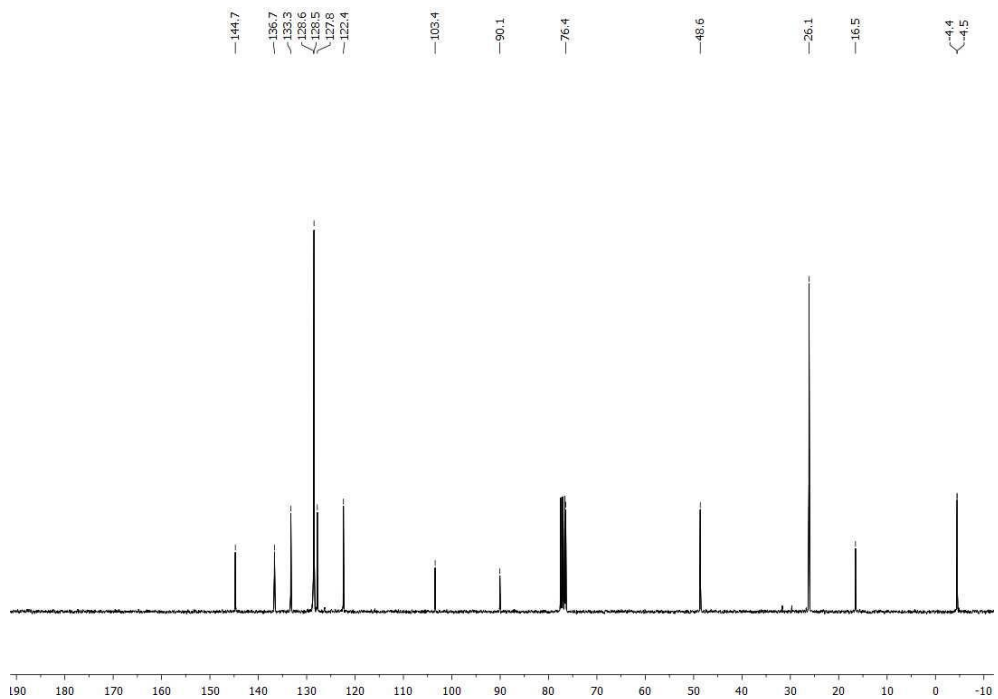
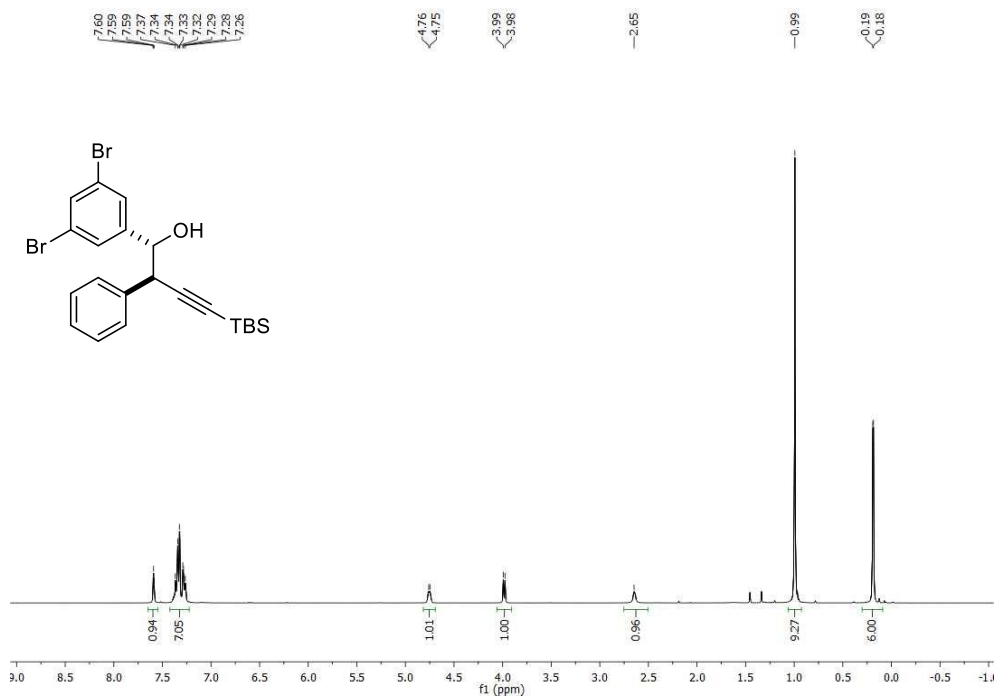
1,3-dimethoxy-6-phenylnaphthalene (3.5)



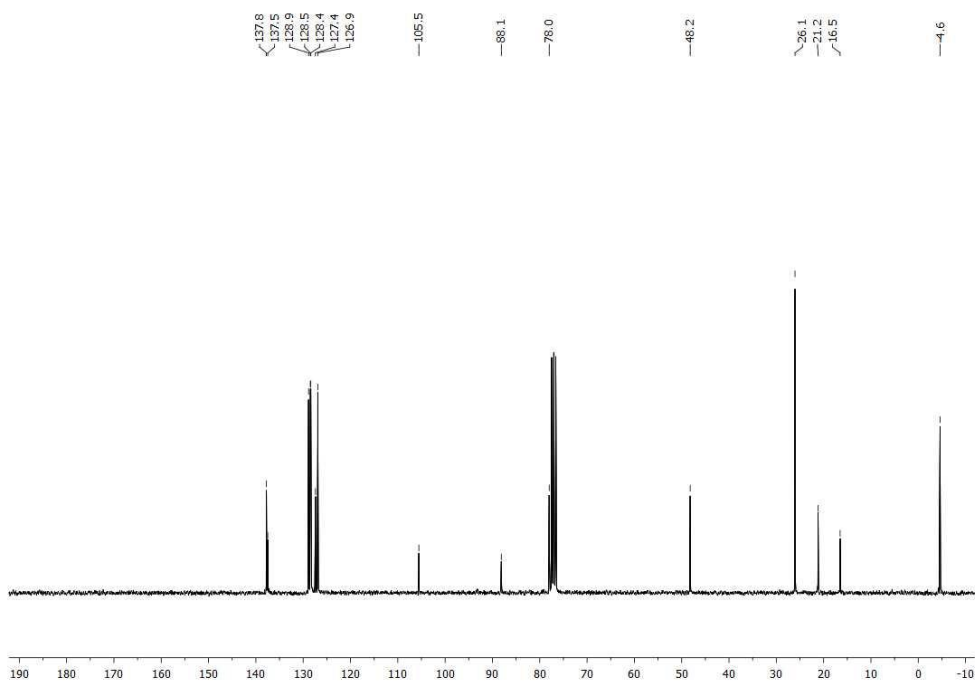
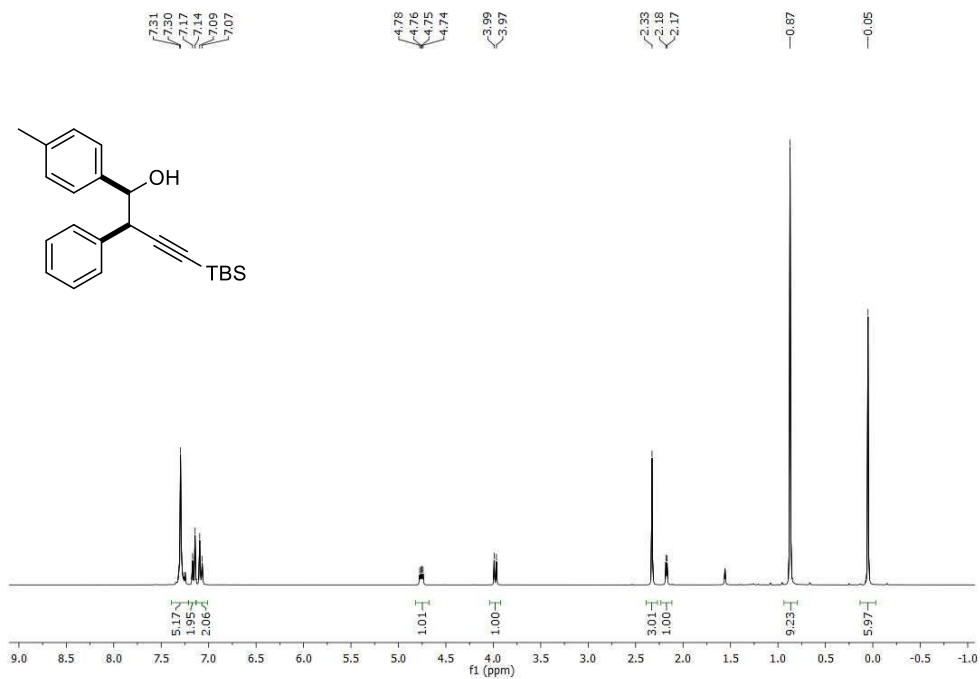
Anti-4-(tert-butyldimethylsilyl)-1-(4-trifluoromethylphenyl)-2-phenylbut-3-yn-1-ol
(anti-3.3i)

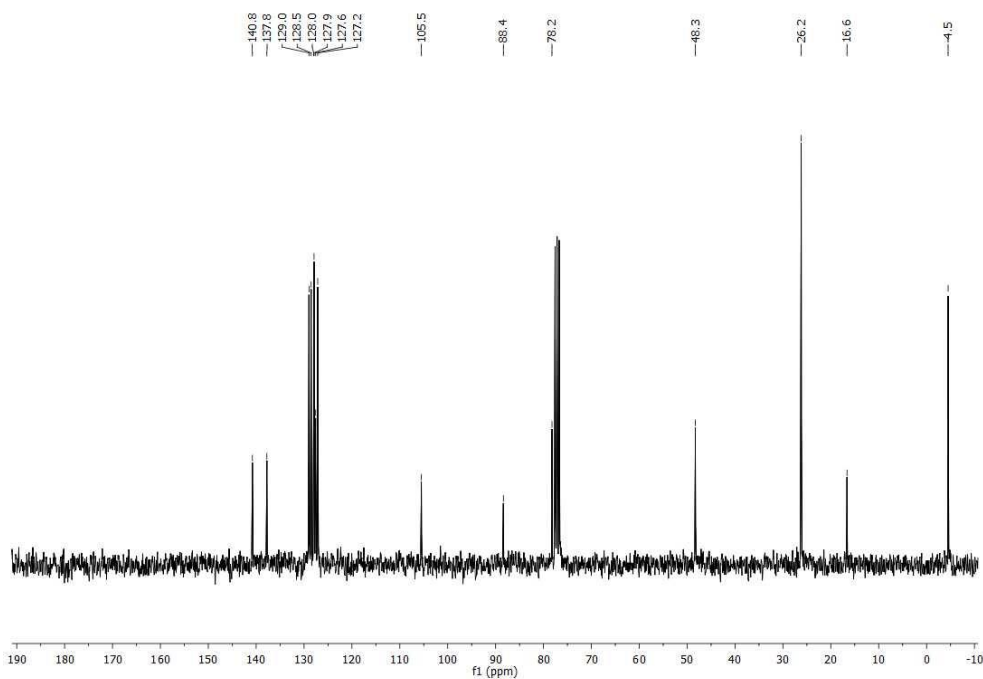
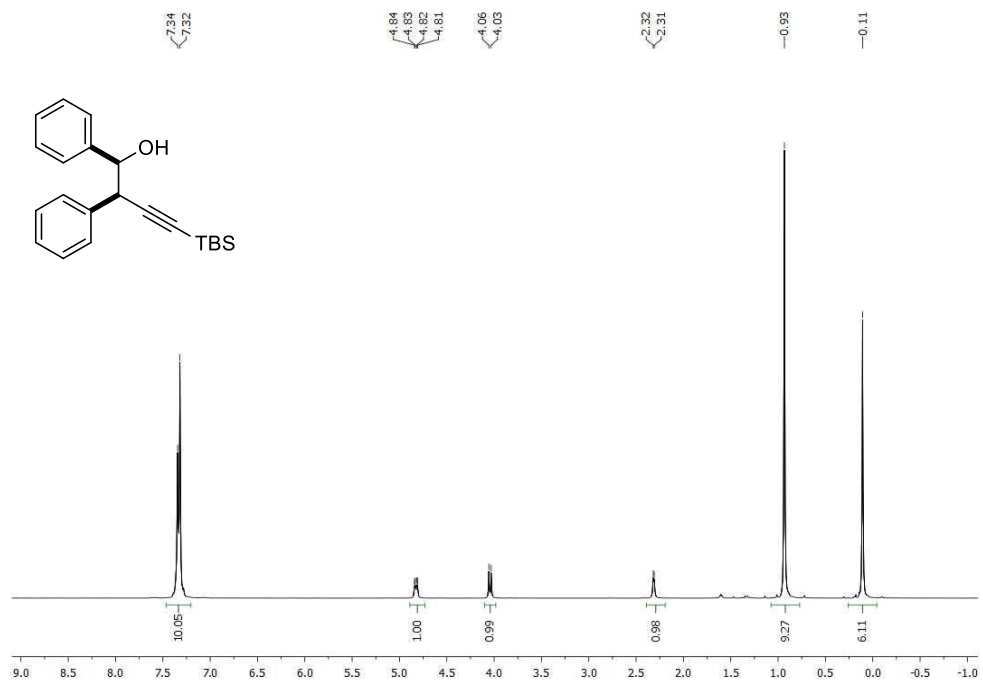
Anti-4-(tert-butyldimethylsilyl)-1-(4-nitrophenyl)-2-phenylbut-3-yn-1-ol (*anti*-3.3j)



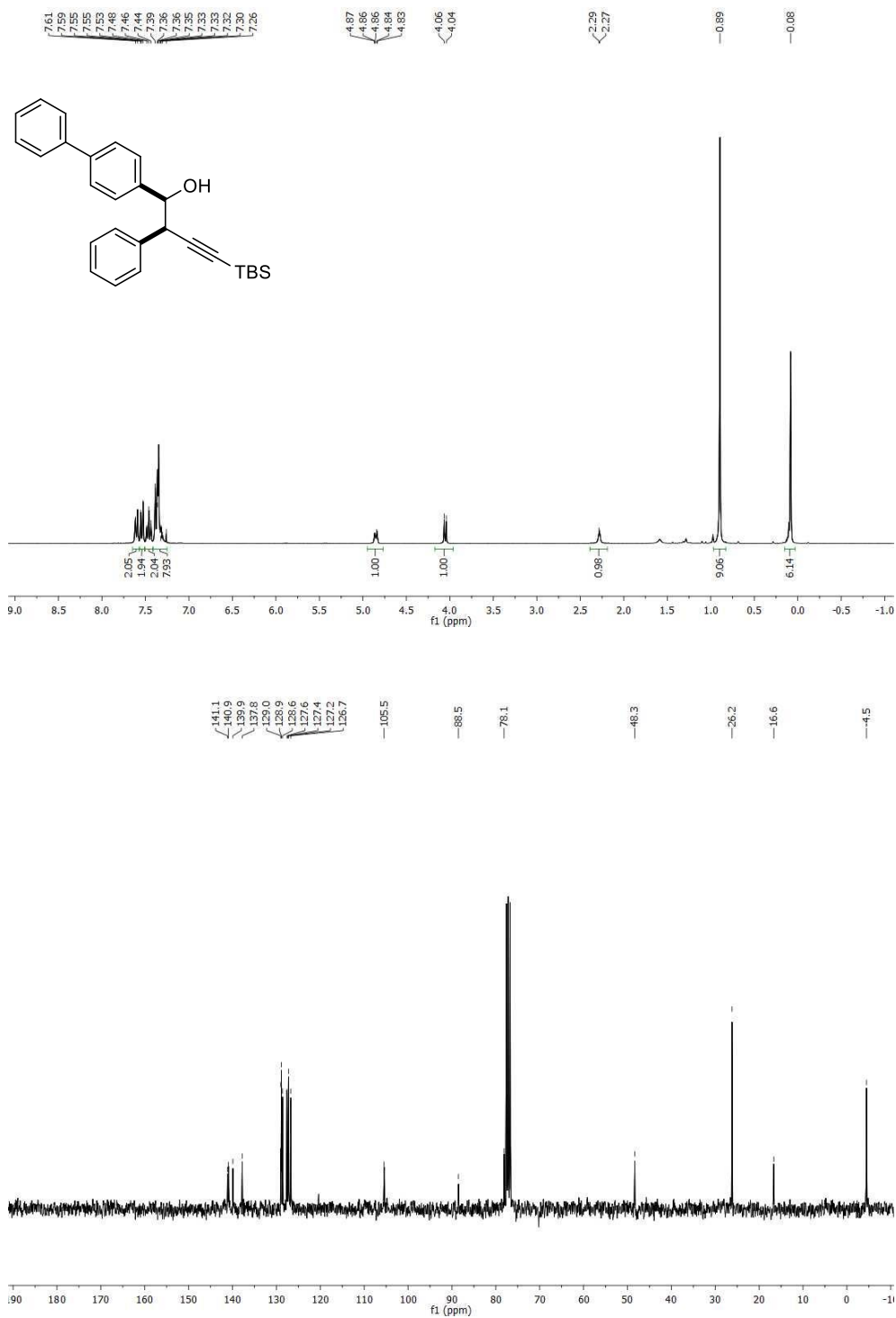
Anti-4-(tert-butyldimethylsilyl)-1-(3,5-dibromophenyl)-2-phenylbut-3-yn-1-ol
(anti-3.3p)

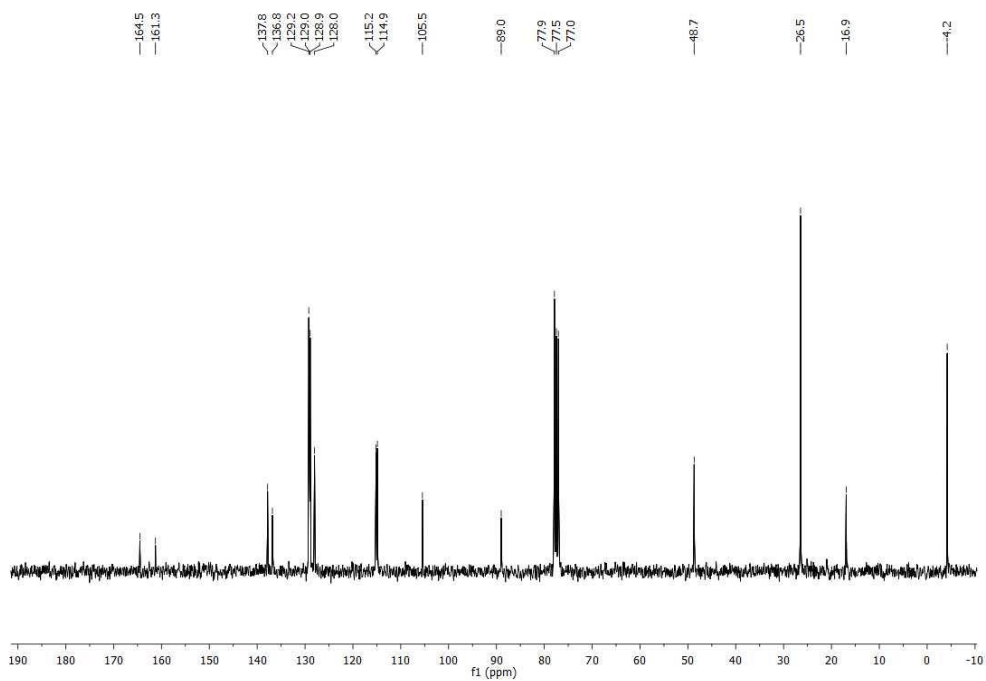
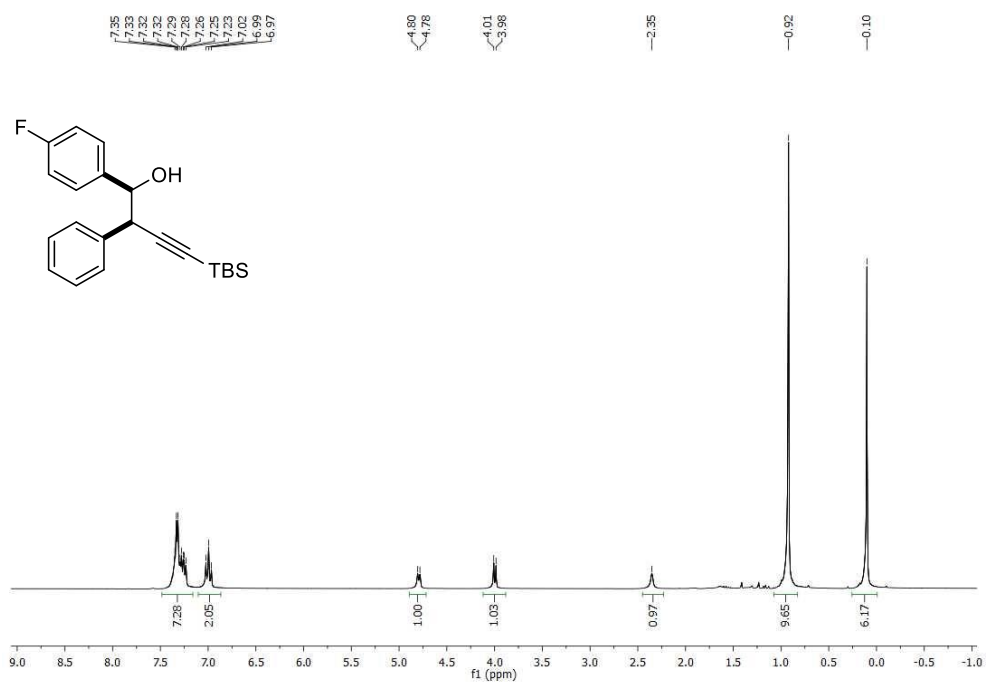
Syn-4-(*tert*-butyldimethylsilyl)-2-phenyl-1-(*p*-tolyl)but-3-yn-1-ol (syn-3.3a)



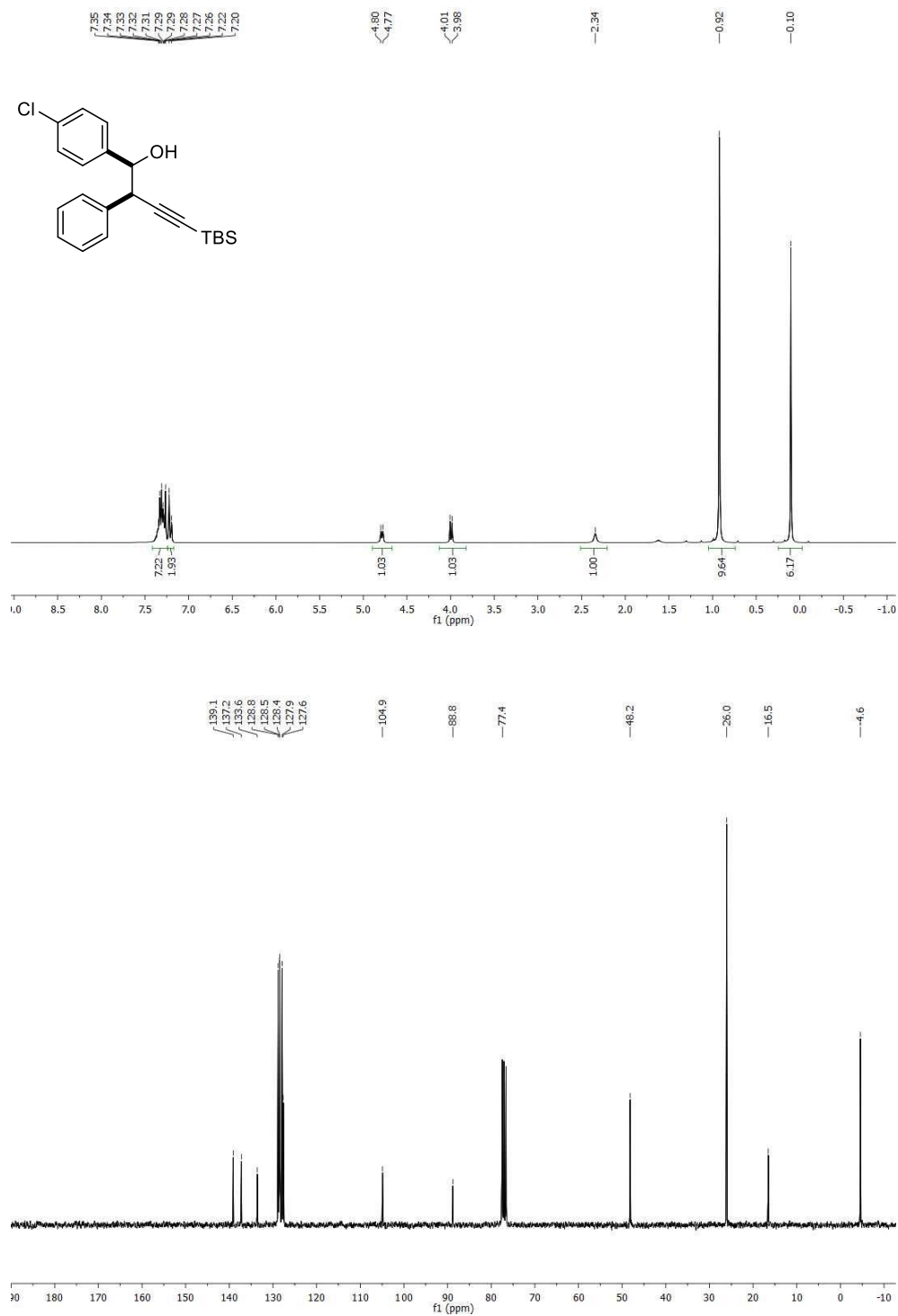
Syn-4-(tert-butyltrimethylsilyl)-1,2-diphenylbut-3-yn-1-ol (syn-3.3b)

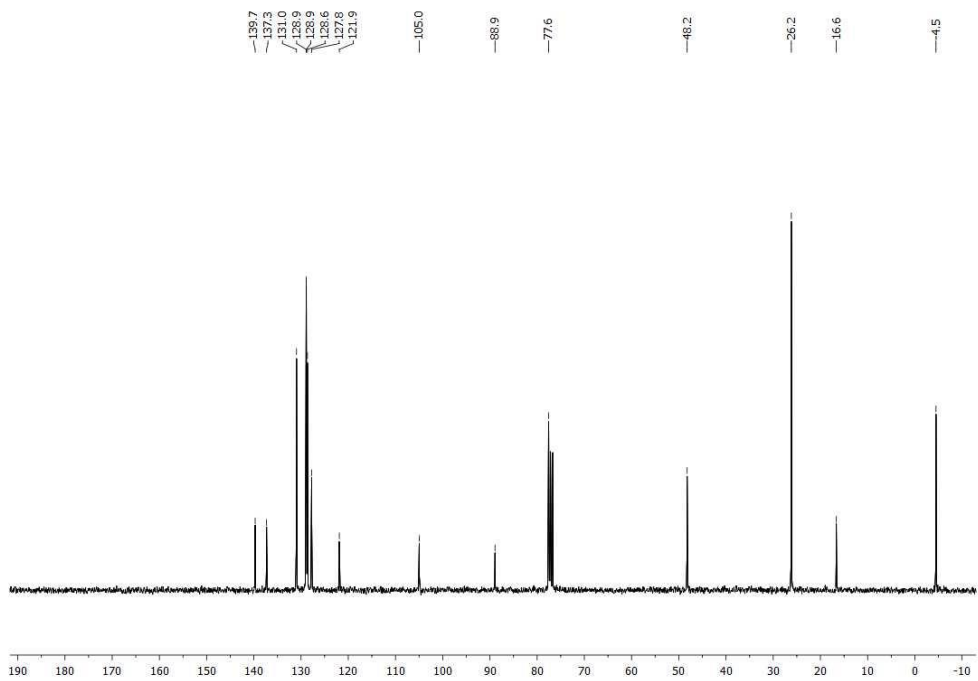
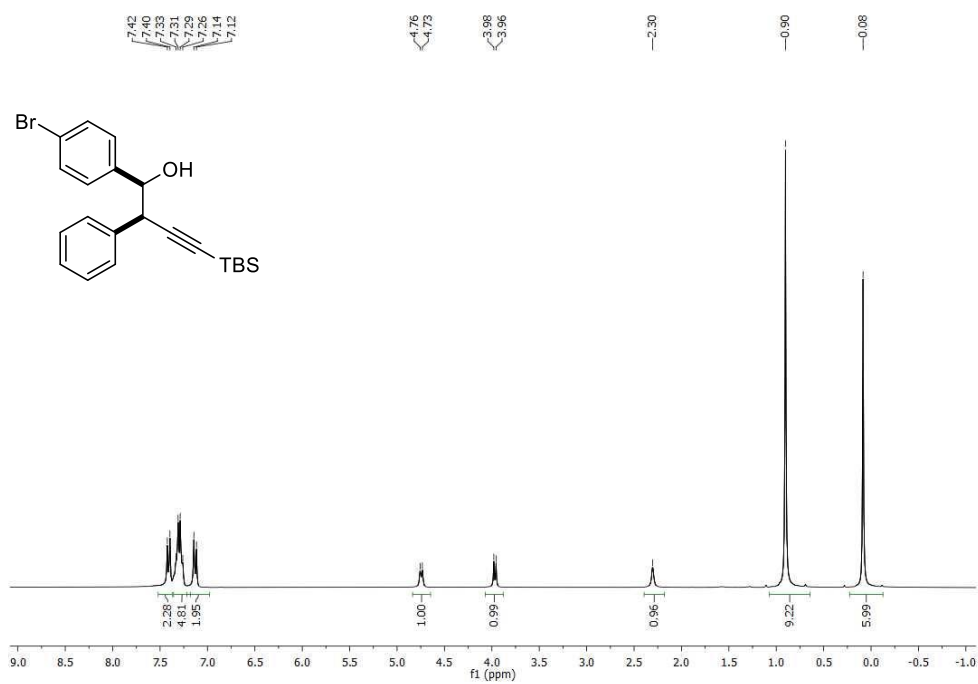
Syn-1-([1,1'-biphenyl]-4-yl)-4-(tert-butyldimethylsilyl)-2-phenylbut-3-yn-1-ol (syn-3.3c)



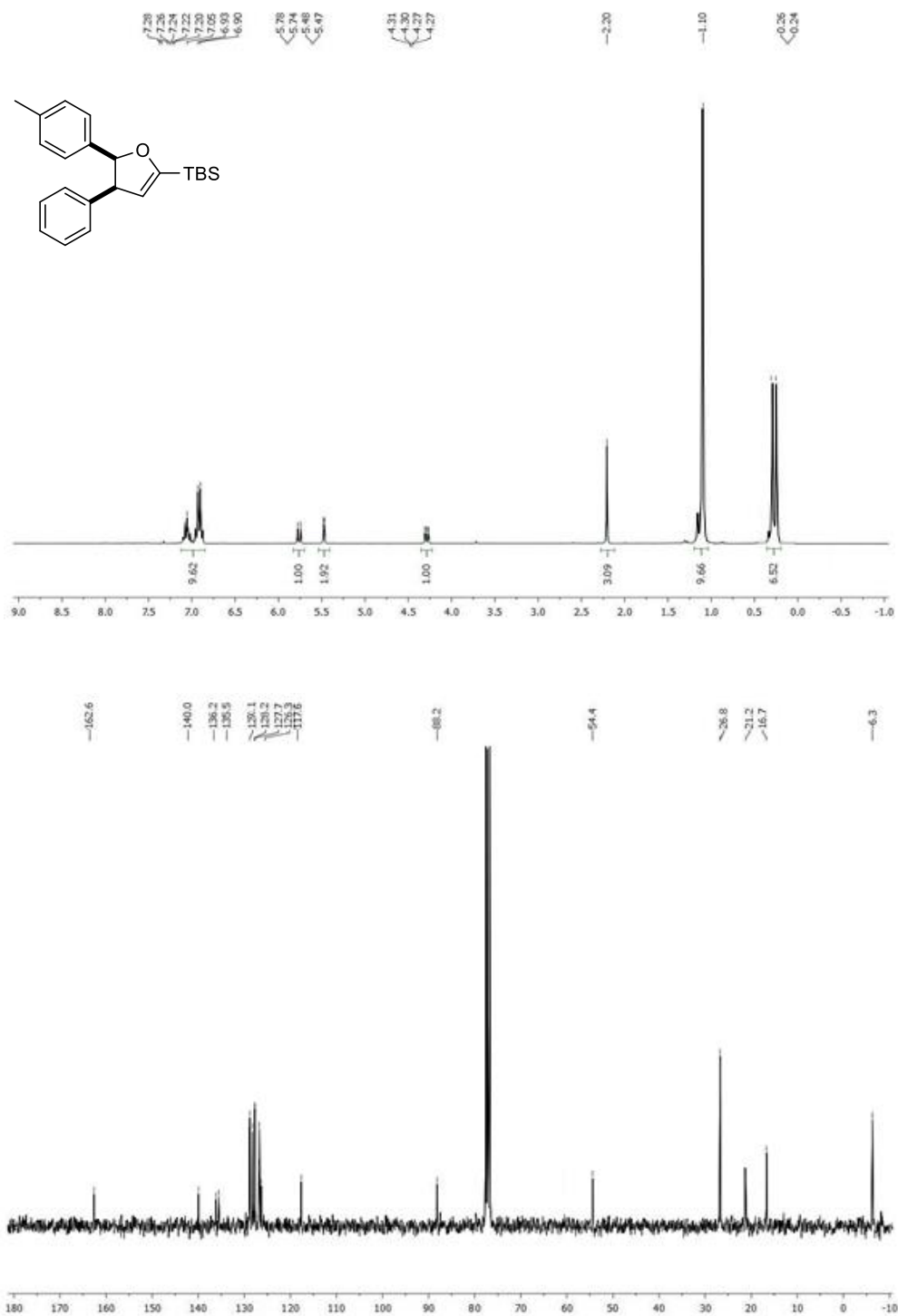
Syn-4-(tert-butyltrimethylsilyl)-1-(4-fluorophenyl)-2-phenylbut-3-yn-1-ol (syn-3.3e)

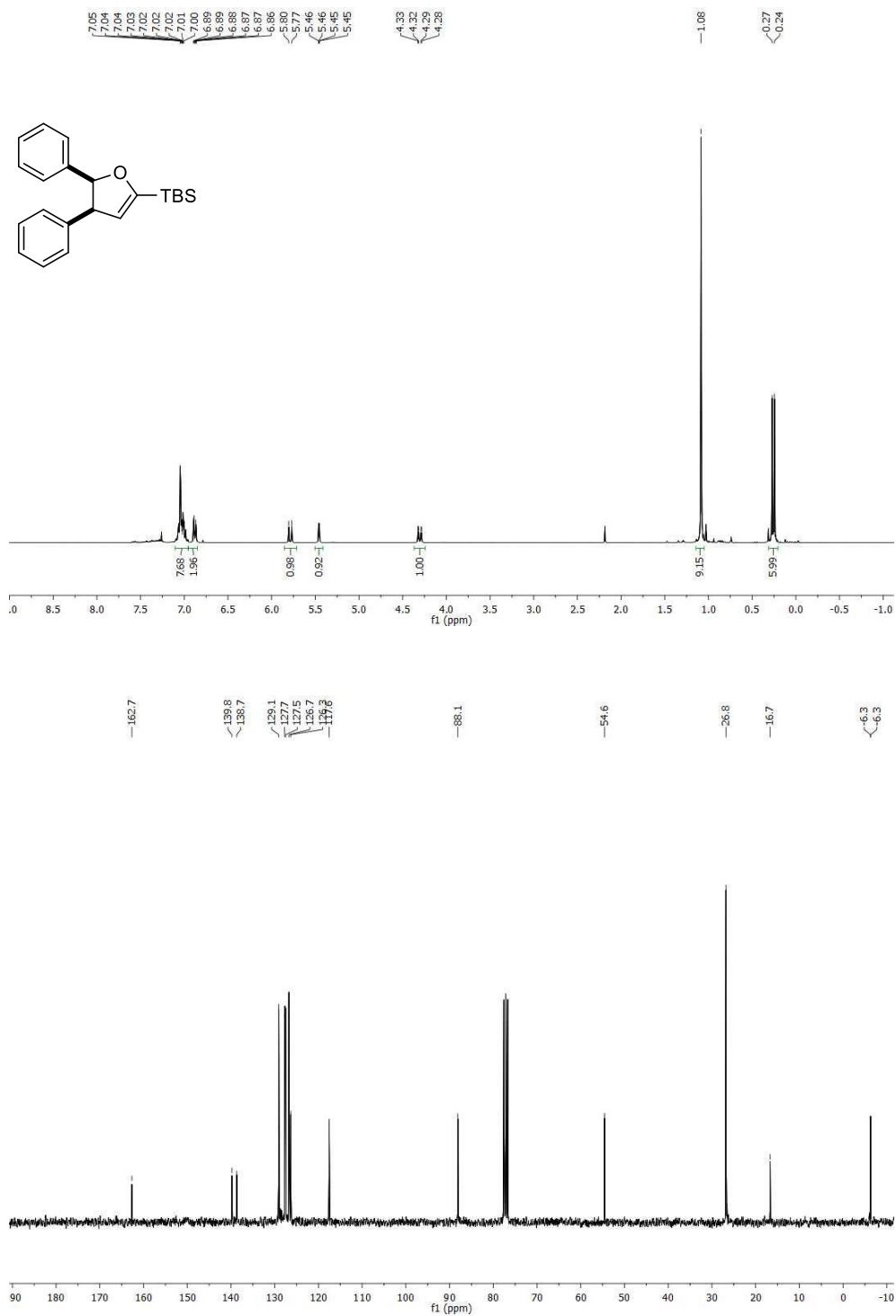
Syn-4-(*tert*-butyldimethylsilyl)-1-(4-chlorophenyl)-2-phenylbut-3-yn-1-ol (syn-3.3f)



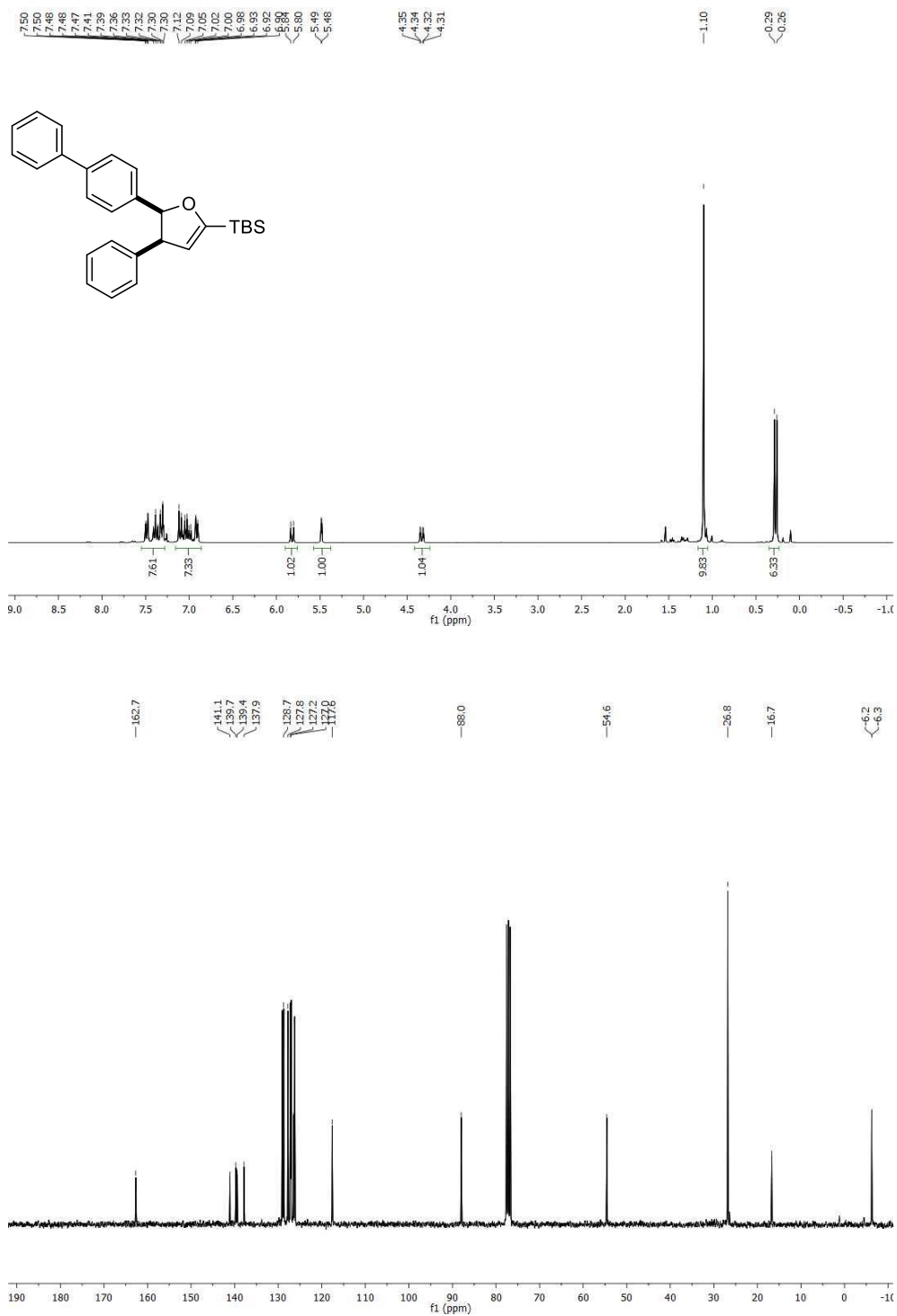
Syn-1-(4-Bromophenyl)-4-(tert-butyldimethylsilyl)-2-phenylbut-3-yn-1-ol (syn-3.3g)

***Cis-tert*-butyldimethyl(4-phenyl-5-(*p*-tolyl)-4,5-dihydrofuran-2-yl)silane (*cis*-3.4a)**

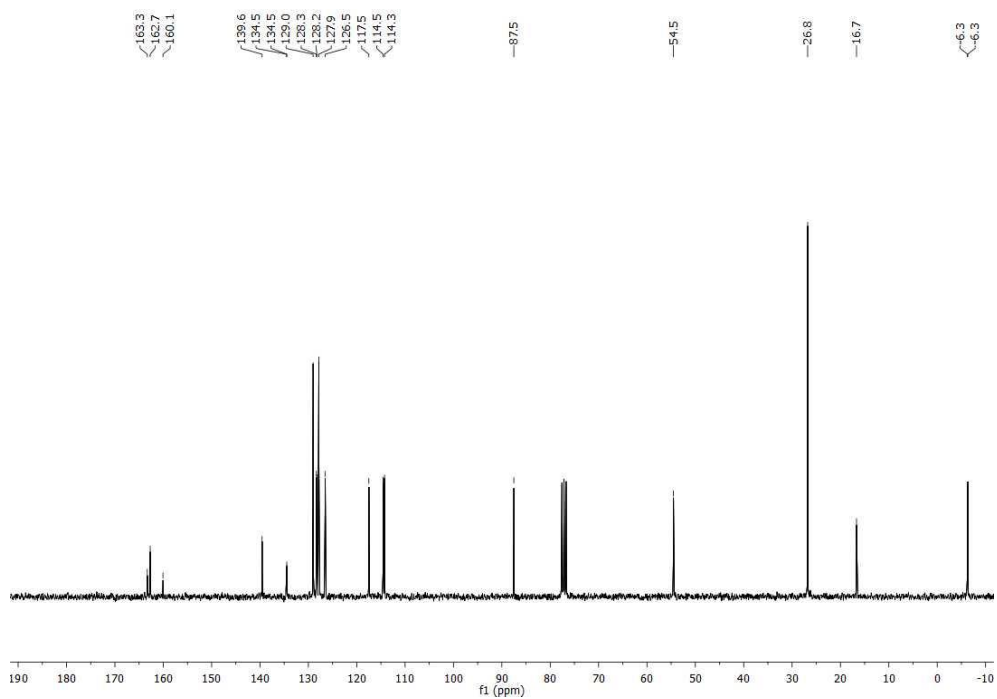
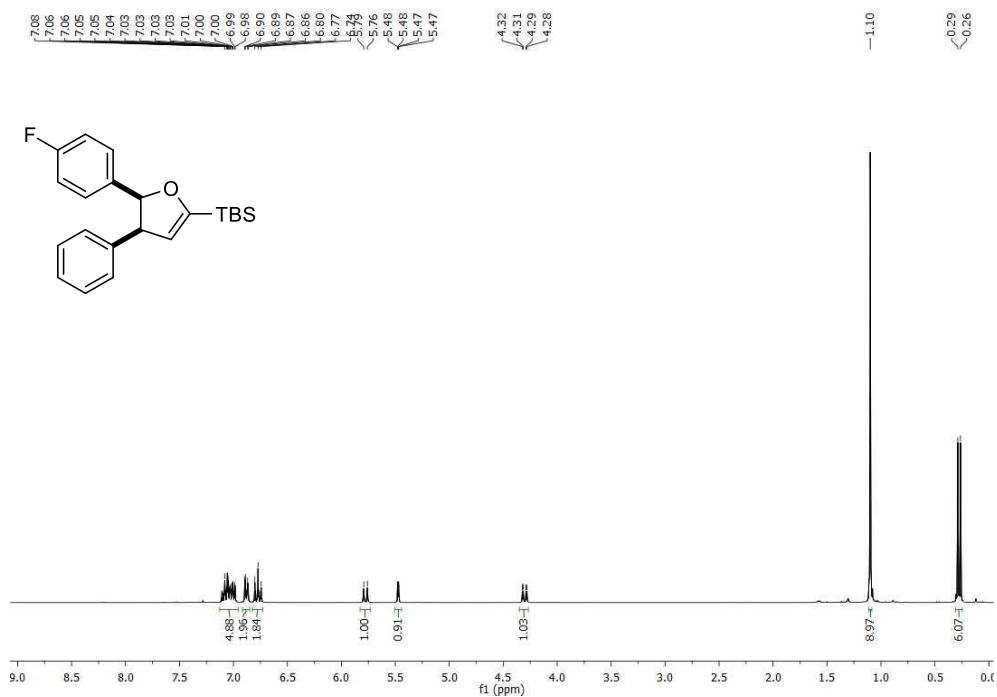


Cis-tert-butyl dimethyl-4,5-diphenyl-4,5-dihydrofuran-2-yl)dimethylsilane (cis-3.4b)

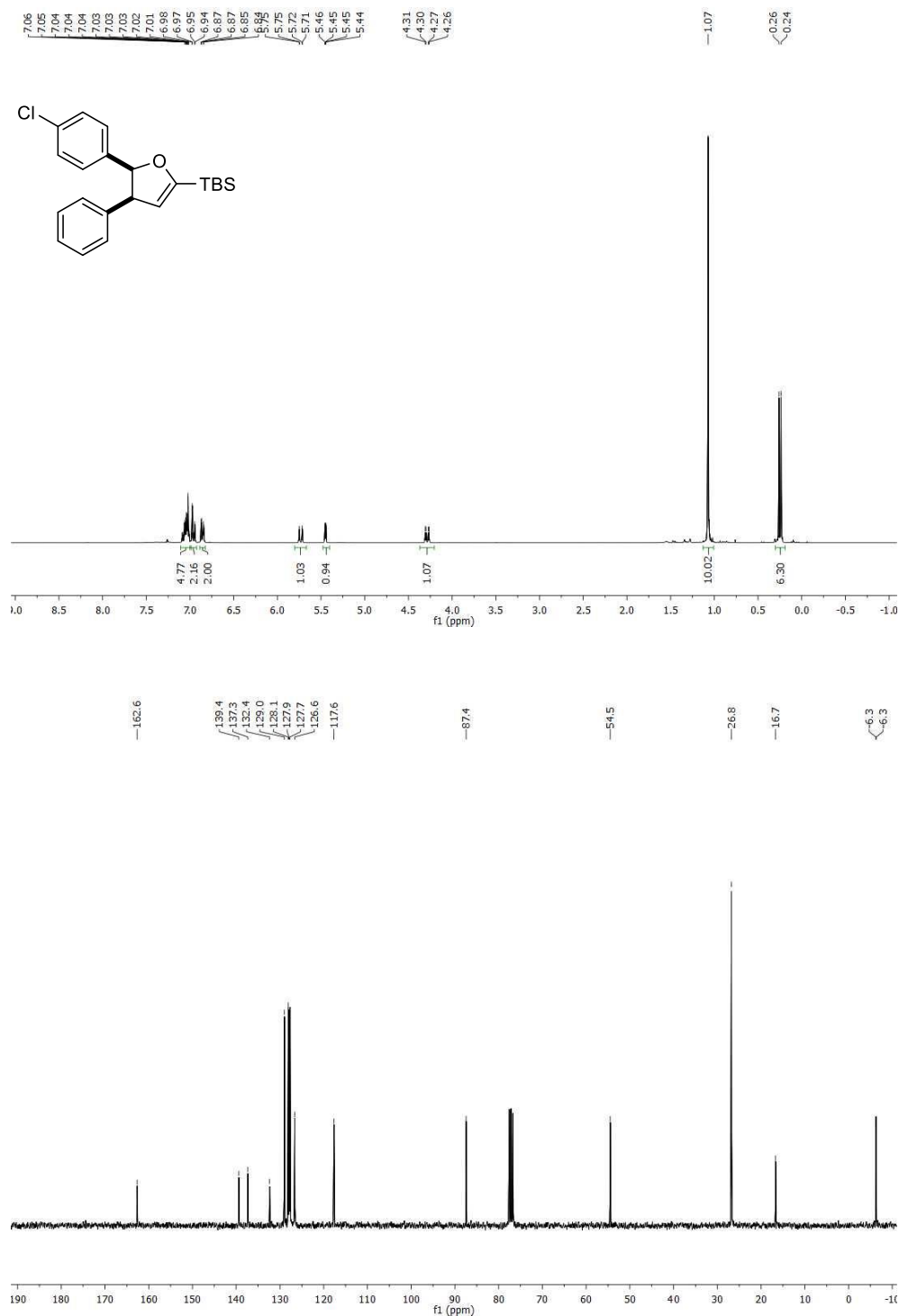
***Cis*-5-([1,1'-biphenyl]-4-yl)-4-phenyl-4,5-dihydrofuran-2-yl)(*tert*-butyl)dimethylsilane (*cis*-3.4c)**

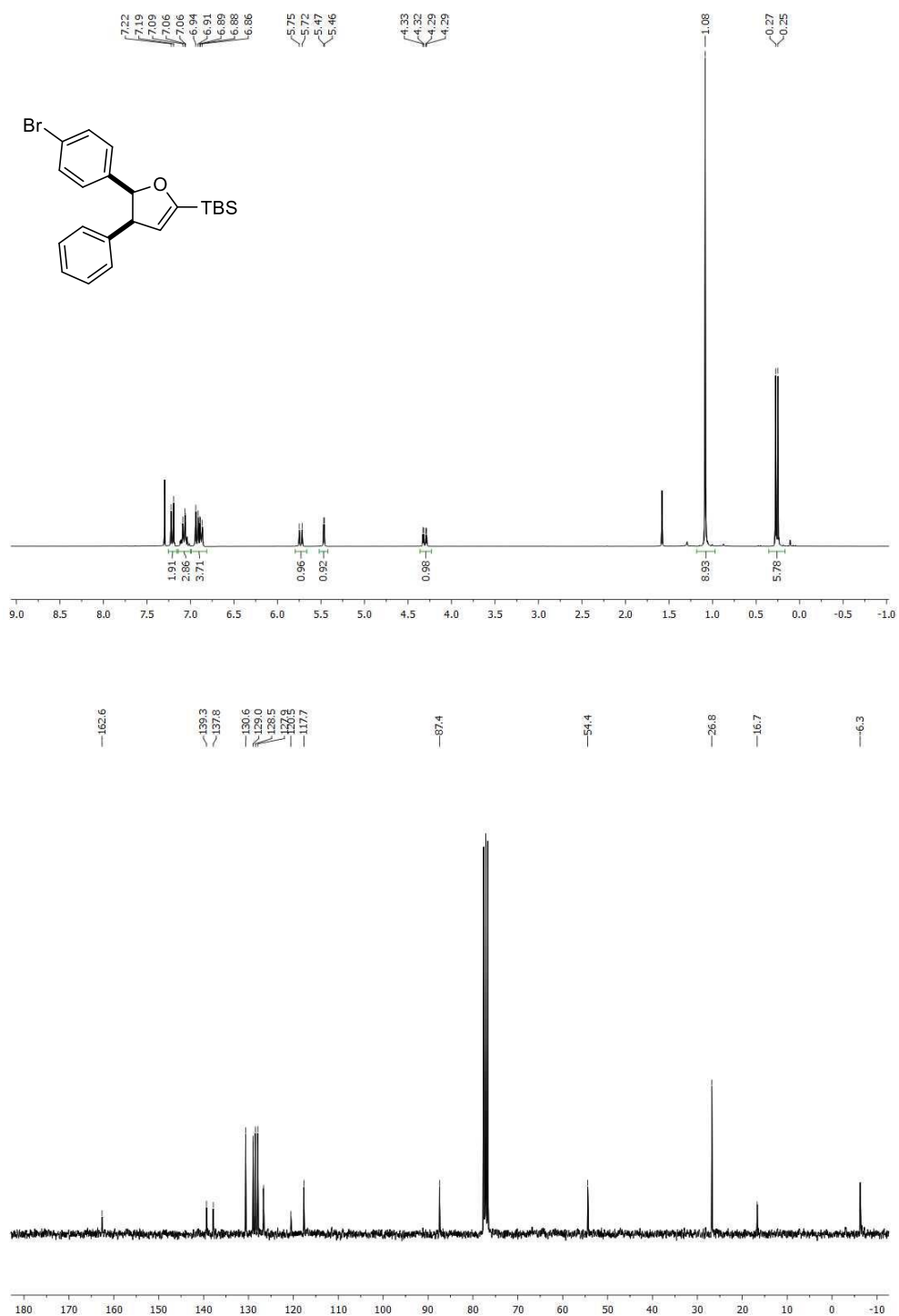


Cis-tert-butyl(5-(4-fluorophenyl)-4-phenyl-4,5-dihydrofuran-2-yl)dimethylsilane
(*cis*-3.4e)



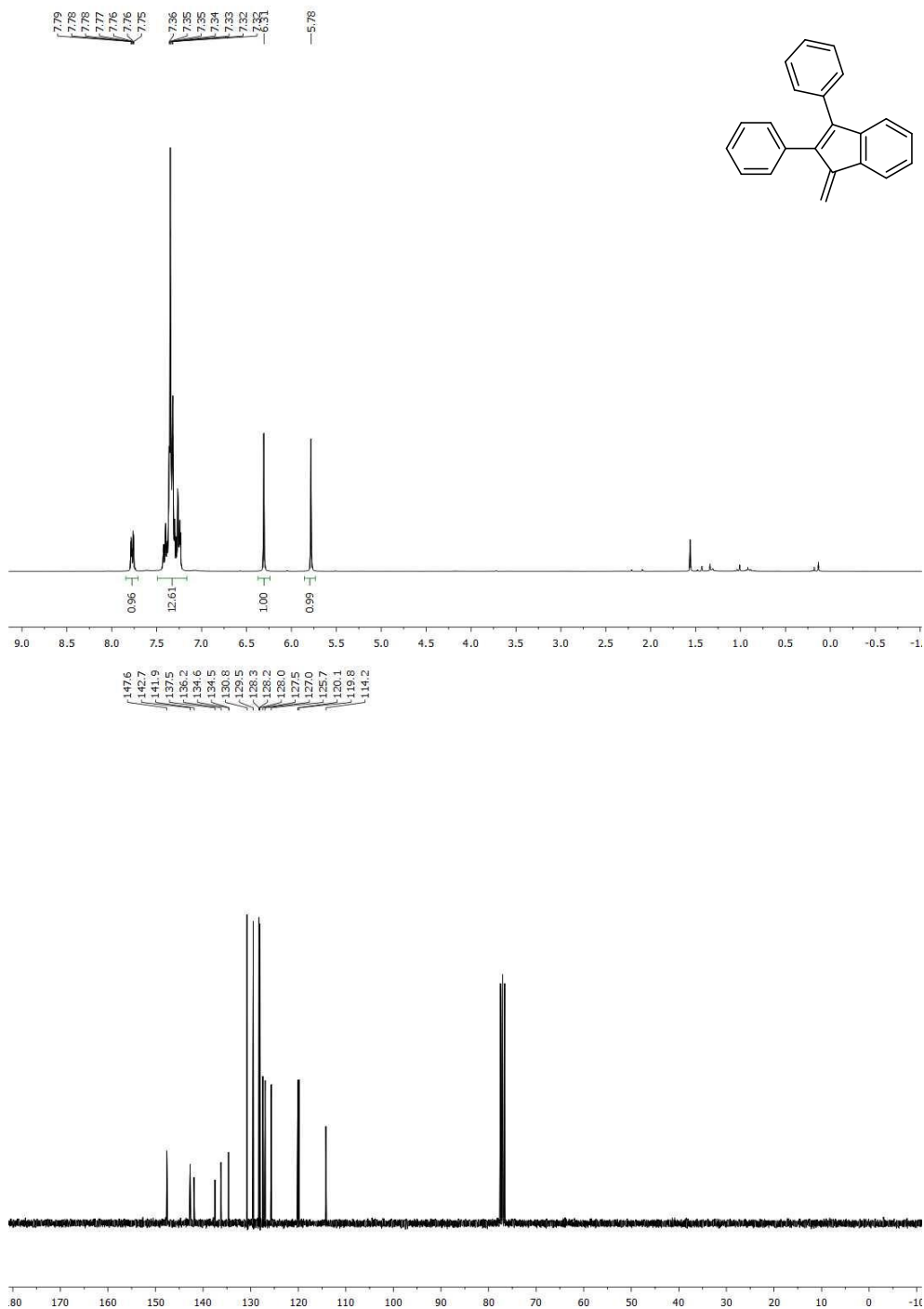
Cis-tert-butyl(5-(4-chlorophenyl)-4-phenyl-4,5-dihydrofuran-2-yl)dimethylsilane
(*cis*-3.4f)

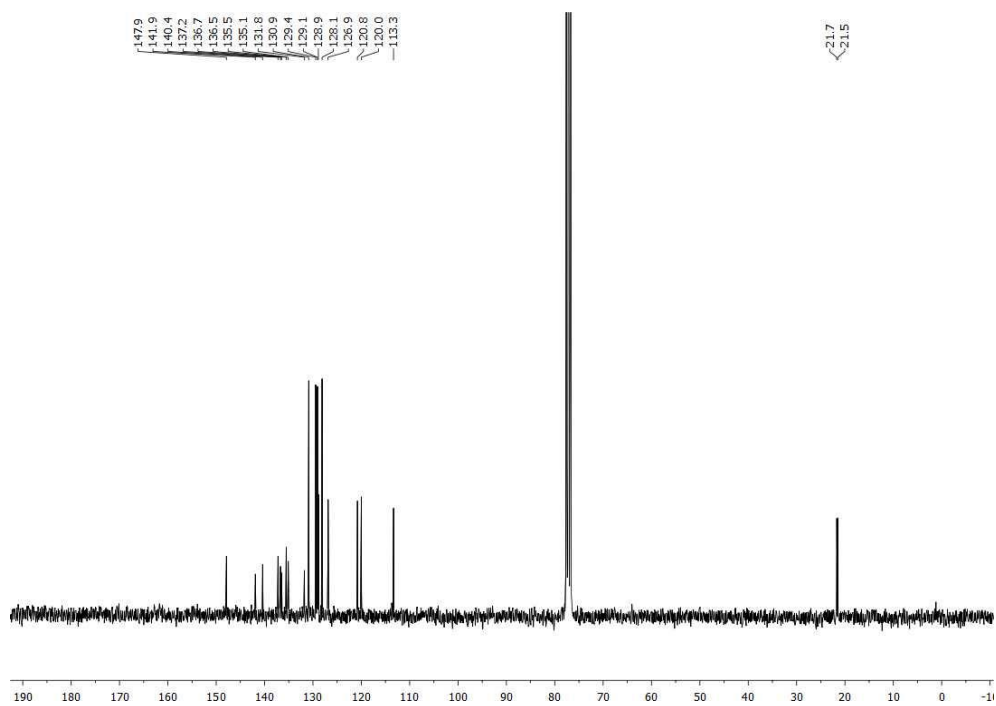
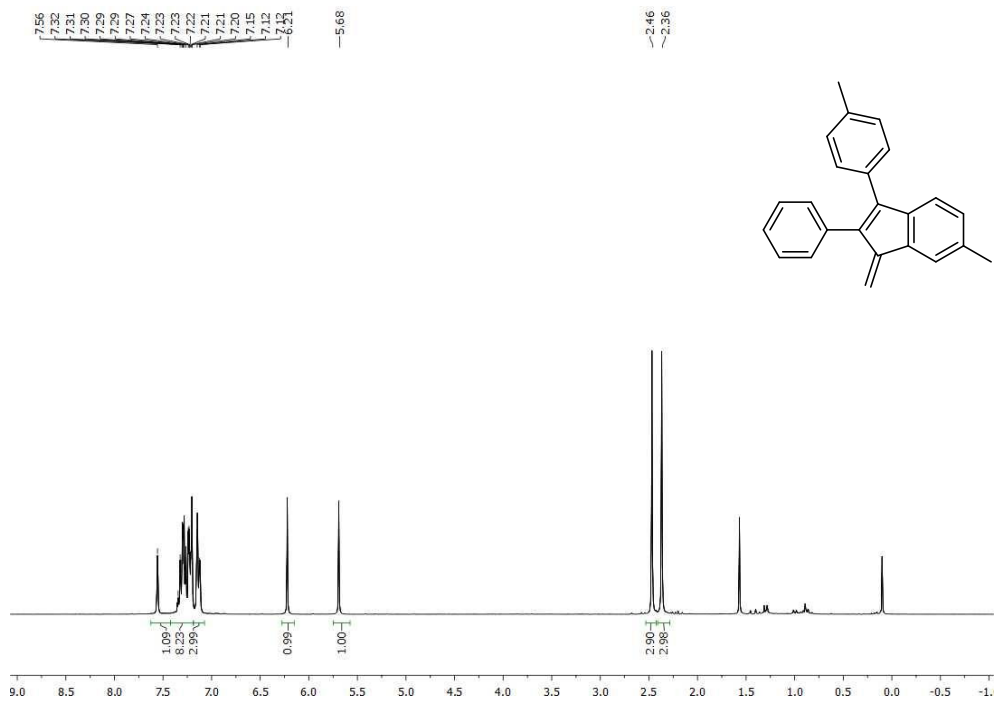


***Cis-tert*-butyldimethyl(5-(*p*-bromophenyl)-4-phenyl-4,5-dihydrofuran-2-yl)silane (*cis*-3.4g)**

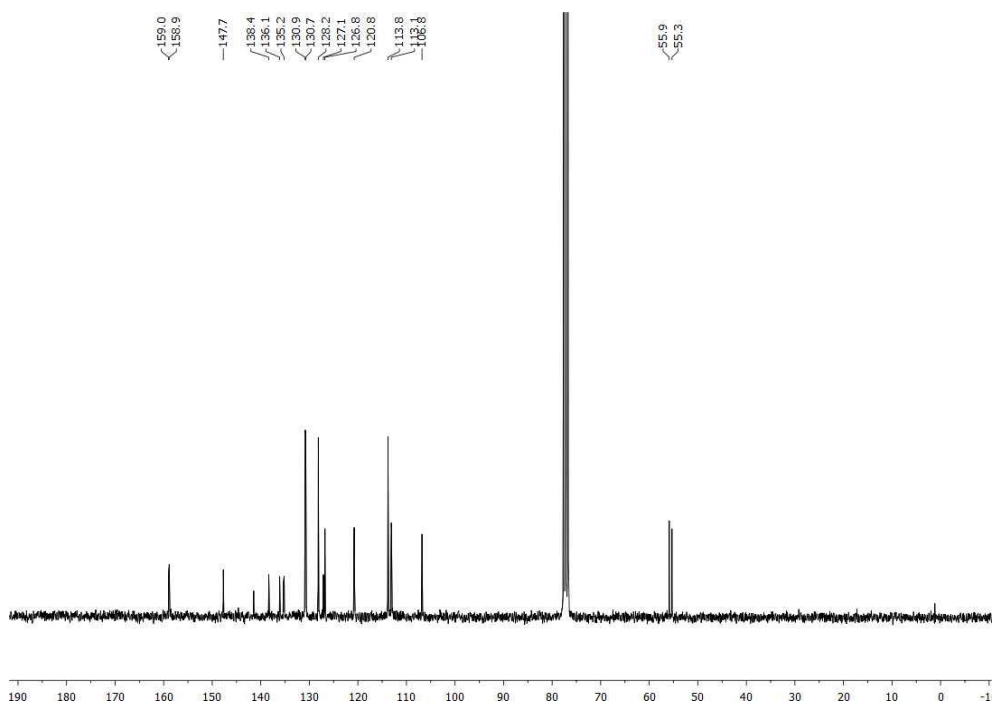
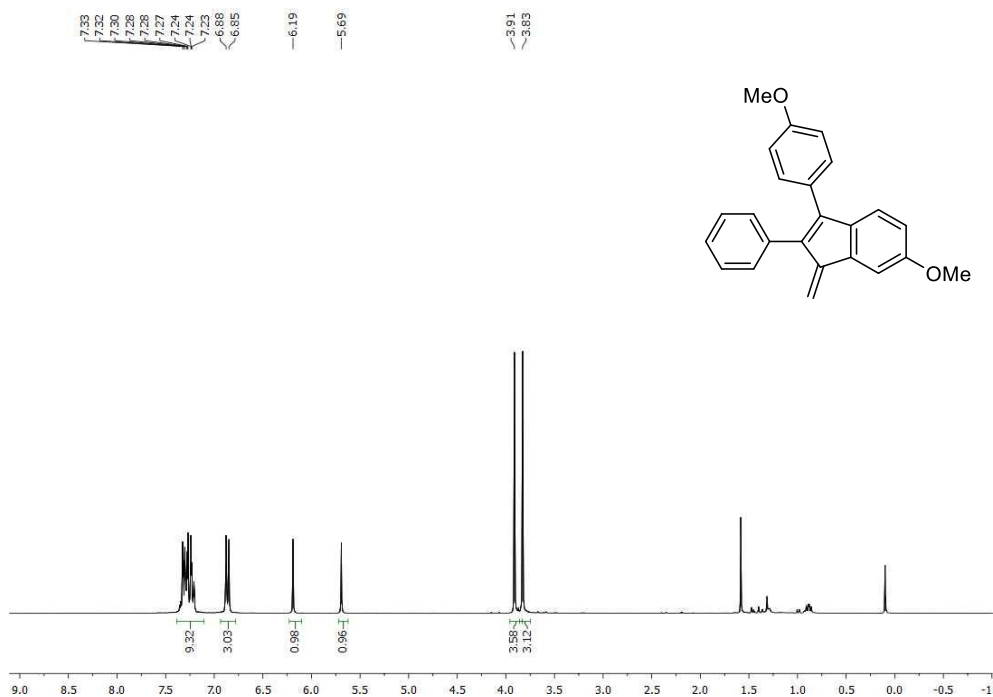
6 Chapter IV

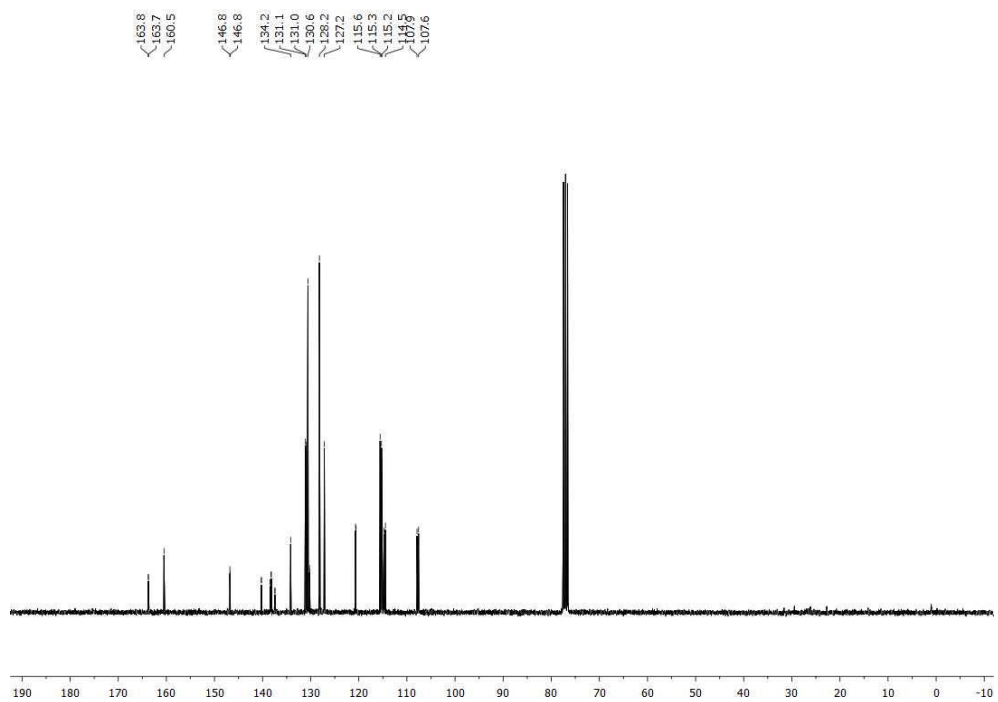
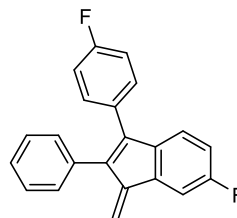
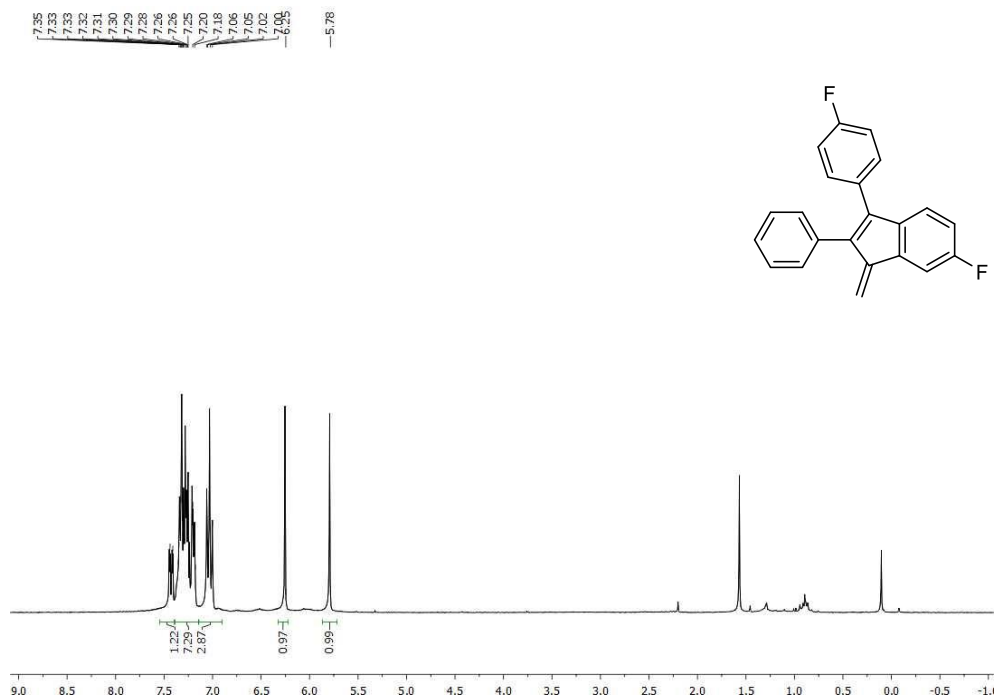
1-Methylene-2,3-diphenyl-1H-indene (4.3a)



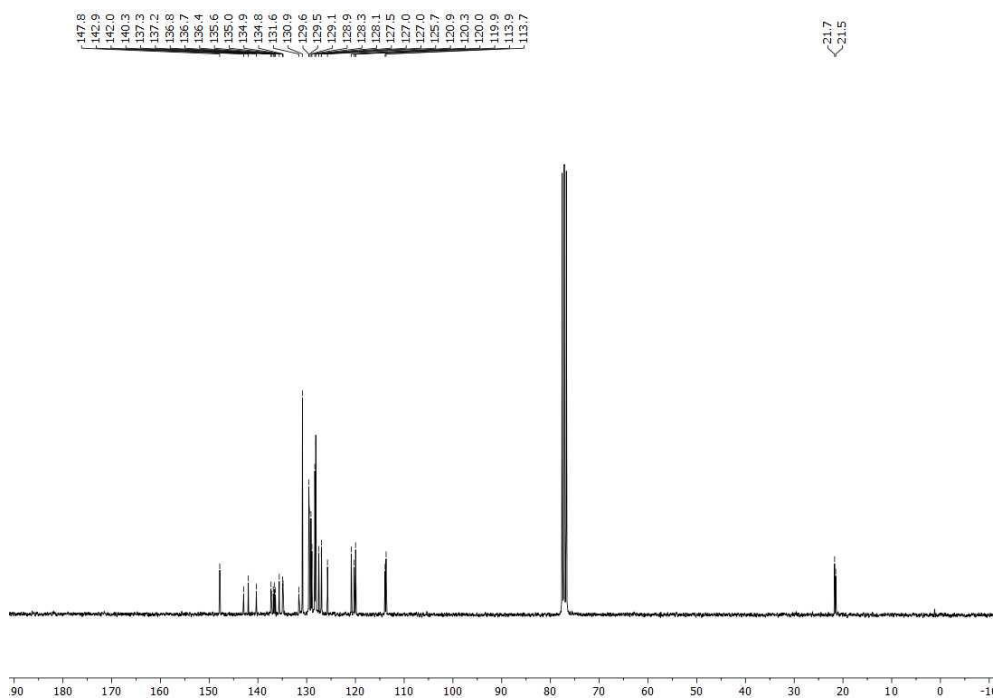
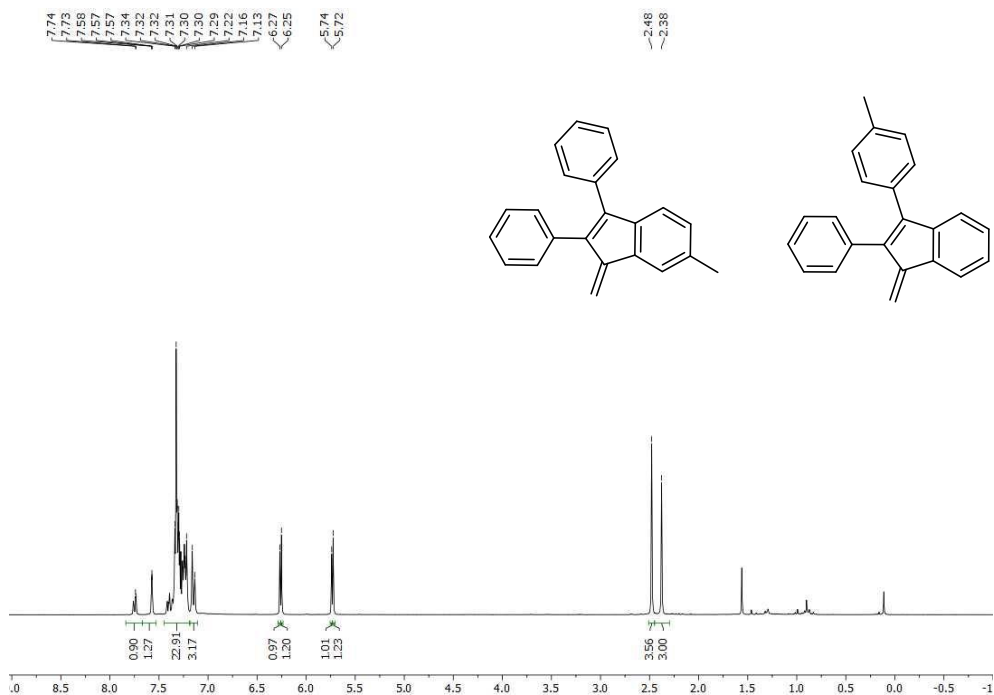
6-Methyl-1-methylene-2-phenyl-3-(*p*-tolyl)-1*H*-indene (4.3b)

6-Methoxy-3-(4-methoxyphenyl)-1-methylene-2-phenyl-1H-indene (4.3c)

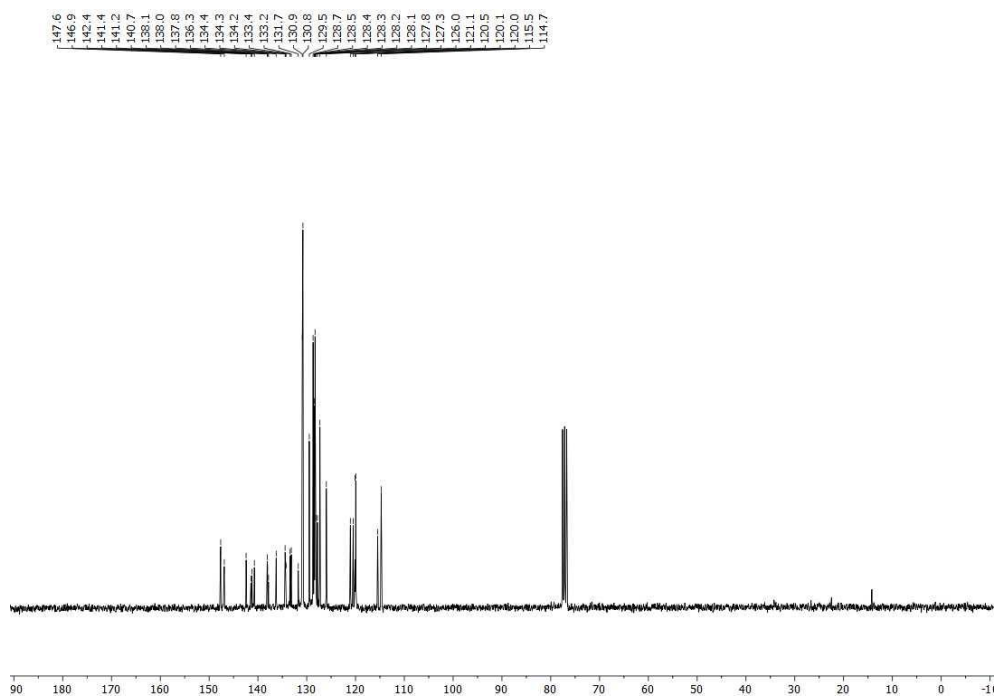
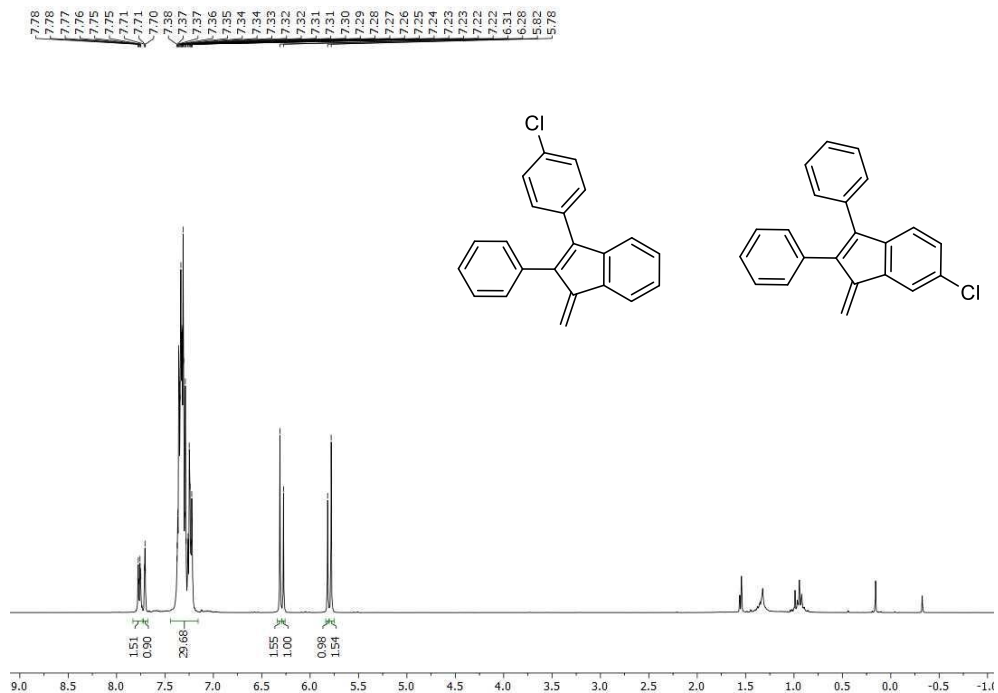


6-Fluoro-3-(4-fluorophenyl)-1-methylene-2-phenyl-1H-indene (4.3d)

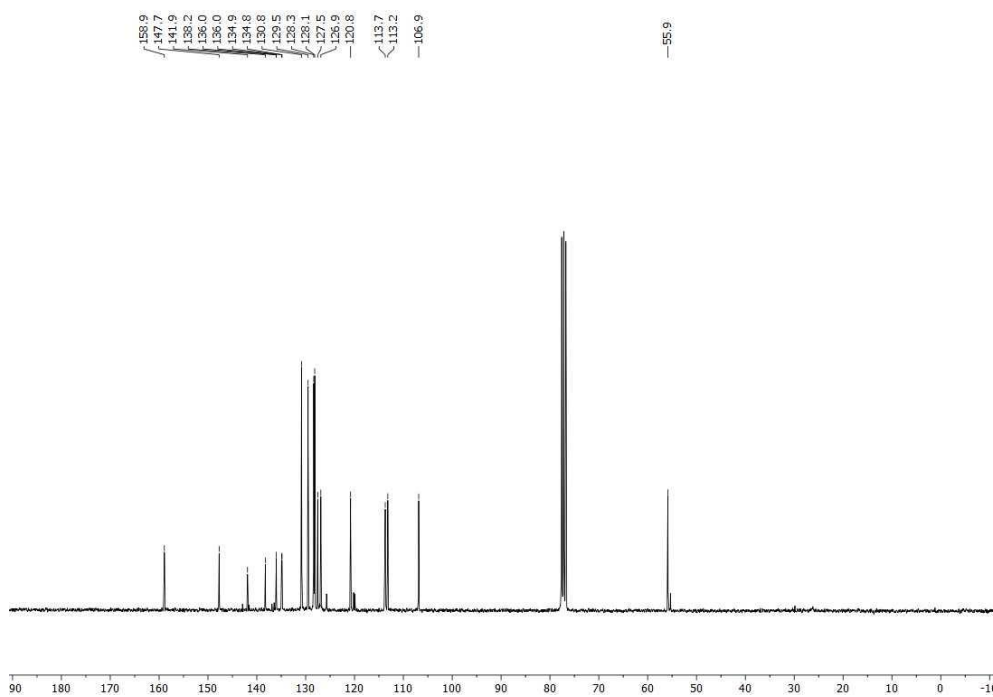
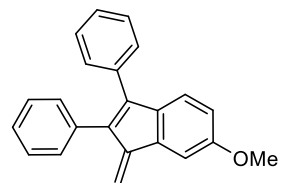
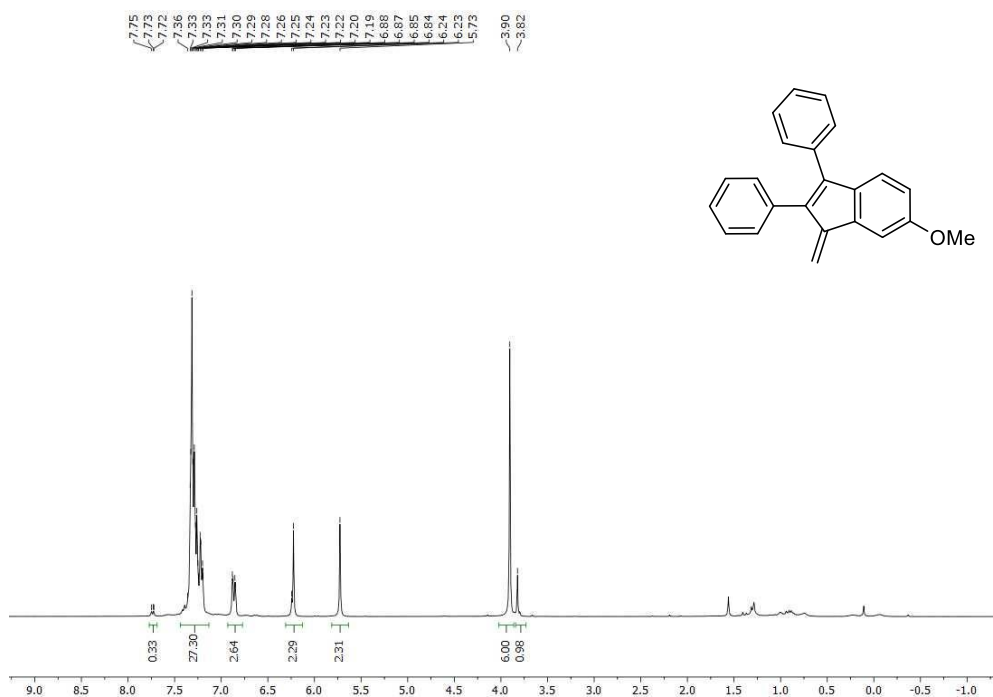
6-Methyl-1-methylene-2,3-diphenyl-1H-indene or 1-Methylene-2-phenyl-3-(p-tolyl)-1H-indene (4.3e)

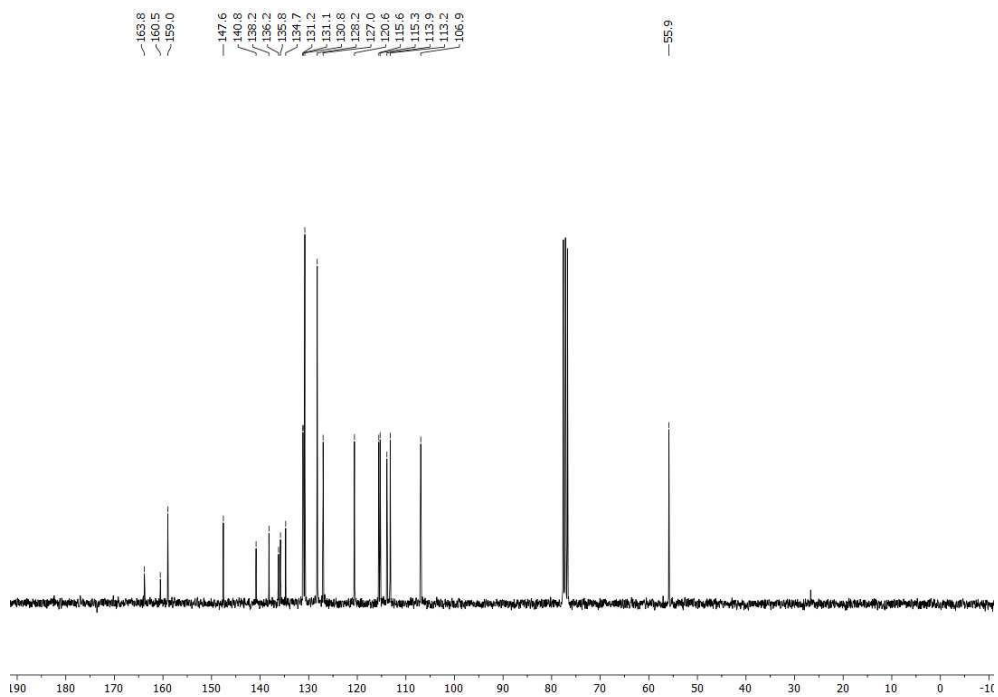
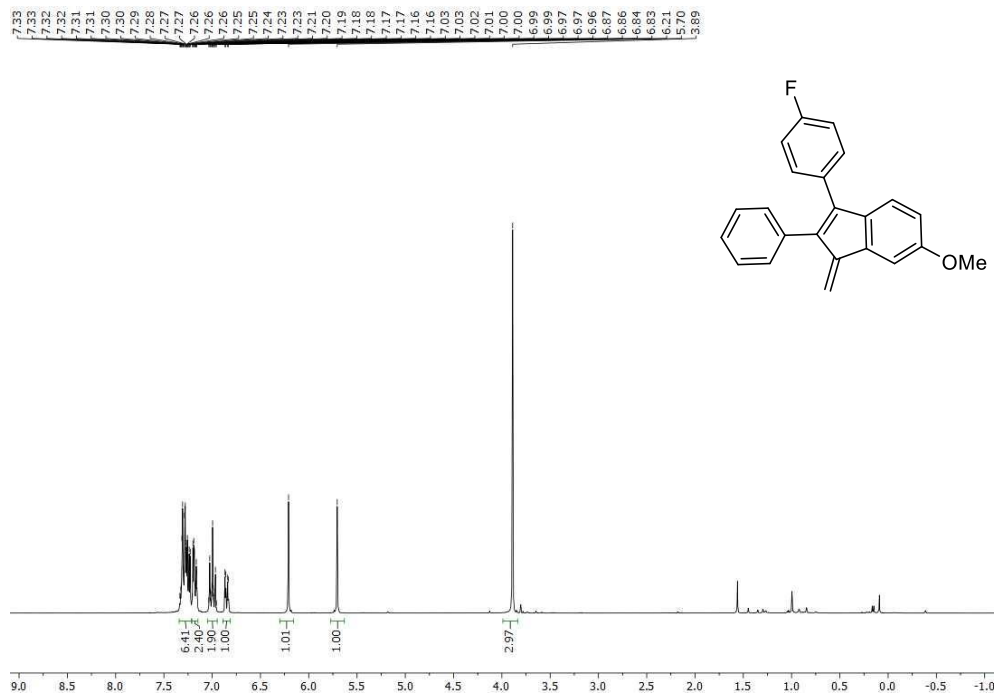


3-(4-Chlorophenyl)-1-methylene-2-phenyl-1H-indene or 6-Chloro-1-methylene-2,3-diphenyl-1H-indene (4.3f)

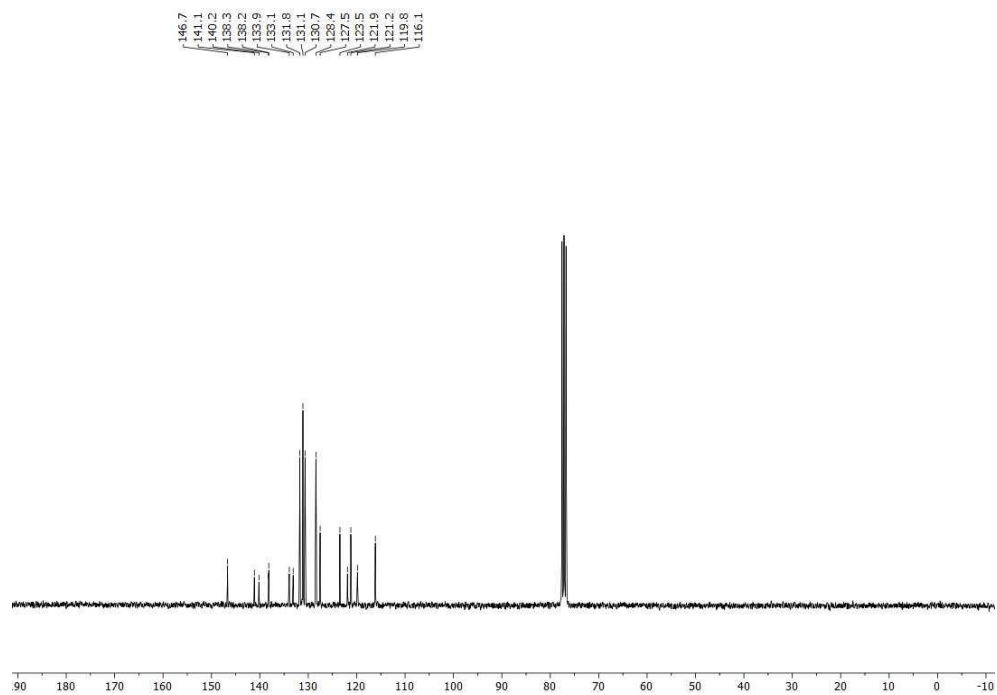
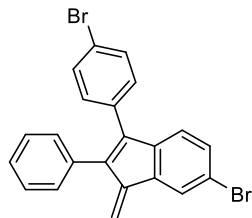
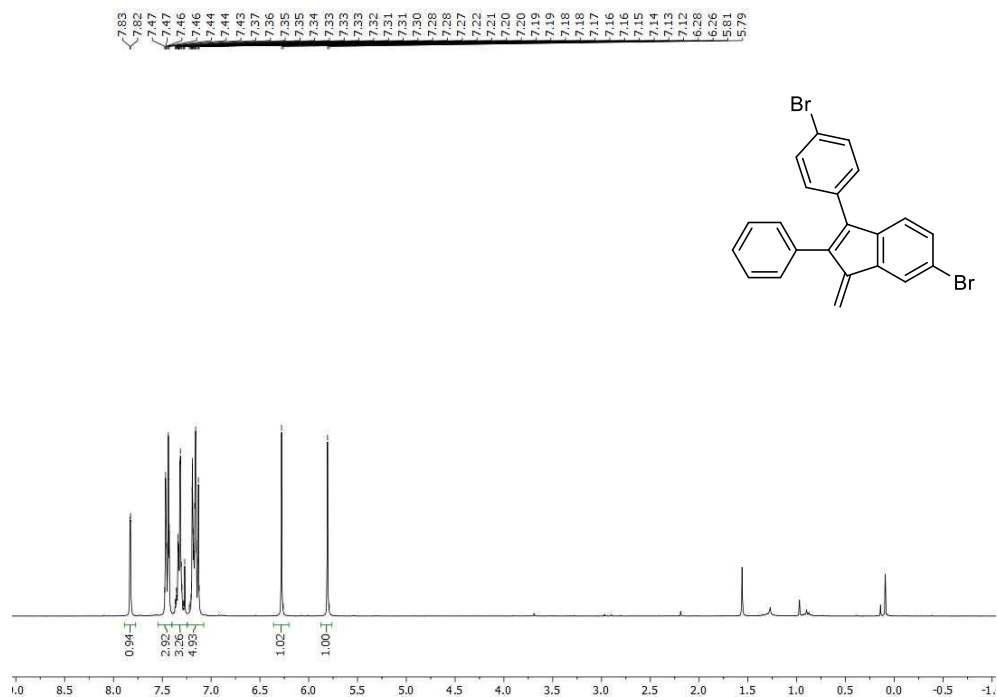


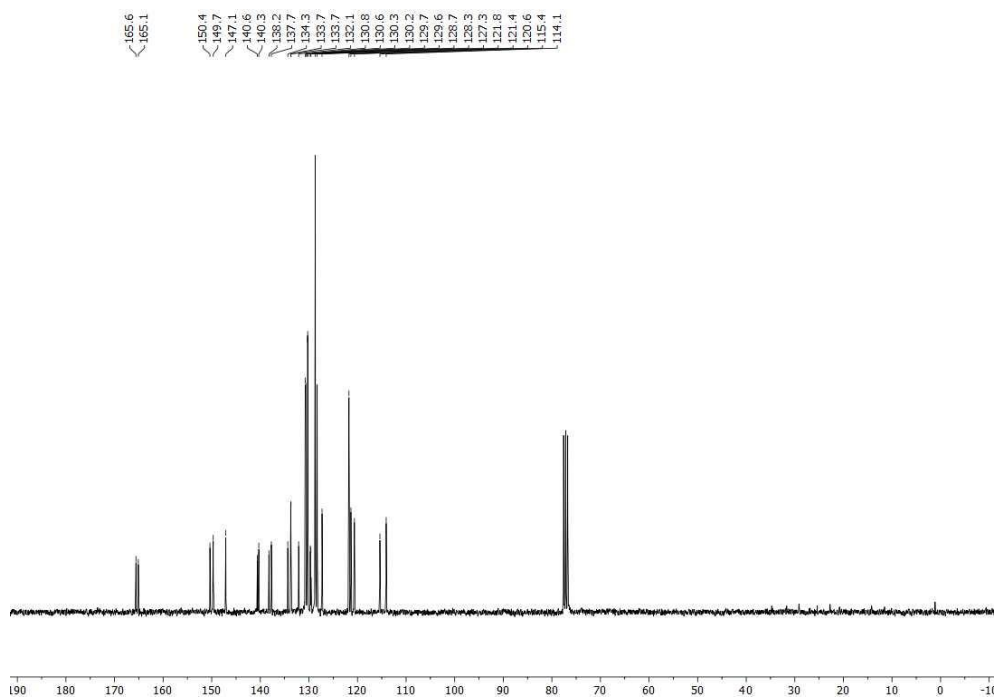
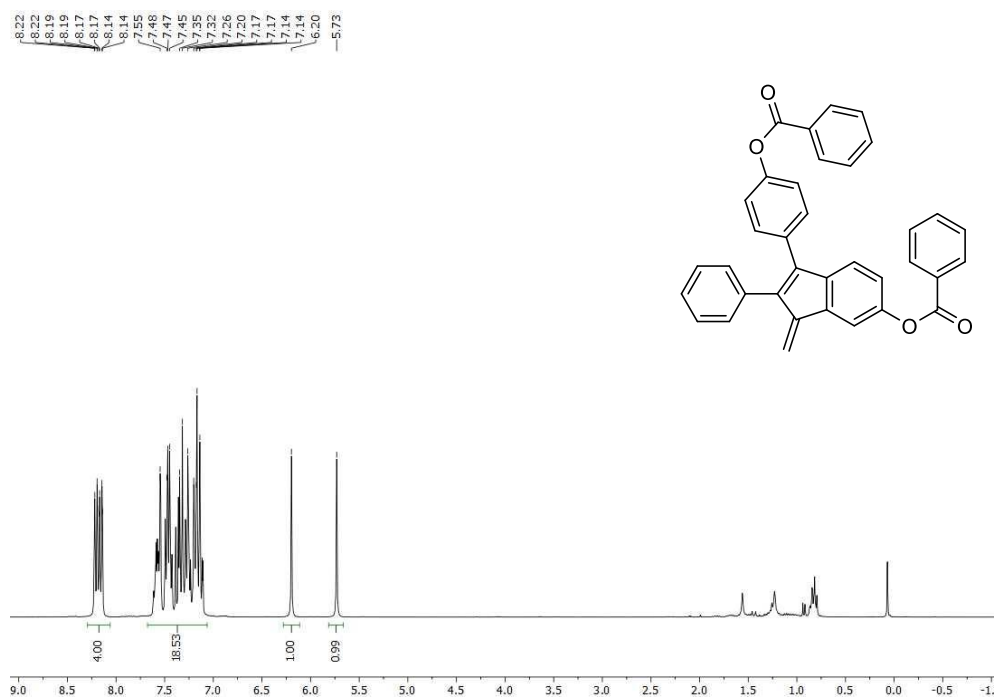
6-Methoxy-1-methylene 2,3-diphenyl-1H-indene (4.3g)



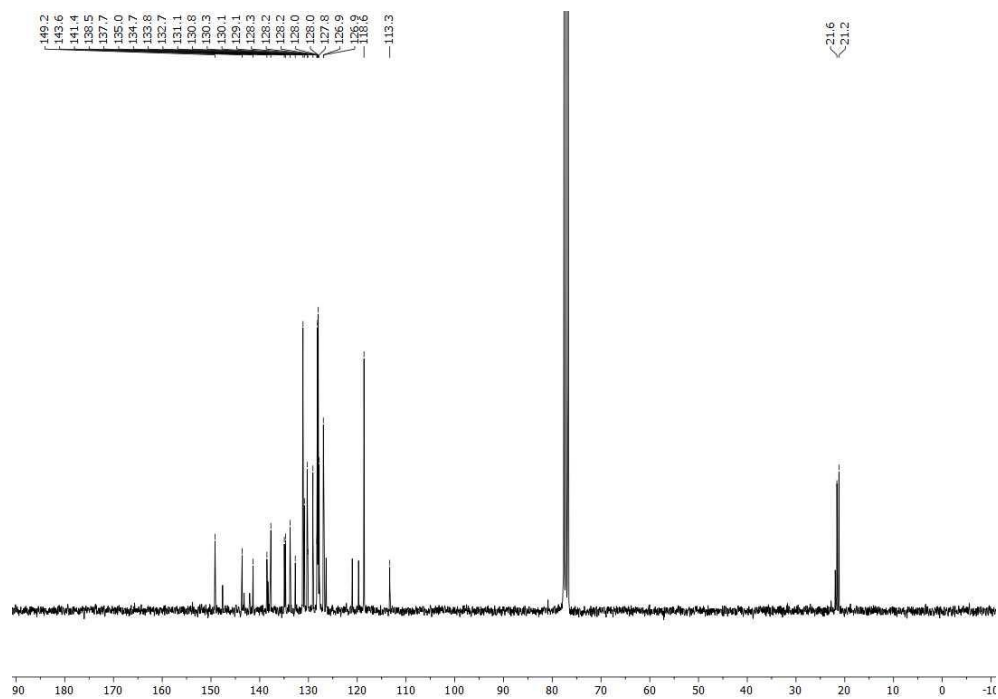
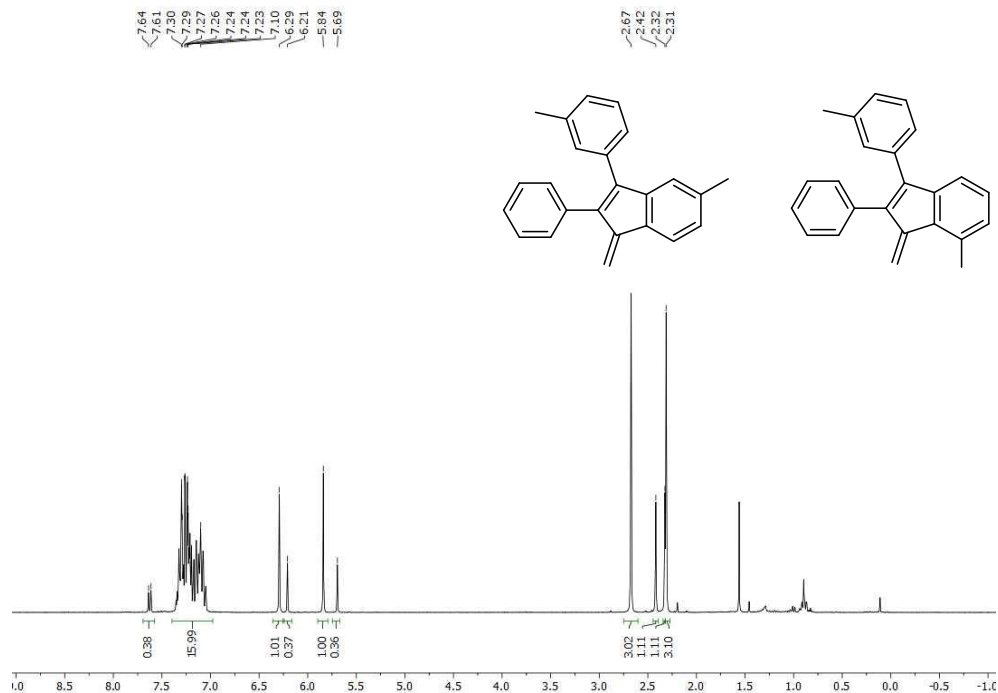
3-(4-Fluorophenyl)-6-methoxy-1-methylene-2-phenyl-1H-indene (4.3h)

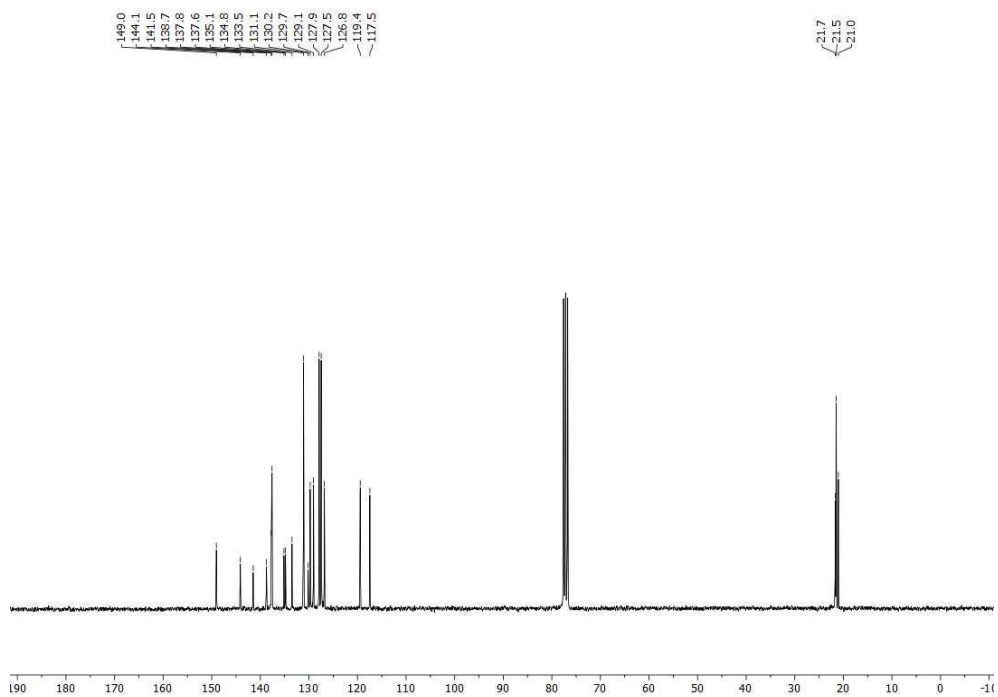
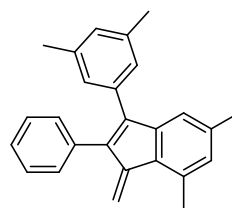
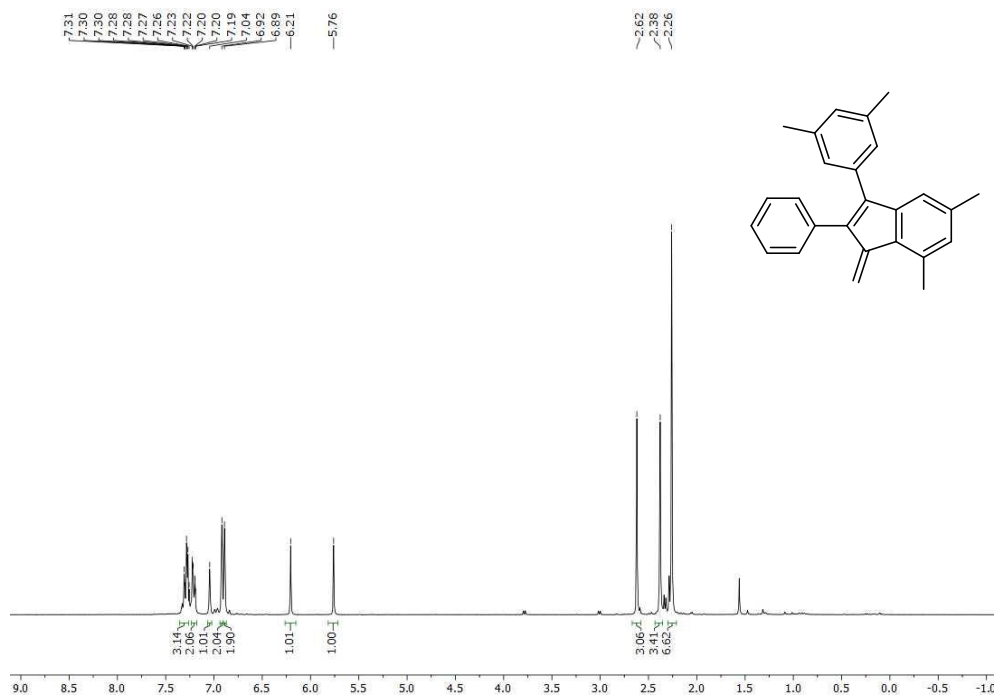
6-Bromo-3-(4-bromophenyl)-1-methylene-2-phenyl-1H-indene (4.3i)



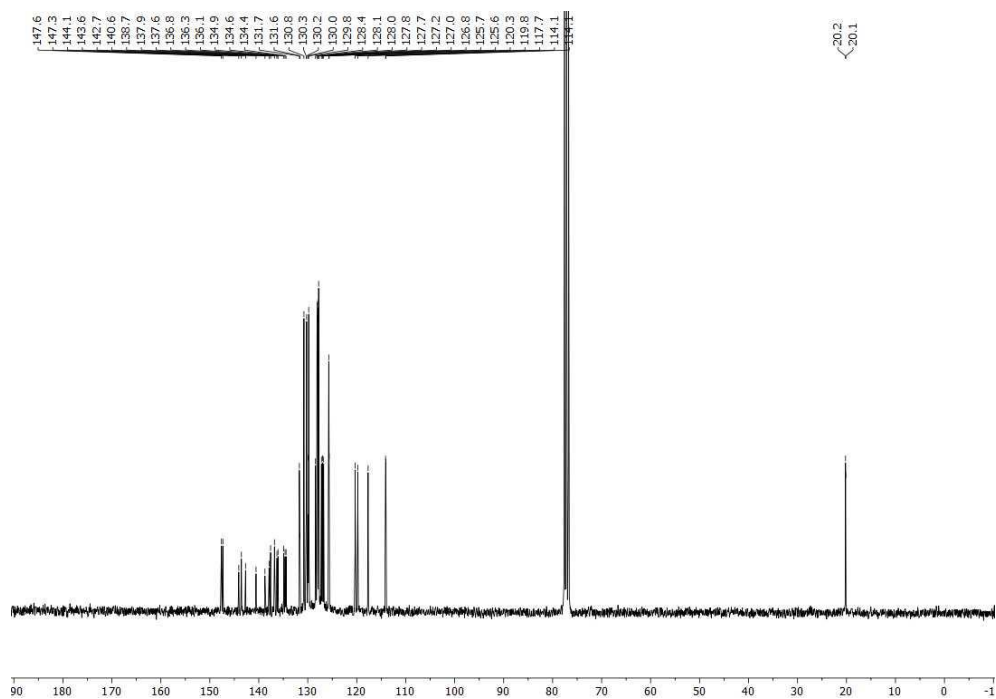
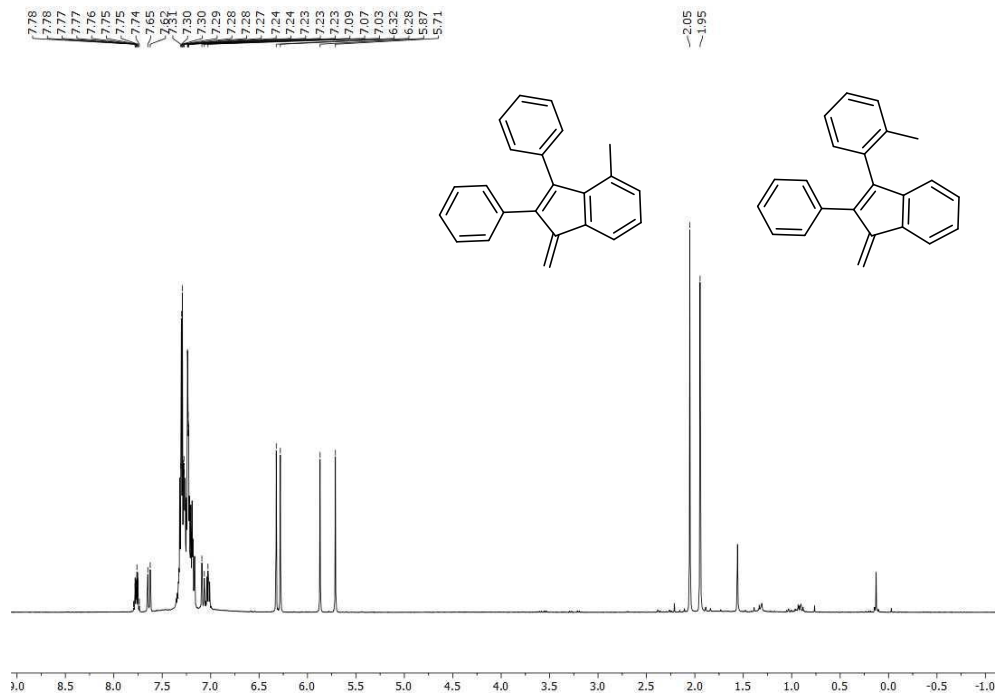
4-(6-(Benzoyloxy)-1-methylene-2-phenyl-1H-inden-3-yl)phenyl benzoate (4.3j)

5-Methyl-1-methylene-2-phenyl-3-(*m*-tolyl)-1H-indene or 7-methyl-1-methylene-2-phenyl-3-(*m*-tolyl)-1H-indene(4.3k)

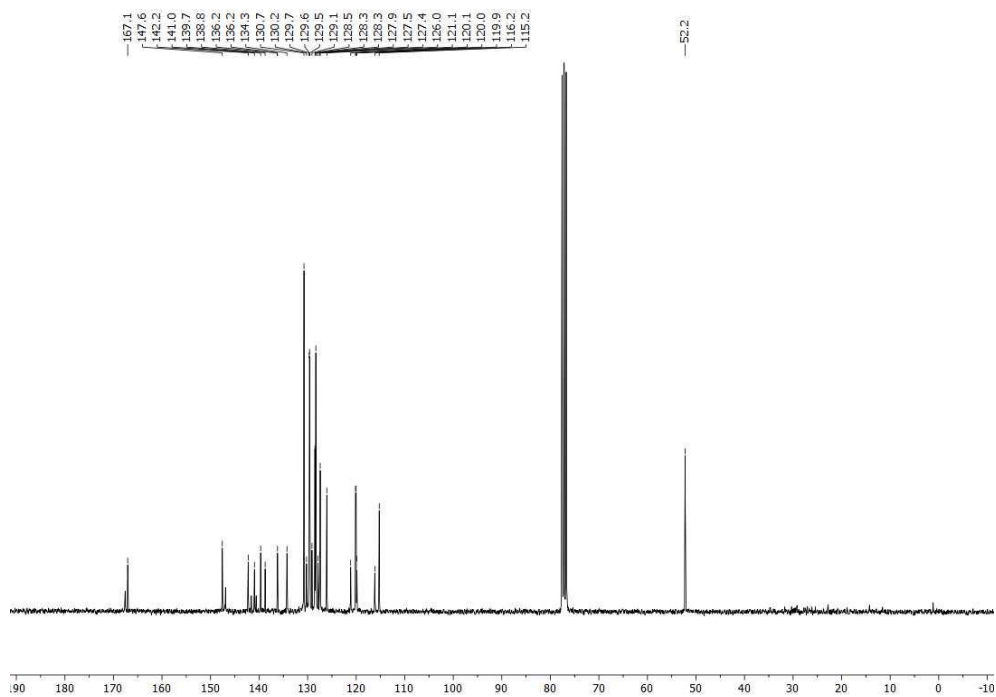
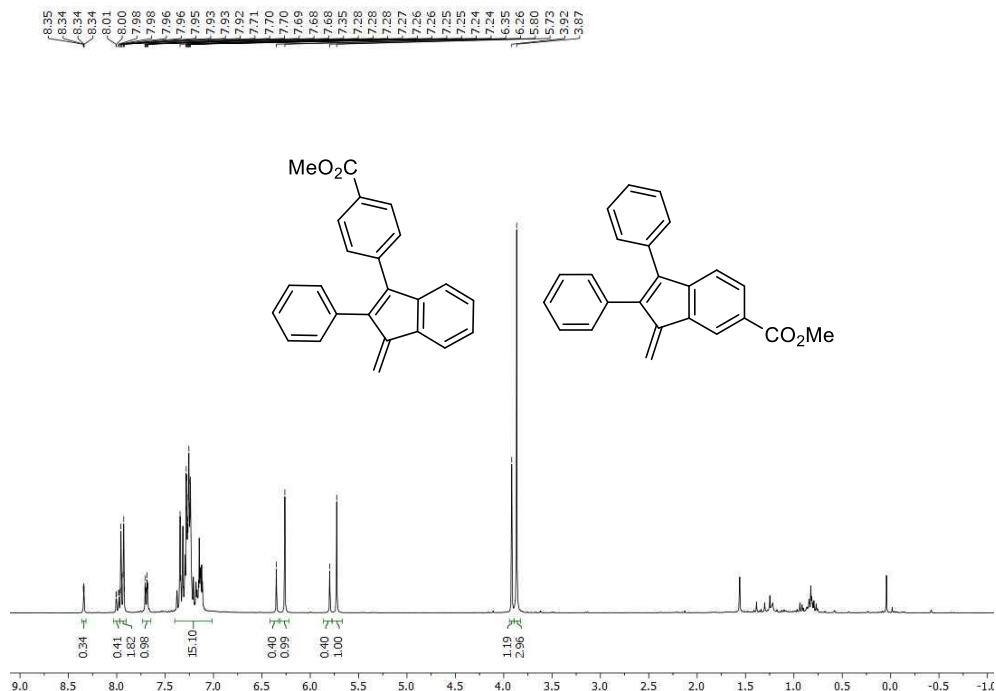


5,7-Dimethyl-1-methylene-3-(3,5-dimethylphenyl)-2-phenyl-1H-indene (4.3I)

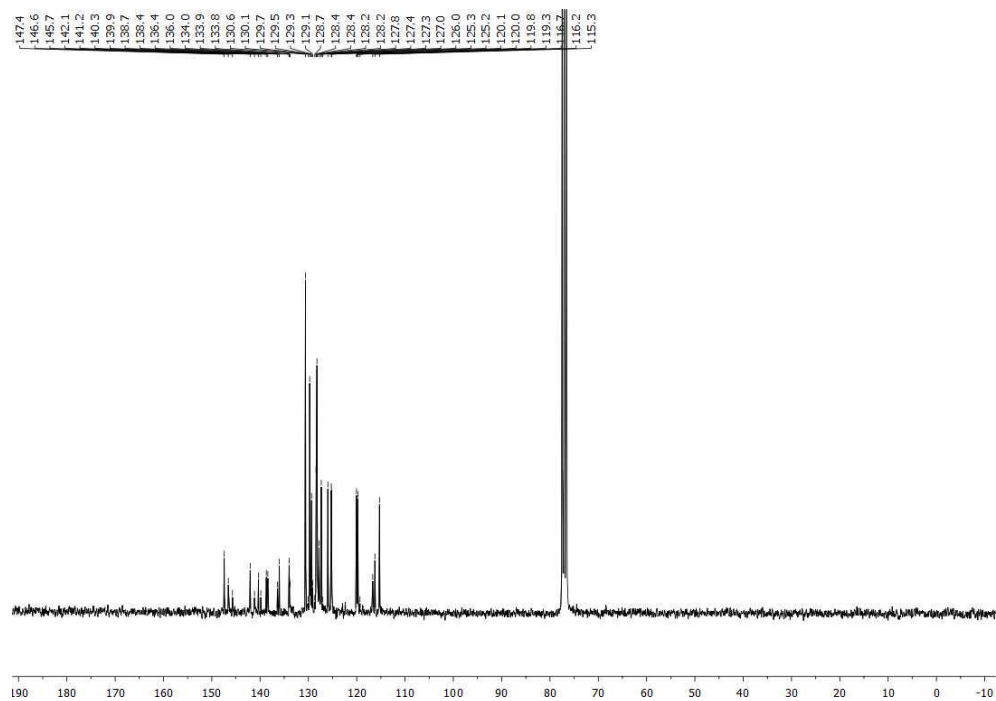
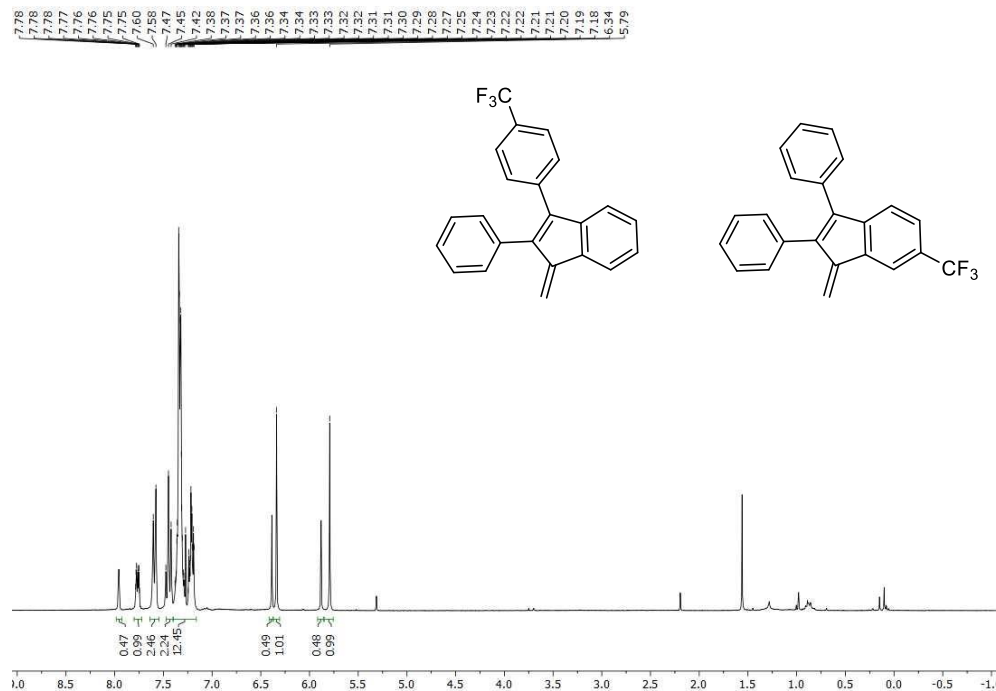
4-Methyl-1-methylene-2,3-diphenyl-1H-indene or 1-methylene-2-phenyl-3-(*o*-tolyl)-1H-indene (4.3m)

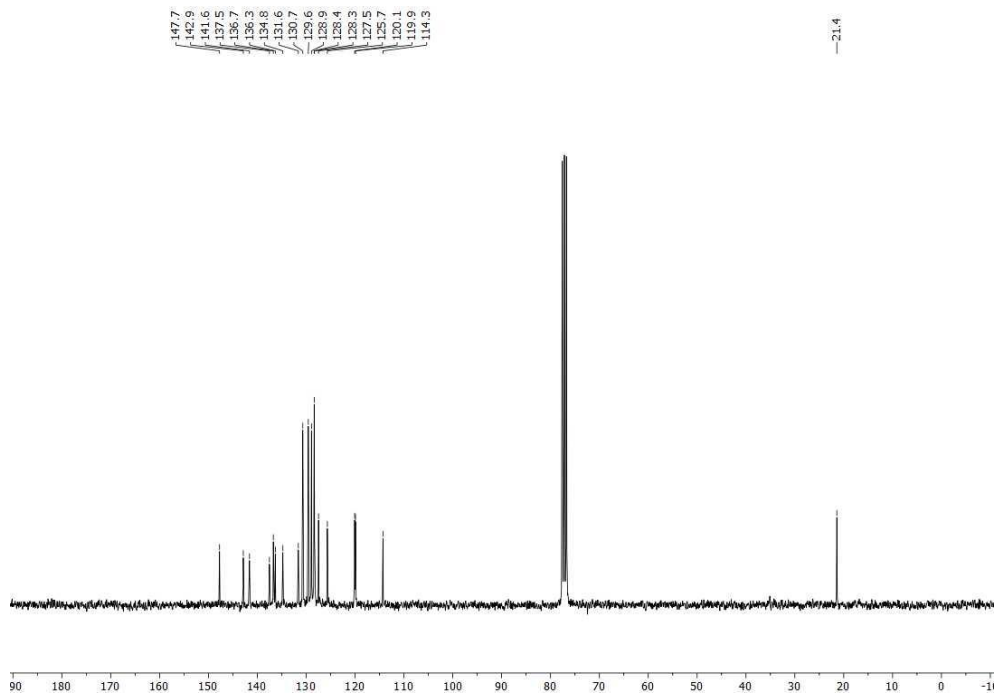
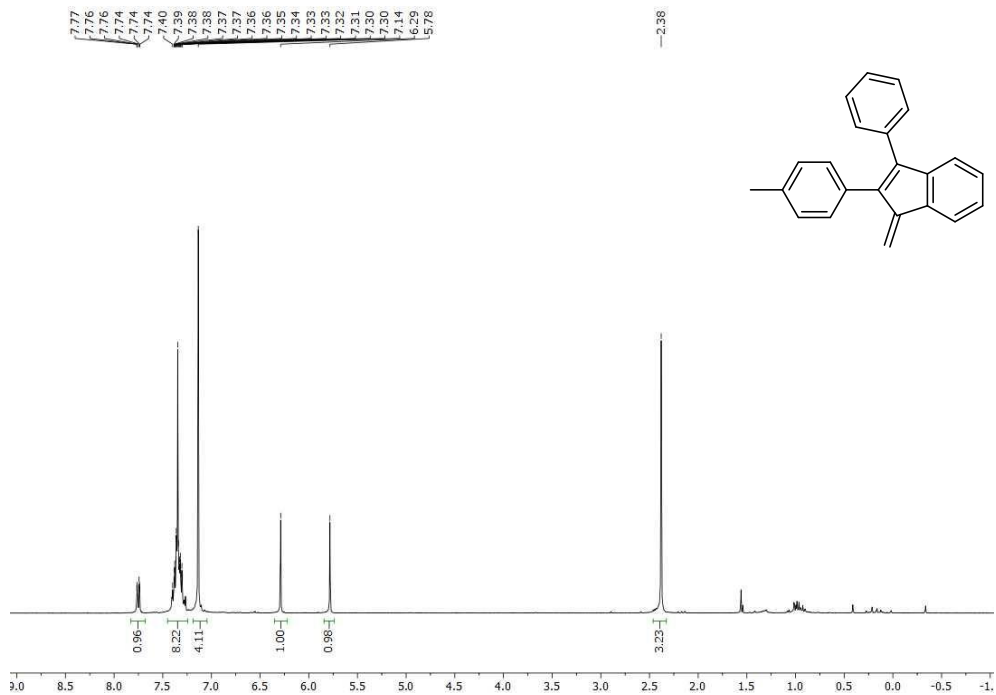


Methyl 4-(1-methylene-2-phenyl-1*H*-inden-3-yl)benzoate or methyl 1-methylene-2,3-diphenyl-1*H*-indene-6-carboxylate (4.3n)

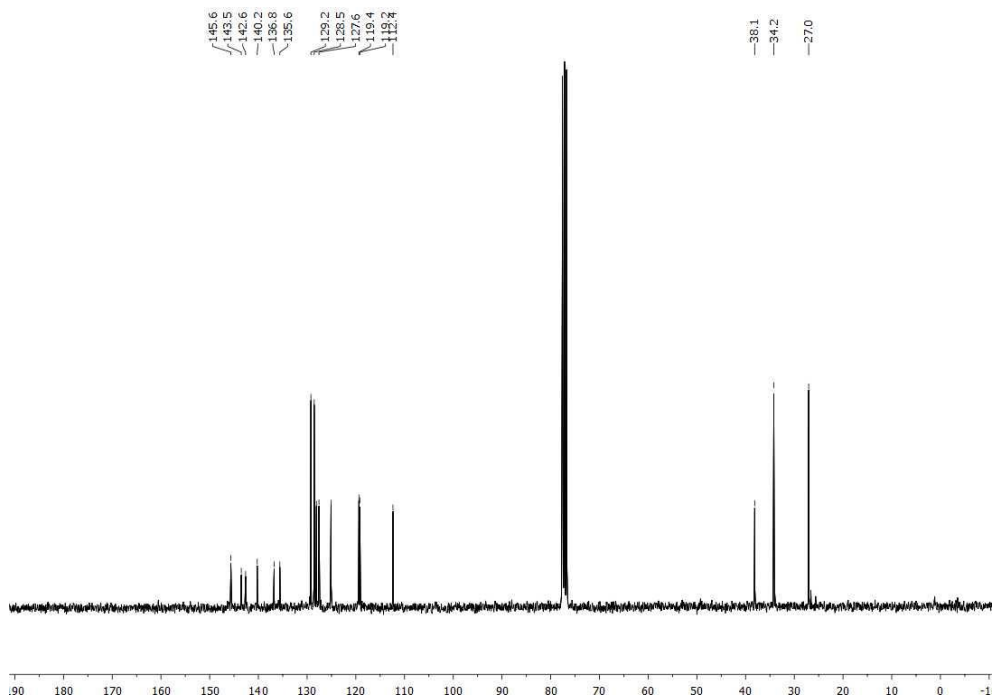
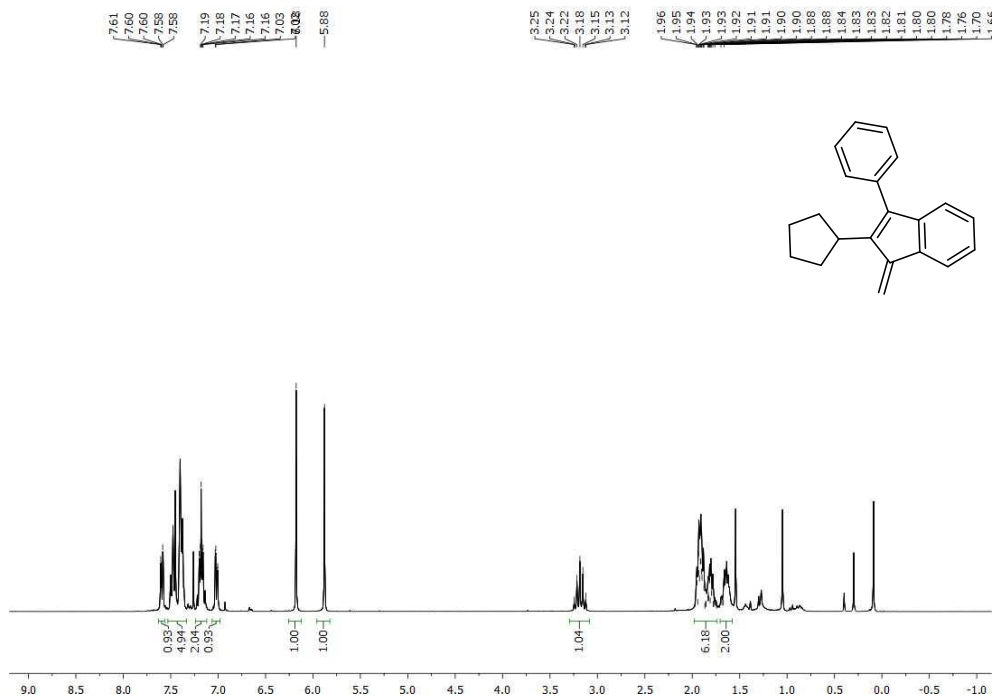


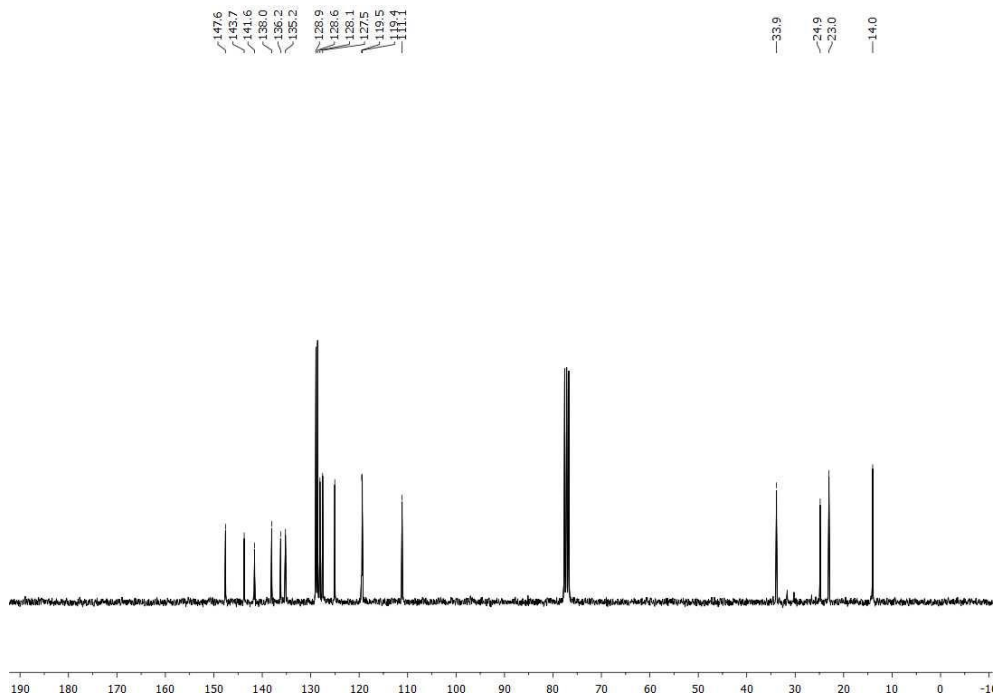
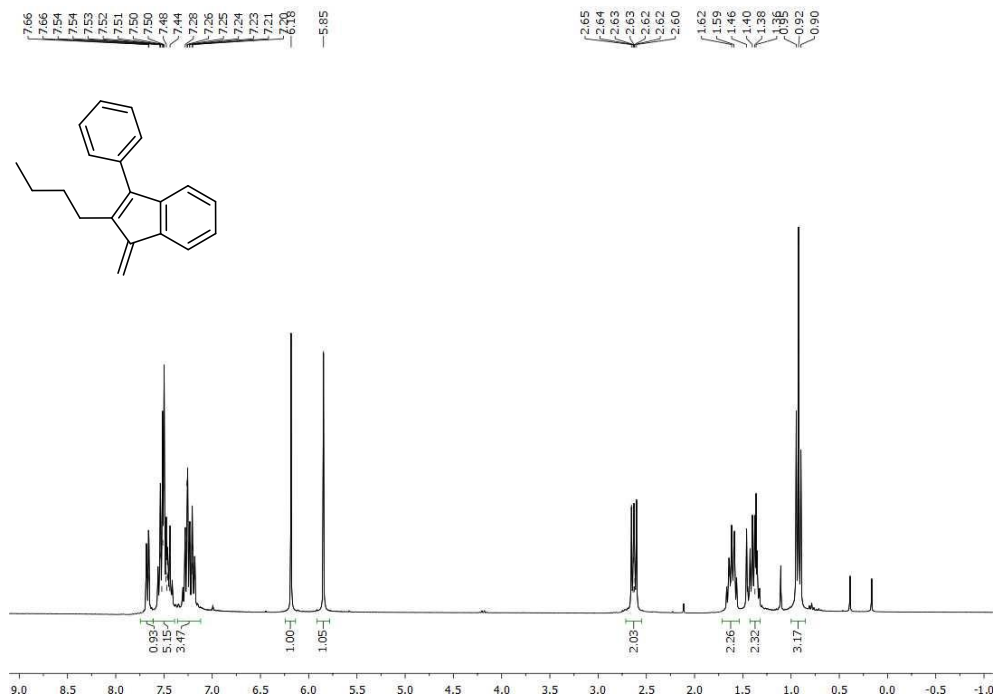
1-Methylene-2,3-diphenyl-6-(trifluoromethyl)-1H-indene or 1-methylene-2-phenyl-3-(4-(trifluoromethyl)phenyl)-1H-indene (4.30)



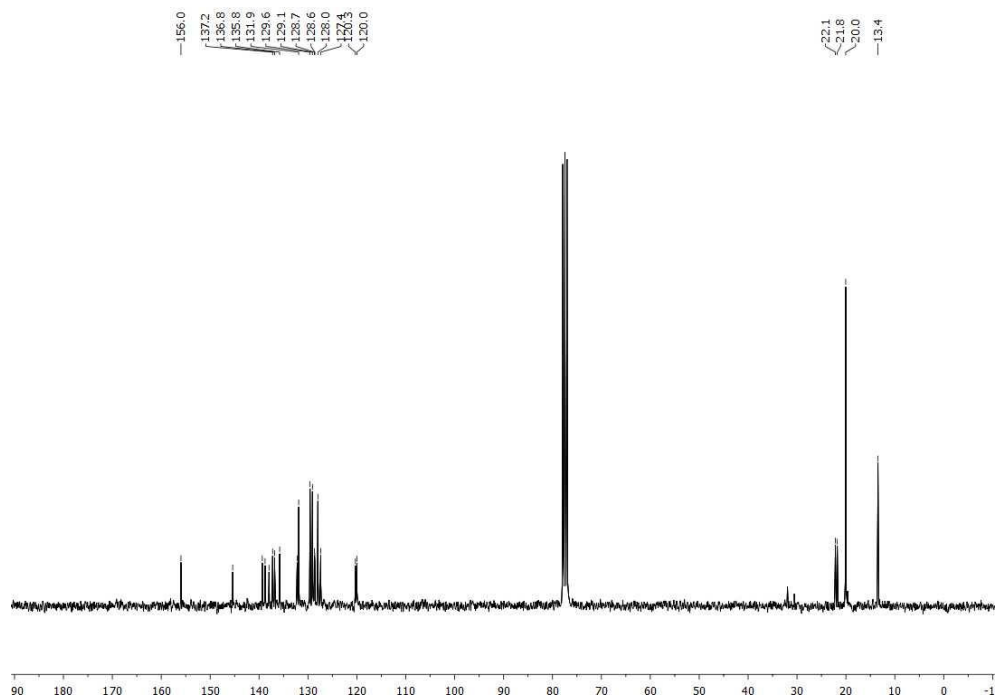
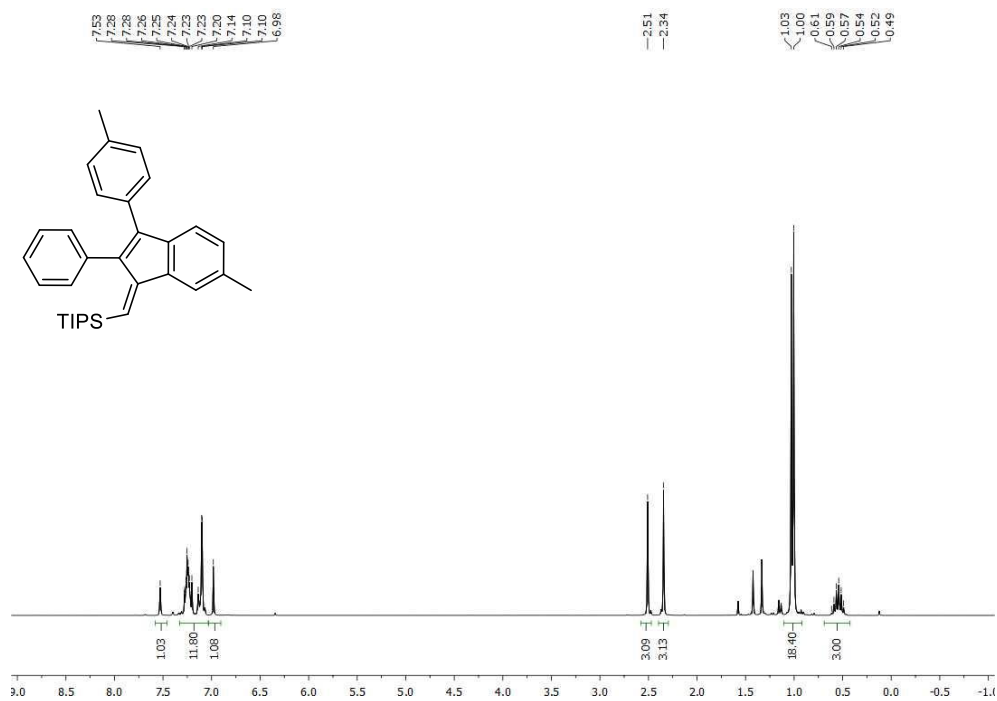
1-Methylene-3-phenyl-2-(*p*-tolyl)-1*H*-indene (4.3p)

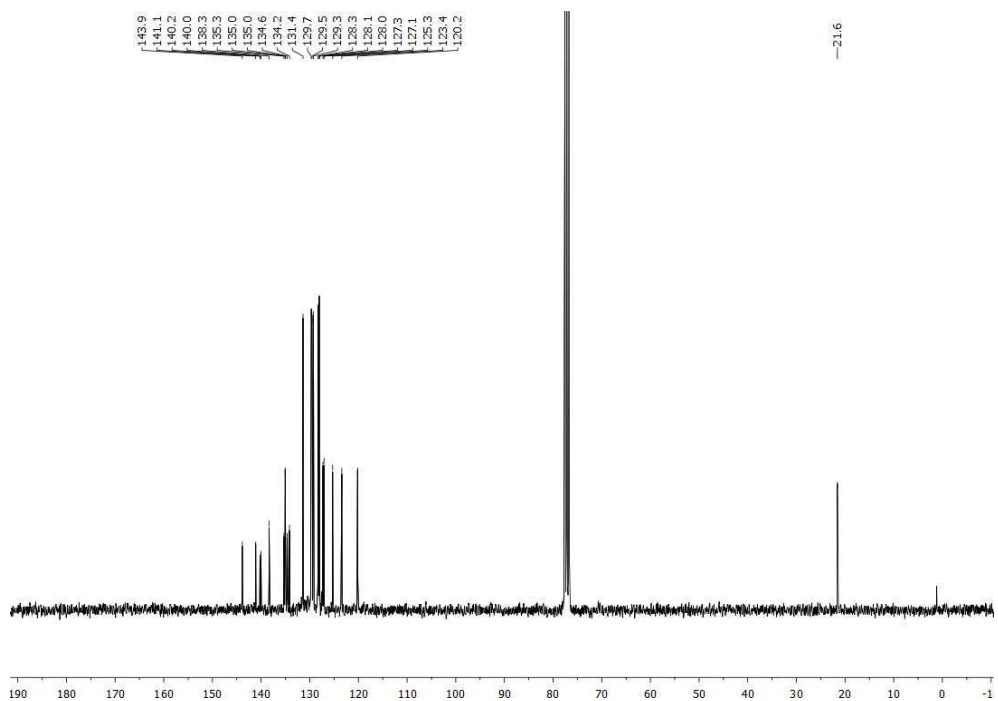
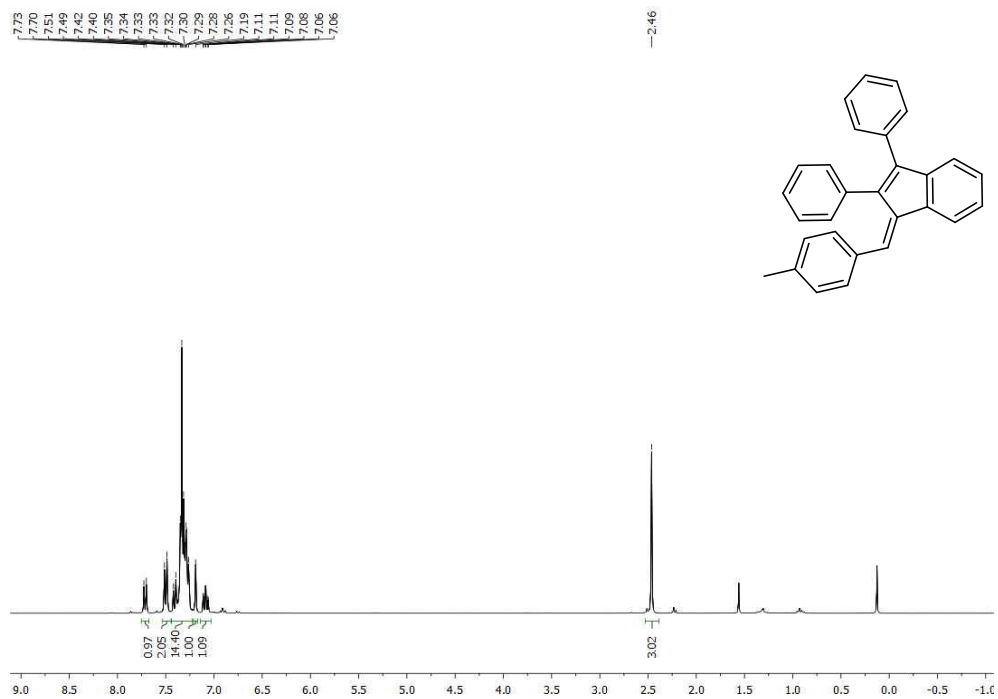
2-Cyclopentyl-1-methylene-3-phenyl-1H-indene (4.3q)



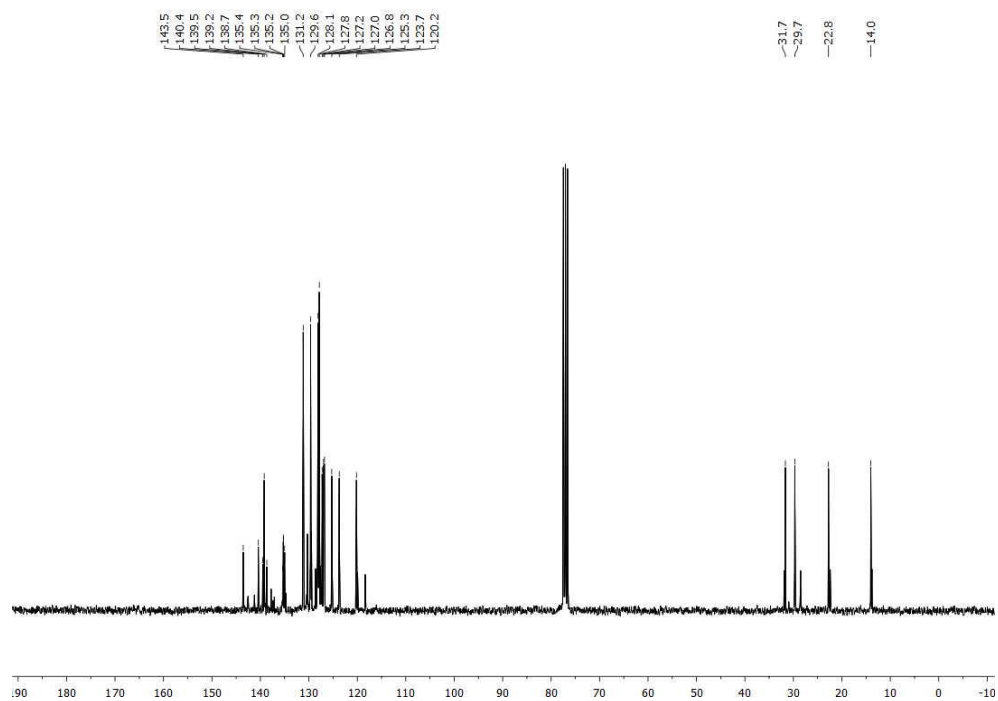
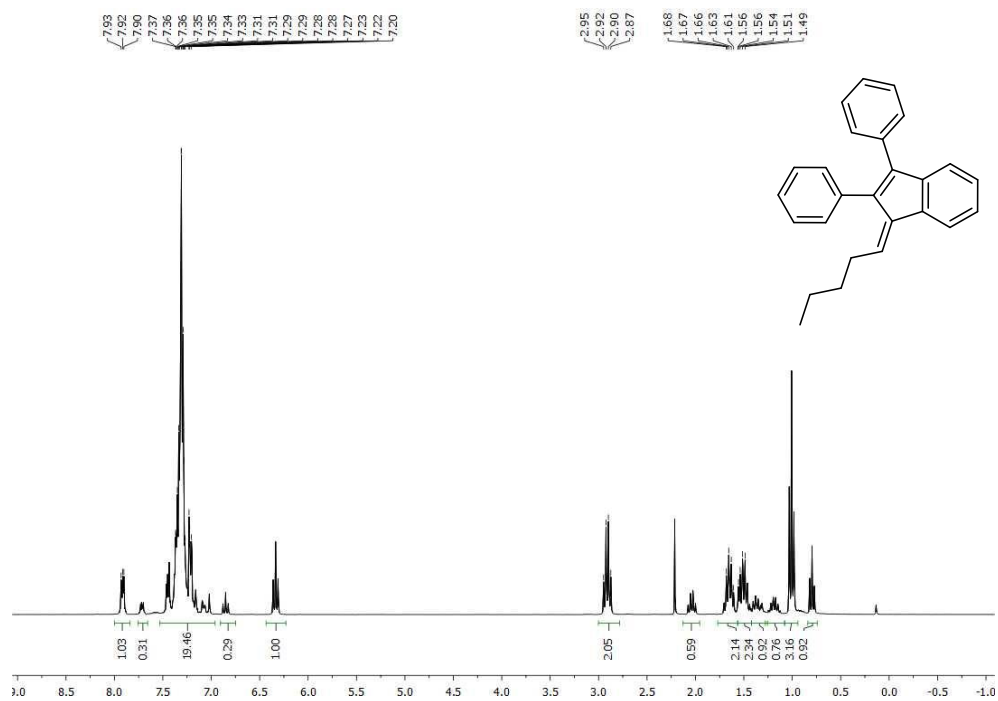
2-Butyl-1-methylene-3-phenyl-1H-indene (4.3r)

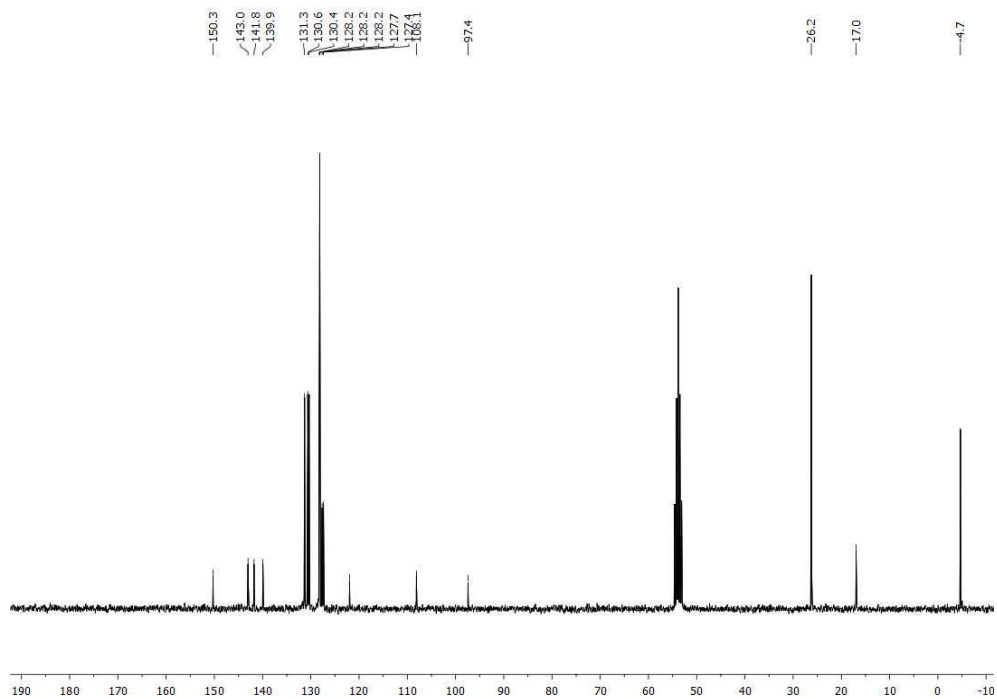
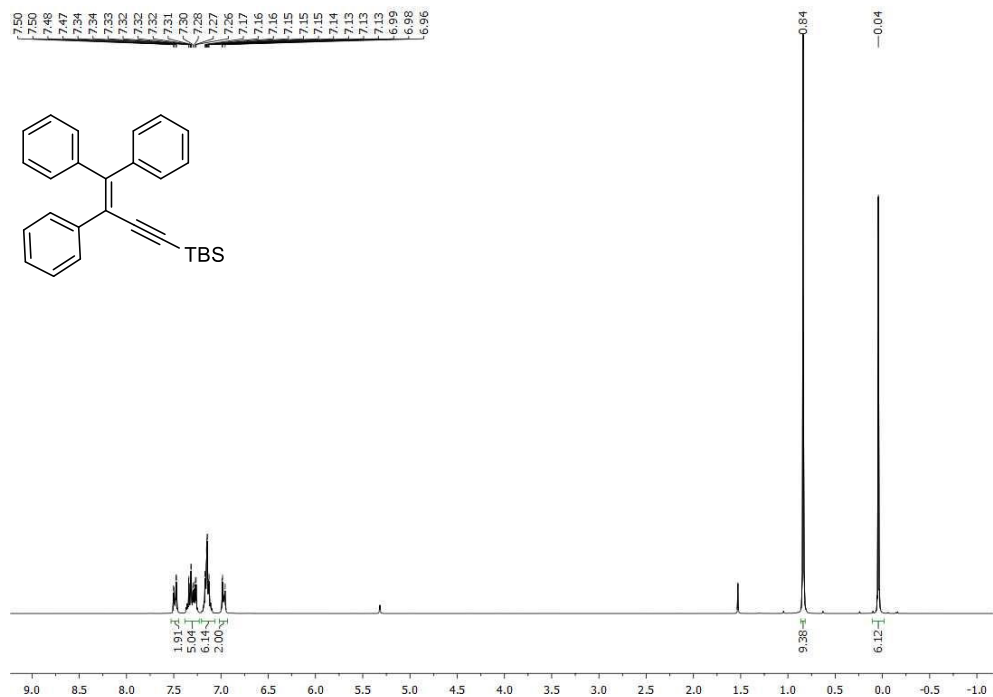
(E)-1-(4-triisopropylsilylmethylidene)-2,3-diphenyl-1H-indene (4.9a)



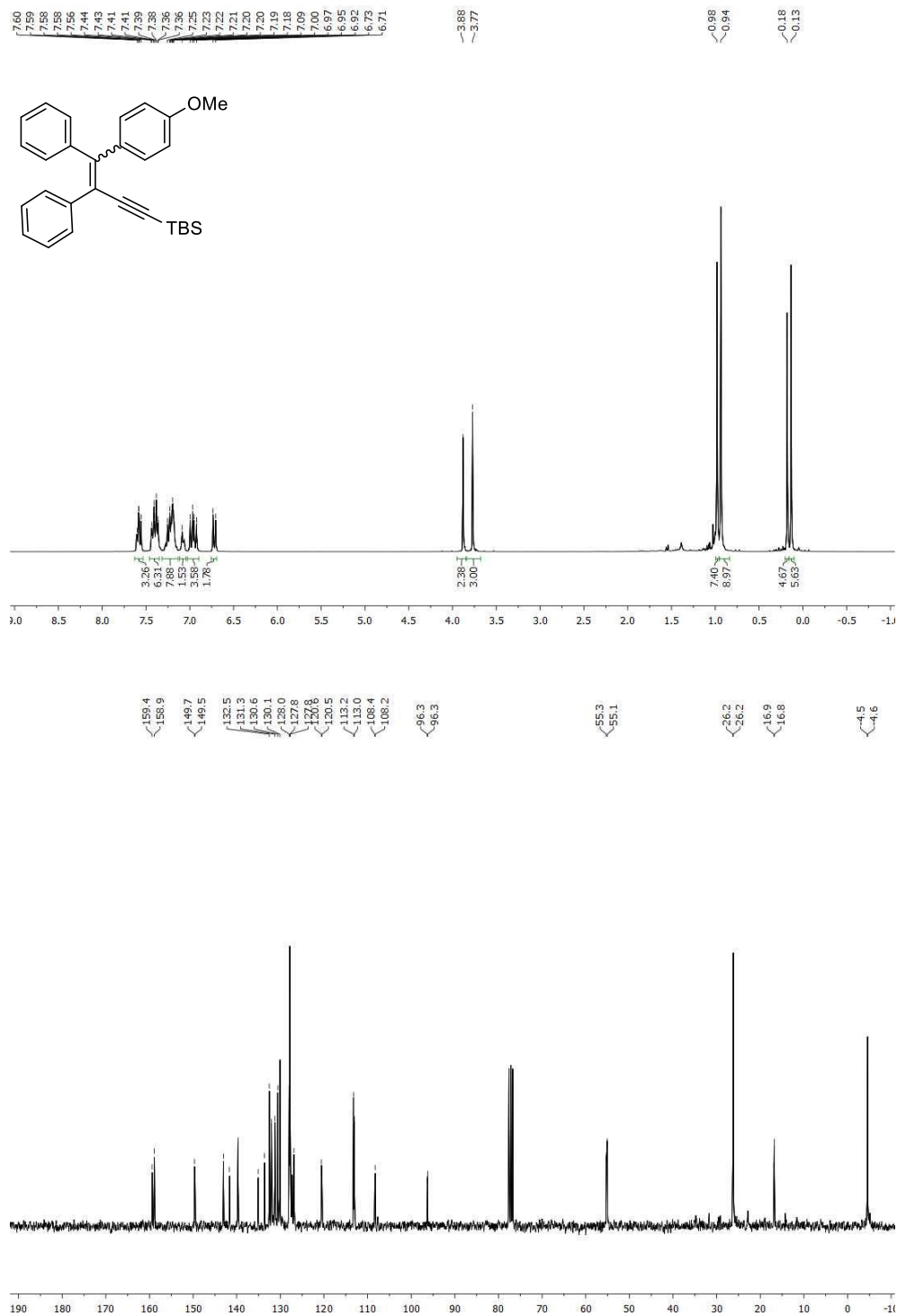
(E)-1-(4-methylbenzylidene)-2,3-diphenyl-1H-indene (4.9b)

1-Pentylidene-2,3-diphenyl-1H-indene (4.9c)

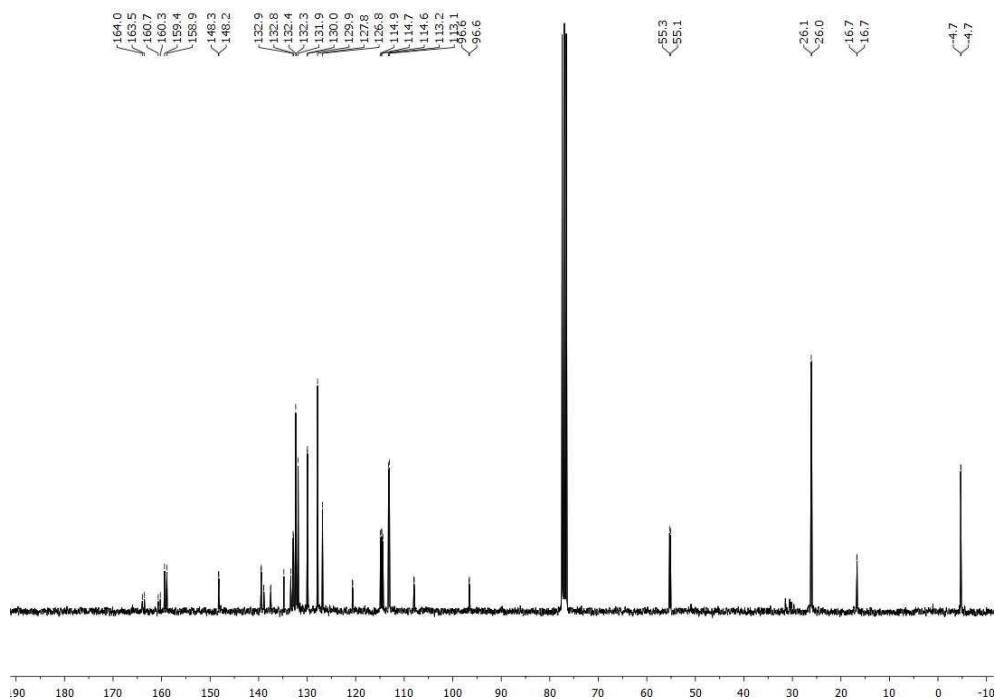
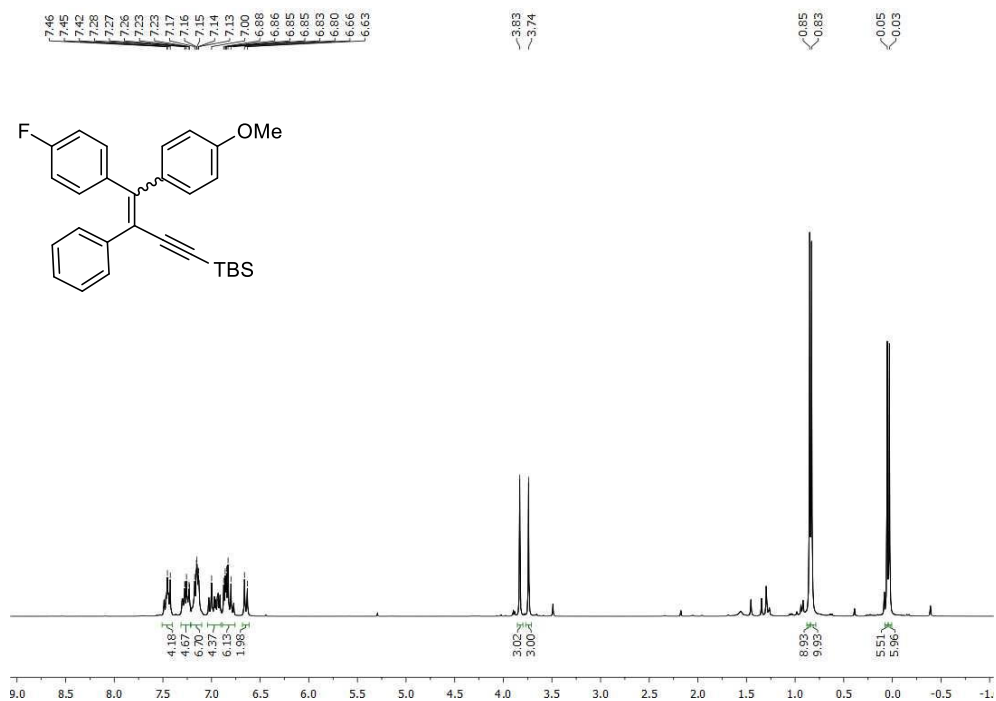


Tert-butyldimethyl(3,4,4-triphenylbut-3-en-1-yn-1-yl)silane (4.4a)

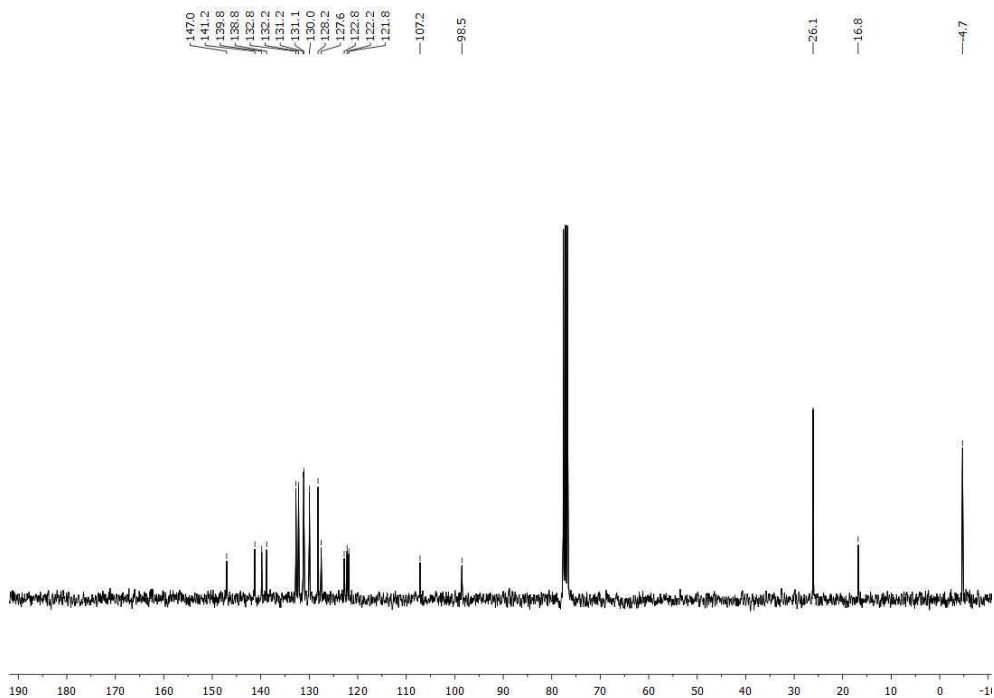
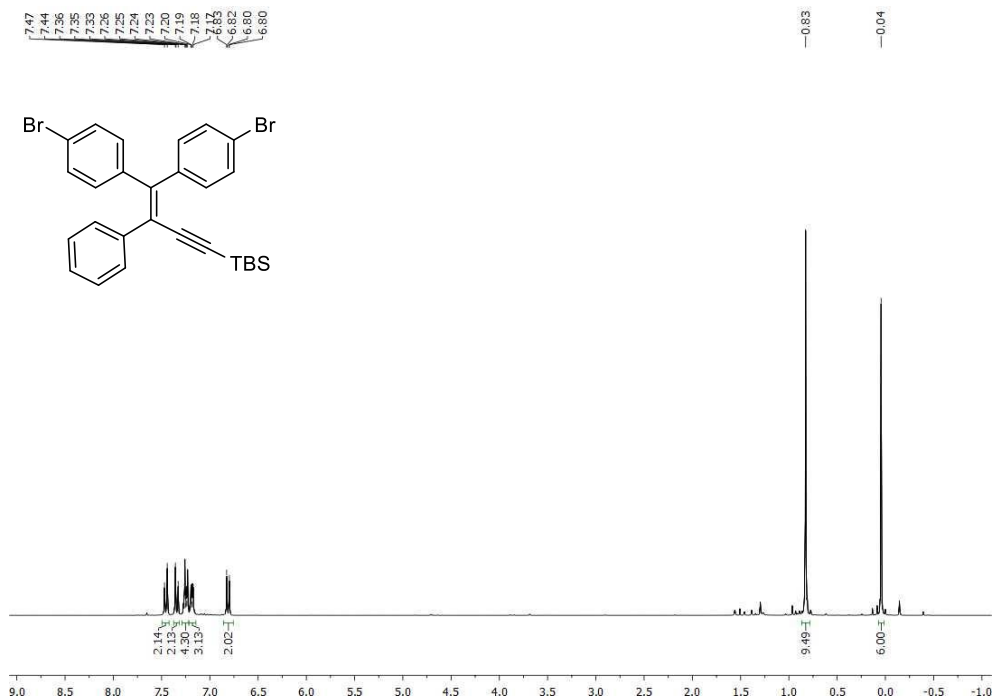
Tert-butyl(4-(4-methoxyphenyl)-3,4-diphenylbut-3-en-1-yn-1-yl)dimethylsilane (4.4g).

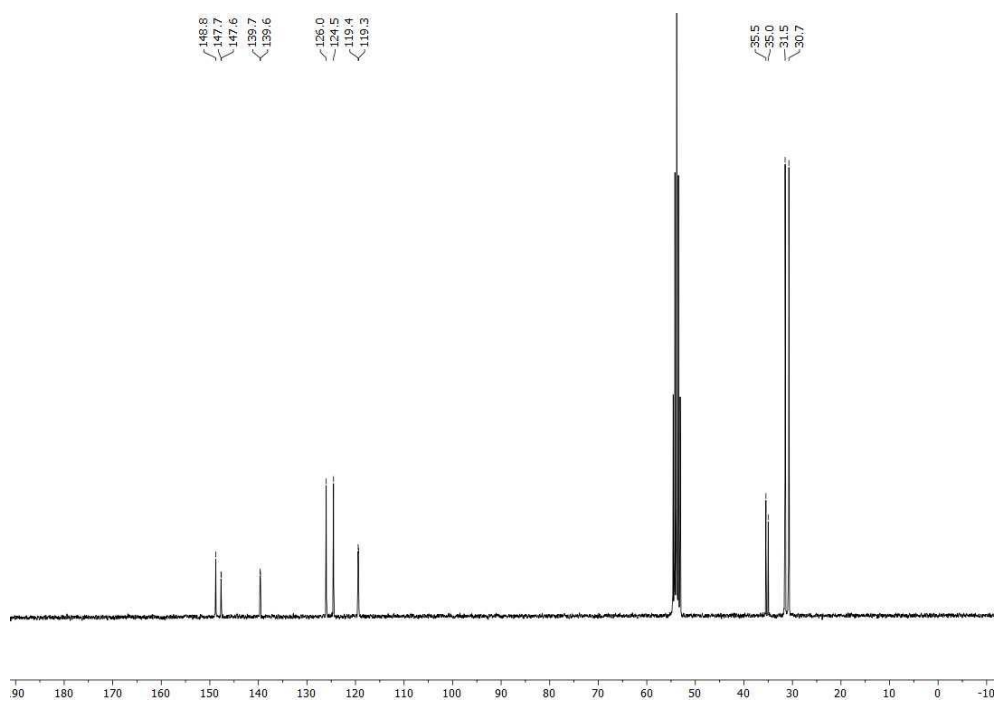
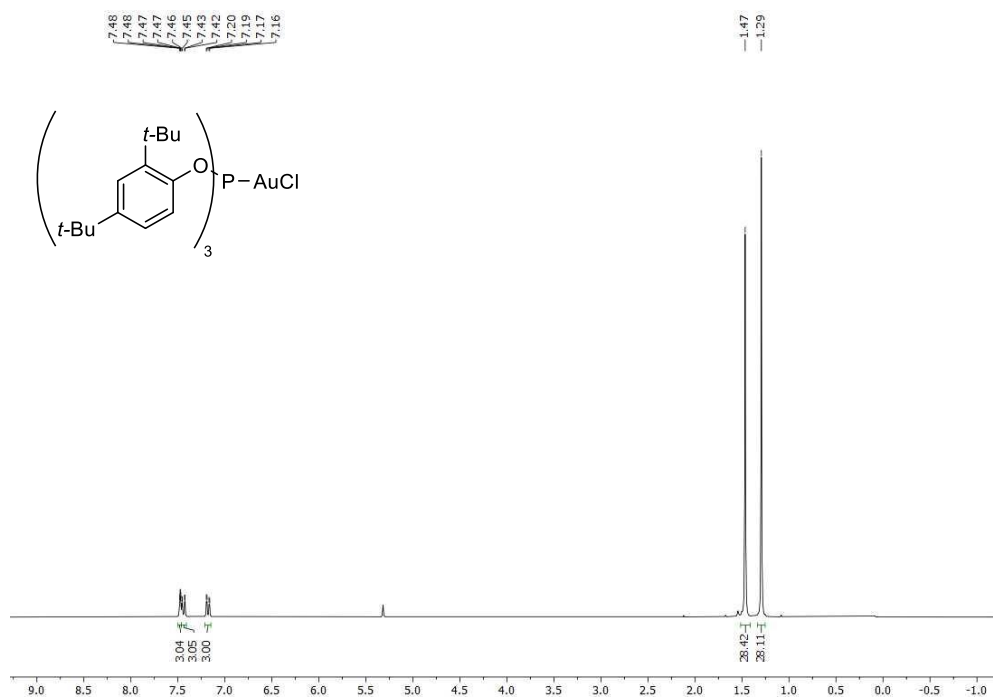


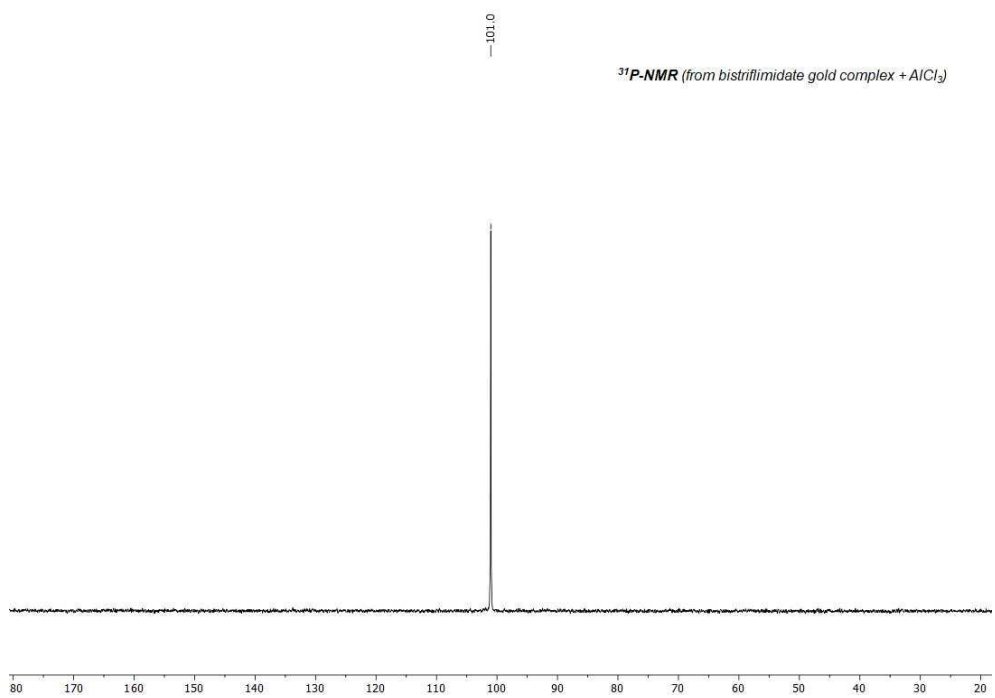
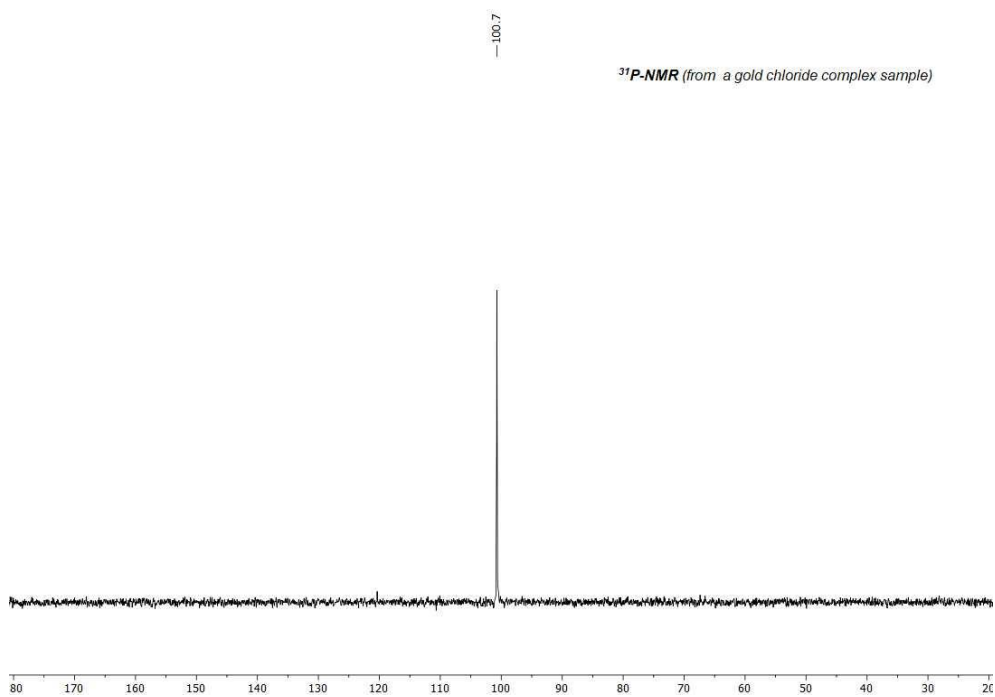
Tert-butyl(4-(4-fluorophenyl)-4-(4-methoxyphenyl)-3-phenylbut-3-en-1-yn-1-yl)dimethylsilane (4.4h).

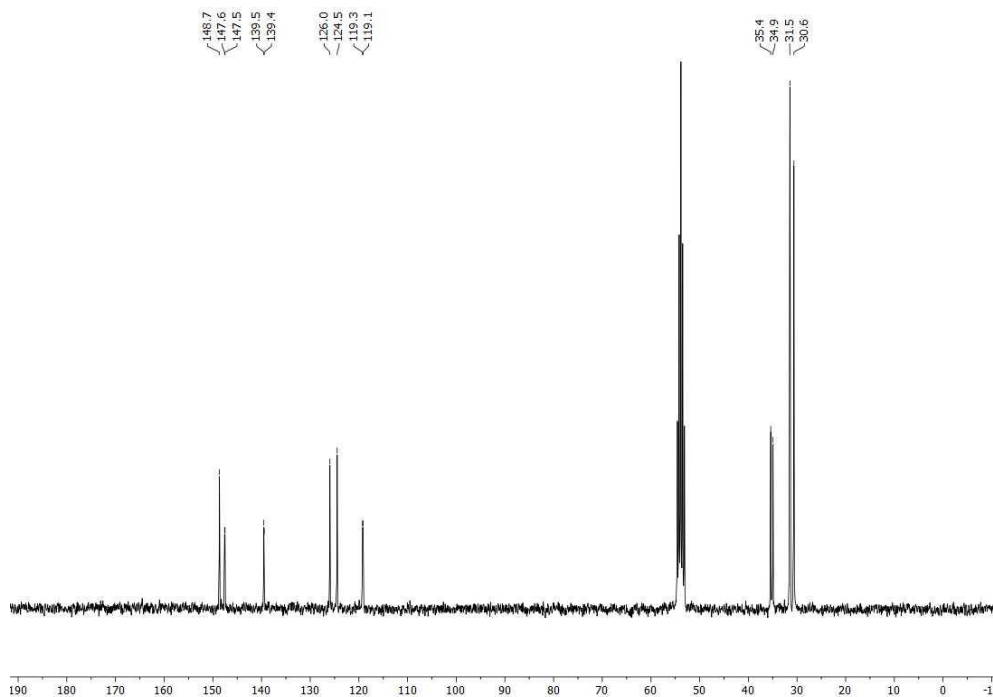
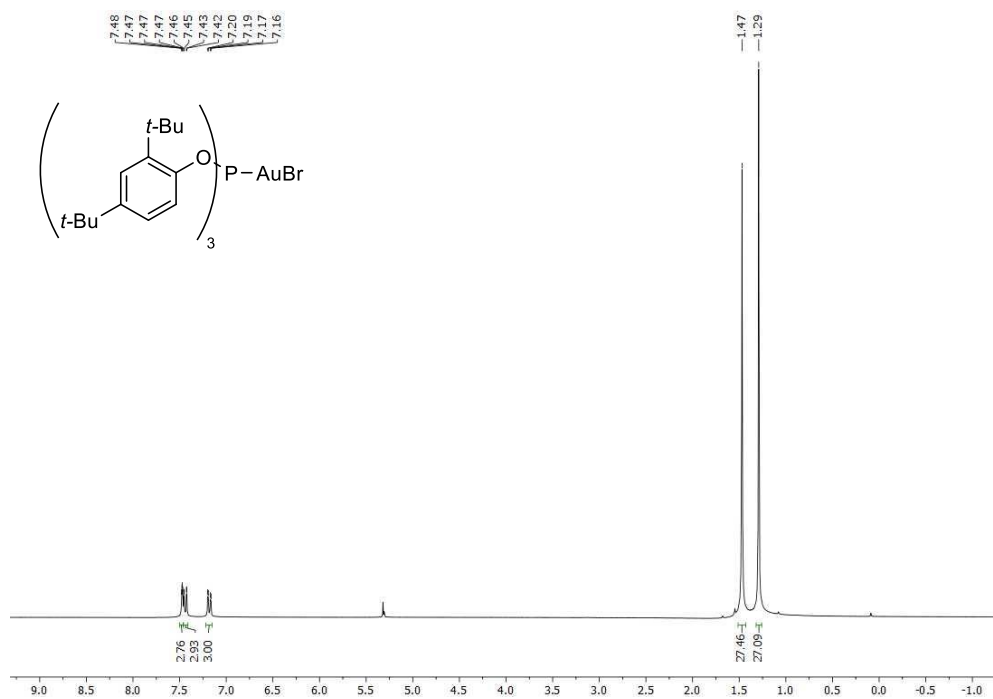


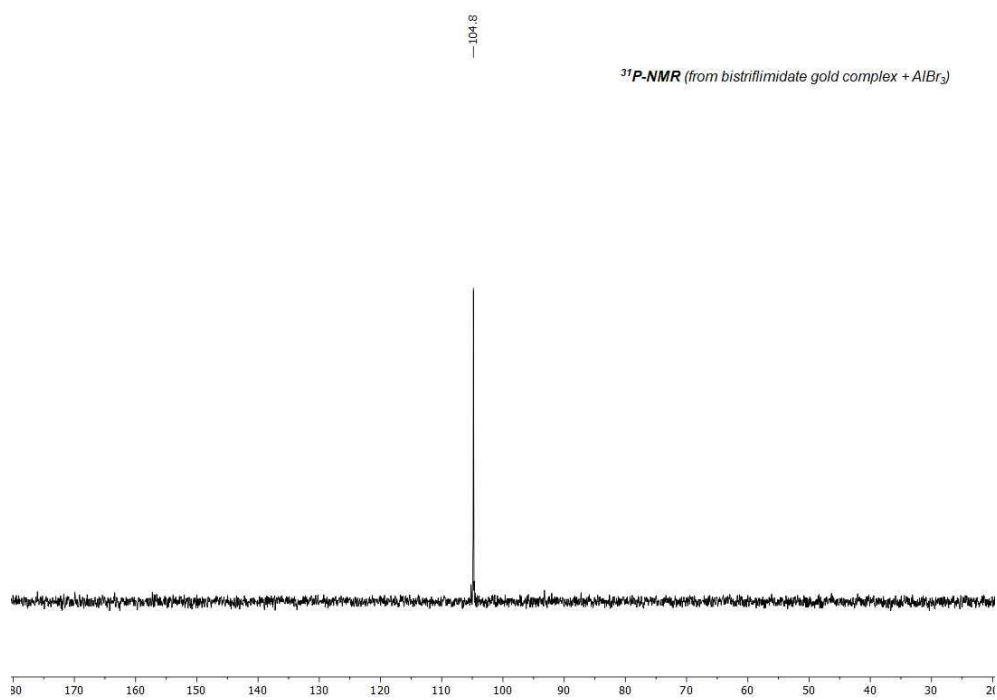
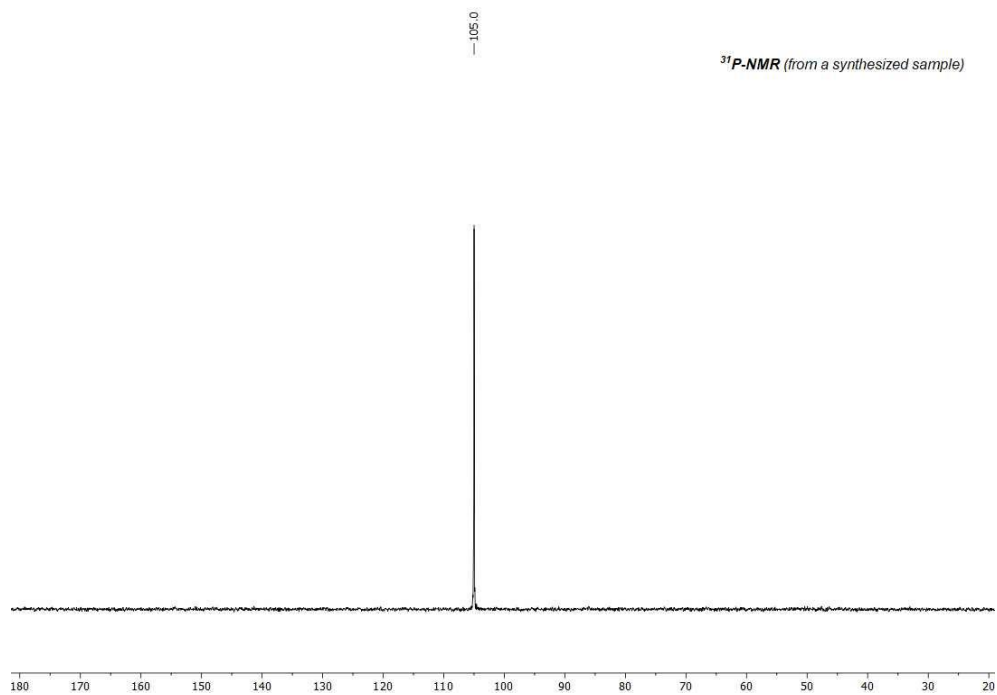
(4,4-Bis(4-bromophenyl)-3-phenylbut-3-en-1-yn-1-yl)(tert-butyl)dimethylsilane (4.4i).

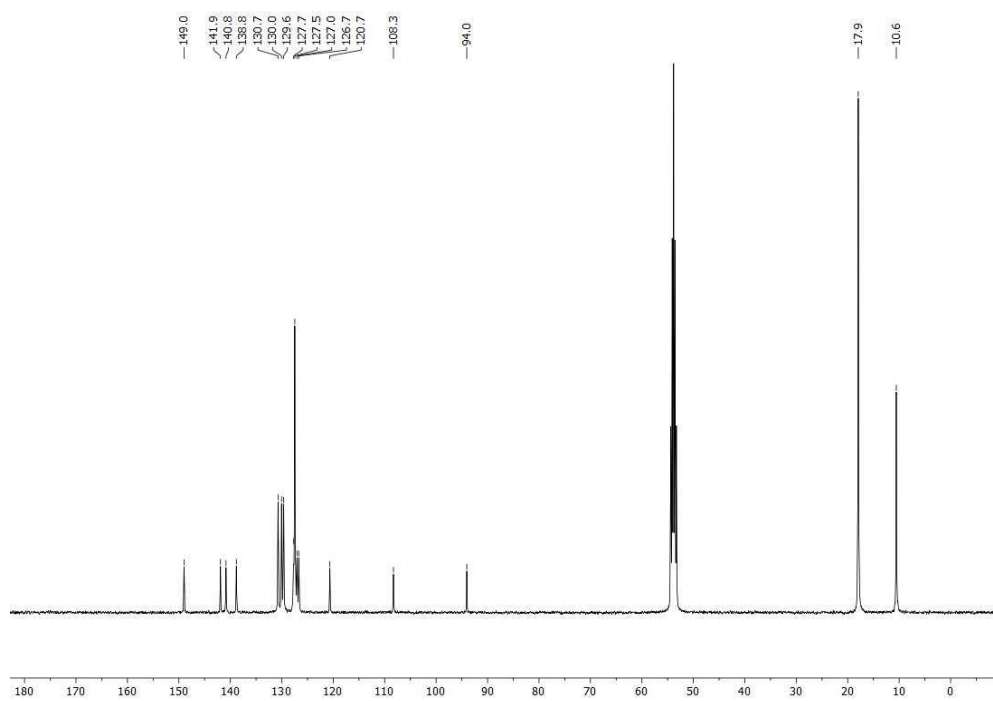
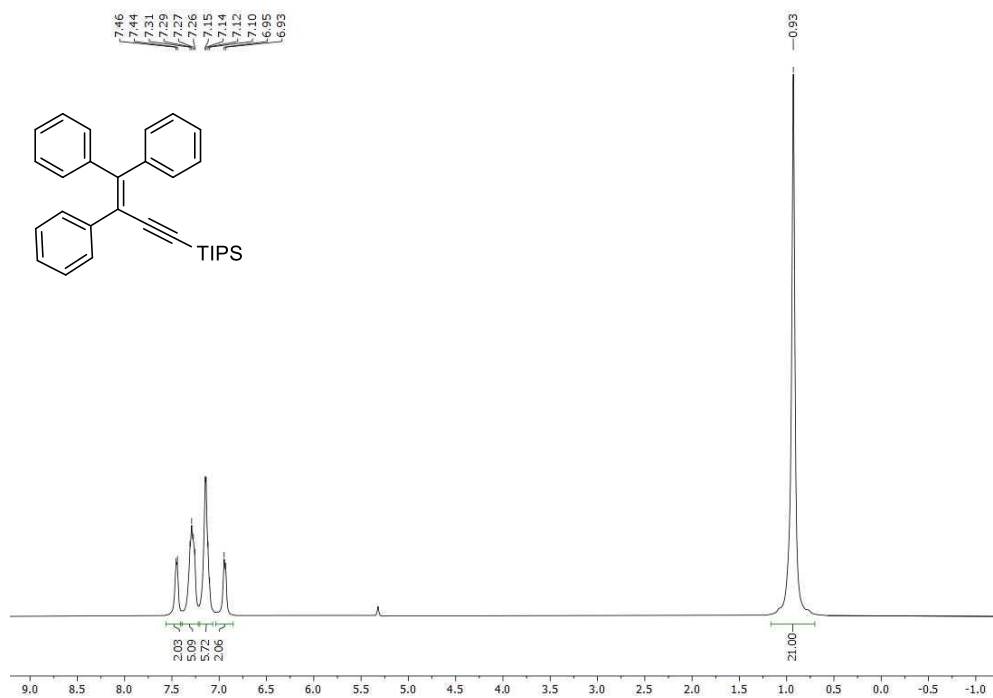


[Tris(2,4-di-*tert*-butylphenyl)]phosphite gold(I) chloride (4.10a)

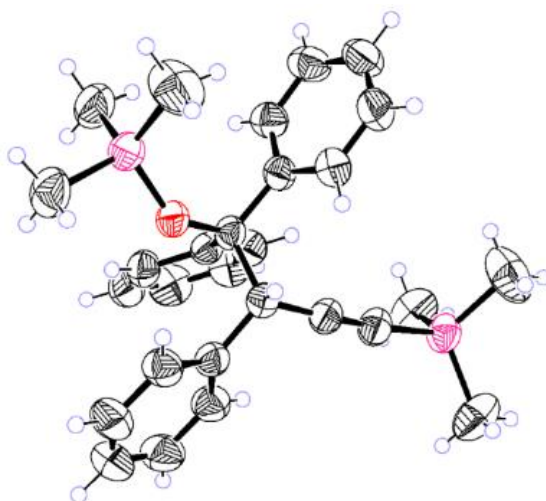


[Tris(2,4-di-*tert*-butylphenyl)]phosphite gold(I) bromide (4.10b)



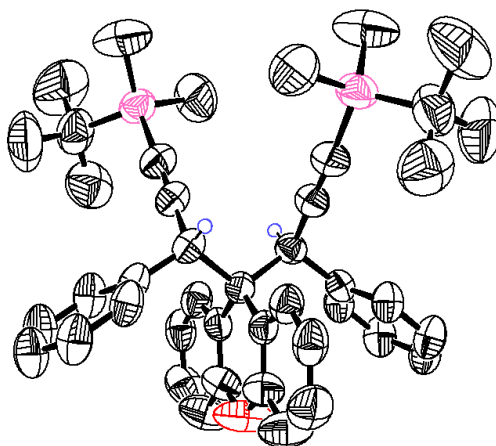
Triisopropyl(3,4,4-triphenylbut-3-en-1-yn-1-yl)silane (4.4s)

Annex II:
Crystallographic data

Trimethyl-4-((trimethylsilyl)oxy-3,4,4-triphenylbut-1-yn-1-yl)silane (1.3b)

Empirical formula:	$C_{28}H_{34}OSi_2$	Formula weight:	442.73
Temperature:	282(2) K	Wavelength:	1.54184 Å
Crystal system, space group:			Triclinic, P -1
Unit cell dimensions:	$a = 10.3767 (7) \text{ \AA}$	$\alpha = 104.806 (4) \text{ deg.}$	
	$b = 11.4452 (6) \text{ \AA}$	$\beta = 104.698 (5) \text{ deg.}$	
	$c = 12.9884 (7) \text{ \AA}$	$\gamma = 105.116 (5) \text{ deg.}$	
Volume:	$1352.26(15) \text{ \AA}^3$	Z, Calculated density:	2, 1.087 Mg/m ³
F(000):	476	Absorption coefficient:	1.299 mm ⁻¹
Crystal size:			0.44 x 0.21 x 0.16 mm
Theta range for data collection:			3.748 to 69.460 deg.
Limiting indices:			$-12 \leq h \leq 12, -13 \leq k \leq 13, -13 \leq l \leq 15$
Reflections collected / unique:			11255 / 4953 [R(int) = 0.0301]
Completeness to theta = 70.000			99.4 %
Absorption correction:			Semi-empirical from equivalents
Max. and min. Transmission:			1.00000 and 0.6974
Refinement method:			Full-matrix least-squares on F ²
Data / restraints / parameters:			4953 / 0 / 392
Goodness-of-fit on F²:			1.034
Final R indices [I > 2σ(I)]:			$R_1 = 0.0396, wR_2 = 0.1100$
R indices (all data):			$R_1 = 0.0450, wR_2 = 0.1159$
Largest diff. peak and hole:			0.231 and -0.222 e.Å ⁻³

((3*S,3'*S*'*)-(9*H*-Xanthene-9,9-diyl)bis(3-phenylprop-1-yne-3,1-diyl))bis(*tert*-butyldimethylsilane) (2.3a)**



Empirical formula: C ₄₃ H ₅₀ OSi ₂	Formula weight: 639.01
Temperature: 296.0(6) K	Wavelength: 1.54184 Å
Crystal system, space group:	Monoclinic, P 2/c
Unit cell dimensions:	a = 21.3771(3) Å α = 90 deg.
	b = 12.24350(10) Å β = 98.3670(10) deg.
	c = 15.5186(2) Å γ = 90 deg.
Volume: 4018.46(8) Å ³	Z, Calculated density: 4, 1.056 Mg/m ³
F(000): 1376	Absorption coefficient: 1.010 mm ⁻¹
Crystal size:	0.353 x 0.338 x 0.274 mm
Theta range for data collection:	3.610 to 69.692 deg.
Limiting indices:	-24<=h<=25, -14<=k<=11, -18<=l<=17
Reflections collected / unique:	21160 / 7453 [R(int): 0.0252]
Completeness to theta = 67.684	99.8 %
Absorption correction:	Empirical, spherical harmonics
Max. and min. Transmission:	0.76395/1.00000
Refinement method:	Full-matrix least-squares on F ²
Data / restraints / parameters:	7453 / 0/ 415
Goodness-of-fit on F²:	1.046
Final R indices [I>2σ(I)]:	R ₁ = 0.0624, wR ₂ = 0.1879
R indices (all data):	R ₁ = 0.0717, wR ₂ = 0.2029
Largest diff. peak and hole:	0.528 to -0.359 e.Å ⁻³

